CHANNEL EROSION on the MISSOURI RIVER, MONTANA between FORT PECK DAM and the NORTH DAKOTA BORDER

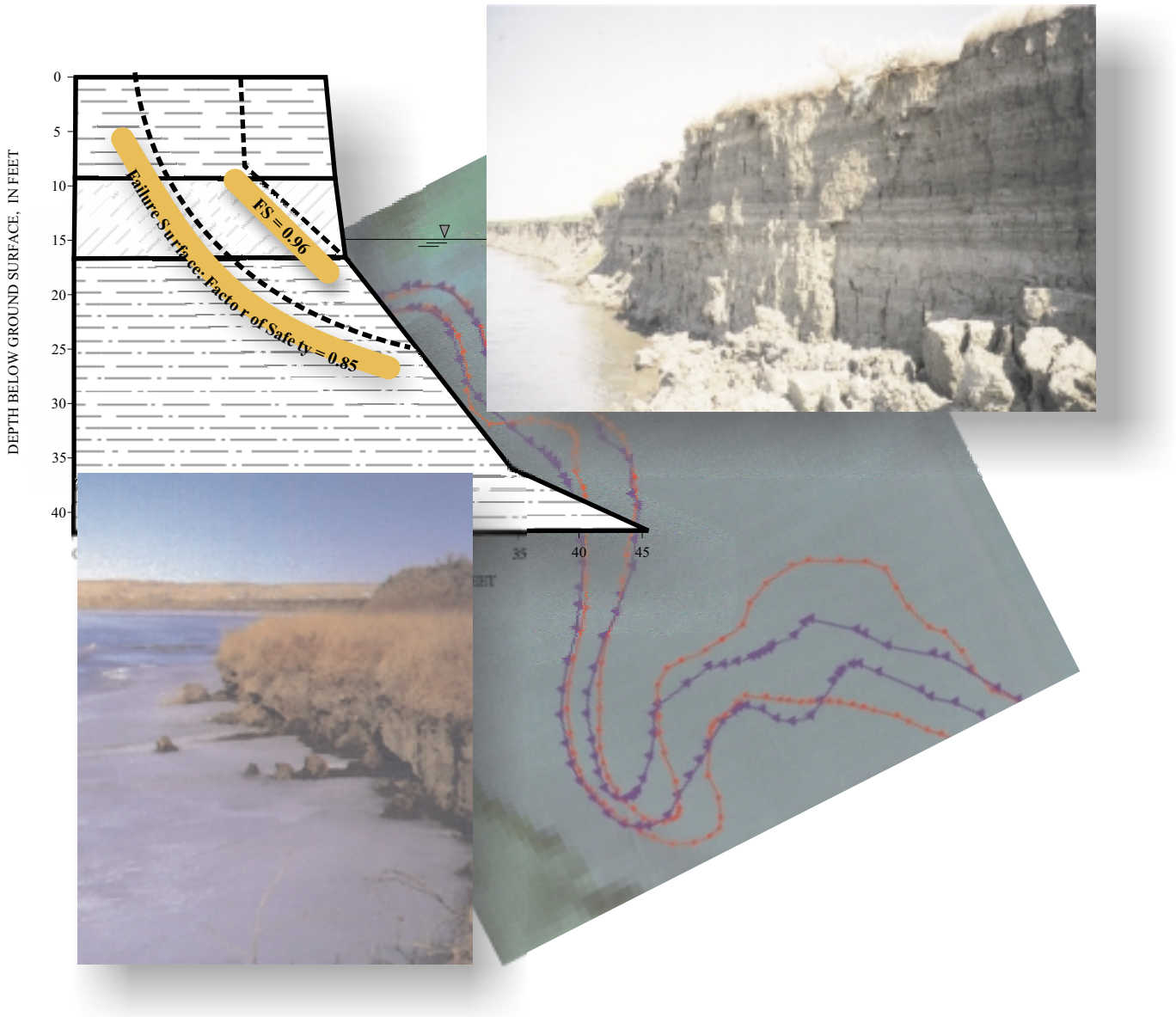

Prepared By:
USDA-Agricultural Research Service
National Sedimentation Laboratory
Oxford, Mississippi

In Collaboration With:
USDA-Natural Resources Conservation Service
Lincoln, NE; Bozeman, MT; Culbertson, MT
Iowa Institute of Hydraulic Research

Prepared For:
Coordinated Resource Management Group - Lower Missouri River CRM
Culbertson, Montana

May 1999

CHANNEL EROSION on the MISSOURI RIVER, MONTANA

between

FORT PECK DAM and the NORTH DAKOTA BORDER

By: Andrew Simon[1], F. Douglas Shields[1], Robert Ettema[2], Carlos Alonso[1], Marie Marshall-Garsjo[3], Andrea Curini[1] and **Lyle Steffen[4]**

Submitted to: Coordinated Resource Management Group-Lower Missouri River CRM
Culbertson, Montana

May, 1999

[1] USDA/ARS, National Sedimentation Laboratory, Oxford, MS
[2] Iowa Institute of Hydraulic Research, Iowa City, IA
[3] USDA, NRCS, Bozeman, MT
[4] USDA, NRCS, Lincoln, NE

LIST OF ILLUSTRATIONS

LIST OF TABLES

PREFACE

"The current ran at five miles per hour usually, but it sped up when it encountered encroaching bluffs, islands, sandbars, and narrow channels. The level was springtime high, almost flood stage. Incredible to behold were the obstacles -- whole trees, huge trees, oaks and maples and cottonwoods, that had been uprooted when a bank caved in; hundreds of large and thousands of smaller branches; sawyers, trees whose roots were stuck in the bottom and whose limbs sawed back and forth in the current, often out of sight; great piles of driftwood clumped together, racing downriver…innumerable sandbars, always shifting; swirls and whirlpools beyond counting. This was worse than the Mississippi" (Ambrose, 1996; p. 140). These are the conditions along the Missouri River as experienced by Captain Meriwether Lewis and the Corps of Discovery in May 1804. Granted that this passage refers to the Missouri River in the reaches just upstream of St. Louis, Missouri but it is interesting to note that almost 200 years ago, near the turn of the 19th century, river observers were referring to the effects of bank erosion.

Near the turn of the 21st century stability of the Missouri River is still an important concern for local landowners. A September 1995 field reconnaissance study of a 160 mile reach of the Upper Missouri River between Fort Peck Dam, Montana and the confluence of the Yellowstone River has indicated that approximately 50% of the river banks in this reach exhibit evidence of recent geotechnical failure and instability (Darby and Thorne, 1996). Riparian landowners and users, organized as the Coordinated Resource Management (CRM) group, have expressed concern that construction of Fort Peck Dam and subsequent operation of the dam for hydropower generation and flood-control functions may have been responsible for triggering changes in flow and sediment regime compared to pre-dam conditions. The CRM group perceive that these changes may have been responsible for triggering accelerated bank erosion, and loss of riparian property.

Previous studies have quantified channel changes, rates of bank erosion and channel migration rates (U. S. Corps of Engineers 1976; 1984; Englehardt and Waren, 1991; Wei, 1997; Pokrefke *et al*. 1998), and identified bank erosion mechanisms and the extent of bank instability (Simon and Darby, 1996; Darby and Thorne, 1996). However, data describing the geotechnical characteristics (mechanical behavior) of representative soil series were unavailable at that time. This had precluded the development of accurate, quantitative analyses of bank stability and other land loss problems associated with mass wasting (bank failures by gravity) for representative reaches on the Missouri River between Fort Peck Dam and the North Dakota border.

SUMMARY

Erosion and deposition are natural processes that occur over short time scales in response to changing flow conditions. Long-term river-channel changes, however, are generally due to a change in environmental conditions that control the supply of water and sediment to a river. The closure of Fort Peck Dam in the mid-1930's caused changes in the delivery of water and sediment to reaches of the Missouri River downstream of the dam in eastern Montana.

The closure of Fort Peck Dam reduced the amount of sediment delivered to downstream reaches and significantly altered the flow regime of the river. Much of the great peak-flows of the spring-summer snowmelt season are now stored behind the dam and replaced with a more constant, annual flow series. To accommodate the storage of the high magnitude snowmelt-runoff flows, average daily discharges over the remainder of the discharge range have been increased. The median of the mean-daily flow has increased from a pre-dam value of 4,830 ft^3/s to a post-dam value of 8,760 ft^3/s. Annual discharge peaks have been shifted to the winter months because of power demands. High flows during winter months, when there is an ice cover on the river have other important implications towards channel erosion along various reaches.

The trapping of sediment behind Fort Peck Dam resulted in channel-bed degradation downstream of the dam. Analysis of bed-level changes shows that this effect was most pronounced in the 30 miles just downstream of the dam. Average bed elevations decreased as much as 8 feet while thalweg (deepest part of the channel) elevations decreased by as much as 15 feet. This effect generally decreased downstream with increasing distance from the dam. The greatest effects were felt in the 55 miles closest to the dam. The effect also decreases with time such that at present (1998) channel-bed degradation as a result of Fort Peck Dam has virtually ceased. Given the average flow conditions, projected future amounts of bed-level lowering due to the dam are less than one foot.

The average rate of channel activity (migration) in the study reach is six-times less than it was before the closure of Fort Peck Dam. This change is at least partially due to a reduction in the frequency and duration of the highest discharges as caused by reservoir operations. The mean rate of pre-dam channel activity between Fort Peck and River Mile 1642 was 32.5 ft/yr, while the mean post-dam rate for the same reach between 1971 and 1991 was 5.7 ft/yr. The rate of activity for the entire reach (Fort Peck Dam to the North Dakota Stateline) was 7.7 ft/yr. The widths measured in the channel activity analysis are not top widths. The widths of the channel as measured from the pre dam, top-bank (flood plain) elevations are greater at present than they were pre-dam.

Empirical analysis of historical information indicates that channel activity tends to be greater in the eastern (downstream) portion of the study reach. Neck cutoffs occur on bends where substantial elongation and neck constriction occur, with low values of bend radius of curvature. There is at least one large meander bend in the study reach at Woods Peninsula (River Miles 1675-1679) for which a future neck cutoff is imminent.

The relative stability of the channel banks was analyzed using three independent techniques, all producing consistent results:

- Banks of low shear strength (generally low cohesive strength) are unstable. These

sites are characterized by sandy or silty soils of the following soil series: Banks, Havre-Harlem, Riverwash, and Trembles.

- Banks with sand or silty-sand bank-toe material are the most unstable. Study sites with sandy bank toes are located at River Miles 1604 (Hardy); 1624-low terrace (Tveit-Johnson); 1624 (Tveit-Johnson); 1631 (Vournas); 1646 (Mattelin); 1676 (Woods Peninsula); 1716 (Pipal); and 1765 (Garwood). The most stable banks are those that have clay in the lowest portion of the bank and/or at the bank toe.
- Banks that are stable during low-water stage often become unstable during periods of high groundwater levels due to the loss of soil suction and the generation of positive pore-water pressures.
- The destabilizing effect of high groundwater levels is produced by maintaining flows greater than 15,000 ft^3/s – 20,000 ft^3/s for 5 to 10 days and has increased in frequency since dam closure.
- The most stable banks are those containing cohesive clays that also are resistant to deep cracking. The site at River Mile 1762 (Milk River) is representative of this.

Banks that are unstable under most hydrologic conditions in any one of the three analyses are considered **unstable**. They are located at River Miles: 1604 (Hardy); 1624 low-terrace (Tveit-Johnson); 1631 (Vournas); 1646 (Mattelin); 1676 (Woods Peninsula); 1716 (Pipal); 1728 (Flynn Creek); and 1765 (Garwood). There are also many other unstable banks that were not studied in detail.

The cycle of river-ice formation, presence, and breakup affects bank erosion, sediment transport, and channel morphology in numerous ways. The mechanisms whereby river ice locally may accelerate bank erosion and change in channel morphology are as follows:

- Elevated ice-cover level;
- Elevated flow rates after freeze up;
- Local scour in regions of locally high flow velocity at ice accumulations or flow deflected by ice accumulations;
- Ice-run gouging and abrasion of channel banks and bars;
- Channel avulsion attributable to ice jams; and,
- Ice-cover influence on bank-material strength and bank stability.

A bank-stability index is developed for concerned agencies and citizens to evaluate erosion conditions along the river. The index uses diagnostic criteria of channel and bank conditions to identify those sites that are likely to have the most intense bank-erosion problems. Assigned values for each criteria are not weighted but simply increase as the condition or value of a given variable indicates a greater tendency for bank instability. Sites with a bank-stability index greater then 20 are generally unstable. Values greater than 25 indicate the potential for rapid bank erosion by mass wasting while sites with an I_s value less than 15 are considered relatively stable under non ice-effected conditions. The maximum possible I_s value is 35. It should be emphasized that this index is not designed to predict rates of bank erosion or to insinuate that a streambank with an index value of 30 is twice as likely to fail as a site with an index value of 15.

The index is tested for the 17 detailed study sites. In support of the more rigorous numerical analyses of bank instability, the bank-stability index successfully identified

banks at River Miles 1631 (Vournas), 1716 (Pipal), 1646 (Mattelin), 1624 (Tveit-Johnson, low terrace), and 1676 (Woods Peninsula) as having the greatest potential for further instabilities. Sites at River Miles 1744 (Little Porcupine) and 1762 (Milk River) ranked as among the more stable sites in the reach.

A significant concern commonly expressed is the substantial rates of flow and flow-rate fluctuations that Fort Peck Dam imposes on the Missouri River during winter. The flows are much larger, and fluctuate more frequently, during winter than occurred prior to the dam. The increased magnitudes of ice-covered flow, increased ice movement up and down banks, bank freezing at a higher level and more frequent freeze-thaw cycles experienced by the bank materials are seen as severely aggravating bank erosion. The effects of these processes become noticeable in spring, when large portions of banks, which have been undercut during winter or early spring, begin to fail.

Freezing and thawing (and/or sublimation) of pore water in riverbanks comprises a second set of mechanisms whereby ice potentially may affect riverbank erosion and channel morphology. An eroding riverbank is especially subject to deep penetration of frost, thereby making more of the riverbank prone to freeze-thaw weakening and erosion.

Freeze-thaw cycles affect soil structure, porosity, permeability, and density. These changes in soil properties substantially reduce soil shear strength and bearing capacity; strength reductions of as much as 95% have been reported in other studies. Soils containing fine sands and silts are especially sensitive, because they are permeable and susceptible to change in soil structure. By virtue of their particle size (about 0.1 mm to 0.06 mm), and the surface tension property of water, fine sandy and silty soils absorb moisture more readily than do coarser or clay-sized sediment. Clayey soils are less sensitive, because of their low permeability.

In general, the soils formed in recent alluvium on low terraces at or near the water level have a higher average percentage of total sand (35.4%; std. error S_e = 4.6) than the more stable alluvial terraces (20.8%; S_e = 8.4), which lie above the present flood plain. Differences are even more striking if the median values are considered. Median sand content for the “new” soils is 27.4% compared to 5% for the upper 5 feet of the “old” soils.

Two of the most important issues regarding streambank erosion along the Missouri River in the study reach are pore-water pressure effects from sustained high flows, ice-related effects, and the direct effects of an ice cover. Ice effects are particularly significant in channel-bed shifting and, therefore, the silting of pump sites along the river. These effects and appropriate designs for mitigation of these effects can be quantified only by undertaking further measuring and monitoring activities that concentrate on those factors that control and dominate channel erosion in the study reach. These variables include groundwater and bank-freezing levels, hydraulics in the near-bank zone, and effects of river ice.

INTRODUCTION

Background

In July of 1994, Paul Johnson, who was Chief of the Natural Resources Conservation Service at that time, met with Dick Gooby, Montana State Conservationist, and the Lower Fort Peck Missouri River Development group in Wolf Point, Montana. Since 1994, the group has formed a Coordinated Resource Management Group, now known as the Lower Missouri River CRM. The group asked for help in solving problems involving erosion of the Missouri River bed and banks. In particular, the CRM group is concerned with the loss of agricultural land due to bank erosion and sedimentation around irrigation-pump sites. The Chief told the group that while the Corps has jurisdiction over the project, the NRCS would look into the erosion problem.

At this time the Chief stated that erosion control and protection of natural resources are included in the mission of our agency, and that the NRCS would take the lead in coordinating an interagency study of erosion process. This project was formed and supported by the NRCS because it is a project with national significance. For example, the Missouri River was placed on the list of North America's ten most endangered rivers by the environmental group American Rivers in April 1997. In July 1998, the group launched a five-year "Voyage of Recovery" for a "healthier and more beautiful Missouri River" that was covered by the Great Falls Tribune on July 7, 1998.

Concerns of the Lower Missouri River CRM

The Lower Missouri River CRM has expanded its original concern of river bed and bank erosion and is also looking at the economic base of northeastern Montana and western North Dakota. The Missouri River is the lifeblood of the region now and has been since the settlement of the western United States.

The CRM's identified concerns are:

- Retain agricultural land threatened by erosion
- Improve aquatic habitat, especially for threatened and endangered species
- Improve overbank habitat, including re-establishment of cottonwood riparian zones
- Add recreation opportunities, parks, boat ramps, wildlife areas, etc.
- Provide stable irrigation pump sites and water intake facilities
- Create communal irrigation systems
- Create an interagency (Federal, State, Local) group to plan, implement, and monitor improvements
- Educate stakeholders and the public

This investigation was carried out with these concerns in mind.

OBJECTIVES AND SCOPE

The overall objective of the study described by this report was to determine the magnitude and extent of channel changes along the Missouri River between Fort Peck Dam and the North Dakota border. Concerns regarding the instability of streambanks and the silting-in of pump sites were identified by the CRM group as being of particular concern. More specifically, the objectives of this study are as follows:

1) Compare flow regimes before and after closure of Fort Peck Dam;
2) Determine if and how changes in flow regime affected bed- and bank- erosion processes;
3) Compare rates of channel change before and after closure of Fort Peck Dam;
4) Estimate future amounts of channel change;
5) Determine the effects of ice and ice-related processes on channel morphology;
6) Determine the controlling factors in streambank stability in the reach;
7) Determine the relative erodibility and stability of the channel banks;
8) Develop and demonstrate methodology for assessing erosion potential of channel banks that can be used by agencies and landowners;
9) Recommend further data and information needs based on the results of this study; and
10) Compile a comprehensive bibliography.

The scope of this study stretches from River Mile 1771.5, at Fort Peck Dam, downstream to the North Dakota border. The temporal scope of the study includes 1890 to the present (1998).

GENERAL VALLEY CHARACTERISTICS

The reach of the Missouri River between Fort Peck Dam and the North Dakota border is between River Mile (RM) 1771.55 and River Mile 1586.63 (U.S. Army Engineer District, Omaha, undated). Descriptions of the dam and the study reach are provided by the Fort Peck District (US Army Corps of Engineers, 1952) and Wei (1997). In the study reach, the Missouri River channel meanders through a broad floodplain from Fort Peck Dam, at River Mile 1771, to River Mile 1659 a few miles west of the town of Brockton. In this reach, the floodplain is nearly three to over four miles wide, and follows the ancestral, pre-glacial channel of the river. In most of this reach the channel lies in the southern portion of the floodplain and the meanders are confined by bedrock exposed on the southern bank.

Between Brockton and River Mile 1621 at Culbertson the floodplain narrows to a width of two to almost three miles. While this reach is narrower than the previous reach, it is still developed in the ancestral channel and the southern bank confines the meanders. At Culbertson, the floodplain narrows to an average width of one mile. This channel was developed during the Pleistocene and does not show the mature morphology of the upper reaches. This younger reach is entrenched into bedrock, which confines meanders on both banks.

At the Shotgun Creek confluence, at about River Mile1604 south of the town of Bainville, the Missouri River rejoins the ancestral channel with its broader floodplain. The older floodplain is two to three miles wide from here to the North Dakota border.

In general, the river is bordered to the north by gently sloping uplands. To the south, the surface rises abruptly and irregularly through rolling prairies and rugged badlands. Distinct terraces 5 to 25 feet above the present day floodplain flank the river.

Several straight reaches occur, although the channel pattern is considered meandering. Islands and bars are quite common in the channel, which has a total width of about 800 to 1,150 feet. The floodplain has many meander scars, some of which have been filled with sediment and organic material and are now broad, shallow swales. Younger meander scars contain standing water all year.

Study Reach

The climate is semi-arid with about 14 inches of annual precipitation, cold winters, and hot summers. Drainage area above the dam is 57,500 mi^2, and drainage area contributing to the reach below the dam is only 36,035 mi^2. About 66% of this is in the watershed of the Milk River, which empties into the Missouri about 10 miles downstream from the dam. The river channel is entrenched and is flanked by distinct terraces, with the highest terrace about 10 feet above the present high water level. The valley is much narrower (~ 1 mile wide) in the reach between about River Mile 1621 and River Mile 1636 where the river is entrenched in sandstones and shales. Elsewhere, despite the greater alluvial valley width, meanders are confined and contact the valley walls at several points (U.S. Corps of Engineers 1984, Wei 1997). Several straight reaches occur, although the overall channel pattern corresponds well to the “sinuous braided” river type (Brice 1984). Islands and bars are quite common in the channel, which has a total width of about 800 to 1200 feet. River slope is about 0.0002 (1-foot per mile) and bed material

is about 0.25 mm (medium to fine sand) with occasional deposits of coarse gravel, cobbles, and dense clay. In 1993, the average median bed sediment grain size varied from about 1.6 mm (coarse sand) in the 70 miles immediately downstream from the dam to about 0.25 mm in the reaches further downstream (Wei, 1997).

Fort Peck Reservoir has a surface area and volume at maximum operational pool level (2,250 feet MSL) of 240,000 acres and 18.7 million-acre feet, respectively. Fort Peck Dam was constructed between 1933 and 1937 and began storing water in November of 1937. It reached minimum operational level in 1942. During the period just prior to dam closure (1929-1936), average discharge at Wolf Point (about 70 river miles down--stream was 7,060 ft^3/s and the average annual peak discharge was 27,000 ft^3/s. These values were 9,900 ft^3/s and 24,000 ft^3/s, respectively, during the period 1937 through 1978 (Williams and Wolman, 1984). The contrast between pre- and post-dam discharges would likely be greater if not for the drought that dominated the short pre-dam period of record. Surveys of Fort Peck Reservoir indicate that sediment retention has resulted in a loss of storage capacity of 869,000-acre feet between 1938 and 1987 (McGregor *et al.*, 1996).

Investigations of downstream channel response to reservoir closure have been performed by the Corps of Engineers (1945) and Williams and Wolman (1984). The major effect of Fort Peck Reservoir on study reach channel geometry appears to have been degradation in the reach immediately downstream from the dam (Williams and Wolman 1984, Pokrefke *et al*. 1998).

Only ten valley cross sections were surveyed at the time of dam construction (1936), and periodic resurveys of four of these were discontinued because they were disturbed by dredging associated with dam construction (US Army Corps of Engineers 1952). Analysis of repetitive surveys of the six remaining cross sections, which were located in the reach between the dam and 47 miles downstream, indicated that mean bed elevation decreased as much as 3 feet by 1951 (US Army Corps of Engineers 1952), and as much as 5.7 feet during the period between dam closure and 1973 (Williams and Wolman 1984). Degradation was most rapid immediately after dam closure. Greatest degradation was observed at cross sections 10 miles and 14 miles downstream from the dam.

Channel widening at the six cross-sections varied considerably (from 0 to 37%). Wei (1997) also examined post-impoundment changes in the geometry of the study reach. Analysis of changes was hindered by the availability of survey data prior to 1956, as only 5 cross sections were surveyed in 1936 and 6 in 1946, and these were located 5 to 47 miles downstream from the dam. In this report, however, additional 1936 data is simulated from 1889 low-water maps. Strangely, survey dates and cross section locations differed from those tabulated by Williams and Wolman (1984) for this reach.

Data provided by Wei indicated that mean bed elevation for the five cross sections decreased 2 to 5.6 feet while channel width changes varied from an increase of 310 feet to a decrease of 213 feet between 1936 and 1994. Contrary to statements by Wei (1997), these data do not show that the overall rates of change were more rapid immediately after dam closure than recently. Water surface profiles for a discharge of 10,000 ft^3/s indicate degradation through 1995 between the dam and about 70 miles downstream, with aggradation further downstream since about 1958 (Wei 1997). Bed

aggradation has been observed only in the most downstream portions of the study reach (Pokrefke *et al*. 1998).

Since little analysis has been done by others of bed elevation changes between pre-impoundment and the present, we plotted 1936 and 1994 average bed elevations provided by Wei (1997) on the same axis with the 1889 low water profile provided in U. S. Corps of Engineers (1933) (Figure 1). Comparison of the two profiles shows 1 to 8 feet of degradation. Evidently, post-impoundment degradation has been most pronounced in the 70 miles immediately below the dam, but an additional zone of degradation is located in the reach 100 to 150 miles downstream from the dam.

Currently part of the flood plain immediately adjacent to the river is intensely cultivated for irrigated sugar beet and grain production. Riparian landowners have contended that their operations are adversely impacted by bank erosion. Darby and Thorne (1996) estimated that about 57% of the banks along the study reach were eroding through mass wasting processes. Another study estimated bank erosion in the reach leads to an average annual loss of land of 0.47 acres per River Mile (U. S. Army Corps of Engineers 1995). However, comparison of aerial photographs taken in 1975 and 1983 led to an annual erosion estimate of only 0.12 acres per river mile (Wei, 1997 and U.S. Army Corps of Engineers, 1984).

Planar failures due to toe scour and oversteepening by fluvial bank erosion is the most common mechanism of collapse. Alleged bank erosion impacts include the loss of agricultural land, irrigation pumping stations and pipelines, damage to roads and bridges, and downstream sedimentation in Lake Sakakawea (Bernard *et al*. 1997). Some landowners contend that the riverine erosion and deposition processes are replacing high quality flood plain lands with lower elevation deposits of soils that are coarser and less fertile, while others simply contend that erosion of arable lands is not balanced by deposition (Rahn, 1977).

Bed-Material Characteristics

Bed material in the study reach is predominantly sand, with gravel generally making up less than 20 percent of the distribution. There are occasional deposits of coarse gravel, cobbles, and dense clay. Bed material tends to be coarser (dominated by gravels) in the reach immediately downstream of Fort Peck Dam.

Available data have been separated into 4 different periods: 1937-1941, 1942-1945, 1960, and 1993 (U.S. Army Corps of Engineers, written commun.; Wei, 1997). Data from 1937-1941 and 1942 –1945 represent an average of 4-11 times that 3 samples were taken at a particular cross-section (range) during each of the periods (Table 1). These averages are plotted with sample data acquired in 1960 and 1993 (Figures 2 and 3). The U.S. Army Corps of Engineers collected all samples.

Downstream of the immediate vicinity of the dam (downstream of River Mile 1765) median bed-material particle size was in the range of 0.2 – 0.3 mm during 1937-1941. Over the span of the next 50-60 years, bed-material sizes did not change much in these reaches, with 1960 and 1993 median particle sizes in the range of 0.3 – 0.4 mm (Figure 3). The coarsest particles comprising the bed in these reaches, represented by the 90^{th} percentile of the distribution (d_{90}), were between 10 and 20 mm. Dredging operations in the vicinity of the downstream side of the dam prior to April 1940 left an irregular

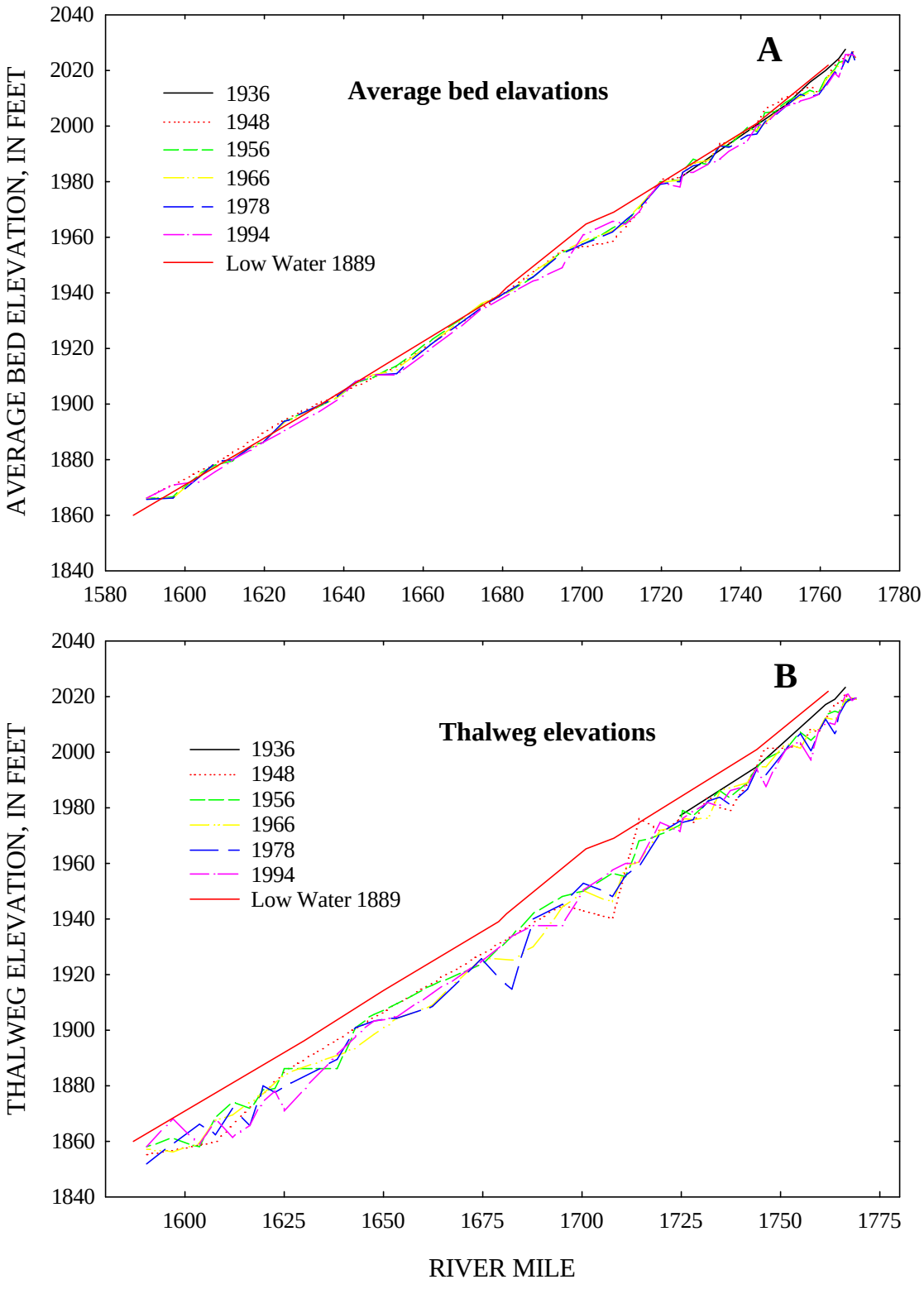

Figure 1--Comparison of 1889 low water profile with 1936, 1948, 1956, 1966, 1978 and 1994 (A) average bed elevations, and (B) thalweg elevations (Wei, 1997).

Table 1--Bed-material data from 1937 - 1945 sampled by the U.S. Army Corps of Engineers

Range 3			**Range 4**	**1763.84**		**Range 5**	**1761.56**		**Range 6**	**1757.58**		**Range 7**	**1743.97**		**Range 8**	**1724.81**		**Range 1**	**1768.89**		**Range 2**	**1768.13**	
7/37-10/41	D90	D50	7/37-10/41	D90	D50	7/37-10/41	D90	D50	7/37-10/41	D90	D50	7/38-10/41	D90	D50	7/38-10/41	D90	D50	7/37-2/38	D90	D50	7/37-4/39	D90	D50
1	0.365	0.072	1	0.475	0.120	1	0.220	0.120	1	0.335	0.098	1	0.315	0.063	1	0.280	0.043	1	0.460	0.090	1	0.415	0.115
2	0.42	0.14	2	0.595	0.155	2	0.425	0.26	2	0.405	0.165	2	0.38	0.14	2	0.31	0.091	2	0.5	0.125	2	0.47	0.275
3	0.45	0.177	3	0.62	0.24	3	0.475	0.3	3	0.45	0.18	3	0.395	0.24	3	0.43	0.099	3	0.54	0.165	3	0.48	0.31
4	0.46	0.22	4	0.73	0.265	4	0.505	0.32	4	0.455	0.22	4	0.49	0.255	4	0.47	0.16	4	3.5	0.185	4	0.5	0.345
5	0.47	0.29	5	4.7	0.29	5	0.55	0.325	5	0.475	0.245	5	0.515	0.275	5	0.505	0.24				5	0.51	0.36
6	0.52	0.305	6	10.5	0.325	6	0.555	0.405	6	0.49	0.295	6	12	0.3	6	0.52	0.255				6	0.52	0.365
7	1.30	0.32	7	12.5	0.41	7	0.605	0.36	7	4	0.305	7	16.5	0.405	7	23	0.39						
8	5.40	0.33	8	13.5	0.45	8	0.62	0.355	8	9	0.33												
9	5.50	0.38	9	15.5	0.475	9	0.65	0.35	9	23	0.39												
10	5.50	0.42	10	23	0.48	10	0.65	0.345	10	24.56	0.405												
11	17.50	0.44	11	37	0.52	11	0.57	0.34	11	32.5	0.43												
Average	**3.44**	**0.281**		**10.829**	**0.339**		**0.530**	**0.316**		**8.697**	**0.278**		**4.371**	**0.240**		**3.645**	**0.183**		**1.250**	**0.141**		**0.483**	**0.295**
Std. Dev.	**5.18**	**0.11708**		**11.4918**	**0.13718**		**0.12487**	**0.07474**		**12.0604**	**0.10711**		**6.87305**	**0.11076**		**8.53526**	**0.12037**		**1.50036**	**0.0423**		**0.03637**	**0.1016**
Std. Error	**1.56**	**0.04**		**3.46**	**0.04**		**0.04**	**0.02**		**3.64**	**0.03**		**2.60**	**0.04**		**3.23**	**0.05**		**0.75018**	**0.02115**		**0.01485**	**0.04148**
																					Range 2A	**1766.92**	
5/42-5/45			5/42-8/45			5/42/8/45			5/42/8/45			5/42/8/45			5/42/8/45						10/42-8/45	D90	D50
1	0.45	0.24	1	0.39	0.081	1	0.29	0.097	1	0.355	0.066	1	0.325	0.215	1	0.19	0.036				1	0.38	0.18
2	0.50	0.25	2	0.525	0.089	2	0.39	0.22	2	0.43	0.165	2	0.36	0.24	2	0.29	0.039				2	0.465	0.185
3	0.52	0.32	3	0.76	0.29	3	0.43	0.3	3	0.455	0.175	3	0.52	0.26	3	0.34	0.069				3	0.57	0.21
4	0.63	0.32	4	6	0.31	4	0.53	0.32	4	0.5	0.245	4	1.2	0.275	4	0.365	0.079				4	11	0.23
5	8.00	0.44	5	14	0.315	5	0.545	0.35	5	0.505	0.305	5	3.2	0.3	5	0.38	0.11				5	20	0.24
6	9.90	0.65	6	44	0.36	6	0.785	0.35	6	0.54	0.31	6	5	0.3	6	0.42	0.14				6	25	0.475
7	20.50	0.26	7	51	0.45	7	1.45	0.385	7	0.36	0.37	7	32	0.32	7	0.44	0.28						
Average	**5.79**	**0.35429**		**16.6679**	**0.27071**		**0.63143**	**0.28886**		**0.44929**	**0.23371**		**6.08643**	**0.27286**		**0.34643**	**0.10757**					**9.56917**	**0.25333**
Std. Dev.	**7.62735**	**0.14718**		**21.6998**	**0.13724**		**0.39303**	**0.09947**		**0.07208**	**0.1048**		**11.5605**	**0.03718**		**0.08499**	**0.08458**					**10.9295**	**0.11116**
Std. Error	**2.88287**	**0.05563**		**8.20175**	**0.05187**		**0.14855**	**0.0376**		**0.02724**	**0.03961**		**4.36946**	**0.01405**		**0.03212**	**0.03197**					**4.46196**	**0.04538**

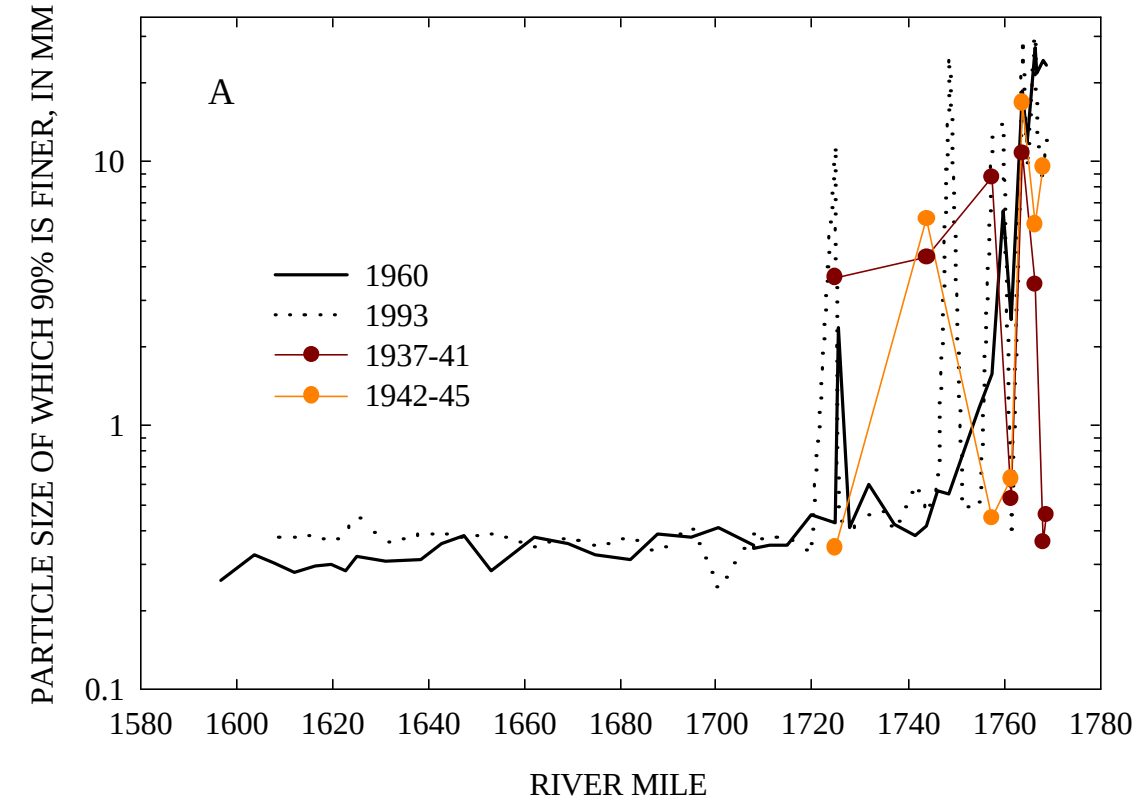

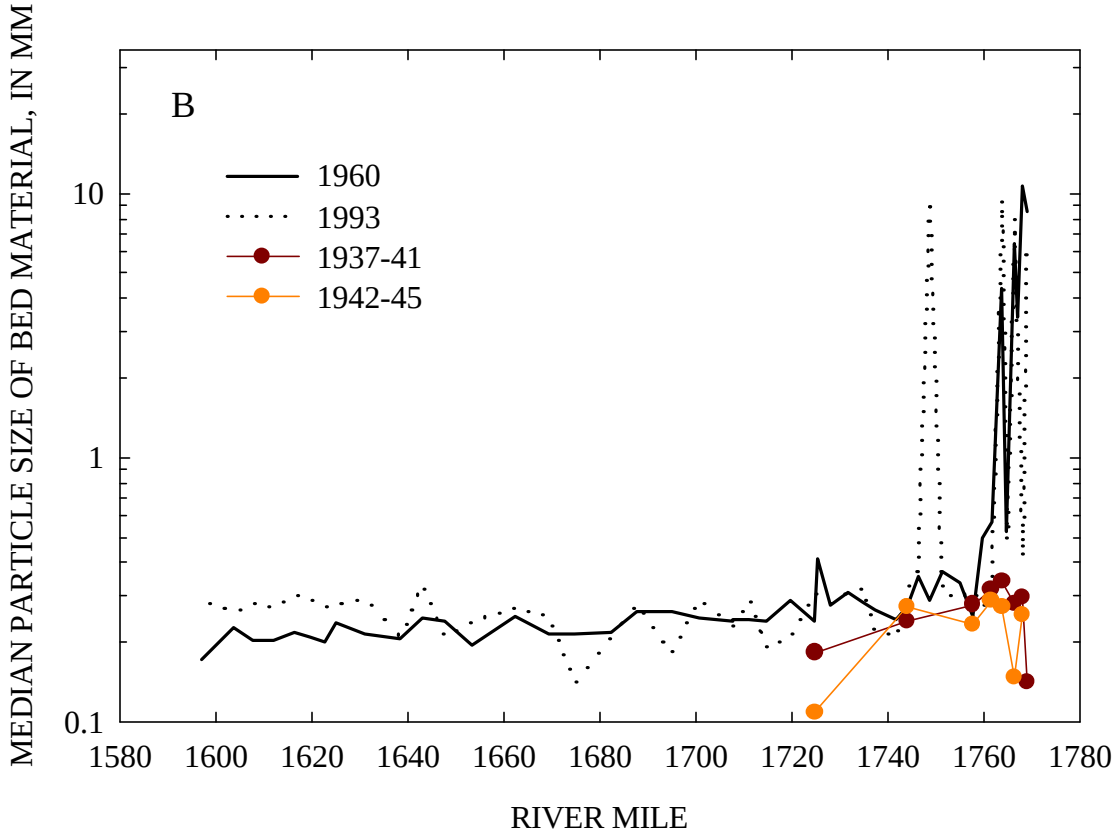

Figure 2--Comparison of median and d_{90} particle size of bed-material for four periods ranging from 1937-1993 for the entire study reach.

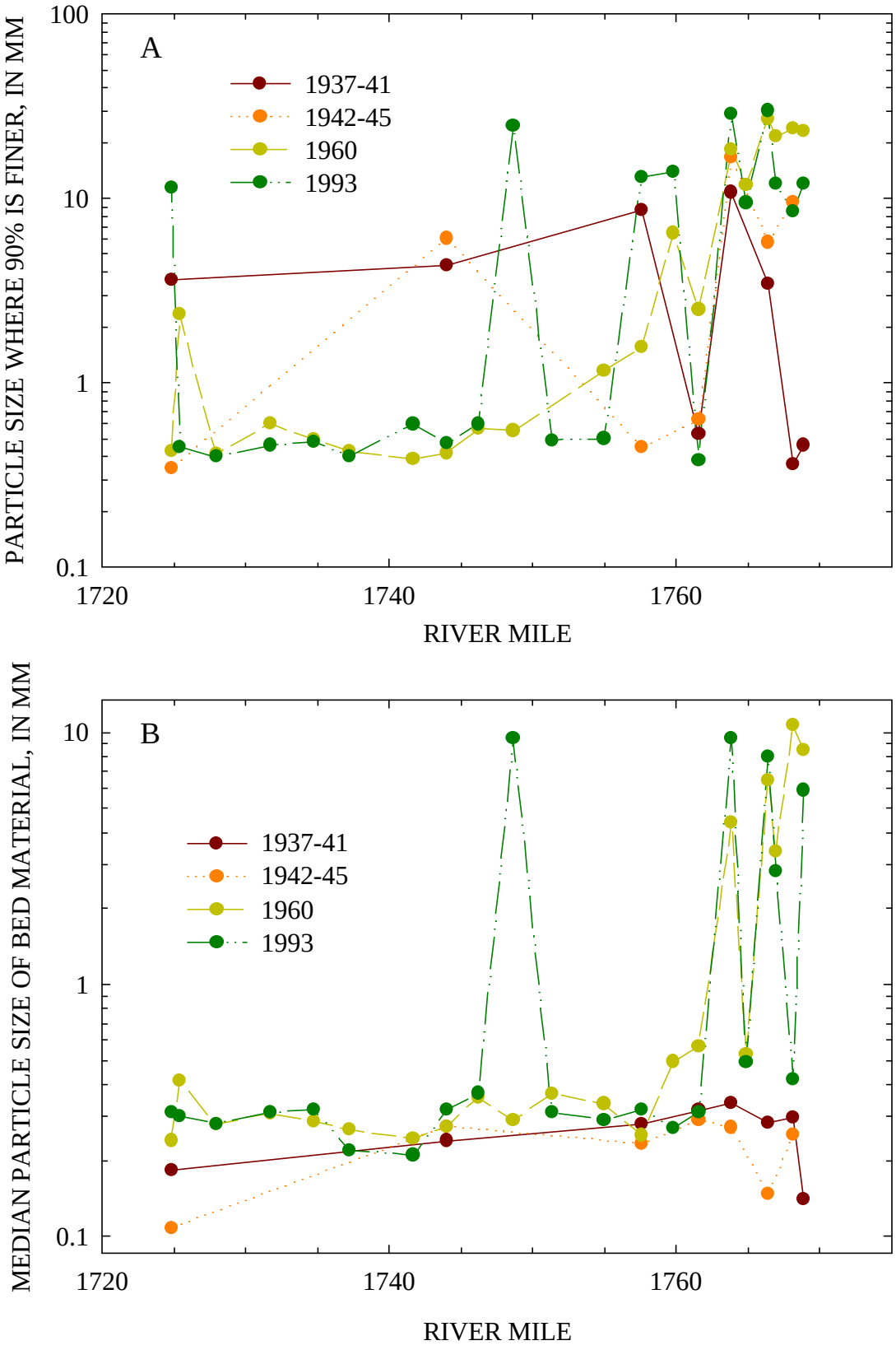

Figure 3--Comparision of median and d_{90} particle size of bed-material for 4 periods ranging from 1937-1993 for the 55 river miles closest to Ft. Peck dam.

channel with numerous islands and high banks. The effects of this are indicated by the smaller d_{90} values for the two ranges furthest upstream in the 1937-1941 data set.

In the reach just downstream from Fort Peck Dam (above River Mile 1765) coarsening of the entire distribution occurred (Figures 2 and 3). By 1960, the coarsest portion of the distribution (d_{90}) contained 20-30 mm gravels, while the medians coarsened from the sand range to the gravel range. This coarsening is termed “armoring” and is due to the erosion of the finer-grained sediments by sediment-free dam outlfows.

Sand beds dominate the reaches below River Mile 1755 (Figure 2). Even the d_{90} is predominantly in the sand range for the later periods (1960 and 1993). Some coarsening can be observed in the reaches furthest downstream between 1960 and 1993. These changes were not drastic, however, and certainly do not have much of an effect on erosion resistance.

GEOLOGIC HISTORY

Bedrock in the study reach river consists of marine and strandline sediments deposited during the Late Cretaceous (63 to 96 million years ago), and fluvial and deltaic sediments deposited during the Tertiary Period (2 to 63 million years ago). This area was only slightly affected by the intense mountain building occurring to the west in the Rocky Mountains, and the sedimentary bedrock is gently folded.

Four major glacial invasions reached into Montana during the Pleistocene Epoch 10,000 – 2 million years ago), covering the northern third of the state during their maximum advance. Prior to glaciation, the ancestral Missouri River flowed north around the Bearpaw Mountains and down the course of the present Milk River. From there, it flowed down the existing channel of the Missouri to what is now the town of Poplar, then northeastward through eastern Roosevelt County and southeastern Sheridan County and across Canada to Hudson Bay. About 50,000 to 70,000 years ago, advancing ice blocked the river near what is now the town of Big Sandy, diverting the flow to the south into its present channel.

Channel dynamics since the early Pleistocene have been extremely varied and complex. At various locations, ice has diverted the flow for both long and short durations as well as re-routing the channel. The addition of glacial meltwater to "normal" runoff volumes resulted in the deposition of coarser-grained sediments and a greater rate of deposition than has occurred since that time. As a consequence, the older alluvium in the lower portion of the deposit is coarser grained.

As the glacial age progressed, downcutting began along drainage courses. As downcutting continued, enough sediment was produced such that the valleys began to aggrade. In the Milk and Missouri River Valleys, aggradation continued until the flood plain level was several feet higher than present. These effects extended far up the tributaries, although they were more pronounced near the confluences with the main valley. It is likely that melt water ceased to contribute a major portion of stream volume well before the end of this period, and the sediment size decreased to predominantly silt- and clay-sized particles. Within comparatively recent times the rivers have resumed downcutting, which has lowered flood plain levels about 25 feet below the highest terrace levels in the valley. Even more recently, closure of Fort Peck Dam resulted in the development of new geomorphic surfaces.

Geologic Units

Structurally, the formations of the high plains have been gently warped into broad, open folds. In the Fort Peck area, they are dipping gently (about 20 to 40 feet per mile, or less than one percent) out of the Bowdoin Dome to the west, and into the Williston Basin to the east. The Poplar Dome is a small anticlinal structure between Poplar and Brockton.

The sedimentary rocks exposed in the area are, from oldest to youngest, the Bearpaw Shale, Fox Hills Sandstone, Hell Creek Formation, and the Fort Union Formation. Unconsolidated glacial deposits and contemporary alluvium overlie them.

The Bearpaw Shale consists primarily of marine, dark-gray clayey shale with thin interbeds of bentonite, and is easily erodible and subject to slumping. The upper part of

the formation is exposed in an almost continuous belt along the southern wall of the Missouri River valley from Fort Peck almost to Brockton. It is also exposed in a few places north of the river between Nashua and Wolf Point.

The lower portion of the Fox Hills Sandstone consists of soft, partially unconsolidated sandstone that characteristically weathers to gentle slopes. The upper portion is more cemented and resistant to erosion, so it tends to form rimrocks that cap many of the hills bordering the reservoir. It crops out in small areas near the Wolf Point bridge on the south side of the river, and is exposed in the northern bank in the Poplar Dome uplift between Tule Creek and Chelsea Creek (RM 1693). It is also exposed on the south side of the river in a thin band at River Mile 1653 west of Brockton.

Both the Hell Creek Formation and the overlying Fort Union Formation consist of soft shale, siltstone, and sandstone. They have similar erosional characteristics to the Fox Hills Sandstone, with rimrock-forming sandstones and gentle slopes eroded into soft shale. The Hell Creek Formation crops out in a thin band above the Fox Hills Sandstone west of Brockton. The Fort Union Formation forms the bedrock from Brockton to the North Dakota border.

There are several younger, unconsolidated deposits which locally overlie the bedrock. Coarse-grained deposits of the Flaxville Gravels cap some of the benches and plateaus north of the river and have contributed gravel to the sediment load. The Wiota Gravels are a younger pre-glacial gravel deposit that occur in many areas north of the river, located between the glacial deposits and the local bedrock. It is discontinuous but widespread, flooring buried stream channels and covering old erosional surfaces that slope toward the Missouri River.

Glacial till blankets the uplands north of the river, while only remnants have been mapped to the south. These deposits are in general fine-grained, consisting primarily of densely compacted clay, with lesser amounts of sand and gravel. It also contains randomly oriented cobbles and boulders up to three feet in diameter, which were derived from igneous and metamorphic sources far to the north. The till here is characterized by the presence of low ridges composed of coarser-grained, gravelly materials that are more resistant to erosion. This dense material is responsible for the gradual rise and gently rolling topography on the north side of the river. The rougher topography to the south of the river was eroded into bedrock.

Most of the alluvium is moderately to well sorted and there are significant vertical and horizontal variations in bedding. Individual beds range in thickness from one inch to four feet and all are lenticular. In general, the upper part of the alluvium is finer grained than the lower part. Exploratory drilling performed by the U. S. Army Corps of Engineers for the construction of Fort Peck Dam shows the alluvial fill to be between 122 and 164 feet thick in the center of the valley at the dam. Within each soil series, there is no significant difference in composition between soils on varying terrace surfaces.

HYDROLOGIC CONDITIONS

Mean daily-flow and peak-flow conditions have undergone changes in magnitude and distribution since the closure of Fort Peck Dam in 1937 (Figures 4 and 5). In general terms, the closure and operation of Fort Peck Dam resulted in a decrease in the magnitude of high flows and an increase in the magnitude of the low flows.

Although the dam was closed in 1937, it was not until 1942 that a minimum operation level was attained (Wei, 1997). Releases from the dam were elevated somewhat between the late 1950's and the mid-1960's to fill downstream reservoirs during an extended drought (Shields *et al*., in press). Hydropower units began operation in 1943 and 1961. Records of mean-daily discharge and peak discharges for the gages at Wolf Point, Montana, located about 64 miles downstream from the dam, and at Culbertson, Montana (RM 1621) were obtained from the U. S. Geological Survey (USGS) for the period 1929 through 1996. Mean-daily flows for the Wolf Point and Culbertson gages are shown in Figures 4 and 5.

Changes in Flow Regime

For ease of comparison, mean-daily discharge data from the Wolf Point stream gage has been split into 4 periods: Pre-dam (1928-1937); Post-dam period I: 1938-1956; Post-dam period II: 1958-1967; Post-dam period III: 1968-1995. Representative years from each of the designated periods are shown in a succession of graphs, with the heavy black line representing the mean over the period (Figures 6-9). Note how the pre-dam natural annual hydrographs displayed in Figure 6 differ significantly in shape from the regulated flows of successive periods (Figures 7-9). In particular, it can be seen that the high flows were shifted from June and July, reflecting snowmelt conditions, to August through October (1940-1956). Subsequent to this, mean-daily flows became more regular (Figures 8 and 9). Peak flows occur now (1970-1995) during the winter months (January and February; Figure 10a). It can also be seen from this figure that flows during the winter months have been steadily increasing through the 4 time periods. The average of the peak winter flows has increased from about 5,000 ft^3/s to about 13,000 ft^3/s through the 1990's (Figure 10a). The data used to generate Figure 10a are included in Appendix A.

The shifting of peak flows into the winter can have significant effects on channel morphology by altering flow distributions and, therefore, the erosive power of a given discharge as well as by direct impacts with channel boundaries such as banks. These effects seem to be the greater with increasing flow discharges. These and other ice-related effects will be discussed in detail in a later section of the report.

Peak-flow data from both the Wolf Point and Culbertson gages show a general decrease in the magnitude of peak flows following closure of the dam (Figure 11). These data indicate successful flood-control and the lack of

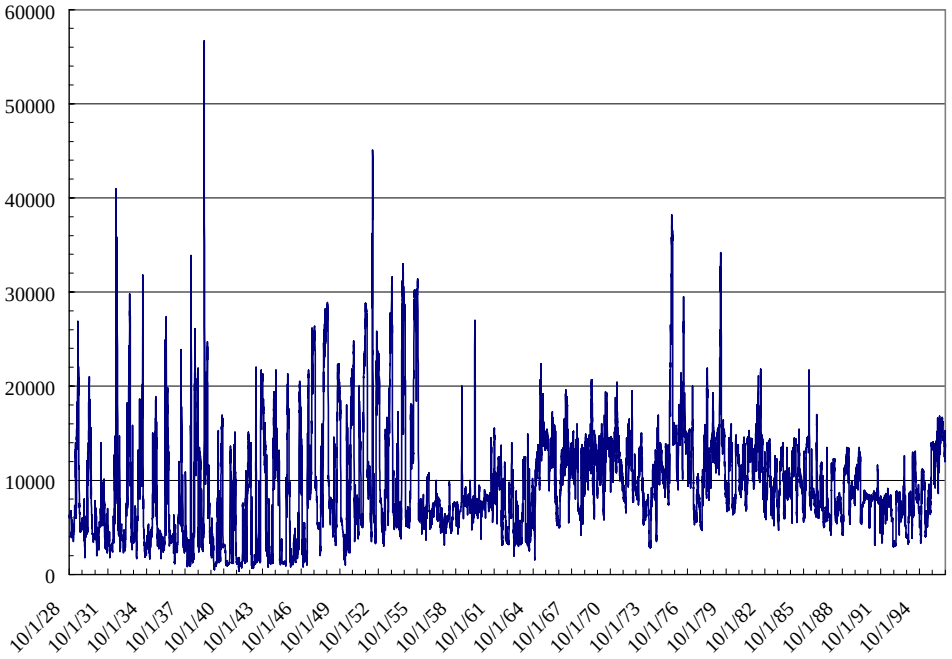

Figure 4--Mean-daily flows for the Missouri River at Wolf Point, Montana between 1928 and 1996.

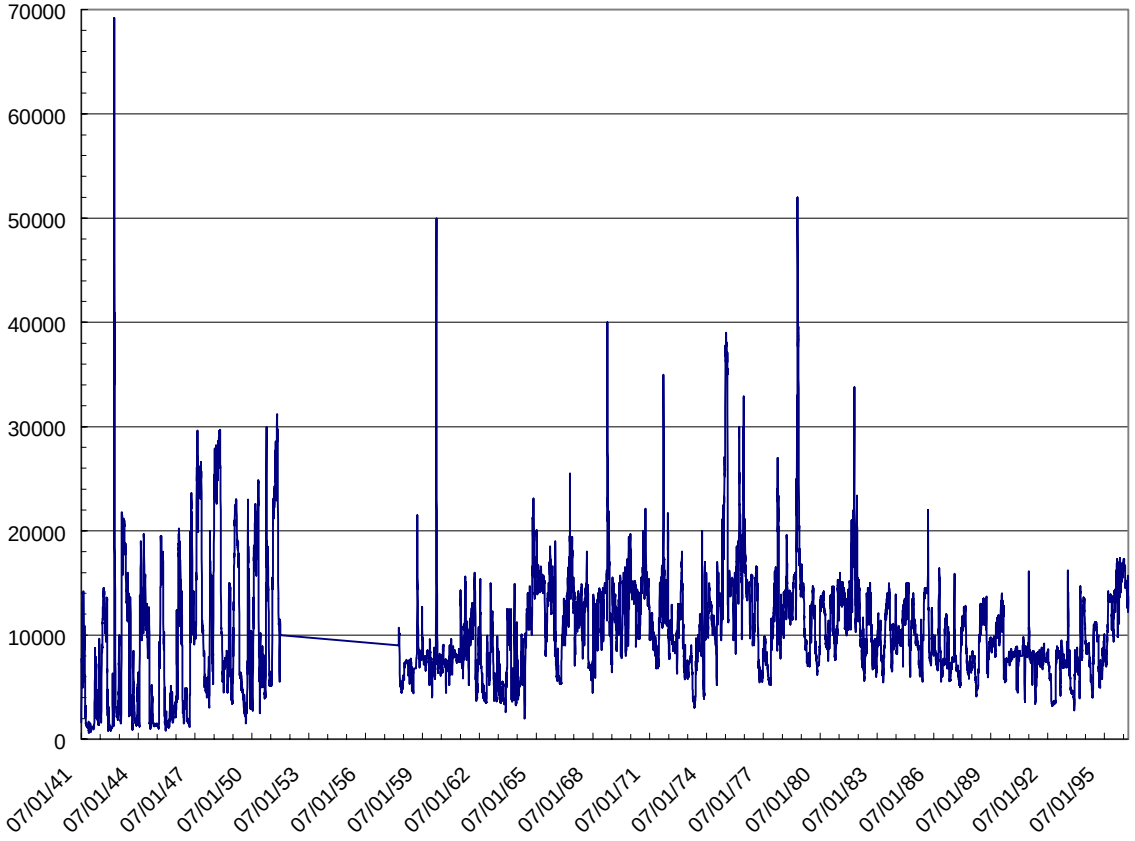

Figure 5--Mean-daily flows for the Missouri River at Culbertson, Montana between 1941 and 1996.

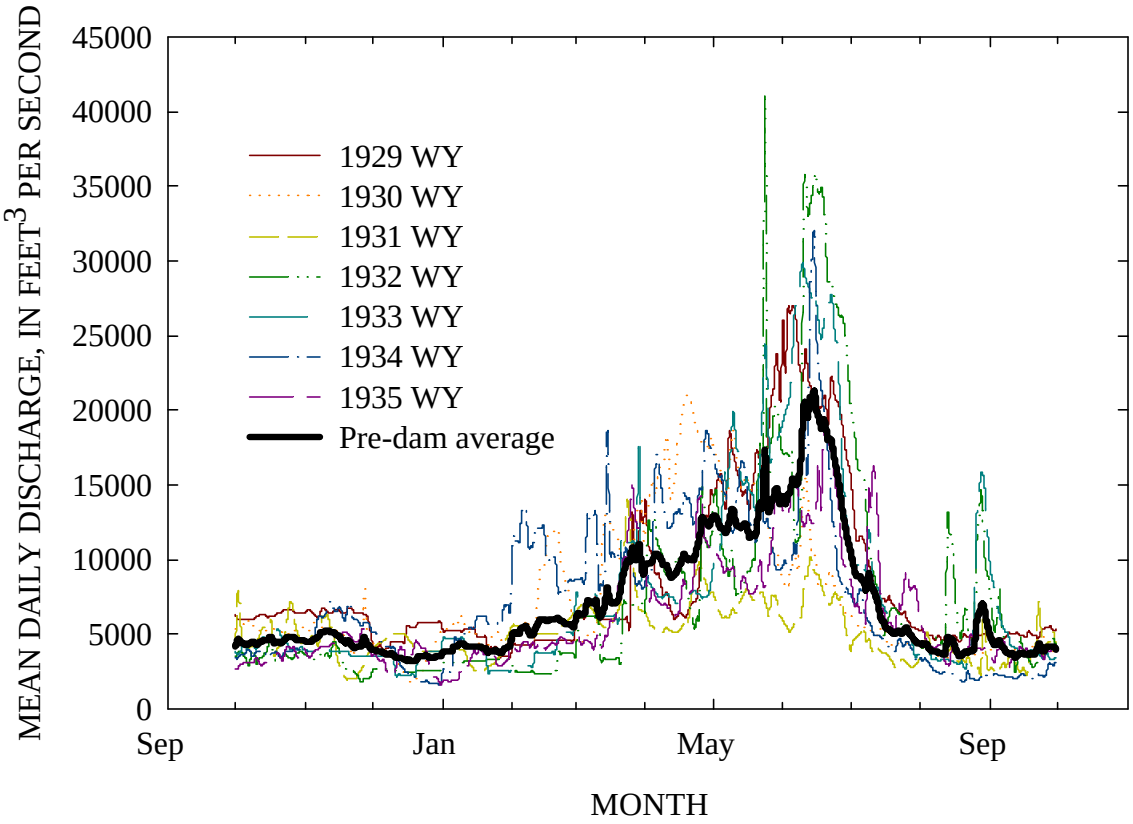

Figure 6--Mean-daily flows for the Missouri River at Wolf Point for the pre-dam period with the highest flows occurring during the late spring-early summer.

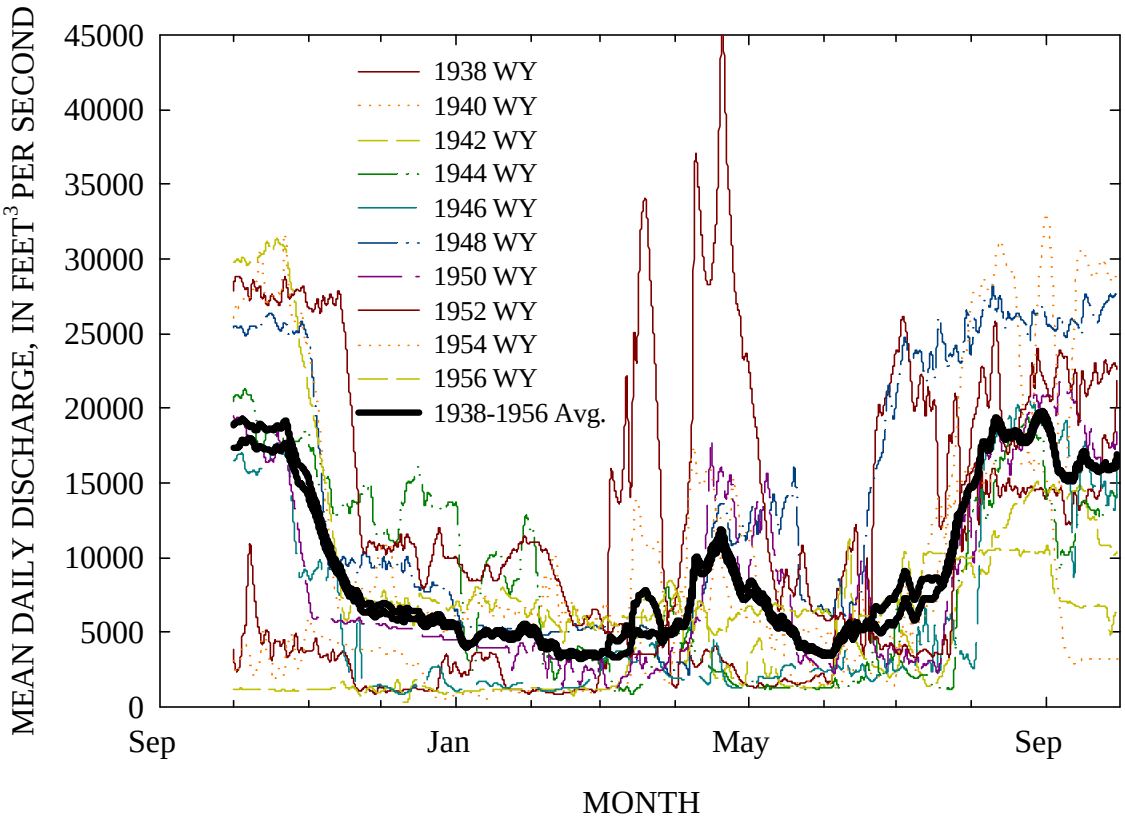

Figure 7--Mean-daily flows for the Missouri River at Wolf Point for post-dam period I: 1938-1956.

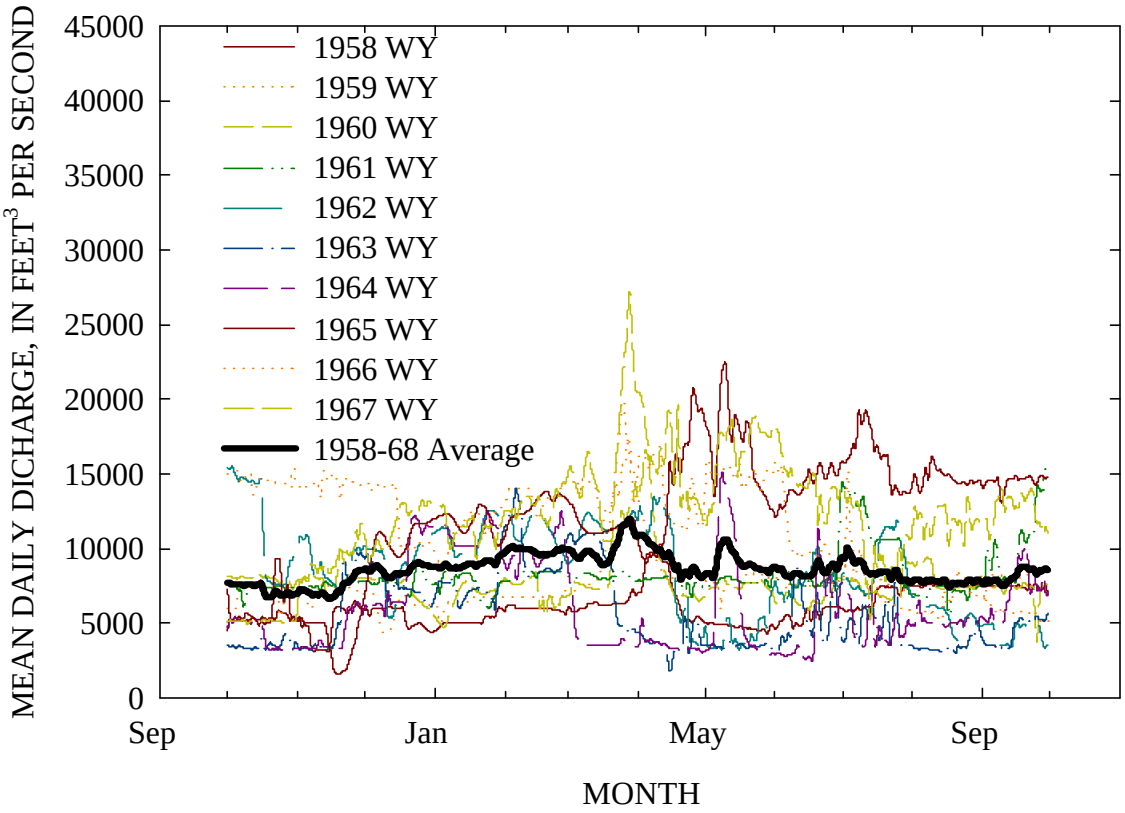

Figure 8--Mean-daily flows for the Missouri River at Wolf Point for post-dam period II: 1958-1967.

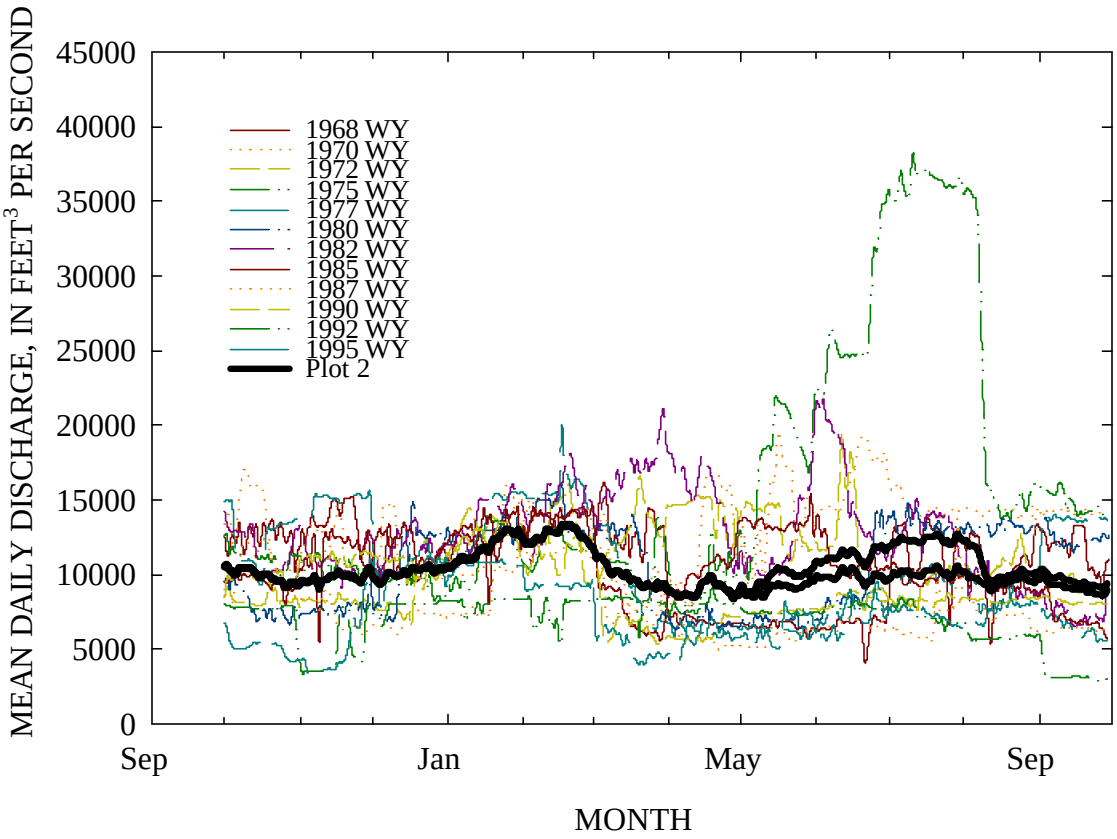

Figure 9--Mean-daily flows for the Missouri River at Wolf Point for post-dam period III: 1968-1995.

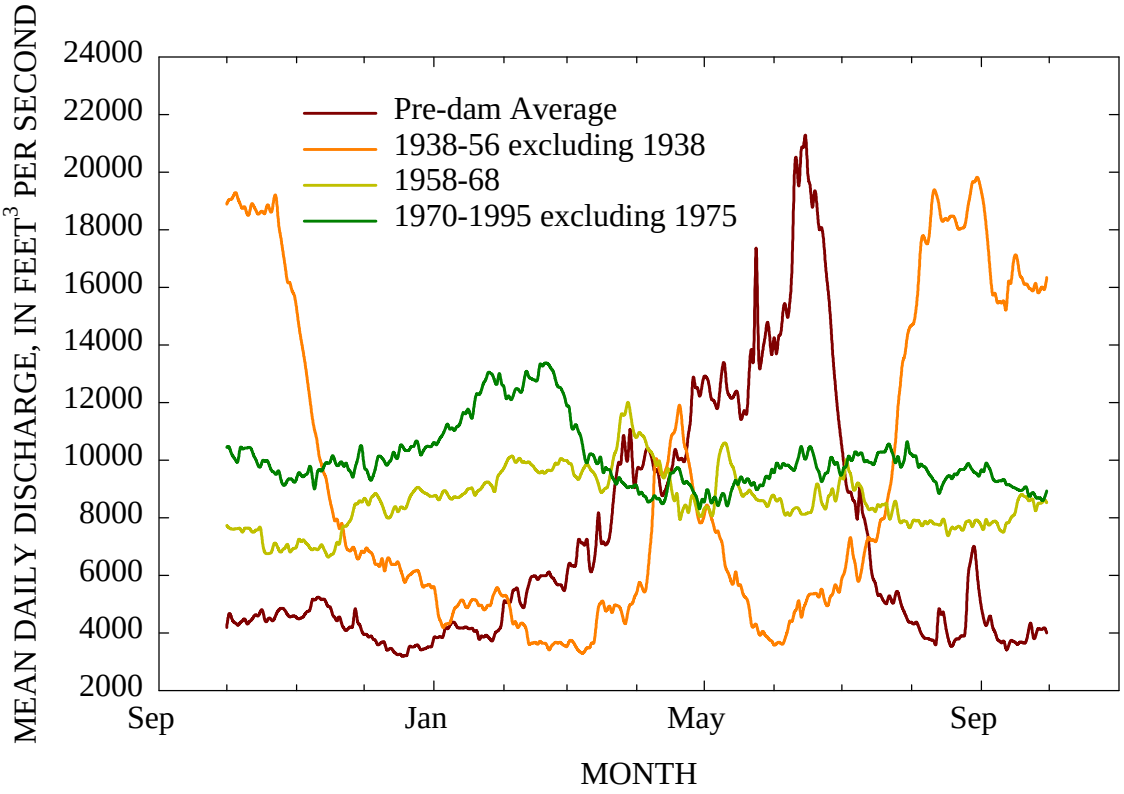

Figure 10a--Average of mean-daily flows for four different periods at the Missouri River at Wolf Point gage showing change in timing of high flow season and the reduction of pre-dam peaks.

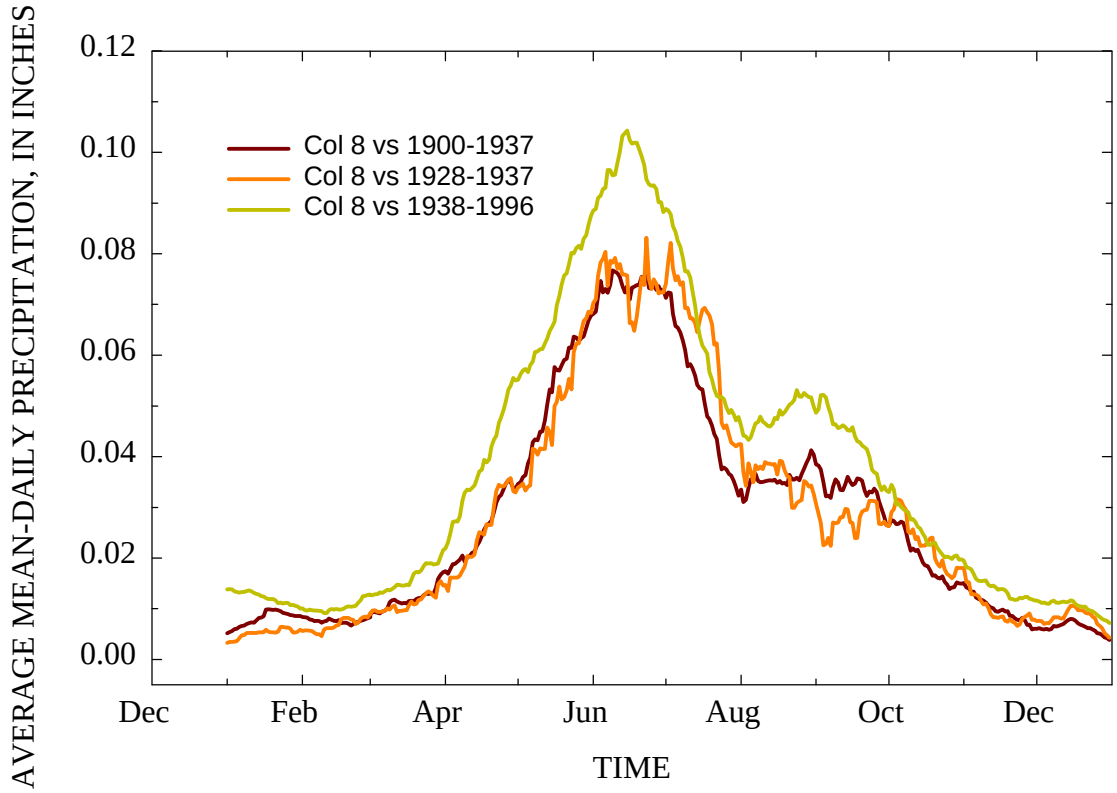

Figure 10b--Average of mean-daily precipitation at Culbertson, Montana for the specified periods based on 30-day moving average. Note that the pre-dam period 1928-1937 is generally about 24% less than the post-dam period.

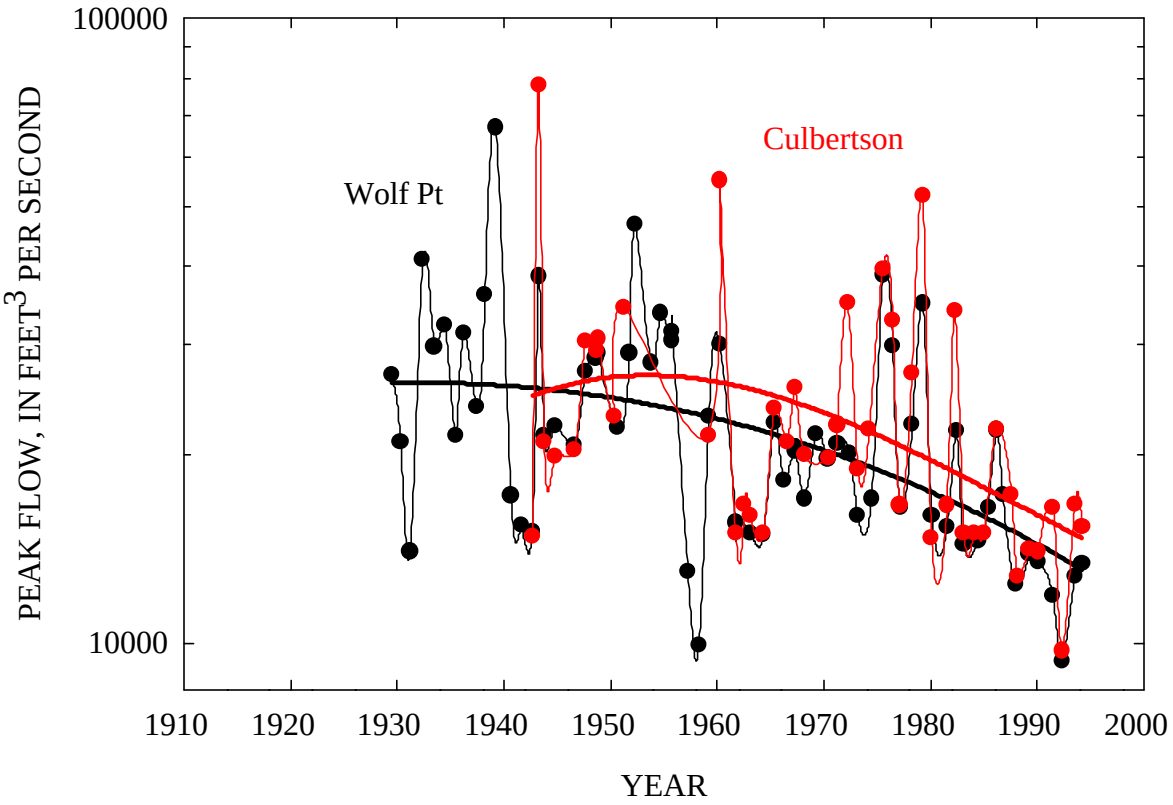

Figure 11. Annual peak flows for the Missouri River at Wolf Point and at Culbertson showing reduction in the magnitude of flows.

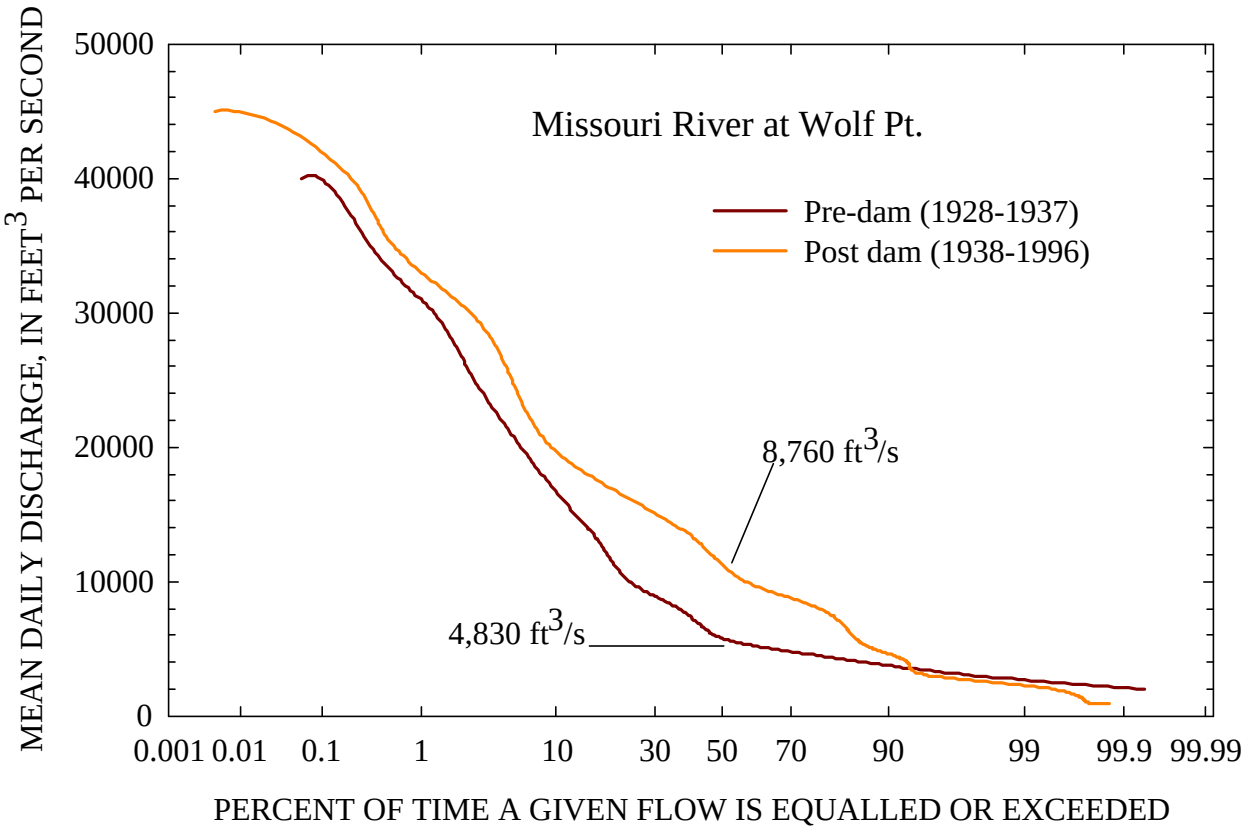

Figure 12--Pre- and post-dam flow duration curves for the Missouri River at Wolf Point.

overbank flooding. Part of this flood control can be associated with channel enlargement downstream from the dam.

Analysis of the flow duration series for mean-daily discharges at the Wolf Point gage show generally higher discharges about 90% of the time (Figure 12). This increase in mean-daily flows after dam closure is supported by visual inspection of the average changes in flow regime shown in Figure 10a. For example, a mean-daily flow of 10,000 ft^3/s was exceeded about 25% of the time pre-dam but about 55% of the time post dam. Similarly, the mean daily flow that is exceeded 50% of the time increased from 4,830 to 8,760 ft3/s. This has been accomplished by storing high spring- runoff flows, distributing them more equally throughout the year such that there are no extended periods of very low flows.

Analysis of pre- (1928-1937) and post-dam (1938-1996) mean-daily precipitation data from Culbertson shows that precipitation was, on average, about 24% less during the pre-dam period (Figure 10b). Increases in flow magnitude from pre- to post-dam periods therefore cannot solely be attributed to changes in precipitation regime.

Rating-Curve Analysis

Work by (Wei, 1997) provides data on stage-discharge relations (rating curves or ratings) with time for 7 gages along the study reach. These data originated from the Omaha District, U.S. Army Corps of Engineers and range in some instances from 1941 to 1994. Gages are located at the following River Miles 1768.96, 1763.5, 1751.33, 1736.64, 1727.56, 1701.22, and 1620.76.

A shift in a stage-discharge relation indicates a change in channel shape and flow capacity. At low discharges, these changes are related to changes on the channel bed (i.e. erosion or deposition). Shifts in ratings for higher discharges, where flows impinge on the channel banks may also indicate channel narrowing or widening. For example, the stage-discharge relations for the gage at River Mile 1767.0 indicate a lower water-surface elevation for a given discharge with time (Figure 13). The channel here has, therefore, been progressively enlargening with time from 1941 through 1994. Similar trends can be observed at the other gages although most are not as pronounced because they represent shorter spans of time (Figures 13-19). Downstream at the Culbertson gage at River Mile 1621 changes in the ratings are minimal (Figure 19). Lowering of the water surface for a given discharge is in the range of 2 to 6 feet. More definitive assessments of changes in channel shape can be obtained through analysis of cross-section surveys and thalweg-profile data.

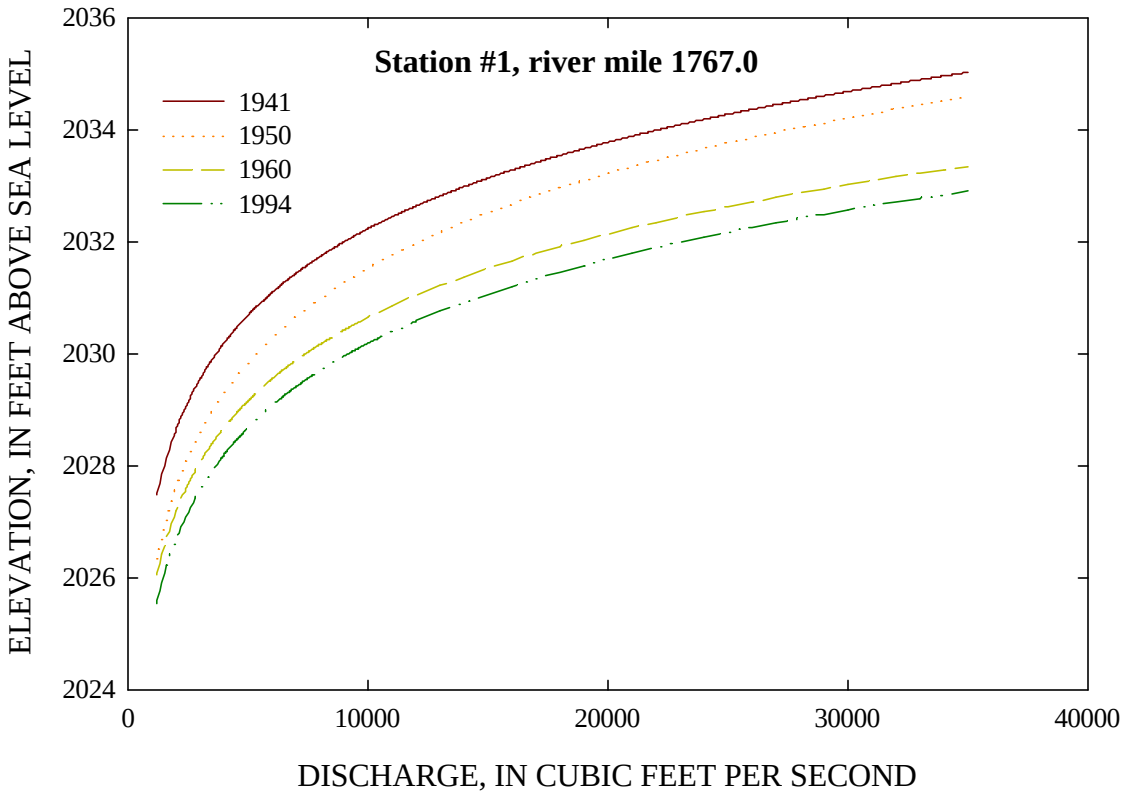

Figure 13--Stage-discharge relation for Missouri River gage at River Mile 1767.0 showing change with time (Modified from Wei, 1997).

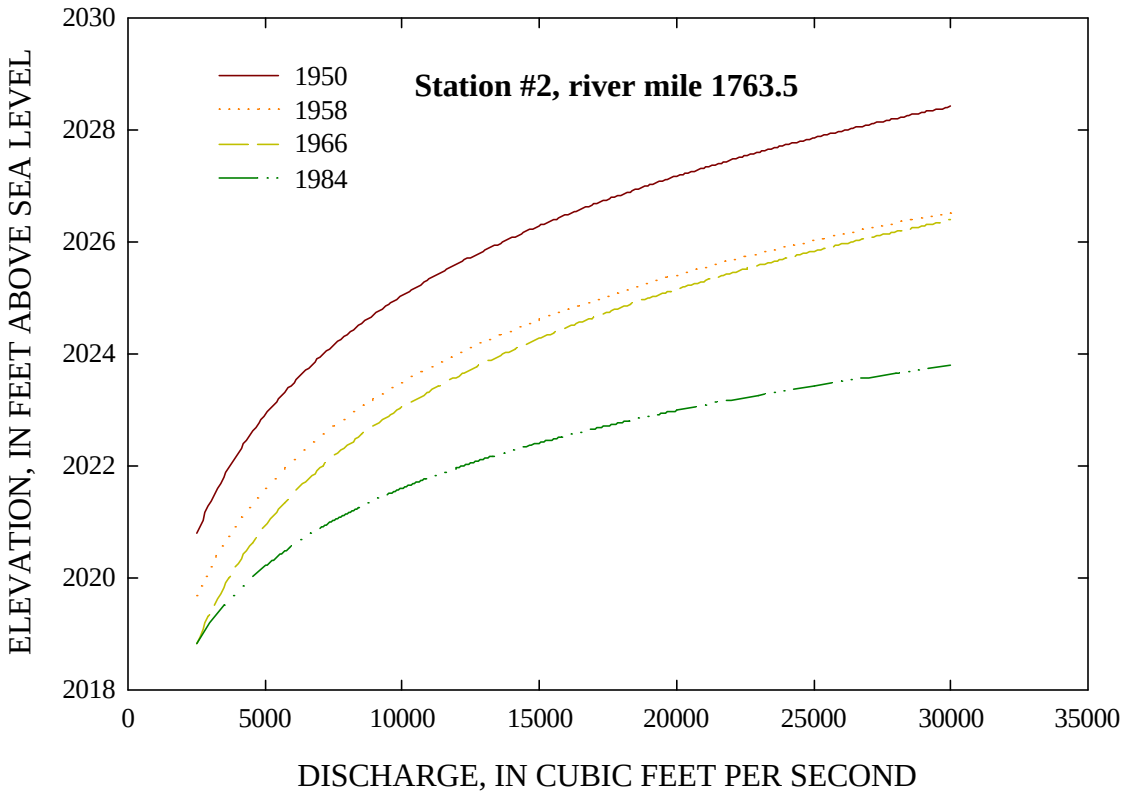

Figure 14--Stage-discharge relation for Missouri River gage at River Mile 1763.5 showing change with time (Modified from Wei, 1997).

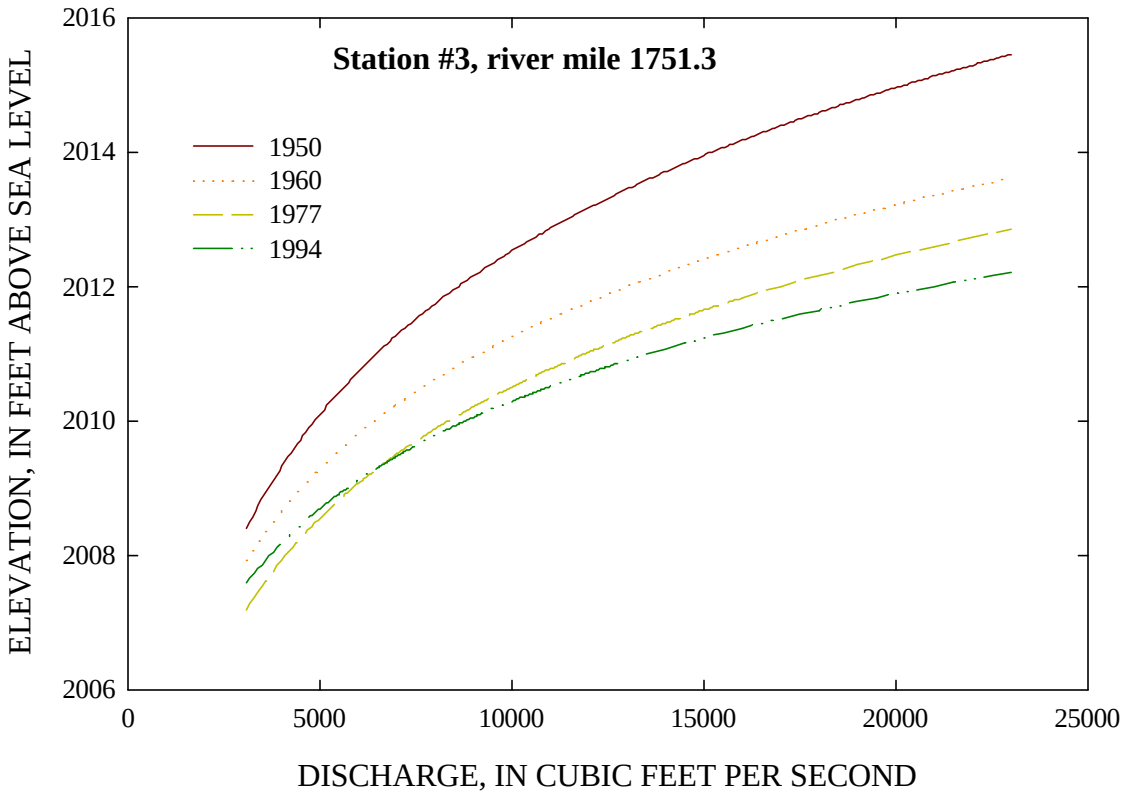

Figure 15--Stage-discharge relation for Missouri River gage at River Mile 1751.3 showing change with time (Modified from Wei, 1997).

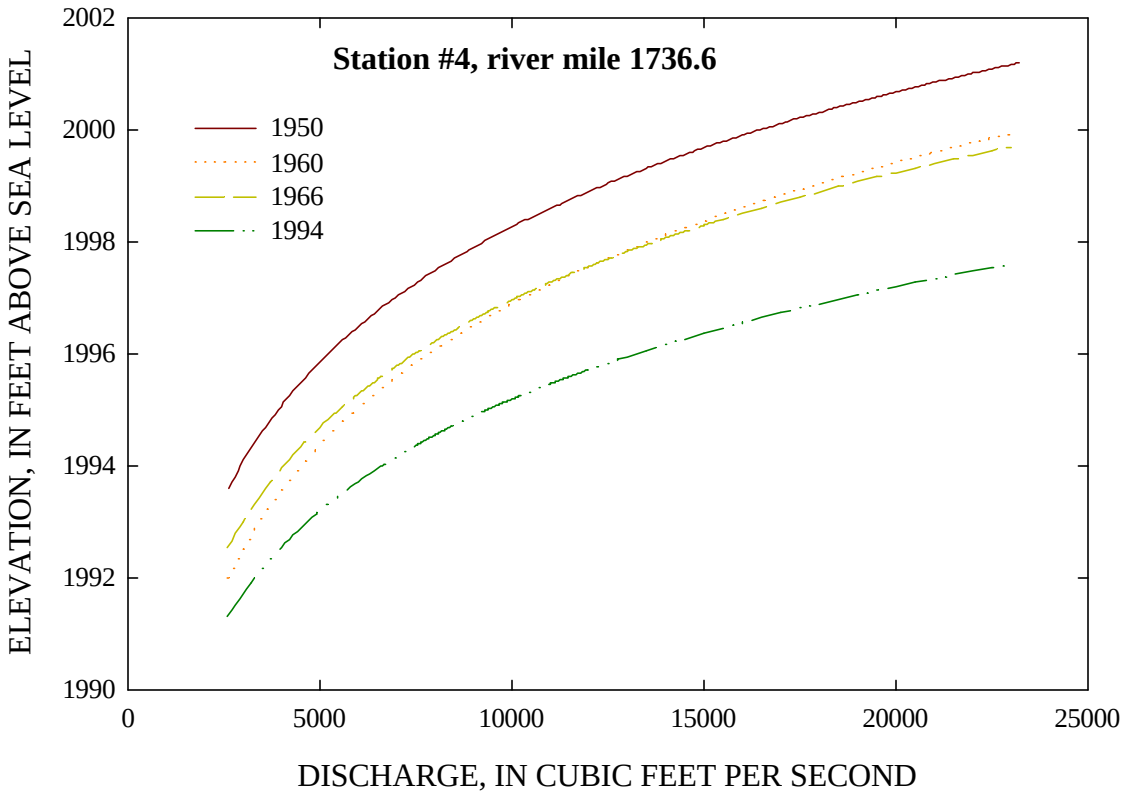

Figure 16--Stage-discharge relation for Missouri River gage at River Mile 1736.6 (Fraizer Pump) showing change with time (Modified from Wei, 1997).

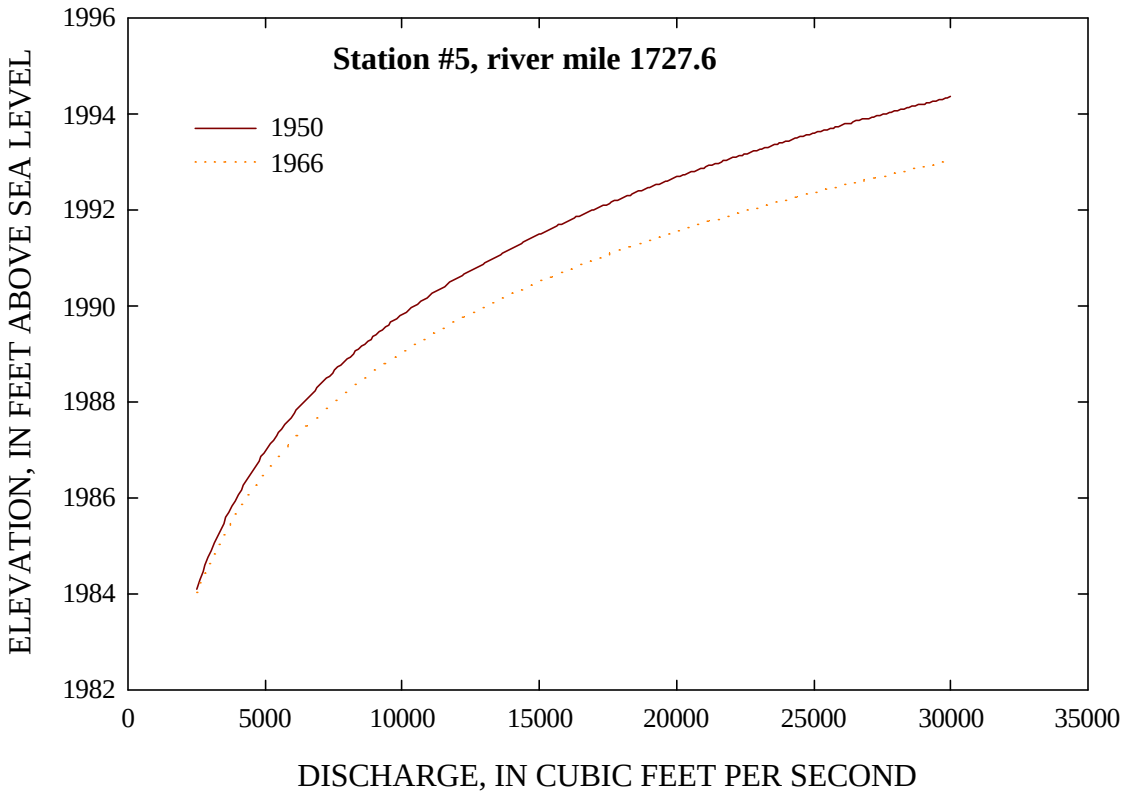

Figure 17--Stage-discharge relation for Missouri River gage at River Mile 1727.6 showing change with time (Modified from Wei, 1997).

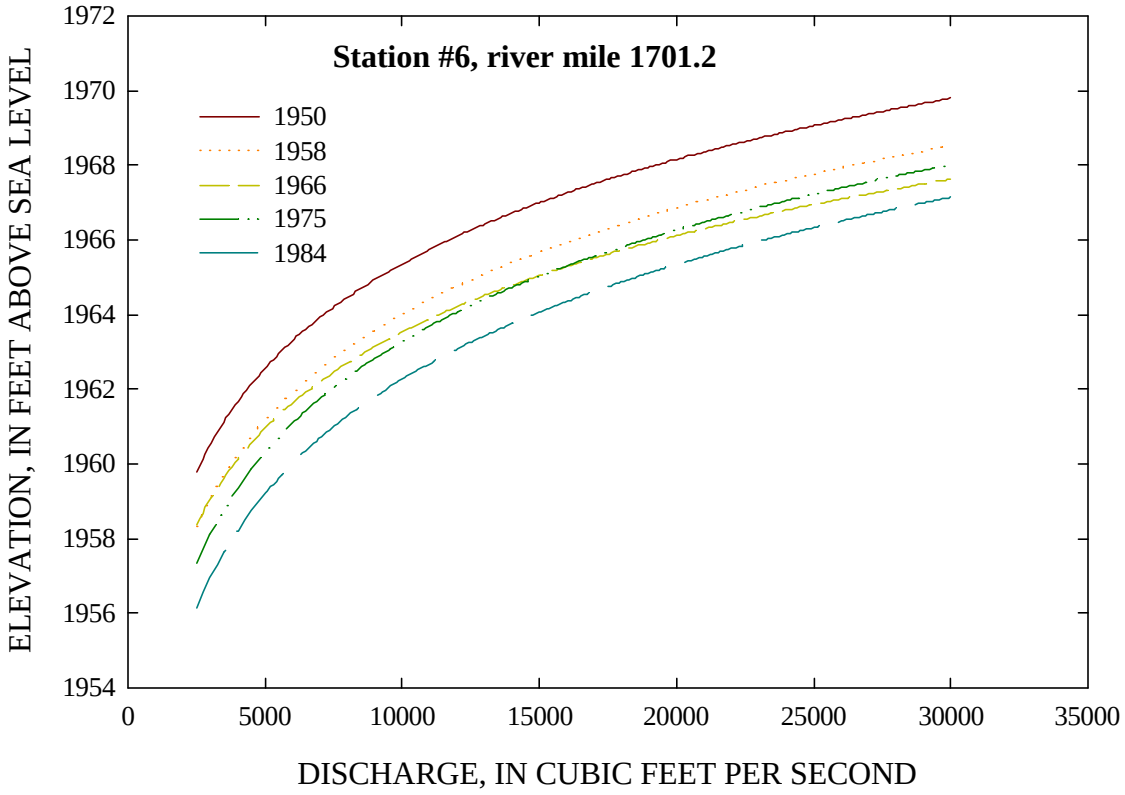

Figure 18--Stage-discharge relation for Missouri River gage at River Mile 1701.2 (Wolf Point) showing change with time (Modified from Wei, 1997).

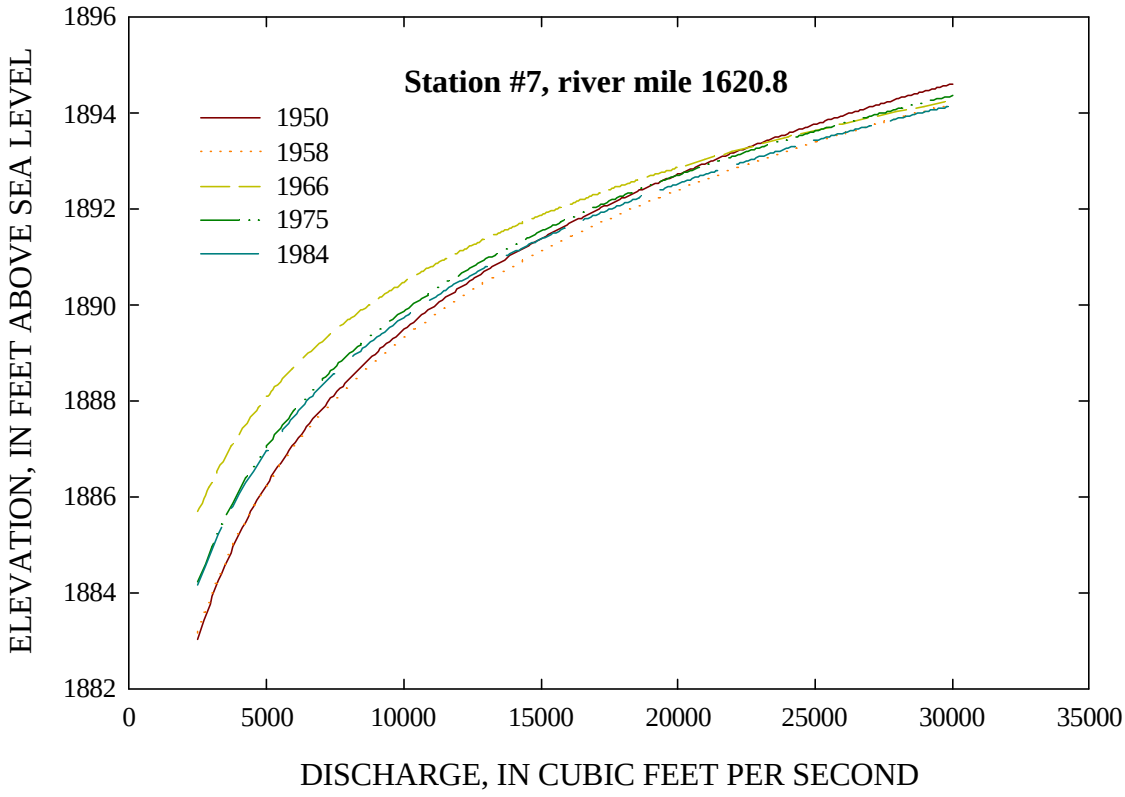

Figure 19--Stage-discharge relation for Missouri River gage at River Mile 1620.8 (Culbertson) showing change with time (Modified from Wei, 1997).

SITE SELECTION AND GENERAL CHARACTERISTICS

To ascertain the general characteristics of the streambanks in the reach between Fort Peck Dam and the North Dakota border, representative sites had to be selected. Given the resources of the study, 17 sites were selected for an in-depth evaluation. Two of the sites, however, are located within the same River Mile (1624). Therefore, at times only 16 sites are referred to in the text. Most of these sites represent terrace surfaces above the incipient flood-plain level. Criteria used for site selection included the following:

- soils from a representative soil series,
- proximity to a stream gage,
- pre-dam historical survey data from the Corps (1920's, 1936, and 1948),
- location on an outside bend,
- moderate to high bank-erosion rates,
- safe site-access and landowner permission and
- good longitudinal coverage of the entire reach

A list of the 17 sites including River Mile, soil-series name, and date sampled and tested is given in Table 2. GIS-based color maps of each of the sites showing the location of the site, the 1971 and 1991 banklines and, in most cases, the representative soil series are included in Appendix B of the report. At the selected sites, data collection centered on characterizing the physical properties and geotechnical strength of the bank materials. Because of this, one of the primary considerations in site selection was that of soil series. However, soil classification as conducted by the NRCS encompasses only the upper 5 feet of the soil. In many locations, the character of the surficial soils as represented by the soil series does not reflect that of the deeper alluvium.

Still, it was felt that by sorting the sites by soil series, information could be provided on strength of the upper part of the bank. Soils from eight soil series were evaluated during the field investigation. These include Gerdrum, Harlem, Havre, Havrelon, Lohler, Riverwash, Shambo, Trembles, Typic Fluvaquents, and Ustic Torrifluvents. A comprehensive description of each series is included below. In general, these soils are fine-grained and consist of silty clay and clay loam, with some fine sand. Only the Riverwash and Trembles series consist primarily of sand-sized materials. The lower, more coarse-grained portion of the alluvium is normally well below the 60-inch depth that is used to classify soils. The distribution of the soil units can be seen on the color maps included in Appendix B.

Soil-Series Descriptions

This summary has been compiled from the NRCS soil surveys of McCone, Richland, Roosevelt and Valley Counties. It includes only those soil series present along the riverbanks that were selected for detailed field evaluation. Because sand is a low-strength unit and is particularly susceptible to freeze-thaw processes, **sandy** intervals are highlighted for easier identification.

Table 2 --List of study sites, representative soil series, and the date visited.

River Mile	Soil Series	Site Name	Date Tested
1589	Havrelon	Nohly	09/09/97
1604	Lohler	Hardy	09/10/97
1621	Havrelon	Culbertson	09/08/97
1624 (Low Terrace)	River Wash	Tveit-Johnson	08/19/96
1624	Lohler	Tveit-Johnson	08/19/96
1630	Haverlon	Iverson	08/20/96
1631	Banks	Vournas	08/20/96
1646	Trembles	Mattelin	08/21/96
1676	Trembles	Woods Peninsula	09/10/97
1682	Shambo	McCrae	09/11/97
1701	Gerdrum	Wolf Point	09/12/97
1716	Havre	Pipal	08/21/96
1728	Harlem	Flynn Creek	08/22/96
1737	Harlem	Fraizer Pump	09/15/97
1744	Harlem/Till	L. Porcupine	09/15/97
1762	Harlem	Milk River	09/16/97
1765	Havre-Harlem	Garwood	09/17/97

Gerdrum Clay Loam

This deep, well drained, salt and sodium affected soil is on fans and terraces and is only recognized in the western and northern parts of McCone County. It formed in alluvium.

Typical profile:	0-7”	CLAY LOAM	light brownish gray
	7-11”.	CLAY	light brownish gray
	11-18”	CLAY LOAM	light brownish gray.
	18-60+”	CLAY LOAM	light brownish gray and pale olive

Permeability is slow, available water capacity is moderate and productivity is low. Most areas of this soil are used as rangeland and a few areas are used for non-irrigated farming.

Harlem Series

The Harlem series consists of deep, well-drained soils that formed in stratified, fine and moderately fine textured alluvium of mixed origin. They occupy flood plains and both low and high terraces along the Missouri River. It is recognized in McCone, Roosevelt, and Valley Counties. Permeability is slow, and available water capacity is high. This soil is used as rangeland and for non-irrigated and irrigated farming. Where irrigated, it is prime farmland.

Harlem Silty Clay

Typical profile:	0-5”	SILTY CLAY	grayish brown
	5-23”	SILTY CLAY	light brownish gray
	23-60+”	SILTY CLAY	grayish brown
		stratified with thin lenses of SILT LOAM.	

Harlem Silty Clay, Protected, soils have the same profile as above, but they occur on high terraces and are protected from flooding by Fort Peck Dam.

Harlem Silty Clay Loam

Typical profile:	0-4”	SILTY CLAY LOAM	grayish brown
	4-60+”	SILTY CLAY	grayish brown

Havre Series

The Havre series consists of deep, well drained, calcareous soils that formed in alluvium, and occupy flood plains and both low and high terraces along streams. This soil is recognized in McCone, Roosevelt, and Valley Counties. Permeability is moderate and the available water capacity is high. This soil is used as rangeland and for non-irrigated and irrigated farming. Where irrigated, it is prime farmland.

Havre Silt Loam

Typical profile:	0-5”	SILT LOAM	light brownish gray
	5-60+”	SILT LOAM	light brownish gray
		and thin stratifications of fine **SANDY** LOAM.	

Havre Silt Loam, Protected, has the same profile as above, but occurs on high terraces and is protected from flooding by Fort Peck Dam.

Havre Silty Clay Loam

Typical profile:	0-9”	SILTY CLAY LOAM	grayish brown
	9-25”	SILTY CLAY LOAM	grayish brown,
		stratified with fine **SANDY** LOAM,	
	25-60+”	FINE **SANDY** LOAM	light brownish gray
		stratified with SILT LOAM	

Havre Silty Clay Loam, Protected, has the same profile as above, but occurs on high terraces and is protected from flooding by Fort Peck Dam.

Havrelon Series

This deep, well-drained soil is on high terraces of the Missouri River and is formed in alluvium. Slope is 0-2 percent. It is recognized in McCone, Richland, and Roosevelt Counties. Permeability is moderate and the soil is calcareous throughout. This soil is used for rangeland and for non-irrigated and irrigated farming. Where irrigated, it is prime farmland.

Havrelon Loam

Typical profile:	0-5”	LOAM	pale brown
	0-60+”	VERY FINE **SANDY** LOAM	pale brown

Haverlon Loam, Protected, has the same profile as above but occurs on high terraces and is protected from flooding by Fort Peck Dam.

Havrelon Silt Loam

Typical profile::	0-13”	SILT LOAM	light brownish gray
	13-34”	SILT LOAM	light brownish gray
	34-56”	SILTY CLAY LOAM	light brownish gray
	56-60+”	SILTY CLAY LOAM	grayish brown

Havrelon Silt Loam, Protected, has the same profile as above but occurs on high terraces and is protected from flooding by Fort Peck Dam.

Havrelon Silty Clay Loam

Typical profile:	0-6”	SILTY CLAY LOAM	light brownish gray
	6-18”	LOAM AND SILT LOAM, stratified	light brownish gray
	18-60+”	LOAM AND SILTY CLAY, stratified.	light brownish gray

Lohler Series

This deep, moderately well drained soil is on flood plains and both low and high terraces along the Missouri River. It formed in alluvium. This soil is recognized in McCone, Richland, and Roosevelt Counties. Permeability is moderately slow to slow and the available water capacity is high. The soil is calcareous throughout. This soil is used mainly for non-irrigated and irrigated farming and is also used as rangeland. Where irrigated, it is prime farmland.

Lohler Silty Clay

Typical profile:	0-7”	SILTY CLAY	grayish brown
	7-10”	SILTY CLAY	light brownish gray
	10-32”	CLAY	light brownish gray
	32-60+”	SILTY CLAY	light brownish gray

Lohler Silty Clay, Protected, has the same profile as above but occurs on high terraces and is protected from flooding by Fort Peck Dam.

Lohler Silty Clay Loam

Typical profile:	0-6”	SILTY CLAY LOAM	dark grayish brown
	6-35”	SILTY CLAY with SILTY CLAY LOAM	grayish brown stratifications
	35-60+”	SILTY CLAY LOAM	grayish brown

Lohler Silty Clay Loam, Protected, has the same profile as above, but occurs on high terraces and is protected from flooding by Fort Peck Dam.

Riverwash

This soil consists of nearly level, unstabilized alluvium on flood plains and is recognized in Richland and Roosevelt Counties. It consists mainly of **sand**, pebbles, and cobbles. It is flooded, washed, and reworked so frequently that it supports little, if any, vegetation. It is typically light gray or very pale brown. Riverwash is used for groundwater recharge, as a source of sand and gravel and for wildlife habitat.

Shambo Series

This deep, well-drained soil is on terraces and fans with 0-4 percent slopes. It formed in alluvium. It is recognized in McCone and Richland Counties. Permeability is moderate and the soil is calcareous below 14 inches. This soil is used as rangeland and for non-irrigated crops.

Typical profile:	0-4”	LOAM	grayish brown
	4-14”	LOAM	brown
	14-22”	LOAM	pale yellow loam
	22-60+”	LOAM	light gray

Trembles Series

This deep, well-drained soil is on low and high terraces and flood plains and formed in alluvium. Slope is 0-2 percent. These soils are recognized in Richland and Roosevelt Counties. Permeability is moderately rapid and available water capacity is moderate to high. This soil is used mainly for non-irrigated and irrigated farming and is also used as rangeland.

Trembles Fine Sandy Loam

Typical profile:	0-6”	FINE **SANDY** LOAM	grayish brown
	6-60+”	FINE **SANDY** LOAM	yellowish brown and light brownish gray

Trembles Fine Sandy Loam, Protected, has the same profile as above, but occurs on high terraces and is protected from flooding by Fort Peck Dam.

Typic Fluvaquents, Frequently Flooded

These deep, poorly drained soils are on flood plains of the Missouri and its tributaries and are formed in **sandy** and gravelly alluvium. Slope is 0-2 percent. These soils are recognized in McCone, Roosevelt and Valley Counties.

Typic Fluvaquents do not have a typical profile. Generally, along the Missouri River they consist of bars of **sand** stratified with thin lenses of loam and silt loam that often have been stabilized by willows and brushy vegetation. They have a water table from 1 foot above to 1 foot below the surface in late winter and spring and are used only as wildlife habitat.

Ustic Torrifluvents

This map unit consists of soils that formed in recent deposits of alluvium on nearly level to gently sloping low terraces, bottomlands, and flood plains. Slopes are 0-5 percent. Soils are well and moderately well drained, but are subject to common flooding.

These soils are recognized in McCone, Roosevelt and Valley Counties. The soil is stratified loam to clay. Soil characteristics are extremely variable and no one kind of soil can be consistently identified and mapped separately. Areas south of the Milk River have little or no gravel in the soil. The soils are suited to range and wildlife habitat.

TESTING AND SAMPLING OF BANK MATERIAL

Bank material samples for particle–size and other mechanical analyses were collected in the field during the summers of 1996 and 1997 with a hand auger at various depths. New samples were taken as different materials were found in the boreholes. A hammer sampler was also used to sample materials of a known volume for analysis of moisture content and unit weight. Tensiometer measurements were also performed during the 1997 fieldwork to determine the magnitude of negative pore-water pressures at various depths in the borehole.

At the center of the field-testing was the determination of the shearing resistance or resistance to failure of the bank materials. To accomplish this, direct measurements were made at each site with an Iowa Borehole Shear Tester (BST). This instrument permits rapid *in situ* determination of important geotechnical parameters required for modeling of bank stability. A series of tests was performed in each borehole at several depths as dictated by the stratigraphy of each bank.

Particle-size distribution was performed on the 1996 samples at the ARS Laboratory in Oxford, Mississippi. Laboratory analyses including particle size distribution, classification using the Unified Soils Classification System and dispersion tests were performed on the 1997 samples at the NRCS Soil Mechanics Laboratory in Lincoln, Nebraska.

It is important to note that some of the clay soils tested at the Lincoln NRCS Laboratory had dispersive characteristics. Dispersive clays have an electrochemical imbalance caused by the presence of sodium cations and tend to repulse each other rather than flocculate. Since the clay particles are very small, they are easily detached and transported by water, giving them an extremely low resistance to erosion. These materials are also subject to piping, thereby creating pathways for the flow of water deep into streambanks. Marine shales, alluvium derived from marine shales, and bentonite beds all tend to have dispersive characteristics and these geologic materials are present in the banks and in the watershed of this reach of the Missouri River.

Identification of Geomorphic Surfaces

To identify broad recent-term (100 years) changes in channel size and shape woody vegetation growing on various levels were sampled for their ages. Dating of riparian vegetation (dendrochronology) is useful in extracting information about the age of a given surface that a tree is growing on. In cases where a bank has failed and a tree was transported with the failure, the subsequent development of eccentric rings, or the germination of vertical sprouts can be used to date the timing of the failure episode. This type of sampling was undertaken at 9 sites along the study reach during the 1997 field season. In particular, efforts were concentrated on determining the ages of various surfaces that could then provide us with a temporal map of channel changes and adjustments to dam closure and altered hydrologic regimes. Interpretations of these surfaces can then be used to advance ideas about their genesis. The following sites were surveyed in the manner described above 1591, 1621, 1676, 1682, 1701, 1737, 1744, 1762, and 1765.

CONTROLS OF CHANNEL EVOLUTION: THEORY

Factors that affect channel stability can be conceptualized in terms of the resistance of the channel boundary to erosion and the forces acting on the channel to erode the boundary. If these opposing tendencies are balanced, the channel is considered to be in equilibrium and no net erosion or deposition will occur with time.

Vertical channel instabilities can be considered to be the result of a disruption to the equilibrium (balance) between available stream power (the discharge-gradient product) and the discharge of bed-material sediment (Lane, 1955; Bull, 1979):

$$Q\,S \propto Q_s\,d_{50} \qquad (1)$$

Where Q = bankfull discharge,
S = channel gradient,
Q_s = bed-material discharge, and
d_{50} = median grain size of bed material.

Equation (1) indicates that if available stream power was increased by an increase in the bankfull discharge or the gradient of the stream, then there would be an excess amount of stream power relative to the discharge of bed-material sediment. Additional sediment would be eroded from the channel bed resulting in: (1) an increase in bed-material discharge to an amount commensurate with the heightened stream power and (2), a decrease in channel gradient and, consequently, stream power as the elevation of the channel bed is lowered.

In the case of a dam such as Fort Peck, trapping of coarse sediment (sand and gravel) on the upstream side of the dam results in the release of sediment-free water on the downstream side of the dam. The result is that there is an excess amount of stream power relative to the amount of sediment being delivered to the flow on the downstream side of the dam. The channel bed erodes (degrades) in response to this imbalance until a new equilibrium condition is achieved. A similar response would be expected from a decrease in the erosional resistance of the channel boundary or a decrease in the size of bed-material sediment (assuming it is not cohesive).

In most alluvial channels, disruption of the dynamic equilibrium generally results in a certain degree of upstream channel degradation and downstream aggradation. In the case of a dam, however, degradation generally extends downstream from the dam with maximum rates and amounts occurring in reaches closest to the dam (Williams and Wolman, 1984). As a result, tributary streams entering the degraded channel have steep channel gradients, an excess amount of stream power and, therefore, degrade headward. Thus the degradation process migrates downstream from the dam but upstream along affected tributaries.

Researchers in fluvial geomorphology have noted that alluvial channels in different environments, destabilized by different natural and human-induced disturbances, pass through a sequence of channel forms with time (Ireland and others, 1939; Schumm and Hadley, 1957; Daniels, 1960; Emerson, 1971; Keller, 1972; Elliot, 1979; Schumm and others, 1984; Simon and Hupp, 1986; Simon, 1989). These systematic temporal adjustments are collectively termed "channel evolution" and permit

interpretation of past and present channel processes, and the prediction of future channel changes and processes (Figure 20).

If we consider the predisturbed channel as the initial stage (I) of channel evolution and the disrupted channel as an instantaneous condition (stage II), rapid channel degradation can be considered stage III (Figure 20). Degradation flattens channel gradients and consequently reduces the available stream power for given discharges with time. Concurrently, bank heights are increased and bank angles are often steepened by fluvial undercutting and by pore-pressure induced bank failures near the base of the bank. Thus, the degradation stage (III) is directly related to destabilization of the channel banks and to channel widening by mass-wasting processes (stage IV) once bank heights and angles exceed the critical conditions of the bank material (as determined by shear-strength and other characteristics).

As degradation migrates further downstream from the dam or upstream along a tributary, aggradation (stage V) becomes the dominant trend in previously degraded downstream sites because the flatter gradient at the degraded site cannot transport the heightened sediment loads originating from degrading reaches upstream. This secondary aggradation occurs at rates roughly 60% less than the associated degradation rate (Simon, 1992). These reduced aggradation rates indicate that bed-level recovery will not be complete and that attainment of a new dynamic equilibrium will take place through (1) further bank widening and the consequent flattening of bank slopes, (2) the establishment and proliferation of riparian vegetation that adds roughness elements and reduces the stream power for given discharges and (3), further gradient reduction by meander extension and elongation. The lack of complete bed-level recovery often results in a two-tiered channel configuration with the original flood-plain surface becoming a terrace. High flows are, therefore, constrained within this enlarged channel below the terrace level resulting in a given flow having greater erosive power than when flood flows could dissipate energy by spreading across the flood plain. Aggradation on the bed slows with time but can ultimately reduce bank heights to such an extent that streambanks become stable again as indicated by the establishment and proliferation of woody vegetation.

Bed-Level Adjustments

In unstable channels, the change in bed elevation with time (years) can be described by nonlinear functions, where change in response to a disturbance occurs rapidly at first and then slows and becomes asymptotic. Plotting of bed elevations with time thus permits evaluation of phase(s) of bed-level adjustment and indicates whether the major phase of degradation (stage III) has passed or is ongoing. This method can also provide valuable information on trends of channel stability at gaged locations where abundant data from discharge measurements are available.

Mathematical Model of Bed-Level Changes

A channel begins to erode its bed following a disturbance to a stream system in which there is an excess amount of stream power for a given flow relative to the amount of bed-material sediment supplied from upstream (equation 1). Construction of a dam can represent such a disturbance. Bed level response is rapid at first and then slows as

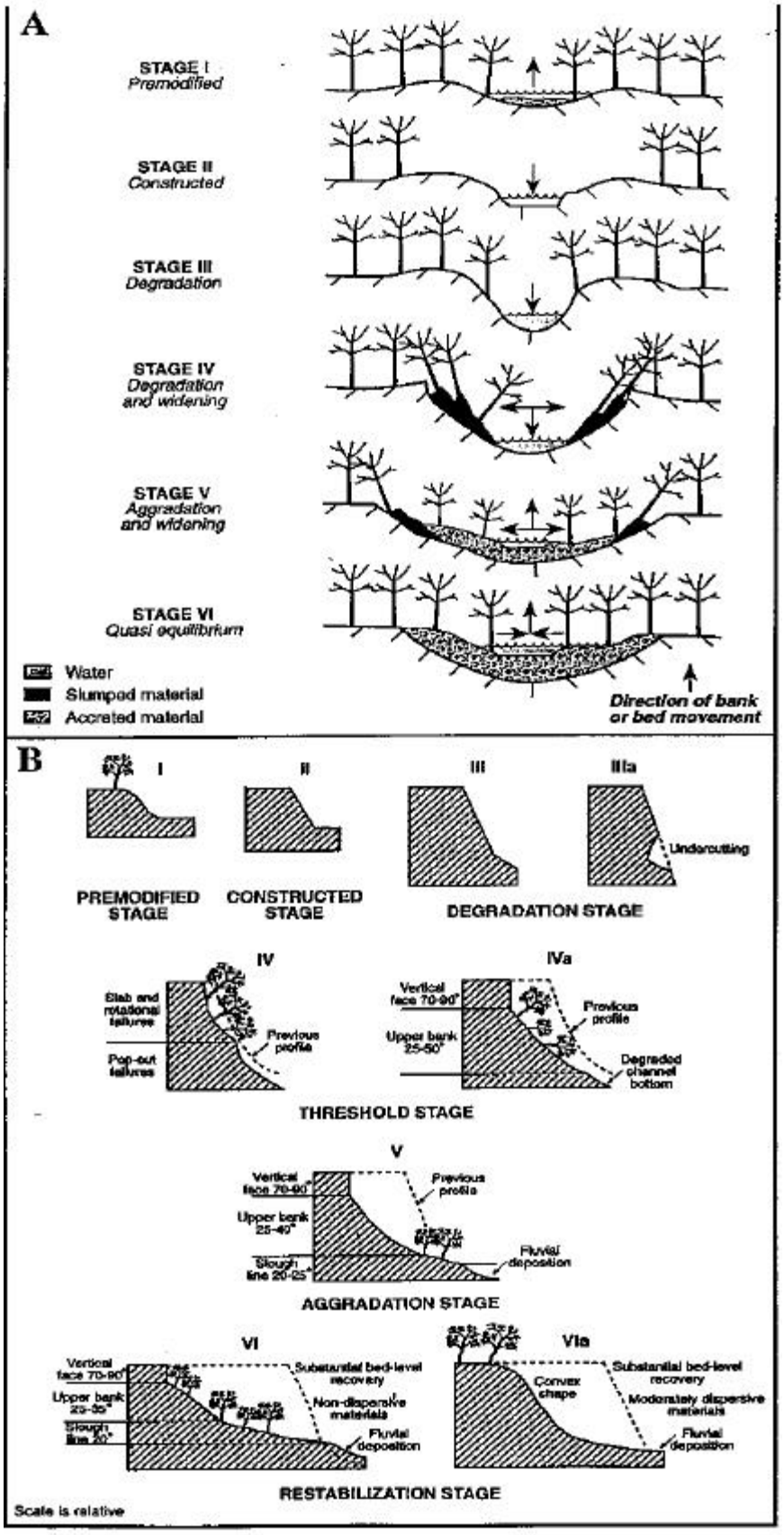

Figure 20--Models of channel evolution (A) and bank-slope development (B) in disturbed channels. From Simon, 1989.

additional sediment is supplied to the flow from bed erosion and equation 1 approaches a balance. The elevation of the channel bed thus changes non-linearly with time and can be described by various types of mathematical functions. Various mathematical forms of this function, including exponential, power, and hyperbolic, have been used to characterize bed-level adjustment at a site with time and to predict future bed elevations (Graf, 1977; Williams and Wolman, 1984; Simon and Hupp, 1986; Simon, 1992). The exponential function converges to an asymptote and is preferred (H. Jobson, U.S. Geological Survey, written commun., 1992); however, the power function is easier to use:

$$E = a\, t^{\,b} \tag{2}$$

where E = elevation of the channel bed, in feet;

a = coefficient, determined by regression, representing the premodified elevation of the channel bed, in feet;

t = time since beginning of adjustment process, in years where $t_0 = 1.0$ (year prior to onset of the adjustment process); and

b = dimensionless exponent, determined by regression and indicative of the nonlinear rate of channel-bed change (negative for degradation and positive for aggradation).

This function can be used for average bed elevations or thalweg (deepest part of the channel) elevations and represents a simplification of the actual scour and fill episodes that occur around a general bed-level adjustment trend. This is displayed graphically with thalweg-elevation data from River Mile 1766.4).

Maximum amounts of degradation are indicated by the most-negative values of b and these generally occur in regions closest to the "area of maximum disturbance" (Simon, 1989; 1992; 1994). In the case of the Missouri River below Fort Peck Dam, the area of maximum disturbance is just downstream from the dam, because it is here that concentrations of bed-material load are probably very low relative to the stream power of the flow being released.

Future elevations of the channel bed can, therefore, be estimated by fitting equation 2 to bed elevations and by solving for the time period of interest. The predisturbed bed elevation, obtained from field survey or from a topographic map, is required along with at least one other bed elevation from a different time period. Statistical significance of the fitted curves improves with additional data. Degradation and aggradation curves for the same site can be fitted separately. For degrading sites, equation 2 will provide projected minimum channel elevations when the value of t becomes large and, by subtracting this result from the flood-plain elevation, will provide projected maximum bank heights.

Abundant data are available at stream gaging stations. At these locations, mean channel-bed elevations can be obtained by subtracting mean flow depth (cross-section area divided by flow width) from water-surface elevation for each discharge measurement where flows are at bankfull stage or below. This method is described in detail by Jacobson (1995). Data scatter can be eliminated by using a 5-point moving average. If this procedure is used for at least several years of record, it should be possible to determine if bed-level adjustment is ongoing. If it is determined that degradation or

aggradation are active, the data can be fitted to equation 2 to estimate future changes. Considerable data scatter around the fitted relation can be expected when this method is used at bridges because of the affects of local scour during stormflow.

BED ELEVATION DATA: APPLICATION

For this study, bed elevation data were obtained from the U.S. Army Corps of Engineers, Omaha District and from Wei, 1997 for the periods 1936, 1948, 1956, 1966, 1978, and 1994. Additional data originally derived from 4 gaging stations along the reach were also obtained from Williams and Wolman (1984). Some of the previous studies of the effect of Fort Peck Dam on downstream channel changes along the Missouri River have been hampered by a lack of pre-dam data on channel morphology. There are only 6 sites with 1936 survey data, all are within 46.5 miles of the dam (River Mile 1725) and 5 are within the first 20.5 miles of the dam (River Mile 1751).

Because bed-level response is most rapid immediately following closure of the dam (Williams and Wolman, 1984), it is imperative to analyze bed-elevation data with respect to the pre-disturbed condition. To accomplish this, pre-dam conditions were estimated for the reach downstream of River Mile 1725. Pre-dam (1936) water-surface slopes and channel elevations over the 46.5-mile reach were compared to low-water water-surface elevations obtained from a set of maps prepared by the Missouri River Commission of 1889 (Figure 21). These 1889 maps extend over the entire reach.

By assuming that the river was vertically stable over the period 1889 to construction of the dam, 1936 bed conditions can be estimated from the 1889 water-surface elevations by adjusting the 1889 level down by 6.3 feet. This average difference was obtained by establishing linear regressions between river mile and elevation for both dates, calculating the area encompassed by the two profiles, and dividing by the reach length. Figure 22 shows the method used to interpolate the pre-dam (1936) profile over the upper 46.5 river miles as well as to extrapolate downstream.

Average bed-elevation data were obtained for pre-dam conditions by the above method. These data were then used (1) as the initial bed elevation (t_0) in development of bed-level trends (using equation 2) following dam closure and (2), to determine net changes in bed elevation along the study reach. These and thalweg-elevation data, together with the data accumulated by (Wei, 1997) from Corps of Engineers records are shown in Tables 3 and 4, respectively.

Bed-Level Response

Results using both simulated and measured 1936 t_0 elevations clearly show a trend of degradation downstream from the dam that was initiated following dam closure. Examples of average bed-level adjustment trends are shown for a number of sites in Figure 23 along with the fitted relation using equation 2. The most negative *b*-values, indicating maximum degradation occur in the reach just downstream from Fort Peck Dam (Figure 24a). Data taken from gaging stations (Williams and Wolman, 1984; Table 5) have been re-analyzed with equation 2 and are shown (open circles in Figure 24A) to be in general agreement with the spatial trends developed here.

The greatest amount of downcutting occurred in the vicinity of the dam and attenuates with increasing distance to about River Mile 1711. Over the period 1936-1994 thalweg elevations decreased as much as 15 feet, while average bed elevations decreased as much as 6-8 feet in the 50- mile reach closest to the dam. Net amounts of bed-level lowering over the period are shown for the entire reach (Figure 25) and for the

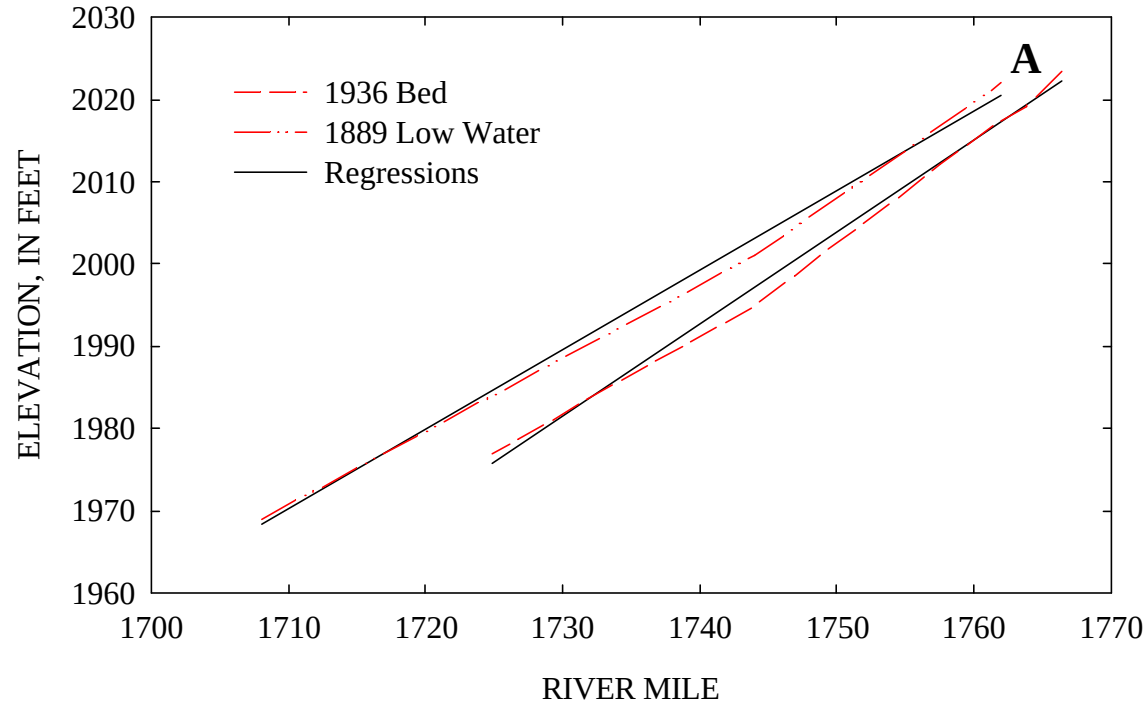

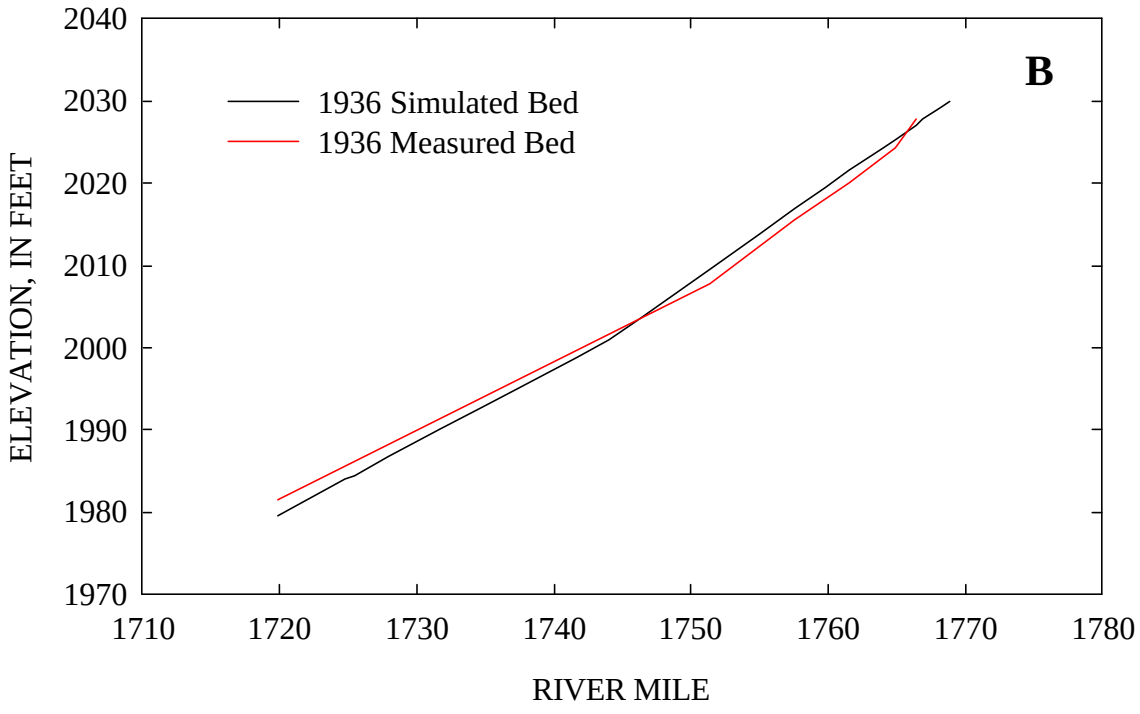

Figure 21--Comparison between (A) 1936 bed elevations and profile with 1889 low-water profile, and (B) comparison of measured and simulated 1936 bed elevations, for the 46.5 mile reach below Fort Peck Dam.

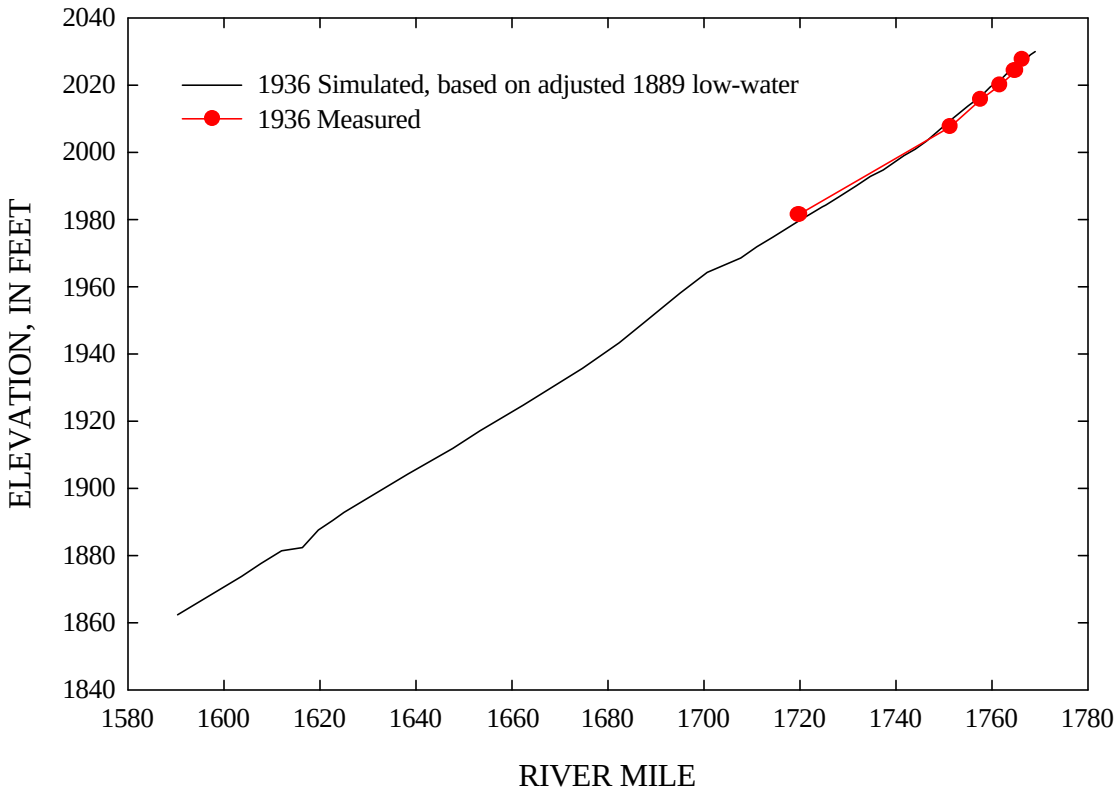

Figure 22--Measured and simulated 1936 average-bed elevations for the entire study reach.

Table 3-- Average channel-bed elevations for 1936, 1948, 1956, 1966, 1978, and 1994. Note that much of the 1936 data are simulated, based on analysis of the 1889 low-water profile.

1960 River Miles	Average bed elevation (feet)						Change in average bed elevation (feet)				
	1936	1948	1956	1966	1978	1994	1936-1948	1948-1956	1956-1966	1966-1978	1978-1994
1768.9	2030**	2024.8	2024.5	2024.6	2023.7	2025.2	-5.21	-0.37	0.12	-0.92	1.52
1768.1	2029.1**	2027.0	2026.4	2026.7	2026.5	2025.9	-2.19	-0.59	0.30	-0.14	-0.65
1766.9	2027.7**		2023.0	2022.8	2022.9	2026.0			-0.22	0.15	3.12
1766.4	2027.8*	2024.5	2023.8	2023.9	2023.7	2025.8	-3.27	-0.78	0.17	-0.25	2.15
1764.9	2024.3*	2023.9	2022.9	2022.7	2018.2	2017.9	-0.39	-0.99	-0.25	-4.43	-0.37
1763.8	2024.2**	2022.1	2020.7	2020.0	2019.5	2019.1	-2.04	-1.41	-0.73	-0.49	-0.38
1761.6	2020.1*	2016.9	2017.0	2016.5	2015.0	2014.4	-3.16	0.10	-0.56	-1.50	-0.57
1759.8	2019.4**	2012.0	2012.4	2011.6	2011.4	2011.7	-7.43	0.39	-0.78	-0.21	0.31
1757.6	2015.6*	2014.4	2012.8	2012.4	2011.1	2010.0	-1.20	-1.61	-0.44	-1.30	-1.09
1755.0	2013.8**	2012.5	2011.2	2010.5	2011.5	2008.9	-1.36	-1.21	-0.77	1.00	-2.53
1751.3	2007.8*	2010.6	2008.8	2007.9	2007.1	2007.1	2.74	-1.74	-0.97	-0.77	0.06
1748.7	2003.6**		2005.3	2004.6	2004.2	2004.1			-0.71	-0.33	-0.10
1746.2	2001**	2006.2	2004.7	2001.2	2001.4	2000.7	5.20	-1.48	-3.49	0.14	-0.66
1744.0	1998.9**	2000.8	1998.3	1998.5	1997.1	2000.1	1.91	-2.56	0.23	-1.41	3.02
1741.7	1995.0**		1999.6	1998.8	1996.8	1994.5			-0.80	-2.02	-2.29
1737.2	1992.8**	1994.1	1993.1	1994.7	1992.3	1991.1	1.38	-1.04	1.57	-2.42	-1.16
1734.8	1990.0**	1993.7	1992.8	1992.6	1992.9	1988.0	3.64	-0.91	-0.20	0.34	-4.93
1731.7	1986.8**	1987.5	1986.1	1987.4	1986.2	1986.3	0.72	-1.37	1.33	-1.25	0.07
1727.9	1984.4**	1986.9	1988.2	1986.6	1986.0	1983.3	2.46	1.32	-1.62	-0.64	-2.66
1725.4	1984.0**		1983.6	1983.9	1983.3	1983.0			0.30	-0.59	-0.28
1724.8	1981.6*	1981.7	1980.6	1980.5	1980.1	1978.1	0.08	-1.01	-0.13	-0.37	-2.07
1719.8	1974.7**	1980.6	1979.9	1979.9	1979.0	1979.8	5.96	-0.78	0.08	-0.92	0.81
1714.4	1971.8**	1969.3	1970.7	1971.2	1970.5	1969.3	-2.51	1.44	0.48	-0.70	-1.22
1711.2	1968.8**		1965.4	1965.0	1966.2	1964.7			-0.45	1.26	-1.56
1707.7	1964.5**	1958.6	1963.4	1962.4	1961.8	1965.7	-5.86	4.82	-1.02	-0.61	3.94
1700.5	1958.0**		1957.7	1958.7	1957.8	1960.9			1.05	-0.92	3.03
1694.9	1949.8**	1955.1	1954.6	1954.6	1954.2	1949.2	5.33	-0.51	0.02	-0.38	-5.07
1687.8	1943.5**		1945.9	1947.2	1945.9	1944.2			1.23	-1.28	-1.69
1682.3	1935.8**	1941.9	1940.9	1941.2	1941.6	1939.9	6.12	-0.99	0.31	0.40	-1.69
1674.7	1924.8**		1935.9	1936.3	1935.1	1934.0			0.34	-1.22	-1.10
1662.2	1917.0**		1923.2	1922.0	1921.8	1920.3			-1.21	-0.16	-1.52
1653.2	1912.1**	1913.3	1913.9	1912.4	1911.2	1910.6	1.21	0.53	-1.44	-1.25	-0.58
1647.6	1908.0**		1909.8	1910.7	1910.3	1910.4			0.90	-0.38	0.02
1643.0	1904.2**		1907.4	1907.8	1907.9	1908.0			0.34	0.14	0.05
1638.5	1892.7**		1902.3	1902.5	1903.0	1901.4			0.20	0.50	-1.53
1625.1	1890.5**	1894.5	1893.6	1893.5	1893.8	1890.5	4.05	-0.91	-0.13	0.26	-3.26
1619.7	1887.8**		1886.3	1886.6	1886.2	1886.4			0.29	-0.45	0.25
1616.5	1882.3**		1884.5	1884.3	1884.5	1883.4			-0.17	0.16	-1.10
1612.1	1881.3**		1879.7	1880.9	1879.9	1879.9			1.23	-1.01	-0.04
1607.7	1877.4**	1878.7	1878.4	1877.2	1879.1	1875.6	1.24	-0.28	-1.18	1.85	-3.48
1603.7	1874.0**		1874.8	1874.7	1874.1	1872.3			-0.14	-0.58	-1.80
1596.9	1868.0**		1866.5	1866.3	1866.3	1870.8			-0.18	0.01	4.51
1590.2	1862.3**	1866.3	1866.4	1866.3	1865.8	1866.2	3.93	0.11	-0.08	-0.54	0.40

* Measured data.
** Simulated data.

Table 4--Thalweg elevations for 1936, 1948, 1956, 1966, 1978, and 1994. Note that much of the 1936 data are simulated, based on analysis of the 1889 low-water profile

1960	Thalweg elevations (feet)						Change in thalweg elevation (feet)				
River Miles	1936	1948	1956	1966	1978	1994	1936-1948	1948-1956	1956-1966	1966-1978	1978-1994
1768.9	2024**	2019.2	2019.0	2019.0	2019.5	2019.7	-4.79	-0.20	0.00	0.50	0.20
1768.1	2023.2**	2019.8	2018.8	2019.5	2018.9	2018.4	-3.35	-1.00	0.70	-0.60	-0.50
1766.9	2021.8**	2019.4	2018.8	2018.2	2018.4	2020.8	-2.38	-0.60	-0.60	0.20	2.40
1766.4	2023.5*	2021.1	2018.6	2018.9	2017.6	2020.4	-2.40	-2.50	0.30	-1.30	2.80
1764.9	2019.4**	2017.4	2014.3	2014.0	2013.2	2013.5	-1.97	-3.10	-0.30	-0.80	0.30
1763.8	2019.2*	2017.4	2014.6	2011.3	2006.7	2009.7	-1.80	-2.80	-3.30	-4.60	3.00
1761.6	2017*	2012.6	2013.6	2012.2	2011.8	2010.3	-4.40	1.00	-1.40	-0.40	-1.50
1759.8	2013.5**	2007.2	2007.0	2008.0	2007.2	2008.0	-6.29	-0.20	1.00	-0.80	0.80
1757.6	2012.1*	2008.0	2004.2	2007.9	2000.5	1997.1	-4.10	-3.80	3.70	-7.40	-3.40
1755.0	2007.8**	2002.0	2007.1	2001.2	2006.4	2003.8	-5.82	5.10	-5.90	5.20	-2.60
1751.3	2003.6**	2001.4	2001.0	2003.0	2001.0	2000.7	-2.22	-0.40	2.00	-2.00	-0.30
1746.2	1997.6**	2001.5	1997.7	1994.8	1991.7	1987.5	3.87	-3.80	-2.90	-3.10	-4.20
1744.0	1994.9*	1995.0	1994.0	1994.3	1994.0	1994.2	0.10	-1.00	0.30	-0.30	0.20
1741.7	1992.9**	1988.5	1989.0	1988.9	1986.8	1988.1	-4.43	0.50	-0.10	-2.10	1.30
1737.2	1988.9**	1979.1	1983.6	1987.2	1980.9	1986.0	-9.83	4.50	3.60	-6.30	5.10
1734.8	1986.9**	1980.1	1985.9	1986.0	1983.6	1980.6	-6.75	5.80	0.10	-2.40	-3.00
1731.7	1984.0**	1984.2	1982.0	1976.0	1982.4	1981.9	0.23	-2.20	-6.00	6.40	-0.50
1727.9	1980.8**	1974.4	1976.9	1975.6	1975.4	1978.5	-6.37	2.50	-1.30	-0.20	3.10
1725.4	1978.5**		1979.0	1976.0	1974.6	1975.9			-3.00	-1.40	1.30
1724.8	1977.0*	1975.9	1973.7	1973.0	1975.0	1971.2	-1.10	-2.20	-0.70	2.00	-3.80
1719.8	1973.6**	1971.4	1970.2	1971.5	1971.0	1974.8	-2.17	-1.20	1.30	-0.50	3.80
1714.4	1968.8**	1976.0	1968.0	1960.5	1958.9	1960.2	7.23	-8.00	-7.50	-1.60	1.30
1711.2	1965.7**		1955.3	1958.8	1955.6	1959.8			3.50	-3.20	4.20
1707.7	1962.9**	1940.1	1956.5	1946.0	1948.2	1957.4	-22.8	16.4	-10.5	2.20	9.20
1700.5	1958.5**		1949.9	1950.0	1952.8	1950.2			0.10	2.80	-2.60
1694.9	1951.8**	1944.9	1947.9	1944.0	1945.0	1937.6	-6.93	3.00	-3.90	1.00	-7.40
1687.8	1943.6**		1942.0	1930.0	1939.7	1937.3			-12.00	9.70	-2.40
1682.3	1937.2**	1933.6	1933.6	1924.9	1914.5	1933.6	-3.58	0.00	-8.70	-10.4	19.1
1674.7	1929.1*		1923.6	1925.8	1925.4	1924.6			2.20	-0.40	-0.80
1662.2	1918.4*		1916.1	1908.7	1908.4	1913.1			-7.40	-0.30	4.70
1653.2	1910.7**	1909.3	1909.2	1904.0	1904.3	1904.8	-1.43	-0.10	-5.20	0.30	0.50
1647.6	1905.8*		1905.6	1898.4	1903.1	1903.1			-7.20	4.70	0.00
1643.0	1901.8*		1900.7	1893.5	1900.9	1897.7			-7.20	7.40	-3.20
1638.5	1898.1*		1886.0	1891.0	1889.6	1891.4			5.00	-1.40	1.80
1625.1	1886.6*	1885.1	1885.8	1884.0	1879.4	1871.0	-1.47	0.70	-1.80	-4.60	-8.40
1622.7	1884.4*		1879.0		1877.7	1877.9					0.20
1619.7	1881.8*		1878.3	1877.0	1880.0	1874.4			-1.30	3.00	-5.60
1616.3	1878.8*		1871.6	1873.9	1865.6	1865.8			2.30	-8.30	0.20
1612.1	1875.3*		1874.1	1869.2	1872.0	1861.4			-4.90	2.80	-10.60
1607.7	1871.5*	1859.6	1868.9	1867.6	1862.5	1868.0	-11.9	9.30	-1.30	-5.10	5.50
1603.7	1868.2*		1857.8	1859.3	1865.9	1858.7			1.50	6.60	-7.20
1596.9	1862.2*		1861.0	1856.2	1858.8	1868.0			-4.80	2.60	9.20
1590.2	1856.5*	1855.0	1858.0	1857.0	1852.0	1858.0	-1.47	3.00	-1.00	-5.00	6.00

* Measured data.
** Simulated data.

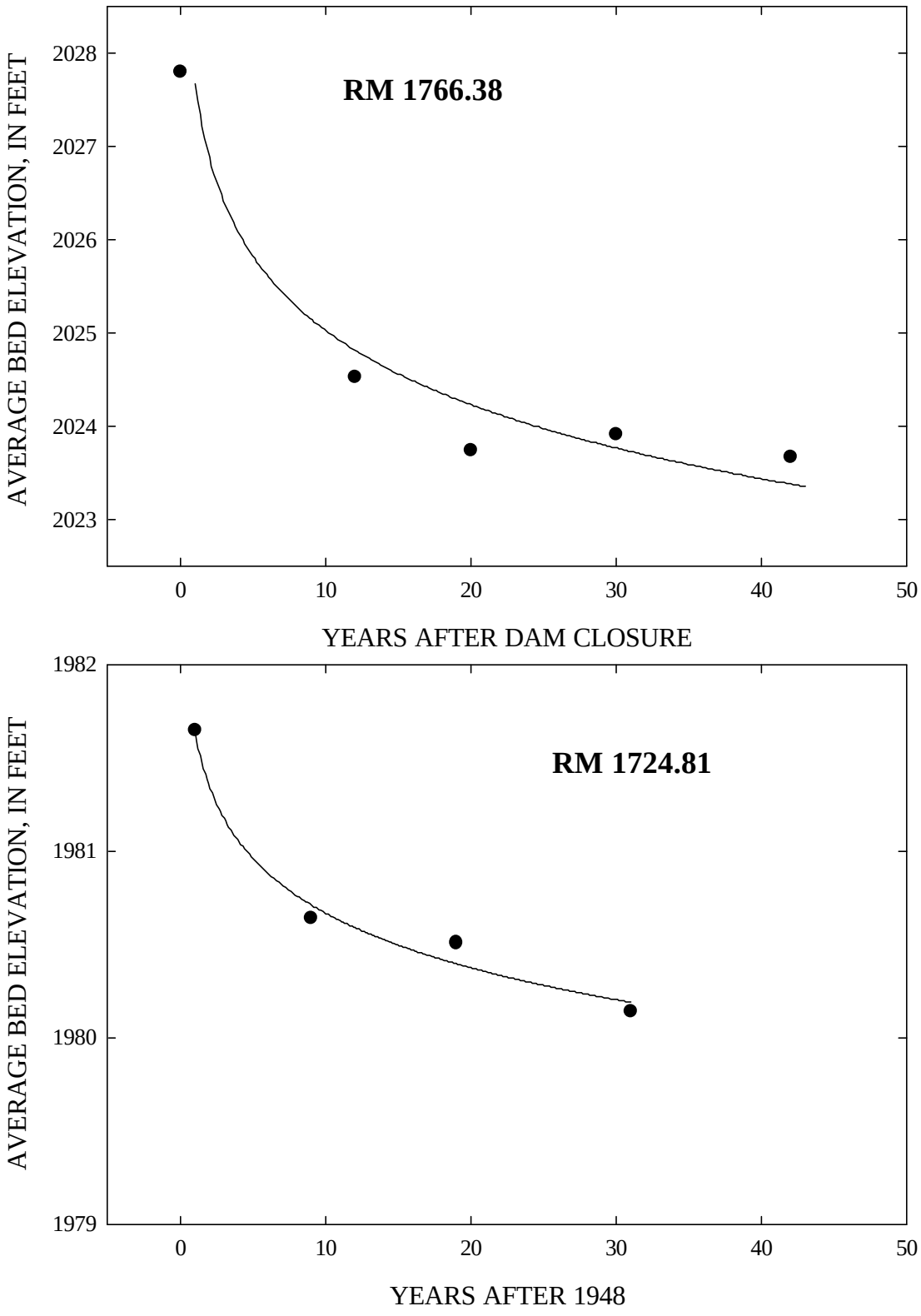

Figure 23--Examples of fitting equation 2 to bed-level adjustment trends.

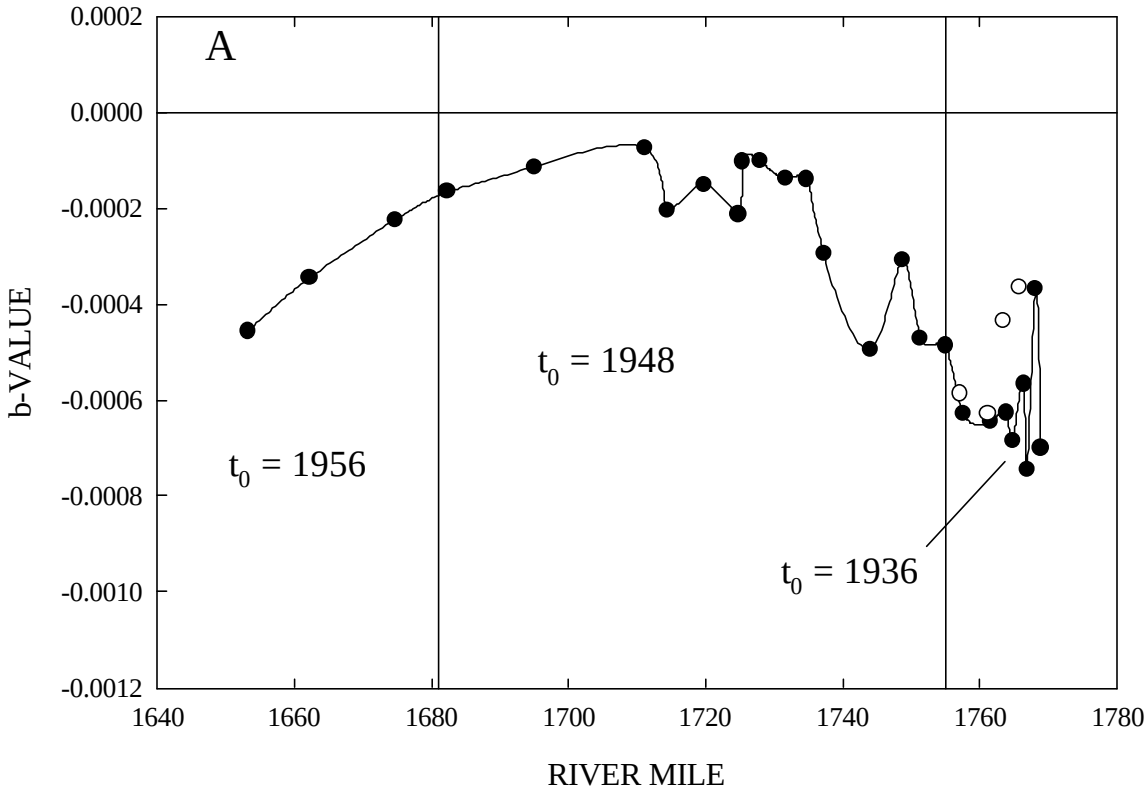

Figure 24--Model of bed-level response for the Missouri River study reach based on exponents from equation 2 plotted against river mile for (A) average bed elevations and, (B) thalweg elevations.

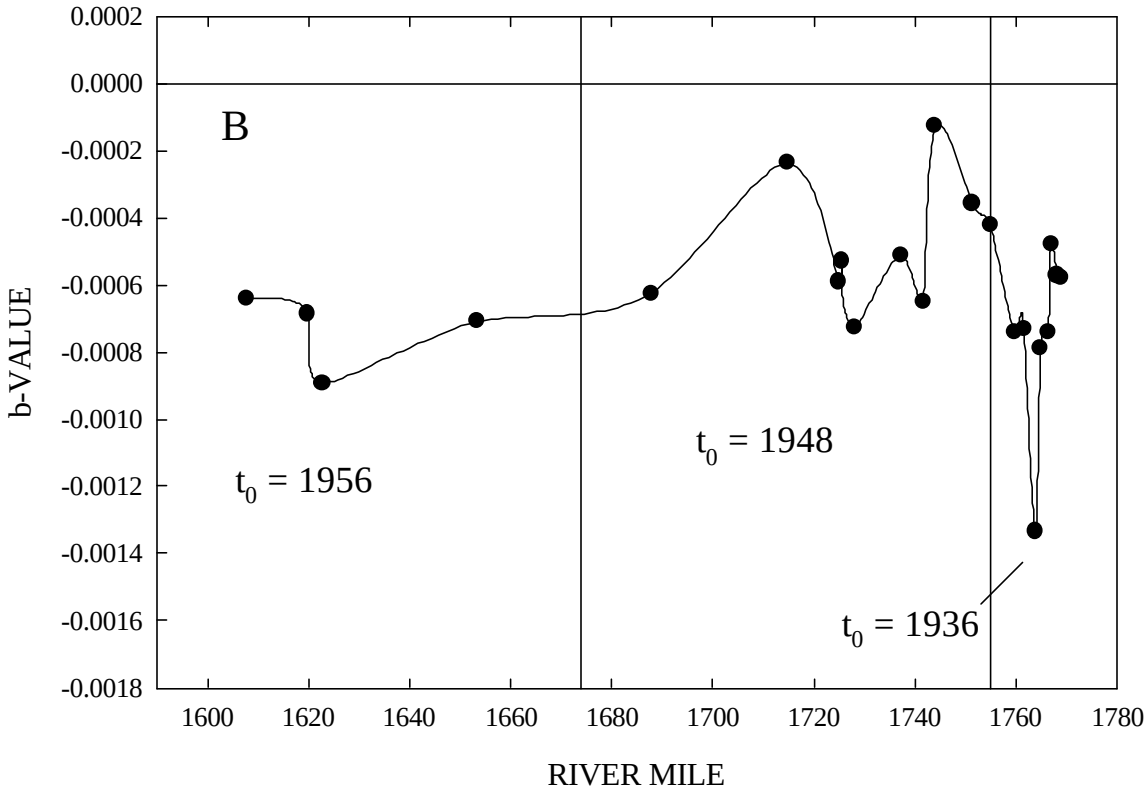

Figure 24--Model of bed-level response for the Missouri River study reach based on exponents from equation 2 plotted against river mile for (A) average bed elevations and, (B) thalweg elevations

Table 5-- Changes in bed-elevations for 4 gaging sites along the study reach. Original data from Williams and Wolman (1984; Table 13) and re-worked in this study according to equation 2.

1960 River Mile	Mean Bed Elevation, in Feet							
	1936	1950	1955	1956	1958	1960	1966	1973
1765.8	2020.4	2017.8	2018.3	2018.1	2018.1	2018.3	2018.0	2017.5
1763.4	2017.7	2015.6	2015.1	2015.2	2015.7	2015.2	2014.4	2014.2
1761.2	2015.1	2011.8	2011.1	2011.8	2011.8	2011.6	2011.3	2009.3
1757.2	2010.4	2008.8	2008.1	2007.2	2007.0	2006.7	2006.7	2005.5
	Mean Bed Elevation Change, in Feet							
	1936-1950	1950-1955	1955-1956	1956-1958	1958-1960	1960-1966	1966-1973	
1765.8	-2.62	0.49	-0.16	0.00	0.16	-0.33	-0.49	
1763.4	-2.13	-0.49	0.16	0.49	-0.49	-0.82	-0.16	
1761.2	-3.28	-0.66	0.66	0.00	-0.16	-0.33	-1.97	
1757.2	-1.64	-0.66	-0.98	-0.16	-0.33	0.00	-1.15	

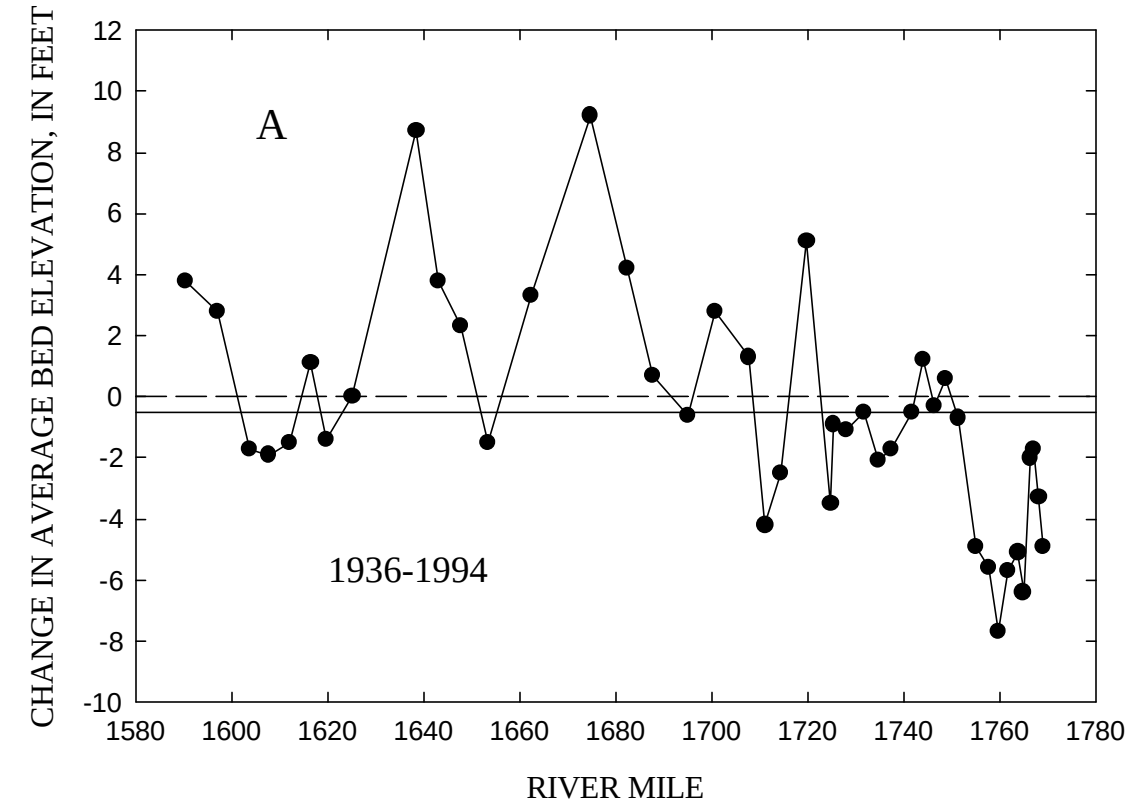

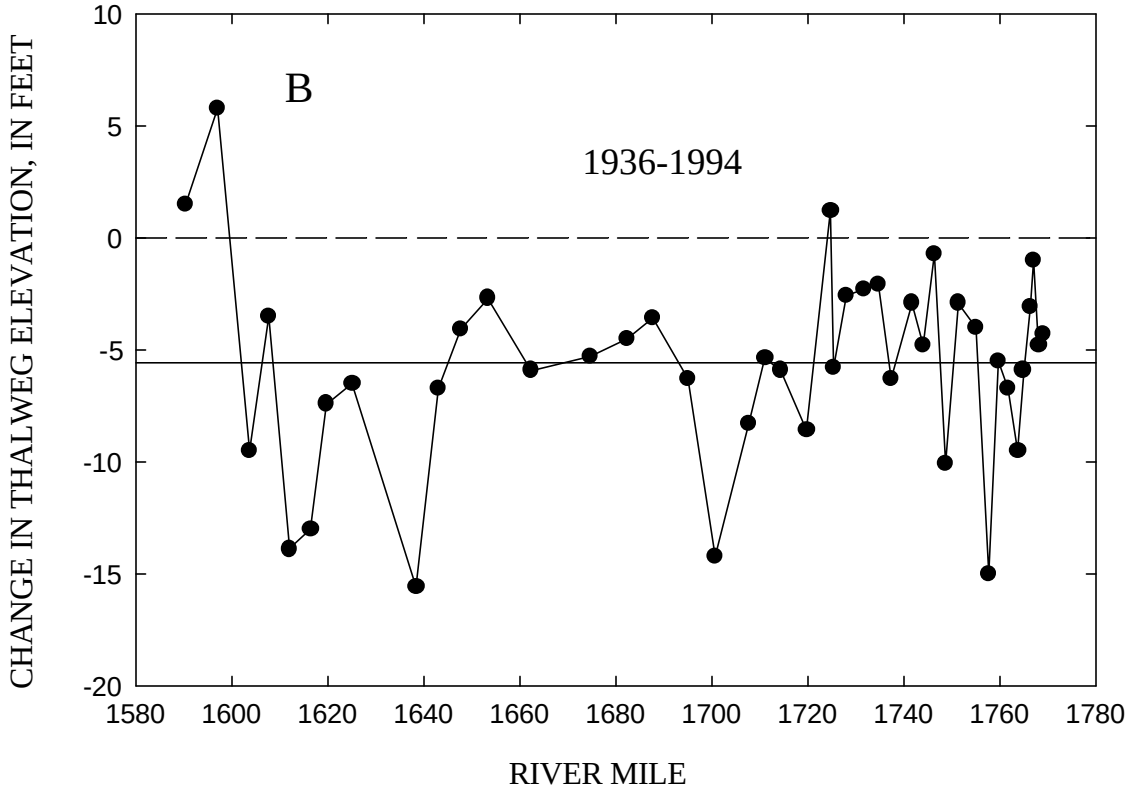

Figure 25--Net amount of average (A) and thalweg (B) bed-level change over the study reach for the period 1936-1994.

50-mile reach closest to the dam (Figure 26). Over the entire reach, the average amount of thalweg erosion was about 5.0 feet and about 5.6 feet in the reach closest to Fort Peck Dam (Figures 25b and 26b). The general attenuation of erosion with increasing distance from the dam can be seen in Figures 25a and 26a.

By plotting the b-values obtained using equation 2 against river mile, a model of average bed-level response for the period following dam closure is obtained (Figure 24a). Recall that each of the points represented on this figure is the culmination of historical bed-level data at a given location along the reach. Only the first 16.5 miles downstream from the dam experienced measurable degradation in the first 12-years after dam closure. For locations downstream from River Mile 1755, the t_0 used to model degradation is represented by 1948 data. Thus, it took about 12 years for the effects of the disturbance to be felt further downstream in the reach between River Mile 1751 and about 1710. Because of this, the simulated 1936 bed elevations were not needed (for this analysis) beyond where direct comparisons with the 1889 profile were possible. By 1956 degradation effects had reached further downstream to include the reach between River Miles 1674 and 1653. Downstream from this location, bed-level adjustment trends are indeterminate with some sites experiencing mild degradation and others experiencing mild aggradation.

A similar bed-level trend analysis was performed using thalweg-elevation data. Again, the most-negative *b*-values occur in the vicinity of the dam but are greater than those calculated using average bed elevations (Figure 24b). Results from the thalweg analysis show considerably more data scatter due to the effects of local boundary and flow conditions, thereby masking overall trends. Still it is the changes represented by the thalweg data, particularly if the thalweg is adjacent to the bank, which can be important in considering the most critical conditions regarding bank stability. Changes in thalweg elevations for the 5 periods are displayed graphically in Appendix C for each site.

Data showing changes in average bed elevation for each of the 5 time periods (1936-1948; 1948-1956; 1956-1966; 1966-1978; and 1978-1994) are displayed in Figure 27 to show (1) the great variability in the reach and (2), the general trend of decreasing amounts of bed erosion with time over the entire study reach. There is, however, an increase in erosion activity displayed by the 1978-1994 period. This could be due to the second of two successive high-flow years occurring in 1978 and 1979. These flow events, as well as the one in 1976 have been identified by dendrochronology as helping to create a new geomorphic surface.

Bed Profiles

Profiles of the channel bed are shown in Figures 1a and 1b. Again as expected the variability of the thalweg profile is seen to be much greater than for the profile based on average bed-elevations. The 1889 low-water profile is plotted on both graphs for comparison. Changes in bed elevation for all sites and for specific time periods are listed in Tables 3 and 4. These data are shown graphically for each site in a series of plots in Appendix C.

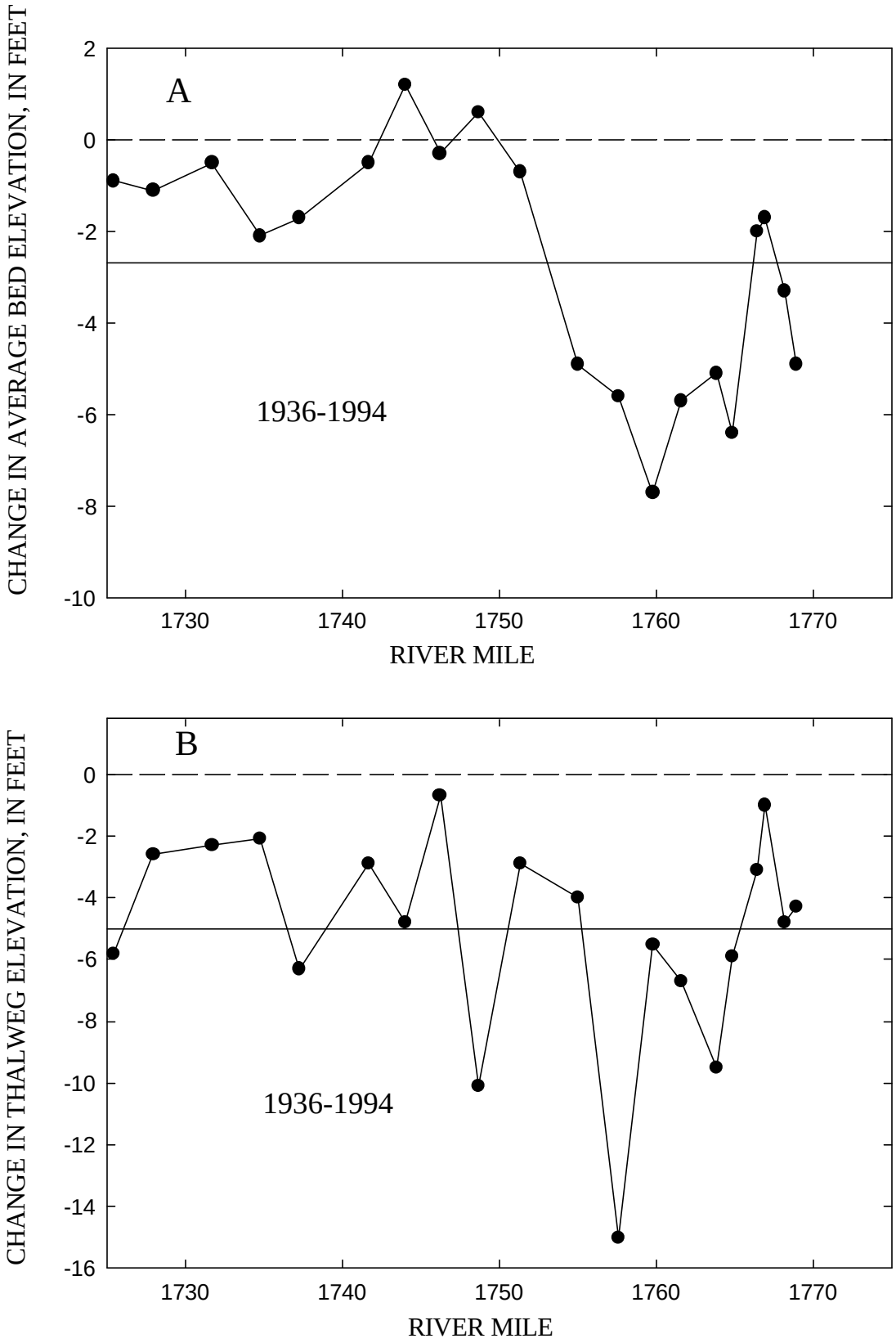

Figure 26--Net amount of average (A) and thalweg (B) bed-level change over the reach between Fort Peck Dam and River Mile 1725 for the period 1936-1994.

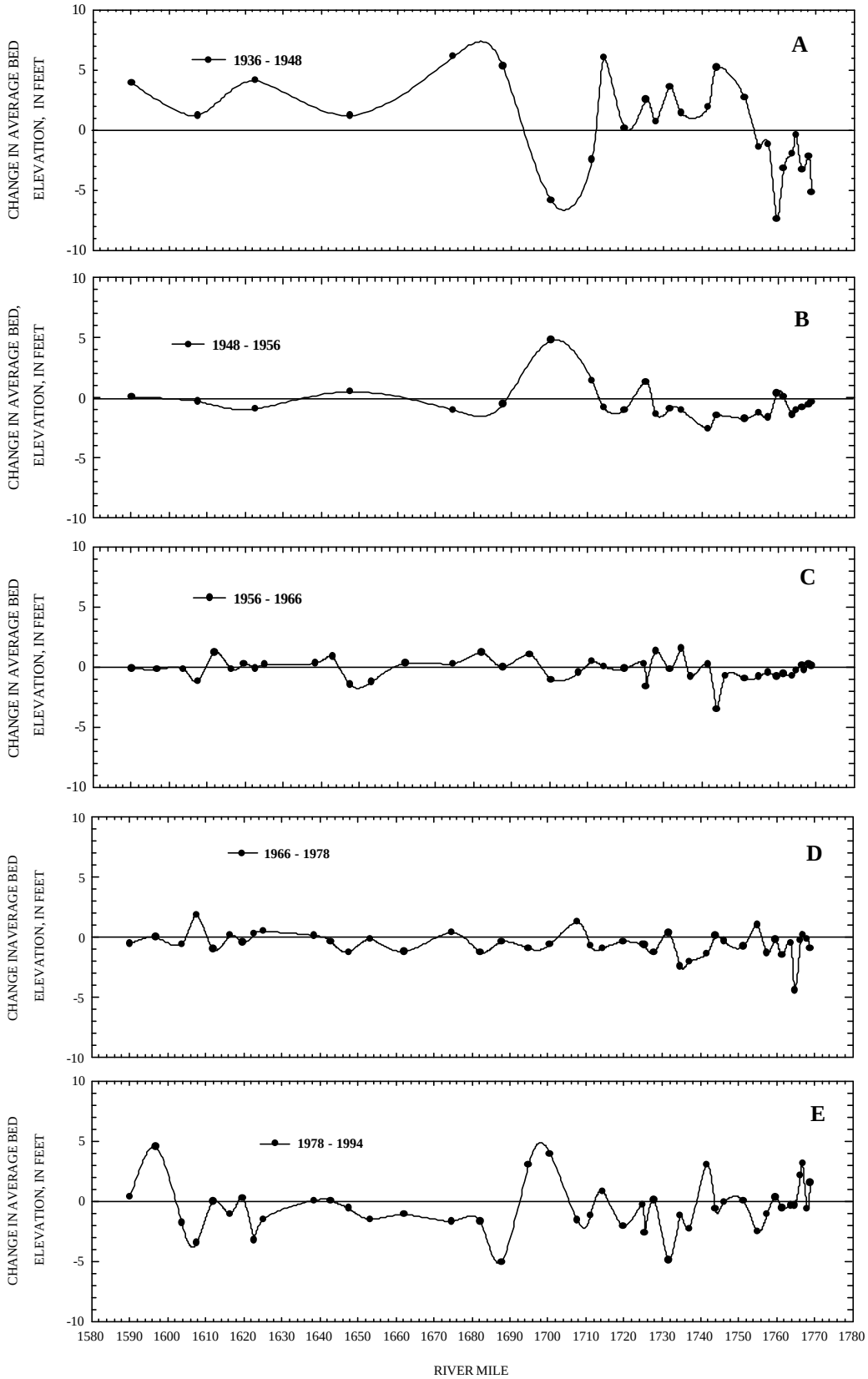

Figure 27--Change in average bed elevation between (A) 1936 and 1948; (B) 1948-1956; (C) 1956-1966; (D) 1966-1978; and (E) 1978-1994.

Total Bed-Level Changes Since Dam Closure

The site-specific relations derived with equation 2 are used to calculate total amounts of bed-level lowering between dam closure and 1998 (Figure 28 and Tables 6 and 7). This is accomplished by calculating the bed elevation for a given site, with $t = 62$ years after dam closure. The value obtained is then subtracted from the 1936 elevation to obtain the amount eroded (Tables 6 and 7). Average bed-elevations decreased as much as 6 feet near the dam and thalweg elevations decreased as much as 11 feet. Reductions in average bed-elevations decrease with distance downstream from the dam to about 1-foot near River Mile 1715 (Figure 28a). Amounts of bed erosion then seem to increase towards River Mile 1640.

The future trend for thalweg elevations is not as clear (Figure 28b). Future changes in both average and thalweg elevations are minimal (generally less than one foot) over the period 1998 to 2008 as calculated from equation 2 (Figure 28). This is not to say that sediment movement from the channel bed will cease. Scour and fill will occur over short time frames in response to changing flow conditions. However, net removal of material over the long term in the reach downstream from Fort Peck Dam seems to have abated. Therefore, it can be generally stated that long-term, channel-bed degradation downstream from Fort Peck Dam as a direct result of dam closure is essentially complete. Results from four sites in this reach published by Williams and Wolman (1984) support these findings.

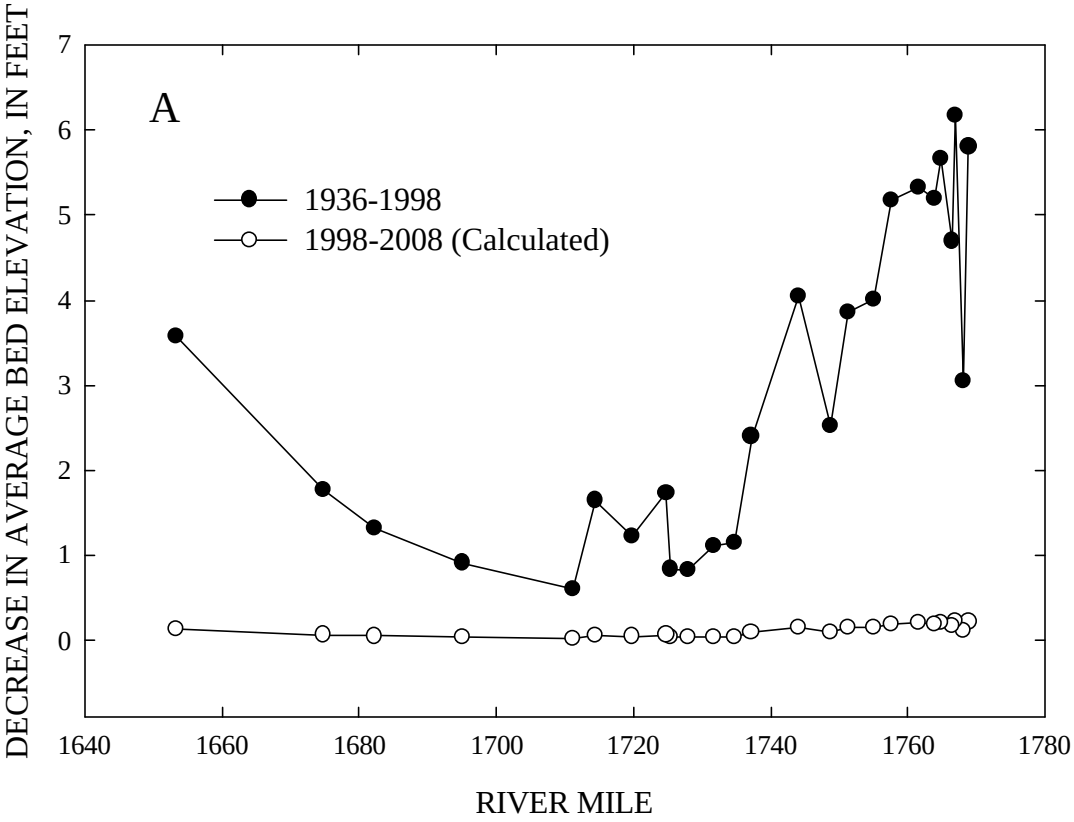

Figure 28--Calculated changes in (A) average and (B) thalweg bed elevations between 1936 and 1998 with predicted erosion to 2008.

Table 6. Summary of data used to develop bed-level response model for average bed elevations.

River Mile	a-value	b-value	t_0	Elev. 1998	Elev. 2008	Amount eroded (feet)					River mile	1960 d_{50}
	from equation 2			in feet		1936-1998	1998-2008					
1768.89	2029.4	-0.000700	1936	2023.6	2023.4	5.81	0.22				1768.89	8.52
1768.13	2029.0	-0.000368	1936	2026.0	2025.8	3.05	0.11				1768.13	10.706
1766.92	2027.8	-0.000744	1936	2021.6	2021.4	6.17	0.23				1766.92	3.385
1766.38	2027.7	-0.000566	1936	2023.0	2022.8	4.69	0.18				1766.38	6.486
1765.8	*	-0.000364	1936									
1764.86	2025.5	-0.000684	1936	2019.9	2019.7	5.66	0.21				1764.86	0.528
1763.84	2024.5	-0.000627	1936	2019.3	2019.1	5.19	0.20				1761.56	4.375
1763.4	*	-0.000434	1936									
1761.56	2020.3	-0.000645	1936	2015.0	2014.8	5.33	0.20				1759.8	0.569
1761.2	*	-0.000628	1936									
1759.8											1757.58	0.494
1757.58	2016.3	-0.000628	1936	2011.1	2010.9	5.18	0.19				1754.97	0.252
1757.2	*	-0.000586	1936									
1754.97	2014.2	-0.000486	1936	2010.1	2010.0	4.00	0.15				1751.33	0.336
1751.33	2010.6	-0.000470	1948	2006.8	2006.6	3.87	0.15				1748.65	0.368
1748.65	2006.5	-0.000307	1948	2003.9	2003.8	2.52	0.09				1746.2	0.289
1746.2	2006.6										1743.97	0.357
1743.97	2000.8	-0.000495	1948	1996.7	1996.6	4.05	0.15				1741.67	0.273
1741.67	2001.8										1737.21	0.244
1737.21	1994.5	-0.000294	1948	1992.1	1992.0	2.40	0.09				1734.75	0.265
1734.75	1993.6	-0.000140	1948	1992.4	1992.4	1.14	0.04				1731.69	0.286
1731.69	1987.4	-0.000137	1948	1986.3	1986.2	1.11	0.04				1727.94	0.309
1727.94	1987.4	-0.000101	1948	1986.5	1986.5	0.82	0.03				1725.41	0.278
1725.41	1984.1	-0.000103	1948	1983.2	1983.2	0.84	0.03				1724.81	0.415
1724.81	1981.6	-0.000213	1948	1979.9	1979.8	1.73	0.07				1719.82	0.24
1719.82	1980.6	-0.000150	1948	1979.4	1979.3	1.22	0.05				1714.78	0.29
1714.4	1971.6	-0.000204	1948	1970.0	1969.9	1.65	0.06				1711.15	0.239
1711.15	1965.8	-0.000074	1948	1965.2	1965.2	0.60	0.02				1707.83	0.242
1694.94	1955.1	-0.000114	1948	1954.2	1954.2	0.91	0.03				1707.7	0.242
1687.79											1707.6	0.241
1682.3	1941.9	-0.000166	1948	1940.6	1940.6	1.32	0.05				1700.54	0.247
1674.72	1936.3	-0.000224	1956	1934.5	1934.5	1.78	0.07				1695.1	0.263
1669.23											1687.79	0.26
1662.23		-0.000345	1956								1682.3	0.219
1653.24	1914.0	-0.000456	1956	1910.4	1910.3	3.57	0.13				1674.72	0.215
											1669.23	0.214
* Sites also studied by Williams and Wolman (1984)											1662.23	0.25
											1653.24	0.195
											1647.55	0.241
											1642.95	0.248
											1638.46	0.205
											1630.96	0.214
											1625.1	0.238
											1622.7	0.2
											1619.73	0.208
											1616.47	0.218
											1612.05	0.204
											1607.65	0.203
											1603.74	0.226
											1596.89	0.172

Table 7. Summary of data used to develop bed-level response model for thalweg elevations.

River mile	a-value	b-value	t_0	Elev. 1998	Elev. 2008	Amount eroded (feet)		River mile	1960 d_{50}
	from equation 2			in feet		1936-1998	1998-2008		
1768.89	2023.36	-0.000579	1936	2018.6	2018.4	4.79	0.18	1768.89	8.52
1768.13	2023.02	-0.000572	1936	2018.3	2018.1	4.73	0.18	1768.13	10.706
1766.92	2021.79	-0.000478	1936	2017.8	2017.7	3.95	0.15	1766.92	3.385
1766.38	2024	-0.000741	1936	2017.9	2017.6	6.13	0.23	1766.38	6.486
1764.86	2020	-0.000789	1936	2013.5	2013.2	6.51	0.24	1764.86	0.528
1763.84	2021	-0.001334	1936	2010.0	2009.6	11.01	0.41	1761.56	4.375
1761.56	2017	-0.000731	1936	2011.0	2010.7	6.03	0.23	1759.8	0.569
1759.8	2013	-0.000742	1936	2006.9	2006.7	6.11	0.23	1757.58	0.494
1757.58								1754.97	0.252
1754.97	2007	-0.000420	1936	2003.6	2003.4	3.45	0.13	1751.33	0.336
1751.33	2003	-0.000357	1948	2000.1	2000.0	2.93	0.11	1748.65	0.368
1746.2	2003		1948					1746.2	0.289
1743.97	1995	-0.000127	1948	1994.0	1993.9	1.04	0.04	1743.97	0.357
1741.67	1993	-0.000651	1948	1987.7	1987.5	5.31	0.20	1741.67	0.273
1737.21	1987	-0.000512	1948	1982.8	1982.7	4.16	0.16	1737.21	0.244
1734.75			1948					1734.75	0.265
1731.69			1948					1731.69	0.286
1727.94	1980	-0.000727	1948	1974.1	1973.9	5.88	0.22	1727.94	0.309
1725.41	1979	-0.000528	1948	1974.7	1974.6	4.27	0.16	1725.41	0.278
1724.81	1976	-0.000590	1948	1971.2	1971.1	4.77	0.18	1724.81	0.415
1719.82			1948					1719.82	0.24
1714.78	1976	-0.000235	1948	1974.1	1974.0	1.90	0.07	1714.78	0.29
1694.94	1949	-0.001103	1948	1940.2	1939.9	8.78	0.33	1711.15	0.239
1687.79	1940	-0.000626	1948	1935.0	1934.8	4.97	0.19	1707.83	0.242
1682.3	1931.58	-0.001100	1948	1922.9	1922.6	8.68	0.33	1707.7	0.242
1674.72			1956					1707.6	0.241
1662.23	1916	-0.001370	1956	1905.3	1904.9	10.72	0.40	1700.54	0.247
1653.24	1909	-0.000709	1956	1903.5	1903.3	5.53	0.21	1695.1	0.263
1622.7	1884	-0.000894	1956	1877.1	1876.9	6.88	0.26	1687.79	0.26
1619.73	1882	-0.000686	1956	1876.7	1876.5	5.28	0.20	1682.3	0.219
1616.47	1880	-0.001562	1956	1868.0	1867.6	11.98	0.45	1674.72	0.215
1612.05			1956					1669.23	0.214
1607.65	1870	-0.000639	1956	1865.1	1864.9	4.89	0.18	1662.23	0.25
1603.74	1867	-0.001018	1956	1859.2	1858.9	7.77	0.29	1653.24	0.195
								1647.55	0.241
								1642.95	0.248
								1638.46	0.205
								1630.96	0.214
								1625.1	0.238
								1622.7	0.2
								1619.73	0.208
								1616.47	0.218
								1612.05	0.204
								1607.65	0.203
								1603.74	0.226
								1596.89	0.172

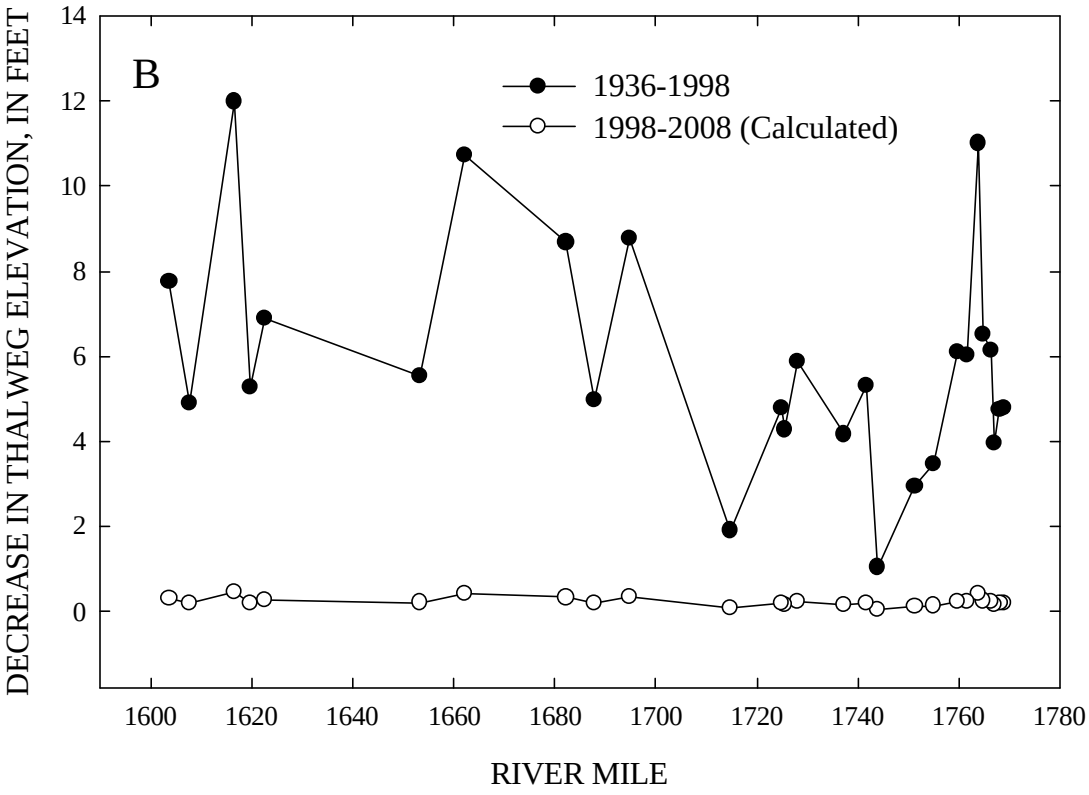

Figure 28--Calculated changes in (A) average and (B) thalweg bed elevations between 1936 and 1998 with predicted erosion to 2008.

MEANDERS AND LATERAL-MIGRATION PROCESSES: THEORY

Meandering rivers erode their banks, leading to migration of the channel across its flood plain. In addition to gradual movement of the channel, rapid avulsions such as neck cutoffs also occur along more active systems. Rates of lateral migration vary widely from river to river and from reach to reach along a given river. Published values representing global conditions range from zero to as high as 2,600 ft/yr (Hooke, 1980). Although patterns of concave bank erosion and convex bank deposition are easily identifiable, prediction of channel behavior at a given point for a given time interval is very difficult (Cherry *et al.,* 1996).

Governing Variables

Meander geometry may be described by a set of variables referred to herein as form variables. These include channel width, meander length, meander wavelength, amplitude, radius of curvature, arc angle and sinuosity. Mean or median values of these variables for a given reach containing multiple bends have been used to generate empirical formulas that take the form of power functions of bed slope, sediment discharge, water discharge and of one another, although considerable scatter exists from one bend to the next. Tables of these relationships (regression formulas) have been published by many workers (e.g., Chitale, 1973, Williams 1986, and Cherry *et al*. 1996). The departure of a given stream reach from these relationships may be diagnostic of systemic instability, which is often associated with accelerated channel erosion.

Meander form and meander migration rate are dependent upon essentially the same set of controlling variables: water discharge, sediment supply, sediment type, boundary (bank) properties and valley slope. If meander form has reached equilibrium with the dominant value of the controlling variables, then variables describing meander geometry should be useful for empirically predicting migration rate. For example, Hooke (1984) found mean migration rates for 54 streams were roughly proportional to the square root of the upstream drainage area, while Brice (1982) correlated mean migration rates for 43 streams with channel width. It is important to note, however, that form variables are not truly independent in the sense of cause-and-effect (Cherry *et al*. 1996). In addition, the migration rate at a particular point along a given river reflects the behavior of adjacent reaches, tributary influences, and overbank drainage (Fischer, 1994). The influence of adjacent reaches (for example, the impact of a rapidly growing bend just downstream) is the most difficult factor to account for in prediction (Hooke, 1995).

Water discharge is one of the most important independent variables governing river migration. Regression analyses have revealed that meander migration may be fit to a simple power function of bank height and channel-forming discharge, but the regression equations typically explain less than half of the variance in the underlying data (MacDonald *et al*. 1991). Garcia *et al*. (1994) developed regression formulas for migration rate (e.g., area of flood plain reworked per channel length per year) as a function of channel width and as a function of two-year recurrence interval discharge using data from small to medium-sized rivers in Minnesota and Illinois. However, observed values of migration rate varied by an order of magnitude for a given value of width or discharge. Prior to reservoir closure, annual thalweg shift for seven reaches of

the braided Hanjiang River in China was highly correlated (r = 0.95) with the ratio of mean annual maximum daily discharge divided by the mean annual discharge (Jiongxin 1997). Prior to reservoir closure, observations on the Missouri River downstream from Fort Peck Dam in Montana indicated that bank erosion increased sharply with discharges greater than about 18,000 ft^3/s, which was equaled or exceeded about 12% of the time before dam closure (U.S. Army Corps of Engineers 1952, p. 37, in Williams and Wolman 1984).

Many investigators have noted relationships between migration rate and the average bend radius of curvature, R_c. Most notable among these are relationships between the maximum erosion rate along a given bend axis and the average radius of curvature for the bend (Hickin and Nanson, 1975; Nanson and Hickin, 1983). Similar relations have been reported for the River Dane (Hooke, 1987), the Red River (Biedenharn *et al*. 1989), and the Sacramento River (Fischer, 1994), amongst others. Data from different reaches are normalized by dividing R_c by the average channel width, W. These data sets show a nonlinear relationship with most rapid bend migration for values of R_c/W between 2 and 3, and less rapid rates for higher or lower values of R_c/W. For example, Nanson and Hickin (1983) fit data from the Beatton River, British Columbia, to the relations:

$$v = 6.6\ W/R_c \text{ for } R_c/W \geq 3.125 \quad (3)$$

$$v = 0.7\ R_c/W \text{ for } R_c/W < 3.125, \quad (4)$$

where v is the migration rate in ft/yr .

A physical explanation for the shape of this relationship has been proposed by Begin (1986). Additional work has been done examining relationships between migration rate and sinuosity of meandering river reaches. Cherry *et al*. (1996) reported no relationship between sinuosity and median erosion rate, while Hooke and Redmond (1992) found that the most unstable reaches in two Welsh rivers had the highest sinuosity (1.4-2.0). Earlier analysis of data from an English river showed maximum rates of migration at sinuosities between about 1.1 and 1.4 (Hooke 1987).

Migration rates are further governed by the nature of boundary materials (Fischer 1994) and vegetation (Odgaard 1987). Families of curves relating migration rate to R_c/W for various values of boundary resistance to erosion have been proposed by Hickin and Nanson (1984). Thorne (1992) drew a bank-material-based family of curves for maximum bend scour depth as a function of R_c/W using data from the Red River. Conflicting reports are found in the literature about the effects of various types of vegetation on the width and depth of natural stream channels. Several authors attest to the value of vegetation and root systems in protecting streambanks from erosion, and note that banks without woody vegetation retreat faster than wooded banks (Odgaard 1987, Beeson and Doyle 1995), while others report that vegetation has no effect on channel migration (Nanson and Hickin 1986), or that grass banks erode more slowly than those with trees (e.g., Hooke 1995). These differences may, in part, reflect the differences in stream size and bank height.

It is important to note that even when the general nature of boundary materials and meander form are taken into account, much scatter remains in observed values of

average migration rate. Furthermore, there appears to be no relationship between point values of migration rate and corresponding point values of bend radius divided by width (Cherry *et al*. 1996). Since channel migration is episodic, migration rates measured over shorter time periods (20-30 yr) exhibit greater scatter than those over 100-200 years (Cherry *et al*. 1996) , particularly for streams with banks that experience mass wasting (Beatty, 1984).

Flow-Field Models

In an effort to obtain more physically-based results, several workers have formulated mathematical models of the flow field in meander bends for predicting meander migration. A review is provided by Mosselman (1995). Meander flow models necessarily involve simplifying assumptions and most require input of a parameter describing the erodibility of the banks (Odgaard, 1987; Hasegawa, 1989). In the models the local bank migration rate is given by the product of this parameter, termed the erosion coefficient, and the local excess velocity (the difference between the near bank velocity and the cross-section mean velocity).

$$v = e * (u_b - u) \qquad (5)$$

where e = the erosion coefficient;
u_b = the near-bank depth averaged mean velocity; and
u = is the reach-averaged mean velocity.

Howard (1992) suggested that the erosion rate include a term for near-bank depth as well as near bank velocity.

The erosion coefficient reflects many factors, but varies with grain size as does critical velocity or shear stress in a Hjulstrom- or Shields-type relation (Hasegawa 1989). Hasegawa suggested that the erosion coefficient is inversely proportional to the number of blows in a standard penetration test with separate relationships evident for sandy or clay banks. The mathematical meander migration models (e.g., Ikeda *et al*. 1981; Johannesson and Parker, 1985) typically contain one-dimensional (streamwise) schemes with implicit representation of the cross-stream variations in flow or vertically averaged two-dimensional representations of the flow field. Major shortcomings of the meander migration models include the inability to predict outward bend growth (although simulation of downstream migration is good) (Garcia *et al*. 1994), reliance on a constant bank erosion coefficient even though bank erodibility may be highly variable in space, assumption of constant discharge and width (Cherry *et al*. 1996), and numerical instability for channels with high width-depth ratios. In addition, these models do not consider mass wasting or piping bank failure.

RESERVOR EFFECTS ON MIGRATION RATES: APPLICATION

Despite the quantity of work done on river response to upstream reservoirs (Richards 1982; Williams and Wolman 1984; and Ligon *et al*. 1995), relatively little work has been done on the effect of dam closure on lateral migration rates. Studies by the U.S. Army Corps of Engineers of bank erosion below the six dams on the main stem of the Missouri River using aerial photography concluded bank erosion rates were lower downstream of Garrison and Fort Randall dams than before dam construction (Patrick *et al.* 1982). Deposition (accretion) patterns were changed also, with accretion now occurring somewhat randomly along the channel rather than by point bar migration, as was the case before the dams.

Two studies of rivers in the north central United States indicate that lateral migration rates were reduced by about 75% following dam closure. Johnson (1992) examined the effects of Garrison Dam on migration rates of the Missouri River in central North Dakota between the dam and the downstream reservoir (Oahe). Between 1881 and 1945 (before dam closure), the mean erosion rate was 230 ac/yr, but only 52 ac/yr following dam closure (1969-1979). Based on the length of the study reach (103 miles), these rates are equivalent to lateral migration rates of 18 ft/yr before and 4.3 ft/yr after dam closure. However, these lateral migration rates are somewhat misleading since much of this reach has experienced net channel widening since dam closure (Williams and Wolman 1984), and thus the stated post-dam migration rate is the composite migration of both banks. Deposition rates for the same time periods were 408 ac/yr and 3.2 ac/yr, respectively.

Changes in meander rates were associated with the effects of the dam on high flows. Mean annual flood and the maximum mean-daily discharge for the 25 years following dam closure were only 30% and 19% as great, respectively, as the mean annual flood for the 25 years preceding dam closure. As described in an earlier section of the report, the timing of peak flows was shifted from the period April to July before dam closure, to February and March after closure. River meandering rates were greater in the wider portions of the flood plain than in more constricted reaches. Additional analysis of this reach was performed by Patrick *et al*. (1982) who concurred that erosion and deposition rates declined after dam closure.

Bradley and Smith (1984) found that the reach of the Milk River downstream from Fresno Dam in northern Montana experienced a reduction in migration rate from 5.7 ft/yr to 1.5 ft/yr following dam closure. Channel width decreased about 25% and the bed degraded about 4.9 feet. The dam had little effect on average discharge, but caused a 60% decrease in the magnitude of the two-year return flood and similar decreases in larger, less frequent events (Bradley and Smith 1984).

In contrast to these findings, Jiongxin (1997) reported that the braided Hanjiang River in China exhibited complex response to reservoir closure. The river experienced an initial reduction in bank erosion intensity of the same magnitude as for the U.S. rivers described above--from about 82 ft/yr during 1955-1960 to about 23 ft/yr during the 17-yr period immediately after dam construction. However, as the riverbed became coarser and less easily eroded, bank erosion rates rebounded to levels (72 to 115 ft/yr) approaching the pre-dam condition. During the period of reduced bank erosion, the river degraded its bed but, after bed coarsening, degradation ceased and widening ensued. This succession

of processes is similar to those documented by Simon (1992) along the Toutle River, Washington.

Methods of Analysis

Channel Planform

A survey of several government agencies and their archives was performed to locate maps of the study reach. In addition to the map coverages, rectified black and white aerial photographs were obtained to provide more recent coverage than the most recent complete mapping (1968-1971). Map and photo coverages selected for data extraction are listed in Table 8 and a complete tabulation of all maps and photos is found in Appendix D. Available maps and photos were organized to provide two pre-dam coverages (1890 and 1913-18) and two post-dam coverages (1968-71 and 1991). Coverage of the study reach by U.S. Geological Survey topographic maps dated 1913-18 was incomplete (Table 8). Therefore comparison of temporal changes in channel activity was limited to the reach from Fort Peck Dam to about River Mile 1642.

A small-scale map of the study reach was obtained from the National Archives, but the quality was so poor that it was used only for sinuosity measurements. References to USGS maps published in the late 1940s were found, but copies of these maps were not. USGS topographic survey maps dated 1972 but photorevised in 1989 were not used because the 1989 coverage was redundant with the 1991 photographs, which provided full coverage. However, these maps were used to register the aerial photos.

The water surface depicted on the maps or aerial photographs was assumed to be the channel. Transects running perpendicular to the channel were constructed at intervals of about 500 feet, or roughly one-half of the stream width. Transects were drawn closer together in bends than in straight reaches to capture detail. Transect endpoints were defined as their points of intersection with the water's edge. Mid-channel bars were ignored, but bars attached to the bankline were treated as part of the bank. Transect endpoint coordinates were determined using a digitizer or a CAD system calibrated to a common coordinate system for each map or photo coverage. Endpoint coordinates were transferred to a spreadsheet for analysis.

For each transect, the width was computed as the distance between endpoints. This approach did not yield any direct information about channel top width, but simply captured the information displayed on the maps and aerial photographs. The resulting widths were representative of water widths displayed on the aerial photographs, but mapping conventions used for deciding where to draw the river boundary were unknown. Coordinates for the channel centerline were determined by averaging the endpoint coordinates. Channel centerlines were used for measuring meander characteristics. The 1890-91 and 1968-71 channel centerlines were plotted on paper and the radii of curvature and belt widths measured manually. Bend lengths (distance measured along the channel) and meander half wavelengths (straight-line distance between inflection points) were computed using centerline coordinates. Bend surface area was determined by numerical integration and average width was computed for each meander as the ratio of surface area to bend length.

Table 8--Maps and aerial photographic coverages used in this study.

Survey or photography dates	Scale	Spatial domain	Source	Physical description
1874	1:253,440	Entire study reach	National Archives, U.S. Northern Boundary Commission	Black and white paper reproduction on two sheets (sheets 3 and 4 of a set of 4).
1890-1891	1:63,360	Entire study reach	Missouri River Commission	Six sheets which were reproductions of engravings printed with black ink on yellow paper
1910-1914	1:62,500	Fort Peck Dam to RM 1642	U.S. Geological Survey	Seven sheets printed from archived microfilm onto photographic paper
1968	1:24,000	RM 1642 to RM 1587	U.S. Geological Survey	11 sheets that were photocopies of color offset prints of maps published in 1969 based on 1968 aerial photos. One of the 11 was a 1950 publication based on 1947 and 1950 surveys.
1971	1:24,000	Fort Peck Dam to RM 1642; Provides coverage of entire reach when combined with 1968 maps.	U.S. Geological Survey	8 color offset prints on paper and 7 photocopies of color offset prints. These are maps published in 1972 based on 1971 aerial photos.
1989	1:24000	RM 1727 to 1707 and RM 1685 to 1587	U.S. Geological Survey	16 color offset prints on paper. These are 1972 maps photorevised based on 1989 aerial photos
1991	1:24,000	Entire study reach	National Aerial Photography Program	39 rectified paper enlargements of black and white aerial photographs

In order to assess the dynamic stability of the study reach before and after dam construction, meander form variables measured from the 1890-91 and 1968-71 coverages were compared with empirical relationships listed in Table 9 using scatter plots and computations based on means of measured values. In addition, data from the study reach were used to evaluate two formulas that have been proposed as planform predictors (Leopold and Wolman 1957; Chang 1988). These formulas are also listed in Table 9. Pre-dam conditions were evaluated using values of discharge, bed sediment size and mean bed slope of 27,000 ft^3/s, 0.2 mm and 1.8×10^{-4}, respectively, while post-dam conditions were evaluated using values of 25,000 ft^3/s, 1.7×10^{-4} and a range of bed sediment sizes between 0.3 and 1.6 mm.

Measurement of Channel Activity

Channel activity, defined here as the average rate of lateral migration along a river reach in dimensions of length per unit time, has been measured several ways by various investigators. Because of the limitations of available data, we determined channel activity by measuring the area enclosed by successive channel centerlines (MacDonald and Parker 1994). Hooke (1987) found that migration rates measured in this way were slightly smaller than those measured between banklines, but were of the same relative magnitude. The area enclosed by successive centerlines was determined by computing the area of the series of polygons defined by the intertwined, digitized centerlines. Channel activity was then computed by dividing the sum of polygon areas for a given reach by the length of the earlier of the two centerlines and the time between the two coverages.

Survey or aerial photography dates for each map were used to date coverages rather than map publication dates. It is important to note that this method of measuring channel activity does not differentiate among various types of centerline migration. For example, gradual migration due to erosion of the outside of a bend, a major avulsion like a neck cutoff and movement of the channel centerline due to attachment of a mid-channel bar to the bank are all treated in a similar fashion.

Means of channel activity for the pre-dam and post-dam periods were computed and compared. These comparisons were limited to the reaches mapped by all four coverages: from Fort Peck Dam (RM 1771) to about River Mile 1642. Simple graphical and statistical approaches (correlation and regression) were used to examine relationships between channel activity and form variables (width, radius of curvature, meander half wavelength, bend length, and valley width) for pre-impoundment and post-impoundment data sets. Two analyses were performed. The first considered relationships between average channel activity rates for each bend and planform characteristic. Since mass failure of banks is related to bank height and since bank height is increased by degradation, it might be reasonable to expect channel activity to be influenced by the magnitude of bed degradation, which in the study reach was inversely related to the channel distance downstream from the dam (Figure 1). Therefore, the distance from Fort Peck to the bend apex was also used as an independent variable in the first type of analysis. The second analysis considered relationships between channel activity and the means of planform characteristics computed for sub-reaches bounded by major tributary confluences. Sub-reach channel activity was determined by summing the area reworked

Table 9--Selected empirical formulas for inter-relationships among morphologic variables for rivers. K = meander bend length/half wavelength[1], B = meander belt width; W = width; R_c = bend radius of curvature; L_m = meander half wavelength; S = bed slope; $Q_{bankfull}$ = discharge at bankfull stage; L_b = meander bend length.

Formula	Basis	Accuracy[2]	Reference
$S > 0.06\ Q_{bankfull}^{-0.44}$	Data from ~63 rivers	Chitale (1973) found this condition held for 18 of 23 braided rivers	Leopold and Wolman (1957) in Chitale (1973)
$Sd^{0.5} \geq 0.00238(Q_{bankfull})^{-0.51}$	Repetitive solution of analytical model using different values of Q, S, and d	unknown	Chang (1988)
$K = 1.145(B/W)^{0.134}$	Data from 42 rivers	Error of estimate = 18.8%	Chitale (1973)
$R_c = L_m K^{1.5} / [13(1-K)^{0.5}]$	Random-walk model	Error of estimate ~ 20%	Langbein and Leopold (1966)
$L_m = 2.27\ R_c$	Data from up to 194 rivers and models	21-17	Williams (1986)
$L_b = 3.77\ R_c$	Data from up to 194 rivers and models	35-26	Williams (1986)
$B = 2.88\ R_c$	Data from up to 194 rivers and models	42-29	Williams (1986)
$W = 0.71\ R_c^{0.89}$	Data from up to 194 rivers and models	48-32	Williams (1986)
$L_m = 3.75\ W^{1.12}$	Data from up to 194 rivers and models	65-39	Williams (1986)
$L_b = 5.1\ W^{1.12}$	Data from up to 194 rivers and models	65-39	Williams (1986)
$B = 4.3\ W^{1.12}$	Data from up to 194 rivers and models	74-42	Williams (1986)
$R_c = 1.5\ W^{1.12}$	Data from up to 194 rivers and models	55-35	Williams (1986)

[1] Note that the reach-average value of K is equal to the sinuosity.

[2] Figures given for Williams (1986) relations are standard deviation of residuals in percent + and -.

within the sub-reach and dividing by the length of the channel centerline and the time between the two coverages.

Contributing drainage area, sinuosity and meander belt width were also used as independent variables in the latter (sub-reach means) analysis. Centerline sinuosity was computed for each sub-reach by dividing the length of the channel centerline by the length of the valley centerline.

Neck cutoffs

Individual river meanders evolve in a cyclical fashion that may include lateral extension, downvalley translation, deformation and cutoff (Hooke 1995). Rates of bend evolution are quite unsteady in time and space. Cutoffs may be chute cutoffs or neck cutoffs. Patterns of channel migration and meander development leading to neck cutoffs have been described by Fisk (1947) and Carson (1986), among others. Neck cutoffs generally occur when meanders elongate to the point that the reduced slope through the bend promotes deposition in the upstream limb, thus diverting higher flows across the neck of the meander. Meander necks gradually become narrower due to differential rates of erosion in upstream and downstream bends (Vanoni 1975).

In order to define morphologic conditions conducive to the occurrence of neck cutoffs within the study reach, historic records of three neck cutoffs were examined (Weismann 1990a; 1990b; 1993). Meander form variables measured from the coverage prior to cutoff were tabulated for each of the three cases. In particular, the ratio of bend radius of curvature to width, the ratio of the bend length to the distance across the narrowest part of the meander neck, bend radius of curvature and channel activity measured prior to cutoff were tabulated for each of the three bends. For neck cutoff analysis, bend length was defined as the distance between points on opposite sides of the narrowest part of the meander neck, measured along the channel. Elsewhere in this study, the bend length is measured between bend inflection points.

Elongated meander bends susceptible to neck cutoff were identified based on visual review of current 1:100,000 scale U.S. Geological Survey Topographic maps. Values of the aforementioned form variables measured from recent coverages were tabulated for each of these bends and compared to the range of values from the three bends that had cut off.

Gross Channel Planform

Gross channel planform varied little over the 117-year period of observation (Tables 10 and 11). Differences in sinuosity between 1874 and 1890-91 appear related to the elongation of four bends between the two coverages and also to the finer detail depicted on the latter, larger-scale maps. The average width of the water surface depicted on the three complete coverages (1890s, 1968-71, and 1991) varied less than 2% for the entire study reach (Table 10). The channel depicted on the 1910-1914 maps was about 20% wider than for the other coverages (Table 11). This difference is likely due to differences in mapping conventions rather than morphologic differences. Changes in channel length, water surface area and centerline sinuosity reflect a neck cutoff that occurred between River Mile 1604 and River Mile 1599 ca. 1980 (Weismann, 1993),

Table 10--Properties of Missouri River channel between Fort Peck Dam and the North Dakota state line.

	1874	1890-91	1968-71	1991
Number of transects drawn		1383	1305	1951
Average distance between transects, ft		677	464	479
Mean water width, ft		1,019	1,005	1,012
Total length of centerline, mi	175	177	181	177
Total area of water surface, acres		21,889	22,068	21,703
Centerline sinuosity	1.41	1.43	1.47	1.43

Table 11-- Properties of Missouri River channel between Fort Peck Dam and Brockton, Montana (RM 1642).

	1874	1890-91	1910-14	1968-71	1991
Number of transects drawn		1010	1297	1305	1340
Average distance between transects, ft		656	512	517	501
Mean water width, ft		1,075	1,261	995	1,023
Total length of centerline, mi	122	125	125	128	127
Total area of water surface, acres		16,342	19,121	15,389	15,745
Centerline sinuosity	1.43	1.47	1.46	1.49	1.48

shortening the channel about four miles and returning these geometric properties to values similar to those observed in 1890-91.

Planform Geometry Relations

The planform prediction formula of Leopold and Wolman (1957) indicated that the study reach should have a meandering planform for both pre- and post-dam conditions (Tables 12 and 13). This prediction holds for values of discharge up to 500,000 ft^3/s. The Chang (1988) formula predicts the study reach will be braided. However, the reach plots very near the boundary between regions labeled "straight braided streams," and, "braided point-bar and wide-bend point-bar streams," in the diagram published by Chang (1988) based on his formulas.

Observed sinuosity values were slightly greater than those predicted by the formula of Chitale (1973), while observed mean values of bend radius were more than three times greater than those predicted by the formula of Langbein and Leopold (1966) (Tables 12 and 13).

Meander form variables measured from the first (pre-dam) and third (post-dam) coverages are plotted against width and bend radius in Figures 29 and 30 with lines representing values predicted by the Williams (1986) regression formulas listed in Table 9. In general, the regression formulas are very poor fits to the measured data, but do appear to pass through the centroid of the data scatter. It is important to note that the formulas were derived using mean or median values from a large number of river reaches and physical models. Mean values of measured form variables were compared with values predicted by the Williams formulas. For the pre-dam coverage of the study reach, predictions are best for mean meander half wavelength and bend length as a function of width, with much greater error in formulas involving bend radius (Table 14). Predictions based on means of the post-dam data were considerably less accurate than for the pre-dam 1890-91 data (Table 15); however, formulas based on width were within the range of accuracy published by Williams (1986) (Table 9). In general, the means of measured values of bend radius were about twice as large as those predicted by empirical formulas (Tables 12-15).

Comparison of Pre- and Post-Dam Channel Activity

Channel activity rates were considerably higher prior to dam closure than afterward (Figure 31 and Table 16). In the reach between Fort Peck and Brockton about 11,400 acres of flood plain were enclosed by the 1890-91 and 1910-14 centerlines. This figure includes areas affected by five channel avulsions that may not have been eroded by the river channel, but probably is a good estimate of the total area of flood plain reworked by the river. Only about 1,700 acres were enclosed by centerlines for the same reach derived from the two post-dam coverages. The mean rate of pre-dam channel activity between Fort Peck and River Mile 1642 was 32.5 ft/yr, while the mean post-dam rate for the same reach between 1971 and 1991 was 5.7 ft/yr. The rate of activity for the entire reach (Fort Peck to the North Dakota Stateline) was 7.7 ft/yr. If the area affected by the 1980 cutoff near River Mile 1600 is excluded from the post-dam calculations, the mean activity rate is only 6.1 ft/yr.

Table 12--Comparison of planforms observed using 1890-91 maps of the study reach and predictions from published formulas.

Variable	Relationship (Table 2)	Observed	Predicted	Percent error
Planform	Leopold and Wolman (1957) in Chitale (1973)	Meandering with numerous mid-channel bars	Meandering	N/A
Planform	Chang (1988)	Meandering with numerous mid-channel bars	Braided point-bar	N/A
Sinuosity	Chitale (1973)	1.71	1.54	-10%
Bend radius of curvature in feet	Langbein and Leopold (1966)	6,515	1,808	-72%

Table 13--Comparison of planforms observed using 1968 and 1971 maps of the study reach and predictions from published formulas.

Variable	Relationship	Observed	Predicted	Percent error
Planform	Leopold and Wolman (1957) in Chitale (1973)	Meandering with numerous mid-channel bars	Meandering	N/A
Planform	Chang (1988)	Meandering with numerous mid-channel bars	Braided point-bar	N/A
Sinuosity	Chitale (1973)	1.66	1.56	-6%
Bend radius of curvature in feet	Langbein and Leopold (1966)	5,223	1,569	-70%

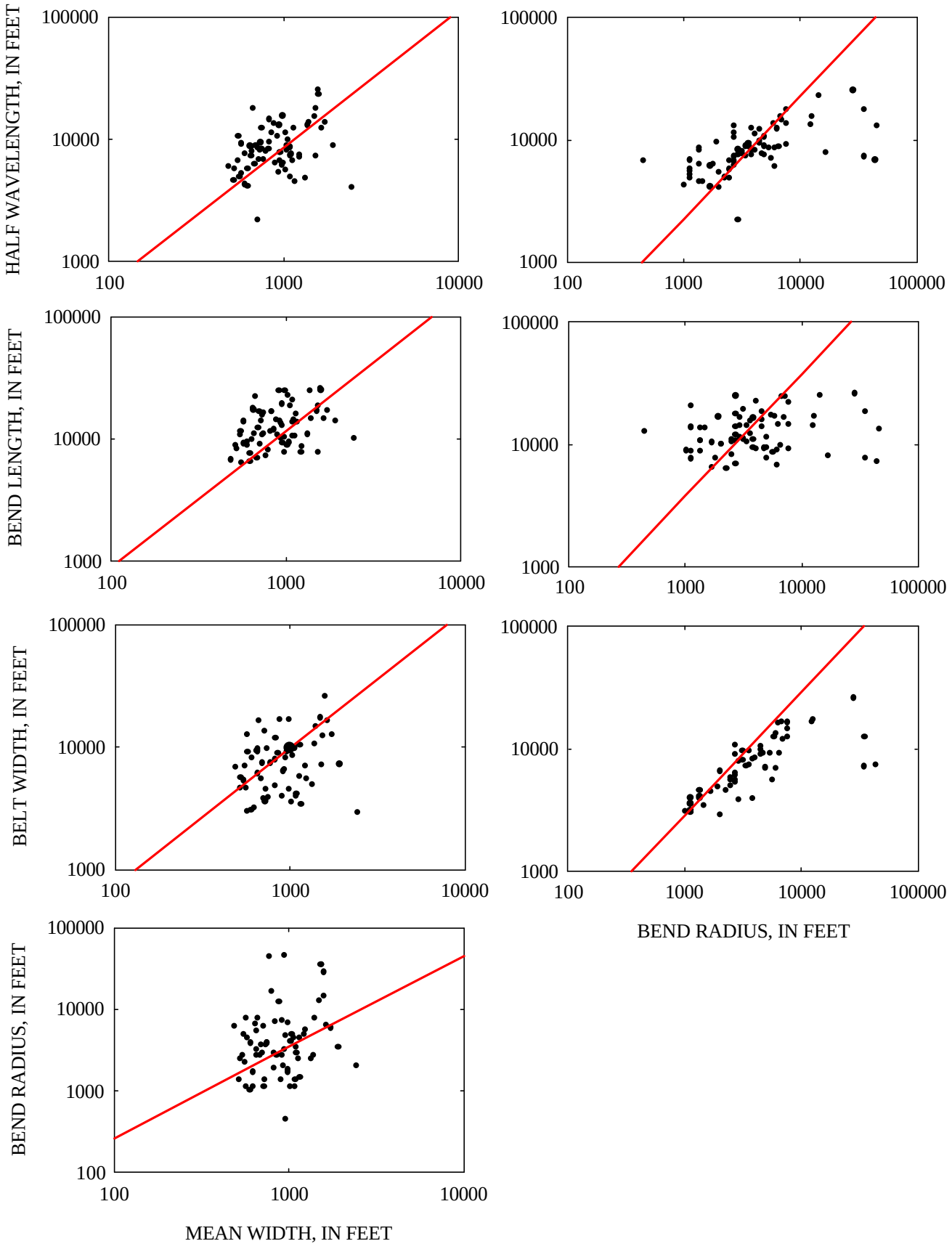

Figure 29-- Relationships among selected meander form variables (Pre dam (1890-91) conditions) and empirical formulas derived using data from other rivers (Williams 1986).

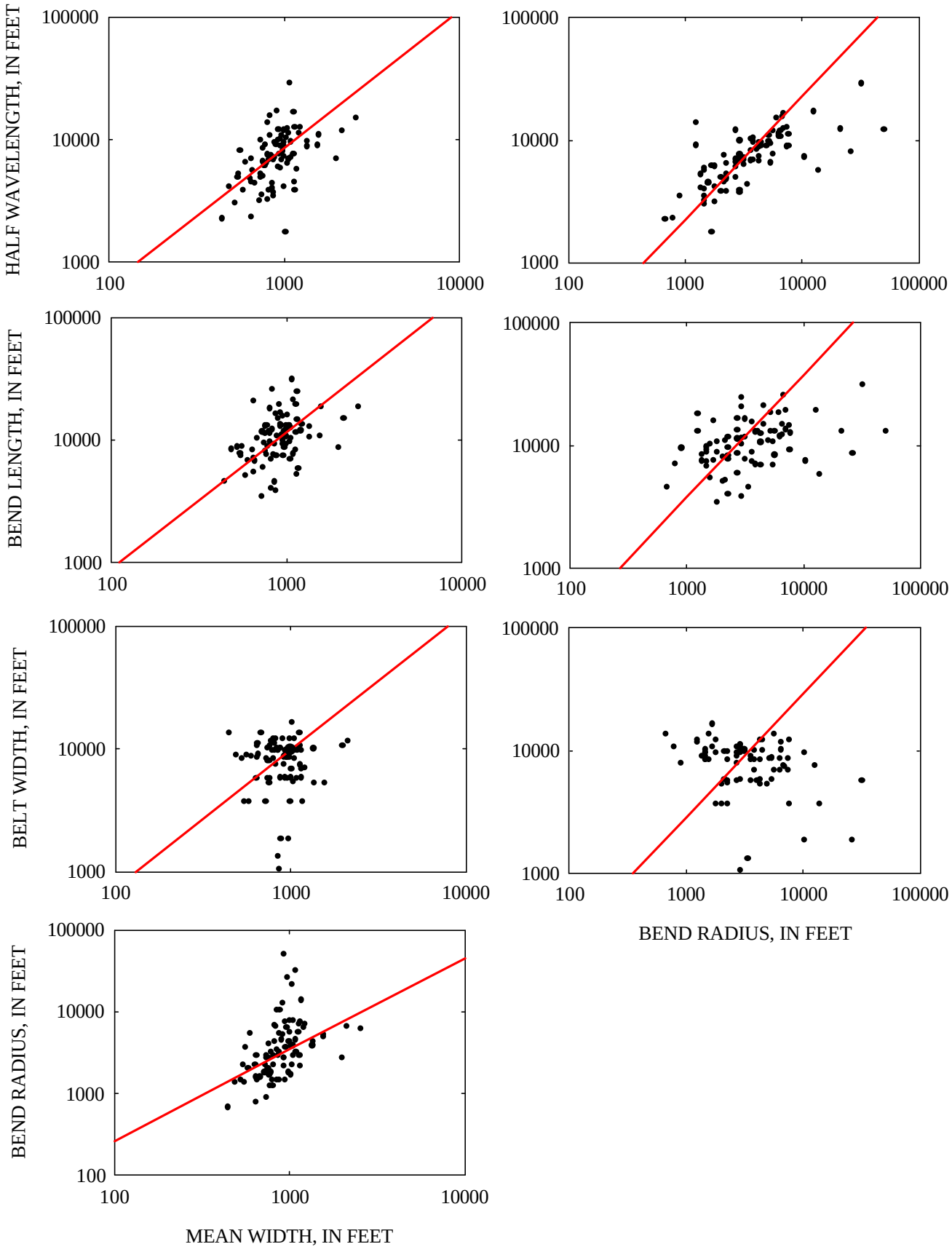

Figure 30-- Relationships among selected meander form variables (Post dam (1991) conditions) and empirical formulas derived using data from other rivers (Williams 1986).

Table 14--Comparison of form variables measured from 1890-91 maps of the study reach and values predicted using Williams (1986) formulas in Table 9.

Variable	Observed mean, ft	Predicted as a function of width, ft	Percent error	Predicted as a function of bend radius, ft	Percent error
W	961			1,763	83%
L_m	9,030	8,219	-9%	14,780	64%
L_b	13,247	11,178	-16%	24,600	84%
B	8,168	9,425	15%	18,793	130%
R_c	6,525	3,288	-50%		

Table 15--Comparison of form variables measured from 1968 and 1971 maps of the study reach and values predicted using Williams (1986) formulas in Table 9.

Variable	Observed mean, ft	Predicted as a function of width, ft	Percent error	Predicted as a function of bend radius, ft	Percent error
W	946			2,179	130%
L_m	5,234	8,069	54%	18,752	258%
L_b	7,910	10,974	39%	31,212	295%
B	11,244	9,253	-18%	23,844	112%
R_c	8,279	3,228	-61%		

Table 16--Mean rates of channel activity, Missouri River downstream of Fort Peck Dam.

Reach	Ft. Peck to Brockton		Ft. Peck to State line
Period	Pre dam	Post dam	Post dam
Area worked, acres	11,431	1,736	3,367
Length of channel, mi	126.3	125.1	181.0
Mean channel centerline migration distance, ft	746.6	114.5	153.5
Mean rate of channel activity, ft/yr	32.5	5.7	7.7
Maximum rate of channel activity for a single bend, ft/yr	93.1	37.7	74.1

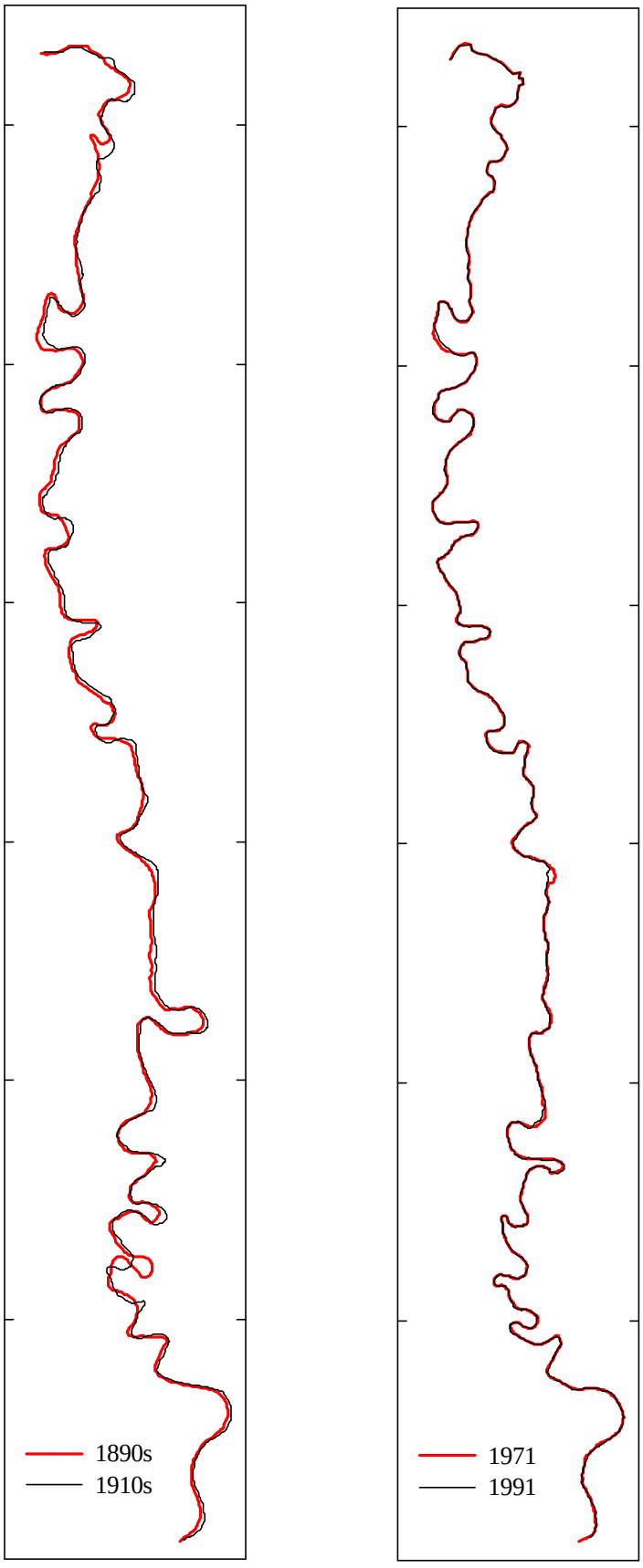

Figure 31-- Successive centerlines of Missouri River downstream from Fort Peck Dam, Montana before and after dam closure. Maps are arranged so that the north direction is horizontal to the right. Tick interval on vertical axes = 16 miles.

Predictors of Future Activity: Bend-Average Values

Forty-eight bends were defined using centerlines developed from the first two coverages, which were limited to the reach from Fort Peck to Brockton (Table 17). Eighty-five bends were defined using the third and fourth (post-dam) coverages, which extended from Fort Peck to the State line (Table 18). During both the pre-dam and post-dam periods, bend-average channel activity was roughly associated with the bend R_c/W in a fashion similar to that described by Nanson and Hickin (1983), Hooke (1987) and others (Figure 32). Considerable scatter is present, but the envelope of maximum values follows the curve proposed by Nanson and Hickin (1983) based on their study of Canadian Rivers if the functions describing the curve (Equations 3 and 4 above) are multiplied by 50 and 30 for pre-dam and post-dam data sets, respectively. Highest levels of channel activity were observed for bends with values of R_c/W between 0.8 and 5.2 (pre dam) and between 1.7 and 3.1 (post-dam).

Bend-average channel activity was slightly correlated with meander wavelength and meander length prior to dam closure but with no other independent variables (Table 19). Bend average channel activity was slightly correlated with width in the post-dam data set (Figure 33). If two outlying points representing bends that experienced high rates of channel activity due to large avulsions are excluded, the correlation between post-dam channel activity and width improves (Figure 33 and footnote following Table 19). Post-dam channel activity also appeared to increase slightly with bend length and with distance downstream from the dam (computed by subtracting the average 1960 River Mile for each bend from the River Mile location of the dam (1771.55)).

The following relationship was derived for post-dam bend-average channel activity using multiple regression (n = 85, $r^2 = 0.14$, standard error of estimate = 7.6):

$$v_{bend} = -4.186 + 0.00771\ W + 0.0366 * Dist \qquad (6)$$

where v_{bend} = average channel activity for a given bend in ft/yr;
W = mean width for the bend in feet; and
Dist = distance along the channel centerline from Fort Peck Dam to the bend apex, in miles.

Predictors of Future Activity: Sub-reach-Average Values

Pre-dam centerlines were divided into five sub-reaches corresponding to segments bordered by major tributary mouths, while six sub-reaches were defined for the post-dam coverage (Tables 20 and 21). Sub-reach channel activity was correlated with the average value of bend radius of curvature divided by width prior to dam closure, and with downchannel distance and sub-reach sinuosity afterward (Table 22). Channel activity was inversely related to sinuosity (n = 6, $r^2 = 0.57$, standard error of the estimate = 1.7):

$$v_{reach} = 24.70 - 12.56\ K \qquad (7)$$

Table 17--Channel activity by bend based on areas enclosed by 1890-91 and 1910-1914 centerlines. Meander geometry based on 1890-91 coverage.

Bend	UTM Easting m	1890 River Mile	Valley width, ft	Half wavelength, ft	Bend length, ft	Width, ft	Rc, ft	Channel activity, ft/yr
1	395,642	1950.6	13,093	22,186	24,520	915	7,216	27.1
2	396,750	1946.0	11,324	7,377	10,484	1,091	3,383	49.6
3	399,048	1944.0	11,934	8,295	11,041	747	3,834	16.0
4	400,803	1941.9	13,746	4,130	6,539	623	1,691	93.1
5	402,395	1940.6	11,571	6,725	12,827	952	451	35.7
6	404,489	1938.2	14,931	7,286	7,752	1,532	35,178	36.9
7	409,376	1936.7	13,818	25,280	25,934	1,581	28,413	21.2
8	414,237	1931.8	10,261	8,856	14,135	1,921	3,383	18.8
9	415,957	1929.2	10,647	6,823	14,059	721	1,128	29.3
10	417,708	1926.5	10,999	8,890	12,293	694	3,608	55.2
11	420,186	1924.2	15,457	9,384	15,581	737	3,608	25.9
12	422,679	1921.2	14,232	7,277	17,819	651	2,706	7.8
13	425,003	1917.8	14,050	8,312	11,507	820	2,932	23.2
14	427,417	1915.7	16,755	8,791	9,854	642	6,540	38.0
15	429,452	1913.8	18,813	6,029	6,736	486	6,089	49.3
16	431,444	1912.5	18,387	7,558	9,500	603	3,834	35.1
17	433,987	1910.7	19,159	9,345	13,925	574	4,510	45.1
18	436,016	1908.1	21,177	4,929	6,392	560	2,255	29.3
19	437,912	1906.9	20,662	9,136	9,144	570	7,667	42.3
20	440,293	1905.1	20,868	8,151	9,164	1,038	4,059	34.6
22	442,046	1903.4	20,350	4,537	13,609	1,159	1,466	38.4
23	445,252	1900.8	21,150	17,718	21,993	666	7,667	34.7
24	449,005	1896.7	18,137	7,993	11,101	656	3,157	30.6
25	450,812	1894.6	16,672	5,228	13,685	571	1,128	24.0
26	454,863	1892.0	20,062	23,126	25,010	1,583	14,432	35.0
27	459,589	1887.2	20,675	8,580	13,583	1,089	1,353	20.4
28	463,053	1884.7	18,725	15,381	16,830	1,499	12,628	42.8
29	467,939	1881.5	15,432	17,800	18,491	1,524	34,953	46.3
30	472,296	1878.0	15,974	13,623	16,954	1,732	5,863	38.3
31	475,000	1874.8	17,577	7,725	19,270	946	3,157	27.6
32	477,733	1871.1	22,283	13,001	24,914	1,377	2,706	18.2

Table continues on next page.

Table 17--(concluded). Channel activity by bend based on areas enclosed by 1890-91 and 1910-1914 centerlines. Meander geometry based on 1890-91 coverage.

Bend	UTM Easting m	1890 River Mile	Valley width, ft	Half wavelength, ft	Bend length, ft	Width, ft	Rc, ft	Channel activity, ft/yr
33	481,240	1866.4	23,407	12,293	14,576	1,639	6,314	32.5
34	484,564	1863.6	28,067	9,811	18,623	1,060	4,510	12.0
35	486,999	1860.1	25,893	6,350	7,738	984	1,804	58.5
36	489,078	1858.6	23,795	7,538	14,205	1,105	2,932	9.3
37	490,802	1855.9	21,902	4,076	10,118	2,437	2,030	56.3
38	493,046	1854.0	20,928	11,233	22,618	1,022	4,059	23.9
39	495,029	1849.7	22,449	2,198	16,621	705	2,932	61.1
40	495,849	1846.6	24,628	6,738	10,535	1,126	2,481	64.7
41	497,088	1844.6	24,628	6,232	6,970	683	2,706	32.4
42	498,925	1843.3	26,279	7,745	9,315	956	4,736	45.8
43	500,731	1841.5	20,568	6,367	10,760	895	1,353	20.2
44	502,201	1839.5	19,787	5,576	8,848	1,018	1,128	39.3
45	504,262	1837.8	16,993	12,275	15,885	1,142	4,510	20.3
46	507,866	1834.8	10,137	15,502	24,587	987	6,765	31.2
47	512,127	1830.1	14,289	13,360	14,325	879	12,403	19.6
48	516,258	1827.4	9,980	14,513	16,557	829	6,991	40.1

Table 18--Channel activity by bend based on areas enclosed by 1968-1971 and 1991 channel centerlines. Meander geometry based on 1968-1971 coverage.

Bend	Easting m	1960 RM	Distance below dam, mi	Valley width ft	L_m ft	L_b ft	Width ft	R_c ft	Channel activity ft/yr
1	394900	1769.80	1.75	13,093	15,140	18,491	2,556	6,096	4.34
2	396583	1766.29	5.26	11,324	10,936	18,568	1,569	5,193	2.20
3	399512	1763.30	8.25	12,522	8,480	12,969	758	4,064	3.19
4	401808	1761.37	10.18	13,818	6,839	7,438	957	3,612	4.63
5	403549	1759.88	11.67	12,028	4,816	8,293	639	2,258	1.92
6	404976	1758.53	13.02	16,518	4,936	4,934	736	2,709	4.01
7	410027	1755.03	16.52	13,818	28,825	31,092	1,076	32,059	2.37
8	414,799	1750.82	20.73	10,838	6,020	13,338	925	2,709	3.97
9	415,851	1748.62	22.93	11,099	5,907	9,875	944	1,467	4.77
10	417,720	1746.28	25.27	10,999	11,898	14,877	2,119	6,547	26.54
11	420,320	1743.63	27.92	15,457	9,084	13,138	773	1,242	1.44
12	422,734	1740.41	31.14	14,232	7,021	20,829	648	2,935	3.98
13	424,874	1737.36	34.19	14,042	7,531	11,389	806	2,935	3.17
14	427,437	1735.08	36.47	16,755	11,233	12,673	1,051	7,676	1.64
15	429,903	1733.23	38.32	18,813	6,798	6,903	817	4,290	1.60
16	431,984	1731.16	40.39	18,387	9,006	14,899	899	4,515	1.43
17	433,690	1728.73	42.82	18,214	4,166	10,749	991	1,806	3.72
18	436,345	1726.01	45.54	21,752	13,834	17,988	802	1,242	2.58
19	439,452	1723.59	47.96	22,016	7,410	7,390	843	10,385	2.44
20	441,134	1722.03	49.52	20,350	6,130	8,890	781	1,806	4.01
21	442,370	1720.31	51.24	20,350	4,006	9,221	849	1,467	2.62
22	443,928	1718.46	53.09	19,774	6,881	10,299	1,054	2,935	3.07
23	446,224	1716.34	55.21	21,802	10,755	12,163	830	6,547	2.78
24	449,033	1714.10	57.45	18,137	9,901	11,518	735	2,935	5.65
25	451,182	1711.45	60.10	16,672	6,859	16,422	871	3,161	5.94
26	452,220	1709.19	62.36	18,893	3,474	7,454	869	1,467	4.91
27	453,660	1707.76	63.79	16,462	7,188	7,672	1,090	3,161	2.65
28	455,418	1706.54	65.01	18,607	4,541	5,205	1,146	2,145	3.24
29	456,671	1705.66	65.89	18,607	3,844	4,039	810	2,258	4.10
30	457,861	1704.76	66.79	18,765	4,503	5,473	644	1,580	3.32
31	459,918	1702.77	68.78	20,668	10,176	15,497	949	3,612	5.48
32	462,422	1700.30	71.25	20,684	7,341	10,677	990	4,290	37.70
33	464,041	1698.92	72.63	18,725	3,719	3,471	864	2,935	12.39
34	465,262	1698.12	73.43	16,220	4,392	4,548	849	3,386	2.43
35	467,136	1696.88	74.67	15,611	8,043	8,598	972	26,189	1.77
36	469,445	1695.36	76.19	16,488	7,156	7,445	880	10,385	2.02
37	471,884	1693.78	77.77	15,974	8,900	9,186	995	7,676	6.74
38	474,559	1691.92	79.63	17,577	8,786	10,454	1,352	4,290	12.23
39	476,658	1690.29	81.26	21,643	5,647	6,748	655	1,467	3.77
40	479,199	1688.41	83.14	20,580	12,085	13,177	934	50,333	4.39

Table continues on following page.

Table 18--(concluded). Channel activity by bend based on areas enclosed by 1968-1971 and 1991 channel centerlines. Meander geometry based on 1968-1971 coverage.

Bend	Easting m	1960 RM	Distance below dam, mi	Valley width ft	L_m ft	L_b ft	Width ft	R_c ft	Channel activity ft/yr
41	482,301	1685.95	85.60	24,691	9,697	12,789	1,351	3,838	27.92
42	485,026	1682.73	88.82	28,067	9,588	21,222	1,083	4,515	5.74
43	486,689	1679.21	92.34	25,893	1,779	15,885	1,015	1,693	11.66
44	488,526	1676.58	94.97	23,795	11,284	11,903	1,205	6,321	4.79
45	490,978	1674.38	97.17	21,902	6,608	11,327	754	2,709	3.77
46	492,338	1672.41	99.14	20,928	3,520	9,507	739	903	3.57
47	493,614	1670.86	100.69	20,928	6,540	6,116	597	5,418	3.26
48	495,325	1669.10	102.45	22,449	6,355	11,634	789	3,161	2.46
49	496,691	1667.09	104.46	24,628	3,233	9,588	800	1,467	3.09
50	498,033	1665.52	106.03	26,279	6,931	7,019	1,049	3,838	7.51
51	499,695	1663.75	107.80	21,796	5,283	11,631	728	2,258	6.21
52	500,871	1661.82	109.73	20,568	3,033	8,762	525	1,467	5.54
53	501,437	1660.16	111.39	20,568	8,176	8,855	560	3,612	2.99
54	502,166	1658.52	113.03	19,787	4,120	8,391	487	1,355	1.50
55	504,201	1656.15	115.40	16,993	12,053	16,706	925	2,709	5.02
56	507,912	1652.11	119.44	10,137	15,584	25,876	825	6,773	4.99
57	512,721	1647.83	123.72	12,212	17,060	19,337	911	12,643	6.32
58	516,709	1644.98	126.57	16,279	9,414	10,768	877	5,418	8.45
59	519,554	1642.79	128.76	18,731	9,555	12,401	1,000	4,290	2.88
60	522,309	1640.58	130.97	16,814	8,982	10,865	1,552	4,967	12.03
61	524,366	1638.79	132.76	18,226	4,993	8,093	754	2,032	3.71
62	525,917	1637.47	134.08	16,515	5,700	5,627	1,167	13,772	4.91
63	527,297	1636.18	135.37	16,178	4,922	7,746	543	2,258	4.38
64	528,124	1634.96	136.59	13,263	3,840	5,156	581	2,032	11.38
65	528,697	1634.15	137.40	13,263	3,160	3,428	721	1,806	15.11
66	529,341	1633.39	138.16	13,228	2,270	4,584	444	677	6.48
67	530,183	1632.16	139.39	14,542	7,664	8,346	1,123	5,644	6.25
68	531,315	1630.40	141.15	10,171	4,454	10,338	679	1,580	1.81
69	533,856	1628.04	143.51	11,077	12,681	14,564	1,148	7,450	6.36
70	536,748	1625.75	145.80	8,335	6,452	9,598	1,034	2,258	5.10
71	539,179	1623.61	147.94	6,707	9,829	12,965	916	5,193	3.86
72	541,470	1621.52	150.03	6,424	8,857	9,184	947	7,450	4.49
73	544,008	1619.42	152.13	6,211	12,343	12,968	1,036	21,222	3.79
74	546,927	1617.07	154.48	7,397	10,798	11,870	965	6,321	6.24
75	549,647	1614.71	156.84	8,202	10,386	12,995	1,021	3,838	3.57
76	552,907	1612.24	159.31	6,105	11,922	13,103	997	5,644	2.54
77	557,201	1609.17	162.38	6,876	16,636	19,324	1,131	6,999	5.85
78	560,311	1605.00	166.55	15,978	3,906	24,647	1,148	2,935	58.09
79	562,002	1601.64	169.91	16,894	7,571	10,899	930	2,145	5.26
80	564,188	1599.51	172.04	12,739	7,634	11,545	1,131	2,935	8.61
81	566,168	1597.60	173.95	10,441	6,982	8,625	1,982	2,709	13.65
82	567,277	1596.12	175.43	10,574	2,335	7,068	645	790	11.25
83	567,294	1594.73	176.82	10,338	6,181	7,556	766	1,693	5.92
84	567,792	1593.31	178.24	10,439	5,245	7,482	548	1,355	1.88
85	570,350	1591.32	180.23	10,456	12,562	13,480	1,223	6,999	11.63

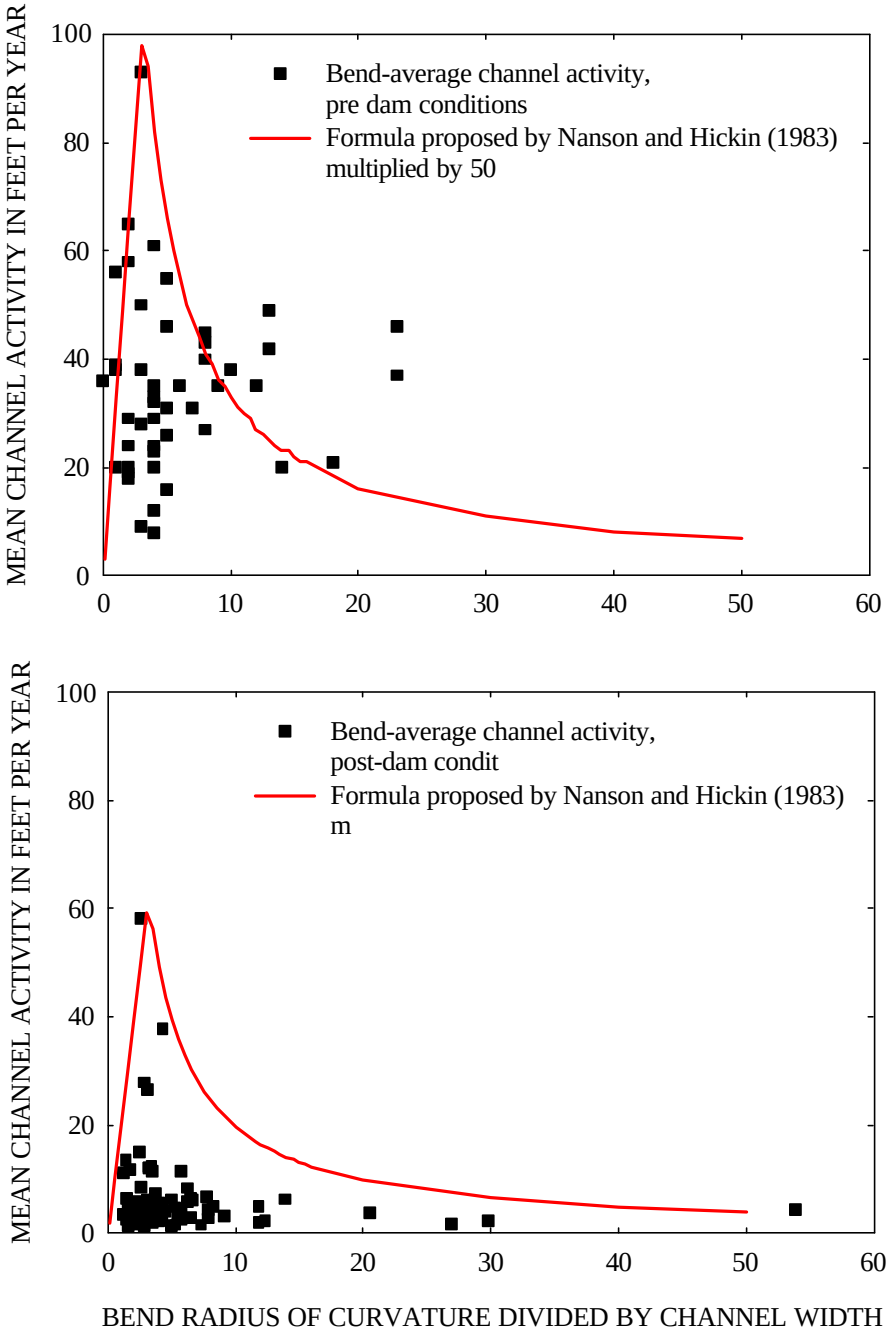

Figure 32-- Bend-average channel activity versus bend radius of curvature divided by bend-average width.

Table 19--Correlation of bend-average channel activity with geometric variables. Table entries are values of coefficients of determination r^2 (p= probability of a value of r^2 this large arising by chance).

Variable	**Pre-impoundment (n = 47)**	**Post-impoundment (n = 85)**
Width	**	0.09 (0.006)*
Meander half wavelength	0.07 (0.09)	**
Length of bend	0.16 (0.006)	0.04 (0.08)
Distance below Fort Peck along channel centerline	**	0.04 (0.07)

*$r^2 = 0.18$, $p < 0.0001$ when two outliers representing bends with extremely high values of activity due to large avulsions are excluded from regression.

** Indicate p values were > 0.10.

a) ALL DATA. ACTIVITY = -0.255 + 0.0071 WIDTH. $r^2 = 0.086$

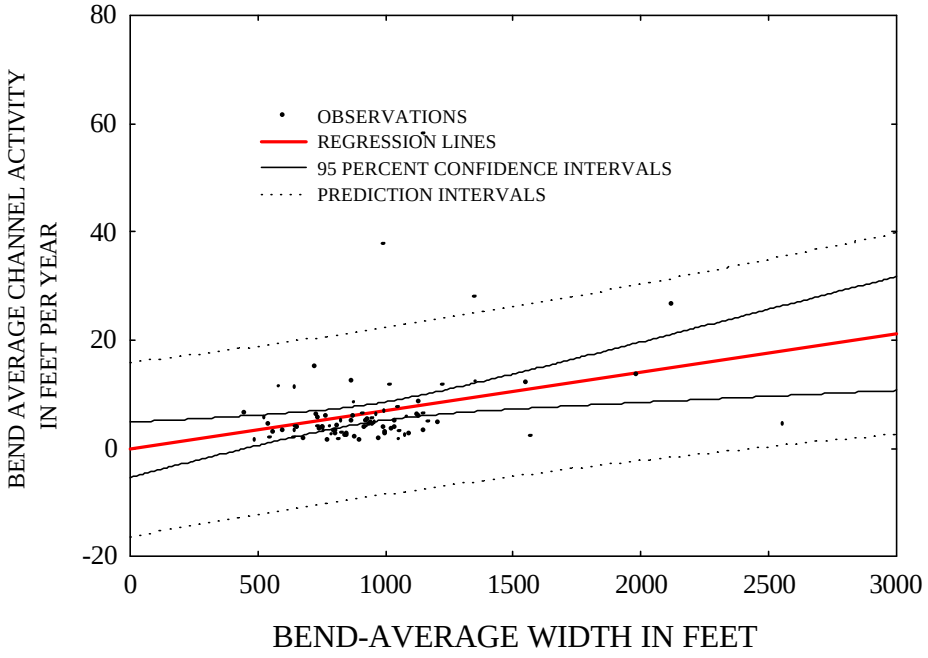

b) OMITTING TWO OUTLYING POINTS REPRESENTING LARGE AVULSIONS.
ACTIVITY = -0.0233 + 0.0059 WIDTH. $r^2 = 0.181$

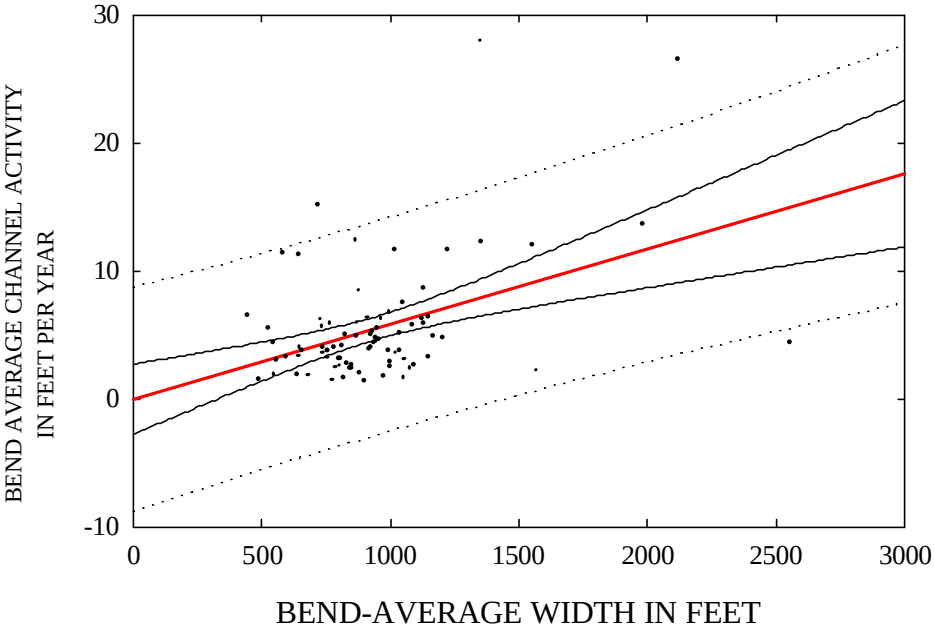

Figure 33-- Post dam channel activity as a function of width.

Table 20--Pre-dam sub-reach means.

Reach	No. of bends in reach	Valley width ft	Drainage area mi^2	Half wavelength ft	Bend length ft	Meander belt width ft	Width ft	Bend radius of curvature ft	Sinuosity	Channel activity ft/yr
Ft. Peck to Milk R.	5	12,333	57,725	9,742	13,082		893	3,315	1.39	37.1
Milk R. to Little Porcupine Creek	5	12,131	81,610	11,427	14,835	11,289	1,331	14,342	1.42	29.5
Little Porcupine Creek to Wolf Creek	14	18,276	82,069	8,171	12,143	8,211	704	4,115	1.59	31.3
Wolf Creek to Poplar River	9	20,245	83,175	13,482	18,695	10,739	1,387	9,546	1.50	30.1
Poplar River to Big Muddy River	14	20,161	89,000	8,550	13,506	8,199	1,035	4,059	1.62	35.2

Table 21--Post-dam sub-reach means.

Reach	No. of bends in reach	Valley width ft	Drainage area mi^2	Half wavelength ft	Bend length ft	Meander belt width ft	Distance below dam mi	Width ft	Bend radius of curvature ft	Sinuosity	Channel activity ft/yr
Ft. Peck to Milk River	3	12,313	57,725	11,518	16,676	5,703	11.1	1,723	5,117	1.52	3.3
Milk River to Little Porcupine Creek	8	13,072	81,610	9,790	12,873	8,171	24.5	1,096	6,575	1.42	6.4
Little Porcupine Creek to Wolf Creek	14	18,664	82,069	7,967	12,238	10,855	52.0	845	3,903	1.67	3.3
Wolf Creek to Poplar River	17	19,310	83,175	7,005	9,039	6,805	79.9	1,008	7,855	1.33	9.3
Poplar River to Big Muddy River	23	19,049	89,000	7,049	10,723	7,272	121.7	857	4,039	1.65	5.7
Big Muddy River to Yellowstone	20	10,157	92,500	8,335	11,557	9,051	165.2	1,031	4,792	1.39	11.5

Table 22--Correlation of reach-average* channel activity with geometric variables. Table entries are values of coefficients of determination r^2 (p= probability of a value of r^2 this large arising by chance).

Variable	Pre-impoundment (n = 5)	Post-impoundment (n = 6)
R_c/W	0.76 (0.05)	**
Distance below Fort Peck along channel centerline	**	0.54 (0.10)
Subreach sinuosity	**	0.57 (0.08)

* Study reach divided into subreaches with endpoints corresponding to major tributary confluences.

** = p values were > 0.10.

where v_{reach} = the average pre-dam channel activity for a given reach in ft/yr and K is the sub-reach sinuosity.

Neck Cutoffs

Examination of the meander geometry for the three historic neck cutoffs indicated that neck cutoff may be imminent when the ratio of bend radius of curvature to width is between about 1.8 and 3, the distance ratio is greater than 6, bend length exceeds about 2.5 mi, and bend radius of curvature is less than about 4,000 feet (Table 23). Data for each of the 85 bends defined from the 1991 aerial photographs were examined in light of these criteria, and five bends were identified with the potential for neck cutoff ranging from severe to moderate (Table 24).

Discussion

The rates of channel activity measured for the study reach are in general agreement with the findings of other studies that used different sources of data and different measurement techniques. Previous efforts based on measurements of the area of bankline eroded between successive aerial photographic coverages (U. S. Corps of Engineers 1976; 1984; Englehardt and Waren, 1991; Pokrefke *et al*. 1998) reported rates of bank erosion in acres per year. If these rates are converted to channel activity rates by dividing the sum of left and right bank areal erosion rates by the length of the reach, mean values of 8.8 ft/yr for the period 1938 to 1975 and 4.0 ft/yr for 1975 to 1983 result (Table 25). The former figure is based on analysis of photos for five sub-reaches with a total length of 91.7 miles, while the latter figure is based on photographs of 185 miles of the 189-mile long study reach.

The higher rate for the period 1938-1975 relative to the later period is reasonable in light of the number and duration of high flows during the two periods (Figure 10). There was an average of 13 days per year with average discharge > 25,000 ft^3/s during 1938-1975, but only 9 days per year during 1975-1983. Bank erosion rates determined from aerial photographs for the period 1938-1975 increase in the downstream direction (Table 25 and Figure 34). The boundary for the upper limit of bank erosion rates in these studies agrees well with the post-dam channel activity rates measured herein. Analyses of changes in cross-sections were used to compute volumes of material eroded from banks within the study reach by Pokrefke *et al*. (1998). If these volumes are converted to bank retreat rates by dividing by mean bank height, the results are comparable to those determined herein (Table 26).

Current and pre-dam channel activity for this reach of the Missouri River is only weakly related to channel form. Other workers have noted the difficulty of relating local channel migration, bank retreat, or channel activity rates to form variables. Due to the large number of variables involved, empirical relationships between channel activity and one or two hydrologic or form variables are best suited to describing the behavior of river channels averaged over large distances and over long periods of time (Cherry *et al*. 1996). Published relationships typically show mean rates of channel migration for long reaches of many rivers plotted against independent variables, which range over several orders of magnitude (e.g., Garcia *et al*. 1994).

Table 23--Conditions at meanders which have experienced neck cutoffs.

Approximate 1960 RM	Date of cutoff	Geometry prior to cutoff				Recent channel activity ft/yr
		Radius of curvature/ Width	Length of bend/distance across neck*	Bend length mi	Radius of curvature ft	
1667	ca. 1915	1.9	6.4	2.8	2,482	61.1
1691	between 1913 and 1936	2.9	6.0	3.1	3,643	27.6
1599-1603	1980	2.6	6.4	3.7	2,935	74.1

* Distances were measured about 10 years prior to cutoff for the bends described in the first and third rows of the table. Cutoff date for the bend described in the second row is uncertain, but distances were likely measured within 20 years of cutoff.

Table 24--Recent conditions at selected bends with relatively high risk of neck cutoff.

Approximate 1960 RM	Radius of curvature/ Width	Length of bend/distance across neck	Bend length mi	Radius of curvature ft	Recent channel activity ft/yr
1675-1679	1.7	10.1	3.0	1,693	11.7
1664	3.1	4.6	2.2	2,258	6.2
1662-1660	3.5	4.4	1.6	2,258	1.9
1711	3.6	3.6	3.1	3,161	5.9
1720	1.7	3.5	1.7	1,467	2.6

Table 25--Rates of study reach bank erosion determined by others using aerial photographs.

Time period	Location RM	Average Rate ft/yr	Source
1938-1975	1739.3 – 1724.7 1721.1 – 1696.3 1688.7 – 1678.4 1651.1 – 1630.0 1605.3 – 1596.9 mean for all reaches	5.9 6.2 8.2 10.1 11.7 8.8	U. S. Corps of Engineers, 1976, Englehardt and Waren, 1991
1975-1983	Entire study reach 1771 - 1582	4.0	U. S. Corps of Engineers, 1984
1933-1983	Entire study reach 1771 - 1582	5.9	Pokrefke *et al*. 1998

Table 26--Rates of study reach bank erosion determined by Pokrefke et al. (1998) for entire study reach (River Miles 1771- 1582) using cross-section surveys.

Time period	Average Rate, ft/yr
1955-1966	6.4
1966-1978	3.4
1955-1978	4.8

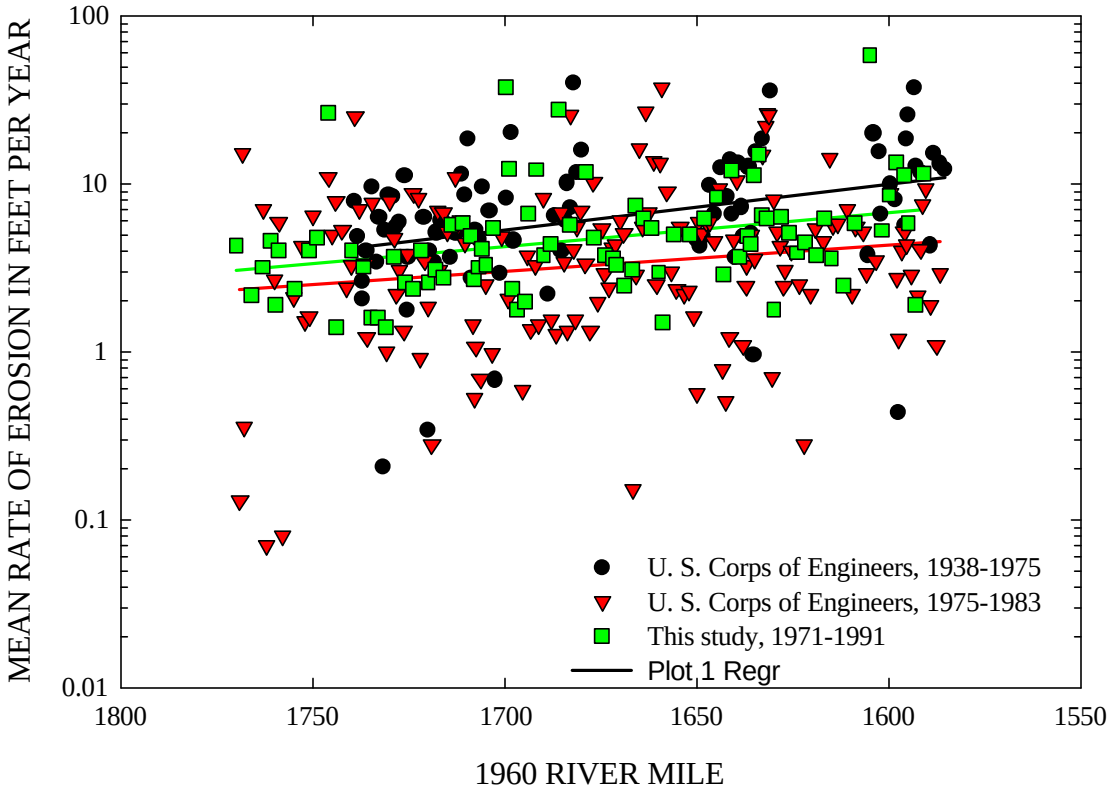

Figure 34-- Erosion rates determined from aerial photographs (U. S. Corps of Engineers 1976 and 1984) with activity rates measured in this study.

Drainage area for the study reach ranges from about 58,000 mi^2 at the dam site to about 94,000 mi^2 at the state line, and spatial variation in mean discharge is confined to a similarly narrow range. Accordingly, variation in drainage area explains less than 3% of the variation in bend-average channel activity in both the pre- and post-dam data. On the other hand, the sixfold reduction in channel activity is almost certainly due to the changes in peak flow levels and frequency following dam closure (Figure 10). Study reach channel activity was 5.7 times greater prior to impoundment than at present, which is comparable to the findings of others studying the effects of reservoirs on alluvial rivers (Table 27).

Form variables are better predictors of channel activity when reach averages are considered rather than bend averages. However, the relationships between meander form and channel activity show stronger correlation for the pre-dam data than for more recent data (Tables 19 and 22). This type of response, uncoupling fluvial form and process, has been observed by other workers comparing channel migration rates on controlled reaches of the Sacramento River with varying amounts of flow control, bank stabilization and bank soil strength (Fischer *et al*. 1994). Rahn (1977) suggested that sediment trapping by Missouri River dams caused erosion along both concave and convex banks and increased the number of mid-channel bars. This is in contrast to the pre-dam regime, which featured roughly equal amounts of concave bank erosion and convex bank deposition. Although data do not uniformly support Rahn's hypothesis, the concept that flow control has disrupted the links between fluvial form and process appears valid.

Comparison of maps and photographs of the study reach indicates that several neck cutoffs and more minor channel avulsions have occurred since 1874. The most recent neck cutoff occurred in 1980 and was triggered by an ice jam during a high flow event (Weismann 1993). Since overbank flows occur much less frequently than prior to dam closure, breaching meander necks will occur less frequently also. Meander neck cutoffs will probably result from gradual narrowing of the meander neck by bank erosion rather than by creation of a chute during an overbank flood. However, rare events, such as floods and ice jams, can trigger neck cutoffs.

Effects on Flood plains

Flow control by Garrison Dam on the Missouri River downstream from the study reach has reduced channel migration rates by a factor of four (Table 27), and this has resulted in major impacts on successional processes in flood plain forests, which depend upon periodic disturbance by floods and riverine erosion for habitat modification and construction (Johnson *et al*. 1976; Johnson 1992). Forecasting based on relationships between channel activity and plant succession rates predicts decline of willow-cottonwood pioneer communities and a general decline in flood plain forest diversity along the Missouri River between Garrison Dam and Lake Oahe, North Dakota.

Similar, but more pronounced impacts have been linked to channel metamorphosis along major European rivers that were formally dynamic braided systems (Bravard *et al*. 1986; 1997; Marston *et al*. 1995). Braided rivers and the ecosystems they support appear to be especially vulnerable to impacts associated with reservoirs. As high flows are suppressed, rivers become less dynamic and physical habitats more homogeneous (Ligon *et al*. 1995). Globally, large temperate-zone rivers have been

Table 27--Comparison of findings on the effects of reservoir impoundment on channel migration rates.

River	Location	Pre dam migration rate, ft/yr	Post dam migration rate, ft/yr	Pre/Post	Reference
Hanjiang	China	82.0	23.0*	3.6	Jiongxin (1997)
Milk	Downstream from Fresno Dam, Montana	5.7	1.5	3.8	Bradley and Smith (1984)
Missouri	Downstream from Garrison Dam, N. Dakota	18.4	4.3	4.3	Johnson (1992)
Missouri	Ft. Peck to Brockton, Montana	32.5	5.7	5.7	this study

* Initial response. Erosion later accelerated following bed armoring.

transformed by the cumulative effects of bank stabilization and river-training structures (Shields *et al*. 1995). Mitigation strategies that preserve rather than limit natural riverine geomorphic processes are preferred to providing habitat for only one (or a few) species (Ligon *et al*. 1995; Interagency Task Force 1998).

Summary of Results

Closure of Fort Peck Dam has resulted in a six-fold reduction of the average rate of channel activity in the study reach. This change is at least partially due to a reduction in the frequency and duration of the highest discharges as caused by reservoir operations. Existing technology for predicting streambank retreat and lateral migration of river channels is not adequate to allow prediction of the future location of study reach banklines. Empirical analysis of historical information indicates that channel activity tends to be greater in the downstream part of the study reach. Channel activity is positively related to channel width and sinuosity. Neck cutoffs occur on bends where substantial elongation and neck constriction occur, with low values of bend radius of curvature. There is at least one large meander bend in the study reach (River Miles 1675-1679) for which a neck cutoff is imminent.

SHEAR STRENGTH AND CHANNEL-BANK STABILITY: THEORY

One of the primary concerns of landowners along the Missouri River in the study reach is the stability of the streambanks. Streambank failures translate directly to a loss in the amount of land available for cultivation. The loss of land associated with bank erosion is a process that can accelerate following channel incision because bank heights are increased. As we have seen earlier, bank erosion and channel widening are processes inherent to channel evolution.

The adjustment of channel width by mass-wasting and related processes can represent an important mechanism of channel response and energy dissipation in incised alluvial streams. For example, bank material contributes as much as 80% of the total sediment eroded from incised channels (Simon *et al*., 1996). In unstable streams, rates of width adjustment by mass-wasting processes can occur over several orders of magnitude: 5 ft/yr in the Obion-Forked Deer River System, West Tennessee (Simon, 1989); 46 ft/yr in the Cimarron River, Kansas (Schumm and Lichty, 1963); about 160 ft/yr in the Gila River, Arizona; and more than 325 ft/yr in some reaches of the Toutle River System, Washington (Simon, 1992). Johnson (1992) found erosion rates on the Missouri River below Garrison dam, on average, to have varied between 4 and 18 ft/yr. The range of rates reflects a diversity of channel-disturbance characteristics, environmental settings and boundary materials.

Conceptual models of bank retreat and the delivery of bank sediments to the flow emphasize the importance of interactions between hydraulic forces acting at the bed and bank toe, and gravitational forces acting on *in situ* bank material (Carson and Kirkby, 1972; Thorne, 1982; Simon *et al*., 1991). Failure occurs when erosion of the bank toe and the channel bed adjacent to the bank have increased the height and angle of the bank to the point that gravitational forces exceed the shear strength of the bank material. After failure, failed bank materials may be delivered directly to the flow and deposited as bed material, dispersed as wash load, or deposited along the toe of the bank as intact blocks or as smaller, dispersed aggregates (Simon *et al*., 1991). If deposited at the bank toe, failed bank material may temporarily increase bank stability by buttressing the bank and protecting *in situ* bank material from attack and entrainment by the flow. The properties of the failed bank material, in tandem with the hydraulic forces acting at the bank toe, control the residence time of failed bank material.

Governing Forces and Processes

The resistance of a channel bank to mass failure is a function of the shear strength of the bank material. Shear strength comprises two components, cohesive strength and frictional strength. For the simple case of a planar failure of unit length the Coulomb equation is applicable:

$$S_r = c' + (\sigma - \mu_w) \tan \phi' \qquad (8)$$

where S_r= shear strength, in pounds per square foot (lbs/ft^2)
c' = effective cohesion, in lbs/ft^2;
σ = normal stress on the failure plane, in lbs/ft^2;

μ_w = pore-water pressure, in lbs/ft^2; and
ϕ' = effective friction angle, in degrees.

Also, $$\sigma = W (cos\ \beta) \quad (9)$$

where W = weight of the failure block, and
β = angle of the failure plane.

The gravitational (driving) force acting on the bank is $W\ sin\ \beta$. Factors that decrease the erosional resistance (S_r), such as excess pore pressure from saturation and the development of vertical tension cracks, favor bank instabilities. Similarly, increases in bank height by bed degradation and bank angle by undercutting favor bank failure by causing the gravitational component to increase. In contrast, vegetated banks are generally drier and provide improved bank drainage, which enhances bank stability (Thorne, 1990). However, recent work by Collison and Anderson (1996) suggests that the effects of roots, at least in the humid tropics may reduce shearing resistance because of enhanced permeability and hence, greater delivery of water to the subsurface. Plant roots provide tensile strength to the soil which is generally strong in compression, resulting in reinforced earth (Vidal, 1969) that resists mass failure, at least to the depth of vegetation roots. However, the added weight of woody vegetation on a bank acts as a surcharge and can have negative effects on bank stability by increasing the downslope component of weight, particularly on steep banks. Matric suction, caused by negative pore pressures that exist above the water table also increases the shearing resistance of the bank in the unsaturated zone. Evaluation of matric suction helps to determine accurate values of effective cohesion, shear strength and stable-bank geometries (Fredlund, *et al*., 1978; Curini, 1998; Simon and Curini, 1998).

Obtaining Shear-Strength Data

In-situ measurements of soil shear strength were obtained using an Iowa Borehole Shear Tester (BST) (Figure 35). The operation and features of the BST have been reviewed by Handy and Fox (1967), Luttenegger and Hallberg (1981), Thorne, *et al*., (1981), Simon (1989), and Simon and Hupp (1992). A summary is provided here.

The shear head of the BST is lowered into a vertical borehole to the desired depth and expanded under gas pressure to provide a normal force acting against the side of the borehole. The soil in contact with the shear head is then allowed to consolidate for at least 20 minutes under the applied normal force. The consolidation time is increased in wet and in clay soils, to allow sufficient time to ensure that positive pore pressures are dissipated and that the test can be considered as drained. The shear head is then pulled vertically by means of a pulling assembly located at the surface. The vertical force provides the shearing force on the walls and is increased until failure of the soil occurs beyond the surface of the borehole. Failure is identified either by a decrease in the shearing-force gauge or by a constant gauge reading over at least 40 turns of the pulling-assembly handle.

The normal force and critical shearing force are plotted on arithmetic graph paper, and the test is repeated several times at increasingly higher normal forces to obtain a series of points delineating the Mohr-Coulomb line:

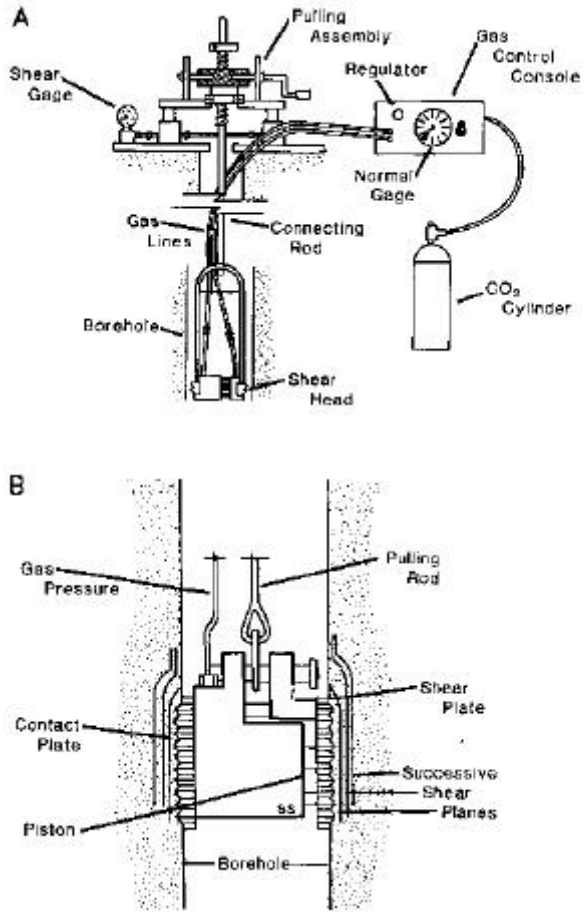

Figure 35--Schematic representation of Iowa Borehole Shear Tester, used for testing of bank material shear strength. Modified from Thorne *et al*., 1981.

$$\tau = c_a + \sigma \tan \phi' \quad (10)$$

where τ = shear strength at failure, in pounds per square foot (lbs/ft^2),
c_a = apparent cohesion, in lbs/ft^2,
σ = normal stress, in lbs/ft^2, and
ϕ' = friction angle, in degrees.

Linear regression is used to define apparent cohesion (y-intercept) and friction angle (slope of regression line), which are two of the required parameters for bank-stability analysis. An example is provided in Figure 36.

Compared to conventional laboratory analyses, which require removal of a sample from the field, the main advantage of the BST is that the soil shear strength values obtained are representative of undisturbed *in-situ* bank material. Another advantage of the BST is that cohesion and friction angle values are updated as the test proceeds in the field, allowing for immediate quality control checks.

Accounting for Both Unsaturated and Saturated Bank Materials

Incised streams generally have high banks where the phreatic surface is usually deep relative to the total bank height during low and even moderate river stages. Thus a large proportion of the streambanks of an incised channel can be characterized as unsaturated. For these circumstances where a good portion of the failure surface might pass through unsaturated soil, slope stability analyses need to incorporate unsaturated shear-strength parameters.

In the part of the streambank above the "normal" level of the groundwater table, bank materials are unsaturated, pores are filled with water and with air, and pore-water pressure is negative. The difference ($\mu_a - \mu_w$) between the air pressure (μ_a) and the water pressure in the pores (μ_w) represents the matric suction (ψ). The increase in shear strength due to an increase in matric suction is described by the angle ϕ^b. Incorporating this effect into the standard Mohr-Coulomb equation produces (Fredlund *et al*., 1978):

$$S_r = c' + (\sigma - \mu_a) \tan \phi' + (\mu_a - \mu_w) \tan \phi^b \quad (11)$$

where $(\sigma - \mu_a)$ = net normal stress on the failure plane at failure;
μ_w = pore-water pressure on the failure plane at failure.

The value of ϕ^b is generally between 10^o and 20^o, with a maximum value of ϕ' under saturated conditions (Fredlund and Rahardjo, 1993). The effects of matric suction on shear strength is reflected in the apparent or total cohesion (c_a) term:

$$c_a = c' + (\mu_a - \mu_w) \tan \phi^b = c' + \psi \tan \phi^b \quad (12)$$

As can be seen from equation 12, negative pore-water pressures (positive matric suction; ψ) in the unsaturated zone provide for cohesion greater than the effective cohesion and, thus, greater shearing resistance. This is often manifest in steeper bank slopes than would be indicated by ϕ'. Negative values of ψ equate to positive values of pore-water pressure

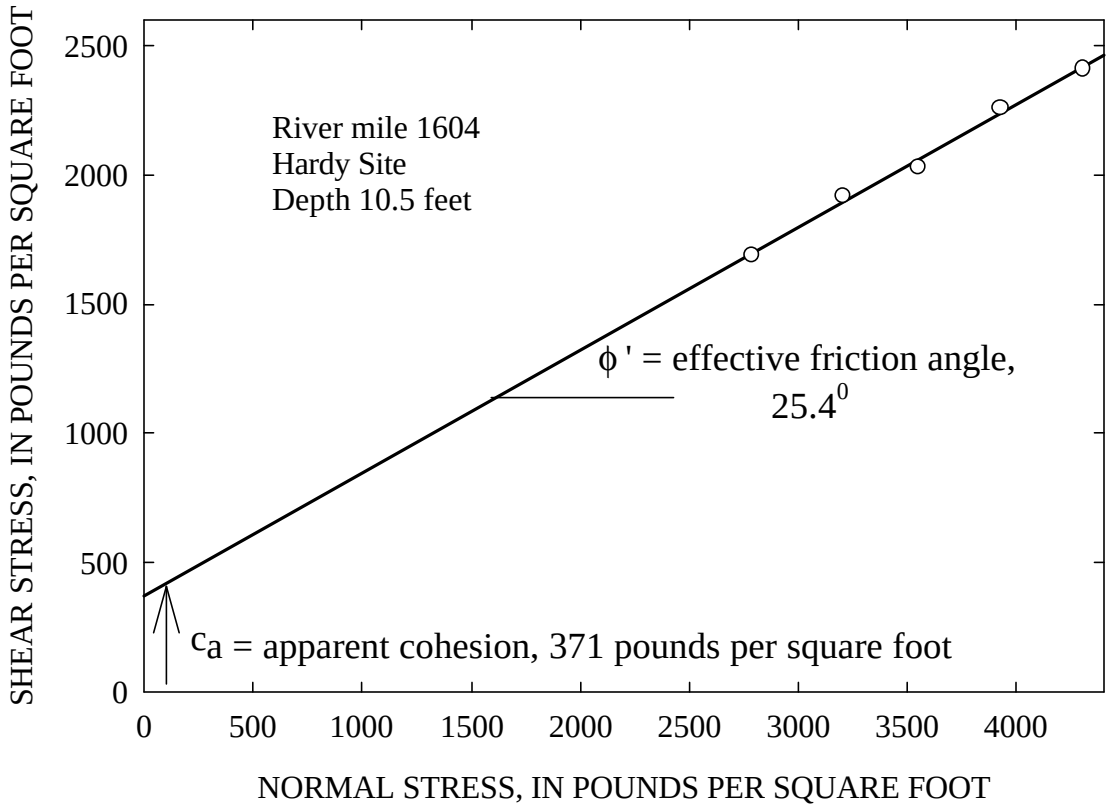

Figure 36--Example borehole shear test showing trials at successively higher normal stresses, fitting of regression line, and calculation of cohesive strength and friction angle.

(μ_w) and consequently, a reduction in shear strength. To quantify the magnitude of this effect, data are required on pore-pressure distributions in the bank. Measurements of matric suction were performed with a portable tensiometer during the 1997 fieldwork to ascertain the variability of pore-water pressure with depth. To account for the lack of these data for the sites studied in 1996, the force imposed by matric suction acting on the failure surface at various depths was calculated by:

$$S = -\gamma_w h^2 / 2 \sin \beta \qquad (13)$$

where h = the height above the water table, in feet.

GEOTECHNICAL CHARACTERISTICS OF THE BANK MATERIAL

A list of all soil materials encountered during the summer fieldwork of 1996 and 1997 is shown in the log of test holes prepared by the NRCS (Table 28). Depths tested and sampled, soil descriptions and field classifications are sorted by river mile. Soils from eight soil series were evaluated during the field investigation. These include Gerdrum, Harlem, Havre, Havrelon, Lohler, Riverwash, Shambo, Trembles, Typic Fluvaquents, and Ustic Torrifluvents. A comprehensive description of each series was included in a previous section of the report (Soil-Series Descriptions).

In general, these soils are fine-grained and consist of silty clay and clay loam, with some fine sand. The classifications shown in Table 28 represent field classifications assigned at the time of sampling. Laboratory classifications are listed in Table 29 along with grain-size statistics and plasticity indices of the materials. Note that the majority of the materials found were low- and high- plasticity clays. In general, the sand to clay ratio (SP/CL) is low (0.82) indicating the general fine-grained, cohesive nature of the bank materials. Only the Riverwash (RM 1624, low terrace) and Trembles (RM 1646 and 1676) series consist primarily of sand-sized materials. The sample data listed in Table 29 are associated with the BST tests.

The lower, more coarse-grained portion of the alluvium is normally well below the 60-inch (5-foot) depth that is used to classify soils. In many locations, the character of the surficial soils does not reflect that of the deeper alluvium. Geotechnical tests were taken at these and greater depths to accurately depict bank strength above low-water levels.

Shear-strength (BST) testing was conducted at all sites from a point considered to be the top of the bank. These tests provide the fundamental data for conducting all of the bank-stability analyses. Results of the BST and other geotechnical tests taken during the summers of 1996 and 1997 are shown in Table 30. Cohesive strengths ranged from 0.0 to 838 lbs/ft^2 with a mean value of 292 lbs/ft^2. Friction angles ranged from 0.0 ^{o}, indicating saturated conditions, to 38.1^o, with a mean value of 25.2^o. Because the geotechnical testing was designed to determine shear strength of the entire streambank and not the shear strength of each soil series, which only represents the upper 5 feet of bank, definitive statements about the strength of a bank composed of a given soil series cannot be made. However, generalizations can be advanced based on the geotechnical testing that took place within given soil series. Often, the lowest shear strengths (weakest materials) are associated with the lowest values of cohesive strength. The lowest cohesion values (0.0 lbs/ft^2) are associated with sands and fissured (cracked) clays. Thus, streambanks containing the Riverwash and Trembles Series tend to be the weakest of all those tested. Some units of the Havre soil series are particularly sandy and provide no cohesive strength (RM 1716). Similarly, dry fissured clays of the Harlem (RM 1728) and Lohler (1631) soil series were found to have no cohesion (Table 30).

Negative Pore-Water Pressures

To obtain data for modeling the magnitude of the shear strength provided by negative pore-water pressures (matric suction), measurements were performed during September, 1997 with a quick-draw tensiometer. To obtain a pore-water pressure profile

Table 28 – Logs of boreholes drilled during August 1996 and September 1997 at 16 sites along the study reach.

U.S. DEPARTMENT OF AGRICULTURE
NATURAL RESOURCES CONSERVATION SERVICE

English units

WATERSHED: Lower Missouri River		PROJECT: Lower Missouri River Channel Erosion Research	
LOCATION: NE Montana		OWNER: STATE Montana	
LOGGED BY: M.Marshall/T.Rolfes	DATE: 8/19-22/96 and 9/8-17/97	PROJECT: Holes drilled for Iowa Borehole Shear testing device, all samples collected w/ hand auger; '97 samples analyzed in Lincoln, NE.	
DRILLING EQUIPMENT: pickup-mounted Simco:	Mark Yerger, 1996 operator Tony Rolfes, 1997 operator	LOCATION OF HOLES: Holes drilled as close to bank as possible. Bank height depends on flow and is subject to change.	

HOLE NO.	STA. & SURFACE ELEVATION	HOLE DEPTH FROM FT.	HOLE DEPTH TO FT.	DESCRIPTION OF MATERIALS	USCS	SAMPLES NO.	SAMPLES * TYPE	SAMPLES FROM FT.	SAMPLES TO FT.	FINES %	SAND %	GRAVEL %
				RICHLAND COUNTY--south bank								
River				Nohly pump site, furthest down river, 9/9/97, Havrelon silt loam, 21' high bank								
mile 1588.5 (1588.6)	1888.1	0	4	Light brown silt, with 20% clay, dry	CL-ML							
				--gradational contact--								
		4	6	Fine sand, dry with 18-20% clay	SC							
				--gradational contact--								
		6	11	Light brown silt as above, dry	ML	98-90		@ 6.6'		75	25	
					CL	98-91		@13.1'		75	20	5
		11	16.8	Dark brown, heavy clay, with precipitated	CH	98-92		@16.1'		100		
				salts and just workable moisture to 15 feet. Wet below 15', contains 40-45% clay.								
		16.8	17	Lightened texture--Dark brown clay with increased sand. Contains saturated pockets.	CL							
				RICHLAND COUNTY--south bank								
River				Hardy site, 9/10/97, Lohler soils (mapped as Havrelon), 20' high banks, 6' from bank								
mile 1603.7	1894	0	2	Brown, silty clay with fine sand, almost dry	CL-ML							
		2	9	Dark brown silty clay, with just workable moisture. Dense, increased water at 8'.	CL	98-93		@ 4.9'		100		
		9	12	Heavy, dark brown clay, with 40-45% clay	CH	98-94		@ 10.2'		90	9	1
		12	13	Thin, stratified beds of heavy clay and silty clay	field CL-CH CH	98-95		@ 12.5'		100		
		13	15	Clay, with increased sand and water	CL							
		15	15.5	Thin CL-CH stratifications as above	CL-CH							
		15.5	23	Fine to medium sand with 15% clay.	SC-SM							
				saturated. Clay decreases with depth to 10-12%. Coarse sand interbed at 16'.								
				ROOSEVELT COUNTY--north bank								
				Culbertson gage site, 9/8/97, Anderson								
River				(heavy) Havrelon silty clay, drilled 13' above river, 35' back from overhanging bank								
mile 1620.8	1904	0	8	Light brown clay, dry at surface, with precipitated salts. Workable moisture	field CL CH	98-88		@ 2.5'		83	17	
				by 2', soft and wet by 4'. Silt content increases with depth below 6'.	CL	98-86		@ 5'		100		
			@7.8	Thin sand lens								
				--gradational contact--	CL	98-89		@ 9.2'		100		
		8	10.5	Dark brown, silty clay, damp but no free water.	CL	98-87		@ 12'		98	2	

*DISTURBED-UNDISTURBED-ROCK CORE Elevations revised 7/22/98

NRCS-ENG-533 U.S. DEPARTMENT OF AGRICULTURE

Table 28 cont.

LOG OF TEST HOLES

English units

WATERSHED: Lower Missouri River				PROJECT: Lower Missouri River Channel Erosion Research									
LOCATION: NE Montana				OWNER: STATE Montana									
LOGGED BY: M.Marshall/T.Rolfes		DATE: 8/19-22/96 and 9/8-17/97		PROJECT: Holes drilled for Iowa Borehole Shear testing device, all samples collected w/ hand auger; '97 samples analyzed in Lincoln, NE.									
DRILLING EQUIPMENT: pickup-mounted Simco:		Mark Yerger, 1996 operator Tony Rolfes, 1997 operator		LOCATION OF HOLES: Holes drilled as close to bank as possible. Bank height depends on flow and is subject to change.									
		HOLE DEPTH		DESCRIPTION OF MATERIALS	U	SAMPLES							
HOLE NO.	STA. & SURFACE ELEVATION	FROM	TO		S C S	NO.	* TYPE	FROM	TO	FINES	SAND	GRAVEL	
		FT.	FT.					FT.	FT.	%	%	%	
River				ROOSEVELT COUNTY--north bank									
mile				Tveit-Johnson lower terrace, Riverwash soils, bank is 6 feet high--hand auger only									
1623.9	1900	0	2	Light brown, silty sand	SM-ML								
(1623.5)		2	5	Clean, fine sand, light brown to brown	SP								
				ROOSEVELT COUNTY--north bank									
				Tveit-Johnson site, 8/19/96									
River				Lohler silty clay, drilled 15.5 feet above river									
mile				Light brown clay, homogeneous. Dry to 6',									
1624	1909	0	13.5	damp and denser below, and relatively	CL								
(1623.8)				consistent with depth. Seems softer ~ 10'. Softer, wetter, no free water yet @ 13'.									
		13.5	16	COLOR CHANGE, soft, blue-gray clay. Water in hole at 15.2 feet.	CL								
		16	18	Sand with high silt content, dark gray.	SM								
				RICHLAND COUNTY--south bank, 8/20/96									
River				Iversen site, Havrelon soils, banks are 12 feet high.									
mile				Brown silty clay, dry at surface, dense and dark									
1630	1908.3	0	6.5	brown below 4', with thin sand lenses < 4"	CL								
(1629.5)		6.5	12	Clean sand with thin clay lenses	SP								
		@12		Clay ledge shows at water surface	CL								
				RICHLAND COUNTY--south bank									
River				Vournas site, Lohler soils, banks are 9 feet high, drilled 8/20/96									
mile													
1631.0	1909.9	0	7	Clay with thin lenses of clean sand	ML-CL								
		7	8	Clean sand	SP								
				ROOSEVELT COUNTY--north bank,									
				Mattelin site, 8/21/96, drilled with hand auger									
River	1926			Trembles soils, the bank is 11" high.									
mile													
1646		0	6	Light brown silty sand with 2-3" thick clay	SM								
(1646.6)				lens at 3 feet. Increase in silt content and thin clay lenses to 6 feet.									
		6	7	Silt with very fine sand, and 3" clay lens at 6 feet.	ML								
		7	9	Fine, silty sand, becomes cleaner with depth.	SM to SP								

*DISTURBED-UNDISTURBED-ROCK CORE Elevations revised 7/22/98

Table 28 cont.

LOG OF TEST HOLES

English units

WATERSHED: Lower Missouri River | PROJECT: Lower Missouri River Channel Erosion Research

LOCATION: NE Montana | OWNER: STATE Montana

LOGGED BY: M.Marshall/T.Rolfes | DATE: 8/19-22/96 and 9/8-17/97 | PROJECT: Holes drilled for Iowa Borehole Shear testing device, all samples collected w/ hand auger; '97 samples analyzed in Lincoln, NE.

DRILLING EQUIPMENT: pickup-mounted Simco: Mark Yerger, 1996 operator; Tony Rolfes, 1997 operator | LOCATION OF HOLES: Holes drilled as close to bank as possible. Bank height depends on flow and is subject to change.

HOLE NO.	STA. & SURFACE ELEVATION	HOLE DEPTH FROM FT.	HOLE DEPTH TO FT.	DESCRIPTION OF MATERIALS	USCS	SAMPLES NO.	SAMPLES * TYPE	SAMPLES FROM FT.	SAMPLES TO FT.	FINES %	SAND %	GRAVEL %
				RICHLAND COUNTY--south bank								
River				Woods Peninsula, 9/11/97, Trembles soils, hand augered, 13' high banks								
mile 1675.5	1956	0	11	Light brown silty sand with non-plastic fines	SM	98-96		@ 5.2'		39	61	
		11	12.5	Brown clay, saturated at 12.5'	CL							
		12.5	13	Clean, brown sand	SP							
				McCONE COUNTY--south bank								
River				McCrae's pump site, 9/11/97, Shambo soils, 23' high banks								
mile 1682.2	1974.2	0	1	Dark brown, organic silt, with 18-20% clay	CL-ML							
		1	4	Light brown, silty clay, 19-20% clay, dry	CL							
		4	7	Lt. brown, silt w/ fine sand and 14% clay, dry	ML	98-98		@ 6.6'		93	7	
		7	11	Light silty clay, just damp at 8', workable water content at 11'.	CL	98-99		@ 10.8'		100		
		11	13.5	Light brown silty sand	SM							
		13.5	23	Dense brown clay, contains 1-3" sand	CL	98-100		@ 23.6'		100		
				lenses, with heavier clay approaching CH at 18-19' and 22-23'. Mottles at 23'.		98-97		@ 30.8'		100		
				McCONE COUNTY--south bank								
River				John Mann site at Wolf Point Bridge, 9/12/97, Gerdrum soils, 16' high banks								
mile 1700.6	1979	0	4	Light brown silty clay, dry	CL							
		4	6.5	Brown sandy clay, increase in fine sand	CL							
		6.5	9	Brown silty clay, 25-27% clay, with workable moisture content	field CL / CH	98-101		@ 6.6'		83	13	4
		9	10	Increased sand, with 22-25% clay	CL							
		10	13	COLOR CHANGE, soft, damp, brown-gray silty clay w/significant mottling. Sand % > @12.5	CL	98-102 98-103		@ 10.2' @ 12.5'		92 86	8 12	 2
		13	18	Gray clay, @ 13.5' soft and wet but no free water. Contains small, saturated pockets of sand. Water at 15.8'.	CL							
		18	19.5	Gray silty sand	SM							
		19.5	22	Sandy clay	CL							

*DISTURBED-UNDISTURBED-ROCK CORE | Elevations revised 7/22/98 | SHEET 3 OF 6 SHEETS

NRCS-ENG-533
REV. 7-98

U.S. DEPARTMENT OF AGRICULTURE
NATURAL RESOURCES CONSERVATION SERVICE

Table 28 cont.

LOG OF TEST HOLES

WATERSHED: Lower Missouri River	PROJECT: Lower Missouri River Channel Erosion Research
LOCATION: NE Montana	OWNER: STATE Montana
LOGGED BY: M.Marshall/T.Rolfes	DATE: 8/19-22/96 and 9/8-17/97
DRILLING EQUIPMENT: pickup-mounted Simco:	Mark Yerger, 1996 operator; Tony Rolfes, 1997 operator
PROJECT: Holes drilled for Iowa Borehole Shear testing device, all samples collected w/ hand auger; '97 samples analyzed in Lincoln, NE.	
LOCATION OF HOLES: Holes drilled as close to bank as possible. Bank height depends on flow and is subject to change.	

HOLE NO.	STA. & SURFACE ELEVATION	HOLE DEPTH FROM FT.	HOLE DEPTH TO FT.	DESCRIPTION OF MATERIALS	USCS	SAMPLES NO.	* TYPE	FROM FT.	TO FT.	FINES %	SAND %	GRAVEL %
River				McCONE COUNTY--south bank								
mile 1716.0	2002	0	1	Pipal site, Havre silt loam soils, 18' high banks, 8/21/96. Hole drilled to 8.5', then bank logged. Light brown silty sand, dry	SM							
		1	3	Brown, low plastic clay	CL							
		3	4	Light brown silty sand	SM							
		4	5	Brown, low plastic clay	CL							
		5	8	Light brown, silty sand with thin, horizontal CL interbeds	SM							
		8	10.5	Clay with increased plasticity, the base of the vertical bank is in this unit.	CH							
		10.5	13	Cemented silty sand	SM							
		13	15	Moist clay	CL							
		15	18	Silty sand, moist	SM							
River				VALLEY COUNTY--north bank								
mile 1728.0	2006	0	8	Lionnel Flynn hayfield, 8/22/96, banks are 14.2 feet high, Harlem clay soils Brownish-gray clay with minor, 2-3" interbeds of lighter brown, less plastic clay	CH							
		8	9	Lighter textured fines: clay grading to fine, silty sand. Saturated at 8 feet.	CL to SM							
		9	12	Dense, dark gray clay, wet and soft @ bottom	CH							
		12	13	Coarse sand, iron-stained. Contains fewer fines than sandy interbed at 8.5 feet.	SM							
		13	14	Dark gray to black silt with fine sand. Smells organic.	ML							
		14	16	Relatively clean, fine-grained sand, light brown with iron staining.	SP							
		16	18	Dark gray to black silt with fine sand. Smells organic :-(	ML							

WATERSHED	PROJECT
Lower Missouri River	Lower Missouri River Channel Erosion Research
LOCATION	OWNER STATE
NE Montana	Montana
LOGGED BY / DATE	PROJECT: Holes drilled for Iowa Borehole Shear testing device, all
M.Marshall/T.Rolfes / 8/19-22/96 and 9/8-17/97	samples collected w/ hand auger; '97 samples analyzed in Lincoln, NE.
DRILLING EQUIPMENT / Mark Yerger, 1996 operator	LOCATION OF HOLES: Holes drilled as close to bank as possible.
pickup-mounted Simco: / Tony Rolfes, 1997 operator	Bank height depends on flow and is subject to change.

HOLE NO.	STA. & SURFACE ELEVATION	HOLE DEPTH FROM FT.	HOLE DEPTH TO FT.	DESCRIPTION OF MATERIALS	USCS	SAMPLES NO.	* TYPE	FROM FT.	TO FT.	FINES %	SAND %	GRAVEL %
				VALLEY COUNTY--north bank								
River				Todd site, 9/15/97, Harlem soils, bank is 12-13' high								
mile 1737.2	2010	0	1.5	Dark brown clay, increased organics to 1', dry	CL							
		1.5	3	Silty clay, lighter color and texture, dry	CL							
		3	4	Dark brown, heavier silty clay. First 0.5' is stratified, then consistent. 40-42% clay.	CH							
		4	5	Silty clay, dry of workable moisture, with visible precipitated salts	CL							
					field CL-ML							
		5	6	Clay with increased fine sand	CL	98-104		@ 5.2'		100		
		6	8.5	Dark brown silty clay, heavier texture	CL							
				(32-35% clay). Silty 3-4" interbed @ 6.5', mottled at 7' soft @ 8'.								
		8.5	12	Dark brown silty clay with fine sand, 27-30% clay	CL	98-105		@ 9.2'		100		
		12	16	COLOR CHANGE to gray, soft and wet, water @ 14.0'	CL							
		16	17	Clay with increased sand, gray	CL-ML							
				VALLEY COUNTY--north bank								
River				Little Porcupine Creek site, (Westland) 9/15/97, Harlem silty clay loam, bank is 23' high								
mile 1743.9	2021	0	6	Dark brown silty clay, sticky, with 35-40% clay. Dense, with thin stratifications of silty clay, and minor sand stringers < 1/2"	CL-CH							
					(on CL-CH line)							
		6	20	Glacial till--dense, dark brown clay	CH	98-106		@ 6.6'		82	18	
				with minor gravels. Soft and gray by 15' but not saturated	CL	98-107		@ 10.8'		100		
				VALLEY COUNTY--north bank								
River				Milk River site, (Toews) 9/16/97, heavy Harlem soils, bank is 15' high								
mile 1761.6	2032	0	14	Dark brown silty clay, very heavy with 40-45% clay. Consistent composition with depth.	CH	98-108		@ 3.6'		87	13	
				except 3-4" sand stringers at 5'. Mottled	CH	98-109		@ 8.5'		68	27	5
				@ 10', increased water at 13'.	CH	98-110		@ 12.8'		84	6	10
		14	16	COLOR CHANGE to gray, water at 14.4'.	CH							

Table 28 cont.

LOG OF TEST HOLES

English units

Lower Missouri River								Lower Missouri River Channel Erosion Research					
LOCATION NE Montana				OWNER STATE Montana									
LOGGED BY M.Marshall/T.Rolfes		DATE 8/19-22/96 and 9/8-17/97		PROJECT: Holes drilled for Iowa Borehole Shear testing device, all samples collected w/ hand auger; '97 samples analyzed in Lincoln, NE.									
DRILLING EQUIPMENT pickup-mounted Simco:		Mark Yerger, 1996 operator Tony Rolfes, 1997 operator		LOCATION OF HOLES: Holes drilled as close to bank as possible. Bank height depends on flow and is subject to change.									
		HOLE DEPTH		DESCRIPTION OF MATERIALS	U	SAMPLES							
HOLE NO.	STA. & SURFACE ELEVATION	FROM	TO		S C S	NO.	* TYPE	FROM	TO	FINES	SAND	GRAVEL	
		FT.	FT.					FT.	FT.	%	%	%	
River				VALLEY COUNTY--north bank Garwood site, 9/17/97, Havre-Harlem silty clays, 16' high bank									
mile 1764.7	2042	0	2	Light brown silty clay, dry	field CL CH	98-111		@ 2.0'		100			
		2	2.5	6" or less sand lens, with 18-20% clay	SC								
		2.5	4.5	Light brown silty clay, dry	CL								
		4.5	7.5	Silty clay, 27-30% clay, with heavier section in middle, dry	field CL ML	98-112		@ 6.5'		100			
		7.5	8.5	Silty clay with increased fine sand, dry	CL-ML								
		8.5	12	Light brown silty sand, dry	SM								
		12	13.5	Sandy clay, almost dry	CL								
		13.5	17	Light brown silty sand, water table at 16'	SM	98-113		@ 14.8'		21	79		
		17	18	Sand with increased fines	SM-SC								
				There is significant internal variation in this deposit, and drilling results can vary within short distances.									

*DISTURBED-UNDISTURBED-ROCK CORE Elevations revised 7/22/98 SHEET 6 OF 6 SHEETS

Table 29-- Summary of particle-size distributions and classifications of bank materials.

River Mile	Date	Site Name	Depth In Feet	% In Size Class				SP/CL	LL	PI	Lab Classification
				Gravel	Sand	Silt	Clay				
1589	1997	Nohly	6.6	0	25	64	11	2.27	-	-	ML
1589	1997	Nohly	13.1	5	20	43	32	0.63	56	38	CL
1589	1997	Nohly	16.1	0	0	15	85	0.00	53	35	CH
1604	1997	Hardy	4.9	0	0	74	26	0.00	37	19	CL
1604	1997	Hardy	10.2	1	9	44	46	0.20	73	51	CH
1604	1997	Hardy	12.5	0	0	50	50	0.00	63	43	CH
1621	1997	Culbertson	2.5	0	27	36	37	0.73	69	47	CH
1621	1997	Culbertson	5.0	0	0	73	27	0.00	47	29	CL
1621	1997	Culbertson	9.2	0	0	81	19	0.00	35	14	CL
1621	1997	Culbertson	12.0	0	0	82	18	0.00	32	13	CL
1624 Low Terrace	1996	Tveit-Johnson	1.0	0	0	67	33	0.00	51	34	CH
1624 Low Terrace	1996	Tveit-Johnson	3.1	0	30	60	10	3.00	-	-	SM
1624	1996	Tveit-Johnson	3.0	0	0	55	45	0.00	62	46	CH
1624	1996	Tveit-Johnson	6.8	0	0	46	54	0.00	82	62	CH
1624	1996	Tveit-Johnson	13.3	0	0	46	54	0.00	76	59	CH
1624	1996	Tveit-Johnson	16.0	0	42	46	12	3.50	-	-	SM
1630	1996	Iverson	5.7	0	17	68	15	1.13	31	14	SC
1630	1996	Iverson	7.8	0	0	80	20	0.00	37	19	CL
1631	1996	Vournas	2.0	0	10	71	19	0.53	31	17	CL
1631	1996	Vournas	6.4	0	0	53	47	0.00	62	42	CH
1631	1996	Vournas	7.2	0	0	80	20	0.00	35	17	CL
1646	1996	Mattelin	3.8	0	0	74	26	0.00	44	22	CL
1646	1996	Mattelin	6.8	0	0	65	35	0.00	47	29	CL
1646	1996	Mattelin	8.0	0	10	78	12	0.83	30	12	CL
1676	1997	Woods Peninsula	5.2	0	61	30	9	6.78	-	-	SM
1682	1997	Shambo	6.6	0	7	81	12	0.58	-	-	ML
1682	1997	Shambo	10.8	0	0	64	36	0.00	44	23	CL
1682	1997	Shambo	23.6	0	0	83	17	0.00	27	10	CL
1682	1997	Shambo	30.8	0	0	61	39	0.00	49	29	CL
1701	1997	Wolf Point	6.6	4	13	54	29	0.45	52	33	CH
1701	1997	Wolf Point	10.2	0	8	74	18	0.44	34	16	CL
1701	1997	Wolf Point	12.5	2	12	58	28	0.43	51	31	CH
1716	1996	Pipal	3.6	0	0	76	24	0.00	42	25	CL
1716	1996	Pipal	9.3	0	0	46	54	0.00	92	70	CH
1716	1996	Pipal	12.0	0	0	80	20	0.00	43	24	CL
1728	1996	Flynn Creek	3.0	0	0	46	54	0.00	78	53	CH
1728	1996	Flynn Creek	9.6	0	0	63	37	0.00	45	30	CL
1737	1997	Fraizer Pump	5.2	0	0	71	29	0.00	43	26	CL
1737	1997	Fraizer Pump	9.2	0	0	67	33	0.00	49	30	CL
1744	1997	L. Porcupine	6.6	0	18	47	35	0.51	50	33	CH
1744	1997	L. Porcupine	10.8	0	0	68	32	0.00	48	32	CL
1762	1997	Milk River	3.6	0	12	39	49	0.24	81	59	CH
1762	1997	Milk River	8.5	5	17	42	36	0.47	77	55	CH
1762	1997	Milk River	12.8	10	6	45	39	0.15	71	49	CH
1765	1997	Garwood	2.0	0	0	53	47	0.00	64	43	CH
1765	1997	Garwood	6.6	0	0	88	12	0.00	-	-	ML
1765	1997	Garwood	14.8	0	79	16	5	15.80	-	-	SM

Table 30-- Summary of geotechnical data collected at the 17 study sites.

c_a = apparent cohesion; c_u = undrained cohesion; ϕ' = angle of internal friction; γ = unit weight; Ψ = matric suction

River Mile	Soil Series	Depth	USCS	c_a	c_u	ϕ'	Moisture	γ_{dry}	γ_{amb}	γ_{sat}	Ψ
		feet		lbs/ft^2	lbs/ft^2	degrees	%	lbs/ft^3	lbs/ft^3	lbs/ft^3	lbs/ft^2
1589	Havrerlon	6.56	ML	372	-	30.1	3.10	87.9	122	136	313
1589	Havrerlon	13.1	CL	111	-	29.0	18.2	97.7	115	144	125
1589	Havrerlon	16.1	CL	269	-	29.1	24.8	89.9	110	138	115
1589	Havrerlon	17.7	CL	-	-	-	31.5	80.6	106	133	41.8
1604	Lohler	5.25	ML-CL	380	-	20.2	13.7	86.3	98.1	135	522
1604	Lohler	10.2	CL	365	-	25.4	22.6	85.9	105	134	188
1604	Lohler	12.5	CL	257	-	21.2	28.0	85.2	109	134	83.5
1604	Lohler	15.7	CL	-	-	-	22.6	84.5	104	129	10.4
1621	Havrerlon	2.53	CL	441	-	29.7	18.3	93.0	110	140	752
1621	Havrerlon	4.92	CL	280	-	29.2	24.6	81.5	101	131	418
1621	Havrerlon	9.19	CL	491	-	26.5	25.0	81.7	102	131	167
1621	Havrerlon	11.2	CL	-	731	0.00	29.3	93.5	96.3	125	0.00
1621	Havrerlon	12.1	CL	-	731	0.00	-	-	-	-	0.00
1624 (Low terrace)	River Wash	0.98	SM	0.00	-	30.9	13.3	73.0	82.7	98.0	-
1624 (Low terrace)	River Wash	2.95	SP	0.00	-	26.4	25.2	85.7	107	134	-
1624	Lohler	2.30	ML-CL	589	-	31.7	13.6	83.6	94.9	132	-
1624	Lohler	3.61	CL	731	-	25.4	12.5	85.3	95.5	134	-
1624	Lohler	6.89	CL	620	1888	23.6	26.5	81.9	104	131	-
1624	Lohler	13.1	CL	674	-	5.50	28.2	83.6	107	132	-
1624	Lohler	14.1	CL	-	1733	-	-	-	-	-	-
1630	Havrerlon	5.58	SM	163	-	29.9	16.4	85.7	107	134	-
1630	Havrerlon	7.87	SC	514	-	26.6	31.2	80.2	93.3	130	-
1631	Lohler	2.30	ML-CL	0.00	1702	32.0	18.1	89.1	105	137	-
1631	Lohler	6.56	ML-CL	666	1514	9.80	20.7	85.3	103	134	-
1631	Lohler	7.22	SP	-	-	-	26.5	86.1	109	135	-
1646	Trembles	3.94	SM	0.00	-	38.1	10.6	77.5	85.8	127	-
1646	Trembles	6.23	SM	-	-	-	20.7	84.7	100	132	-
1646	Trembles	7.87	SP	96.0	-	35.4	19.8	87.5	105	136	-
1676	Trembles	5.25	SM	45.9	-	26.9	4.50	88.2	92.1	136	125
1676	Trembles	10.2	SM	-	-	-	8.00	80.8	87.2	130	125
1682	Shambo	6.89	CL	192	-	33.6	6.00	84.3	89.8	133	637
1682	Shambo	11.2	CL	60.6	-	37.6	21.8	88.4	108	136	52.2
1682	Shambo	17.7	CL	689	-	14.0	23.3	88.3	109	136	52.2
1682	Shambo	23.3	CL	-	-	-	20.8	90.8	110	139	-
1701	Gerdrum	6.9	SC	173	-	27.6	16.3	87.9	102	136	397
1701	Gerdrum	10.2	SC	4.18	-	35.0	14.6	85.5	98.0	134	125
1701	Gerdrum	13.5	CL	424	-	14.5	31.1	81.2	107	130	73.1
1716	Havre	3.94	SM	0.00	-	37.7	10.8	85.2	94.4	134	-
1716	Havre	9.19	CL-CH	524	1401	13.4	25.0	87.8	110	136	-
1716	Havre	12.1	SM	0.00	-	37.9	15.5	83.9	97.0	133	-
1728	Harlem	2.95	CL-CH	0.00	-	32.0	18.7	85.9	102	134	-
1728	Harlem	9.51	CL-CH	438	-	26.1	27.5	84.5	108	133	-
1737	Harlem	5.25	SC	125	-	28.1	18.3	82.3	97.4	131	219
1737	Harlem	9.84	CL	192	-	28.8	21.9	80.2	97.8	130	73.1
1744	Harlem	4.43	CL-CH	213	-	33.2	13.6	83.0	94.4	132	355
1744	Harlem	6.56	CH	-	-	-	13.2	88.0	99.6	136	355
1744	Till	10.8	CH	361	-	37.8	12.2	82.1	92.1	131	271
1744	Till	21.3	CH	382	-	7.10	45.2	68.7	99.8	120	0.00
1762	Harlem	3.94	CL	-	-	-	22.6	74.4	91.2	98.9	480
1762	Harlem	8.53	CH	839	-	10.8	30.7	94.8	118	138	146
1762	Harlem	12.8	CH	399	-	8.90	41.4	72.4	102	97.4	125
1765	Havre-Harlem	1.97	CL	163	-	33.8	10.8	80.5	89.2	130	710
1765	Havre-Harlem	6.56	CL	-	-	-	7.60	76.8	78.8	84.7	-
1765	Havre-Harlem	14.8	SM	23.0	-	28.9	3.50	86.3	89.2	135	334

of the streambank, the device was inserted into cores extracted from the bank at several depths. Values as high as 752 lbs/ft^2 were obtained.

An example of the data collected from two different clay soils at River Miles 1589 (Nohly) and 1604 (Hardy) using this method are shown in Figures 37 and 38. An example from a sandy soil at River Mile 1676 (Woods Peninsula) is shown in Figure 39. Generally, the largest values of matric suction were measured near the top of the bank as a consequence of the low moisture content produced here by a dearth of precipitation and high evapotranspiration.

Transpiration of water by grass roots creates a primary or secondary maxima of matric suction at the base of the root zone (Figures 37 and 38). In the banks tested, the maximum depth of dense grass roots ranged from about 2 – 3.5 feet. Values of matric suction generally decrease non-linearly with depth until reaching zero at the water table, which is often equivalent to the water-surface elevation in the channel. This trend is only interrupted by the presence of lenses of contrasting permeability. Note that for the sandy soil at River Mile 1676 (Woods Peninsula), the grass roots have a pronounced effect on removing moisture in the upper 1.5 feet (Figure 39).

The rate of increase in shear strength due to increasing values of matric suction is defined by the parameter f^b and is a required input parameter in the type of advanced bank-stability modeling undertaken in this study. Little field data is available from riverine environments on parameter values. Typical values range from 10^o to 25^o, with an average value of 17.5^o generally being accepted as a good estimate (Fredlund and Rahardjo, 1993). An attempt was made here to estimate the parameter f^b for a Havrelon soil. Several BST tests, accompanied by tensiometer measurements, were performed over a range of matric suctions. The relation between shear strength at failure and matric suction at a given normal stress is plotted in Figure 40. Linear regression is then used to determine the f^b angle at 18.6º.

The additional cohesion provided by matric suction can be important in maintaining bank stability and as a possible strategy in mitigation against bank failures. The contribution of matric suction to apparent cohesion is shown in Figure 41 for an assumed average f^b angle of 17.5^o. Recent experimental evidence indicates that the value increases to a maximum value of f' at saturation (Fredlund and Rahardjo, 1991; Simon *et al*, 1999). Cohesion due to matric suction is also shown at a maximum rate, thus providing an envelope of values (Figure 41). If the soil has a value of matric suction of 25,000 lbs/ft^2 and an angle of f^b of 17.5º it gains an additional cohesion of 7,880 lbs/ft^2.

Since the matric suction profile and f^b varies within the bank, the shear strength of the bank material is dependent on these forces that are directly related to moisture content. Moisture content varies from near 0% to about 45% dry weight. Saturation of the Missouri River bank materials occurs at about 30% (Figure 42). Thus the effects of negative pore-water pressures (matric suction) are applicable at moisture contents less than 30% dry weight. For homogeneous materials matric suction reaches a maximum value within the first 3.3 feet below the bank top.

Bank-toe materials

Field observations, sampling and laboratory testing of bank-toe material showed a range of material types from clay to sand. In-situ clays have greater resistance to erosion by

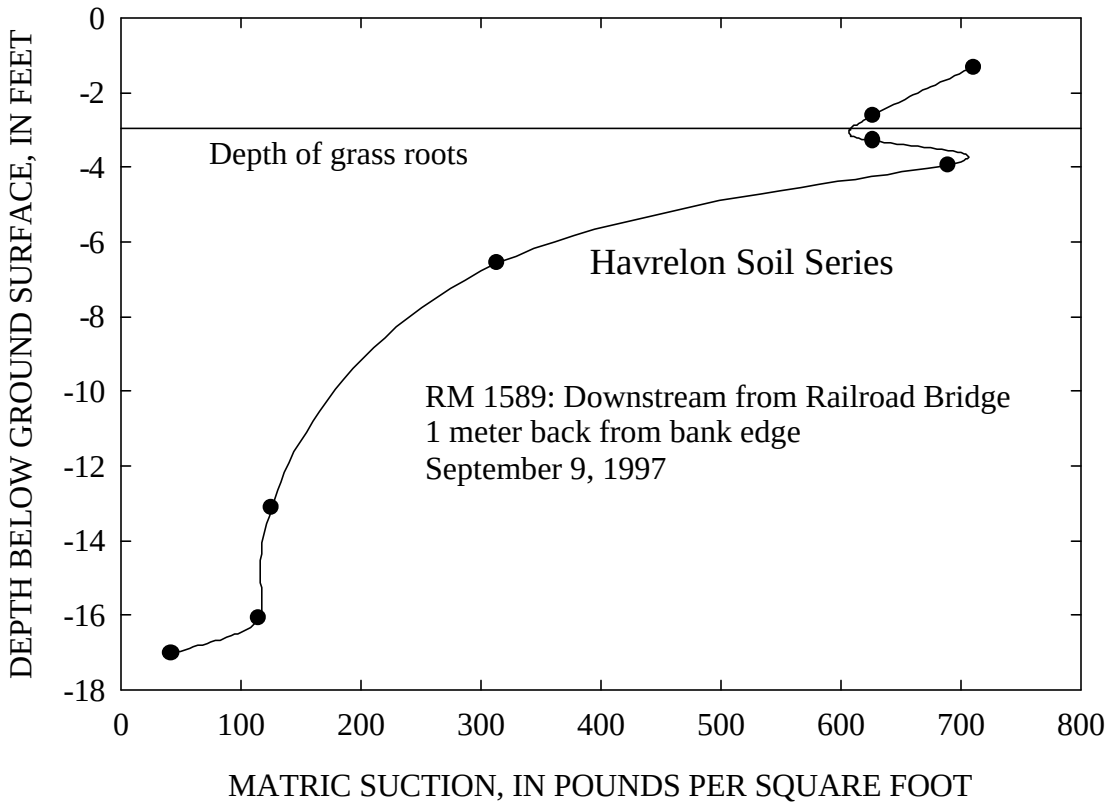

Figure 37--Example of matric suction (negative pore-water pressure) profile for a clay Havrelon soil with grass roots from River Mile 1589 showing variability with depth.

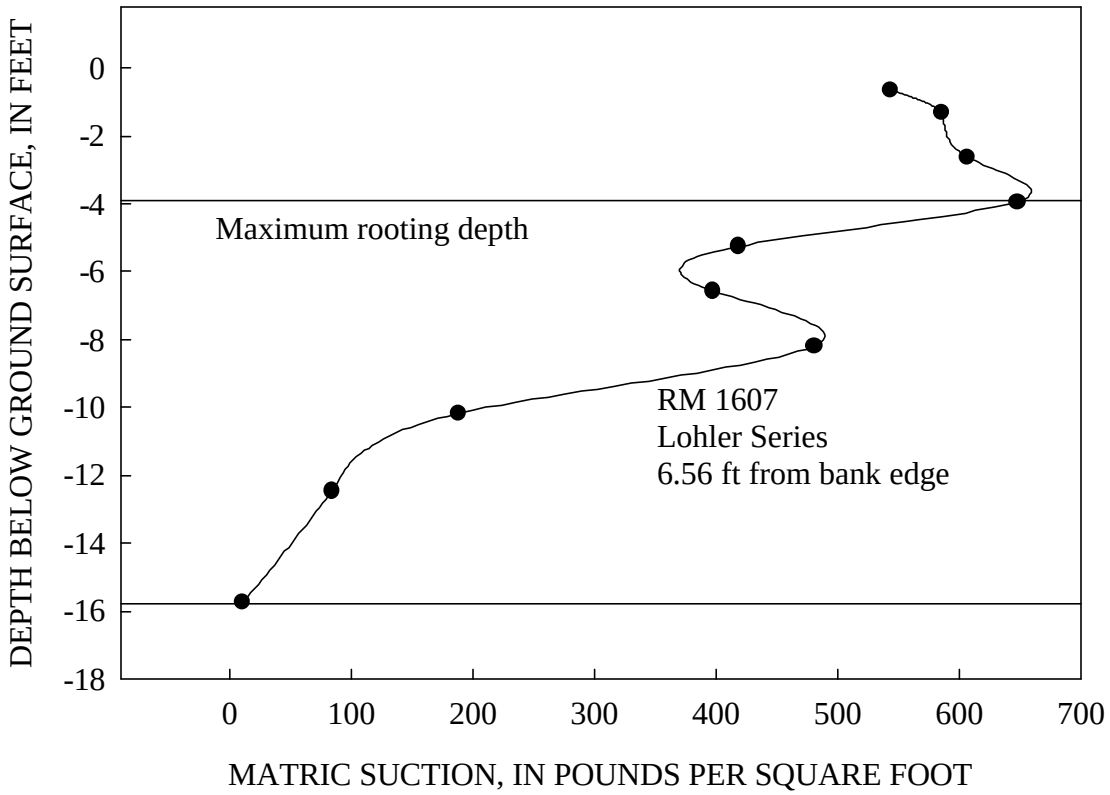

Figure 38--Example of matric suction (negative pore-water pressure) profile for a Lohler clay soil with grass roots from River Mile 1604 showing variability with depth.

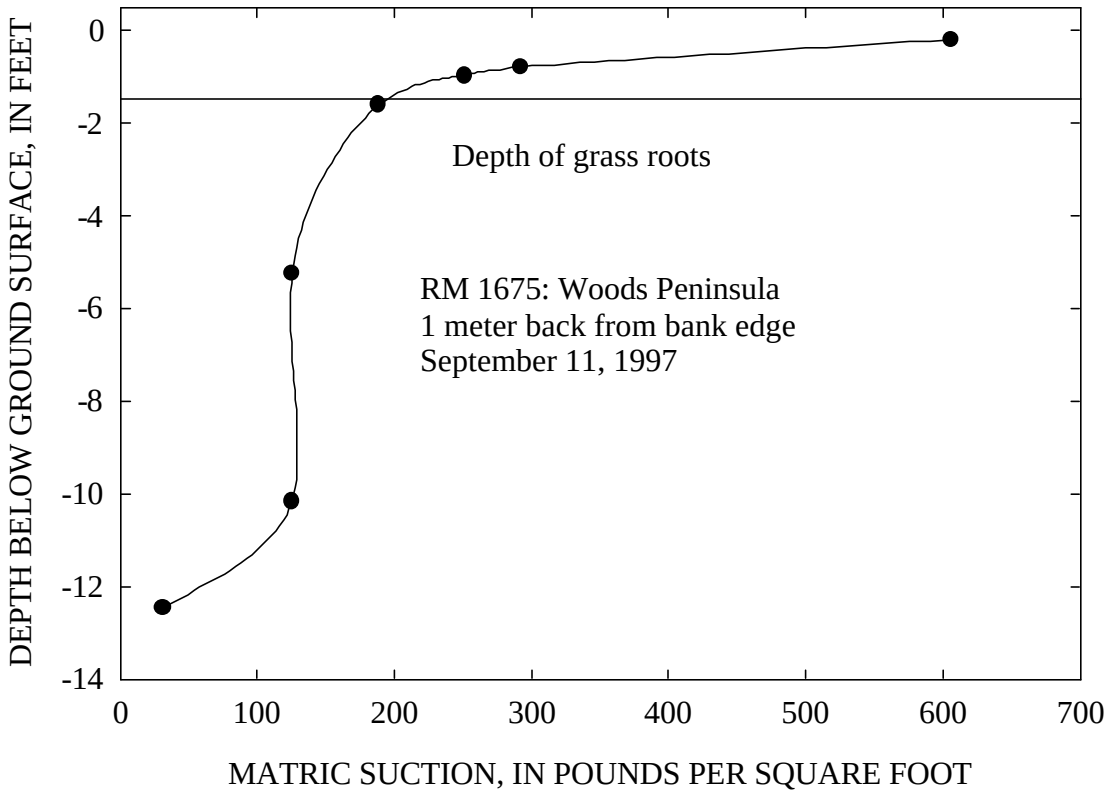

Figure 39--Example of matric suction (negative pore-water pressure) profile for a sandy soil from River Mile 1676 showing variability with depth

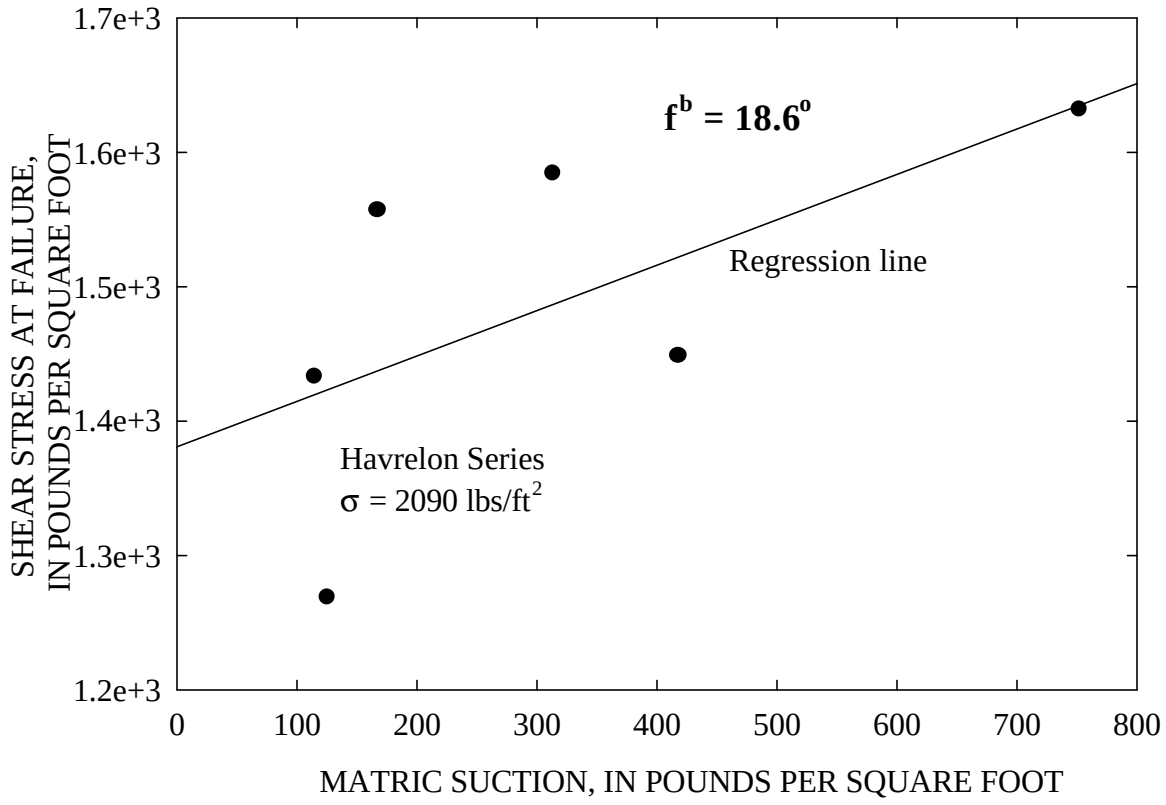

Figure 40--Results of shear–strength tests at different values of matric suction in Havrelon soil showing calculation of the parameter ϕ^b.

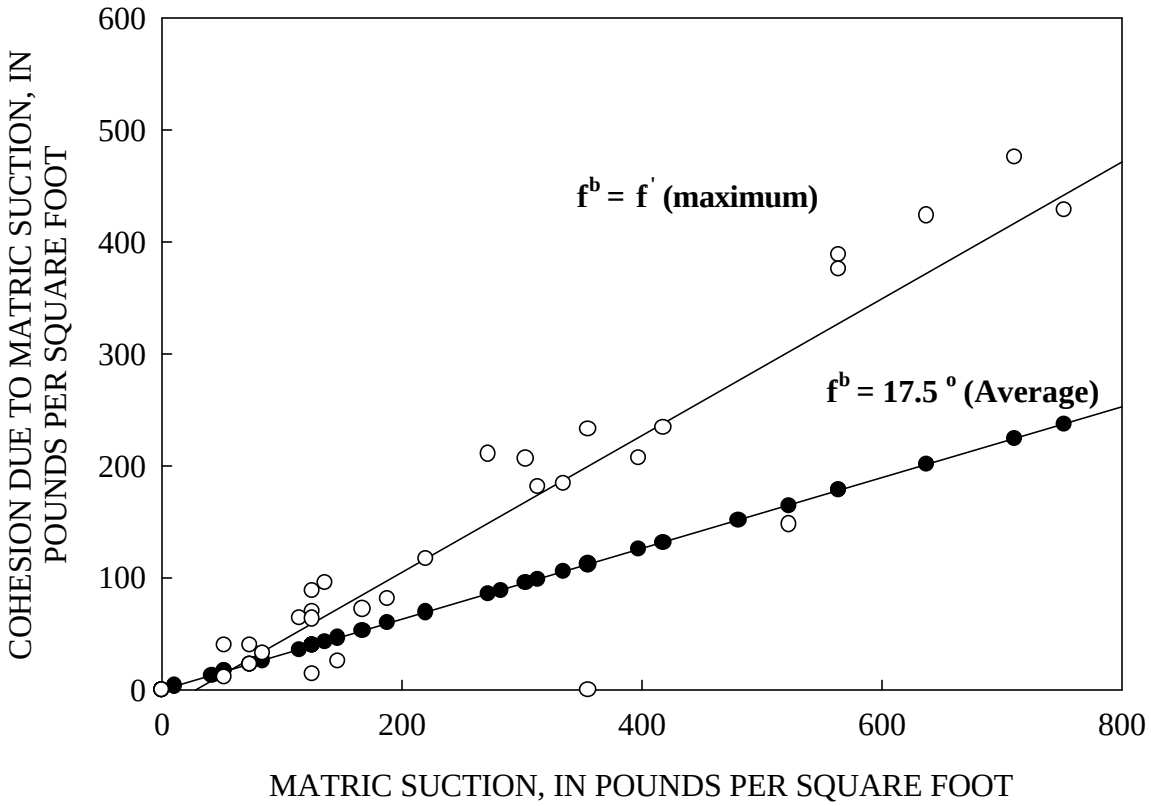

Figure 41--Contribution of matric suction to apparent cohesion assuming an average ϕ^b-angle of 17.5° compared with maximum possible value near saturation when $\phi^b = \phi'$.

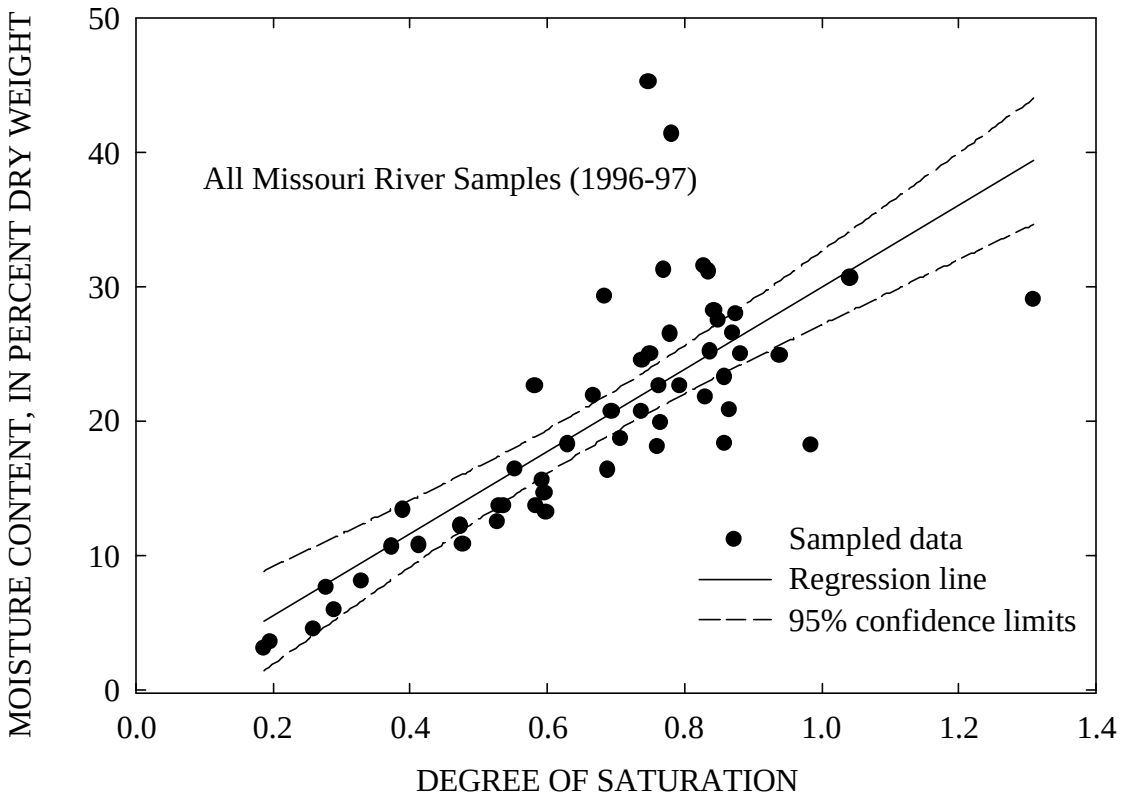

Figure 42--Relation between degree of saturation and moisture content showing range of moisture contents where negative pore-water pressures can develop.

flow than sand-sized materials that have no cohesive strength. Those streambanks with sandy bank-toe materials are more susceptible to bank failure for a given bank height and bank strength because of the likelihood that this material will be eroded, resulting in steeper or undercut banks. Sites with sandy bank toes are located at River Miles 1604 (Hardy); 1624-low terrace (Tveit-Johnson); 1624 (Tveit-Johnson); 1631 (Vournas); 1646 (Mattelin); 1676 (Woods Peninsula); 1716 (Pipal); and 1765 (Garwood). Silty bank-toe material occurs at River Mile 1728 (Flynn Creek).

BANK STABILITY ANALYSES

Three types of bank-stability analyses were conducted in this study to evaluate the stability of the sites. All three analyses take into account measured soil properties of the bank materials, while only two consider directly the magnitude of forces acting on the bank under different hydrologic conditions. Results are expressed in terms of critical bank height (above which there is bank failure) as in the Culman analysis, or as a ratio between the driving and resisting forces acting within a bank along a potential failure surface. The ARS-method (Simon and Curini, 1998; Simon *et al*., 1999) is used to model planar failures, the most commonly observed failure type in the reach. Advanced commercial software (Geo-Slope, 1991) is used to model rotational failures.

Type I: Culman Wedge-Type Analysis: Theory

A factor of safety (F_s) is expressed as the ratio between the resisting and driving forces acting on a streambank. A value of unity indicates the critical case and imminent failure. Another way of computing imminent bank failure is to define the critical height of a particular streambank for a given bank angle. By calculating the critical height (H_c) for a range of bank angles, bank stability charts of critical bank height versus bank angle are developed for each site, to evaluate the relation between bank-stability conditions and past and present bank heights and angles.

Bank-stability charts are based on the Culman wedge-type analysis, which is particularly well suited for streambanks. The Culman analysis is limited to steep banks with or without tension cracks, which fail along approximately planar failure surfaces. Use of this analysis is appropriate for the sites visited in this study because (1) the banks visited exhibited evidence of recent geotechnical failures by this mechanism; and (2) tension crack development was observed at many of the sites visited.

For this type of analysis, Selby (1982) states that the critical bank height is a function of cohesion, friction angle, soil unit weight, and bank angle:

$$H_c = [4c_a \sin\beta \cos\phi'] / [\gamma (1 - \cos(\beta - \phi'))] \qquad (14)$$

Where H_c = critical bank height, in feet,
c_a = apparent cohesion, in pounds per square foot (lbs/ft^2),
γ = soil unit-weight, in pounds pounds per cubic foot (lbs/ft^3),
β = bank angle, in degrees, and
ϕ' = effective friction angle (degrees).

In soils where tension cracks are present or may develop, the critical bank height is reduced by the tension crack depth so that:

$$H_{cz} = H_c - z \qquad (15)$$

where H_{cz} = critical bank height with tension crack, in feet, and
z = tension crack depth, in feet.
The maximum depth of the tension crack is given in Selby (1982) by the formula:

$$z = (2c'/\gamma) \tan [45 + (\phi'/2)] \quad (16)$$

or by :

$$z = 2\, c_u / g_{sat} \quad (17)$$

where c_u = undrained cohesive strength.

Determination of Weighted-Mean Parameter Values

A drawback of the Culman analysis for layered streambanks is the requirement to input only one value for each of the geotechnical parameters: cohesion, friction angle, and soil unit weight. To overcome this, a weighted-mean value for each parameter was calculated as follows for each bank and failure scenario. First, measured values of cohesion, friction angle and soil unit-weight were assigned to each unit comprising the streambank (Table 31). If a particular unit had not been field tested, an assumed value was assigned to that unit based on the average of the tests for that material type (Table 32). Each value was then multiplied by the percentage of the bank height comprising each unit and summed to obtain the weighted-mean values for a given streambank. A summary of these values is provided in Table 32. An average value of f^b was assumed to be 17^0. Finally, the assignation of geotechnical parameter values for each unit was used for the Culman as well as subsequent analyses, where the effects of the individual units are numerically considered.

Using the weighted-mean values of apparent cohesion, friction angle and ambient unit weight (Table 33) outlined in the above procedure, bank-stability charts for ambient field conditions are constructed by iterating equation 14 for bank angles of 90, 80, 70, 60, 50 and 40^o (Figure 43). This procedure is then repeated assuming that the banks are undrained (completely saturated). Critical-bank heights (H_c) for worst-case conditions (undrained) are assessed using unconsolidated undrained strength parameters (f_u = friction angle = 0^o and c_u = cohesion) and the saturated unit weight (γ_s). However, without undrained strength data it was assumed that frictional strength is reduced to zero under saturated conditions because of excess pore-water pressures, leaving only the effective cohesive-strength to resist mass failure (Lutton, 1974). Effective cohesion (c') is used for saturated conditions. This procedure results in the lower, solid line of the figures 43-58. Tension crack depths for each site obtained either from equations 16 or 17, or from direct field evidence are used to obtain H_{cz} for both ambient and saturated conditions (dashed lines in Figure 43). The critical-bank conditions denoted by the lines in Figure 43 do not directly account for the effects of positive or negative pore-water pressures in the banks, or the confining pressure afforded by the water in the channel. This latter factor becomes important in assessing the effect of changing river levels .

At each study site, the geotechnical parameters of each representative soil series vary through time as a function of soil moisture content. To account for these changes and the presence of tension cracks, sensitivity analyses were undertaken to estimate a range of critical bank heights corresponding to the effects of tension crack development and variability in effective cohesion and effective friction angle. Thus four scenarios are represented for each site:

TABLE 31-- . Geotechnical values used for each soil unit for bank-stability modeling.

River Mile	Depth	Base of Failure Surface F.T.B.	USCS	c_a	c_u	c'	ϕ'	ϕ^b	ψ	γ_{amb}	γ_{sat}
	feet	feet		lbs/ft^2	lbs/ft^2	lbs/ft^2	degrees	degrees	lbs/ft^2	lbs/ft^3	lbs/ft^3
1589	11.0	-	ML	372	-	276	30.1	17.0	313	90.6	136
1589	16.8	15.3	CH-CL	190	-	153	29.1	17.0	120	114	141
1589	Assumed *	-	CH-CL	190	-	153	29.1	17.0	-	114	141
1604	8.99	-	CL	380	-	222	20.2	17.0	522	98	135
1604	16.1	-	CH-CL	311	-	270	23.3	17.0	136	107	134
1604	23.0	21.9	SM	38.7	-	35.5	32.9	17.0	10.4	104	133
1604	Assumed *	-	SM	38.7	-	35.5	32.9	17.0	-	104	133
1621	7.87	-	CH-CL	361	-	182	29.5	17.0	585	106	135
1621	10.5	-	CL	491	-	474	8.80	17.0	55.7	98.2	127
1621	Assumed *	17.1	CL	491	-	474	8.80	17.0	-	98.2	127
1624 (Low terrace)	2.00	-	SM-ML	0.00	-	0.00	30.9	17.0	-	82.7	98.0
1624 (Low terrace)	4.99	-	SP	0.00	-	0.00	26.4	17.0	-	107	134
1624 (Low terrace)	Assumed *	15.1	SP	0.00	-	0.00	26.4	17.0	-	107	134
1624	13.5	-	CL	648	-	196	26.9	17.0	-	98	131
1624	16.0	-	CL	675	-	659	5.50	17.0	-	107	132
1624	17.9	-	SM	38.7	-	38.7	32.9	17.0	-	129	146
1624	Assumed *	19.2	SM	38.7	-	38.7	32.9	17.0	-	129	146
1630	7.22	-	CL	339	-	262	28.3	17.0	-	100	132
1630	12.0	-	SP	0.00	-	0.00	35.0	17.0	-	115	138
1630	24.6	12.0	CL	-	1626	-	0.00	17.0	-	134	137
1631	6.99	-	ML-CL	333	-	177	20.9	17.0	-	106	135
1631	7.97	-	SP	0.00	-	0.00	35.0	17.0	-	85.8	135
1631	Assumed *	15.1	SP	0.00	-	0.00	35.0	17.0	-	85.8	135
1646	6.00	-	SM	0.00	-	0.00	38.1	17.0	-	85.8	127
1646	6.99	-	ML	372	-	211	30.1	17.0	-	100	132
1646	8.99	-	SP	96.1	-	0.00	35.4	17.0	-	105	136
1646	Assumed *	12.3	SP	96.1	-	0.00	35.4	17.0	-	105	136
1676	11.0	-	SM	46.0	-	7.52	26.9	17.0	125	92.1	136
1676	12.5	-	CL	-	1626	-	0.00	17.0	125	134	137
1676	13.0	-	SP	0.00	-	0.00	35.0	17.0	0.00	115	138
1676	Assumed *	19.3	SP	0.00	-	0.00	35.0	17.0	0.00	115	138
1682	11.0	-	CL	192	-	0.00	33.6	17.0	626	89.8	133
1682	13.5	-	SM	60.6	-	44.7	37.6	17.0	52.2	108	136
1682	23.0	23.0	CL	690	-	673	14.0	17.0	52.2	109	136
1682	Assumed *	-	CL	815	-	799	11.9	17.0	-	109	136
1701	8.99	-	CL	173	-	52.0	27.6	17.0	397	102	136
1701	9.97	-	SC	4.18	-	0.00	35.0	17.0	125	98.0	134
1701	22.0	19.9	CL	424	-	401	14.5	17.0	73.1	107	130
1716	8.01	-	CL	0.00	-	0.00	37.7	17.0	-	94.4	134
1716	12.5	-	CL-CH	525	-	466	13.4	17.0	-	110	136
1716	18.0	18.0	SM	0.00	-	0.00	37.9	17.0	-	97.0	133
1716	Assumed *	-	SM	0.00	-	0.00	37.9	17.0	-	97.0	133
1728	8.99	-	CL-CH	0.00	-	0.00	32.0	17.0	-	102	134
1728	12.0	-	CH	439	-	178	26.1	17.0	-	108	133
1728	18.0	18.0	CH	38.7	-	0.00	35.0	17.0	-	92.5	128
1728	Assumed *	-	SM	38.7	-	0.00	35.0	17.0	-	92.5	128
1737	2.99	-	CL	192	-	170	28.8	17.0	-	97.8	130
1737	4.00	-	CH	125	-	58.1	28.1	17.0	219	97.4	131
1737	16.0	-	CL	192	-	170	28.8	17.0	73.1	97.8	130
1737	Assumed *	17.0	CL	192	-	170	28.8	17.0	-	97.8	130
1744	6.00	-	CL-CH	213	-	104	33.2	17.0	355	97.0	134
1744	20.0	-	CL	372	-	330	22.5	17.0	136	95.9	126
1744	Assumed *	20.9	CL	372	-	330	22.5	17.0	-	95.9	126
1762	16.0	-	CH	620	-	579	9.90	17.0	136	104	128
1762	Assumed *	21.3	CH	620	-	579	9.90	17.0	-	104	128
1765	9.02	-	CH	163	-	43.2	33.8	11.0	616	85.9	128
1765	12.3	-	SM	38.7	-	38.7	32.9	11.0	-	92.5	128
1765	13.9	13.9	CL	23.0	-	23.0	28.9	11.0	334	89.2	135
1765	27.1	-	SM	38.7	-	38.7	32.9	11.0	-	92.5	128

Assumed * - Values assumed below the termination depth of the boring.

Table 32-- Assumed geotechnical values for untested soil units of a given soil type.

Material type	***c'* (lbs/ft^2)**	**ϕ' (degrees)**	**γ_{amb} (lbs/ft^3)**
SP (sand)	0.0	35.0	115
SM (silty sand)	39.2	32.9	92.0
ML (silt)	350	30.1	100
CL* (clay)	1650	0.0	134

* = undrained parameter values c_u; ϕ_u, and γ_{sat}

TABLE 33 - Weighted mean values used in Culman analysis.

River Mile	**Soil Series**	**c_a**	**c'**	**ϕ'**	**γ_{amb}**	**γ_{sat}**
		lbs/ft^2	lbs/ft^2	degrees	lbs/ft^3	lbs/ft^3
1589	Havrelon	322	242	29.9	96.8	138
1604	Lohler	357	278	19.2	103	134
1621	Havrelon	462	334	22.6	103	127
1624	Riverwash	0	0			
1624	Lohler	631	305	24.4	118	134
1630	Havrelon	203	157	31.0	106	134
1631	Banks	153	81.7	28.5	94.9	135
1646	Trembles	71.0	16.9	36.6	95.5	131
1676	Trembles	156	135	27.6	104	137
1682	Shambo	432	332	25.1	99.3	132
1701	Gerdrum	357	290	22.6	104	134
1716	Havrelon	131	117	29.8	98.0	128
1728	Harlem	87.5	30.1	32.1	99.9	136
1737	Harlem	188	161	28.8	98.0	130
1744	Harlem/Till	325	264	25.6	96.1	128
1762	Harlem	796	718	8.60	104	128
1765	Havre-Harlem	118	39.9	33.0	87.8	129

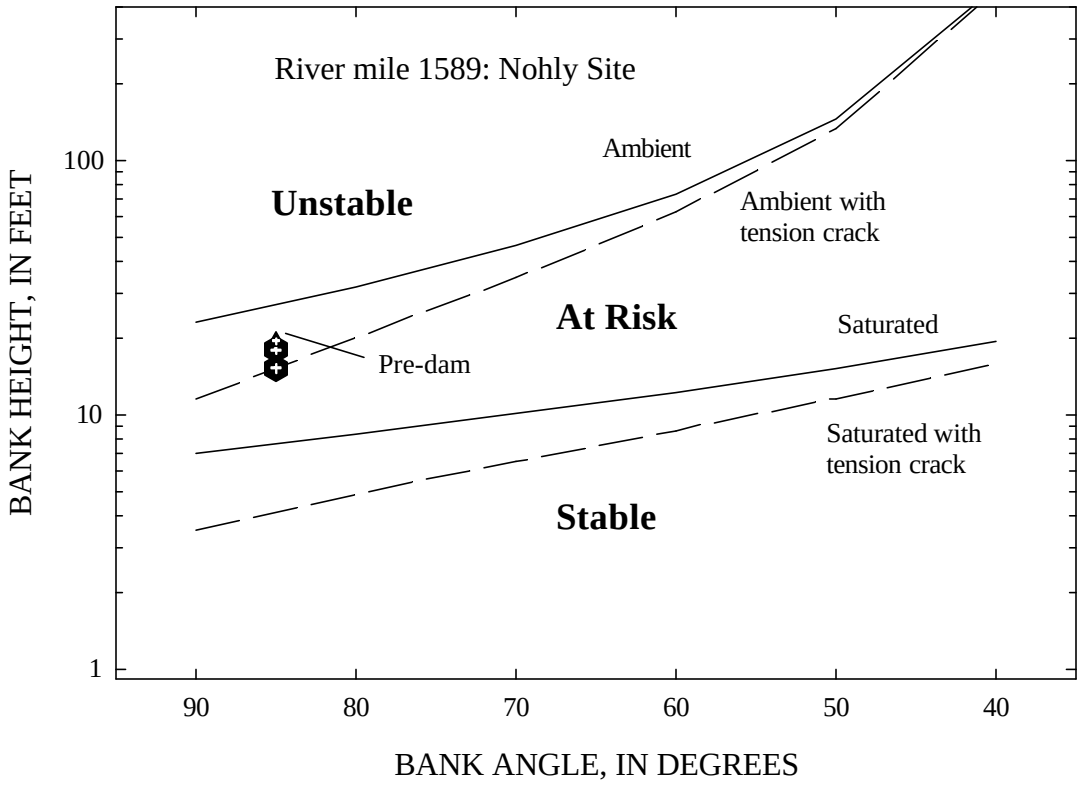

Figure 43--Bank-stability chart for River Mile 1589 (Nohly) developed with the Culman analysis and showing pre-dam and post-dam bank heights and angles.

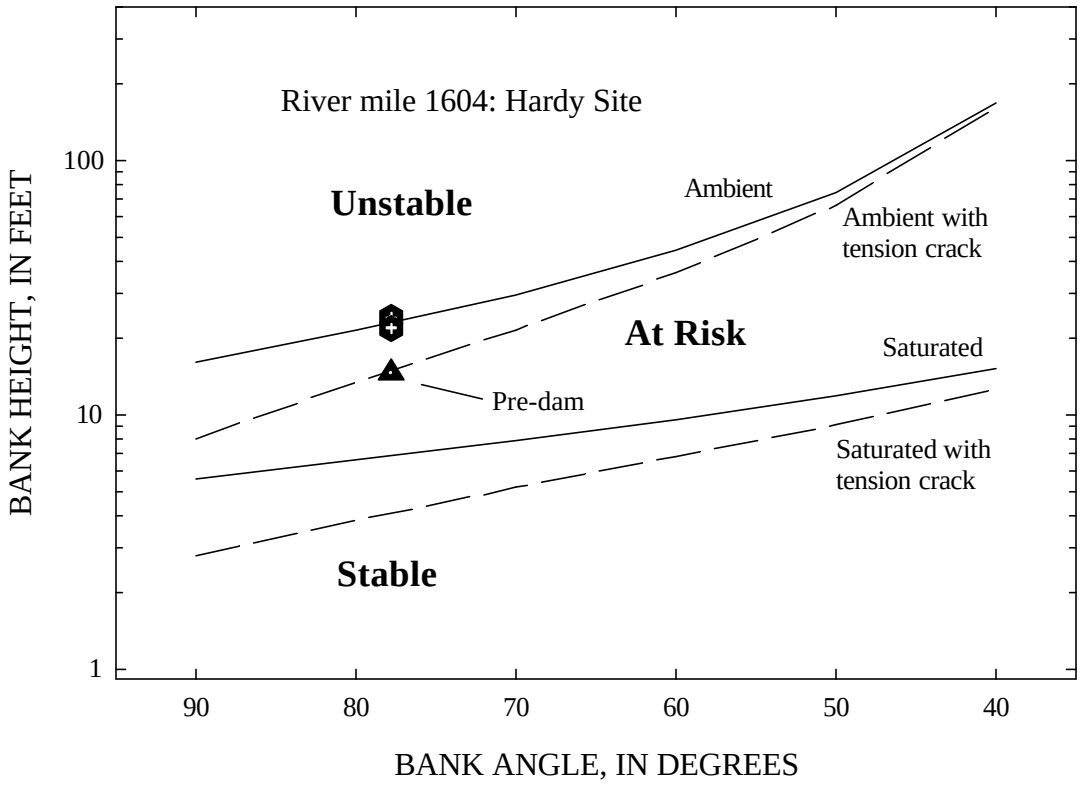

Figure 44--Bank-stability chart for River Mile 1604 (Hardy) developed with the Culman analysis and showing pre-dam and post-dam bank heights and angles.

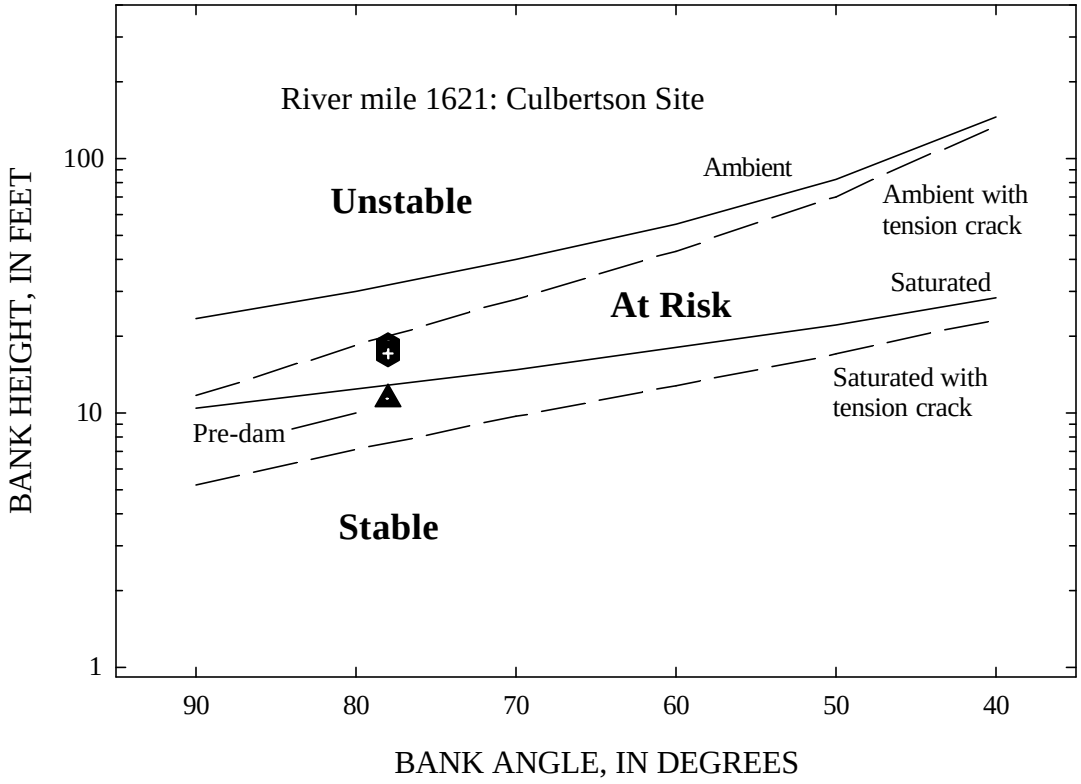

Figure 45--Bank-stability chart for River Mile 1621 (Culbertson) developed with the Culman analysis and showing pre-dam and post-dam bank heights and angles.

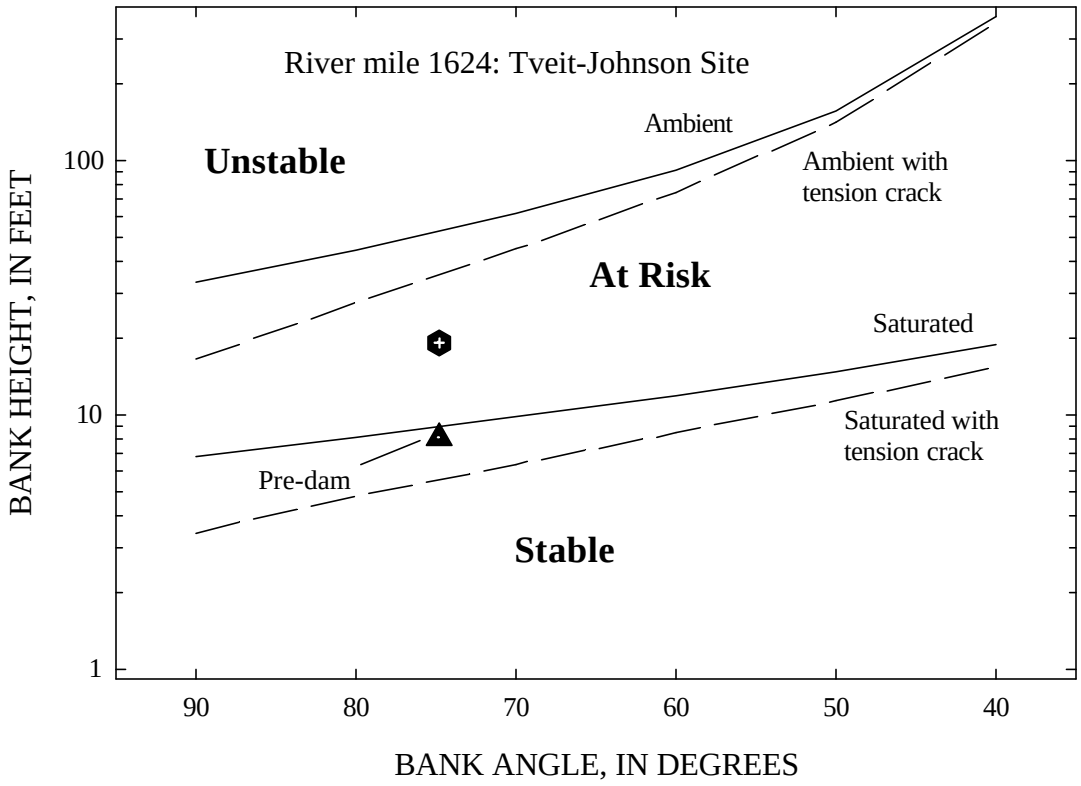

Figure 46--Bank-stability chart for River Mile 1624 (Tveit-Johnson) developed with the Culman analysis and showing pre-dam and post-dam bank heights and angles.

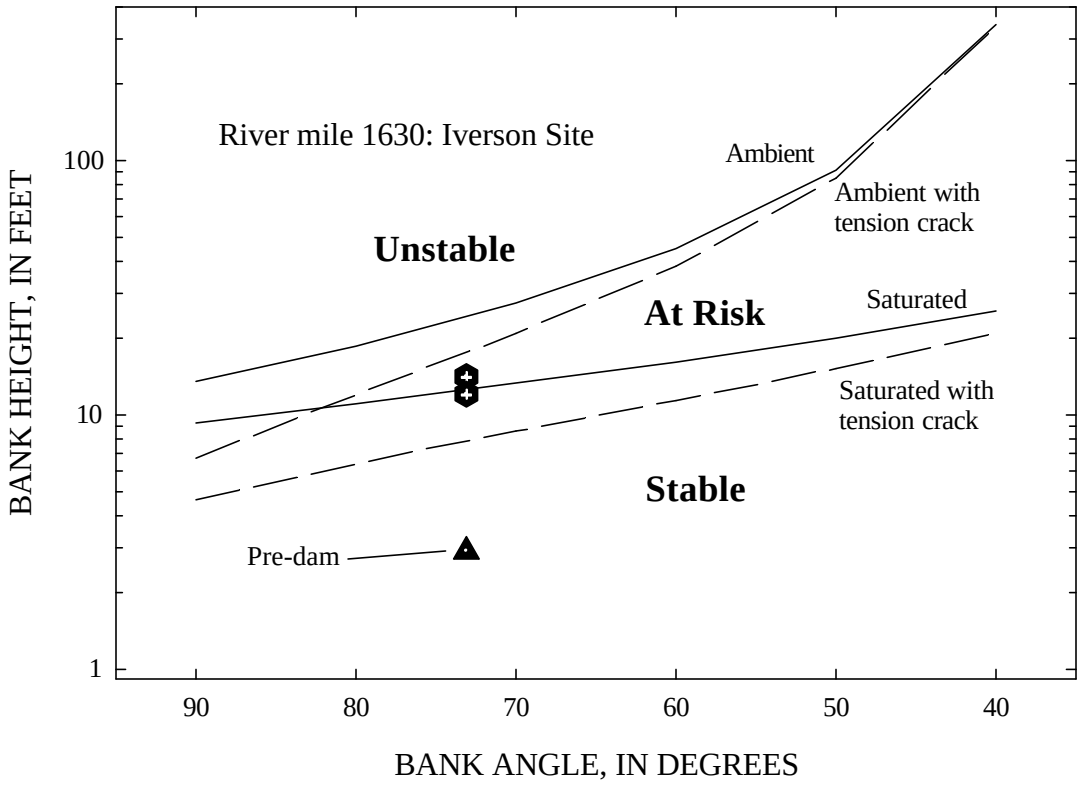

Figure 47--Bank-stability chart for River Mile 1630 (Iverson) developed with the Culman analysis and showing pre-dam and post-dam bank heights and angles.

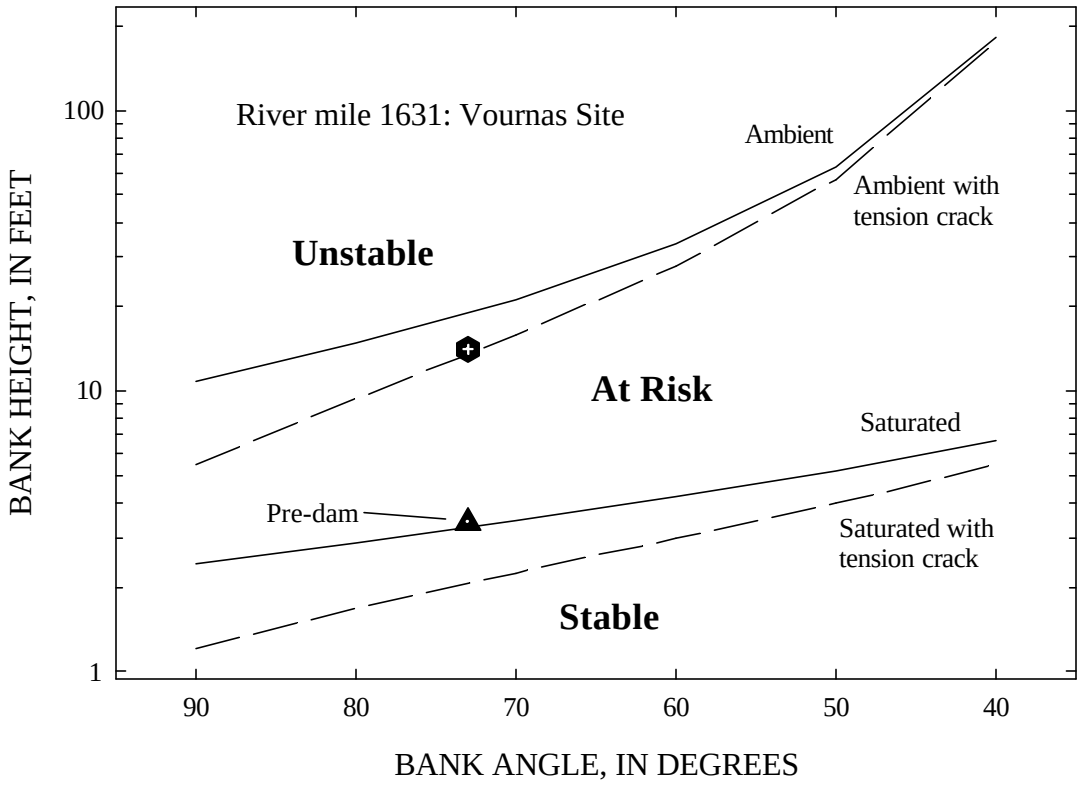

Figure 48--Bank-stability chart for River Mile 1631 (Vournas) developed with the Culman analysis and showing pre-dam and post-dam bank heights and angles.

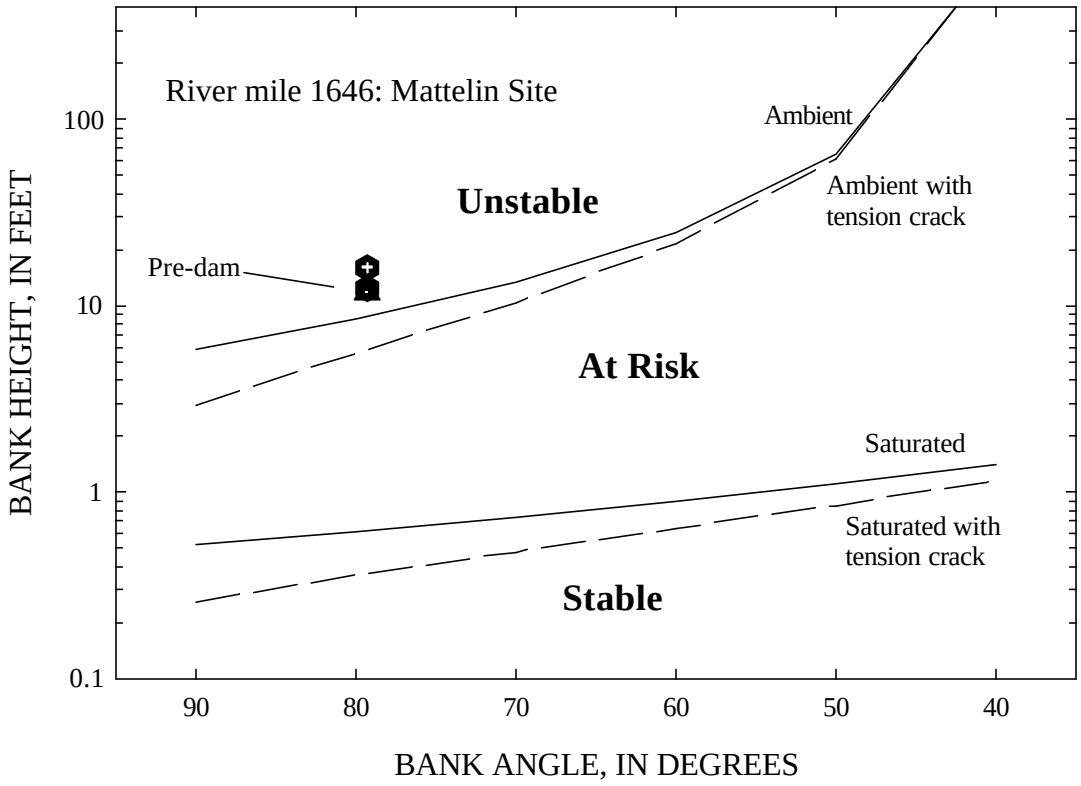

Figure 49--Bank-stability chart for River Mile 1646 (Mattelin) developed with the Culman analysis and showing pre-dam and post-dam bank heights and angles.

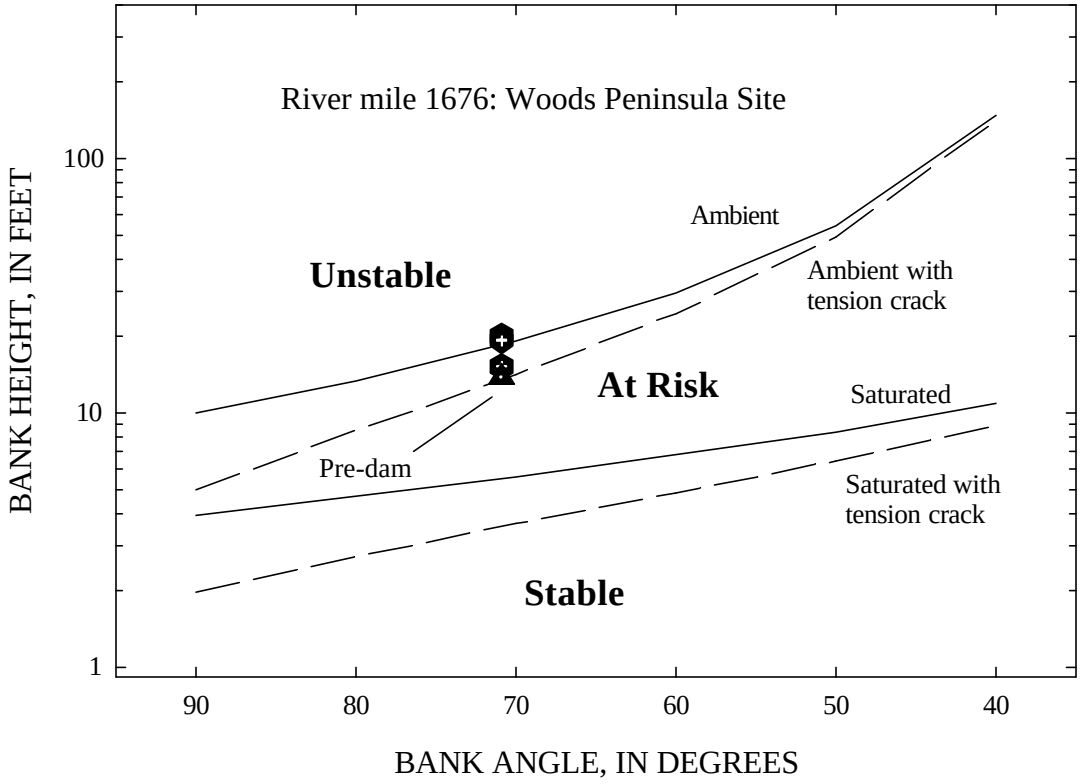

Figure 50--Bank-stability chart for River Mile 1676 (Woods Peninsula) developed with the Culman analysis and showing pre-dam and post-dam bank heights and angles.

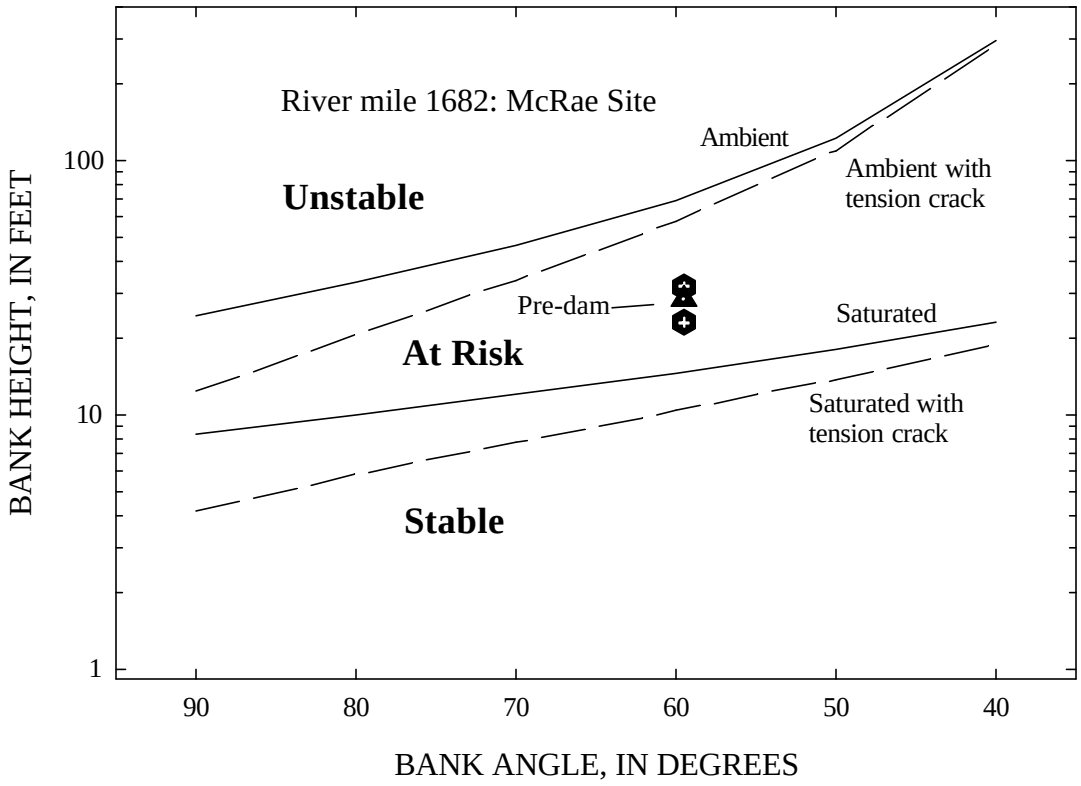

Figure 51--Bank-stability chart for River Mile 1682 (McRae) developed with the Culman analysis and showing pre-dam and post-dam bank heights and angles.

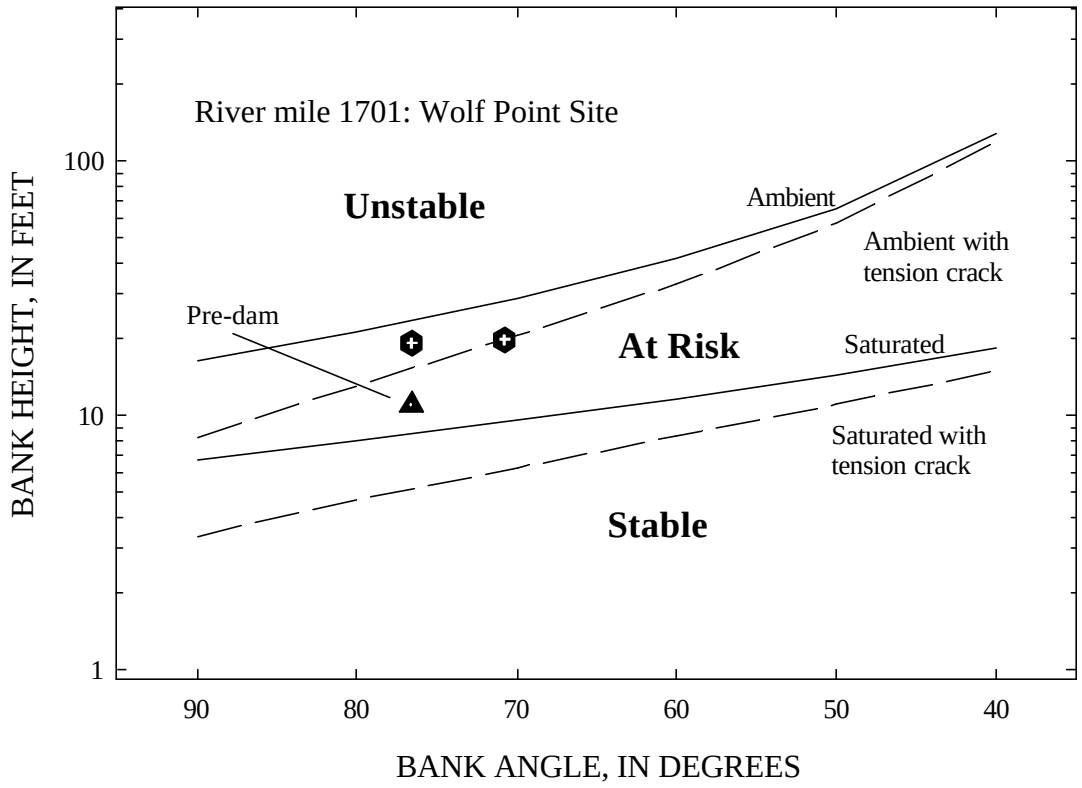

Figure 52--Bank-stability chart for River Mile 1701 (Wolf Point) developed with the Culman analysis and showing pre-dam and post-dam bank heights and angles.

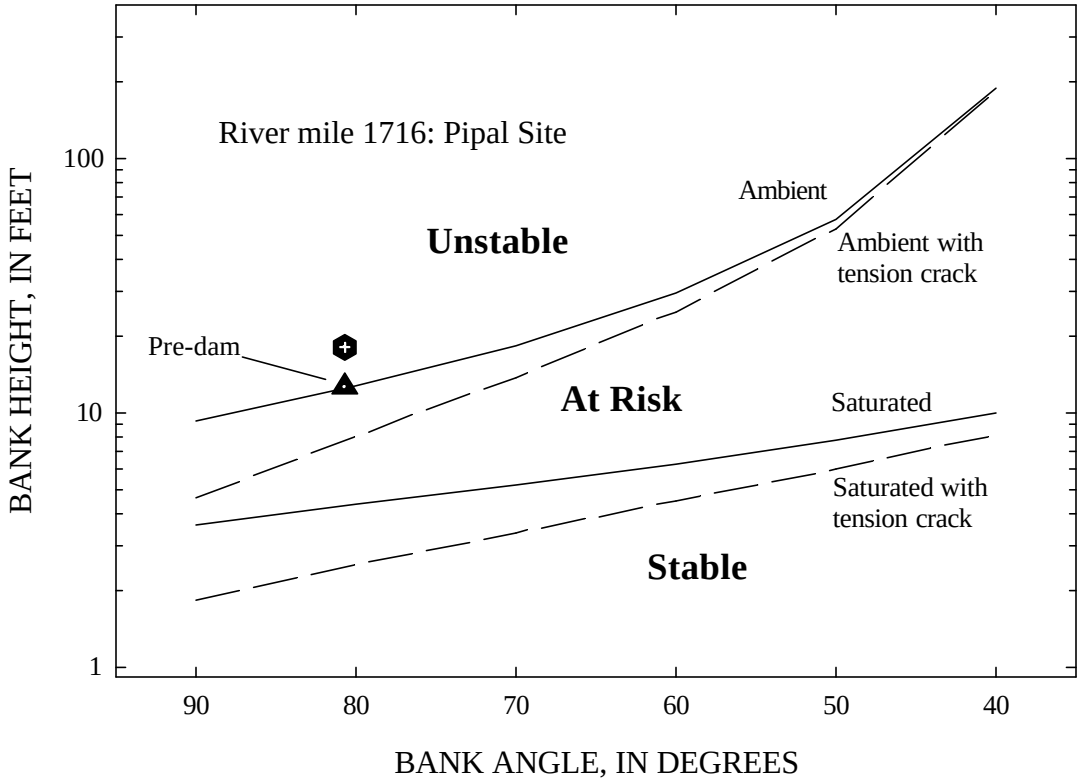

Figure 53--Bank-stability chart for River Mile 1716 (Pipal) developed with the Culman analysis and showing pre-dam and post-dam bank heights and angles.

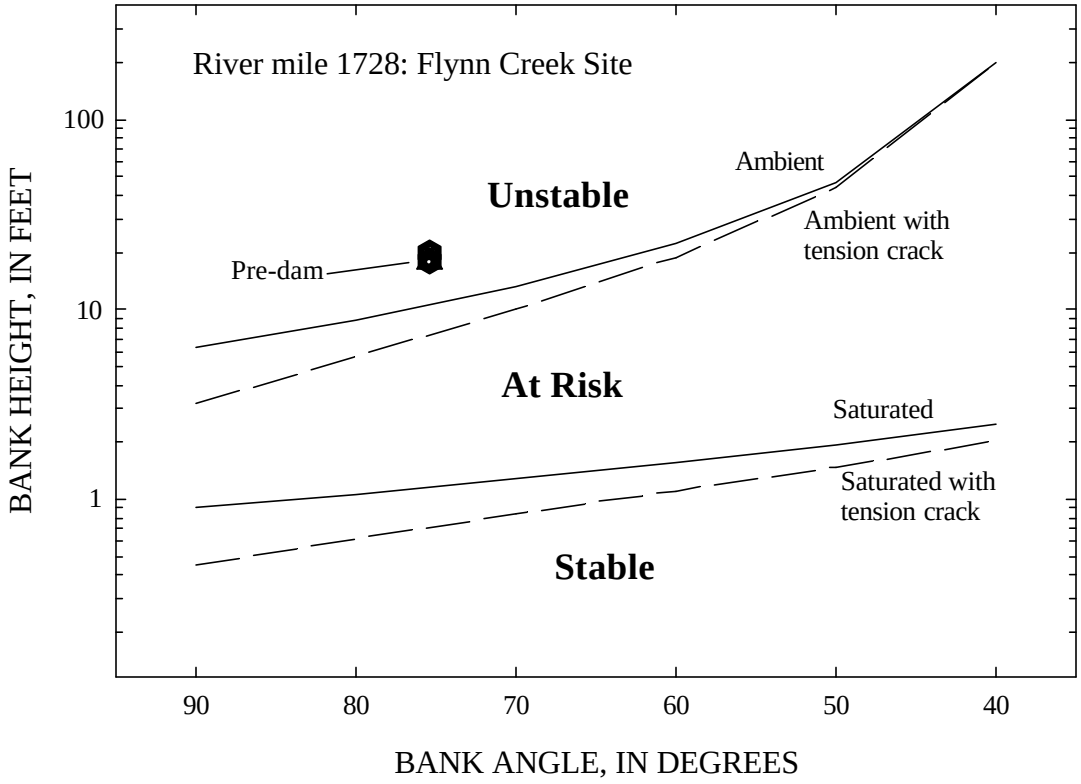

Figure 54--Bank-stability chart for River Mile 1728 (Flynn Creek) developed with the Culman analysis and showing pre-dam and post-dam bank heights and angles.

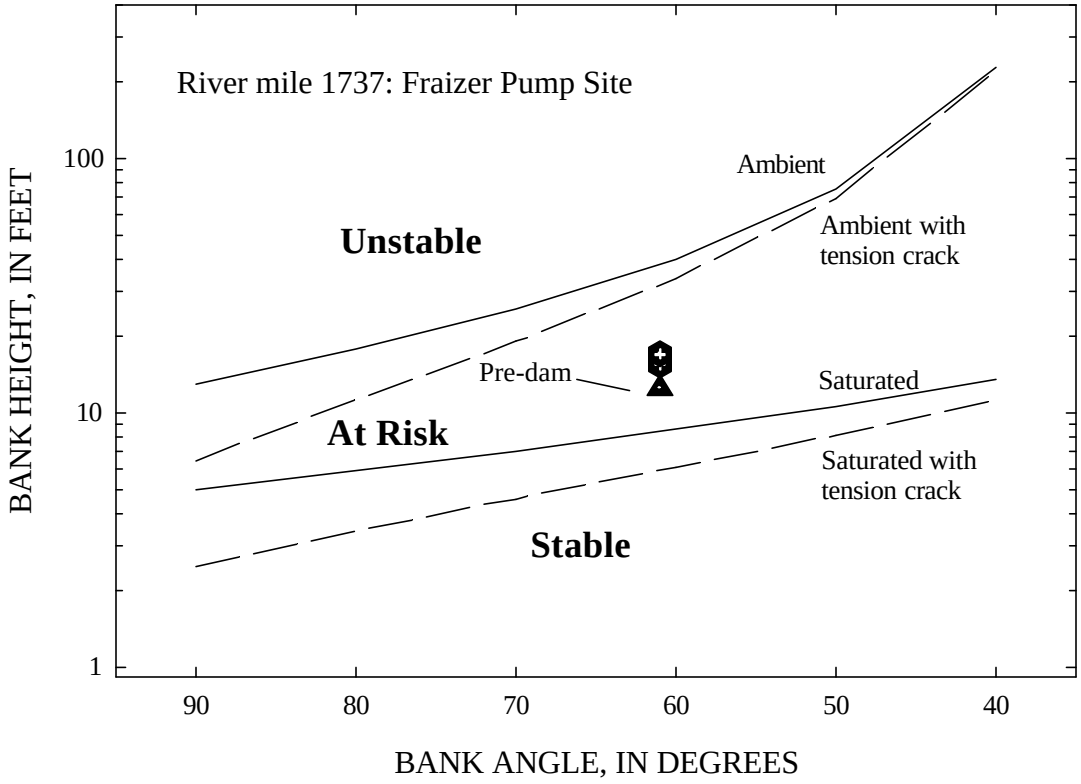

Figure 55--Bank-stability chart for River Mile 1737 (Fraizer Pump) developed with the Culman analysis and showing pre-dam and post-dam bank heights and angles.

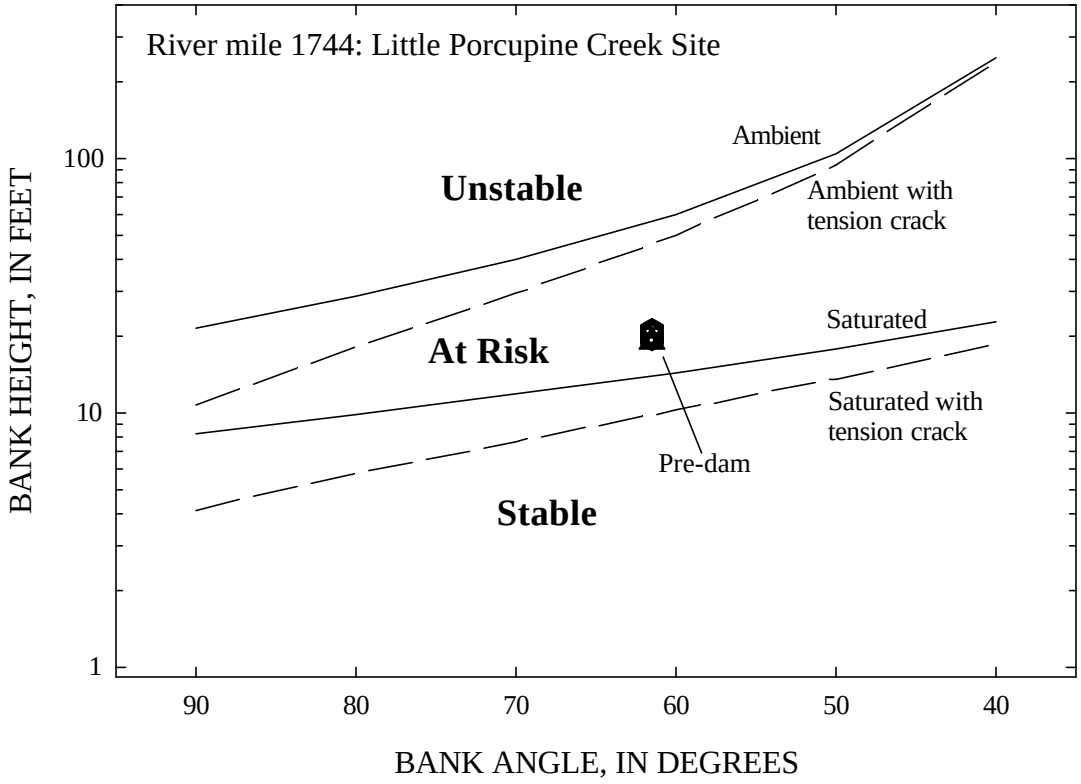

Figure 56--Bank-stability chart for River Mile 1744 (Little Porcupine) developed with the Culman analysis and showing pre-dam and post-dam bank heights and angles.

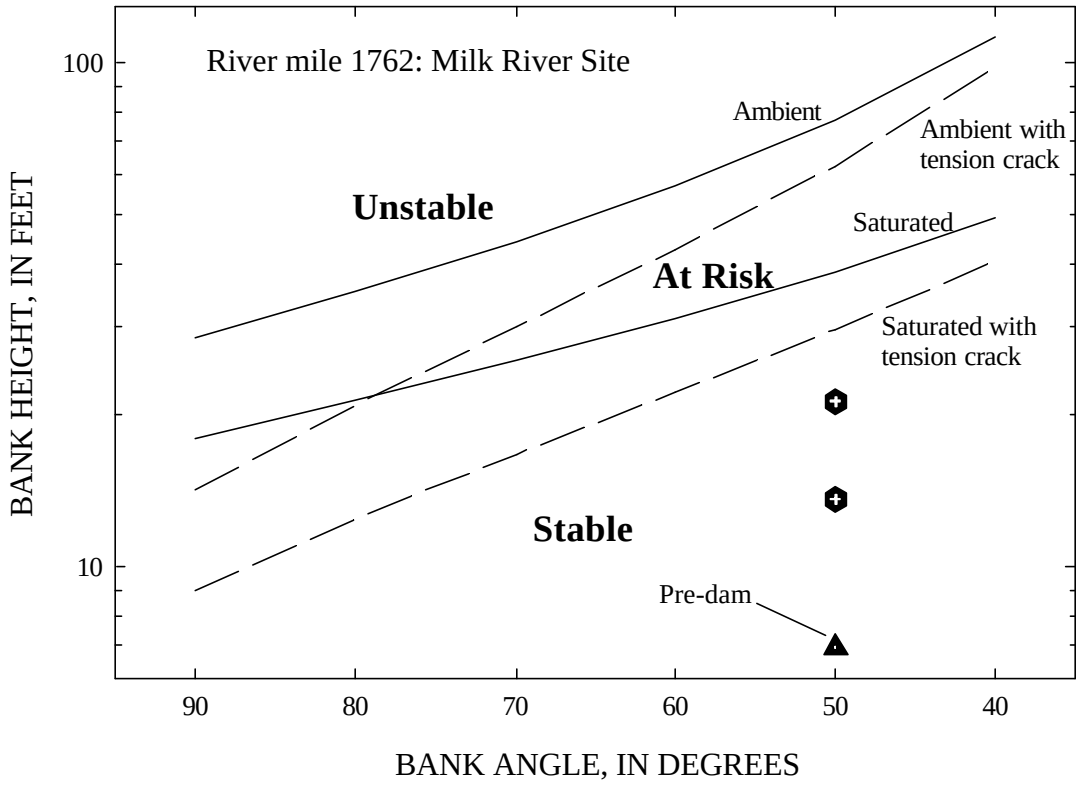

Figure 57--Bank-stability chart for River Mile 1762 (Milk River) developed with the Culman analysis and showing pre-dam and post-dam bank heights and angles.

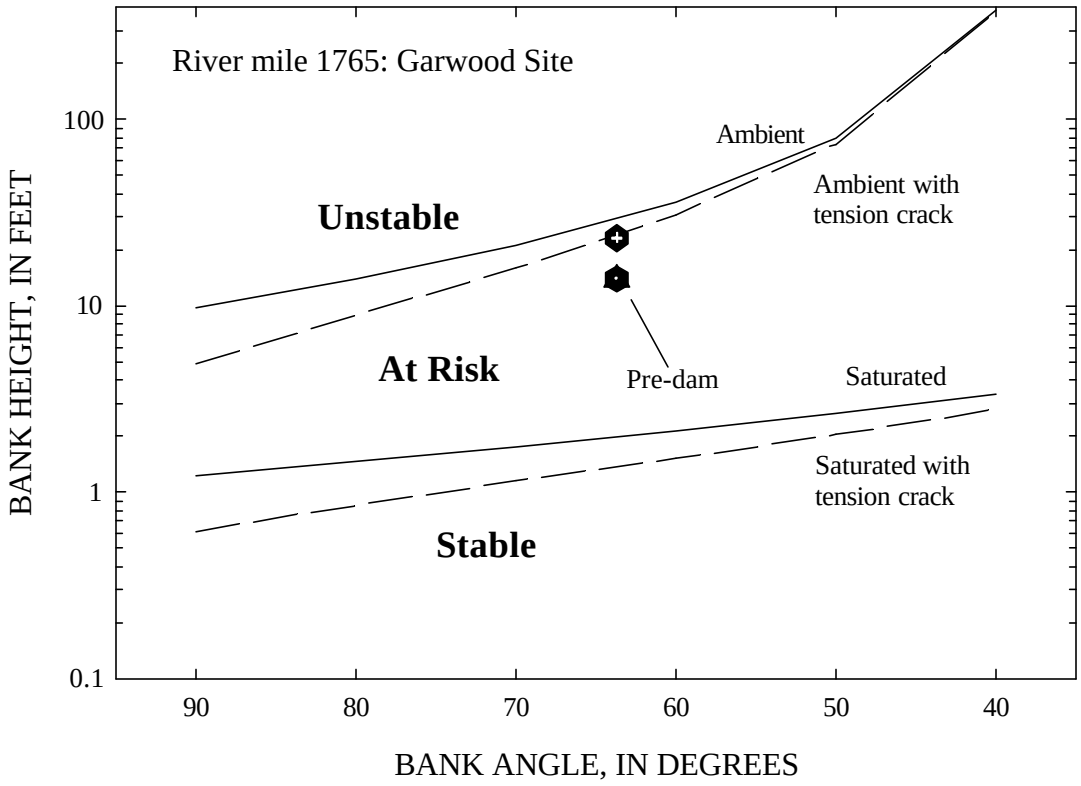

Figure 58--Bank-stability chart for River Mile 1765 (Garwood) developed with the Culman analysis and showing pre-dam and post-dam bank heights and angles.

(1) ambient conditions without tension crack development;
(2) ambient conditions with tension crack development;
(3) worst-case conditions without tension crack development, and;
(4) worst-case conditions with tension crack development.

The term "ambient conditions" refers to values of effective cohesion, effective friction angle and unit weight measured in the field at the time of the site visits. The term "worst-case" conditions refers to estimated values when the soil is fully saturated, as might occur after prolonged or heavy rainfall, or after prolonged periods of inundation.

The frequency of bank failure for the four stability classes is subjective but is based on extensive empirical field data from eastern Nebraska, northern Mississippi, western Iowa, and West Tennessee. An "unstable" channel bank can be expected to fail at least annually and possibly after each major flow event (assuming that there is at least one in a given year). "At-risk" conditions indicate that bank failure can be expected every 2-5 years, again assuming that there is a runoff event that is sufficient to saturate the channel banks. "Stable" banks by definition do not fail by mass-wasting processes. Although channel banks on the outside of meander bends may widen by particle-by-particle erosion and this may ultimately lead to collapse of the upper part of the bank, for the purposes of this discussion, stable-bank conditions refer to the absence of mass wasting.

During the majority of the year, when the banks are relatively dry, ambient conditions can be used to assess streambank stability. However, it is the relatively short-lived periods where critical conditions such as high water tables and low river levels may occur that are conducive to bank instabilities. This stability analysis and the others to follow cannot take into account the various effects of river ice. The impact of freezing and thawing of bank materials can potentially be evaluated with additional data on freezing depth, soil temperature, and pore-water pressures.

Results of Culman Analysis: Application

Results of the Culman analysis are in general agreement with field observations of failure frequency. Bank geometries (height and angle) are represented in two different ways: (1) the distance from the bank top to the 5,000 ft^3/s water surface and (2), the distance from the bank top to the base of the modeled failure surface. Of the 16 bank-stability charts (all but the low terrace of River Mile 1624), only the Milk River site at River Mile 1762 is stable under all modeled scenarios (Figures 43-58). This is not surprising given the relatively high weighted-mean cohesive strength of 796 lbs/ft^2 calculated for this site (Table 33). The plotted points on each of the bank-stability charts represent 2 different bank heights, pre-dam and current.

Sites at River Miles 1646 (Mattelin), 1716 (Pipal), and 1728 (Flynn Creek) are shown to be unstable even under ambient conditions. These sites have the lowest weighted-mean cohesion values amongst the sites studied. The upper units of these banks contain weak silts and sands in the former case, and dried, fissured clays in the latter two cases. The sites at River Miles 1716 and 1728 also have sand units at the bank toe, making them particularly susceptible to undercutting and oversteepening. Banks at River Mile 1604 (Hardy) are also particularly unstable due to high banks. Streambanks at all of the remaining sites are in the “at risk” category indicating that there are various scenarios

of oversteepening, tension-crack development, and saturation that will cause them to fail at the given bank height.

It can be seen, then, that by moving downward (decreasing bank height) and to the right (flattening of bank angle) in any of the bank-stability charts the relative stability of a given bank will improve. In this way, the bank-stability chart can be used to determine a stable geometry under certain moisture and tension-crack scenarios. These are the types of considerations that are necessary in attempting to design a stable-bank alignment. However, it is unrealistic to assume that bank protection could be achieved by lowering of bank heights because this would mean filling the channel. The other option involves reducing bank angles. Of course, this also involves the loss of land. However, if the bank toe can be protected and not permitted to steepen, a stable bank angle can be sustained. With the average bank height for the studied sites being 18.4 feet (standard error = 1.14), completely stable angles would need to be about 40 degrees for most sites.

Effects of Bed Degradation and Dam Closure

In a similar manner, the effects of bed degradation on bank heights and bank stability can be evaluated for each site using the bank-stability charts. Comparison of 1936 and 1994 bed-elevation data permits us to estimate the changes in bank height if we assume that the changes (either maximum or average) occur adjacent to the streambank (Table 4). This is of course not always so but, in the case of a degrading channel bed and increasing bank heights, it provides a mechanism by which to estimate the maximum potential effects of dam-induced degradation. Maximum possible values are obtained by comparing thalweg elevations while more moderate changes are derived from average bed elevations. Negative values indicate that bank height was reduced over the period 1936-1994 (Table 34). For example, at River Mile 1621 (Culbertson site), the maximum possible increase in bank height was 7.0 feet since dam closure (assuming the thalweg is against the bank). If 7.0 feet is subtracted from the points plotted on the bank-stability chart for River Mile 1621 (Figure 45), the indicated bank-stability class would change from “at risk” at 18.3 feet-high in 1994 to “stable” at 11.3 feet in 1937. By analogy, the Iverson site at River Mile 1630 was “stable” pre-dam at 14.1 – 11.2 = 2.9 feet above low water and is currently “at risk” at 14.1 feet (Figure 47). At River Mile 1716 (Pipal site) the estimated 5.5-foot increase in bank heights turned an “at risk” bank into an “unstable” bank (Figure 53). In many of the cases studied, the post dam bank-stability class as determined by the Culman analysis is more critical than the pre-dam bank-stability class (Table 34). However, in less than half of the sites did the stability class worsen.

Estimated Widening

Future amounts of widening for a given bank (assuming stability or protection of the bank toe) can be estimated using the technique described above. This is done by projecting the current (1998) bank height and angle horizontally to the right until it intersects one of the “stable” lines. This will provide the stable bank angle. This is then plotted on the bank cross-section and extended to the elevation of the top of the bank. The horizontal distance between the existing bank edge and the point where the plotted

Table 34. Pre- and post-dam bank-stability classes for each study site according to changes in thalweg elevation between 1936 and 1994, and results of the Culman analysis (Figures 43-58).

River mile	Site name	Estimated change in bank height, in feet 1936-1994		Pre-dam bank height, in feet	Post-dam bank height, in feet*	Pre-dam classification using Culman	Post-dam classification using Culman
		Maximum Possible	Average				
1589	Nohly	-1.50	-3.80	19.5	18.0	At risk	At risk
1604	Hardy	9.50	1.70	14.6	24.1	At risk	Unstable
1621	Culbertson	7.00	-0.70	11.3	18.3	Stable	At risk
1624 (LT)	Tveit-Johnson	-	-	-	11.2	-	-
1624	Tveit-Johnson	11.1	0.00	8.09	19.2	Stable	At risk
1630	Iverson	11.2	-4.30	2.91	14.1	Stable	At risk
1631	Vournas	10.5	-4.40	3.38	13.9	At risk	At risk
1646	Mattelin	4.30	-2.00	11.8	16.1	Unstable	Unstable
1676	Woods Peninsula	5.50	-6.60	13.8	19.3	At risk	Unstable
1682	McCrae	3.60	-4.20	28.4	32.0	At risk	At risk
1701	Wolf Point	8.30	-2.80	11.0	19.3	At risk	At risk
1716	Pipal	5.50	-1.80	12.6	18.1	At risk-unstable	Unstable
1728	Flynn Creek	2.30	1.10	17.7	20.0	Unstable	Unstable
1737	Fraizer Pump	2.90	1.70	12.5	15.4	At risk	At risk
1744	L. Porcupine	0.70	-1.20	19.1	19.8	At risk	At risk
1762	Milk River	6.70	5.70	6.95	13.6	Stable	Stable
1765	Garwood	5.90	6.40	13.9	19.8	At risk	At risk

* Bank height above the 5000 ft^3/s discharge elevation in 1994.

line intersects the top bank surface represents the projected amount of future widening on that side of the river. Table 35 lists amounts of projected widening calculated by the above method and the stable angle that was used. Projected amounts of widening range from 0-2 feet at River Mile 1630 to more than 100 feet at River Miles 1676 and 1716. The site at River Mile 1630 (Iverson) shows limited future widening because of the relatively low bank heights (12-14 feet) at this location. Sites having the greatest maximum projections of future widening are characterized by weak bank materials and tall banks (Tables 33 and 35).

The Culman analysis is a static-type analysis in that the frequency of occurrence of "worst-case" or "ambient" conditions is not considered. A more dynamic analysis can be accomplished by considering the effect of changing moisture content, pore-pressure distributions and unit weights in the streambank.

Dynamic Modeling Scenarios: Theory

To provide a more physically based analysis of bank-failure occurrence, conditions and frequency, planar and rotational failures were modeled using geotechnical data specific to each bank layer (Table 31) and assumed hydrologic condition. Each bank was modeled under five different hydrologic conditions in an attempt to represent the spectrum of possible combinations of pore-water pressures in the banks and confining pressures in the channel. This was accomplished by varying the level of the groundwater (phreatic) surface relative to the elevation of the water in the channel. All elevations are referenced to the water-surface elevation of a given flow discharge (i.e. 5,000, 10,000, and 26,000 ft^3/s).

The five different modeling cases are:

1) river stage (RS) 26,000: groundwater stage (GW) 26,000;
2) RS 10,000: GW 26,000;
3) RS 10,000: GW 10,000;
4) RS 5,000: GW 10,000; and
5) RS 5,000: GW 5,000

Case 2, with high groundwater levels and relatively low flows in the channel are considered to be a worst-case, rapid-drawdown condition. Case 4 represents another drawdown case, but not as severe as Case 2. Conversely, Case 5 with low groundwater and surface-water levels is considered the most conservative because of the important effects of negative pore-water pressures on enhancing bank strength.

Elevations of the 10,000 and 26,000 ft^3/s water surfaces were obtained for each study from measured water-surface profiles reported in Wei (1997). Elevations of the 5,000 ft^3/s water surface were obtained by interpolating rating curves developed by Wei (1997) for seven gages in the reach. The gages are located at the following River Miles: 1766.96; 1763.5, 1751.33; 1736.64; 1727.56; 1701.22; and 1620.8.

Assumed Groundwater (Bank Saturation) Levels

There are probably numerous intermediate cases (not modeled here) where the phreatic surface along the Missouri River is below the 26,000 ft^3/s elevation but above the 10,000 ft^3/s elevation where loss of suction and generation of positive pore-water

Table 35. Projected amounts of future widening based on bank-stability charts and projection of existing bank height to a “stable” bank angle, and by assuming stability at the bank toe.

Site	Projected Widening[a], In Feet		Angle, In Degrees		Bank heigh	Bank height [f]
	Low Point	High Point	Low Point	High Point		
1589	11.9	15.6	49.0	42.0	18.0	15.3
1604	55.7	77.3	20.0	15.0	24.1	21.9
1621	5.85	7.05	61.0	58.0	18.3	17.1
1624	18.0	18.0	40.0	40.0	19.2	19.2
1630	0.16	2.07	74.0	66.0	14.1	12.0
1631	-[b]	-[b]	-[b]	-[b]	13.9	15.1
1646	-[b]	-[b]	-[b]	-[b]	16.1	12.3
1676	103	103	10.0	10.0	19.3	19.3
1682	11.7	27.4	40.0	23.0	32.0	23.0
1701	22.7	23.7	36.0	35.0	19.3	19.9
1716	110	110	9.00	9.00	18.1	18.0
1728	-[b]	-[b]	-[b]	-[b]	20.0	18.0
1737	16.7	23.9	33.0	27.0	15.4	17.0
1744	6.77	9.35	46.5	43.0	19.8	20.9
1762	-[c]	-[c]	50.0 [d]	50.0 [d]	13.6	21.3
1765	-[b]	-[b]	-[b]	-[b]	19.8	13.9

[a] Assumes a stable bank toe

[b] Unstable for all angles

[c] Bank is always stable

[d] Angle of existing bank (always stable)

[e] Above 5,000 ft^3/s water surface

[f] Above base of failure surface (ft)

pressures cause bank failures. In fact, for most of the banks all groundwater levels above the elevation of the 10,000 ft^3/s water surface would generate positive pore-water pressures on the assumed failure planes. Flow-duration data give only an indication of the frequency of river flows at or greater than specified discharges and not the frequency of groundwater levels (Figure 12). However, if a given stage is held for a prolonged period, water will move from the river a certain distance into the bank.

Regulated rivers such as the Missouri do maintain given stages during different times of the year more than a non-regulated river or the pre-dam Missouri River. If a moderate or high stage is released and maintained from the dam there is opportunity for the near-bank region to become saturated at levels above low water. If stage is then decreased relatively rapidly, a drawdown condition can occur, resulting in bank failures. If stage is reduced slowly, permitting positive pore-water pressures to dissipate, streambanks can sometimes maintain their strength and stability. It is interesting to note, however, that modeling results of Case 1 (RS and GW = 26,000 ft^3/s) reveal that about one third of the banks would be unstable ($F_s \leq 1.0$). This again emphasizes the importance of pore-water pressures in the weakening and de-stabilization of streambanks, even though confining pressures are at work and a drawdown condition is not in effect.

The data shown in Table 36 indicate that mean-daily flows equal to or greater than 10,000 ft^3/s occur about 57% of the time (on average, 207 days/yr), up from about 24% of the time for pre-dam conditions. Flows of 26,000 ft^3/s occur 5.2% of the time (on average, 19 days/yr). This does not mean that modeled worst-case conditions (Case 2) occur at these frequencies, only that there is a good potential for excess pore-water pressures to develop in the banks if discharges greater than 10,000 ft^3/s are maintained for prolonged periods.

To put these scenarios into perspective, clay banks have extremely slow hydraulic conductivity. A value of 10^{-8} m/s is a reasonable representation for solid beds of clay without cracks or fissures. This means that the infiltration of 3.3 feet (1.0 meter) landward would occur in 100,000,000 seconds. Considering that there are 86,400 seconds in a day, it would take over three years to cover that distance. However, considering that the banks along the Missouri River are full of cracks from desiccation, freeze-thaw, tension, rotted vegetation etc., it is not difficult to assume that hydraulic conductivity is significantly faster, with a value of 10^{-6} m/s being a reasonable estimate for silty materials and fissured clays. If this were the case, infiltration and saturation of a zone 3.3 feet into the bank can take place in about 10 days; 5 days for 1.67 feet (0.5 meters) while the river stage remains high over that period. This scenario provides a mechanism for the wetting and weakening of streambanks in the study reach.

To quantify this concept, an analysis of the percentage of time that discharges of 10,000; 15,000, 20,000, and 26,000 ft^3/s or greater are maintained for 5- and 10-day periods at the Wolf Point and Culbertson gages was conducted. Results indicate how often the maintained surface-water levels could cause ground-water levels of equal elevation, 1.67 and 3.3 feet into the bank. At the Wolf Point gage, data show that before the dam the modeled worst-case hydrologic conditions (Case 2) could not have caused 3.3 feet of saturation into the bank as a result of high-steady flows of 26,000 ft^3/s (Table 37). During the post dam period, however, Case 2 hydrologic conditions for 3.3 feet of infiltration can occur 0.9% of the time, or on average, about 3 times per year. The occurrence of steady flows is 4-5 times more frequent since dam closure. Phreatic levels at the 20,000 ft^3/s

Table 36-- Occurrence of range of discharges used in bank-stability modeling.

Discharge (ft^3/s)	**Percent of time equaled or exceeded**	
	Pre-dam	**Post-dam**
5,000	64.7	87.7
10,000	23.5	56.8
26,000	2.8	5.2

Table 37-- Average number of occurrences of 5- and 10-day duration flows at Wolf Point and Culbertson gages, showing increase in the occurrence of long-duration high flows after closure of Fort Peck dam.

Wolf Pt.												
Discharge	**Pre-dam 1928-1937**						**Post dam 1938-1996**					
($1,000's ft^3/s$)	**10-day duration**			**5-day duration**			**10-day duration**			**5-day duration**		
	n	Percent of time	n/yr	n	Percent of time	n/yr	n	Percent of time	n/yr	n	Percent of time	n/yr
26	0	0	**0.0**	13	0.4	**1.4**	198	0.9	**3.2**	305	1.4	**5.1**
20	17	0.5	**1.8**	47	1.4	**5.1**	593	2.8	**10.1**	805	3.8	**13.7**
15	59	1.7	**6.1**	117	3.5	**12.6**	1363	6.4	**23.1**	1875	8.7	**31.4**
10	245	7.3	**26.4**	370	11	**39.7**	6346	29.6	**107**	7603	35.4	**128**
Culbertson												
Discharge	**Pre-dam 1928-1937**						**Post dam 1941-1996**					
($1,000's ft^3/s$)	**10-day duration**			**5-day duration**			**10-day duration**			**5-day duration**		
	n	Percent of time	n/yr	n	Percent of time	n/yr	n	Percent of time	n/yr	n	Percent of time	n/yr
26	-			-			82	0.5	**1.8**	133	0.7	**2.5**
20	-			-			370	2.1	**7.6**	519	2.9	**10.5**
15	-			-			1157	6.5	**23.5**	1660	9.3	**33.6**
10	-			-			5947	33.2	**120**	7009	39.2	**142**

elevation, 3.3 feet into the bank can occur, on average 10 times per year compared to about 2 times per year pre-dam.

Similar post-dam results are shown for the Culbertson gage (Table 37). These results are particularly significant in that they provide a mechanism by which relatively high bank-saturation levels can reach critical conditions in a semi-arid environment. Finally, it should be noted that the last time flow levels were maintained above 20,000 ft^3/s for 5 to 10 days at the Wolf Point Gage was 1986. In the past 23 years this occurred in 1976, 1978, 1979, and 1982. 1979 was a particularly high-flow year with discharge levels above 26,000 ft^3/s for about a month. It is likely that bank instabilities were considerable that year.

The increase in the frequency of moderate and high-duration flows during the post-dam period is mostly attributable to dam operation and not the increase in precipitation during this period (Figure 10b). This is shown by the average annual frequency of the 5- and 10-day duration flows (Table 37), which are 66% and 82% less for the pre-dam period when compared to the post-dam period. These values are significantly greater than the difference in precipitation between the two periods, which is only 24% less in the pre-dam period.

Type 2: ARS Method for Planar Failures: Theory

An analytic method that accounts for variations in bank material as well as the effects of pore-water and confining pressures was required to obtain a better understanding of the failure conditions in the study reach. The effect of excess pore-water pressures on reducing bank strength under saturated conditions has long been identified as an important contributor to streambank and hillslope instability. Streambank failures are observed to occur on the recessional limb of storm hydrographs. This has been attributed to a rapid-drawdown condition in the channel banks where positive pore-water pressures are not counteracted by confining pressure afforded by the flowing water in the channel. Recently it has been found that positive or excess pore-water pressures may not be required to establish a rapid-drawdown condition that results in mass failure. In fact, data indicate that the loss of negative pore-water pressures, or suction, plays an important role in initiating bank instabilities following periods of rainfall (Casagli *et al*., 1997; Curini, 1998; Simon and Curini, 1998; Simon, *et al*., 1999; Casagli *et al*., in press).

A bank-stability algorithm for cohesive, layered banks has been developed by the ARS (Simon and Curini, 1998; Simon, *et al*., 1999) incorporating both the failure criterion of Mohr-Coulomb for the saturated part of the failure surface and the failure criterion modified by Fredlund *et al*., (1978) for the unsaturated part of the failure surface. The algorithm, based on the Limit Equilibrium Method, accounts for several additional forces acting on a planar failure surface. These include the:

1. force produced by matric suction on the unsaturated part of the failure surface (*S*);
2. hydrostatic-uplift force due to positive pore-water pressures on the saturated part of the failure plane (*U*), and
3. hydrostatic-confining force provided by the water in the channel (*P*)

(Casagli *et al*., 1998; Curini, 1998; Simon and Curini, 1998; Simon *et al*., 1999; Casagli *et al*., in press).

The confining force (P) provided by the water in the channel is the primary reason bank failures often occur after the peak flow and on the recession of flow hydrographs. The magnitude of this force acting on the bank surface is calculated by:

$$P = \gamma_w h^2 / 2 \sin \theta \qquad (18)$$

Multiple layers are incorporated through summation of forces in a specific (i^{th}) layer acting on the failure plane. The factor of safety (F_s) is then given by Simon *et al*., (1999):

$$F_s = \frac{\sum c_i' L_i + (S_i \tan \phi_i^b) + [W_i \cos \beta - U_i + P_i \cos(\alpha-\beta)] \tan \phi_i'}{\sum W_i \sin \beta - P_i \sin(\alpha-\beta)} \qquad (19)$$

where L_i = the length of the failure plane incorporated within the i^{th} layer;
S = the force produced by matric suction on the unsaturated part of the failure surface, in pounds per foot, (lbs/ft);
U = the hydrostatic-uplift force on the saturated portion of the failure surface, in lbs/ft; and
P = the hydrostatic-confining force due to external water level, in lbs/ft.

The algorithm described represents the continued refinement of bank-failure analyses by incorporating additional forces and soil variability (Osman and Thorne, 1988; Simon *et al*., 1991; Casagli, 1994; Darby, 1994; Rinaldi, 1994; Casagli *et al*., 1997; Curini, 1998; Simon and Curini, 1998; Simon *et al*., 1999.

Results of ARS Method for Planar Failures: Application

The idealized bank sections (Figures 59-74) display the modeled critical failure surface, F_s, river stage and groundwater levels, the location of BST tests and the differentiated soil units for each study site. All but four sites are unstable with a factor of safety (F_s) less than 1.0 under the worst-case, rapid-drawdown conditions (Case 2) described above (Table 38). The four sites, located at River Miles 1621 (Culbertson), 1682 (McCrae), 1744 (Little Porcupine), and 1762 (Milk River) are among the soils exhibiting the greatest cohesive strengths in the reach. In addition, each of these sites contains relatively resistant, cohesive bank-toe material rather than sand, which is more susceptible to erosion by fluvial entrainment.

Under the less critical drawdown scenario, Case 4, all of the modeled banks are stable, with the site at River Mile 1631 (Vournas) approaching a condition of instability. Saturation of only the lower portion of the bank, as happens with Case 4, generally is below the elevation of the base of the failure plane (i.e. Figures 59 and 64). Because of this, the loss of suction at the base of the bank does not affect bank strength and calculations of the factor of safety along the potential failure plane. It is interesting to note that where both river stage and groundwater levels are at the 26,000 ft^3/s level (Case 1), more than one-third of the banks are unstable. This occurs regardless of the confining pressures provided by the flow and is due to weakening of the banks by reduction of apparent cohesion and generation of positive pore-water pressures.

Figure 38-- Minimum factor of safety for planar failures under the given set of hydrologic conditions. Worst-case modeled conditions are represented by the second case where RS = the elevatioon of the 10,000 ft^3/s water surface and GW = the elevation of the 26,000 ft^3/s water surface.

Site	Planar Failures Minimum Factor Of Safety For Given Hydrologic Conditions				
	RS-26000 GW-26000	**RS-10000 GW-26000**	**RS-10000 GW-10000**	**RS-5000 GW-10000**	**RS-5000 GW-5000**
1589	1.36	0.85	1.60	1.54	1.75
1604	1.00	0.80	1.29	1.29	1.29
1621	1.64	1.41	1.83	1.83	1.84
.624 (Low Terrace	0.52	-	0.81	-	0.91
1624	1.23	0.83	1.58	1.50	1.67
1630	1.49	0.61	1.92	1.92	1.92
1631	0.77	0.11	1.12	1.09	1.20
1646	1.05	0.80	1.43	1.43	1.43
1676	1.20	0.95	1.56	1.56	1.56
1682	1.52	1.52	1.52	1.52	1.52
1701	1.23	0.99	1.44	1.42	1.52
1716	0.94	0.57	1.27	1.26	1.36
1728	0.81	0.60	1.16	1.16	1.16
1737	1.63	0.97	1.88	1.82	2.01
1744	1.92	1.57	2.15	2.11	2.28
1762	2.85	2.41	2.90	2.89	2.91
1765	0.99	0.64	1.30	1.30	1.35

RS = Elevation of river at given discharge
GW = Elevation of groundwater equal to specified river discharge

As pore-water pressures are increased and encompass larger portions of the failure surface, factors of safety will decrease towards the worst-case, Case 2 values. A significant amount of wetting in the bank mass is required to reduce matric suction and shear strength sufficiently to trigger mass failures. As shown previously, this can be accomplished by maintenance of high river stages. Again the direct and indirect effects of ice on bank erosion and land loss cannot be understated yet are not accounted for in these analyses.

Detailed Results from Each Site

This section details conditions and planar-failure modeling results for each study site. The idealized bank profiles of each site showing the bank-material units, levels of the 5,000, 10,000, and 26,000 ft^3/s water surfaces and the most-critical failure surface are shown in Figures 59-74. Bank heights referred to here are referenced to the elevation of the 5,000 ft^3/s water surface. Additionally, "RS" refers to elevation of the river and "GW" refers to elevation of the groundwater surface.

River Mile 1589--Nohly

The streambank is 18-feet high and is composed of a basal 6-feet thick layer of dark brown clay and an upper layer of light brown silt, 11-feet thick. The borehole was augered to 17 feet. The bank is unstable under the worst-case condition (Case 2) with a factor of safety of 0.85. Given the same failure dimensions, the factor of safety is greater than 1.0 (stable) for the other hydrologic cases modeled. The highest factor of safety (1.75) is reached during the low water stage (Case 5). Such a high factor of safety is due to high negative pore-water pressures and low soil unit weight.

Observations of fresh failure surfaces and failed blocks at the bank toe confirm the occurrence of recent failures at this site. The average block size of the failed material is 1.6 feet.

River Mile 1604-- Hardy

The streambank is 24.1 feet high and is composed of a basal layer of sand 7-feet thick, a middle 7-feet thick layer of dark brown clay and an upper 9-feet thick layer of silty clay. The borehole was augered to a depth of 23 feet. The bank is unstable under the worst-case condition (Case 2) with a factor of safety of 0.8. Given the same failure dimensions, the factor of safety is greater than 1.0 (stable) for the other hydrologic cases modeled. As is shown in Table 38, three different hydrological conditions have identical factors of safety (1.29) because the failure plane is above the 5,000 and 10,000 ft^3/s stages. Therefore, changes in head do not affect the stability of the bank. Unstable conditions are also reached when groundwater and river stage elevations are at 26,000 ft^3/s (F_s = 1.0). This is because the confining pressure afforded by the flow is insufficient to counteract the loss of shear strength caused by pore-water pressures. The presence of failed blocks at the bank toe confirm the occurrence of recent failures at this site. The average width of the failed blocks is 3.6 feet.

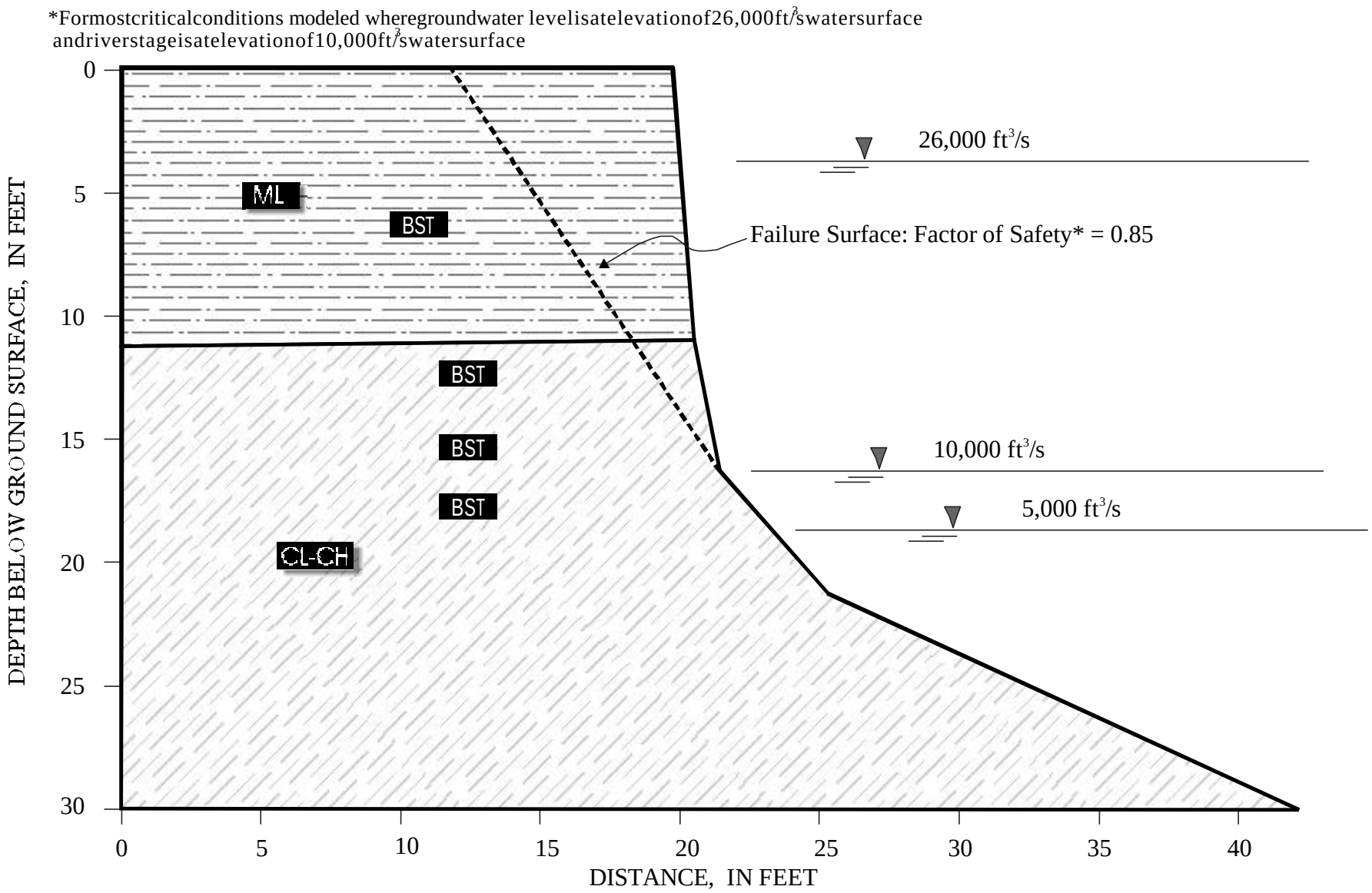

Figure 59--Idealized bank section at River Mile 1589 (Nohly) showing the modeled critical failure-surface, factor of safety (F_s), river stage and groundwater levels, location of BST tests, and differentiated soil units.

Idealized Profile Used for Planar Bank-Failure Analyses
River Mile 1604

*For most critical conditions modeled where groundwater level is at elevation of 26,000 ft³/s water surface and river stage is at elevation of 10,000 ft³/s water surface

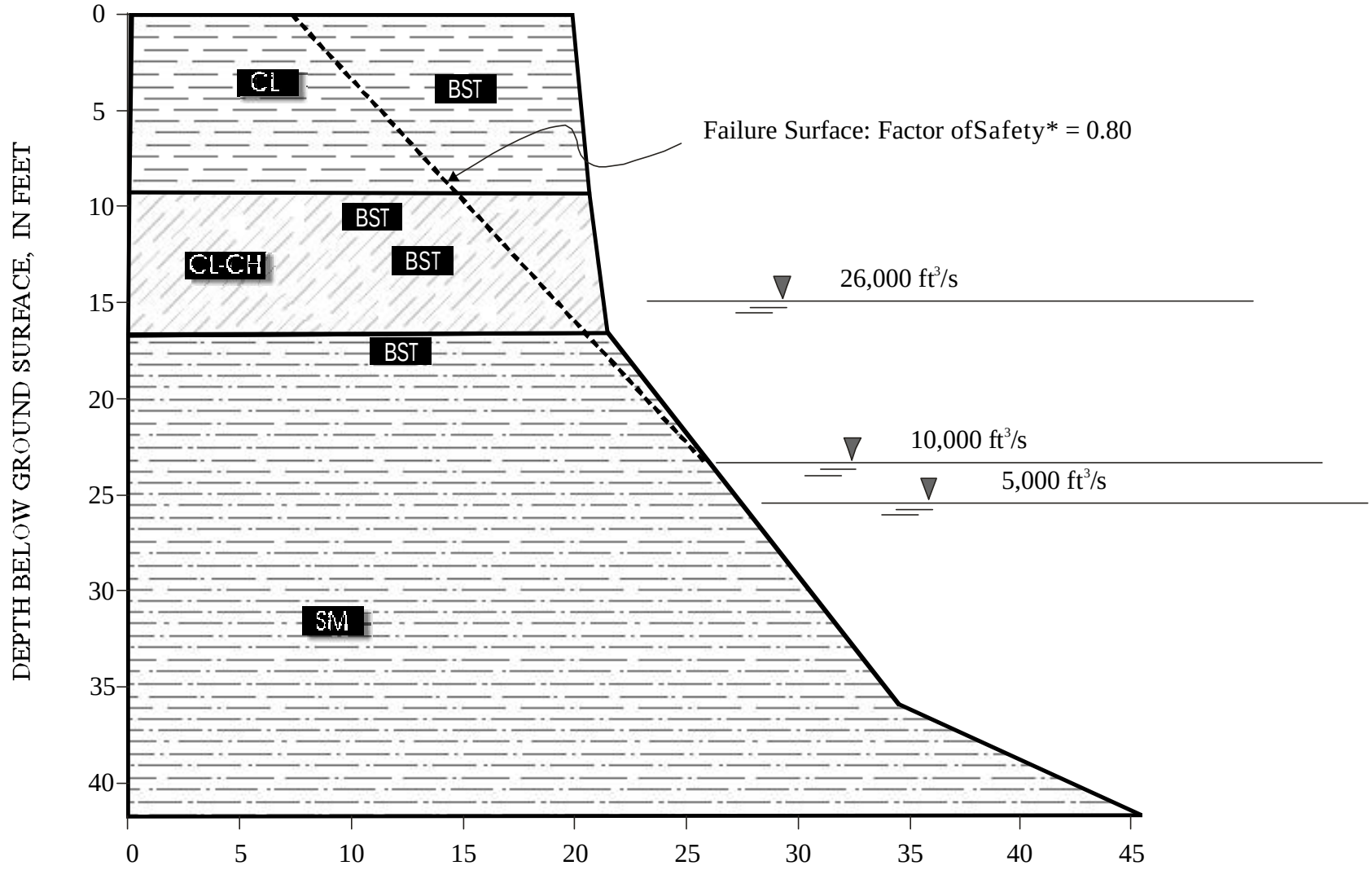

Figure 60--Idealized bank section at river mile 1604 (Hardy) showing the modeled critical failure-surface, factor of safety (F_s), river stage and groundwater levels, location of BST tests, and differentiated soil units.

River Mile 1621-- Culbertson

The riverbank is 18.3-feet high and is composed of a basal 5-feet thick layer of clay, and an upper 8-feet thick layer of silty clay. The borehole was augered to 13 feet from the top of the bank. Therefore, 5.3 feet of clay has been assumed in the lowest part of the bank. The bank is stable under both of the two drawdown conditions analyzed. The high values of factor of safety are strictly related to the high values of cohesion for the 2 units (361 and 491 lbs/ft^2, respectively). The high F_s values evaluated for the lowest RS and GW levels is because of relatively high negative pore-water pressures. Suction values of 585 lbs/ft^2 were measured at this location during the 1997 field survey (Table 30).

That evidence of past bank failures were observed in 1997 and that the model does not predict instability can be due to other forces that have not been taken into account. This could include bank-toe erosion from 1) hydraulic forces, which would provide a steeper bank profile than the one modeled and 2), by floating or rafted ice causing a similar effect.

River Mile 1624-- Low terrace-- Tveit-Johnson

The streambank is 11.2 feet high and is composed of a basal 3-feet thick layer of well sorted fine sand and an upper layer of light-brown silty sand 2 feet thick. The borehole was hand-augered at this location. The bank is unstable under all the hydrological conditions analyzed due to the very weak bank materials.

River Mile 1624-- Tveit-Johnson

The river bank is 19.2 feet high and is composed of a basal 2.5-feet thick layer of sand, a middle 2.5-feet thick layer of blue-gray clay and a 13-feet thick upper layer of brown clay. The borehole was augered to a depth of 18 feet from the top of the bank. Therefore, additional sand has been assumed to continue in the lowest part of the bank.

The bank is unstable under Case 2 drawdown conditions (F_s = 0.83). Given the same failure dimensions, F_s values are greater than 1.0 for the other hydrologic conditions modeled. The highest F_s values (1.67) are reached during the low-water stages for both river stage and groundwater. High F_s values in this bank with only moderate cohesive strength are caused by high negative pore-water pressure and low soil unit weight.

Field surveys confirm the occurrence of recent failures at this site including failed blocks and recently exposed grass-root hairs. At the time of observation in August 1996 failures were observed on the opposite, inside bank in recently-formed soils.

River Mile 1630-- Iverson

The streambank is 14.1-feet high and is composed of a basal layer of clay, a middle 5-feet thick layer of well-sorted sand and an upper 7-feet thick layer of brown sandy-clay. The borehole was hand augered to a depth of 12 feet. Therefore, an additional two feet of clay was assumed in the lowest part of the bank for modeling purposes. The bank is unstable under Case 2 drawdown conditions (F_s = 0.61). Given the

Idealized Profile Used for Planar Bank-Failure Analyses
RM 1621

*For most critical conditions modeled where groundwater level is at elevation of 26,000 ft³/s water surface and river stage is at elevation of 10,000 ft³/s water surface

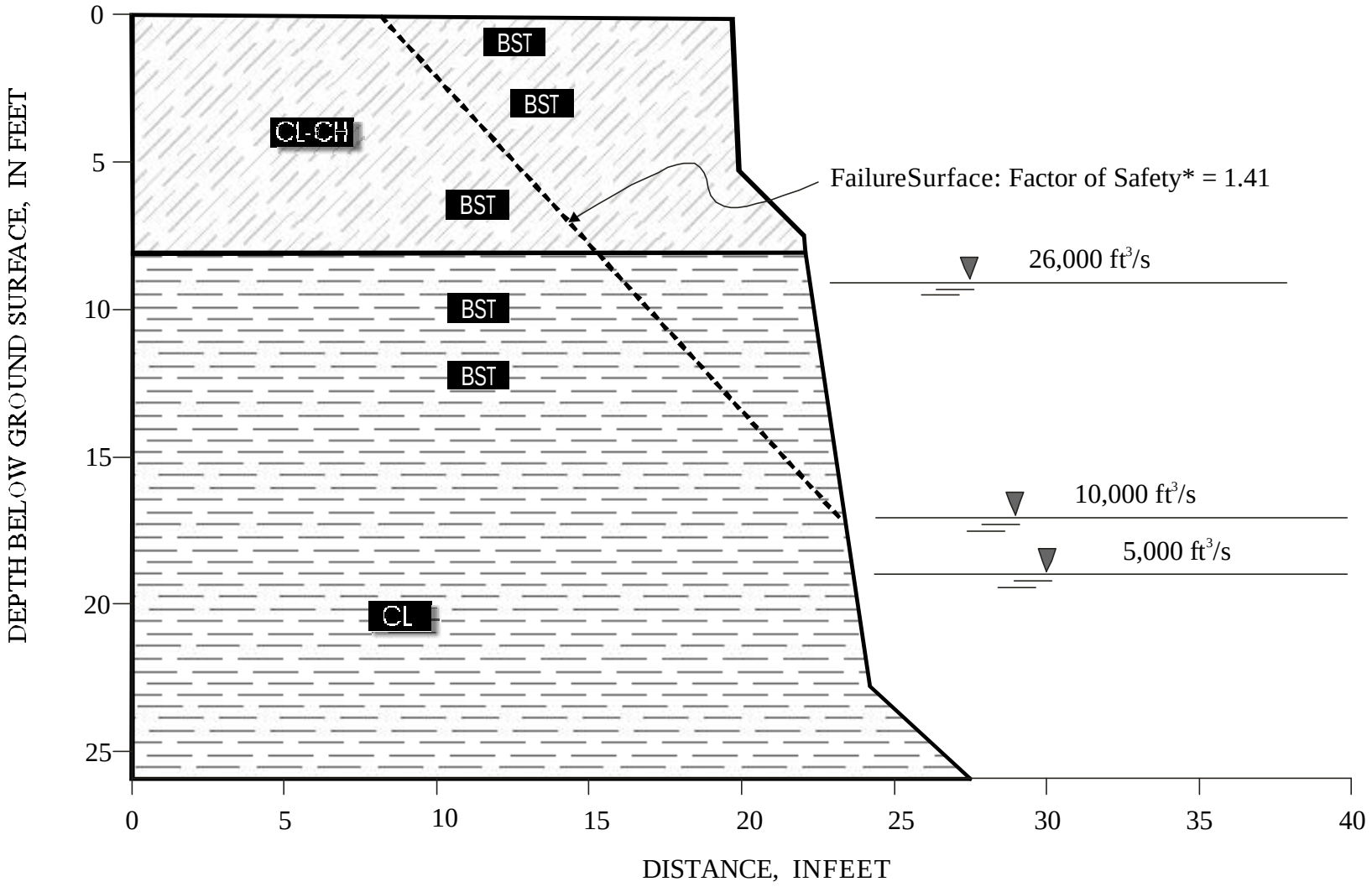

Figure 61--Idealized bank section at river mile 1621 (Culbertson) showing the modeled critical failure-surface, factor of safety (F_s), river stage and groundwater levels, location of BST tests, and differentiated soil units.

Idealized Profile Used for Planar Bank-Failure Analyses
RM 1624

*For most critical conditions modeled where groundwater level is at elevation of 26,000 ft^3/s water surface and river stage is at elevation of 10,000 ft^3/s water surface

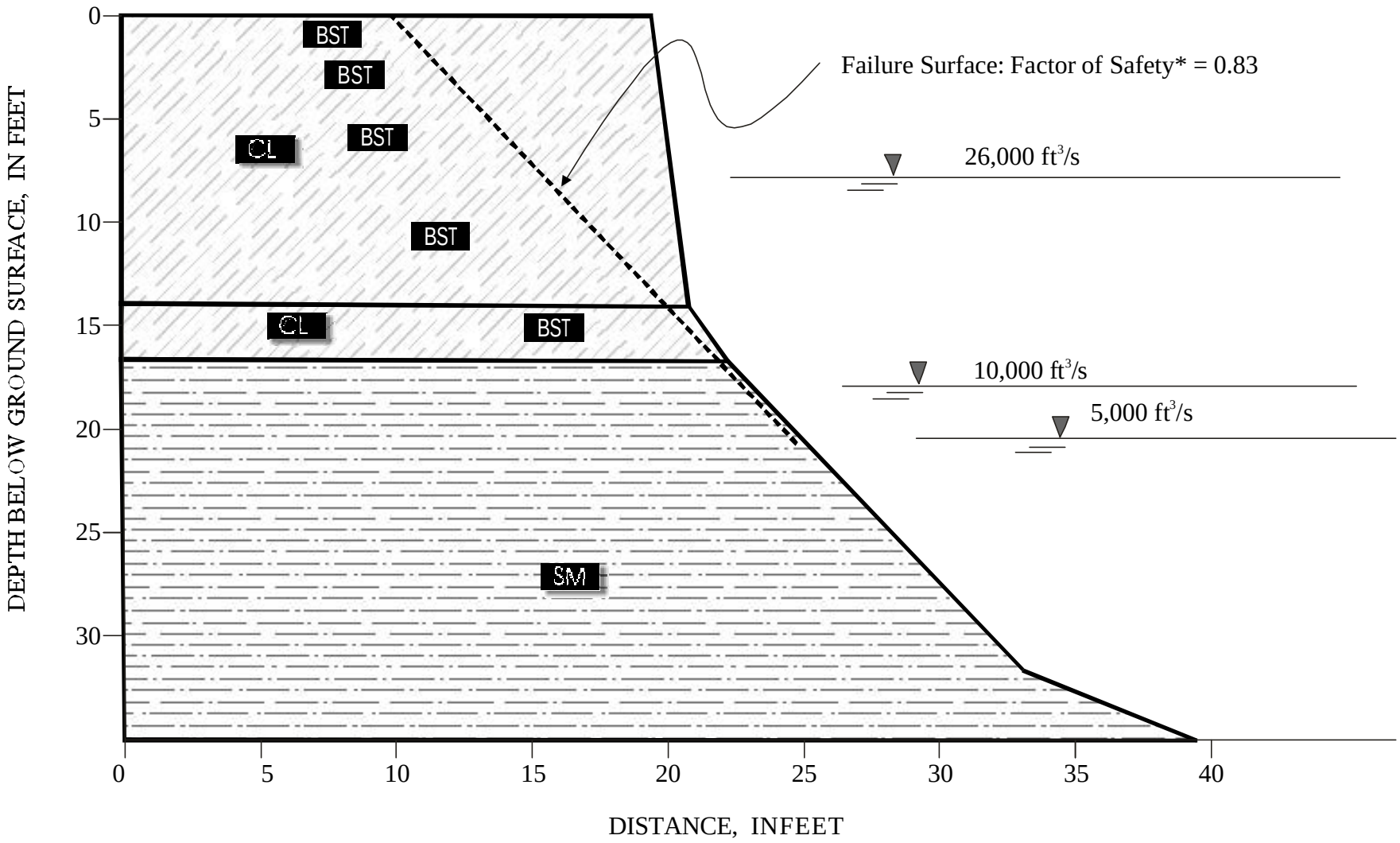

Figure 62--Idealized bank section at river mile 1624 (Tveit-Johnson) showing the modeled critical failure-surface, factor of safety (F_s), river stage and groundwater levels, location of BST tests, and differentiated soil units.

Idealized Profile Used for Planar Bank-Failure Analyses
RM 1630

*For most critical conditions modeled where groundwater level is at elevation of 26,000 ft³/s water surface and river stage is at elevation of 10,000 ft³/s water surface

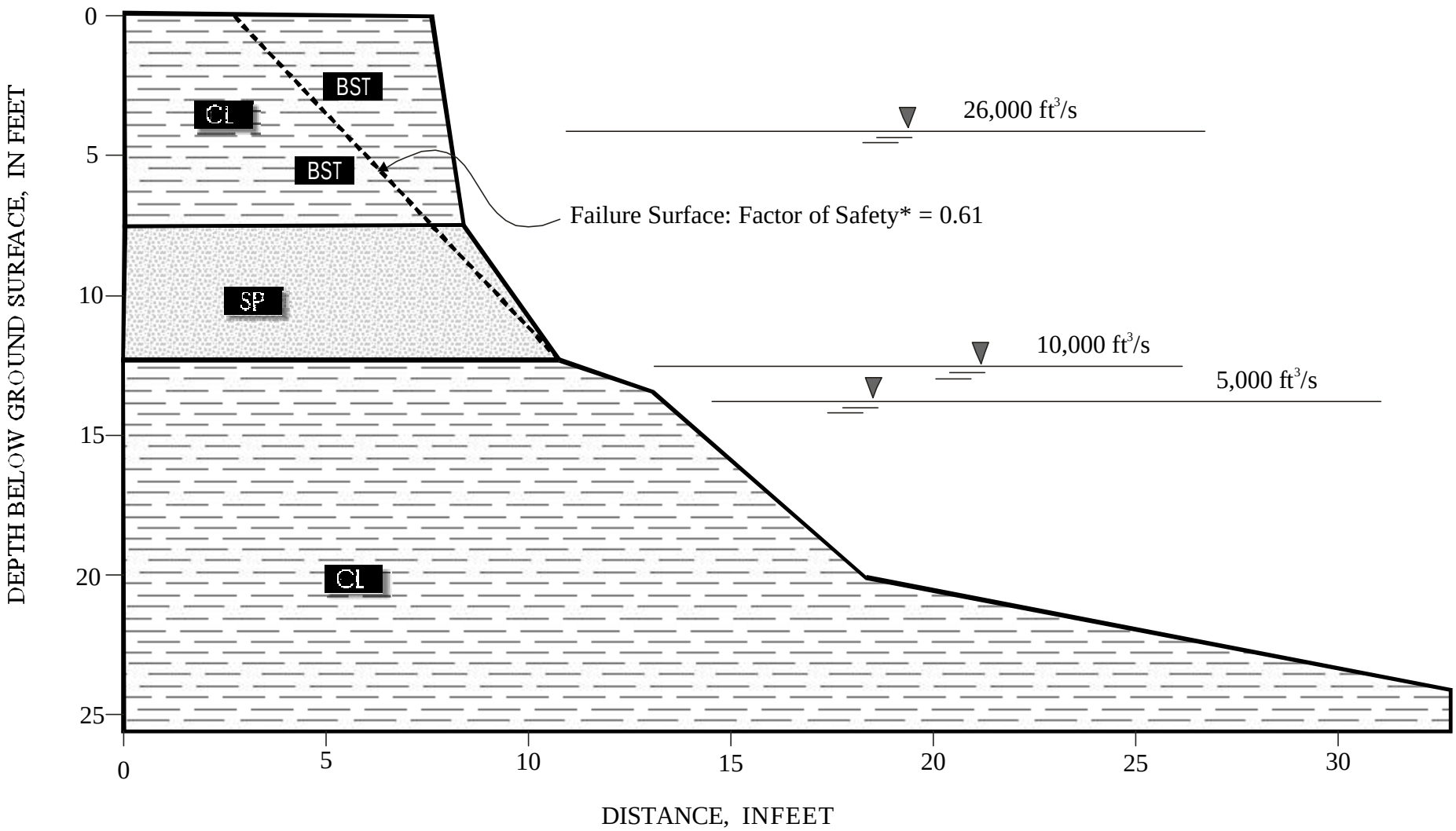

Figure 63--Idealized bank section at river mile 1630 (Iverson) showing the modeled, planar critical failure-surface, factor of safety (F_s), river stage and groundwater levels, location of BST tests, and differentiated soil units.

same failure dimensions, F_s values are greater than 1.0 for the other hydrologic conditions modeled. The large range in F_s values between the worst-case drawdown condition and the other hydrological conditions is explained in terms of the large range of heads displayed by the 26,000 and 10,000 ft^3/s elevations. Three cases have the same factor of safety because the RS and GW levels are below the base of the failure surface. Observations of failed blocks at the bank toe confirm the occurrence of recent failures at this site. The average block width of the failed material is 2.3 feet.

River Mile 1631—Vournas

The streambank is 13.9 feet high and is composed of a 1-foot thick basal layer of well-sorted sand and an upper 7-feet thick layer of clay with interbedded lenses of sand. The borehole was augered to a depth of 8 feet. Almost 6 additional feet of sand are assumed in the lowest part of the bank for modeling purposes.

The bank is unstable under Cases 1 and 2 (high GW) and only marginally stable under the other cases where RS and GW levels are low (Table 38). The bank geometry as well as the soil properties play a fundamental role in the stability of this bank. The weighted bank angle over the length of the planar failure surface is steep, 73º and the bank is composed primarily of sandy materials that exhibit no cohesion. Failed blocks were observed at the bank toe, indicating recent failures. The average block width of the failed material is 2.3 feet.

River Mile 1646-- Mattelin

The streambank is 16.1 feet high and is composed of a basal 2-feet thick layer of fine silty- sand, a middle 1-foot thick layer of silt and an upper 6-feet thick layer of brown silty sand. The borehole was augered to a depth of 9 feet from the top of the bank. An additional 7-feet of fine silty sand was assumed in the lowest part of the bank.

The bank is unstable under the worst drawdown condition (Case 2; $F_s = 0.80$) and very close to unstable at RS and GW levels equal to the 26,000 ft^3/s elevation ($F_s = 1.08$). From this analysis it is possible to denote the relevance of the hydrological conditions in bank stability. Saturated banks are clearly weaker in comparison to dry banks. Failed blocks were observed at the bank toe, indicating a recent failure episode.

River Mile 1676-- Woods Peninsula

This site is located in a very tight meander where a neck cutoff may be likely in the near future. The analysis described here accounts for bank-material conditions in the "neck". The streambank is 19.3-feet high and is composed of a basal 1-foot thick layer of well-sorted brown sand, a middle 1.5-feet thick layer of brown clay and an upper 11-feet thick layer of brown silt. The borehole was augered to a depth of 13.5 feet from the top of the bank. Therefore, about 5 feet of sand is assumed in the lowest part of the bank.

The bank is unstable during the worst of the two falling stage conditions analyzed (Case 2; $F_s = 0.95$). Field surveys confirm the occurrence of recent failures at this site with failed blocks at the bank toe.

Idealized Profile Used for Planar Bank-Failure Analyses
RM 1631

*Formostcriticalconditions modeled where groundwater levelisatelevationof26,000ft^3/swatersurface andriverstageisatelevationof10,000ft^3/swatersurface

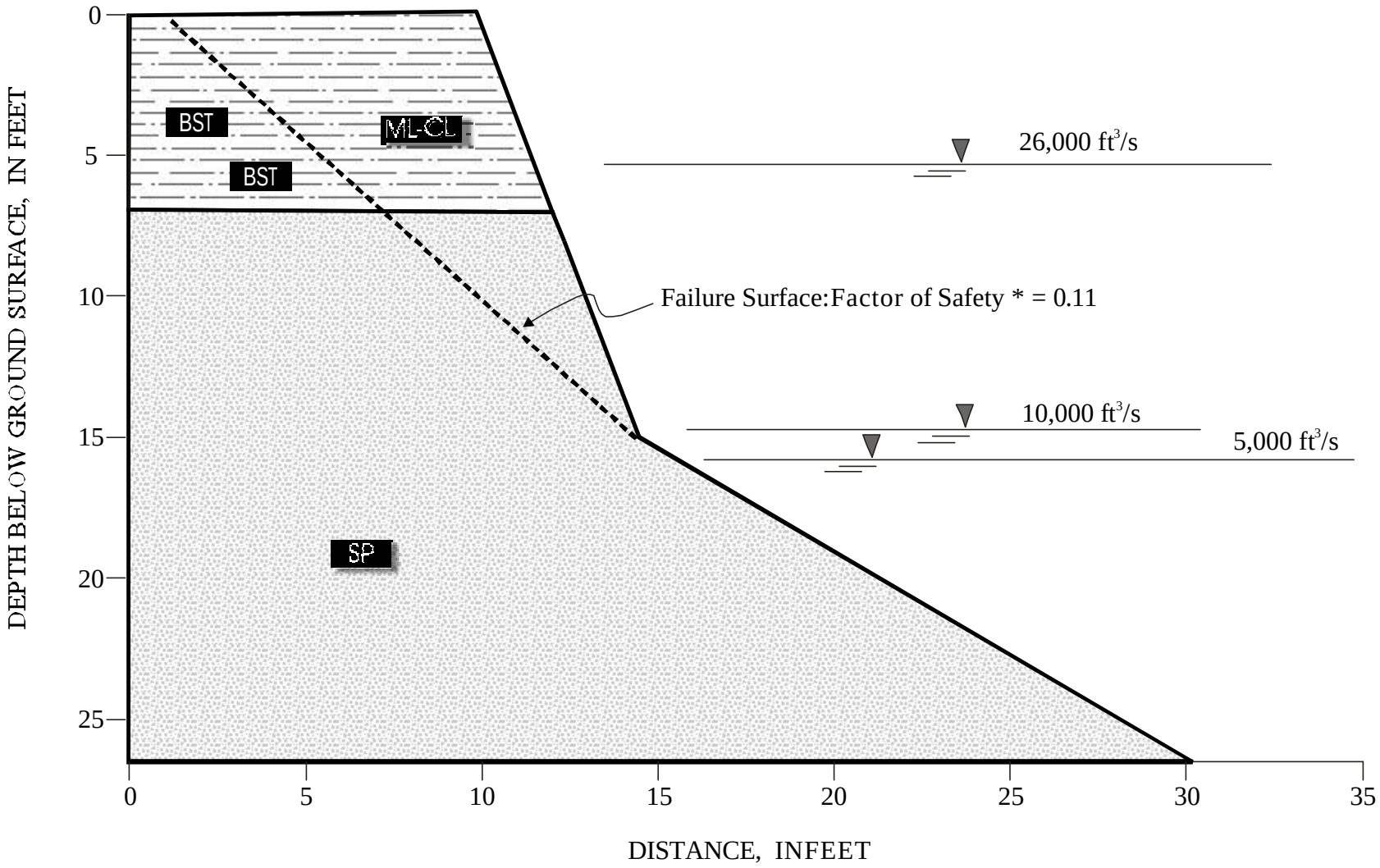

Figure 64--Idealized bank section at river mile 1631 (Vournas) showing the modeled, planar critical failure-surface, factor of safety (F_s), river stage and groundwater levels, location of BST tests, and differentiated soil units.

Idealized Profile Used for Planar Bank-Failure Analyses
RM 1646

*For most critical conditions modeled where groundwater level is at elevation of 26,000 ft³/s water surface and river stage is at elevation of 10,000 ft³/s water surface

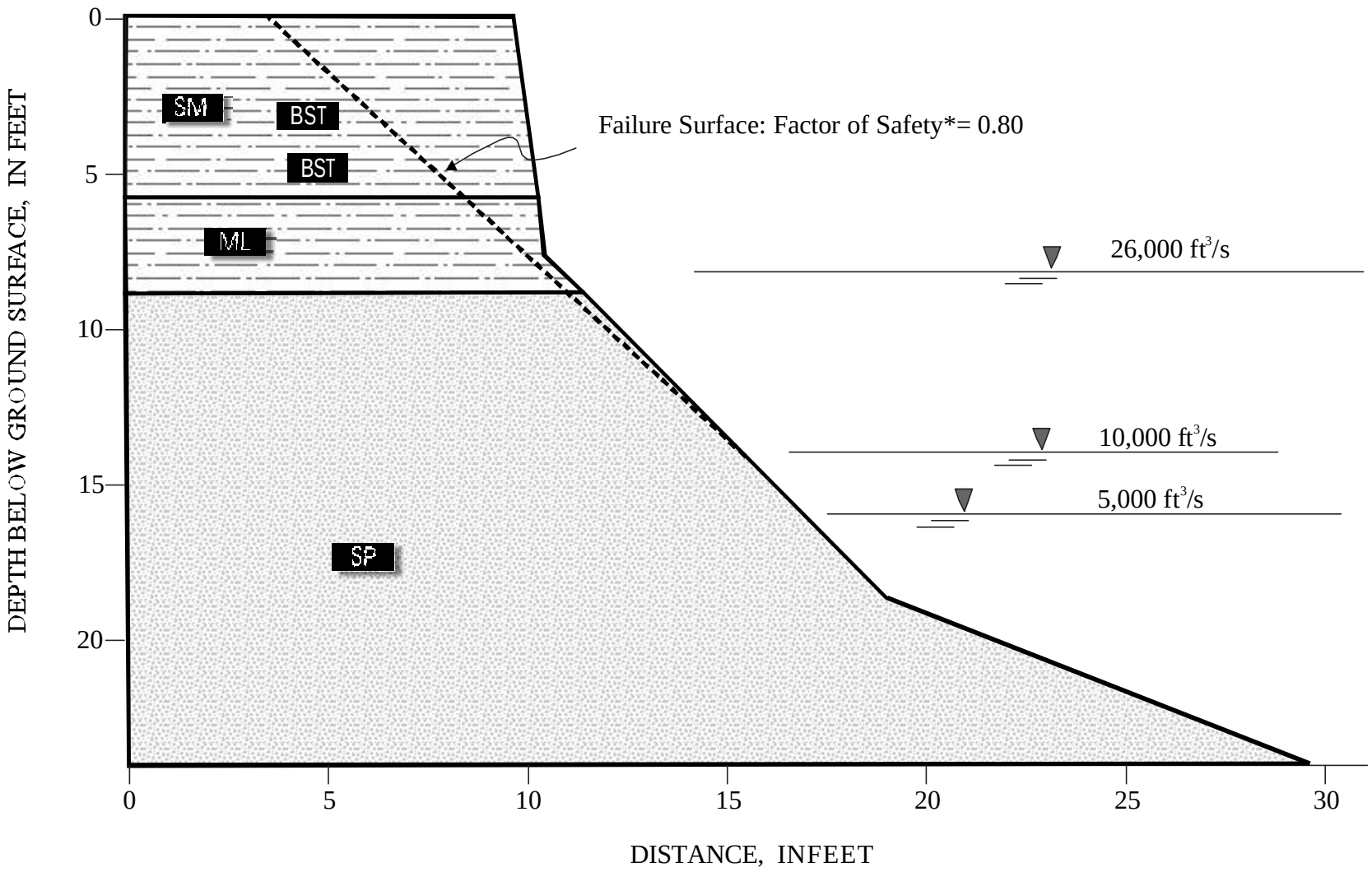

Figure 65--Idealized bank section at river mile 1646 (Mattelin) showing the modeled, planar critical failure-surface, factor of safety (F_s), river stage and groundwater levels, location of BST tests, and differentiated soil units.

Idealized Profile Used for Planar Bank-Failure Analyses
RM 1676

*Formostcriticalconditions modeled where groundwater levelisatelevationof26,000ft^3/swatersurface andriverstageisatelevationof10,000ft^3/swatersurface

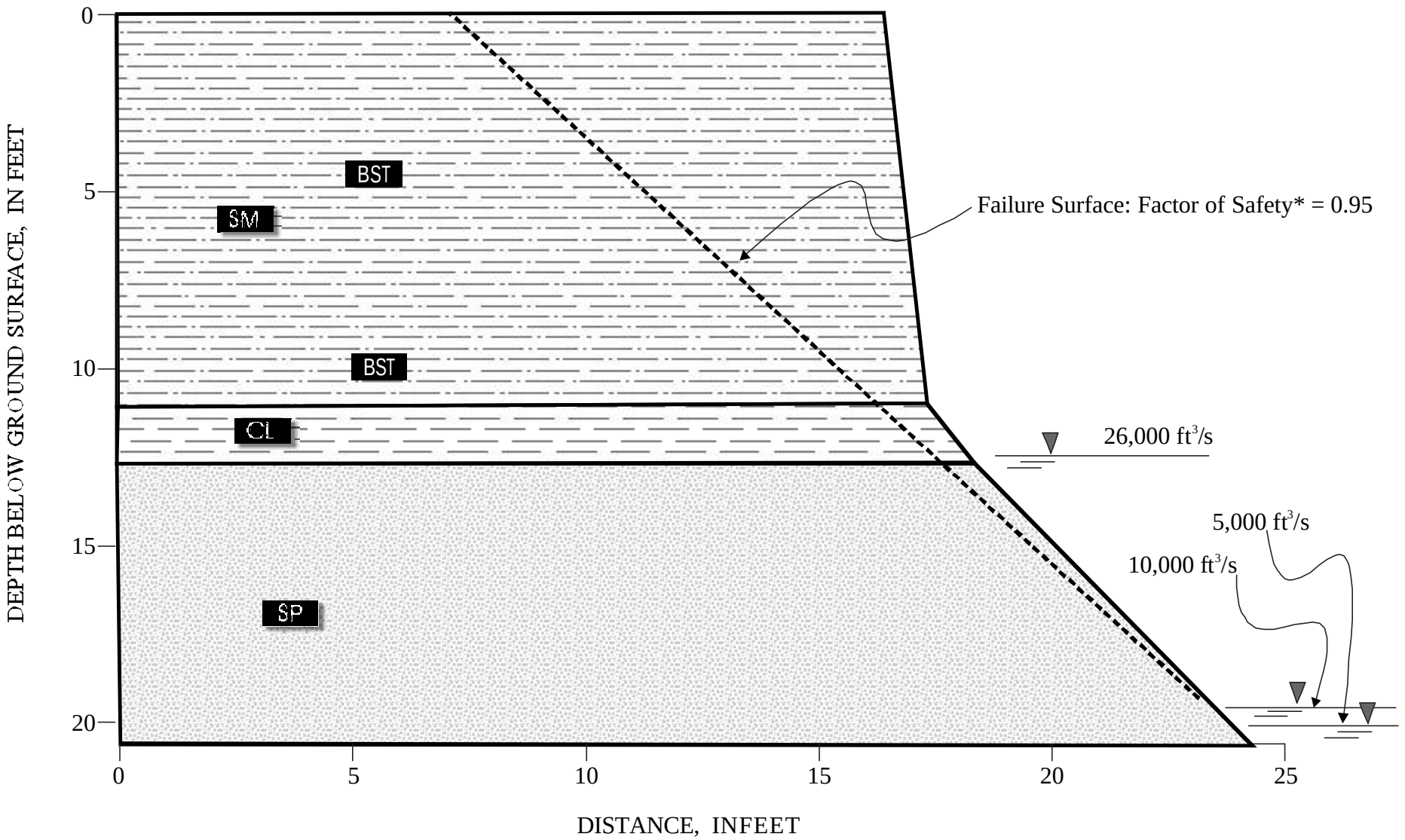

Figure 66--Idealized bank section at river mile 1676 (Woods Peninsula) showing the modeled, planar critical failure-surface, factor of safety (F_s), river stage and groundwater levels, location of BST tests, and differentiated soil units.

River Mile 1682--McCrae

The streambank is cut into a high terrace and is 32-feet high. The bank is composed of a basal 9.5-feet thick layer of dense brown clay, a middle 2.5-feet thick layer of silty-sand and an upper 11-feet thick layer of brown silty-clay. The borehole was augered to a depth of 23 feet from the top of the bank, therefore about 9 feet of dense brown clay is assumed in the lowest part of the bank.

Two different failure geometries were modeled for this site: (1) the base of the failure surface has been placed at the interface between the sand and the dense clay and (2), the base of the failure surface has been placed in the lower part of the bank 23 feet from the top of the bank. The bank is stable under all of the modeled hydrologic conditions for both failure geometries. F_s values obtained for the worst of the two drawdown conditions are 1.52 and 2.3, respectively.

The stability of the bank is controlled by high frictional strength and suction in the upper part of the bank, and high cohesion values in the basal unit (Table 31). This is shown by the higher values obtained in the second analysis where the lower clay layer is taken into account. The factor of safety obtained for the first failure geometry is the same for all the hydrological conditions because the base of the failure surface is located above the river stage corresponding to 26,000 ft^3/s. Even for the second geometry, only a small fraction of the failure is affected by the high level of modeled groundwater.

Field surveys, however, confirm the occurrence of recent failures at this site. discrepancies between observed and modeled conditions is probably due to improper assumptions regarding the location of the phreatic surface and, consequently, positive pore-water pressures. We suspect that perched water tables occur at the interface between the silty sand and clay at depths of about 12 feet. This effect would cause positive-pore water pressures in the bank mass that would reduce shear strength and could result in mass failure during particularly wet periods. Of course there is always the possibility of additional effects that are not accounted for in the analysis, such as ice and undercutting at the bank toe.

River Mile 1701-- Wolf Point

The streambank is 19.3 feet high and is composed of a basal 11-feet thick layer of sandy clay, a thin middle 1-feet thick layer of silty-sand and an upper 9-feet thick unit of light-brown clay. The bank is unstable during the worst-case hydrologic condition (Case 2); $F_s = 0.99$) and is stable under all other modeled hydrological conditions. Observations confirm the occurrence of recent failures.

River Mile 1716-- Pipal

The streambank is 18.1-feet high and extremely steep. The bank is composed of a basal 5-feet thick layer of silty-sand, a 5-feet thick intermediate layer of clay and an upper 8-feet thick layer of light brown, fissured silty clay. The upper unit and the bank face are highly fissured from desiccation. The borehole was augered to a depth of 18 feet from the top of the bank. The U. S. Army Corps of Engineers has constructed a demonstration erosion control project at this site in an attempt to reduce bank erosion.

Idealized Profile Used for Planar Bank-Failure Analyses
River Mile 1682

*For most critical conditions modeled where groundwater level is at elevation of 26,000 ft³/s water surface and river stage is at elevation of 10,000 ft³/s water surface

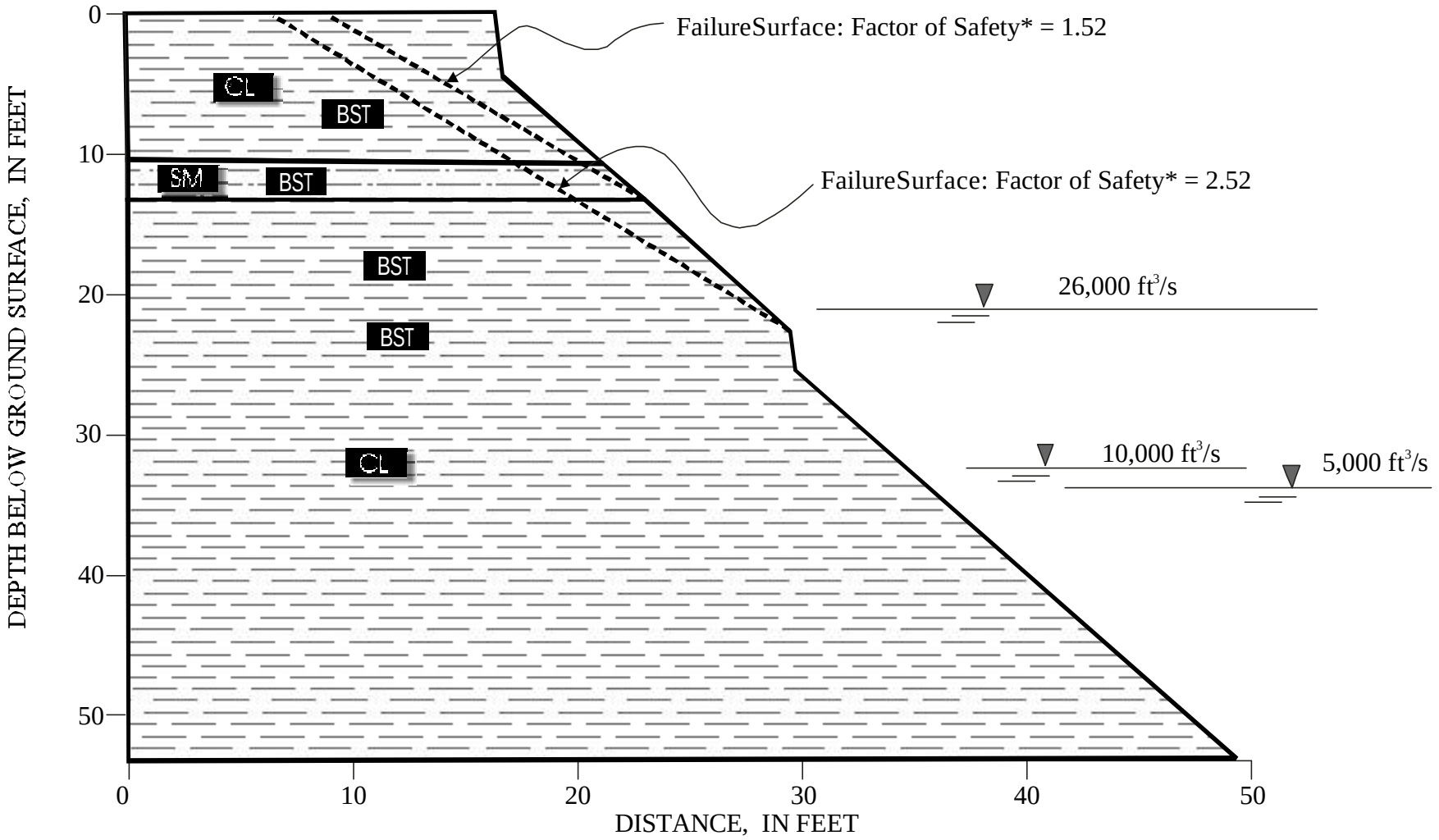

Figure 67--Idealized bank section at River Mile 1682 (McRae) showing the modeled, planar critical failure-surface, factor of safety (F_s), river stage and groundwater levels, location of BST tests, and differentiated soil units.

Idealized Profile Used for Planar Bank-Failure Analyses
RM 1701

*For most critical conditions modeled where groundwater level is at elevation of 26,000 ft^3/s water surface and river stage is at elevation of 10,000 ft^3/s water surface

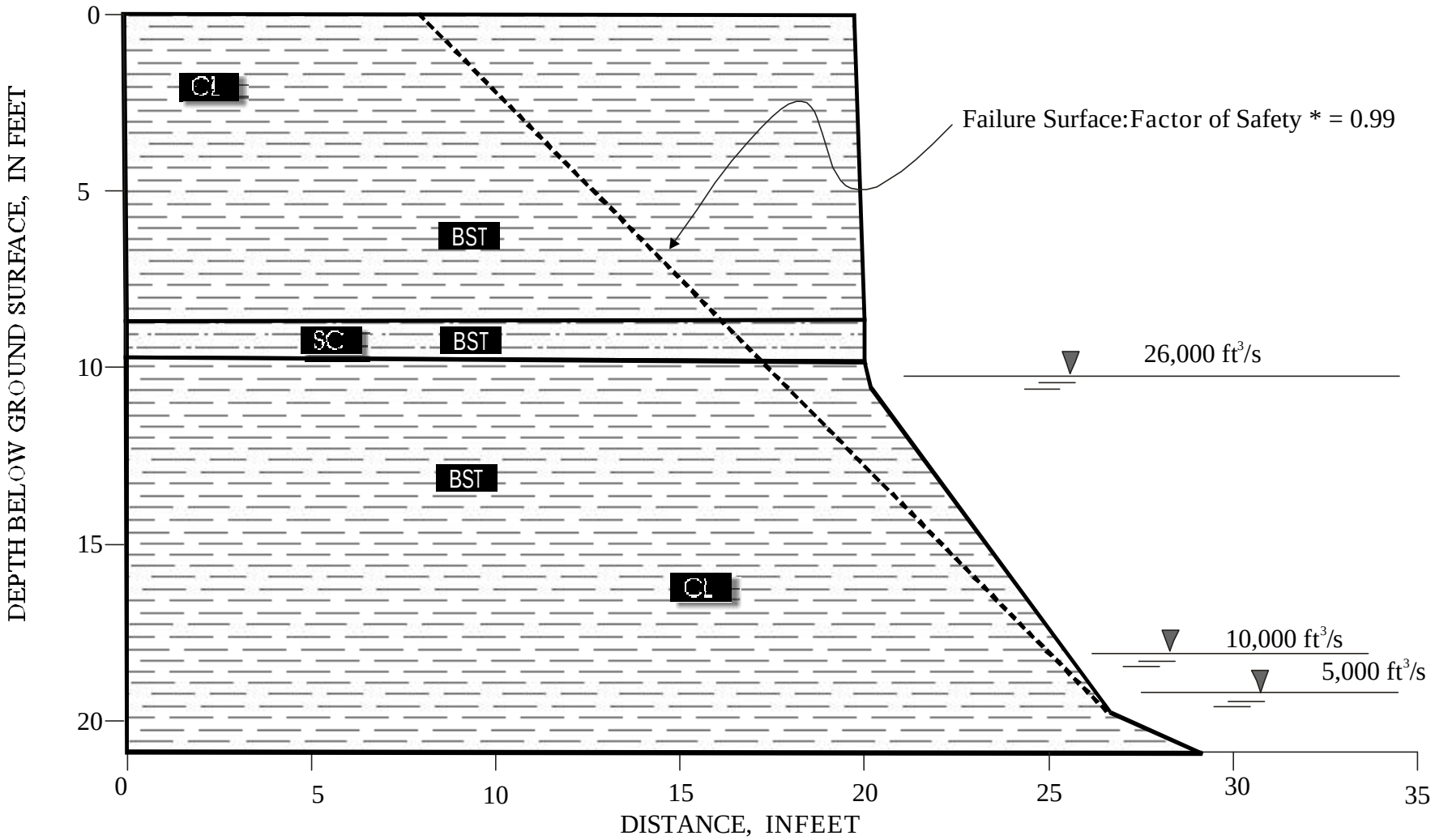

Figure 68--Idealized bank section at river mile 1701 (Wolf Point) showing the modeled, planar critical failure-surface, factor of safety (F_s), river stage and groundwater levels, location of BST tests, and differentiated soil units.

Idealized Profile Used for Planar Bank-Failure Analyses
RM 1716

*Formostcriticalconditions modeled where groundwater levelisatelevationof26,000ft^3/swatersurface andriverstageisatelevationof10,000ft^3/swatersurface

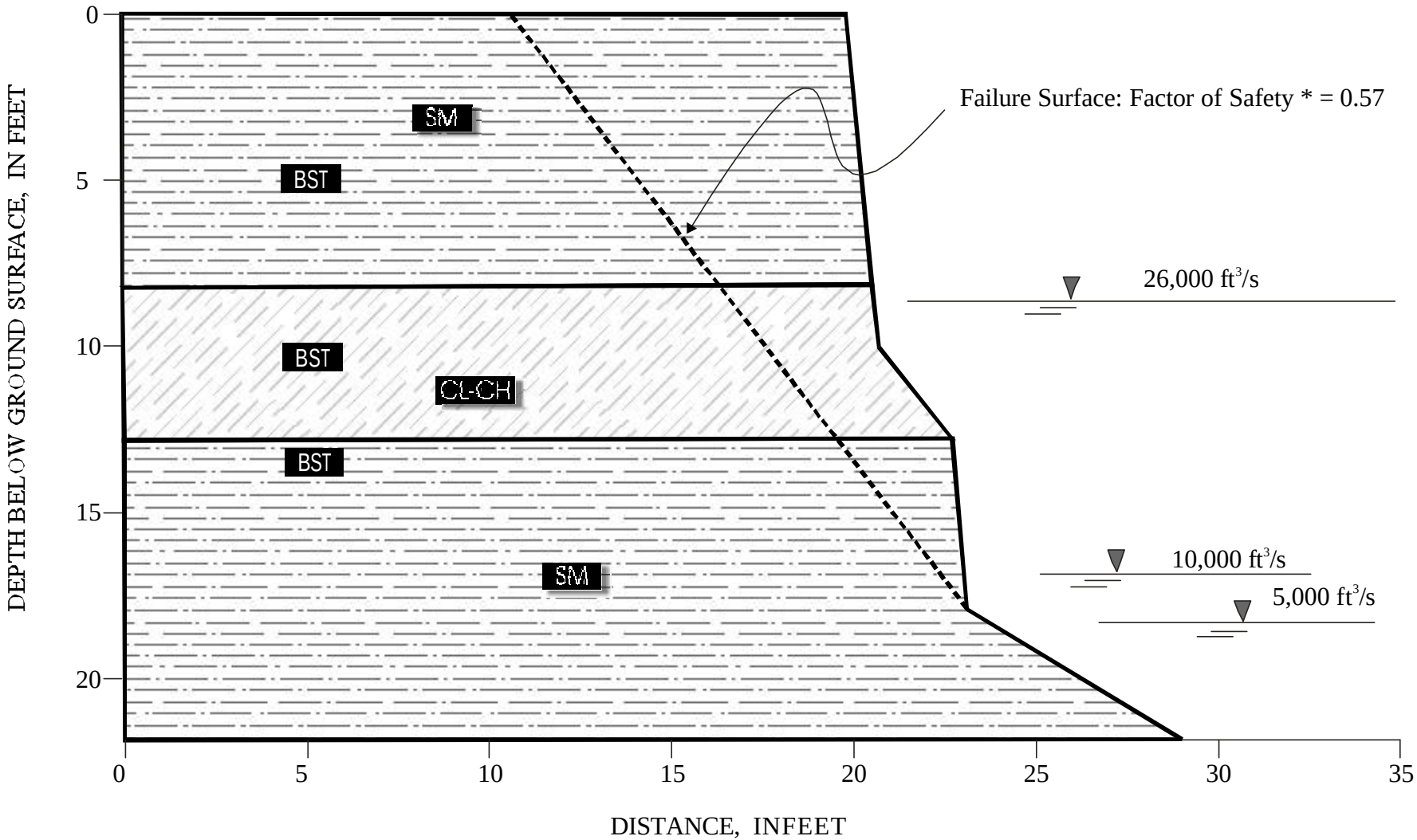

Figure 69--Idealized bank section at river mile 1716 (Pipal) showing the modeled, planar critical failure-surface, factor of safety (F_s), river stage and groundwater levels, location of BST tests, and differentiated soil units.

The bank is unstable during the worst-case drawdown condition (Case 2; F_s = 0.57) as well as when high RS and GW levels occur together (Case 1; F_s = 0.94). Field surveys confirm the occurrence of recent failures at this site as well as the removal of most of the failed debris from the bank-toe region.

River Mile 1728-- Flynn Creek

The streambank is 20 feet high and is composed of a 6-feet thick basal layer of fine sand, a middle layer 3-feet thick of dark gray clay and an upper layer 9-feet thick of light brown clay. The borehole was augered to a depth of 18 feet from the top of the bank, therefore 2 feet of silty-sand was assumed in the lowest part of the bank.

The bank is unstable during the worst of the two drawdown cases (F_s = 0.6) and during high water stage and high water table (F_s = 0.81). Because the lower RS and GW levels are below the base of the failure surface, F_s values for the other hydrologic cases are identical (1.16). Field surveys confirm the occurrence of recent failures at this site. The average block width of the failed material is 1.8 feet.

River Mile 1737-- Frazer Pump

The streambank is 15.4-feet high and is composed of an 11.4-feet thick basal layer of dark brown silty-clay, a 1-foot thick middle layer of dark brown clay, and a 3-feet thick layer of silty clay. The borehole was augered to a depth of 17 feet from the top of the bank.

The bank is unstable during the worst of the two falling stage conditions analyzed (F_s = 0.97). Similar failure dimensions have F_s values significantly greater than 1 for the other sets of hydrologic conditions. In fact, this bank is among the most stable under drier conditions because of the large proportion of relatively cohesive materials and the small proportion of the failure plane that is saturated during non high-flow cases.

River Mile 1744-- Little Porcupine

The stream bank is 19.8-feet high and is composed of a 14-feet thick basal layer of glacial till (dark-brown clay with minor gravels) and an upper layer 6-feet thick of dark brown silty clay. The borehole was augered to a depth of 20 feet from the top of the bank. The bank is stable under all of the modeled hydrologic conditions because the bank material is highly cohesive. Field surveys confirm the absence of recent failures at this site. The block width of the failed material is 4.6 feet.

River Mile 1762-- Milk River

The streambank is 13.6 feet high and is homogeneous, composed of 16 feet of dark brown silty clay. The bank is stable under all the modeled hydrologic conditions because the bank material is highly cohesive and the bank height above the 5,000 ft^3/s surface (representative low water) is not great. The average value of effective cohesion is 579 lbs/ft^2, the highest average value assessed along the study reach. Furthermore the weighted bank angle over the length of the planar failure is the flattest of those modeled

Idealized Profile Used for Planar Bank-Failure Analyses
RM 1728

*For most critical conditions modeled where groundwater level is at elevation of 26,000 ft^3/s water surface and river stage is at elevation of 10,000 ft^3/s water surface

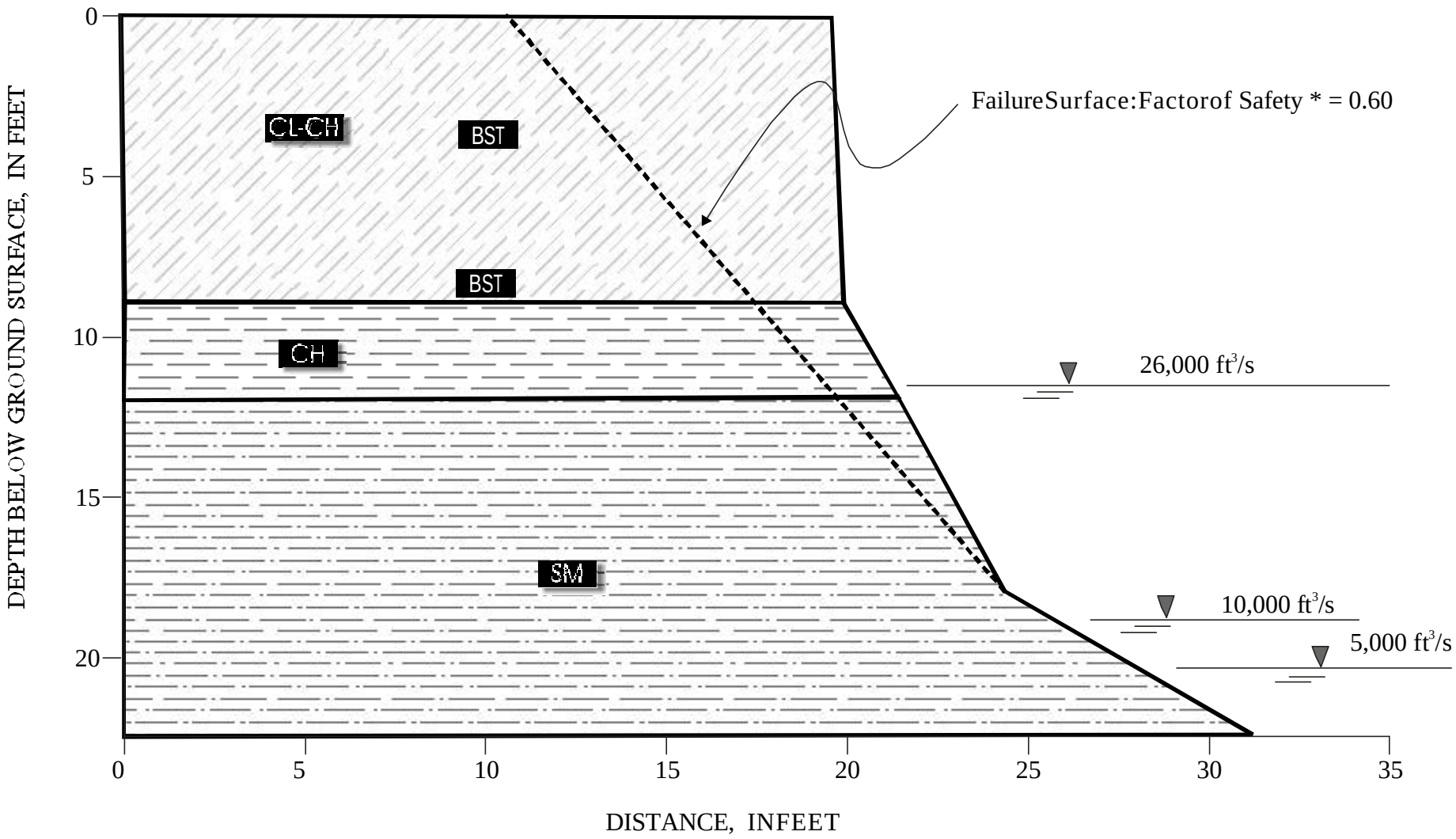

Figure 70--Idealized bank section at river mile 1728 (Flynn Creek) showing the modeled, planar critical failure-surface, factor of safety (F_s), river stage and groundwater levels, location of BST tests, and differentiated soil units.

Idealized Profile Used for Planar Bank-Failure Analyses
RM 1737

*For most critical conditions modeled where groundwater level is at elevation of 26,000 ft³/s water surface and river stage is at elevation of 10,000 ft³/s water surface

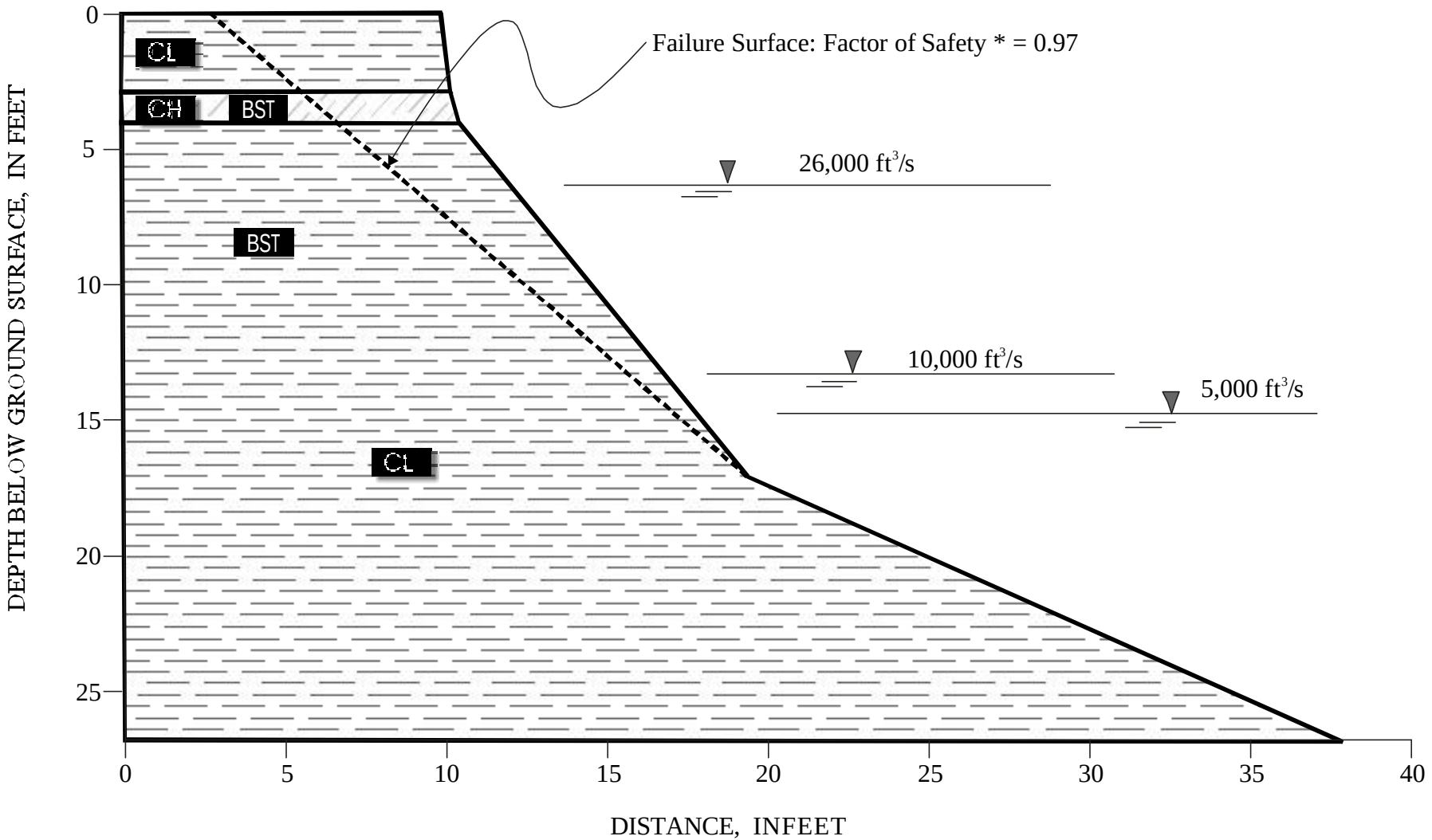

Figure 71--Idealized bank section at river mile 1737 (Fraizer Pump) showing the modeled, planar critical failure-surface, factor of safety (F_s), river stage and groundwater levels, location of BST tests, and differentiated soil units.

Idealized Profile Used for Planar Bank-Failure Analyses
RM 1744

*For most critical conditions modeled where groundwater level is at elevation of 26,000 ft^3/s water surface and river stage is at elevation of 10,000 ft^3/s water surface

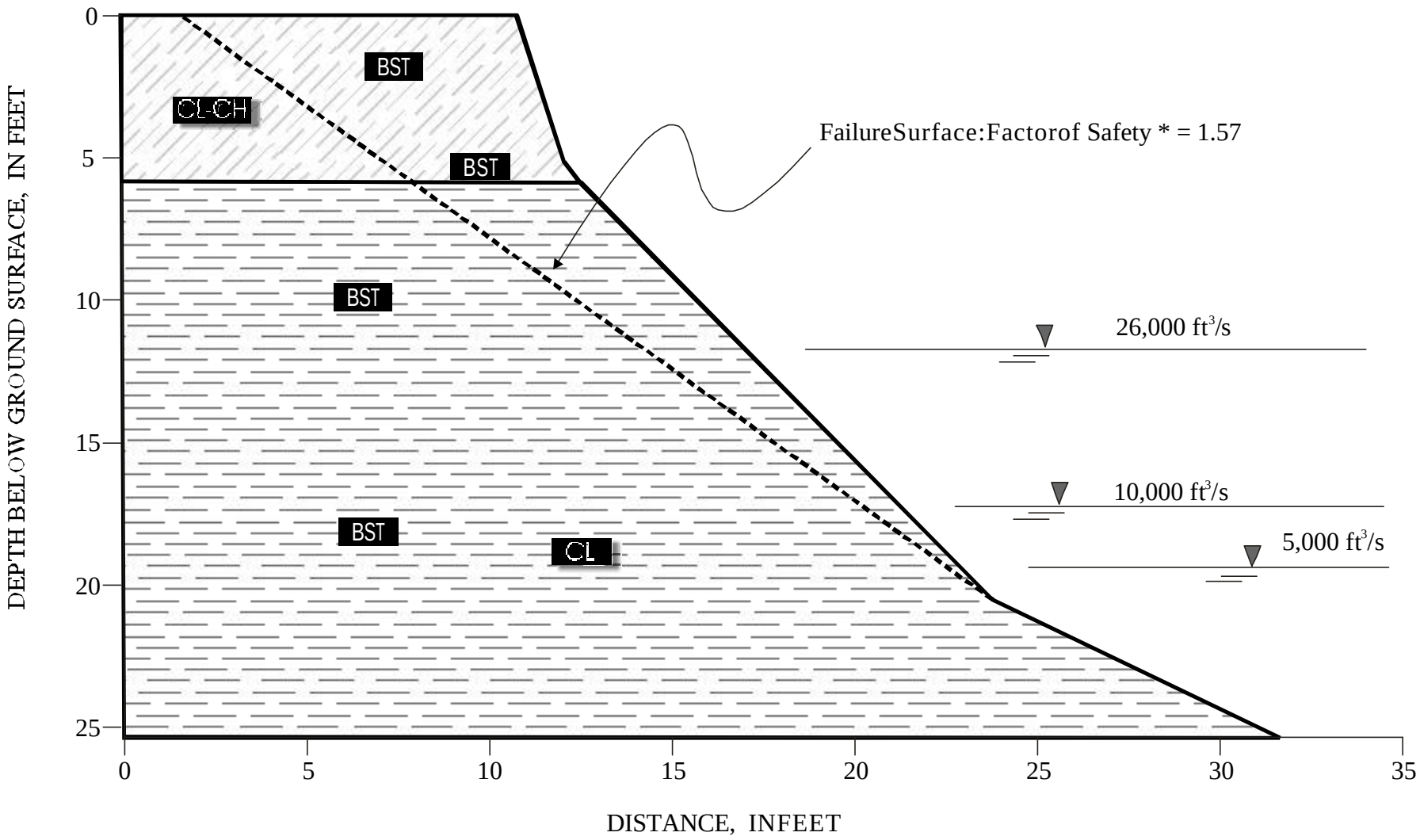

Figure 72--Idealized bank section at river mile 1744 (Little Porcupine) showing the modeled, planar critical failure-surface, factor of safety (F_s), river stage and groundwater levels, location of BST tests, and differentiated soil units.

Idealized Profile Used for Planar Bank-Failure Analyses
RM 1762

*Formostcriticalconditions modeled where groundwater levelisatelevationof26,000ft^3/swatersurface andriverstageisatelevationof10,000ft^3/swatersurface

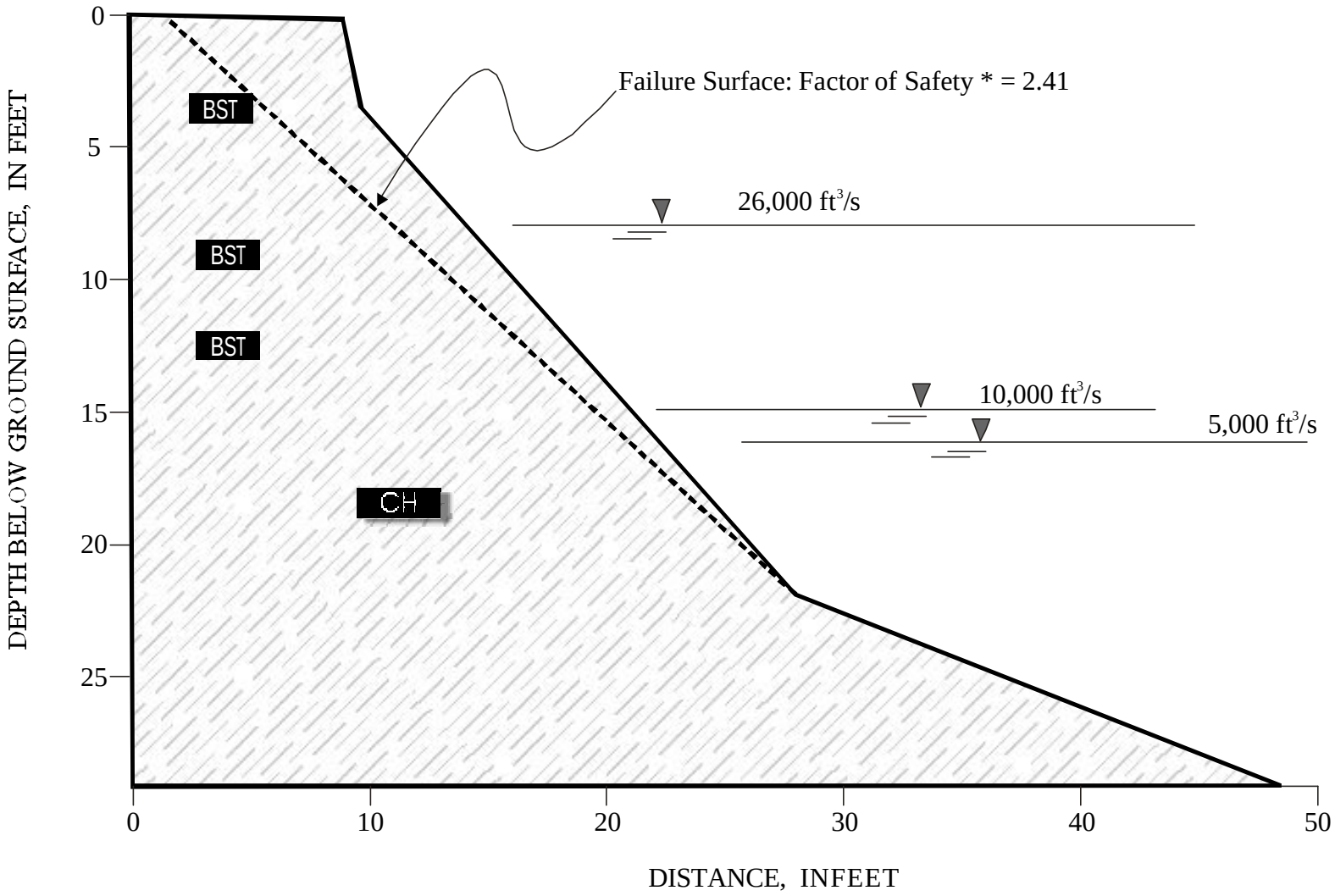

Figure 73--Idealized bank section at river mile 1762 (Milk River) showing the modeled, planar critical failure-surface, factor of safety (F_s), river stage and groundwater levels. location of BST tests. and differentiated soil units.

(50º). Field surveys confirm the absence of recent failures at this site.

River Mile 1765-- Garwood

The streambank is 19.8-feet high and is composite with a 5.5-feet thick basal layer of silty-sand, a 6-feet thick middle layer of silty clay with increased fine sand and a 6.5-feet thick upper layer of light brown silty-clay. The borehole was augered to a depth of 18 feet from the top of the bank, therefore 2.0 feet of silty-clay was assumed in the lowest part of the bank. The bank is unstable during the worst of the two drawdown conditions analyzed (F_s = 0.64) as well as during simultaneous high levels river stage and groundwater (F_s = 0.99).

Type 3: Rotational Failures: Theory

Although generally not as common as planar or wedge-type failures, rotational failures tend to occur on the highest banks and do considerably more damage than those failure types previously discussed. In cohesive materials, shear stress increases more rapidly with depth than does shear strength and at greater depths may be larger than the shear strength, leading to rotational failure (Carson and Kirkby, 1972). Non-vertical and compound-slope banks are also subject to rotational failures due to the variable nature of the direction of the major principle plane.

Rotational failures are analyzed using SLOPE/W, a product of Geo-Slope, Canada. This commercial software product is used for computing the factor of safety of earth and rock slopes. Stability analysis of the Missouri River banks was performed using the Bishop limit-equilibrium method, which is the most widely used. This method allows us to evaluate the stability of layered banks for a variety of slip-surface shapes and for a variety of pore-water pressure conditions and soil properties. In the Bishop method, the method of slices is employed to evaluate the forces between two adjacent slices. The assumption in this method that the inter-slice forces are horizontal and that all moment- and vertical-forces are in equilibrium is satisfied.

Idealized Profile Used for Planar Bank-Failure Analyses
RM 1765

*Formostcriticalconditions modeled wheregroundwater levelisatelevationof26,000ft³/swatersurface andriverstageisatelevationof10,000ft³/swatersurface

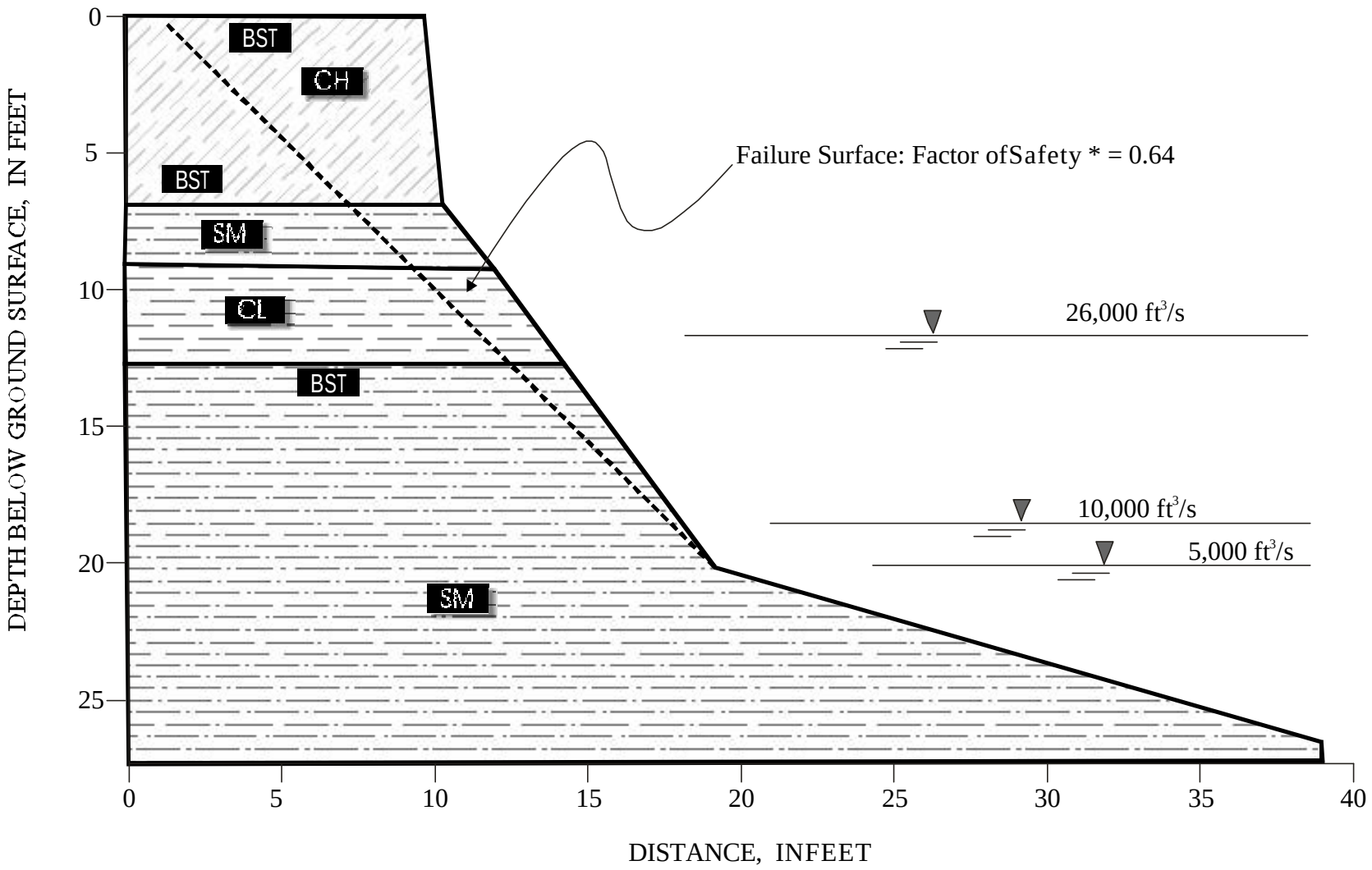

Figure 74--Idealized bank section at river mile 1765 (Garwood) showing the modeled, planar critical failure-surface, factor of safety (F_s), river stage and groundwater levels, location of BST tests, and differentiated soil units.

Governing Equations for Rotational Failures

Neglecting seismic, loading, and confining forces and considering a circular failure surface, the moment equilibrium equation is the summation of the moments for all the slices about a common point:

$$\sum Wx - \sum S_m R = 0 \qquad (20)$$

Where W = the total weight of a slice of width a and height h

x = the horizontal distance from the centerline of each slice to the center of rotation or to the center of moments.

S_m = represents the magnitude of the shear force mobilized on the base of each slice.

R = the radius for a circular slip surface or the moment arm associated with the mobilized shear force, S_m for any shape of slip surface.

.

$$S_m = \frac{S_r \, b}{F_s} = \frac{b\left(c' + \left(\sigma - u_w\right)\tan\phi'\right)}{F_s} \qquad (21)$$

Where S_r = shear strength (equation 8), in lbs/ft^2,

b =length of each slice at the base, in feet.

The average normal stress at the base of each slice (N) is:

$$\sigma = \frac{N}{b} \qquad (22)$$

Substituting equation (21) into equation (20) and solving for the factor of safety for the moment equilibrium (F_s) gives:

$$F_s = \frac{\sum \left(c'bR + \left(N - u_w b\right)R\tan\phi'\right)}{\sum Wx} \qquad (23)$$

Based on the equilibrium of all the forces in the vertical direction, N can be found:

$$\Sigma W - \Sigma N\cos\alpha - \Sigma S_m \sin\alpha = 0 \qquad (24)$$

Knowing N, the factor of safety can be determined from equation (23). For the portion of the bank that is unsaturated, cohesion due to the negative pore-water pressures (matric suction) is taken into account and equation (23) becomes:

$$F_s = \frac{\sum \left(c'bR + \left[N - u_w \, b \frac{\tan \phi^b}{\tan \phi'} - u_a b \left(1 - \frac{\tan \phi^b}{\tan \phi'} \right) \right] R \tan \phi' \right)}{\sum Wx} \qquad (25)$$

Specific Procedures

To evaluate the stability of each of the study sites the following procedure was employed:

1) Sketch the bank, soil units and water surface with a CAD-based finite-element mesh, using the data obtained from field survey conducted by the NRCS, borings logs, and the measured and calculated water-surface profiles.
2) Input required modeling information such as the method of stability analysis (Bishop); soil parameters obtained from field and laboratory tests (Tables 30 and 31) and the specific seepage case.
3) Define the slip search. The slip search setting for a circular slip consists of a group of centers about which a series of radii will be extended, to define the size and shape of the failure surface. A boundary is also described beyond which a slip surface cannot pass.
4) Run the program. The program based on the input generates a series of circular failure surfaces of various radii and calculates the factor of safety for each. By default, the program then displays the slip surface having the minimum factor of safety.
5) Re-run program using the five different hydrologic scenarios described for the planar-failure analyses (Cases).

Results of Rotational Analysis: Application

Under the worst-case modeling scenario (River Stage (RS) 10,000 ft3/s and Groundwater Stage (GW) 26,000 ft3/s) all but 3 of the streambanks modeled are found to be unstable. As with the planar-failure analyses, sites at River Miles 1682 (McRae), 1744 (Little Porcupine), and 1762 (Milk River) appear to be stable (Table 39). All of these sites have cohesive materials making up the bank toe, thereby slowing fluvial erosion and steepening of the lower part of the bank. It is encouraging that totally different analytic techniques (ARS method and SLOPE/W) show the same sites to be stable (or unstable) under similar conditions.

The sites most susceptible to rotational failures, that is, are unstable under all of the simulated conditions are located at River Miles 1604 (Hardy); 1624-low terrace (Tveit-Johnson); 1631 (Vournas); 1646 (Mattelin); and 1765 (Garwood). The values presented in Table 39 represent the factors of safety obtained from the Bishop method for all sites under the five hydrologic scenarios. The most critical failure surface, generated by the model for the worst-case hydrologic scenario (Case 2) is plotted for each site in Figures 75-90. Comparisons between factors of safety in Table 39 may not represent failures of equal size because the program selects the most critical failure surface for the specified hydrologic conditions. Thus, failure sizes and corresponding block widths are of different sizes (Table 40).

Table 39-- Minimum factor of safety for rotational failures under the given set of hydrologic conditions. Worst-case modeled conditions are represented by the second case where RS = the elevation of the 10,000 ft^3/s water surface and GW = the elevation of the 26,000 ft^3/s water surface.

Site	Rotational Failures Minimum Factor Of Safety For Given Hydrologic Conditions				
	RS-26000 GW-26000	**RS-10000 GW-26000**	**RS-10000 GW-10000**	**RS-5000 GW-10000**	**RS-5000 GW-5000**
1589	1.12	0.61	1.09	0.90	1.19
1604	0.78	0.50	0.87	0.79	0.90
1621	1.05	0.81	1.07	1.02	1.08
1624 (Low Terrace)	0.52	0.10	0.56	0.52	0.68
1624	0.96	0.79	1.27	0.95	1.07
1630	1.29	0.34	1.52	1.50	1.67
1631	0.83	0.34	0.87	0.78	0.89
1646	0.76	0.75	0.80	0.75	0.96
1676	0.91	0.88	1.52	1.53	1.63
1682	1.64	1.29	1.57	1.65	1.59
1701	0.97	0.97	1.60	1.59	1.69
1716	1.06	0.83	1.17	1.17	1.25
1728	0.75	0.63	1.06	1.06	1.15
1737	1.32	0.95	1.40	1.32	1.48
1744	1.53	1.23	1.59	1.54	1.68
1762	2.45	2.13	2.31	2.25	2.29
1765	0.72	0.51	0.94	0.94	0.97

RS = Elevation of river at given discharge
GW = Elevation of groundwater equal to specified river discharge

Table 40. Change in failure width of most-critical rotational failure under different hydrologic conditions.

Site	Rotational Failures Failure Block Width For Given Hydrologic Conditions, In Feet				
	RS-26000 GW-26000	RS-10000 GW-26000	RS-10000 GW-10000	RS-5000 GW-10000	RS-5000 GW-5000
1589	10.8	5.77	8.40	8.79	10.1
1604	8.20	7.84	11.6	10.7	11.9
1621	16.3	13.3	13.4	11.6	12.0
1624 (Low Terrace)	6.66	6.30	2.30	3.02	3.94
1624	10.9	8.92	10.4	10.8	12.0
1630	6.23	4.95	7.48	6.89	6.59
1631	9.48	4.33	9.78	9.71	6.43
1646	5.61	3.61	6.30	7.94	4.13
1676	6.50	5.28	9.61	9.15	7.28
1682	17.7	14.0	13.2	12.4	14.1
1701	5.64	5.71	10.6	10.0	13.6
1716	4.69	8.24	6.17	6.17	7.45
1728	6.17	6.73	6.33	6.69	6.89
1737	7.05	4.76	4.82	4.82	4.66
1744	10.2	8.27	7.35	7.58	9.32
1762	22.3	22.3	22.3	22.3	22.3
1765	4.49	4.59	7.09	7.19	7.02

RS = Elevation of river at given discharge
GW = Elevation of groundwater equal to specified river discharge

Detailed Results from Each Site: Rotational Analysis

This section covers details of the rotational analysis but does not include specifics about the bank morphology and field observations as that material was covered in the detailed write up of the planar failures. The reader should refer to the idealized bank profiles of each site showing the bank-material units, levels of the 5,000, 10,000, and 26,000 ft^3/s water surfaces, and the most-critical failure surface (Figures 75-90). Because the rotational analysis finds the most critical failure surface for each set of given hydrologic conditions, failure dimensions can vary. The failure widths corresponding to a given modeled scenario for each site are listed in Table 40. Again, it is important to mention here that comparisons between different hydrologic scenarios are difficult for the rotational failures, because they represent failures of different dimensions that possibly cut through different units of variable strength.

River Mile 1589-- Nohly

The minimum factor of safety (F_s = 0.61) occurs during the modeled worst-case drawdown condition (Case 2) when the RS is 10,000 ft^3/s and GW is at the level of the 26,000 ft^3/s water surface. The width of this failure as measured between the bank edge and intersection of the failure plane with the flood-plain surface is 5.8 feet. The bank is also unstable at the lesser drawdown condition (Case 4) where RS is at the 10,000 ft^3/s-and GW is at 5,000 ft^3/s-levels. This failure encompasses a greater portion of the bank with a failure width of 8.4 feet.

River Mile 1604-- Hardy

This site is unstable for all hydrologic conditions tested. Failure widths range from 7.8 – 11.9 feet with an average of 10.0 feet.

River Mile 1621-- Culbertson

This site is unstable under the most critical case (Case 2) with an F_s value of 0.81. The other cases are only marginally stable and unstable, with F_s values from 1.02 to 1.08. Because of the relatively high cohesive strengths, failure widths are large, ranging between 11.6 and 16.3 feet.

River Mile 1624-Low terrace-- Tveit-Johnson

The sandy Riverwash soil at this site is extremely unstable with F_s values less than 1.0 for all cases. Because of the low cohesive strengths, failure widths are relatively small, ranging from 2.3 to 6.7 feet. The average failure is 4.4 feet.

Idealized Profile Used for Rotational Bank-Failure Analyses
RM 1589

*For most critical conditions modeled where groundwater level is at elevation of 26,000 ft³/s water surface and river stage is at elevation of 10,000 ft³/s water surface

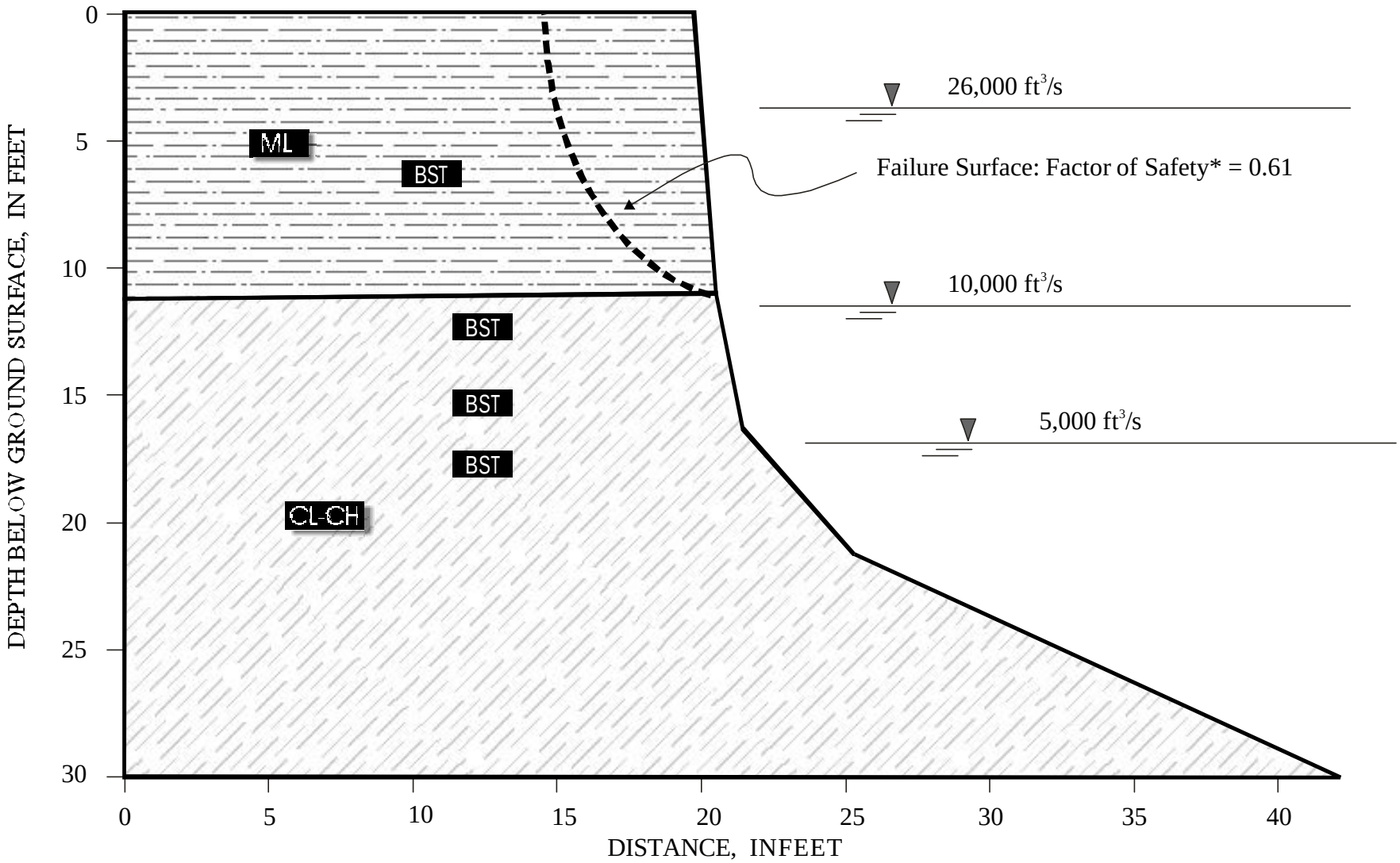

Figure 75--Idealized bank section at river mile 1589 (Nohly) showing the modeled, rotational critical failure-surface, factor of safety (F_s), river stage and groundwater levels, location of BST tests, and differentiated soil units.

Idealized Profile Used for Rotational Bank-Failure Analyses
RM 1604

*Formostcriticalconditions modeled where groundwater levelisatelevationof26,000ft³/swatersurface andriverstageisatelevationof10,000ft³/swatersurface

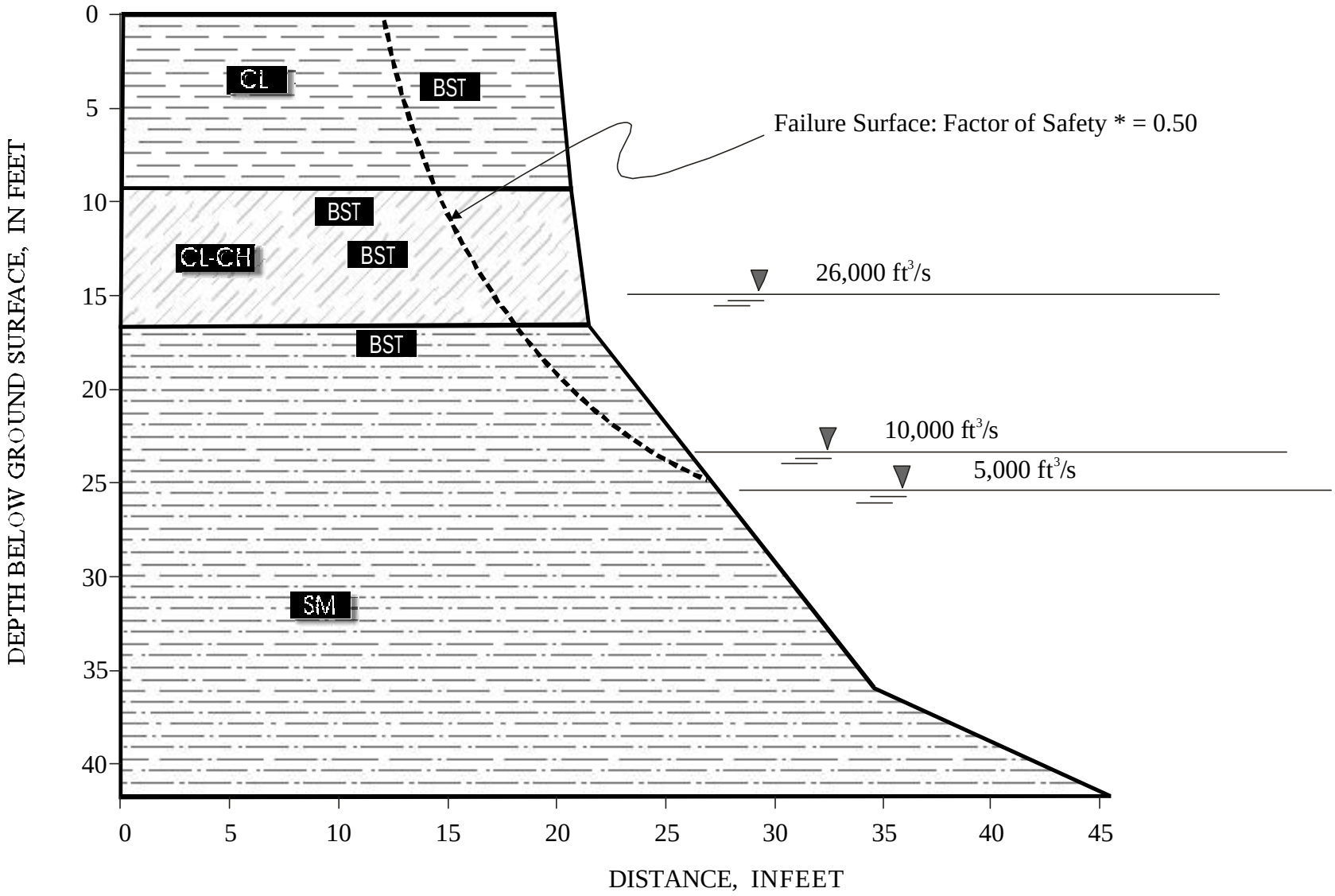

Figure 76--Idealized bank section at river mile 1604 (Hardy) showing the modeled, rotational critical failure-surface, factor of safety (F_s), river stage and groundwater levels, location of BST tests, and differentiated soil units.

Idealized Profile Used for Rotational Bank-Failure Analyses
River Mile 1621

*For most critical conditions modeled where groundwater level is at elevation of 26,000 ft³/s water surface and river stage is at elevation of 10,000 ft³/s water surface

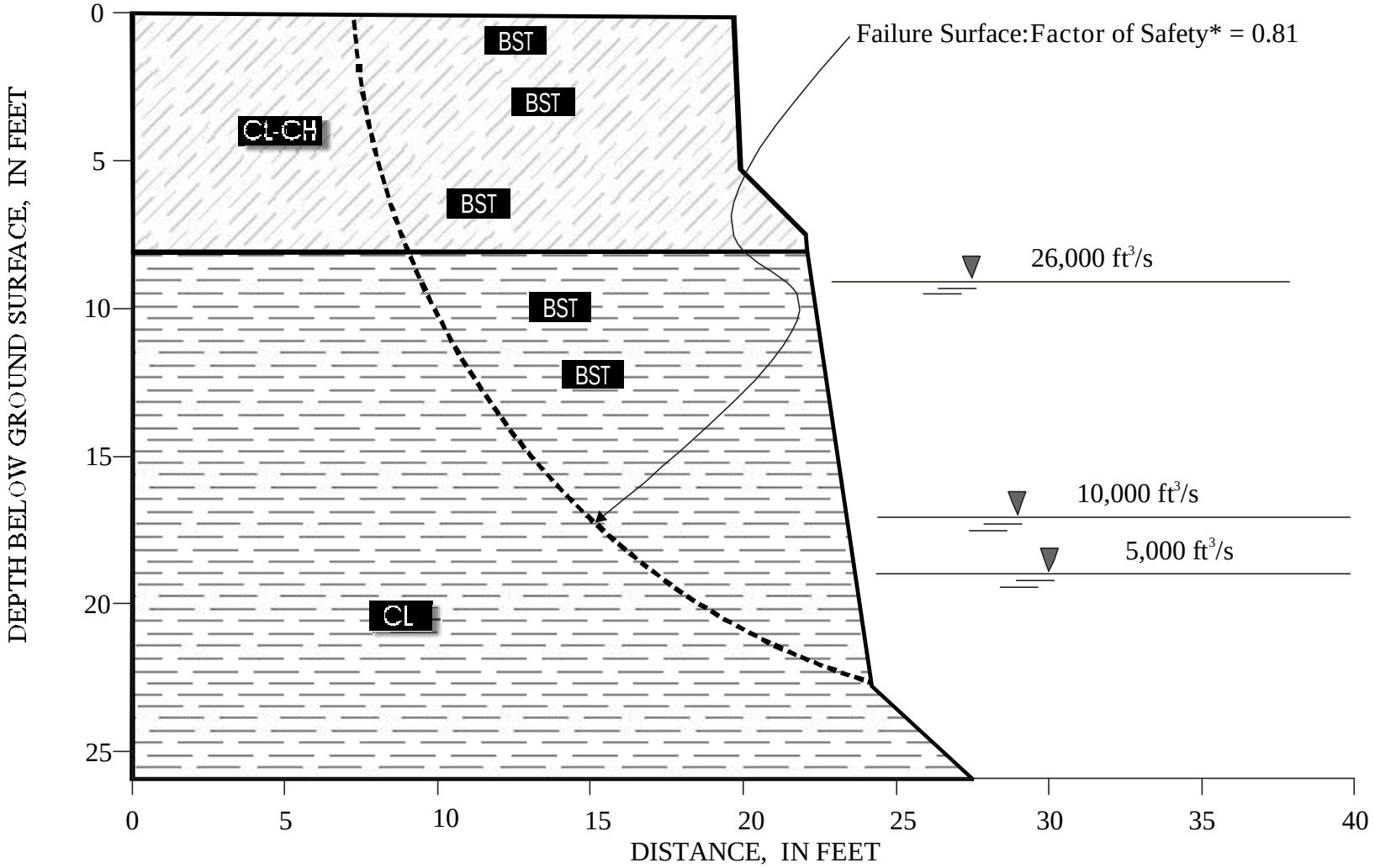

Figure 77--Idealized bank section at river mile 1621 (Culbertson) showing the modeled, rotational critical failure-surface, factor of safety (F_s), river stage and groundwater levels, location of BST tests, and differentiated soil units.

Idealized Profile Used for Rotational Bank-Failure Analyses
RM 1624

*For most critical conditions modeled where groundwater level is at elevation of 26,000 ft^3/s water surface and river stage is at elevation of 10,000 ft^3/s water surface

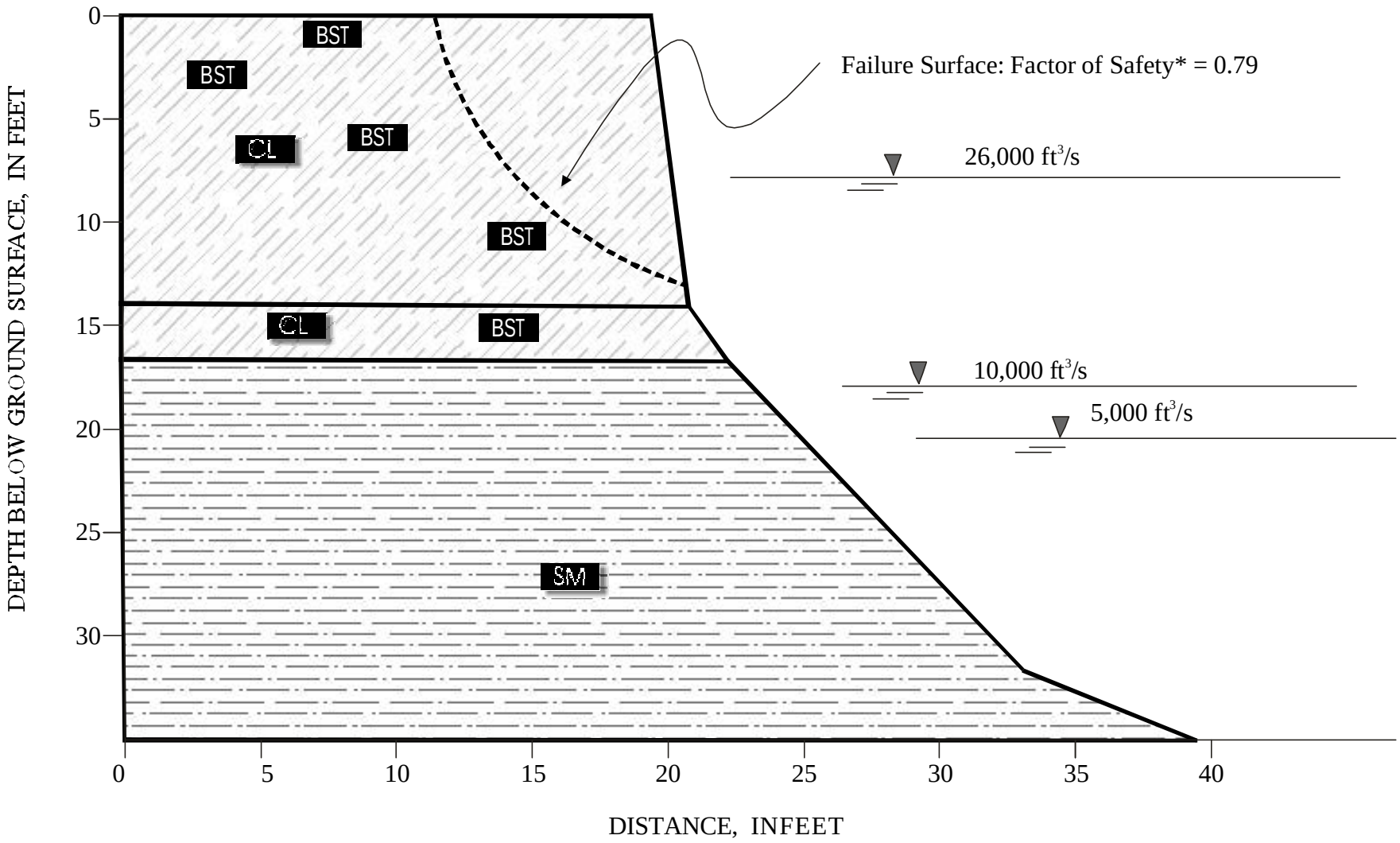

Figure 78--Idealized bank section at river mile 1624 (Tveit-Johnson) showing the modeled, rotational critical failure-surface, factor of safety (F_s), river stage and groundwater levels, location of BST tests, and differentiated soil units.

River Mile 1624—Tveit-Johnson

This site is unstable for three of the five modeled scenarios, the two drawdown conditions, as well as the simultaneous high RS and GW levels. Failure widths for the critical hydrologic conditions range from 8.9 to 10.9 feet.

River Mile 1630-- Iverson

This site is unstable only under the modeled worst-case hydrologic conditions having a factor of safety well below 1.0 and a failure width of about 5.0 feet. The stability of this site under the other hydrologic conditions reflects the fact that lower water levels are below the base of the failure surface and that the bank toe is composed of clay materials.

River Mile 1631-- Vournas

This site has sand at the toe and is unstable under all conditions. Under worst-case conditions, there is only about 3.3 feet of bank that is not saturated. Failure widths range from 4.3 to 9.8 feet with an average failure width of 8.0 feet.

River Mile 1646-- Mattelin

This site has sand at the toe and is unstable under all conditions. The low factors of safety are due to low cohesive strengths, a relatively steep upper bank angle and bank-toe material composed of sand. Failure widths range from 3.6 to 7.9 feet.

River Mile 1676-- Woods Peninsula

Because of the low strength of the sandy banks, both cases where GW levels are at the 26,000 ft^3/s elevation are modeled as unstable at this site. Failure widths for those cases are between 5.3 and 6.5 feet.

River Mile 1682-- McCrae

Although this streambank is very high (32 feet) the cohesive strengths of the bank materials in combination with a large unsaturated portion even during high GW levels result in a stable site. If water could become perched at the interface between the silty-sand and clay at depths of about 12 feet, it is possible that instabilities could result. This scenario was not modeled here. However, if instability developed at this site, failure widths would be relatively large because of the cohesive nature of the banks, ranging from 5.3 to 9.6 feet.

River Mile 1701-- Wolf Point

During periods of high GW levels (Cases 1 and 2), this site is modeled as marginally unstable (F_s = 0.97). However, the 26,000 ft^3/s level is below the base of the

Idealized Profile Used for Rotational Bank-Failure Analyses
River Mile 1630

*For most critical conditions modeled where groundwater level is at elevation of 26,000 ft³/s water surface and river stage is at elevation of 10,000 ft³/s water surface

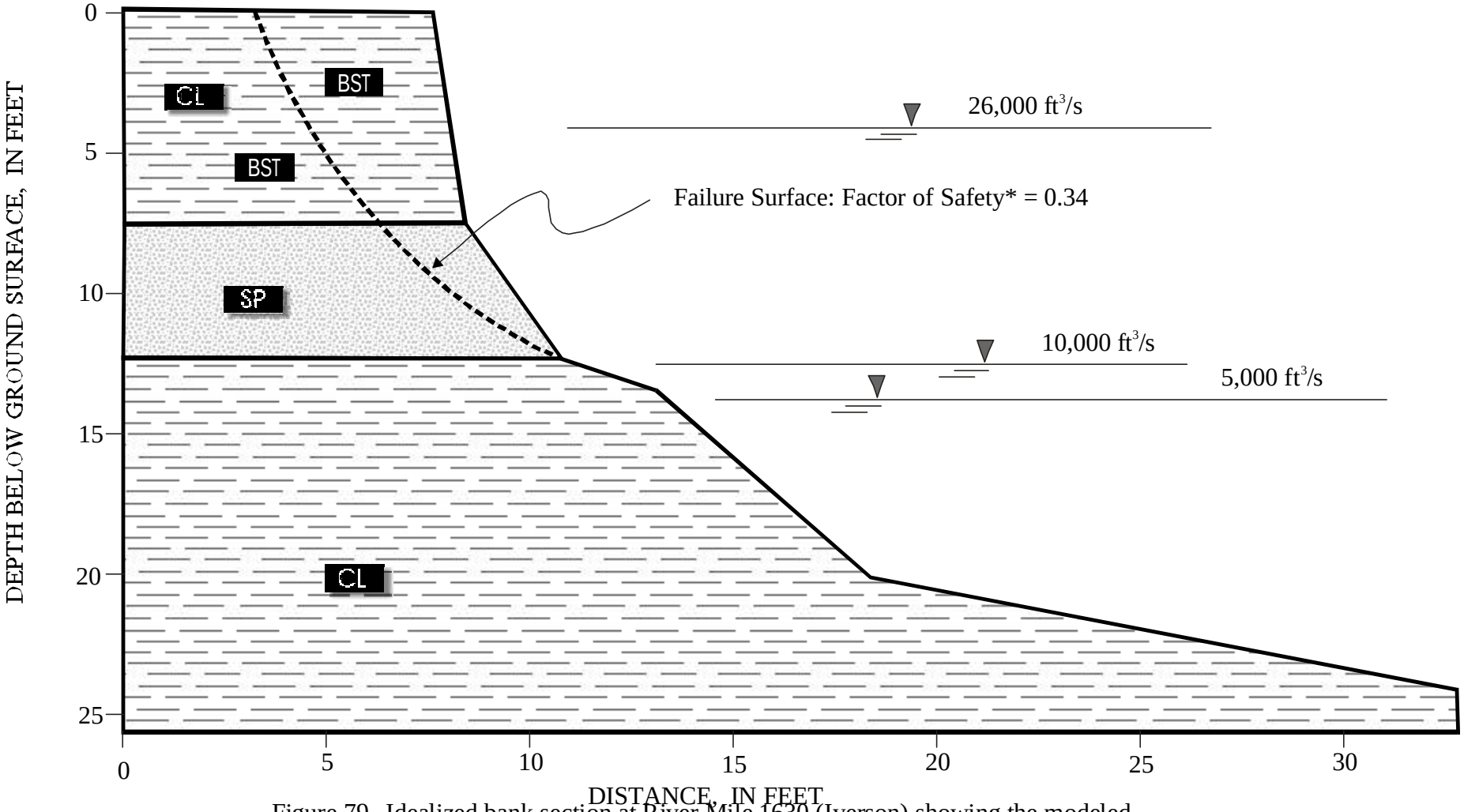

Figure 79--Idealized bank section at River Mile 1630 (Iverson) showing the modeled, rotational critical failure-surface, factor of safety (F_s), river stage and groundwater levels, location of BST tests, and differentiated soil units.

Idealized Profile Used for Rotational Bank-Failure Analyses
RM 1631

*For most critical conditions modeled where groundwater level is at elevation of 26,000 ft³/s water surface and river stage is at elevation of 10,000 ft³/s water surface

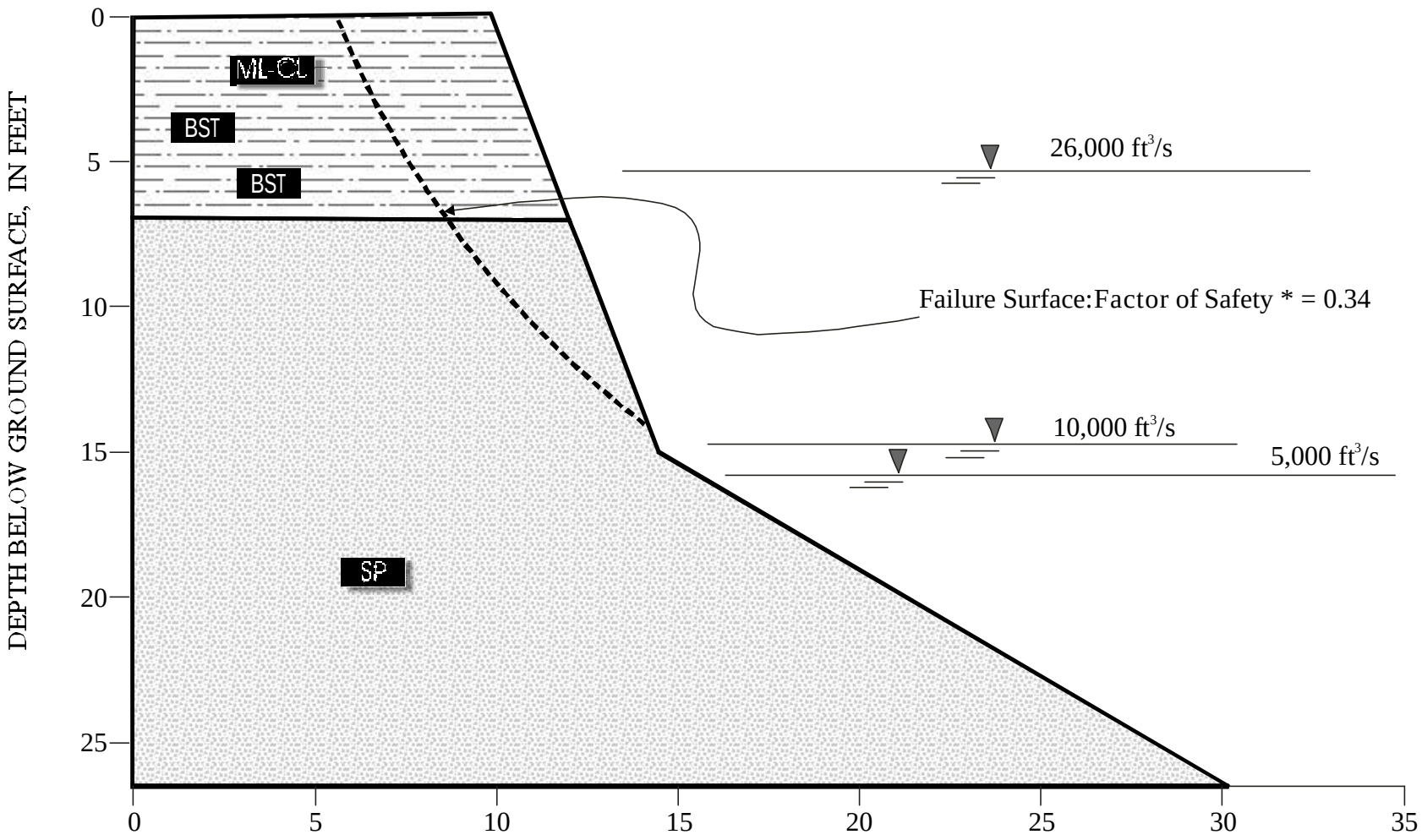

Figure 80--Idealized bank section at river mile 1631 (Vournas) showing the modeled, rotational critical failure-surface, factor of safety (F_s), river stage and groundwater levels, location of BST tests, and differentiated soil units.

Idealized Profile Used for Rotational Bank-Failure Analyses
RM 1646

*For most critical conditions modeled where groundwater level is at elevation of 26,000 ft³/s water surface and river stage is at elevation of 10,000 ft³/s water surface

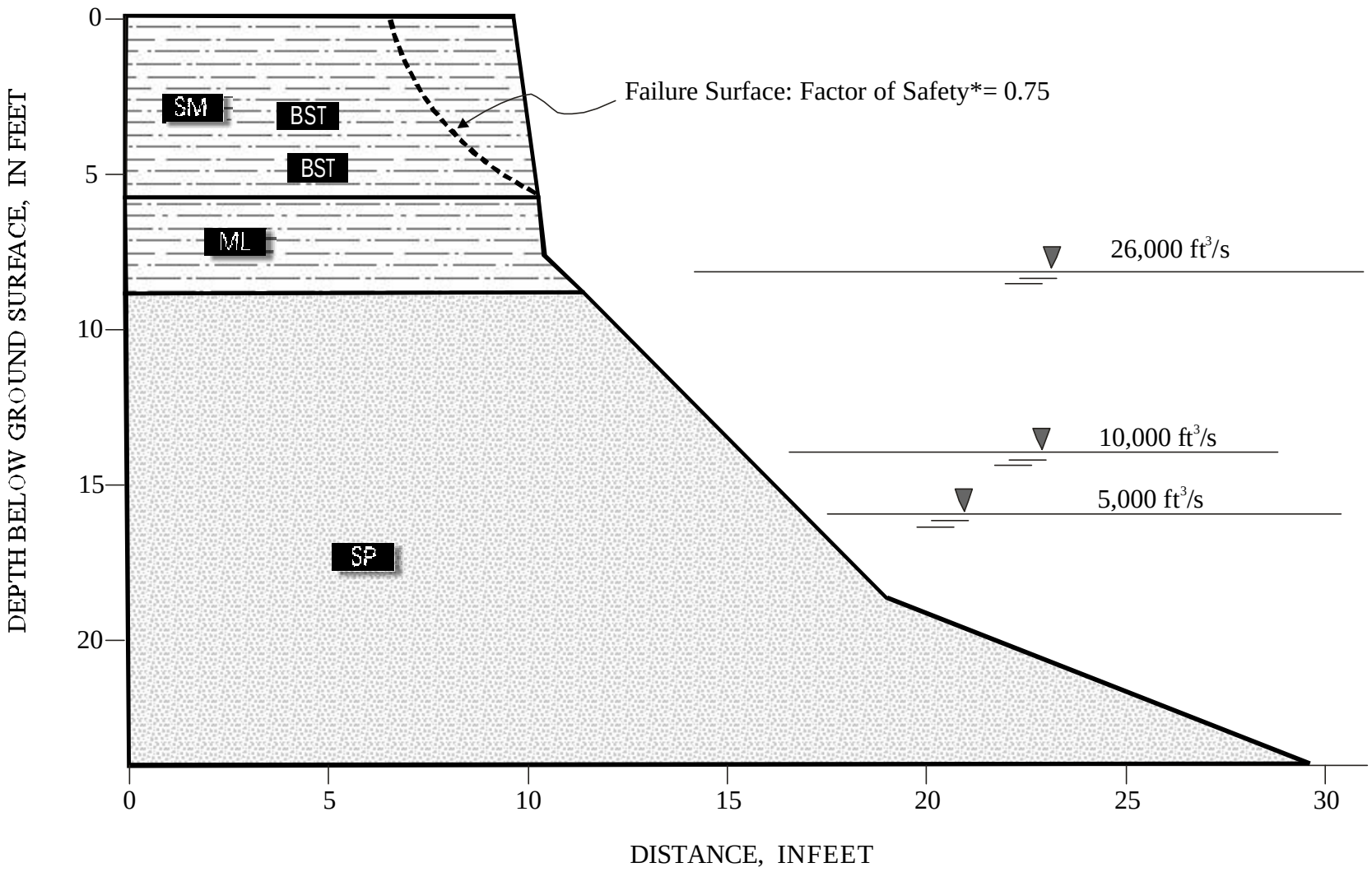

Figure 81--Idealized bank section at river mile 1646 (Mattelin) showing the modeled, rotational critical failure-surface, factor of safety (F_s), river stage and groundwater levels, location of BST tests, and differentiated soil units.

Idealized Profile Used for Rotational Bank-Failure Analyses
RM 1676

*For most critical conditions modeled where groundwater level is at elevation of 26,000 ft³/s water surface and river stage is at elevation of 10,000 ft³/s water surface

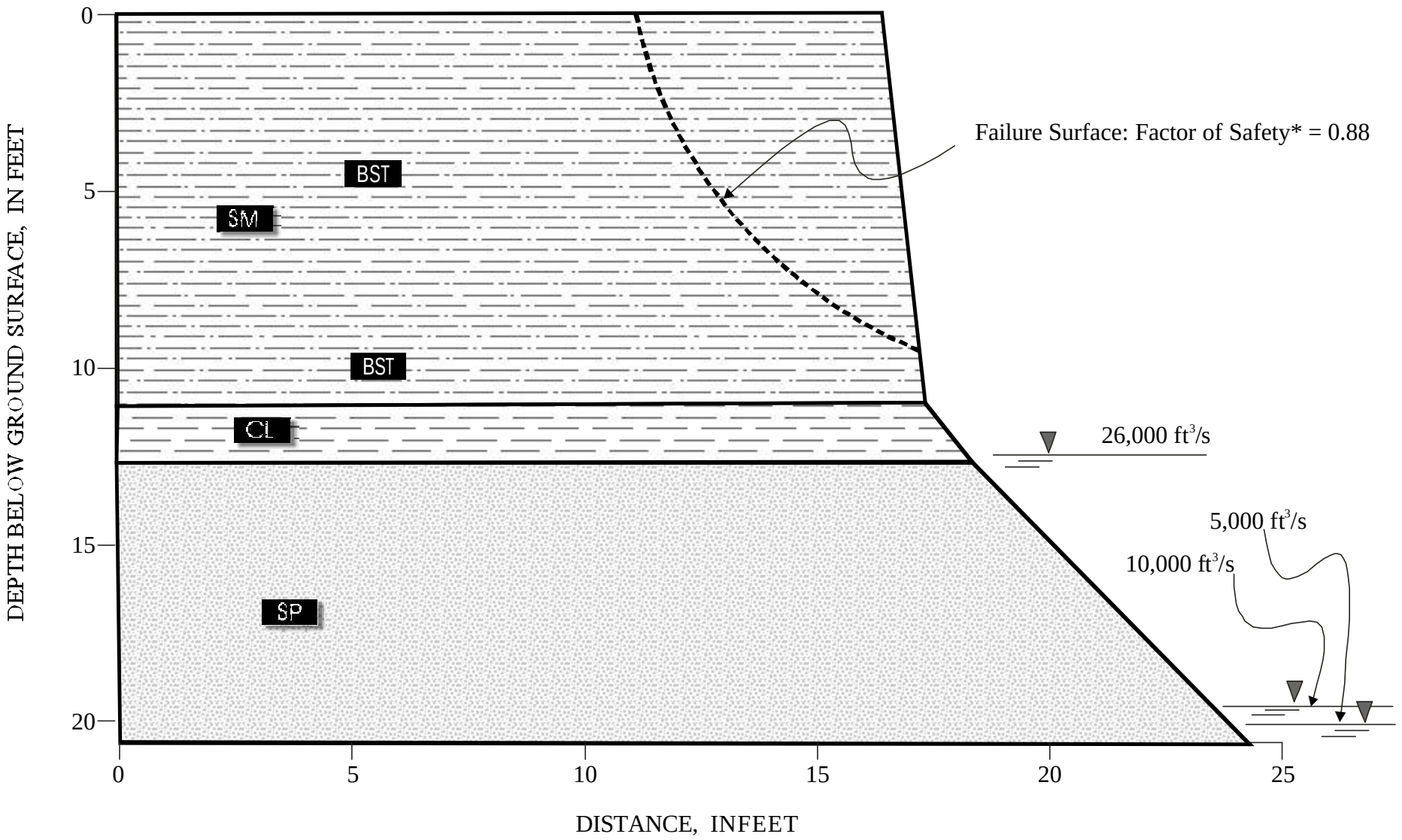

Figure 82--Idealized bank section at river mile 1676 (Woods Peninsula) showing the modeled, rotational critical failure-surface, factor of safety (F_s), river stage and groundwater levels, location of BST tests, and differentiated soil units

Idealized Profile Used for Rotational Bank-Failure Analyses
RM 1682

*For most critical conditions modeled where groundwater level is at elevation of 26,000 ft³/s water surface and river stage is at elevation of 10,000 ft³/s water surface

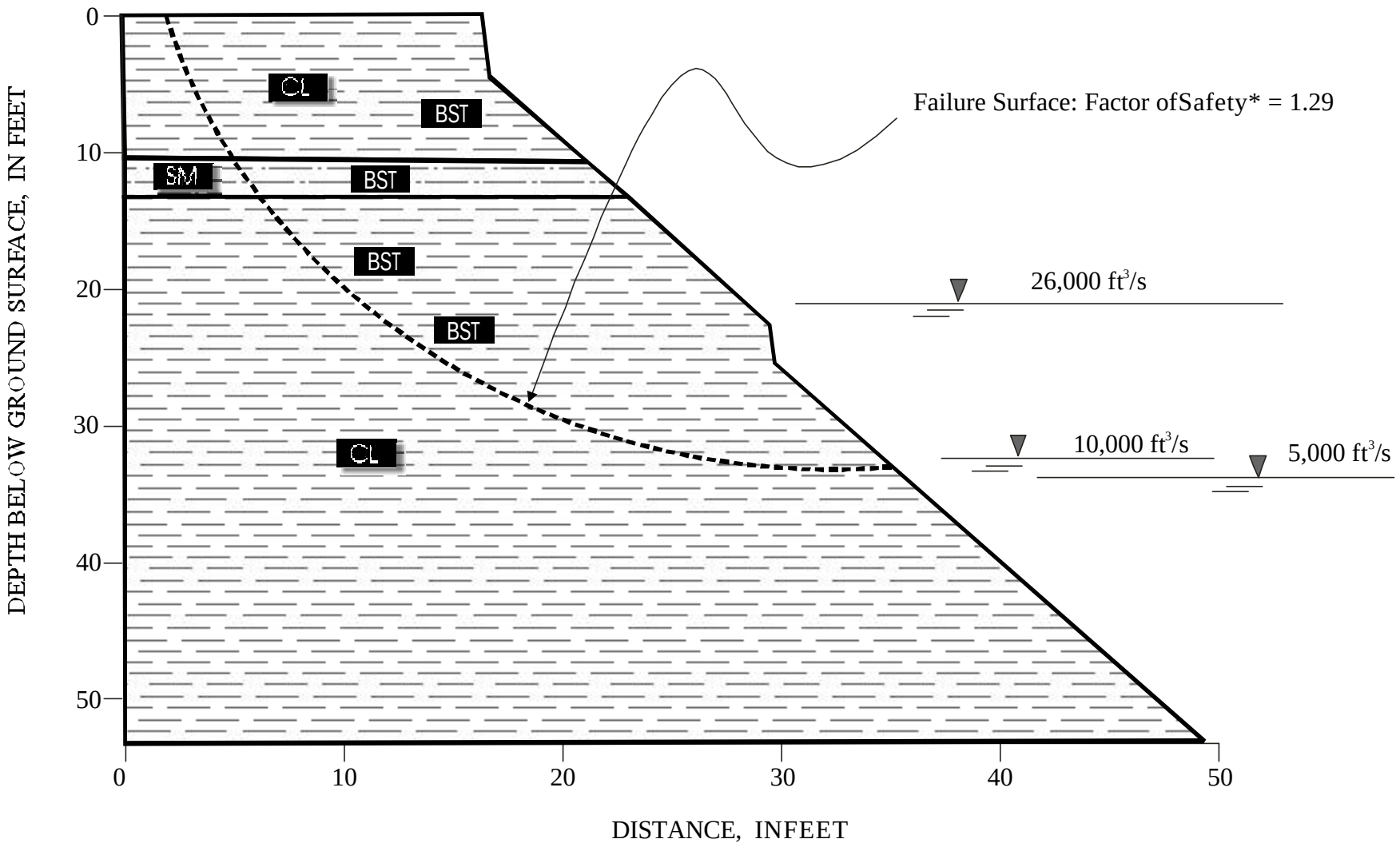

Figure 83--Idealized bank section at river mile 1682 (McRae) showing the modeled, rotational critical failure-surface, factor of safety (F_s), river stage and groundwater levels, location of BST tests, and differentiated soil units.

Idealized Profile Used for Rotational Bank-Failure Analyses
RM 1701

*For most critical conditions modeled where groundwater level is at elevation of 26,000 ft^3/s water surface and river stage is at elevation of 10,000 ft^3/s water surface

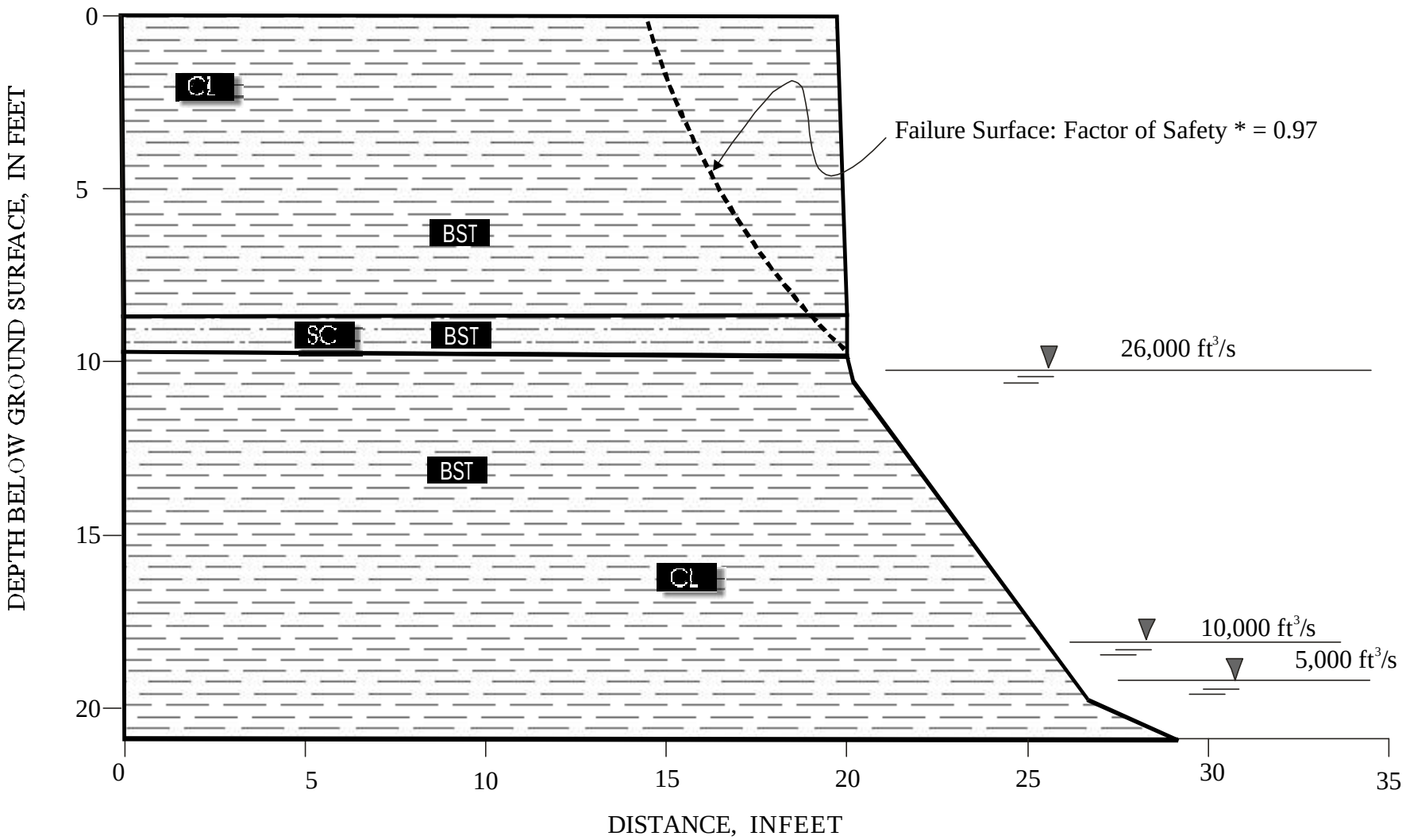

Figure 84--Idealized bank section at river mile 1701 (Wolf Point) showing the modeled, rotational critical failure-surface, factor of safety (F_s), river stage and groundwater levels, location of BST tests, and differentiated soil units.

failure surface for this scenario. In these cases the block width is about half (5.6 to 5.7 feet) that of the other three cases, that manifest drier banks. This bank may reflect another case where perched water tables are possible because of a sand unit confined between two clay units at a depth of about 9 feet.

River Mile 1716-- Pipal

In the high GW cases (Cases 1 and 2) the site is unstable, as about half of the bank is saturated. The remaining three cases are unaffected by the modeled groundwater levels because the base of the failure plane is above them. Failure widths for these unstable cases are 4.7 and 8.2 feet respectively, indicating a substantial difference in the size and shape of the failure surface for even these two cases.

River Mile 1728-- Flynn Creek

The streambank at this site is modeled as having low F_s values for the high GW cases (Cases 1 and 2; F_s values = 0.75 and 0.63, respectively). Cases 3 and 4 are at risk of failure with F_s values of 1.06. The relative instability at this site is related to both the fissured clays that make up the surficial layer of the bank and the sand unit at the bank toe. The "summer" case of low RS and GW levels is relatively stable. The failure width in all cases is about the same, ranging from 6.2 to 6.9 feet.

River Mile 1737-- Frazer Pump

The lowest F_s value at this site is 0.95 in the worst-case drawdown scenario (Case 2). The Case 1 scenario, where both RS and GW are at the 26,000 ft^3/s level is modeled as stable even though more than half of the failure surface is experiencing positive pore-water pressures. This is due to the larger failure dimensions for the Case 1 failure bringing it into contact with a large portion of the stronger cohesive unit at depth. Failure width for the unstable case is 4.8 feet.

River Mile 1744-- Little Porcupine

This site is stable for all modeled cases because of the great cohesive strength of the glacial till that makes up the majority of the bank.

River Mile 1762-- Milk River

Geotechnically, this is a very stable site. The lowest F_s value is 2.13 for the worst-case drawdown condition. The average value of effective cohesion here is 579 lbs/ft^2, the greatest in the study reach. Because of these strengths, if the banks were to become unstable, failure widths would be quite large, about 22.3 feet.

Idealized Profile Used for Rotational Bank-Failure Analyses
RM 1716

*Formostcriticalconditions modeled where groundwater levelisatelevationof26,000ft^3/swatersurface andriverstageisatelevationof10,000ft^3/swatersurface

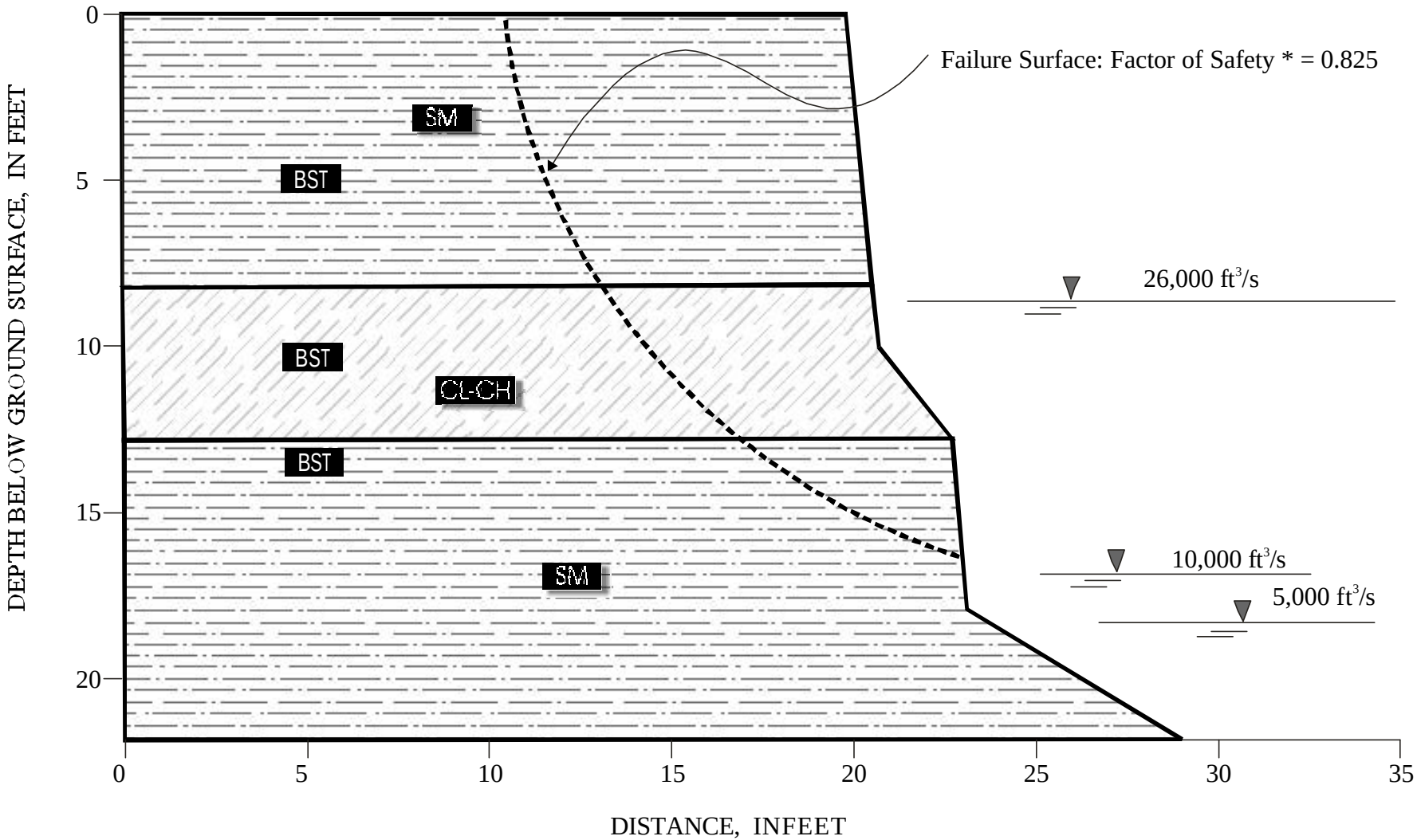

Figure 85--Idealized bank section at river mile 1716 (Pipal) showing the modeled, rotational critical failure-surface, factor of safety (F_s), river stage and groundwater levels, location of BST tests, and differentiated soil units.

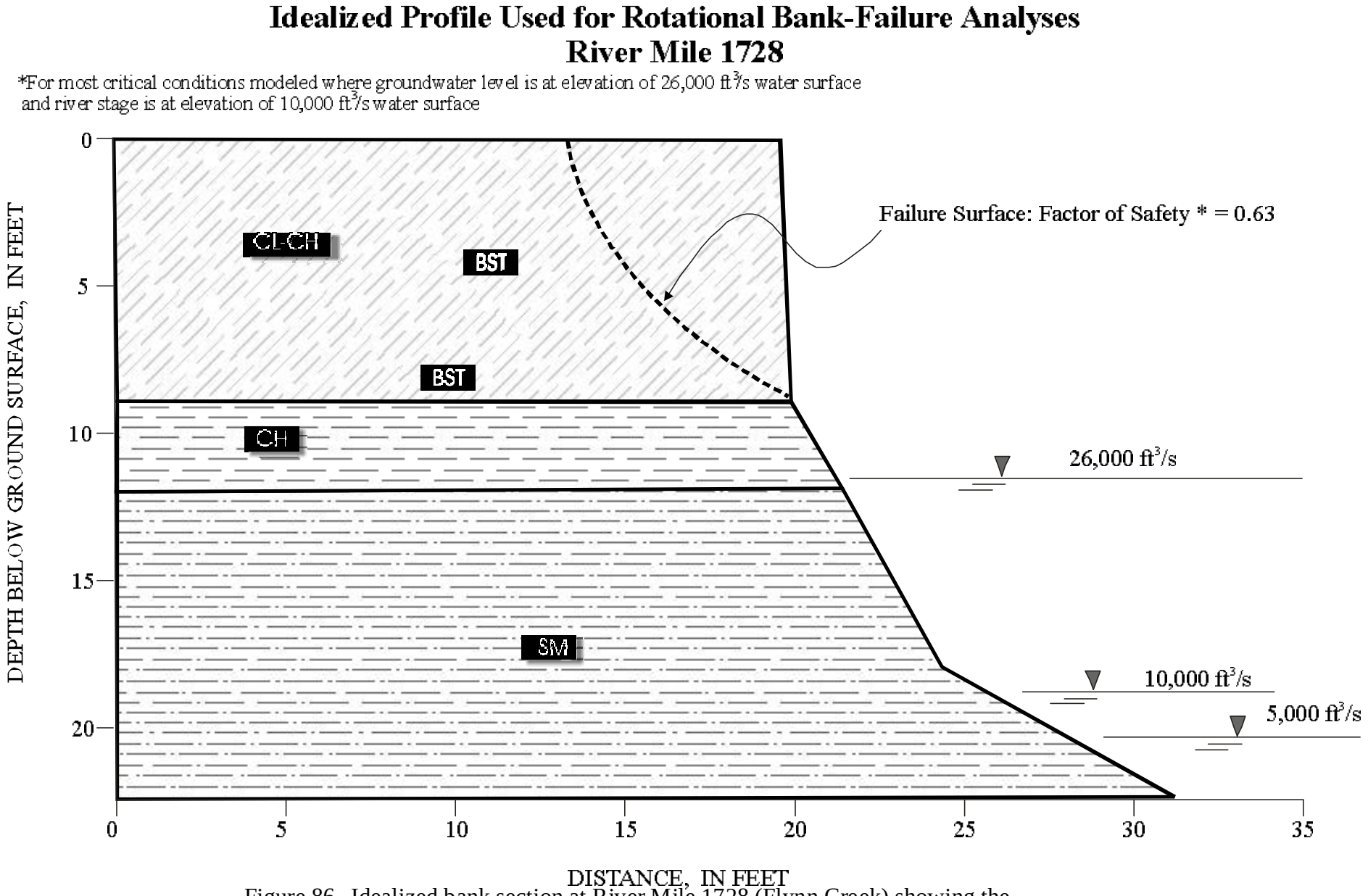

Figure 86--Idealized bank section at River Mile 1728 (Flynn Creek) showing the modeled, rotational critical failure-surface, factor of safety (F_s), river stage and groundwater levels, location of BST tests, and differentiated soil units.

Idealized Profile Used for Rotational Bank-Failure Analyses
RM 1737

*Formostcriticalconditions modeled where groundwater levelisatelevationof26,000ft^3/swatersurface
andriverstageisatelevationof10,000ft^3/swatersurface

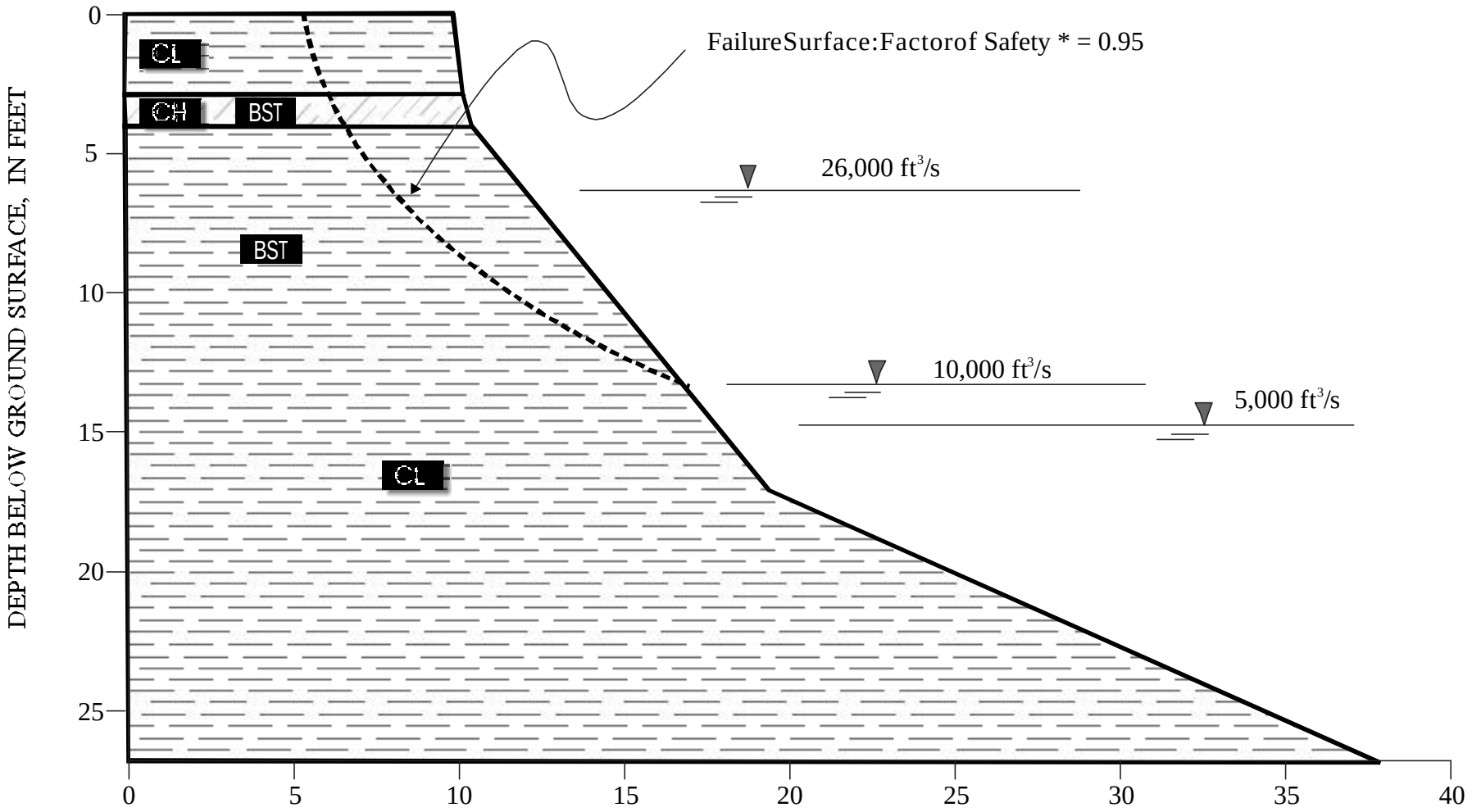

Figure 87--Idealized bank section at river mile 1737 (Fraizer Pump) showing the modeled, rotational critical failure-surface, factor of safety (F_s), river stage and groundwater levels, location of BST tests, and differentiated soil units.

Idealized Profile Used for Rotational Bank-Failure Analyses
RM 1744

*For most critical conditions modeled where groundwater level is at elevation of 26,000 ft^3/s water surface and river stage is at elevation of 10,000 ft^3/s water surface

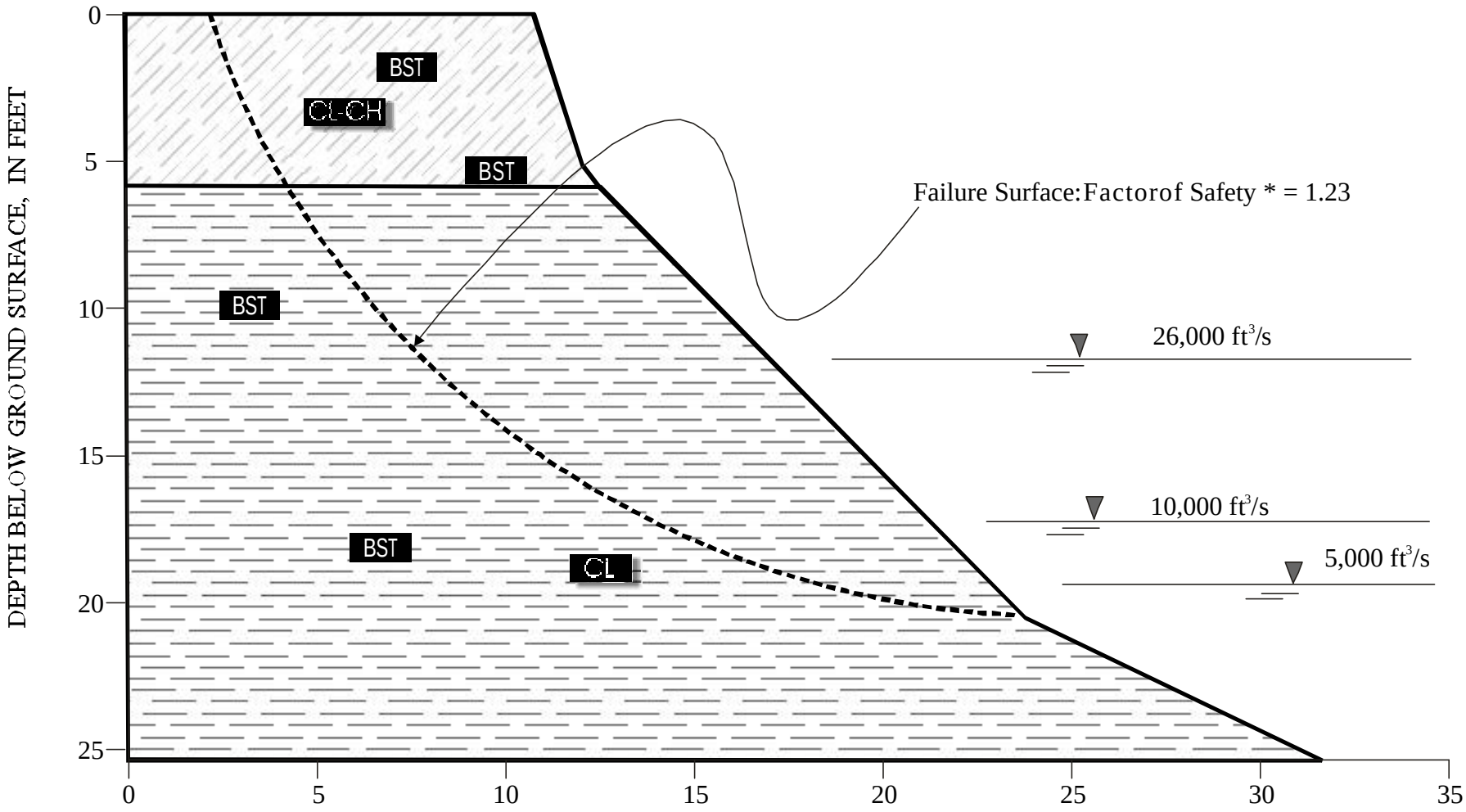

Figure 88--Idealized bank section at river mile 1744 (Little Porcupine) showing the modeled, rotational critical failure-surface, factor of safety (F_s), river stage and groundwater levels, location of BST tests, and differentiated soil units.

Idealized Profile Used for Rotational Bank-Failure Analyses
RM 1762

*Formostcriticalconditions modeled where groundwater levelisatelevationof26,000ft^3/swatersurface andriverstageisatelevationof10,000ft^3/swatersurface

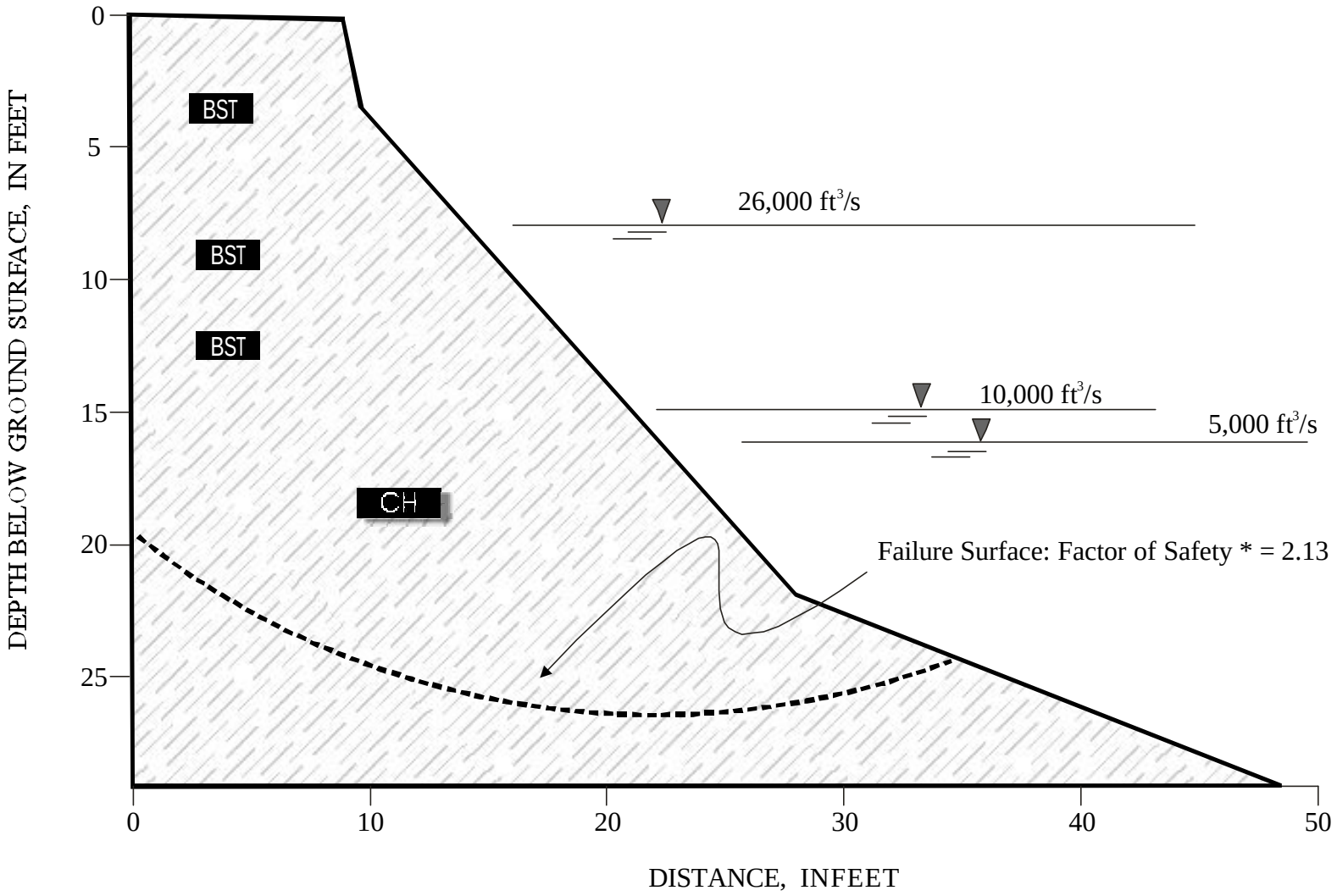

Figure 89--Idealized bank section at river mile 1762 (Milk River) showing the modeled, rotational critical failure-surface, factor of safety (F_s), river stage and groundwater levels, location of BST tests, and differentiated soil units.

River Mile 1765-- Garwood

F_s values for all modeled cases examined are less than 1.0. Weak materials (silty sand) along the base of the failure plane and at the bank toe contribute to the general instability here. Failure widths are similar in the cases of high GW levels at 4.5 feet. Failure widths for the drier cases are larger because of the greater shear strengths (7.0 to 7.2 feet).

Failure-Block Widths

Failure-block widths represent the linear extent of land loss associated with a single failure episode. Individual block widths observed in the field during the summers of 1996 and 1997 ranged from 1.6 to 4.6 feet (average of 2.6 feet). The most critical rotational failures that were simulated are somewhat smaller than originally expected in that they did not encompass greater amounts of land than the modeled planar failures. In fact, the average failure-block width for the modeled rotational failures is 7.2 feet compared to 9.8 feet for the planar failures. This is probably because the more resistant clay materials are often not the surficial layer of bank material. As such, the failure-plane searches for the rotational failures encompass a greater proportion of the lower units than do the planar failure surfaces. Because of this, the most critical rotational failure surface is often above these more resistant materials, resulting in smaller block widths. In contrast, the location of the planar failure planes are fixed by model input parameters. Direct comparisons are, therefore, difficult. One can either compare failures of similar size as an academic exercise or, as we have done here for practical considerations, compare the failures that are the most likely to occur.

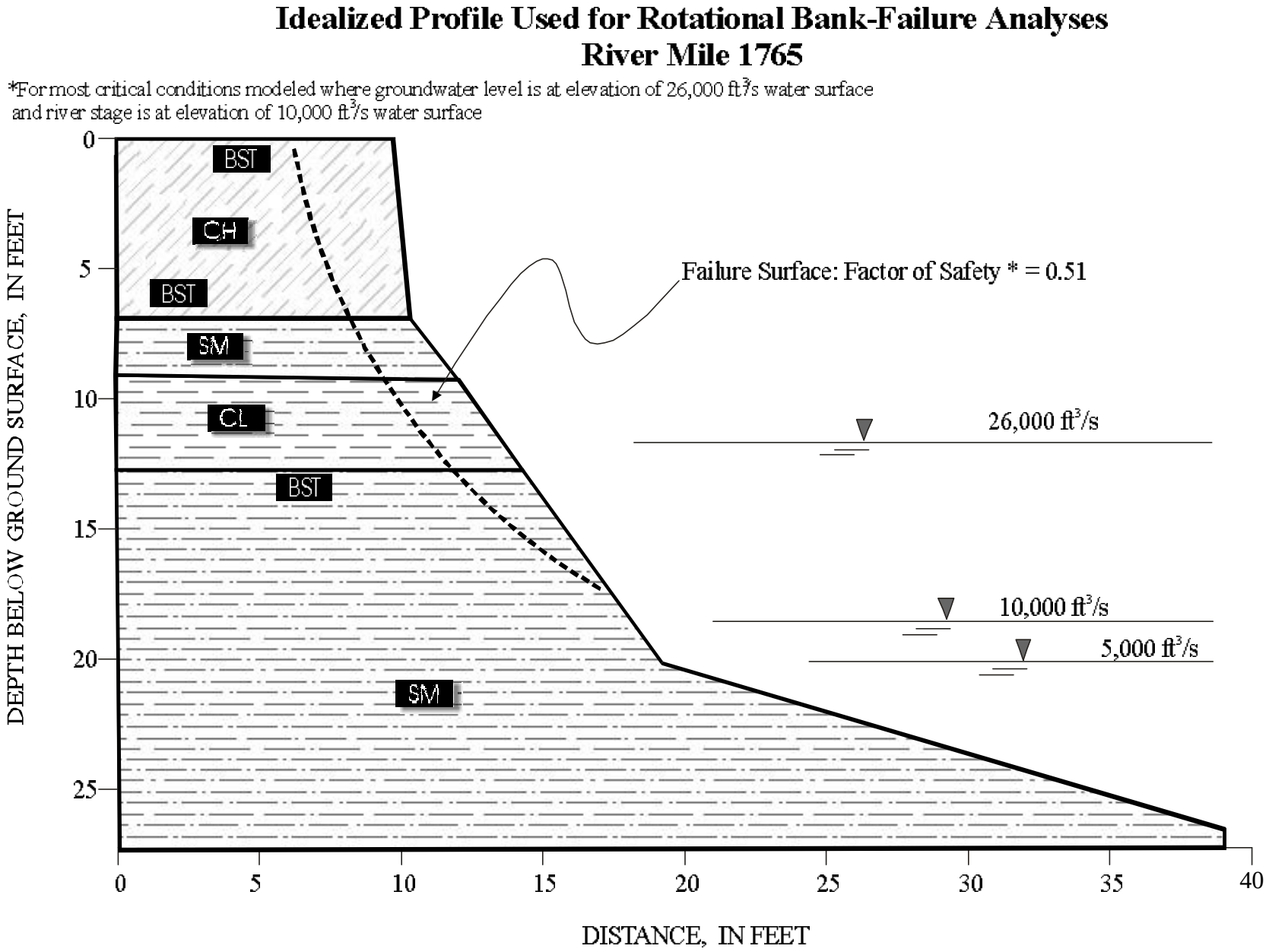

Figure 90--Idealized bank section at River Mile 1765 (Garwood) showing the modeled, rotational critical failure-surface, factor of safety (F_s), river stage and groundwater levels, location of BST tests, and differentiated soil units.

SUMMARY OF BANK-STABILITY ANALYSIS RESULTS

Bank-stability analyses have been carried out using three different methodologies yet all results indicate the following:

1) Banks of low shear strength (generally low cohesive strength) are the most unstable. These sites are characterized by sandy or silty soils of the following soil series: Banks, Havre-Harlem, Riverwash, and Trembles.
2) Banks with sand or silty-sand bank-toe material are the most unstable. Sites with sandy bank toes are located at River Miles 1604 (Hardy); 1624-low terrace (Tveit-Johnson); 1624 (Tveit-Johnson); 1631 (Vournas); 1646 (Mattelin); 1676 (Woods Peninsula); 1716 (Pipal); and 1765 (Garwood). The most stable banks are those that have clay in the lowest portion of the bank and/or at the bank toe;
3) Banks that are stable during low-water stage often become unstable during drawdown conditions as a consequence of the increase of driving forces such as soil unit-weight and the reduction of resisting forces such as negative pore-water pressure, suction and confining pressure.
4) The highest factors of safety are reached during the low water stage, represented by a river stage corresponding to 5,000 ft^3/s and a groundwater height corresponding to 5,000 ft^3/s. The lowest factors of safety are reached during the worst of the two drawdown cases analyzed, represented by a river of stage corresponding to 10,000 ft^3/s and a groundwater height corresponding to 26,000 ft^3/s.
5) The destabilizing effect of high groundwater levels can be produced by maintaining flows greater 15,000 ft^3/s – 20,000 ft^3/s for five - ten days and has increased in frequency since dam closure.
6) The most stable banks are those containing cohesive clays that are also resistant to deep cracking. The site at River Mile 1762 (Milk River) is representative of this.

The hydrologic conditions that often result in bank instability are related to the frequency and duration of moderate and high flows. The elevation of flows greater than 10,000 ft^3/s impinges on banks above the level of the base of the failure surface. The higher the flow level, the greater the proportion of bank that is subject to saturation and positive pore-water pressures. Surface-water elevations associated with the 20,000 ft^3/s and greater flows will have a significant negative impact on the shear strength of the bank material if the flow level is maintained for at least five days. It is assumed that after ten days, bank saturation has occurred 3.3 feet (1 meter) into the bank mass. Thus, in a region where bank saturation is required to produce bank instability and limited rainfall is available to saturate the banks, maintenance of high flow levels creates the mechanism for failure. It is reasonable to assume that these types of effects would be greatly amplified during the winter months due to the effects of river ice and high-flow releases.

Banks that are unstable under all conditions in any one of the three analyses are considered **unstable** and are located at River Miles:

1) 1604 (Hardy);

2) 1624 low-terrace (Tveit-Johnson);
3) 1631 (Vournas);
4) 1646 (Mattelin);
5) 1676 (Woods Peninsula);
6) 1716 (Pipal);
7) 1728 (Flynn Creek); and
8) 1765 (Garwood).

Banks stable only during partially-saturated or dry conditions are those at River Miles:

1) 1589 (Nohly);
2) 1621 (Culbertson);
3) 1621 (Tveit-Johnson);
4) 1630 (Iverson);
5) 1682 (McCrae);
6) 1701 (Wolf Point);
7) 1737 (Fraizer Pump); and
8) 1744 (Little Porcupine).

Banks that are always stable are located at River Mile:

1) 1762 (Milk River).

Streambanks between study sites at River Miles 1589 and 1676 are generally unstable. Banks are generally less unstable between River Miles 1682 and 1701. Between 1716 and 1728 the results indicate that banks are very unstable while from River Mile 1737 to 1744 the banks are unstable only during drawdown conditions. Banks beyond River Mile 1762 are stable during all hydrological conditions.

ICE EFFECTS ON BANK EROSION AND ALLUVIAL-CHANNEL MORPHOLOGY

Introduction

Ice is a prominent feature of the lower Missouri River. It typically grips the river and its banks for an extensive period of the year and, therefore, may potentially influence bank erosion and channel morphology. This section is a preliminary evaluation of the ways in which ice (as river ice and water frozen in banks) may affect bank erosion and channel morphology along the lower Missouri River. It is prepared in response to concerns that ice, in conjunction with elevated flow levels during winter, may aggravate bank erosion and shifts in channel thalweg along the river. A typical scene, such as that shown in Figure 91, indicates the rawness of the contact between exposed bank, river, and ice.

This section of the report begins with an introductory overview of ice effects on bank erosion and channel morphology. The overview briefly presents some of the complexities faced when attempting to evaluate the overall consequences of those effects, which can be diverse; some effects amplify bank erosion and channel shifting, other effects dampen them. The section then briefly reviews and explains the typical processes associated with ice-cover formation, ice-cover presence and ice-cover break-up on rivers. It subsequently describes the typical mechanisms whereby ice may affect riverbanks and channels. Of particular interest are ice effects on bank erosion and channel morphology of rivers whose inflow is regulated by an upstream dam, as is the case for the lower Missouri River. Each description of typical processes or mechanisms is followed by a discussion of the evidence of them at work in the study reach below Fort Peck Dam. The section ends with a short discussion of methods to mitigate the adverse effects of ice, and an outline of the tasks needed to confirm the extents to which the ice affects the banks and channel of the lower Missouri River.

Most aspects of the ice cycle and ice effects on bank erosion and channel morphology are not documented for the lower Missouri River, at least not for the reach from Fort Peck Dam to the river's confluence with the Yellowstone River. A modicum of information is documented for the river between its confluence with the Yellowstone River and Lake Sakakawea (Wuebben and Gagnon, 1995). It must, therefore, be stated that most of the ice effects described in this section have yet to be confirmed. The likely extent to which they are active along the lower Missouri River are deduced tentatively using general knowledge about river-behavior in cold regions and observational evidence obtained from a field trip to the river in mid-February, 1998.

Overview

The literature dealing with ice effects on bank erosion and channel morphology is not extensive. Moreover, what exists contains a fair amount of hypothesis and conjecture. There is a noticeable lack of rigorous investigation into most ice effects. Indeed, the whole subject of whether ice reduces or amplifies bank erosion and modifies channel morphology is still a matter of considerable debate. Inevitably, therefore, this section also contains its share of hypothesis and conjecture. An unavoidable difficulty is

Figure 91--The lower Missouri River at River Mile1624, February 10, 1998. As at many other locations along the river, an eroding bank and shifting channel are in direct contact with river ice.

that ice can have various and, at times, apparently contradictory effects. General conclusions about the net effects of ice are not at all straightforward to state, except to say that ice effects are closely related to velocity and elevation of flow; i.e. higher flows incur higher impacts for ice-covered conditions than they do for openwater conditions.

It is also important to mention that a prevailing opinion holds that river-ice processes likely do not significantly affect channel morphology overall (e.g., Neill, 1976, Kellerhals and Church, 1980). That opinion is based on observations of a few rivers in Canada. It may be correct, at least in terms of ice effects on the morphology of long reaches of rivers. Ice adds an additional set of variables that further complicates the already complex and diverse interactions of channel geometry, inconstant flow conditions, bed-sediment and bank conditions, and possible geologic factors such as rock outcrops and fault lines or zones. Consequently, it may indeed be difficult to discern a clear imprint of ice on the channel morphology of most reaches. And yet, the effects of ice on bank erosion and channel morphology are evident locally within channels and they can be deduced for idealized channel conditions. Ice effects, therefore, may be important locally, but they may not dominate other factors influencing the overall morphology of alluvial channels.

The degree to which the ice cycle modifies alluvial-channel morphology and bank erosion depends on a combination of factors related to the cycle's duration, its intensity, the seasonal availability of flow, the ways whereby ice affects channel flow and bank erodibility, and other diverse factors. The overall impacts of these factors on channel morphology and bank erosion vary widely from river to river and from reach to reach. The impacts may be distinct and clearly observable for rivers in permafrost or those annually subjected to severe ice runs following ice-cover breakup in spring. They may be obvious from stunted riparian vegetation, scarred trees, or gouged channel features. They may be subtle and blurred by the inherent complexities and apparent irregularities of alluvial-channel flow. They may also be intermittent, being significant at one site on one occasion, but not the next. A good deal of the variability of ice impacts is attributable to variability in flow conditions.

The impact of ice on channel morphology may be noticeable over varying scales of time and channel length. On the scales of months and miles of channel, for instance, ice alters the relationships between flow rate, flow depth and sediment transport rates. As it forms, an ice cover usually increases a channel's resistance to flow and reduces its overall capacity to move water and sediment. In a sense, because the channel's bed roughness does not actually increase (in fact it may reduce; Smith and Ettema, 1997), the effect on channel morphology of an ice-cover may be likened to the effect produced by a reduction in energy gradient associated with flow along the channel. More precisely, it may be likened to a change in thalweg geometry; the additional flow energy consumed overcoming the resistance created by the ice cover offsets the portion of the flow's energy that the channel dissipates by thalweg lengthening or bifurcation. This sort of postulation, though possibly sound theoretically, may be difficult to verify practically because ice covers vary in length, thickness and roughness along most rivers.

At the local scale, an ice cover over a short reach may re-distribute flow laterally across the reach, locally accentuating erosion in one place and deposition in another place. Such local changes of the bed may develop during the entire cycle of ice formation, presence, and release. They may develop briefly, lasting slightly longer than

the ice cover, and disappear shortly after the cover breaks up. Or, they may trigger a change that persists for some time. In any event, they should be verifiable from a site investigation.

Ice may dampen or amplify the erosion processes locally. Obvious dampening effects of ice are reduced runoff from a watershed, cementing of bank material by frozen water, and ice armoring of bars and shorelines by ice-cover set down with reduction in flow rates. Yet ice may amplify erosion and sediment-transport rates, notably when the channel conveys flows greater than that for which the ice cover originally formed and when the ice melts.

The present section is an attempt to describ how ice (especially river ice) may affect bank erosion and channel morphology, locally as well as over long reaches. Thus far, there has not been a comprehensive attempt at such an explanation. For example, the prevailing opinion regarding ice effects does not differentiate between river channels whose wintertime flow is regulated and channels whose flow is unregulated. The difference is likely significant, given that flow rate is an important factor determining the erosive effects of ice.

Ice-Cover Formation

This section briefly describes the processes usually involved in ice formation, presence and break up. The general processes are discussed first, then the processes are discussed in the specific context of the lower Missouri River between Fort Peck Dam and the North Dakota border.

General Processes

During fall and into winter, river water cools. In cold regions it cools to the water-freezing temperature or to a fraction below it (super-cooling before initial ice formation), whereupon ice forms. For a river whose inflow rate is regulated by a large reservoir, water temperature decreases with distance of flow downstream. Initial ice-cover formation develops commensurably at some distance downstream of the reservoir.

Ice-cover formation over a river comprises two main processes. One process is static and could be called the border-ice process. It is evident as ice growth out from the river's banks. The second process is dynamic and could be termed the frazil-ice process. It starts with the super-cooling of water and the formation of frazil-ice crystals throughout the entire body of flow. The crystals agglomerate as slush, form ice pans that drift at the water surface, then accumulate as a continuous cover. The processes are summarized in Figure 92, which outlines the usual processes whereby ice forms in rivers and streams. The terms indicated in Figure 92 are explained further in the following sections. The frazil-ice process usually dominates ice-cover formation on rivers.

Border-Ice Process

As indicated in Figure 92 and sketched in Figure 93, border ice is the first type of ice to appear in a river. It forms in low-velocity zones along banks. The top layer of the water adjacent to the bank minimally mixes with lower layers and soon becomes

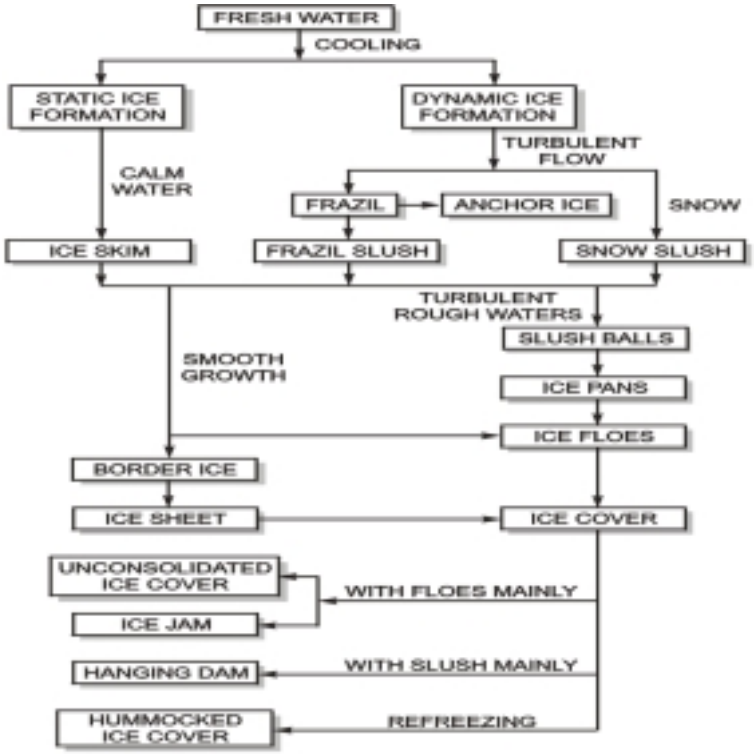

Figure 92--Schematic of general ice-formation processes in rivers and streams.

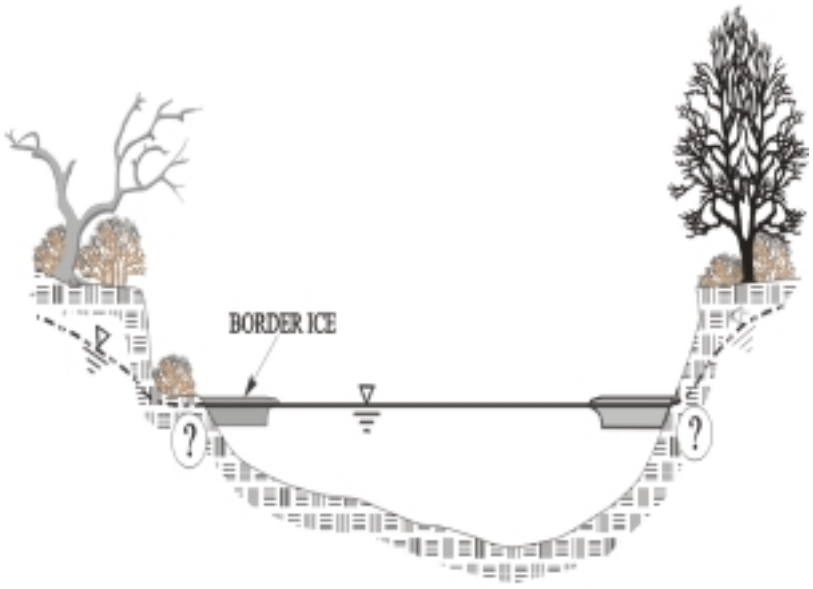

Figure 93-- Sketch of border-ice growth along the banks of a river. The question mark pertains to uncertainties regarding the connection between the border ice, the bank material, and the water table in the bank.

supercooled in frigid air, while water elsewhere is still above the freezing temperature. Ice fragments in the bank surface nucleate the supercooled water at the surface. The nucleated water propagates an ice sheet on the water surface outwards from the bank. The edge of the ice sheet eventually extends to a zone of turbulent water, whereupon its further progress depends on thermal atmospheric exchange. The growth does not stop just because the water is above the freezing temperature, though it slows. It continues growing by virtue of net heat loss of water fringing the border-ice edge. Border-ice extension accelerates when drifting frazil slush and small pans lodge against it. The slush and pans fuse in rows to the dendrite crystals extending from the border-ice edge and they may form successive layers in the outward progressing border ice.

Border-ice growth is the dominant ice-formation process in small rivers and streams with mild slopes. It is also the static type of ice growth that occurs in lakes in calm weather. In the context of bank-erosion concerns, the effects of border ice on bank-material strength and loading are not well understood. For instance, not much is known about how border-ice growth affects freezing of groundwater within a riverbank; hence the question marks in Figure 93.

Frazil-Ice Process

Border-ice formation is a comparatively slow process. It does not account for the rapid progression of ice covers in large rivers. The frazil-ice process (dynamic ice formation) begins with the formation of frazil-ice crystals throughout the depth of flow at an ice-generation zone. It is an especially striking and dominant feature of river behavior in cold regions.

The river flow must first super-cool before ice formation begins, as indicated in Figure 94. Frazil ice first appears in a flow when the flow is supercooled to a fraction of a degree below the freezing temperature of water; i.e. nominally about -0.01 to -0.05^{o}C. For river flow in a watershed unregulated by dams, factors related to channel size and air-temperature variation with altitude and latitude determine rate of water cooling and where ice first appears and gradually envelops a channel. Though exceptions exist, ice first forms in the upper reaches of a watershed for most rivers in the continental United States.

An important factor influencing first ice formation in a channel whose flow is regulated by an upstream reservoir is the temperature of the water released into the channel. In most situations, the reservoir changes the temperature of the flow entering the channel; besides storing water volume, a reservoir stores heat. During freeze-up conditions in late fall and winter, the flow entering the channel is warmer than the flow in the channel prior to construction of the reservoir. Consequently, the reservoir likely will cause ice formation to begin further downstream along the channel than it did prior to construction of the reservoir.

The thermal influence of a reservoir on ice-cover formation can be demonstrated quite readily. Consider, for example, a flow 10-feet deep with an average velocity of 3 ft/s and exposed to representative conditions of air at about -20^{o}C and mild wind. If, prior to construction of the reservoir, the flow entering the channel was at the freezing temperature of water (0^{o}C), an ice cover potentially could begin forming throughout the full length of the channel. With a reservoir in operation and releasing 4^{o}C water (the temperature at which water is most dense and likely to be at the reservoir outflow

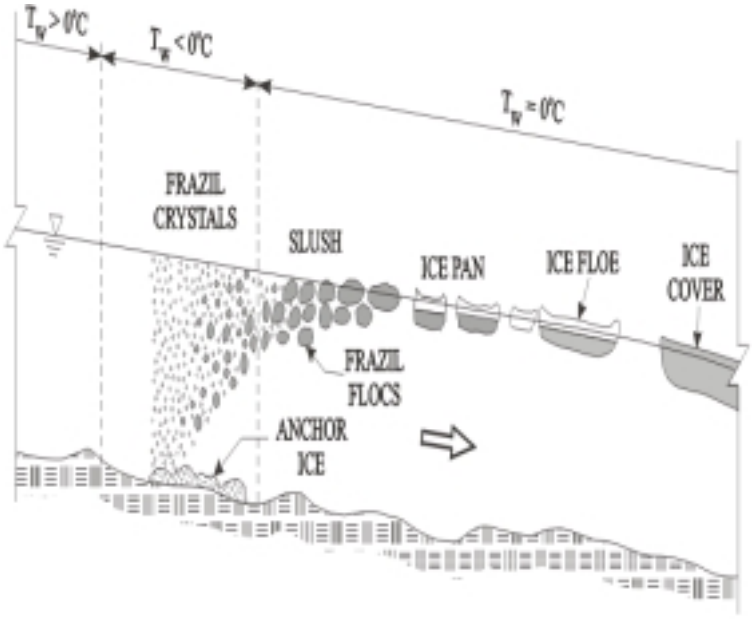

Figure 94--The genesis of frazil ice in a river or stream. The water cools until slightly supercooled, whereupon frazil ice crystals rapidly appear, agglomerate as slush, develop as ice pans, which then may align juxtaposed as an ice cover. T_w = temperature of water.

conduit), it would take almost 70 miles of flow downstream from the reservoir before it is cooled to the freezing temperature. If the initial temperature of the water leaving the reservoir is 1°C, the distance reduces to about 18 miles. Therefore, as the water in the reservoir cools during winter, the ice cover on the river may progress further upstream.

The variation of water temperature along the streamwise axis of a river in frigid air is shown in Figure 94. A volume of water moving with the flow cools until supercooled, whereupon frazil ice crystals quickly start to appear across the full flow cross section. As frazil crystals form, the latent heat of fusion they release gradually raises the water temperature to 0°C. During this period, the frazil is in what is termed the "active" state, in which it fuses readily with solid objects it contacts (e.g. other frazil ice crystals, sediment on the river bed, boulders). The zone of active frazil formation may be fixed in a river and extend only a few hundred feet, producing frazil conveyed downstream by the flow. The continuous variation in weather conditions in nature (notably, fluctuations in air temperature, wind speed and net heat loss by means of radiation) causes the zone to shift. A lowering of air temperature or water flow rate, for example, cause the zone to move upstream. Supercooling could occur at the same river site for several days, depending on daily fluctuations in weather and flow.

Frazil crystals grow rapidly in size, fuse to each other, form slush, and (owing to ice buoyancy) rise to the water surface if able to drift for a sufficient distance. When initially in supercooled water, frazil crystals fuse to almost any solid boundary in the flow. As frazil slush drifts, it rises to the water surface, agglomerates, crusts over, and forms ice pans, which have a hard, flat circular top and an approximately hemispherical accumulation of slush below. At this stage, the water is no longer supercooled and the frazil is termed inactive frazil; it has lost its propensity to fuse readily.

Long reaches of rivers may become covered with drifting slush, pans and floes formed of fused pans. In deep sections with relatively low surface velocity, or in other locations with low surface velocities, the ice coverage concentrates. The pans and floes drift with the flow until becoming congested (like in a traffic jam) or lodging against some constriction. Once a cover has started, it progresses upstream rapidly as a juxtaposed layer of pans and floes cemented with frazil slush. It is typical for ice covers on large rivers to progress upstream at a rate of about 25 miles per day in this manner (e.g., Michel, 1978). Alternately, a pile up of ice may occur and form what is termed a freeze-up jam. Freeze-up jams retard flow and raise water levels, possibly causing flooding upstream of the jam toe.

Several flow-related variables influence the upstream progression of a level cover comprising juxtaposed pans and floes. However, an approximate rule of thumb is that a level cover may develop when the Froude number for flow at the site is about 0.1 or less; i.e., Froude number = $V/\sqrt{(gY)} < 0.1$, in which V = bulk flow velocity, Y = flow depth, and g = gravity acceleration. For typical rivers, it is easier to use simple velocity criteria; e.g., frazil slush passes under the front of an ice cover when flow velocity exceeds about 2 ft/s, frazil pans will go under when velocity exceed about 6 ft/s. The cover may still progress upstream when ice passes under its front, if the rate of ice arrival at the front exceeds the rate at which ice is subducted beneath it.

When the upstream front of the cover reaches a high-velocity section of a river, large amounts of slush and pans are forced under the front and conveyed beneath it.

They may come to rest and accumulate in zones of lower velocity beneath the cover. Large accumulations of ice may develop under the cover and be resistant to shoving. In some situations, they may form a feature known as a hanging dam. Ice moving under the cover progressively accumulates in locations of reduced flow velocity, concentrating the flow in such a way that it locally scours the river's bed (a later section further discusses this concern) and increases flow area. The hummocking of an ice cover can be a clue to the presence of a hanging dam. As hanging dams and similar accumulations increase in size, they increase flow resistance, raise water level, reduce and possibly redistribute flow velocity and enable the cover to continue progressing upstream. Figure 95, taken from Beltaos and Dean (1981), depicts typical aspects of a hanging dam in the Smoky River, Alberta.

For steep highly turbulent streams, a somewhat analogous process occurs. Weirs of anchor ice (frazil ice bonded to the bed, not the ice cover) may extend up from the streambed, reducing flow velocity and enabling the cover to progress upstream. The anchor-ice weirs retard the flow and eventually help a cover form over the flow.

In relatively steep, swift-flowing channels, frazil ice may not develop to the level cover of juxtaposed pans (as illustrated in Figure 94) or covers with hanging dams. Instead, the larger flow velocities associated with steeper channels, pans and slush, sometimes mixed with snow, form a jumbled accumulation known as a freeze-up jam. Such jams may be free floating or partially grounded on the bed. The remnants of such a jam in a reach of the Yellowstone River, Montana, are depicted in Figure 96. The jam clogged much of the reach, especially in shallower, slower current portions to the side of the river's thalweg.

A cover of pans and slush solidifies contiguously between the ice pieces and may thicken thermally. The contiguous solidified cover resists the hydrodynamic drag exerted by the water and the streamwise component of the cover's weight. The cover may locally buckle, shove, hummock and bummock at weak spots as it progresses upstream, the flow rate may fluctuate and/or air temperatures may change.

Ice-Cover Formation on the Lower Missouri River

During late fall and into winter, the lower Missouri River between Fort Peck Dam and Lake Sakakawea may be likened to a large ice-making and ice-assembly machine. Frazil ice is generated at certain locations, from which it is then conveyed downstream to collection points where it is assembled with border ice into an ice cover. The cover subsequently thickens thermally. The amount of ice made, its conveyance and accumulation along the river, depends on the amount of thermal energy entering the river from the reservoir and the amount of thermal energy lost from the river to the frigid air above, as indicated in Figure 97. For given weather conditions, the amount and distribution of ice depends on the flow rate in the river. The river usually runs quite smoothly as an ice-making machine until the weather warms or the flow rate increases substantially. Then, the ice-assembly operation may break down.

Before it was constrained by Fort Peck Dam and Lake Sakakawea, the lower Missouri River comprised an unregulated channel whose inflow rate and water temperature reflected seasonal variations. The river then typically conveyed flows of smaller magnitude and thermal-energy content. For example, the flow rates at Wolf

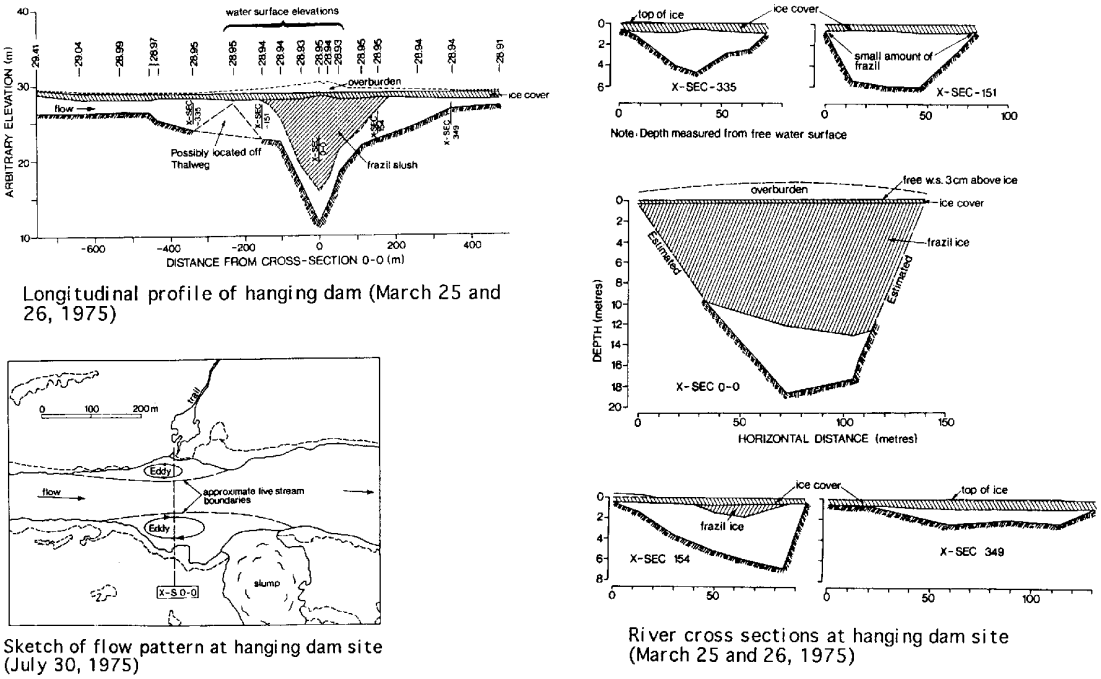

Figure 95--A hanging jam of frazil ice may develop under an ice cover when flow velocities exceed those needed to form an ice cover of juxtaposed pans. This example, taken from Beltaos and Dean 1981, shows a hanging dam in the Smoky River, Alberta.

Figure 96--The remnants of a freeze-up jam in the Yellowstone River, Montana, February 9, 1998. The jam comprised frazil slush and pans, mixed with snow, and it is partially grounded.

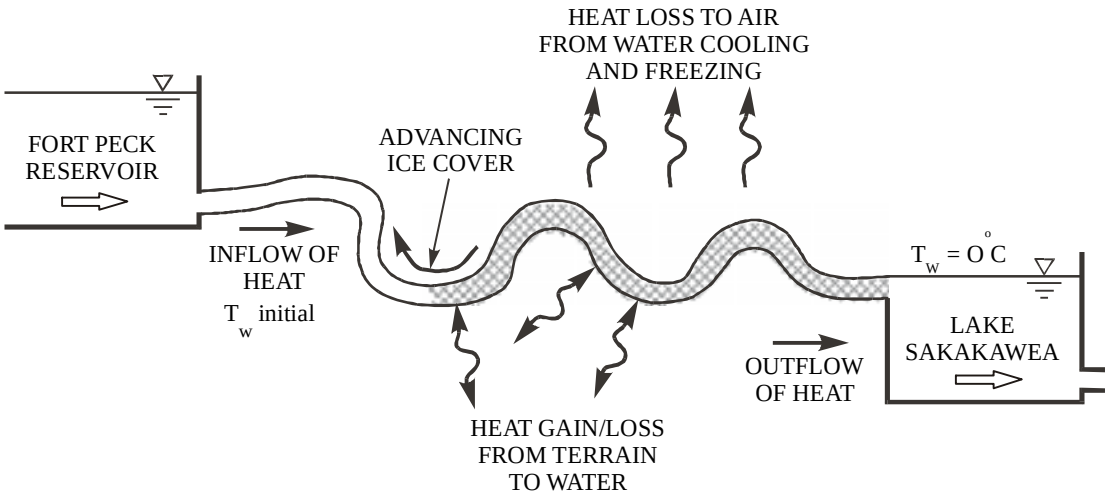

Figure 97--Schematic of the lower Missouri River, between Fort Peck Dam and Lake Sakajawea, as an ice making and ice-cover assembly machine.

Point reportedly ranged between 3,000 to 9,000 ft^3/s during winter (Engelhardt and Waren 1991) and they were likely of water near or at the freezing temperature. Consequently, the ice cover likely formed quicker and earlier during winter and it likely covered the entire river. It typically formed at a low elevation in the river channel, occupied less surface area and was thicker.

Regulated by Fort Peck Dam, the lower Missouri River is still subject to all of the border-ice and frazil-ice processes just described, but it typically receives a greater inflow of water and thermal energy during early winter than in years prior to the dam. Figure 98 compares flow records for two years, one prior to and one after the dam. The river's regulating reservoir, at Fort Peck Dam, prescribes the inflow rate, temperature and thereby energy content of the flow entering the river. Flow resistance controls flow depth along most of the river. The downstream reservoir, Lake Sakakawea, controls the downstream elevation of flow in the channel.

The river channel itself is approximately 190 miles-long and 800 to 900-feet wide (nominal average width) between Fort Peck Dam and Lake Sakakawea. The channel's average slope is about 1.6×10^{-4}. Its sinuous-point-bar and sinuous-braided morphologies ensure that the flow is well mixed over the flow depth, such that its temperature and thermal energy are practically homogeneous over its depth. It also produces substantial variations in flow velocity within reaches and provides numerous locations for frazil-ice slush and pans to congest and form an ice cover or a jam. Inflow from a tributary, the Milk River, just below the dam is usually small during winter.

Winter flow rates typically range from about 3,000 to 14,000 ft^3/s and may undergo substantial daily fluctuations. Daily rates may vary by as much as 50%. With Fort Peck Reservoir as the source of flow at these rates, the river gradually begins forming its ice cover at several locations considerable distances downstream of the dam. For given weather conditions, the flow rate and temperature of water released from Fort Peck Reservoir, along with channel morphology, influence where and how ice covers form on the lower Missouri. The higher the flow rate and temperature of flow released into the river, the greater the distance of flow before ice-cover formation begins. Local channel morphology influences where the river actually begins forming its ice cover. The river's mild slope (about 1.6×10^{-4}) and relatively moderate average velocities facilitate the formation of an initial cover of juxtaposed ice pans and floes over most reaches; average velocities at Wolf Point and Culbertson are about 2.3 and 2.0 ft/s, respectively (Pokrefke *et al*. 1998). At some sections and flow rates, velocities may be high enough (nominally in excess of 6 ft/s) that ice pans are subducted under the ice-cover front, causing a thickened accumulation to develop. The average flow velocities seem not to get so large that a severe freeze-up jam occurs. The velocities are such that frazil slush may accumulate under the cover. On the whole, bulk flow velocities increase upstream, with the likely consequence that cover formation becomes progressively more difficult at upstream locations.

Borland (1959) gives a sense of ice formation on the Missouri River prior to construction of Fort Peck Dam. He describes the relatively frequent occurrence of freeze-up ice jams (termed gorges by him) and the flooding they caused in the vicinity of Townsend, which is a considerable distance upstream of the reach presently being considered. In some respects the jams he describes are similar to the freeze-up jam

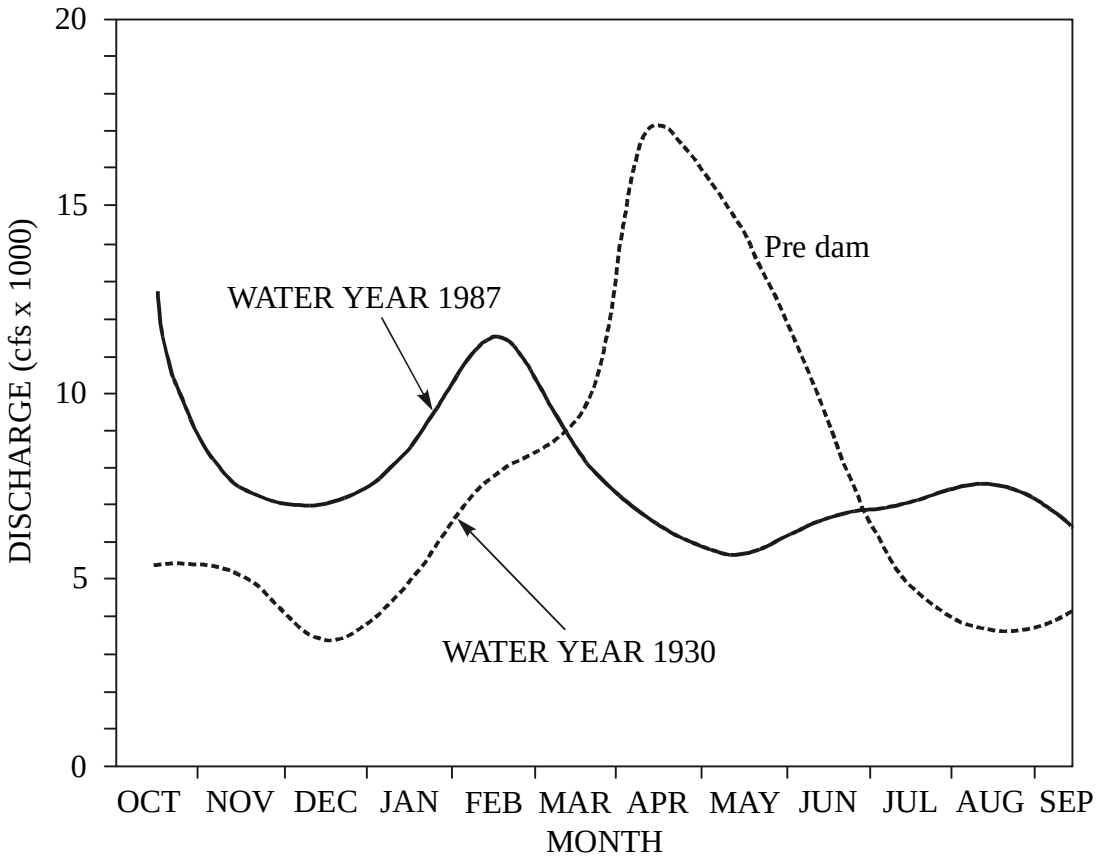

Figure 98--An example of changes in the annual distribution of mean daily discharge in the Lower Missouri River since the closure of Fort Peck Dam. This figure is taken from Engelhardt and Waren (1991).

depicted by Figure 96 for the Yellowstone River. His description nicely captures the way in which ice may grip a river:

> "*The main river channel breaks up into a network of smaller, shallow channels, and there are a great many low brush-covered islands, sand bars, and innumerable obstructions to flow. With the accumulation of frazil ice and anchor ice, the channels become completely choked with or 'gorged' and the river is virtually dammed with ice. Flooding from overflow is, therefore, inevitable. While the cold continues, the frazil ice, exposed to the air, solidifies in huge masses. There is practically no limit to the extent of overflow or ice accumulation that may occur as long as the critical degree of cold continues."*

Actual ice-cover formation on the lower Missouri River in recent times apparently has yet to be documented. Indeed, the typical progression of ice formation of Plains rivers like the lower Missouri River has yet to be documented. At present, only anecdotal descriptions of ice cover progression and conditions are available. For example, the river usually becomes ice covered late in November in the vicinity of Culbertson, about River Mile 1624. The ice cover apparently attains a maximum thickness of about 24 to 36 inches by spring (Iverson, personal communication); the greater thickness usually occurs at locations where the ice cover is layered, due to over-cover flow and freezing. The river usually becomes ice covered at River Mile 1716 (Pipal site) about one month later than at Culbertson (Iverson, personal communication). During a mild winter, such as the winter of 1997-98, freeze-up did not begin until January and the ice thickness was about 18 inches at Culbertson. For the reach between the Yellowstone River confluence and Lake Sakakawea, Wuebben and Gagnon (1995) provide useful observations and data.

Most of the typical features of ice formation on the lower Missouri River are evident in any of its reaches. Figure 99, for instance, depicts border ice growth along the northern bank of the river near River Mile 1624. The reach between River Mile 1623 and River Mile 1622 (just downstream of the Tveit-Johnson Site and conveniently viewed from a local road elevated along a bluff) is depicted in Figures 100a and b. It is representative of the river. The processes of border-ice growth, ice accumulation and cover solidification are evident in Figures 100 a and b, which give upstream and downstream views of the reach during mid-February 1998.

The channel morphology of this reach may be characterized as varying between sinuous point bar and sinuous braided. The channel winds downstream around a bend, with a large point bar extending from the inner bank of the bend. A chute channel cuts through the point bar. Large bars are located upstream and downstream of the bend. The upstream end of the reach is about 157 miles downstream from Fort Peck Dam. Therefore, under many winter conditions, the flow entering the reach would readily have attained the freezing temperature. Ice formation may begin with border-ice growth in regions of low velocity along the banks, over the shallow point bar and in the sheltered lee of other channel features. The process that dominates ice-cover formation is the accumulation of drifting ice, notably frazil ice slush and pans and pieces of border ice possibly detached from upstream reaches. As the border ice encroaches into the reach and as the volumetric discharge of drifting ice increases, a channel section becomes

Figure 99--Border ice growth developing from the north bank of the lower Missouri River near River Mile 1624, February 10, 1998. Note that slight fluctuations in flow elevation have caused several layers of growth.

A

B

Figure 100--Ice formation on the lower Missouri River in the vicinity of River Mile1622 (downstream of the Tveit-Johnson site), February 10, 1998; (A) view upstream, and (B) view downstream. The ice cover comprises border ice along the bank in the foreground and around the bars. It also comprises accumulated frazil slush and pans along the main thalweg of the channel. The accumulation ridges in the center of the top figure indicate how frazil slush and pans accumulated to form the cover.

congested; the chute channel becomes ice covered, while the main thalweg continues to maintain sufficient width to convey the amount of drifting ice entering it. Eventually, the velocity of drifting ice decreases as ice congests the section. In due course, the congested ice accumulates to form a cover over the main thalweg. Once ice covers the channel, it thickens and solidifies thermally.

The regions of higher velocity usually become ice-covered last. The ice cover gradually encroaches on them as border ice extends into the flow and as the front of accumulated ice progresses upstream. This gradual envelopment of higher-velocity regions may cause ice covers to be of non-uniform thickness at a site, with consequences for local distribution of flow.

Ice-Cover Effects on Flow Distribution

General Processes

Ice cover imposes an additional resistant boundary that decreases a channel's flow capacity and vertically redistributes streamwise velocity of flow in a channel. In so doing, an ice cover may reduce the erosive force of flow in the channel and thereby act to reduce rates of bank erosion and channel shifting. However, cover presence may also laterally re-distribute flow, usually concentrating it along the thalweg. If the thalweg lies close to one side of a channel, flow concentration may locally increase bank erosion and channel shifting. On the other hand, if the thalweg is more-or-less centrally located in a channel, the cover may reduce bank erosion and channel shifting. The variability of flow response to ice-cover presence makes it difficult to draw simple overall conclusions about ice-cover effects on a river's banks and channel. The net effects will vary from site to site.

If the flow rate and channel slope were assumed constant, the main individual effects of a uniformly-thick ice cover on a straight, uniformly-deep, alluvial channel are as follows:

1. Raised water level (ice-covered depth exceeds open water depth for the same flow rate);
2. Reduced bulk velocity of flow (bulk flow velocity, V = discharge/flow area);
3. Reduced drag on the channel bed;
4. Reduced velocity of secondary currents (i.e., currents associated with transverse circulation of flow in the channel);
5. Reduced rates of bed-sediment transport; and,
6. Reduced size of bedforms (notably dunes).

The effects are evident in the comparison of Figures 101 a and b and the ensuing explanation, which considers cover effects on flow distribution (items 1 through 4). The effects on sediment transport (items 5 and 6) are discussed in the next section.

The typical changes in depth and velocity distribution over the flow depth are indicated in Figure 101. Depth usually increases in the range of about 10 to 30 percent; i.e., the covered flow is about 10 to 30 percent deeper than the openwater flow at the same discharge, as indicated in Figure 101. Bulk velocity of flow decreases by the same

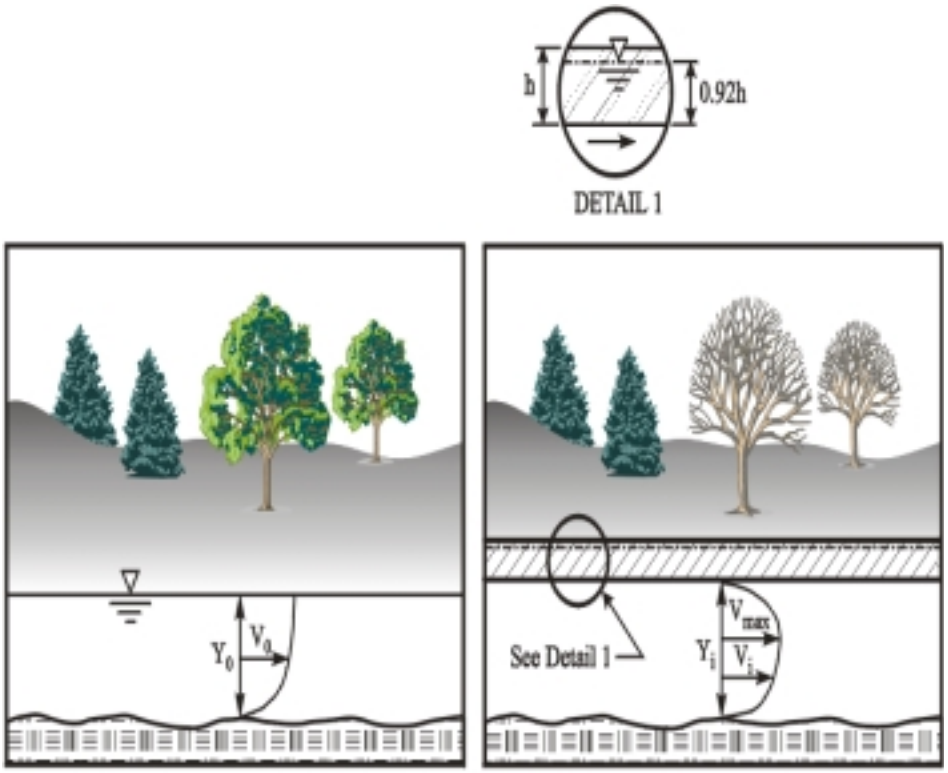

Figure 101--Ice-cover effects on flow depth and vertical distribution of flow. Y = flow depth, V = flow velocity, subscript ‘o’ = initial time, subscript ‘i’ = an additional time, h = ice thickness.

amount. The actual piezometric water level in the channel would be about 0.92 times the ice-cover thickness, h, above the cover underside; the relative densities of solid ice and water = 0.92. The cover floats with a freeboard of about 0.08h above the water level.

Flow drag along the ice cover shifts the location of maximum velocity lower within the flow, instead of being close to the water surface as occurs with openwater flow. The magnitude of the maximum velocity is reduced, more-or-less in proportion with the reduction in bulk velocity of flow.

The reduction in flow drag on the bed is nominally in proportion to the square of the reduction in bulk velocity; i.e., boundary shear stress, $\tau \propto V^2$. As is explained below, reduced bed drag leads to reduced rates of bed-sediment transport and altered bedform geometry.

Cover presence may cause significant lateral re-distribution (sideways shifts) of flow in the following situations:

1. lateral variations in channel depth; and,
2. lateral variation in ice-cover thickness.

An ice cover imposes an additional flow-retarding boundary that decreases the flow-conveyance capacity of a channel and redistributes flow vertically and laterally. Vertical redistribution of flow is marked by flow depth increase (usually) and by a null flow velocity at the cover underside. Lateral re-distribution of flow, though, depends on how the ice cover forms, how it is attached to the channel banks and how it thickens. It can be explained using a flow-resistance equation, such as the Darcy-Weisbach equation:

$$Q_o = Y_o B\left(8gR_o S_o / f_o\right)^{1/2} = K_o S_o^{1/2} \qquad (26)$$

where Q_o = flow rate per unit width of channel;
Y_o = flow depth;
B = flow width;
f_o = Darcy-Weisbach resistance coefficient;
K_o = unit conveyance; and
subscript '*o*' refers to openwater flow.

Cover presence may laterally re-distribute or concentrate flow in accordance with lateral variations in flow depth and/or ice-cover thickness. This impact can be illustrated using a simple, idealized channel comprising two bottom elevations of equal width, as in Figures 102a-d, and may be described approximately in terms of two conveyance components, K_{o1} and K_{o2}, one component associated with each bottom elevation. For constant flow, a free-floating, uniformly thick ice cover reduces the relative magnitudes of the two conveyance components. It smears flow over the full channel width, as $K_{i1}/K_{i2} < K_{o1}/K_{o2}$ (Fig. 102b); the subscript '*i*' denotes ice-covered. However, if the ice cover were fixed to the channel banks and thickened, the reverse occurs; $K_{i1}/K_{i2} > K_{o1}/K_{o2}$ (Fig. 102c), because flow depth reduces more in the shallower portion. Under this condition, cover presence squeezes or concentrates flow along a thalweg where the flow is deeper. If the thalweg lies close to one side of a channel (e.g., near the outer bank of a bend), such a

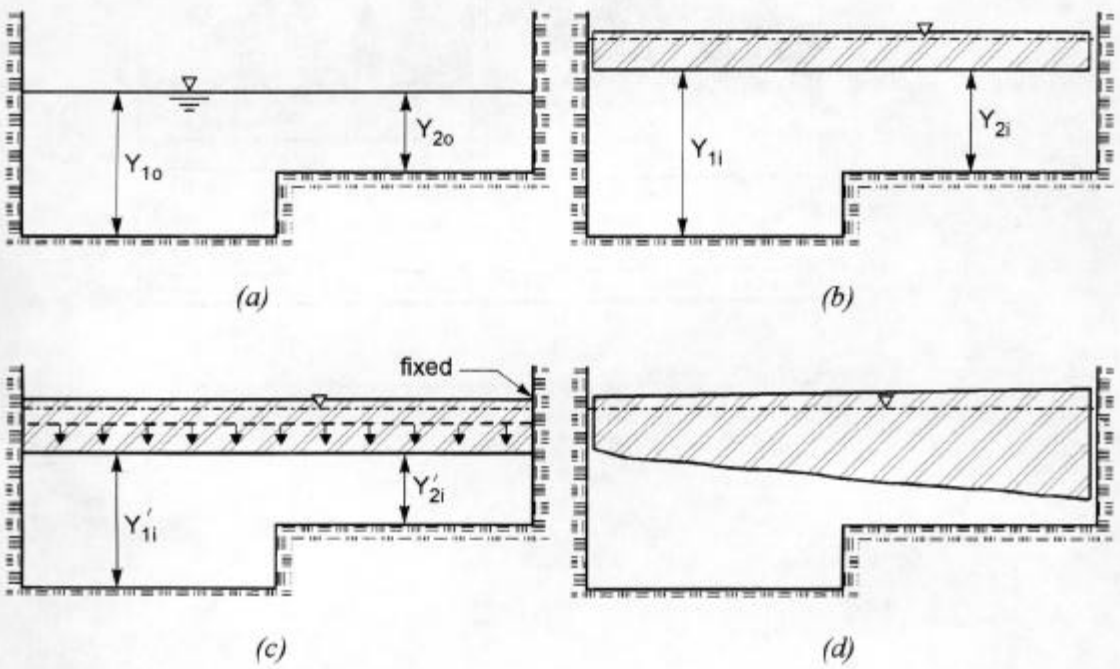

Figure 102. An ice cover may reduce openwater proportions (a) of flow conveyance in lateral segments of a two-part, compound channel if the cover is level and free floating (b), increase them if the cover is fixed and thickens (c), and increase them if the cover is not level (d).

concentration of flow may promote thalweg shifting and deepening. On the other hand, if the thalweg is located more-or-less centrally in a channel, a fixed cover may deepen or entrench the thalweg. An important further point is that the cover, by reducing flow through the shallow portion, may trigger further reductions in conveyance through the shallower portion by promoting ice accumulation (frazil slush or pans) and/or bed-sediment deposition there. Additional flow concentration is possible if the cover were not uniformly thick (Fig. 102d), if ice grounded on the channel bed, or if shore-fast/accumulated ice developed from one or both banks.

A level ice cover, by reducing bulk flow velocity and altering the vertical distribution of streamwise flow, reduces the centrifugal acceleration exerted on flow around a river bend. Only one study has investigated this effect (Tsai and Ettema, 1995). It found that cover presence alters patterns of lateral flow distribution in a channel bend. The two sketches in Figures 103 a and b show the main alteration, which is a splitting of the large secondary flow spiral into two weaker spirals; owing to centrifugal acceleration acting on moving water, a large secondary flow spiral is typical of many curved channels. The presence of a level ice cover reduces radial components of velocity and lateral bed slope in channel bends, causing the bed level to rise near the outer bank. Tsai and Ettema (1995) found a reduction in lateral bed slope of about 10%. This ice-cover effect would tend to retard bank erosion in channel bends, because it may result in reduced flow velocities near the outer bank of a bend. In other words, this effect of cover presence may dampen streamwise oscillations in bed elevation and oscillations in channel position. The dampening effect that an ice cover is calculated to have on the angle of transverse slope of the bed around a 180^{o} bend is evident in Figure 104, taken from Tsai and Ettema (1995).

Lateral variations in cover thickness, however, may further concentrate flow in a channel of non-uniform depth and may override the more subtle effects to those just described for a level ice cover. Significant lateral and streamwise variations in cover thickness may occur in channels with significant variations in flow depth and velocity. Because flow velocities decrease with decreasing flow depth, velocities usually are lower in regions of shallower flows and often in the wake of flow obstructions, such as bars. Ice covers whose formation involved substantial amounts of frazil-ice slush may become thicker in regions of shallower flow. Lower values of flow conveyance in those regions also result in faster border-ice formation. Also, because flow velocities are lower, ice (frazil slush and ice pieces) is less readily conveyed through those regions and is prone to accumulate. Figure 105 illustrates the accumulation of ice at a cross-section of the Tanana River, Alaska, at two times during winter (Lawson *et al*. 1986). That river is comparable to the lower Missouri River in flow rates, but is of steeper slope, is more braided in channel morphology, and its flow is not regulated.

Further concentration of flow is possible if an ice cover is not free to float upwards with increasing flow rate. It is usually assumed in hydraulic analyses (e.g., Michel 1978; Beltaos, 1995) that ice covers are free floating. Actually, they may not always be free floating. A stationary cover exposed to very frigid air may fuse to the channel banks. The cover then becomes constrained from freely floating up or down with changes in the flow, at least initially. Therefore, increasing flow is forced partially beneath the ice cover, initially pressurizing it and increasing flow velocities, which may locally erode the bed beneath the cover. The extent to which a flow may be pressurized

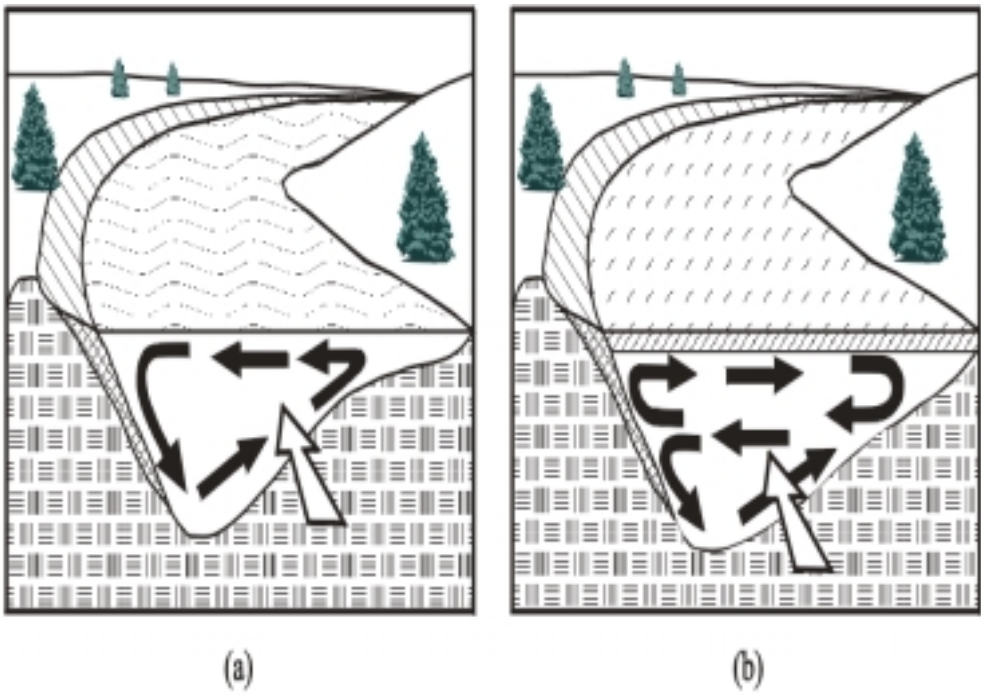

Figure 103--Ice-cover effects on secondary currents in a channel bend.

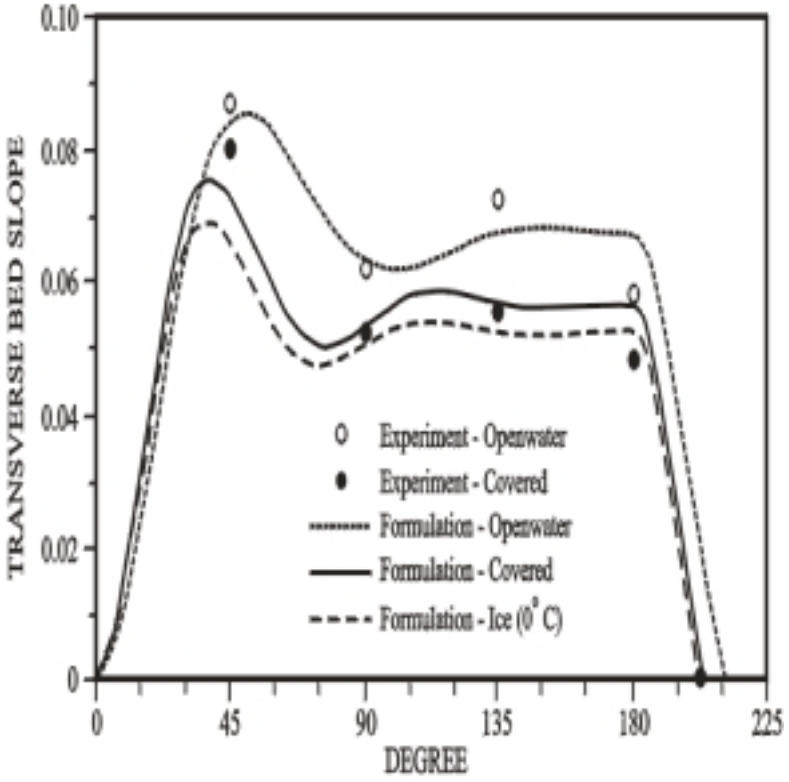

Figure 104--Ice-cover effects on transverse bed slope around an alluvial-channel bend (numerical and experimental results from Tsai and Ettema 1994). The cover reduces fluctuations in transverse slope. Increased water viscosity associated with frigid water (0^{o}C) further reduces slopes slightly.

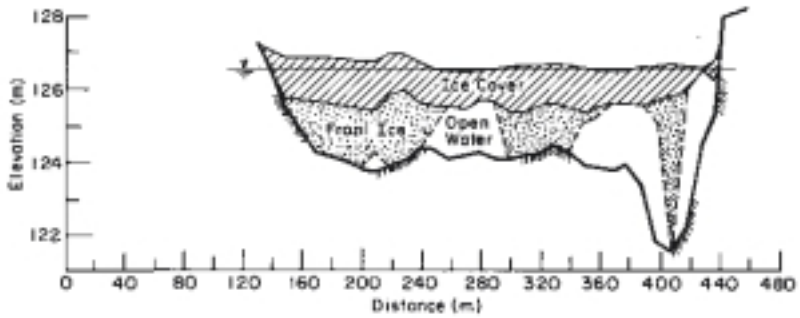

a. 28 February 1984.

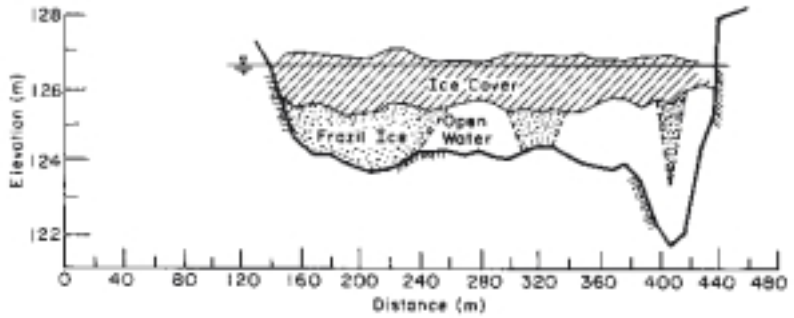

b. 30 March 1984.

Figure 105--Non-uniform ice accumulation across a section of the Tanana River, Alaska. This figure is taken from Lawson *et al.* (1986).

beneath a cover apparently has not yet been measured because the usual assumption is that covers are free floating. An estimate would suggest that the pressure-head increase above the hydrostatic would be approximately equal to the ice thickness, the increment in water depth retained by the upstream end of the cover. Therefore, the thicker the cover, the greater the pressurization possible. Eventually, the pressure would force the cover to bow upward. Also, as flow rises at the upstream end of the cover, some of it will pass over the cover. As the flow further increases, the upward pressure causes the cover to develop cracks parallel to the banks and to float freely on the water surface. Very little information exists on this flow condition, especially with regard to how it may locally affect the channel bed and banks.

Ice-Cover Effects on Flow Distribution in the Lower Missouri River

All of the ice-cover effects on flow distribution described above likely occur in the lower Missouri River. There are, however, no observations or data formally documenting them, a situation that prevails for most rivers in cold regions. The river's fairly complex bathymetry makes it difficult to determine the exact influence of ice cover on flow stage, and that influence may vary from reach to reach. The variability of flow rates and frigid-air conditions also complicate matters. The morphology of sinuous point-bar and sinuous braided channels, such as typify the lower Missouri River, is markedly three-dimensional. It has pronounced lateral and streamwise variations in depth. The channel in some reaches contains a single thalweg aligned near mid-channel; e.g., at RM 1676 (at Wood's Peninsula). At other locations it has a single thalweg aligned close to an outerbank, e.g. at RM1624 (Tveit-Johnson site). At further sites, the channel apparently has two possible thalwegs; e.g., at RM 1631 (Vournas site) and RM 1646 (Mattelin site). Two or more thalwegs commonly develop in channels with in-channel bars and islands. Channel cross-sections at the three sites mentioned are shown in Figures 106 a-c.

Bathymetry variations influence ice-cover formation and lead to thickness variations. The manner of ice-cover formation also affects flow distribution. Channel locations that are the last to become ice covered usually coincide with the channel's prominent thalweg alignment, especially along an outer bank. There the flow gradually concentrates, as the cover forms and pinches off shallower flow areas. Where a second channel thalweg cuts through a bend chute, for example, it is likely that that thalweg becomes ice covered first and partially blocks off with ice.

Some anecdotal evidence exists to suggest that, at times, flow becomes pressurized beneath ice-covered reaches of the lower Missouri River. The evidence suggests that the cover is not always free-floating and may concentrate flow when flow rate increases beyond that at which the cover was formed. Pressurized flow conditions likely occur when flow rate begins to increase during a period of particularly frigid weather that has enabled the ice cover to freeze to the riverbanks; i.e., the ice cover is not free floating. For substantial flow-rate increases, flow also likely spills over the top of the ice cover (personal communication, Iverson), thereby somewhat limiting the extent of pressurization beneath the cover. Flow pressurization beneath an ice cover amplifies bed scour. It also may result in longitudinal (streamwise) and transverse crack development in the ice cover.

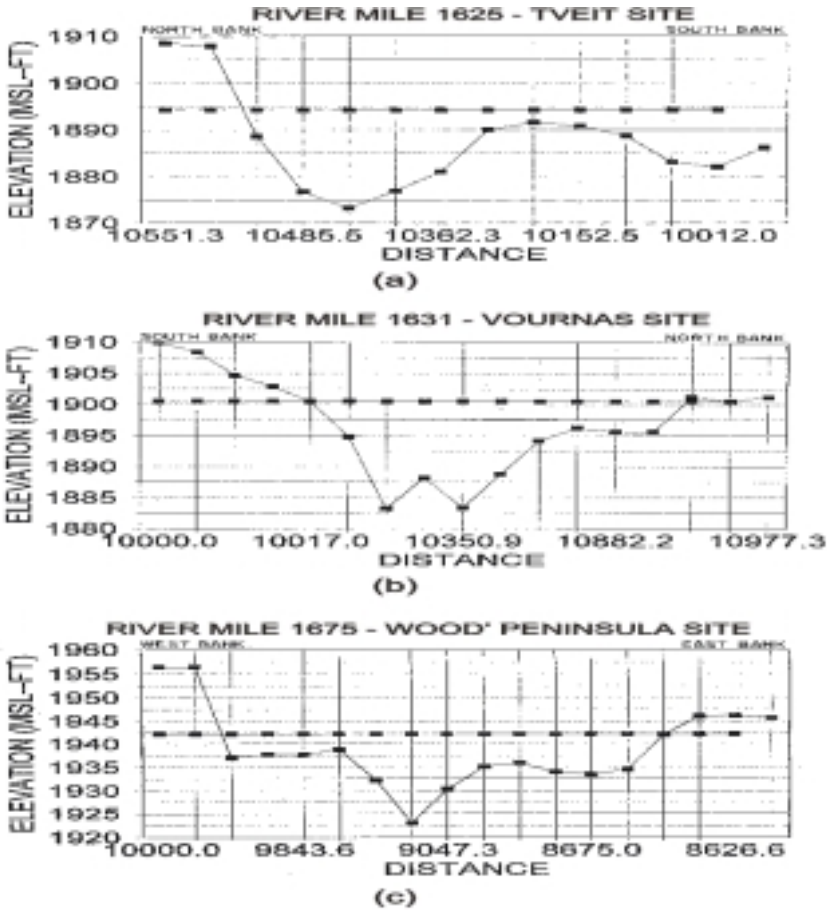

Figure 106--Example cross sections of the lower Missouri River: (A) River Mile 1675, Woods Peninsula; (B) River Mile 1631, Vournas Farm; and (C) River Mile 1625, Tveit-Johnson Site.

Flow spilling over the initial ice cover may itself freeze over, locally causing the cover to be wafered (ice-water-ice) or locally coated with *aufeis* (a form of icing).

Though no data exist on ice-cover effect on flow distribution, some anecdotal evidence exists that the ice cover causes local changes to occur within the channel. For example, there are accounts of thalweg changes at pump sites during winter (e.g., Mattelin, personal communication). There are also accounts of significant hummocks and bummocks in the ice cover as it bows upward or sags downward, in response to flow being forced under it or to a decrease in flow. The anecdotal evidence expresses a perception among people living along the river that the changes are substantial.

Ice-Cover Effects on Sediment Transport Rates

Sediment-transport rates relate sensitively to water-flow rates and flow distribution. Insofar that an ice-cover affects flow distribution, it markedly affects rates and distribution of sediment transport.

General Observations

The topics of sediment transport under ice and ice runs (which may accompany ice-cover break up or ice-jam collapse) have received little general attention in the past. In the last few years, however, they have risen in importance due, in part, to the recent growth of interest in the winter environment of rivers in cold regions. As is the case for all but a few rivers, there seem to be no data on sediment transport rates in the lower Missouri River during winter, since these data are difficult to obtain. Moreover, the subject of sediment transport in alluvial channels is broad and involves many complex physical processes that have yet to be adequately understood. A substantial number of empirical or semi-empirical predictive methods have been developed for estimating sediment transport in openwater flow. The methods are useful for obtaining approximate, openwater estimates of transport rates. Only one method exists for estimating rates of sediment transport in channels with free-floating ice covers (Ettema and Braileanu, 1998). No study has yet been conducted to expressly investigate sediment transport in pressurized flow beneath an ice cover.

The presence of a free-floating ice cover and reduced water temperature alter a channel's capacity to convey sediment during frigid conditions. Reduced water temperature increases the kinematic viscosity of water (it increases 100% when water cools from 25^{o}C to 0^{o}C) and slightly changes water density (it increases about 0.3% when water cools from 25^{o}C to 0^{o}C, but attains a maximum at 4^{o}C). For constant water discharge and channel slope, increased viscosity increases the flow's drag on the channel bed and banks, increases the flow's capacity to convey suspended sediment transport, and thereby increases sediment-transport rate (Straub, 1955; Colby and Scott, 1965; Hong *et al.* 1984). This effect can be taken into account using openwater methods for estimating sediment-transport rates.

By virtue of its reduction of channel conveyance, *K*, and redistribution of flow, a free-floating ice cover typically reduces a channel's capacity to transport bed sediment. At certain zones within a channel, however, where the cover concentrates flow, sediment-

transport rates may increase locally. Several laboratory studies have investigated cover-presence effects on sediment transport rate (Sayre and Song, 1978; Wuebben, 1986; Smith and Ettema, 1995; Ettema and Braileanu, 1998). They have all involved a free-floating cover that rises and subsides with changing flow rates. Their findings confirm that cover presence reduces rates of sediment transport. The rates decline rapidly with cover presence. Bedload-transport rate, for instance, can be almost halved by an ice cover that raises flow depth 15%, for a constant flow rate; this estimate assumes, reasonably, that bedload-transport rate $\propto \tau^2 \propto V^4$, with V decreasing by 15%; τ is shear stress acting on the bed, V is bulk velocity of flow. An important point here is that sediment eroded under an ice cover may not be transported far from the erosion location.

Field data on sediment-transport rates in ice-covered channels are scarce. Only about three field studies have been conducted in which rates of sediment transport were measured for ice-covered channels. The studies indicate the inherent difficulty of obtaining such measurements and of interpreting them. The study carried out by Tywonik and Fowler (1972) focused on measurement of suspended-sediment load in several rivers in the Canadian Prairie (e.g., Assiniboine River, Red River); rivers similar in some respects to the lower Missouri River in size and ice processes prior to Fort Peck Dam. They report that periods of ice cover on these rivers coincide with periods of low discharge and, therefore, low rates of suspended-sediment transport. In addition, they experienced considerable difficulty in making the suspended-load measurements, because of the frigid conditions in which they were made and the presence of slush ice. Lawson *et al*. (1986) conducted an extensive study of flow and sediment movement at a reach of the Tanana River, Alaska. They obtained measurements of bed-load and suspended-load rates at one cross section. The rates were comparable in magnitude to rates measured during a survey conducted about a year earlier at two cross sections in close proximity to that used by Lawson *et al.*,(1986). Burrows and Harrold (1983) describe the earlier survey. Together, these data sets indicate a great reduction in the ratio of suspended load relative to the bed-load from summer to winter. The reduction is attributed tentatively to reduced flow of melt water from glaciers drained by the Tanana River. Laboratory data obtained by Ettema and Braileanu (1998) show the opposite result, which they attribute to cover under-damping of turbulence generated by flow over bedforms.

Alterations in flow distribution complicate evaluation of ice-cover effects on transport rates for many. This difficulty is evident in Figure 107, which shows an ice cover over the Yellowstone River, near Fallon, Montana, and from figures such as Figure 105, which shows non-uniform ice accumulation across the Tanana River. The series of shear lines in the ice cover marked on Figure 107 indicates how the flow area has gradually narrowed. Flow-width alteration is more difficult to predict than flow depth change due to ice. The formation of sub channels within an ice-covered channel may accentuate narrowing of the flow area, especially if the channel is not prismatic. The sub channels form when accumulations of frazil slush or other ice pieces develop under the ice cover. In effect, they duct the flow in a manner that significantly alters the flow distribution from that attributable to the imposition of a level ice cover.

For most cold-regions rivers, the major sediment-transport event each year occurs during the large flows associated with ice runs resulting from the dynamic breakup of an ice cover or the release of a breakup ice jam, if a jam develops. In addition to the large

Figure 107--Lateral changes in flow area complicate estimation of sediment transport rates in an ice-covered river, such as the Yellowstone River shown here. The lines indicate how the flow area reduced laterally as the cover formed.

flow rates usually involved, these events may produce severe gouging and abrasion of banks by moving ice. To date, no systematic investigation has been conducted of bed-sediment transport and bank erosion during ice runs.

Ice-Cover Effects on Sediment Transport Rates in the Lower Missouri River

In short, there exists no documented observations or information concerning ice-cover effects on sediment transport (suspended load or bedload) in the lower Missouri River, a situation that prevails for all rivers throughout the Great Plains. There is only anecdotal evidence that the river's thalweg(s) or bars may shift at certain locations during winter (e.g., Mattelin, personal communication). Such evidence circumstantially indicates that the flow moves significant amounts of sediment at certain locations. However, at present, little more than that can be said.

Ice-Cover Breakup and Breakup Jams

Periods of ice-cover breakup and clearance from a river, by virtue of their coincidence with substantial increases in water-flow rates, are periods of substantial sediment movement in alluvial rivers. For many rivers in cold regions (notably those in permafrost), breakup flows are considered to be the dominant channel-forming flows. The processes attendant to breakup and jamming are reasonably well understood; not so the impacts of breakup and jamming on channel erosion and sediment transport.

General Processes

With the onset of warmer weather, ice-cover strength and thickness decrease. Ice strength usually decreases more significantly than does ice thickness. In most situations, an ice cover may "rot" or "candle," becoming porous and greatly weakened before thinning. Also with the onset of warmer weather, flow increases as snow melts and possibly is accompanied by rain. Increased flow rate and depth increase the hydraulic load exerted against an ice cover, increasing uplift pressure and drag that result in hinge cracks and transverse cracks, respectively. Additionally, increased water elevation creates more surface area for ice to move.

Ice-Cover Breakup

The breakup of a river ice-cover may be considered in three phases. Not all of them may occur. The phases are the pre-breakup weakening of the cover, breakup and ice run, and the breakup jam. For most river reaches, an ice cover weakens, disintegrates or breaks up, then its fragments drift downstream. In some rivers, ice-cover breakup is followed by the development of breakup ice jams. For one of several reasons, certain reaches in those rivers have insufficient capacity to convey the broken ice.

The pre-breakup begins with the start of runoff from the watershed, when solar radiation begins snow-cover melt, even before the average daily air temperature exceeds 0^{o}C. The discharge in the river begins increasing, exerting an uplift pressure on the ice cover, possibly with water flowing over the cover as well as under it. With increasing

discharge, the ice cover fractures at several places. For a long reach with low velocities, the break usually occurs first along the banks. The central part of the cover floats freely, but the border ice may be flooded. In areas of high flow velocity, water may rise and flow over the cover through numerous uplift fractures. Several pieces of ice may detach and begin to move downstream on the ice cover. As the discharge increases and is accompanied by fluctuations responding to daytime variations in air temperature and solar radiation, ice pieces detach themselves at regions of highest flow velocity and accumulate at the front of regions of the stronger ice cover over the low-velocity reaches.

The occurrence of an ice run depends on combinations of flow conditions and ice-cover strength. In this regard, the direction of flow can be important. Rivers flowing into warmer regions usually begin cover breakup at the downstream end of the ice cover. The cover then progressively breaks up in an upstream direction, with the ice moving downstream in an orderly manner, provided it does not develop a jam at some congested location. Rivers flowing into colder regions (e.g., rivers flowing north) usually begin breakup near the upstream end. Breakup may also begin for river reaches for which the inflow hydrograph includes a large peak flow rate than does the outflow hydrograph, owing to flow-resistance attenuation of the hydrograph.

Breakup Ice Jams

It is not uncommon for ice to clear a river by means of a series of breakup jams. An initial jam forms from ice first broken over a reach upstream. Increased flow and warming cause the jam to release, then dislodge and break more ice, forming new jams downstream. Eventually, by means of this stop-go process, the flow shunts ice from the river. In the continental United States, breakup jams may occur at any time once an ice cover has formed on a river. Though spring is the usual time for breakup to occur, mid-winter thaws may cause a river to experience a series of freeze-up and break-up events.

Many aspects about breakup-jam formation and release remain inadequately understood. An inherent difficulty with ice jams is that they radically alter the stage-discharge relationship for a river reach; a moderate flow rate in a jam-covered channel usually produces a flow stage much higher than that produced by the same flow under openwater conditions. Jam formation and release may occur in fairly gentle or gradual manners. They may also occur rapidly, especially if they involve a steep hydrograph of flow or a surge. Jam releases can also be gradual or abrupt, with an abrupt release creating a surge similar to that obtained with dam-break flow; surges and ice runs have been clocked at speeds in excess of 15 ft/s (Beltaos, 1995).

The net effects (detrimental and beneficial) of ice-jam on channel morphology and river ecosystems have not been extensively investigated and, therefore, are not well understood. Subsequently in this section, several hypotheses regarding the effects are discussed briefly.

Ice-Cover Breakup and Breakup Jams on the Lower Missouri River

As with other aspects of ice in the lower Missouri River, information on ice breakup and breakup jam formation along the river is not well documented. Only anecdotal information (e.g., Iverson, personal communication) exists on how the river's

ice cover breaks up and is moved through the river. The little information that exists on ice-cover breakup indicates the following features:

1. The ice cover usually weakens and disintegrates in place;
2. The channel usually releases the ice cover around between mid to late March, to early April;
3. Breakup usually begins, or occurs more frequently, at upstream reaches; and,
4. Breakup is less dynamic (dramatic) than breakup of ice on the Yellowstone River.

The control of spring flood flows by Fort Peck Reservoir and the relatively mild slope of the lower Missouri River in the reach of present interest, enable the river's ice cover to remain intact. The steeper slope of the Yellowstone River and the higher velocities of its flow, cause that river to experience more dramatic episodes of ice-cover breakup. Borland (1959) provides an interesting description of breakup ice jams on the Missouri River upstream of Fort Peck Dam.

As with many rivers in the continental United States, the seasonal cycle of ice-cover formation and breakup on the lower Missouri River is subject to shorter period cycles governed by fluctuations in weather and flow conditions. Ice covers may form and breakup more than once during winter. Therefore, initial ice covers may break up, thereby releasing broken ice that may accumulate and help form a cover at some location downstream.

Breakup Jams on the Lower Missouri River

Breakup jams occur on the lower Missouri, but their frequency and severity are reduced by flow regulation at Fort Peck Dam. There seems to be little or no documentation on the jams, what factors triggered them, their extent, or the prevailing flow, weather, and ice conditions associated with them.

The following observations about the jams are drawn from observations of the river and from anecdotal accounts:

1. Small breakup jams have occurred along the river. The frequency with which they result in over-bank flow seems to be approximately once in five to ten years (Iverson, personal communication);
2. The frequency and severity of the jams may increase downstream, because the volume of ice increases downstream; and,
3. A significant jam forms frequently in the vicinity of the river's confluence with the Yellowstone River and the head of Lake Sakakawea (Wuebben and Gagnon, 1995; Tuthill and Mamone, 1997).

Breakup jams apparently have occurred in the vicinity of River Mile 1632, River Mile 1603, and River Mile 1581. The first two locations approximately correspond to the lee of a meander bend. The last location coincides with the confluence with the Yellowstone River and the delta region of Lake Sakakawea. The jams at River Mile 1632 and River Mile 1603 resulted in flow topping the channel bank and going over the neck

of the downstream meander. Figure 108 indicates the approximate location of the jam at River Mile 1632, near the Vournas site.

Wuebben and Gagnon (1995) and Tuthill and Mamone (1997), provide useful summaries of ice jams in the reach extending from the confluence of the lower Missouri River and the Yellowstone River to Lake Sakakawea. The jams occur because ice runs from the Yellowstone River become blocked by ice cover at the river's confluence with the lower Missouri River or by diminished flow velocities and ice-cover presence at the head of Lake Sakakawea, downstream of the confluence.

River-Ice Effects on Bank Erosion and Channel Morphology

The cycle of river-ice formation, presence, and breakup potentially affects bank erosion, sediment transport, and channel morphology in several ways. This section describes the mechanisms in general terms first, then considers the extents to which they likely affect the lower Missouri River.

Most of the mechanisms, in themselves, are quite straightforward to identify and describe. However, their net effects may not be quite so straightforward. River ice may have dramatic and discordant effects locally. However, those effects may not alter the average geometric relationships defining the morphology of a long reach of channel, but they will increase the variability of those relationships. In other words, they may clutter data on channel geometry and obscure trends reflecting channel response to flow and slope changes.

The mechanisms whereby river ice may affect channel morphology act over a range of length and at different rates. Some processes amplify flow-induced changes of channel morphology. Other processes dampen them. The ice-related erosion mechanisms discussed below potentially may affect the manner and rates of bank erosion and morphology of an alluvial river. Under some conditions, ice may slow erosion and change in channel morphology. Those conditions are pointed out in the discussion. For example, an ice cover may increase flow depth and decrease bulk flow velocity. While frozen, a bank will not usually erode and the formation of border ice along a bank may reduce near-bank flow velocities.

Flow rate is an important factor common to all of the erosion mechanisms. As mentioned throughout this section, increased flow rate usually increases the potential erosive severity of river ice. This factor is of special concern for regulated rivers in cold regions. They must typically convey flows substantially greater in magnitude and possibly duration than they did under natural conditions prior to regulation. It is also an important factor for unregulated rivers whose maximum flow rates coincide with spring snowmelt.

Erosive Effects of River Ice

The mechanisms whereby river ice locally may accelerate bank erosion and changes in channel morphology are as follows:

- Elevated ice-cover level;
- Elevated flow rates after freeze up;

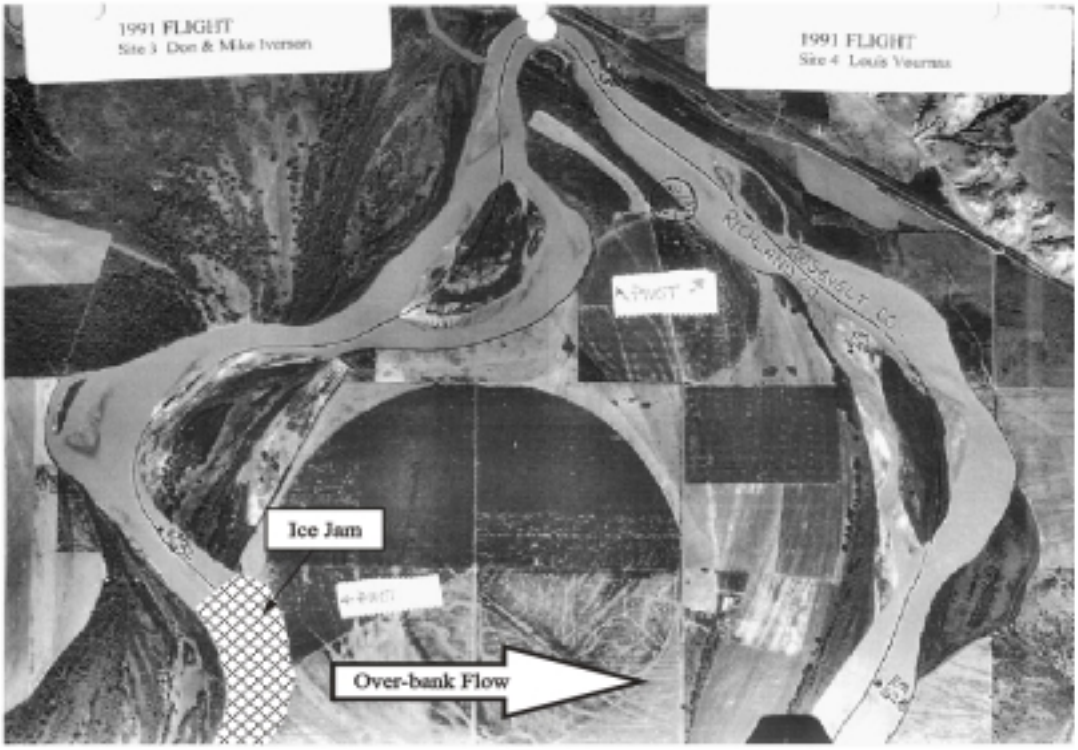

Figure 108--Approximate location of a recurrent ice jam in the vicinity of River Mile 1632, the Vournas site.

Local scour in regions of locally high flow velocity at ice accumulations or flow deflected by ice accumulations;

- Ice-run gouging and abrasion of channel banks and bars;
- Channel avulsion attributable to ice jams; and,
- Ice-cover influence on bank-material strength and bank stability.

Aspects of these mechanisms are illustrated in Figures 109 through 114.

The ensuing description first discusses in general terms how the mechanisms may aggravate bank erosion and local changes in channel morphology. The subsequent section then discusses the overall effects of these mechanisms on a long reach of a channel that includes several cycles of morphologic features of a sinuous channel, such as meander loops. The topic of freeze-thaw (sublimation) weakening of banks is then discussed.

Though it is convenient to describe the listed mechanisms separately, several of them are related and may occur together or in sequence. For example, ice-run gouging and abrasion may precede or follow a breakup jam; an ice run may result in a jam, or the collapse of a breakup jam may result in an ice run. A jam may constrict flow at one channel location, but greatly increase flow velocities at another location. A composite of ice-related erosion mechanisms may occur, depending on the river reach, flow and ice conditions. Also, the erosive effects of river ice may be indirect; e.g. stunted riparian vegetation may have an adverse effect on bank insulation and overall protection.

Elevated Ice-Cover Formation

Flow regulation by means of a reservoir may elevate flow rates and levels above those that occur naturally in a river prior to regulation. Elevated flow stage delays ice-cover formation when river water is above the freezing temperature, because the flow contains a greater amount of thermal energy. An elevated ice cover, once formed, may enable the channel to convey elevated flows throughout winter, and thereby mitigate erosion problems that may result when larger flows are released into a channel with an ice cover formed at a low-flow stage. However, elevated ice-cover formation may incur the following erosion-promoting effects:

1. Riparian vegetation damage;
2. Border-ice weakening of bank material; and,
3. More ice produced in the channel.

The first two effects are potentially the more severe. Riparian vegetation frozen into an ice cover or submerged by it may have difficulty getting established along banks. This problem has been noticed for several regulated rivers in cold regions (e.g., Uunila, 1997).

Border-ice weakening of banks is likely significant for steep banks, typically those comprising sufficient clay to be termed cohesive. It is also likely significant for banks whose water table declines in elevation away from flow levels in a channel, because the border ice is less securely anchored into the bank. This erosion mechanism has not been reported heretofore, but was observed along the lower Missouri River.

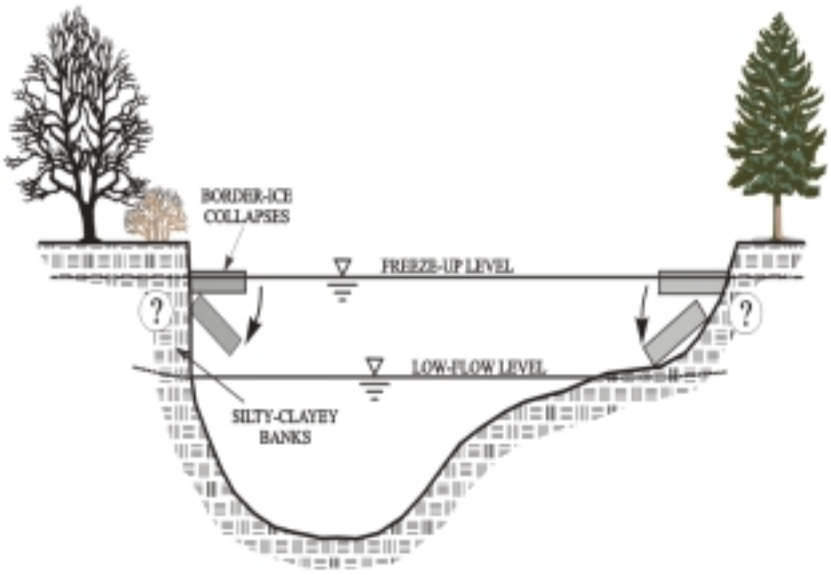

Figure 109--Sketch of border-ice collapse with lowered flow level. At present, the effects on bank erosion of border-ice collapse are not known.

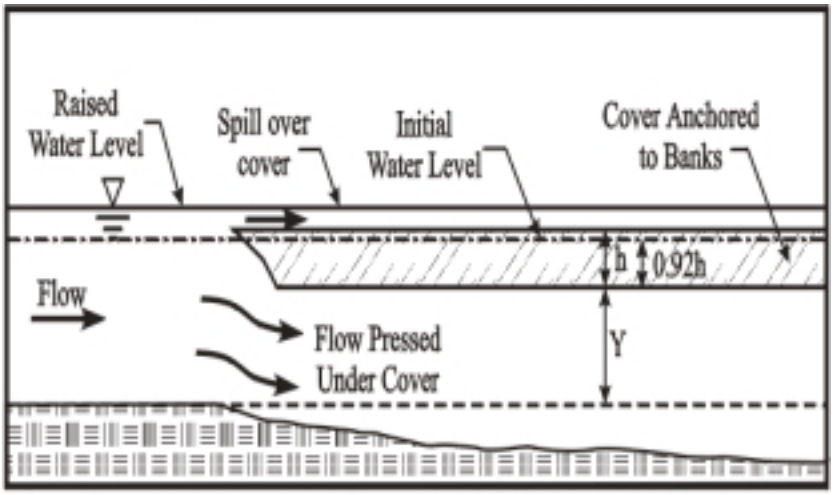

Figure 110--Flow constricted through a channel reach with fixed ice cover may locally scour the reach until the cover cracks, floats upwards and relieves the constriction.

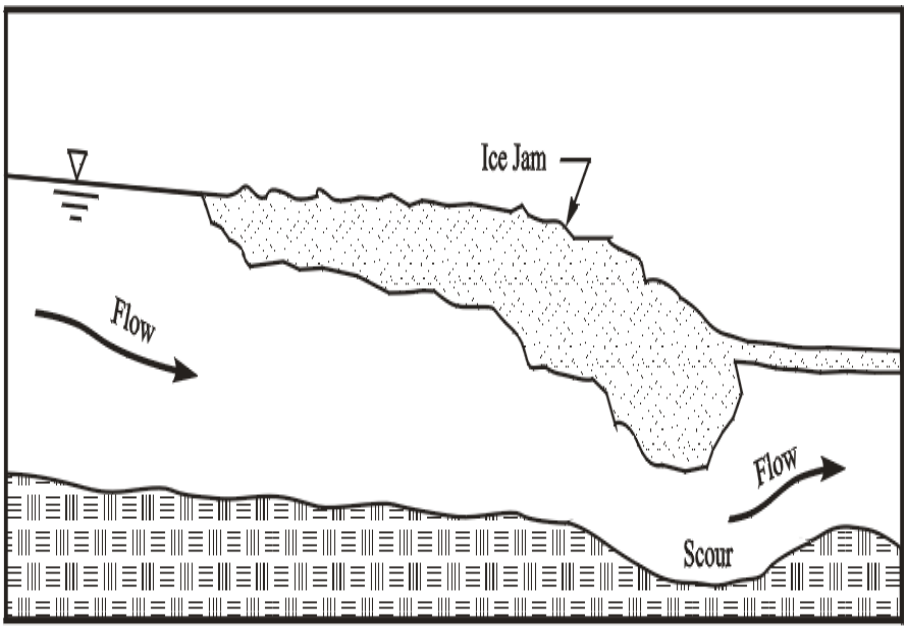

Figure 111--Flow acceleration beneath an ice accumulation, such as a jam, may locally scour a riverbed.

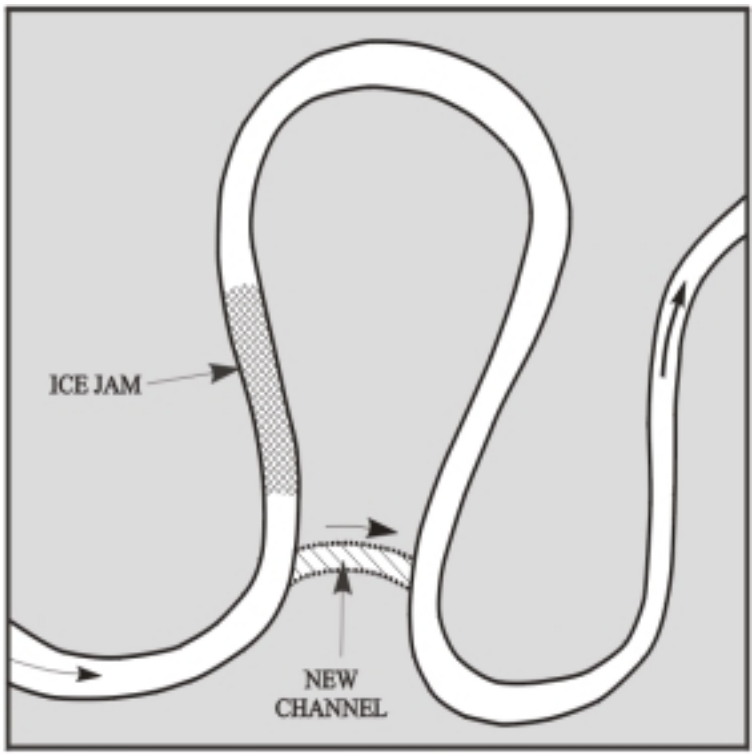

Figure 112. Ice-jam formation in a tight meander loop, and consequent over-bank flow, may result in the formation of a new channel that cuts off of the meander loop.

Figure 113. Stranded ice rubble along a bank of the Yellowstone River attest to the potential erosiveness of an ice run, February 9, 1998. Note the sediment attached to the ice rubble

Figure 114. A shear plane often separates moving ice and a layer of ice pressed against a riverbank. Though the shear plane may partially protect the upper portion of the bank, moving ice may erode the bank toe.

Figure 109 illustrates how border ice might weaken a bank. The ice cover freezes into the bank. The extent of the root is limited by the elevation of the water table and its coincidence with the ice-cover elevation. When the water level in the channel drops, and the ice cover breaks up, ice attached to the bank is cantilevered out from the bank, rotates and tears a portion of the bank as it drops. It is difficult to get direct field observations of this mechanism for border ice attached to vertical banks. For the moment, evidence is circumstantial. There is evidence for a related mechanism commonly termed plucking, which is used with regard to the loss of riprap stones frozen to an ice sheet. Wuebben (1995), for instance, extensively discusses plucking concerns in the design of riprap for bank protection.

Elevated Flow Rate in an Ice-Covered Channel

When the flow rate is greater than that at which the cover formed and the cover constricts the flow, flow velocities may increase and thereby locally increase the rate of bed-sediment transport beneath the cover. This mechanism becomes significant for channels whose available flow area is substantially redistributed or reduced by ice cover presence. It is especially acute for flow in channels with a non-uniform distribution of ice thickness or with an ice cover restrained from free floating. The latter situation, which is sketched in Figure 110, may result in unusually high flow velocities near the bed. It is a condition that seems to have not yet been investigated.

On the other hand, for a constant flow rate in a channel of uniform depth, the presence of a level, free-floating ice cover may decrease flow velocities and retard sediment-transport rates. It does so by raising the water level and diminishing bulk flow velocity, compared to the openwater flow situation. Though this effect would not immediately or energetically promote local bank or bed erosion, it nonetheless may gradually influence channel morphology over a relatively long reach (i.e., a reach containing several cycles of channel forms) and over long duration. The long-reach and long-term effects of a floating ice cover are discussed further in a later section.

Lateral variations in cover thickness amplify lateral variations in flow depth and velocity, thereby concentrating flow in deeper sections of the channel, notably along the channel's thalweg. For low flow rates during winter, the concentration of flow may not result in significant changes in channel morphology. However, significant changes may begin to occur when flow rate increases. The changes are likely local, within short reaches of a channel. For flows unregulated by a dam they would most usually occur during spring, when flow rate increases while the ice cover has not broken. For flows regulated by a dam, the changes could occur at any time when the cover is in place.

By concentrating flow along the channel's thalweg, lateral variations in ice-cover thickness may result in the following two effects on channel morphology:

1. Entrench the thalweg, when the thalweg is more-or-less centrally located in a channel and depth variations are approximately symmetrical about the thalweg; and,
2. Laterally shift the thalweg, when it is close to one side of the channel.

The effect of concentrating flow along a thalweg may cause ice-cover presence to alter the planform geometry of channels. As discussed shortly in the section on long-reach

effects, the extent of planform alteration depends on the channel's initial plan form. In this regard, cover presence may either diminish channel sinuosity or tend to increase it. In either event, the consequence is thalweg shifting, local change in channel morphology, and the prospect of increased bank erosion at certain sites.

These ice-covered-flow effects on channel morphology are plausible, but conjectural; this section is the first occasion that they have been proposed. They have yet to be investigated. It may be conjectured further that, by promoting shifting of thalweg towards the outer bank, cover presence can promote channel-bend migration, at least in terms of thalweg departures from usual openwater alignment. In this sense, ice-cover presence tends to amplify, not dampen, planform oscillations of channel geometry. No observations or data exist to confirm this conjecture.

It is likely that elevated-flow effects on bank erosion entail sequences of steps. The steps may involve cover formation and flow redistribution, thalweg shifting, bank undercutting (all prior to breakup), then bank collapse occurring immediately after ice-cover breakup and during an ice run (e.g. the Yukon River at Galena, Alaska, [UASCOE-Alaska, 1983]). Alternately, the severely eroded bank may collapse once the flow subsides and reduces its support, thus leaving high pore-water pressures in the bank.

Local Scour in Regions of Locally High Flow Velocity at Ice Accumulations

The erosive behavior of a flow may increase locally at an ice accumulation if the accumulation concentrates flow, increasing the magnitude of its velocity and turbulence. Also, an accumulation of ice may deflect flow, altering its direction in a manner that aggravates bank erosion or channel shifting. This mechanism locally increases flow velocity and it may occur when flow and ice pieces are forced beneath an ice accumulation, such as an ice jam or an ice cover. Localized scour of an alluvial bed or bank of a channel may occur in the vicinity of an ice cover when the flow field at the cover locally increases flow velocities and, therefore, increases flow capacity to erode bed or bank sediment. There are several conditions in which this mechanism may occur.

The most severe condition typically occurs near the toe of an ice jam (freeze-up or breakup), as illustrated in Figure 111. There, where jam thickness is greatest and flow most constricted, increased flow velocities may locally scour the bed (Neill, 1976; Mercer and Cooper, 1977; Wuebben, 1988). Channel locations annually subject to ice jams may develop substantial scour holes. Tietze (1961) and Newbury (1968), for example, suggest instances of such scour holes at sites of recurrent freeze-up jams. In most circumstances, the scour hole would have no lasting or adverse effect on channel morphology, because it would gradually fill once the jam was released. It is conceivable that, in certain circumstance, the localized scour could have a longer-term effect on channel morphology; e.g., if it promoted bank erosion at the jam site, or led to the washout of the channel feature triggering the jam; e.g., an island or bar.

To a lesser extent, local scour of bed and banks may also occur when ice pieces collect at the leading edge of an ice cover or at some channel feature (e.g. a set of channel bars) that impedes their drift. These situations are quite marginal in extent, likely occurring more-or-less randomly along a channel, and are short-lived. However, they may potentially trigger more severe erosion in some situations.

Ice-Run Gouging and Abrasion of Channel Banks

During heavy ice runs resulting from ice-cover break-up or ice-jam release, large pieces of ice may potentially gouge and abrade channel banks. There exists significant evidence showing that this substantially affects channel-bank morphology in reaches subject to dynamic ice runs (Marusenko, 1956; Smith, 1979; Hamelin, 1972; Uunila, 1997; Martinson, 1980; USACOE-Alaska, 1981; Doyle, 1992; Wuebben, 1995). Such channels usually are relatively steep and convey high-velocity flows. Moreover, their ice-covers typically break up fairly dramatically in concert with a sudden rise in flow due, for example, to rapid snowmelt and/or rain. The resultant ice rubble comprises hard, angular blocks of ice. Figure 112, for instance, shows such ice rubble lodged against a bank of the Yellowstone River. Note the gravel and sediment attached to the ice blocks; it attests to abrasion of bar and bank by the ice when moving.

The significance of gouging and abrasion with respect to channel morphology is unclear, mainly because it has yet to be thoroughly investigated and because its significance varies. In many circumstances, this mechanism has a slight and intermittent overall effect on channel morphology. The channel simply re-adjusts once openwater conditions have re-established. Ice locally gouges sediment from a bank at some location. In other situations the effect may be longer term and seasonal variation in flow rate is an important consideration in this regard. If the major flow events for a channel coincide with ice runs, the effect is significant. If they do not, the channel-shaping properties of the other flow events probably obscure the effects.

One study of twenty-four rivers in Alberta (Smith 1979) led to the intriguing hypothesis that ice runs enlarge channel cross sections at bank-full stage by as much as 2.6 to 3 times those of comparable flow rivers not subject to ice runs. The hypothesis is based on a comparison of the recurrence interval of bank-full flows in the twenty-four rivers and an empirical relationship between the cross-section area and flow rate for bank-full flow. The channel-widening effect of ice runs is plausible. However, the extent of widening indicated seems overly large and requires further confirmation. Kellerhals and Church (1980), in a discussion of Smith (1979), argue against Smith's hypothesis. They suggest that other factors have led to an apparent widening of the channels analyzed by Smith; e.g. recent entrenchment of major rivers in Alberta and ice-jam effects of flow levels. Moreover, it is possible that the banks are somewhat protected by a band of ice forming a shear wall flanking the riverbanks. It is interesting to contrast Smith's hypothesis with a further hypothesis mentioned above that ice jams may promote channel narrowing by causing over-bank flow (e.g., Uunila 1997). For channels whose dominant channel-forming flow coincides with ice-cover breakup, over-bank loss of flow reduces the flow rate to be accommodated by the channel.

In many situations, notably those in which an ice run is sluggish, a shear wall of broken ice fends off moving ice from the bank. Figure 113 shows a fairly typical shear wall and shear plane between moving ice and the bank of a Midwest River. The shear plane usually is smooth and helps the river move the ice. Running ice, if sufficiently thick, may still gouge the lower portion of a bank, as indeed is indicated by the muddied ice along the shear plane in Figure 113.

Ice gouging and abrasion, though, can be severe for channel features protruding into the flow. In addition, channel locations with a substantial change in channel

alignment are especially prone to ice-run gouging and abrasion; e.g. sharp bends, point bars, and portions of channel confluences. There is a little information on how ice runs affect the local morphology of these sites. Two features have been observed in gravely rivers; ice-push ridges and cobble pavements. Ice-push ridges form when a heavy ice run gouges and shoves sediment along the base of banks (e.g., Bird 1974). The gouged sediment piles up as ridges beneath the ice run as it comes to rest as a jam. The finer sediments eventually get washed out, leaving the more resistant gravel and boulders in ridges. The ridges usually develop in the vicinity of locations subject to recurrent ice jams.

Cobble pavements may cover bars and the lower portion of banks subject to ice gouging and abrasion. Essentially, an over-riding mix of ice and cobbles removes the finer material from the surface of the bars or banks. The resultant cobble surface comprises cobbles whose major axis is aligned parallel to the channel and whose size gradually decreases downstream (Mackay and Mackay, 1977). The resultant cobble pavement may extend for many miles along the banks of large northern rivers, such as the Mackenzie and Yukon (Kindle, 1918; Wentworth, 1932).

The gouging and abrasion of the lower portion of banks, in conjunction with over-bank sediment deposition during ice-jam flooding, may produce an elevated ridge or bench feature along some northern rivers. These features have been dubbed *bechevniks* for Siberian rivers (Hamelin, 1979). The word *becheva* means towrope. A bechevnik is the marginal strip comprising the lower portion of a riverbank and exposed portion of adjoining river bed that, in days gone by, formed convenient paths for towing boats upstream manually or by horse. Figure 114 illustrates the main features of a bechevnik, which may form partly from ice abrasion and partly from the deposition of sediment and debris left by the melting of ice rubble stranded after ice runs.

Moving ice may also grind banks formed of soft rock (e.g., sandstone, mudstone, shale or limestone) or stiff clay. Danilov (1972) and Dionne (1974), for instance, describe how moving ice has affected rock banks of rivers like the St. Lawrence. The extent of erosion, though, doubtless is less than for banks formed of alluvial sediment.

Ice-run gouging and abrasion have an important, though as yet not quantified, effect on riparian vegetation that, in turn, may affect bank erosion and channel shifting. Where ice runs occur with about annual frequency, riparian vegetation communities have difficulty becoming established. Ice abrasion and ice-jam flooding may suppress certain vegetation types along banks, as illustrated in Figure 114 (for a bechevnik) or more generally in Figure 115, possibly exacerbating bank susceptibility to erosion. This aspect of river ice has yet to be further investigated. Scrimgeour *et al*. (1994) and Prowse (in press) provide useful early reviews.

Jam-Initiated Channel Avulsion and Meander-Loop Cutoff

Channels with tight meander loops or sub-channels around numerous bars or islands are prone to ice-jam formation (Ettema, *et al*. in press). Such channels typically have insufficient capacity to convey the incoming amount of ice. Their morphology may be too narrow, shallow, curved, or irregular to enable drifting ice pieces to pass. Jam formation may greatly constrict flow, causing it to discharge along an alternate, less

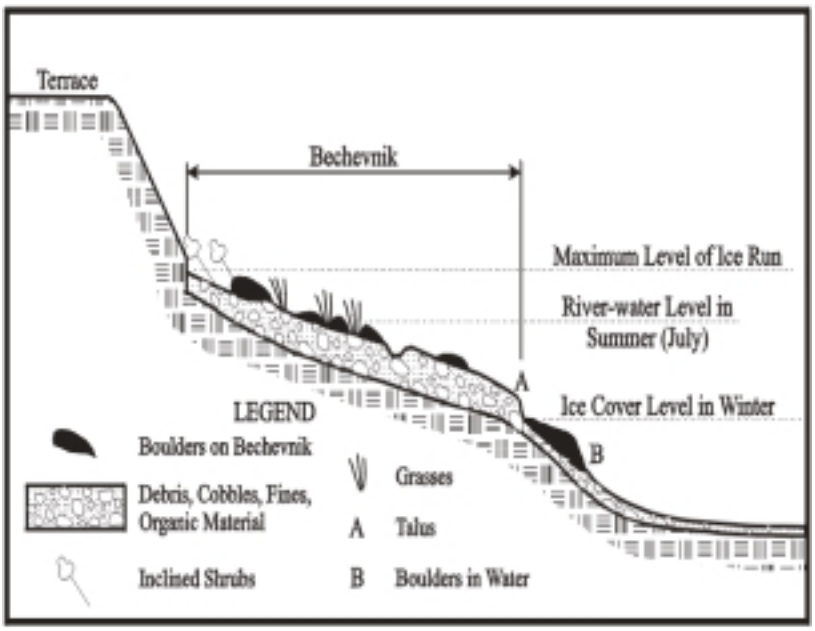

Figure 115. Sketch of a depositional bechevnik. The sketch is modified from Hamelin (1979).

resistant course. Prowse (1998) and Dupre and Thompson (1979) suggest that ice-jam induced avulsion plays a major role in shifting the distributary channels of river deltas.

When an ice jam forms in a meander loop, upstream water levels may rise to the extent that flow proceeds over-bank and across the neck of a meander loop. If the meander neck comprises readily erodible sediment and the flow is of sufficient scouring magnitude, flow diverted by the jam may result in a meander-loop neck cut whereby a new channel forms through the neck and the former channel is left largely cutoff. This situation is illustrated in Figure 116 for a jam formed in a meander loop. A meander cut off shortens and steepens a channel reach, the consequences of which are felt upstream and downstream of the cut off reach. The net effect of ice jams, in this regard, is to reduce channel sinuosity. Williams and Mackay (1973) and Mackay *et al*. (1974) cite examples of such events.

If, on the other hand, the meander loop is wide and not easily eroded, over-bank flow resulting from an ice jam may have the reverse effect. Rather than the net consequence being the erosion of channel through the meander loop, over-bank flow may deposit sediment, thus raising bank height and reinforcing the meander loop. Eardly (1938) reports that ice jams cause substantial sediment deposition on the flood plain of the Yukon River. Over-bank deposition of sediment, together with ice-run gouging and abrasion (see next section) from the lower portion of a bank, may over-steepen riverbanks.

River-Ice Influence on Strength of Streambank Material

A riverbank comprising fine sediments and with a high water table may be subject to freeze-thaw cycles that weaken the bank to the extent that failure occurs due to inadequate slope stability. This ice effect on bank erosion is discussed later in the section. The point to be made here, however, is that river level fluctuations influence the freeze-thaw weakening of a bank. The formation of border ice is closely linked to freezing of water along the water table within the bank. Border-ice formation likely leads to freezing of water at the surface of the water table, because the water table is somewhat insulated by the overlying bank material and border ice thereby influences the extent to which the water table freezes. At present, the relationship between border-ice formation and water-table freezing has not been extensively investigated.

River-Ice Erosion Processes at Work in the lower Missouri River

The erosion mechanisms described above occur to varying extents in the lower Missouri River. The extent of erosion attributable to a particular mechanism, though, is difficult to determine at present. Evidence is observational and anecdotal and suggests that the two most active mechanisms are elevated flow levels at freeze-up and during ice-cover presence.

A significant concern commonly expressed is the substantial rate of flow and flow-rate fluctuations that Fort Peck Dam imposes on the river during winter. The flows are much larger and fluctuate more frequently during winter than occurred prior to the dam. The increased magnitudes of ice-covered flow, increased ice movement up and

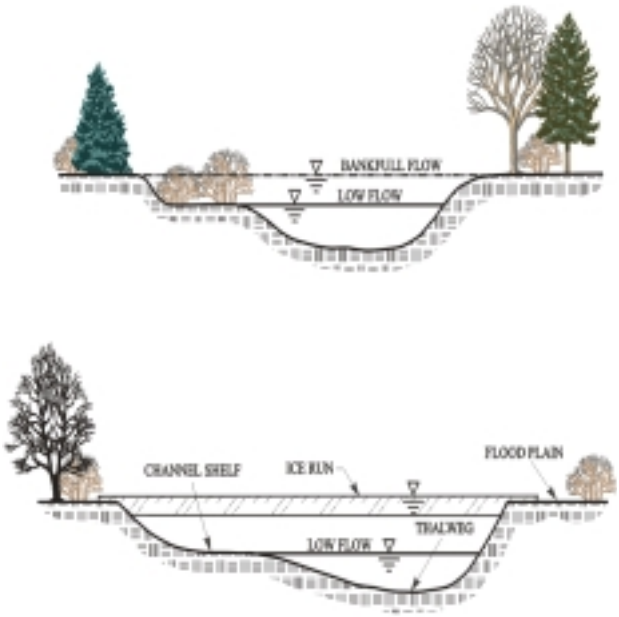

Figure 116. Severe ice runs may inhibit riparian vegetation growth along morphologic features (e.g., on a channel shelf) within a river and on the bank adjoining the river.

down banks, bank freezing at a higher level and more frequent freeze-thaw cycles experienced by the bank materials are seen as severely aggravating bank erosion. The effects of these processes become noticeable in spring, when large portions of banks, which have been undercut during winter or early spring begin to fail (Engelhardt and Waren 1991).

It must also be said that the dam serves to reduce peak flow rates during spring, when snow melt and rain fall produce higher amounts of runoff. An exact estimate of the net effect on channel formation and bank erosion of flow regulation by the dam is not a straightforward matter. The severity of some ice effects is possibly aggravated by higher flows in winter, yet the severity of other ice effects is diminished by lower peak flows during spring.

Elevated Freeze-Up in the lower Missouri River

A noticeable feature of river ice in the lower Missouri River is the rotation of border ice. Rotated and collapsed pieces of border ice delineate locations of substantial drops in flow level. Border-ice rotation and collapse occur due to a lowering of the flow stage to a level below that at which the border ice formed. To date, the extent to which collapsed border ice adversely affects bank erosion has not been determined. It is difficult at this moment to say more than that border-ice rotation and collapse aggravate bank erosion.

Figure 117 shows sagging and rotation of the ice cover at about River Mile 1623 (immediately downstream of the Tveit-Johnson site). Note that the flow level has slightly increased from that associated with cover formation and some flow has partially inundated the ice cover. The most dramatic evidence of border ice rotation and collapse observed during February 1998 was at about River Mile 1716 (near the Pipal site) as illustrated in Figure 118. Shortly before the photo was taken, the reach had been ice covered and the water level higher. The drop in water level was about 4 feet, as is evident from the photograph. Figure 118 suggests that the flow had likely continued eroding the bank toe. Though no firm evidence is available at this point, it can be conjectured (on the basis of relative increase in flow resistance of an ice-covered compound channel) that the ice cover would have concentrated the flow in the channel thalweg, which lies close to the outer (eroding) bank. It is possible to conjecture further from Figure 118 that the collapsed border ice would have weakened the bank and plucked material from it.

Elevated Flow Rates in the lower Missouri River

Flow regulation at Fort Peck Dam may cause winter flow rates in the lower Missouri River to be considerably larger than those occurring prior to dam closure, e.g. Figure 98. It is common for flow rates to be greater than those at which the ice cover initially formed. The effects on bank and channel stability of elevated flow rates are accentuated by lateral variations in channel bathymetry and ice-cover thickness. The lateral variations in channel conveyance concentrate the flow.

The significant variations in flow depth throughout the sinuous point bar and sinuous braided morphology of the lower Missouri River cause significant variations in

Figure 117--Sagging and rotation of the ice cover at about River Mile 1624, near the Tveit-Johnson site, February 10, 1998.

Figure 118--Rotation and collapse of elevated border ice in the vicinity of River Mile 1716, near the Pipal site.

the flow conveyance. An ice cover accentuates those variations and will entrench the thalweg. At locations where a thalweg lies more or less in the middle of a channel, thalweg entrenchment may not affect channel morphology. At locations where a thalweg lies to one side of a channel, thalweg entrenchment promotes local lateral shifting of the channel and bank erosion.

Ice-cover influence on flow distribution at channel cross sections and the extent to which an ice cover may concentrate flow along the channel thalweg, can be estimated for the lower Missouri River in terms of the conveyance ratio, K_1/K_2, described earlier in this section. However, estimation would not indicate the full flow distribution. Several considerations associated with the three-dimensionality of flow, bathymetry and ice-cover thickness at each site influence flow concentration:

1. The ice cover may not be uniformly thick over the cross section;
2. The cross section is part of a three-dimensional domain;
3. Bed sediment and bank material may influence flow concentration; and
4. Scour or deposition of sediment upstream and downstream of the cross section.

Other than to suggest that these effects may occur and to indicate the sensitivities, the lack of direct observations and data at this moment make it difficult to predict the net effect of cover-induced flow redistribution on the channel at these sites. Table 41, nevertheless, comments on the likely trends at selected cross-sections, three of which are shown in Figures 106 a-c. The trends do not take into account the three-dimensional nature of the channel at each site.

Ice Jams in the lower Missouri River

In several instances, ice jams have caused flow to go over-bank, pass over a meander loop and re-enter at the downstream side of the loop. At one location (River Mile 1603), flow over the bank apparently led to the cutoff of a meander loop during the spring of 1979. Figure 119 depicts the altered channel morphology. As mentioned earlier, on one occasion during the early 1980's a jam at about River Mile 1632 caused water to flow over the wider meander loop at the Vournas Farm. The location is shown in Figure 118. This event did not result in a loop cutoff, likely because of the loop's large width. Instead, the over-bank flow apparently deposited a thin layer of sediment wherever it went (Iverson, personal communication).

As noted earlier, in the section on ice jams in the lower Missouri, jams occur more frequently between the confluence with the Yellowstone River and Lake Sakakawea. The main consequences of those jams is sediment deposition associated with the over-bank flow.

Localized Scour in the lower Missouri River

In concept, local scour of a channel bed or bank is easily envisioned; increased flow velocities around an obstructing ice accumulation locally erode the bed or bank. In practice, however, it is difficult to observe owing to the short distance and duration over which it typically occurs. It can be significant beneath major ice jams that severely

Table 41--Comments on possible thalweg shifting at selected sites.

River Mile Site name	Main thalweg position 1991	Comment on thalweg shifting (for cross section)
1675 Wood's Peninsula	channel center	thalweg likely to remain in central position
1682 McRae site	channel side	thalweg likely to shift toward adjoining bank
1631 Vournas site	slightly off center	Slight tendency for thalweg to shift toward outer bank
1646 Mattelin site	two thalwegs	Flow capacity of one thalweg may reduce relative to that of the other thalweg.

Figure 119—River Mile 1603, a reach where an ice jam resulted in a meander-loop cutoff.

congest flow. Local scour likely does not significantly affect channel morphology and bank erosion in the lower Missouri River, which experiences few severe ice jams. Nonetheless, it may aggravate bank erosion under certain circumstances.

Figure 120 shows one circumstance. The head of the ice cover at about River Mile 1624 (in the vicinity of the Tveit-Johnson site) coincides with the downstream end of a bank-erosion arc. Pieces of drifting ice, together with ice broken from the sagged ice cover (cover sagging had occurred due to a reduction in river flow), locally increased water velocities near the bank. Though the site visit was not long enough to monitor for accelerated bank erosion, the configuration of ice at this location could likely accelerate lengthening of the eroding bank, especially if flow increases. An important aspect of the present observation is that the location of the head of an ice cover within a complex channel may accelerate channel shifting by locally altering flow resistance and direction. This bank-erosion mechanism (if it is indeed significant) has never before been investigated.

Ice Gouging and Abrasion in the lower Missouri River

Moving ice may gouge and abrade the banks of the lower Missouri River along certain reaches of the river. Figure 121, for instance, depicts a thick layer of ice moving through the river at about River Mile 1631. However, because ice-cover breakup in the lower Missouri River apparently is a rather gentle process, gouging and abrasion of the river's banks likely are not as severe as may occur for other rivers, such as the Yellowstone River, in which ice-cover breakup and ice jam formation are more dramatic. Other than the instance depicted in Figure 121, there seems to be little information available with which to assess the significance of ice gouging and abrasion. All that can be said is that, when it occurs, it is another factor that aggravates bank erosion.

Effects of River Ice on Channel Planform

The long-reach effects on channel planform of river ice are intriguing to contemplate. Knowledge about them may help explain shifts in thalweg position(s) at some sites along the lower Missouri River. They may be difficult to discern over long distances of the river, though. River morphology over long reaches reflects the influences of numerous variables besides those related to ice. Ice likely does not provide the dominating influence.

General Processes

The effects of ice on channel plan form over long reaches of rivers have barely been investigated. Consequently, the greatest amount of speculation greets any analysis of ice effects on channel morphology over long reaches (plan form and channel cross section). Therefore, let the reader beware. This section is highly speculative.

The following speculations can be argued on the basis of known influences of ice on flow resistance and of flow resistance on sediment transport and channel morphology:

Figure 120--Ice pieces collecting at the head of an ice cover locally increase flow velocities near the bank.

Figure 121--A thick layer of broken ice moves slowly downstream in the vicinity of River Mile 1631, near the Vournas site.

1. The erosive effects of ice increase with increased flow rate;
2. Because an ice cover imposes additional flow resistance, it diminishes the effective gradient of flow energy available for sediment transport and alluvial-channel shaping;
3. Through its effects on local redistribution of channel resistance and, therefore, flow distribution, ice-cover formation and breakup add processes that complicate the regularity of meander wavelengths developed in accordance with the under openwater flow conditions;
4. By reducing a channel's capacity to transport bed sediment, an ice cover will redistribute sediment in the channel. Whatever local-scale effects an ice cover may exert in accentuating erosion, an ice cover reduces the channel's overall capacity to convey the eroded sediment a significant distance from the erosion location. Consequently, bars may develop in response to flow conditions under an ice cover, and be soon washed out shortly after the cover breaks up. In situations where a significant load of bed sediment enters a long reach, a cover may tend to cause mild aggradation of the channel it covers; and,
5. By making it difficult for vegetation to become established along extensive lengths of bank and bar, ice-cover formation and breakup may accelerated bank erosion and lateral shifting of the channel.

Two further effects associated with river ice should be kept in mind. First, a cold flow of water at about 0^oC is twice as viscous, and therefore likely more erosive, than water at about 25^oC. Second, the flow stages during the processes of freeze-up, cover growth, and cover breakup influence bank freezing.

The importance of flow rate in the relationship between river ice and channel morphology is readily evident for a given river reach. Flow rate directly influences flow velocities and the velocities of fragmented river ice during cover breakup. It also influences the amount of ice formed in the reach, through the influence of flow velocities on ice-cover formation and the surface area of flow to be covered; higher flow rates produce more ice and are accompanied by a larger surface area of flow.

The influence of an ice cover on the effective gradient of flow energy available for sediment transport and channel formation requires a little more explanation. The following explanation is ventured using Figure 122, which relates channel sinuosity and channel slope, and Figure 123, which essentially converts an ice-covered flow to an equivalent openwater flow in a channel of reduced slope (actually reduced energy gradient). The explanation is novel. It does not exist in the literature on ice-covered channels. The main point of the explanation is that ice-cover presence may alter thalweg sinuosity of alluvial channels.

For a given flow rate and bed-sediment composition, thalweg sinuosity and channel planform may change as channel slope changes. The planform changes noted on Figure 122 indicate that, for a given flow rate and bed sediment size, the channel lengthens or branches into sub-channels as channel slope increases. Channel slope prescribes the amount of energy available for flow along a given distance of channel; i.e. it prescribes a rate of elevation drop that may be considered a gradient of energy expenditure. Channel lengthening and branching are mechanisms whereby an alluvial-channel flow seeks to increase flow resistance (and thereby energy use) to offset increased flow energy associated with a larger channel slope.

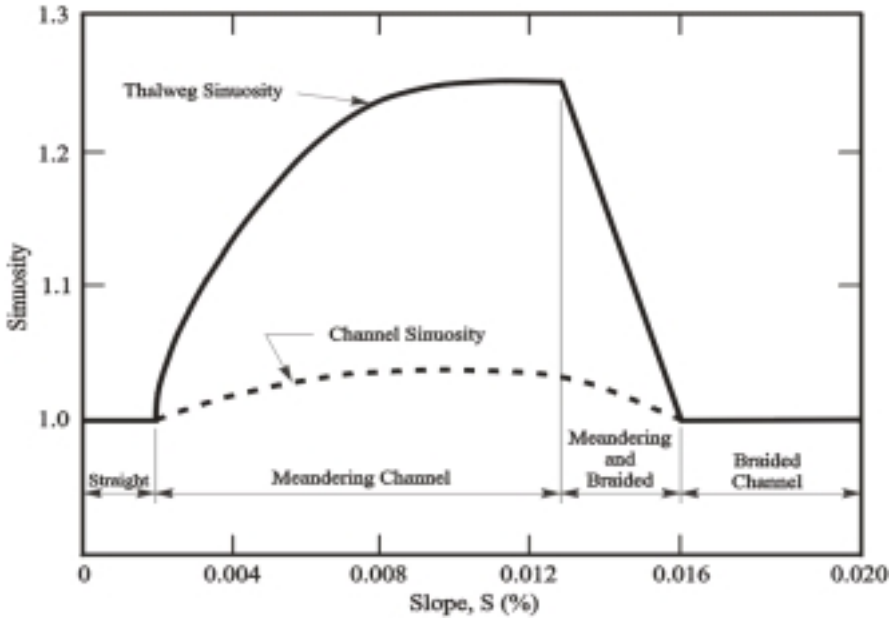

Figure 122--Variation of channel and thalweg sinuosity with channel slope. Figure adapted from Schumm and Khan (1972).

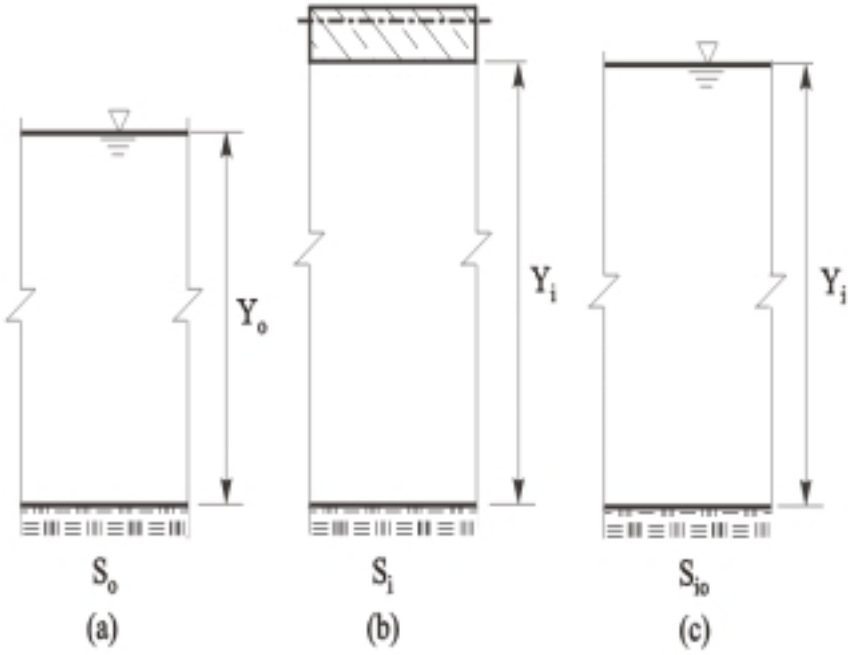

Figure 123--A simplified sketch of how the flow depth in an initial openwater flow (A) may be increased by an ice-cover; (B), for the same flow rate; and (C) the river channel and banks essentially experience flow at a raised flow depth.

The energy gradient of a flow is the rate at which the flow expends energy per unit length of flow along a channel. It is equivalent to channel slope for a flow of uniform depth along a channel. The following relationship (see Table 42 for details) approximately shows the extent to which the rate of energy use available for sediment transport and channel forming decreases when a channel becomes ice covered:

$$\frac{S_{io}}{S_o} \approx \left(\frac{Y_o}{Y_i} \right)^{10/3} \tag{27}$$

where S_{io} = the energy gradient associated with sediment transport and channel forming under ice-covered flow conditions (Figure 123b); and

S_o = the energy gradient for openwater flow in the channel (Figure 123c).

As ice-covered flow depth, Y_i, usually exceeds openwater depth, Y_o, the ratio S_{io}/S_o is less than 1. For a typical value of $Y_o/Y_i \approx 0.8$, $S_{io}/S_o \approx 0.5$; in other words, for a given flow rate in a channel of given length, approximately only half the amount of energy is available for sediment transport and channel formation. The effect of an ice cover, therefore, is to trigger a shift in thalweg sinuosity and alluvial-channel planform so as to balance flow-energy availability and use.

The shifts will vary for channels of different openwater morphology and sinuosity. The following description of thalweg shifts is conceptual and it assumes that substantial flows continue to pass through the channel when ice covered. The descriptions, nonetheless, may shed useful light on channel-shift tendencies. The full extent of the conjectured shifts may not eventuate for several reasons. Most notably, there is the simple fact that the ice cover is present for relatively short duration; no more than a half a year for the most northerly of rivers.

Figure 122 suggests, for instance, that a reduction in slope for a meandering channel (say from 0.008% to 0.004%) may reduce thalweg sinuosity; i.e. the thalweg attempts to straighten and the meander wavelengths shorten, as sketched in Figure 124. A reduction in energy gradient for a sinuous channel with pronounced point bars (say a slope change of about 0.016% to 0.012%) may tend to increase sinuosity, as the flow concentrates in the single thalweg and accelerates erosion of the outer bank of bends.

This effect can be visualized readily if ice cover thickness is greatest in regions of shallowest flow (Figure 125, section A-A). A consequence would be the tendency, as indicated in Figure 125, for the loops to skew. For sinuous-braided channels, such as drawn in Figure 126, ice-cover formation and associated decreases in energy gradient may cause flow to concentrate in a single thalweg of greater sinuosity than the openwater thalwegs. For a braided channel, such as shown in Figure 127, ice-cover presence may concentrate flow into the larger sub-channels. Numerous factors may limit the extent to which the shifts in thalweg and changes in channel plan form occur over long reaches. However, the tendencies for thalweg shift and channel morphology change may be quite evident at local sites along a reach.

Table 42--Details of energy gradient estimate.

The following relationship often is used to relate energy gradient (channel slope for uniform flow), flow depth, flow rate, and channel resistance for flow in a wide channel:

$$q_o = \frac{Y_o Y_o^{2/3} S^{1/2}}{n_o} \qquad (1)$$

in which q_o is flow rate per unit width of channel, and n_o is the value of Manning's *n* associated with openwater flow at rate q_o in the channel.

For flow at the same rate in the channel now ice-covered,

$$q_o = \frac{Y_i Y_i^{2/3} S_i^{1/2}}{n_i} \qquad (2)$$

in which n_o is the value of Manning's *n* associated with openwater flow at rate q_o in the channel. If the ice-covered flow were viewed as an equivalent openwater flow at rate q_o and depth Y_i, the equivalent openwater slope would be S_{io}, with $S_{io} < S_i$. For flow at this equivalent slope,

$$q_o = \frac{Y_i Y_i^{2/3} S_{io}^{1/2}}{n_i} \qquad (3)$$

From Equations (2) and (3), and setting $n_i \approx n_o$, gives

$$\frac{S_{io}}{S_o} \approx \left(\frac{Y_o}{Y_i} \right)^{10/3} \qquad (4)$$

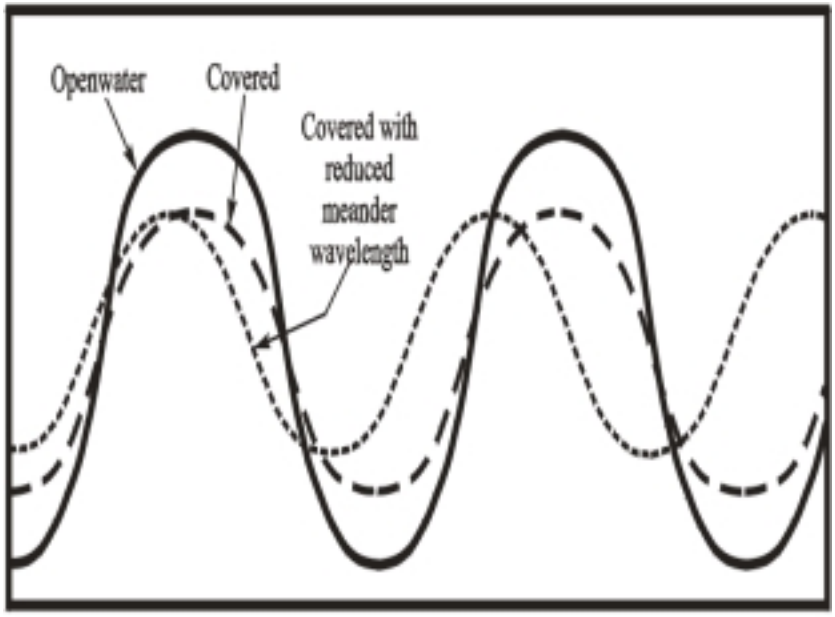

Figure 124--Conceptual influence of an ice cover on a meandering channel of uniform flow depth. The cover may cause the channel to begin straightening and meander loops to shorten.

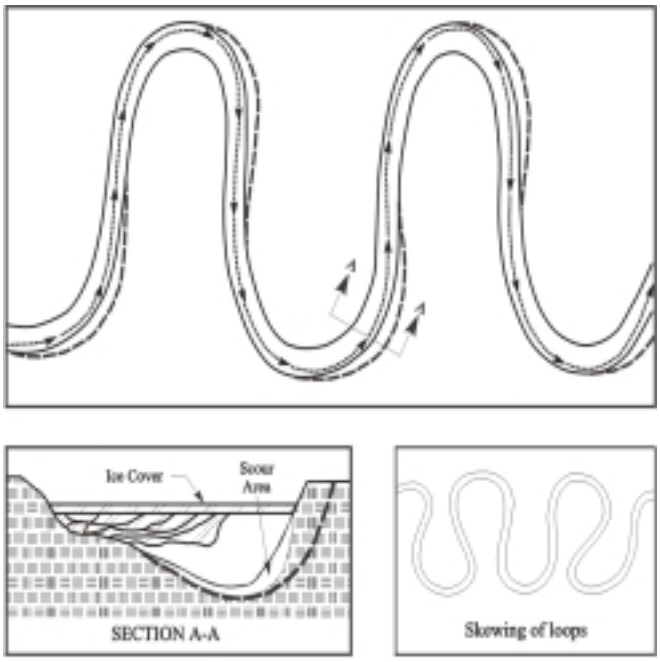

Figure 125--Conceptual influence of an ice-cover on a sinuous-point-bar channel. The cover may cause the channel's thalweg to begin increasing slightly and skew (insert).

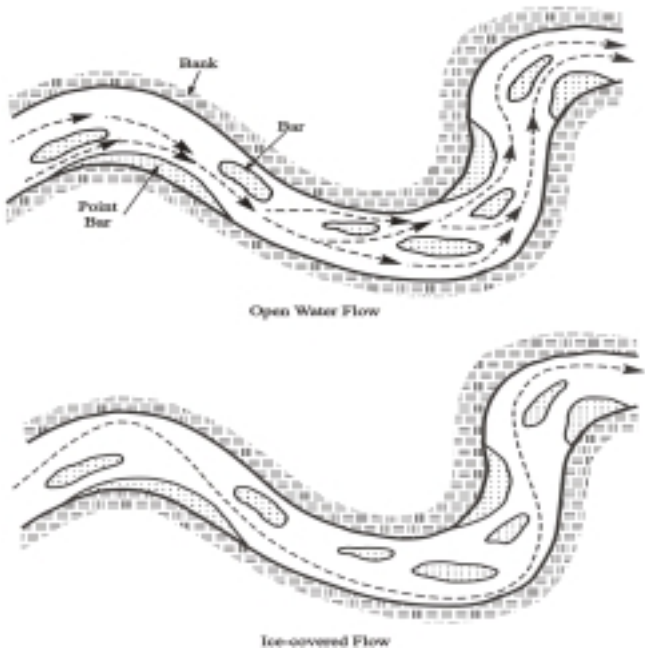

Figure 126--Ice-cover influence of an ice cover on a sinuous-braided channel. The cover may cause the channel's thalweg to begin increasing.

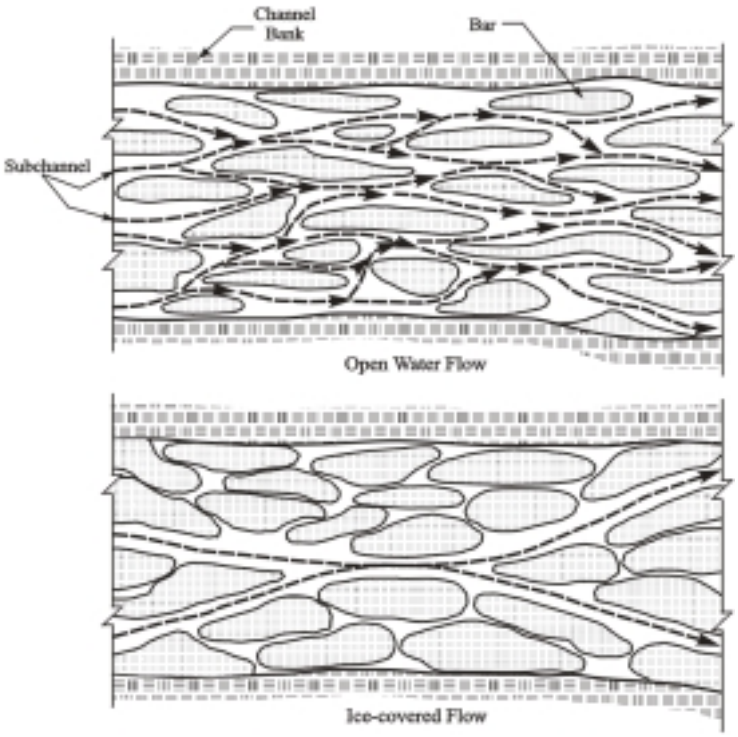

Figure 127--Ice formation over a braided channel may concentrate flow in several larger sub-channels.

Long-Reach Effects for the Lower Missouri River

Ice-cover effects on the morphology of the lower Missouri River have not been investigated. The general effects listed above likely prevail.

In terms of the preceding discussion on changes in thalweg sinuosity, it is possible to conjecture that ice-cover presence would promote changes in thalweg position and, therefore, thalweg sinuosity. If the slope of a representative reach of the lower Missouri River were taken to be $S_o = 1.6 \times 10^{-4}$, and $S_{io}/S_o \approx 0.5$, then $S_{io} = 0.8 \times 10^{-4}$. Figure 122 suggests that, for a constant discharge, this reduction in operative energy gradient would cause thalweg sinuosity to increase, and channel morphology to revert to that of a meandering channel. Though this ice-cover effect is speculative (and the numbers cited in Figure 122 are subject to discussion) it is supported by the effect of flow redistribution due to ice-cover formation. This latter effect causes flow to concentrate in the main thalweg(s), reducing flow in shallower portions of a channel.

Bank Freezing

Freezing and thawing (and/or sublimation) of pore water in riverbanks comprises a second set of mechanisms whereby ice may potentially affect riverbank erosion and channel morphology. It should be considered in conjunction with river-ice effects insofar that those effects influence bank water-table elevation, water temperature and seepage rates. Additionally, as discussed earlier in this section, river ice may mechanically load a bank.

The geotechnical and openwater-flow factors related to bank erosion are discussed more fully in previous sections of the report. The ensuing brief discussion focuses on the ways in which pore-water freezing may affect riverbank erosion.

General Processes

It is well known that the freezing and thawing of soil affects the erosion of banks adjoining rivers and lakes. Lawson (1983, 1985) and Gatto (1988, 1995), among others, provide extensive reviews of the subject. In short, because frozen soil is more resistant to erosion than unfrozen soil, banks are less erodible while frozen. The freezing and thawing of soil, however, usually weakens soils, making thawed (or thawing) banks more susceptible to erosion. The net consequence on the overall rate of bank erosion, therefore, remains a matter of debate. Most likely, the net consequence varies regionally and from site to site.

Gatto (1995) suggests that an eroding riverbank is especially subject to deep penetration of freezing, thereby making more of the riverbank prone to freeze-thaw weakening and erosion. Figure 128 illustrates several features of riverbank freezing along an eroding bank. The absence or stunted extent of vegetation that characterizes many eroding riverbanks results in diminished insulation protection of the bank and increased heat loss to air. In addition, the crest region of a riverbank experiences greatest heat loss, owing to the crest's exposure to air on at least two sides. Because of its exposure to wind, the crest may also accumulate less snow. Less snow, in turn, means deeper frost penetration during winter and faster thawing in spring. However, less snowmelt would be available to percolate into the bank.

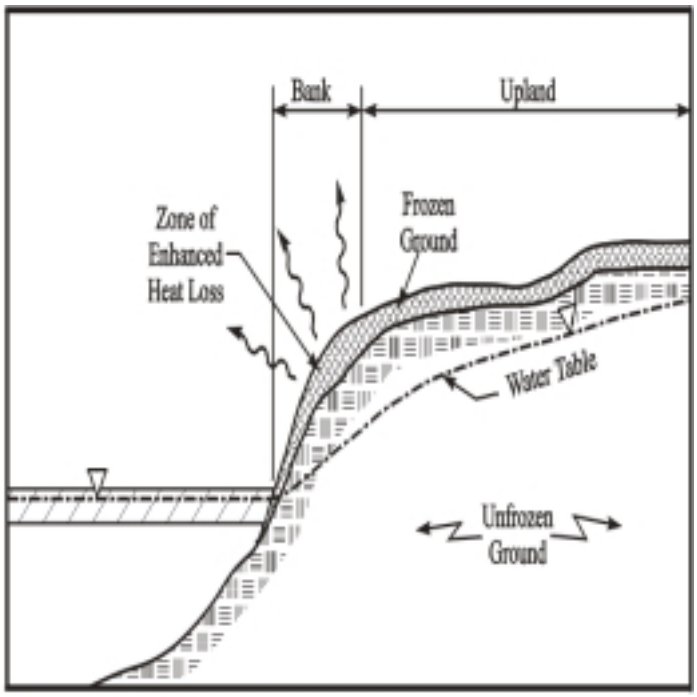

Figure 128--Several features of riverbank freezing. Depth of ground freezing may be thickest at the bank crest, owing to the crest's exposure. Figure adapted from Gatto (1995).

Questions exist about the exact manner in which border ice is anchored to the bank, and other factors (notably, variations in water-table [or piezometric] surfaces and moisture content of the top zone of the bank) would modify the extent of the frozen zone and its connection with river ice. Presumably, if the top portion of the bank and upland were dry, the bank crest might be the zone of least heat loss, as the distance between air and water table is greatest there.

The gradual thawing and seepage of melt water through an eroding bank are sketched in Figure 129. As the upper zone of frozen ground thaws, melt water likely drains down over the surface of the still frozen ground. The bank, weakened by thaw expansion of ground and subject to the seepage pressures, is at its least stable condition of the year.

Several studies (Harlan and Nixon, 1978; Reid, 1985) have found that south-facing banks experience lesser thickness of freezing, all else being the same, than do north-facing banks. The explanation for this is that south-facing banks (in the northern hemisphere) receive more insolation (energy in the form of short-wave radiation from the sun). South-facing banks may also undergo more frequent diurnal freeze-thaw cycles (Gatto, 1995). The net effect on weakening of bank material of bank aspect has yet to be determined.

Freeze-thaw cycles affect soil structure, porosity, permeability and density. These changes in soil properties can substantially reduce soil shear strength and bearing capacity; strength reductions of as much as 95% are reported (Andersland and Anderson, 1990). Such adverse effects on soil strength depend on soil-particle size and gradation, moisture content, the number and duration of freeze-thaw cycles and several other factors. Though there is no single, standard test to determine whether a soil is prone to significant weakening due to freeze-thaw (Chamberlain, 1981), particle size is commonly used as an approximate indicator of soil sensitivity to freeze-thaw weakening. Soils containing fine sands and silts are especially sensitive, because they are permeable and susceptible to change in soil structure. By virtue of their particle size (about 0.1 mm to 0.06 mm) and the surface tension property of water, fine sandy and silty soils absorb moisture more readily than do coarser or fine sediment. Clayey soils are less sensitive because of their low permeability. The variability of soil properties along a riverbank and within a specific bank location, causes the effects of bank freezing to differ along a reach.

Freezing typically results in expansion or heaving of soil as pore-water freezes and expands. Heaving and expansion followed by thawing or sublimation of ice may lead to soil creep, whereby gravity moves soil down-slope. Slope, therefore, plays an important role in freeze-thaw erosion. For banks of low or mild slope, heaving and thawing weaken the soil, making it more readily eroded when subsequently submerged by flowing water. For banks of steep or vertical slope, heaving followed by thawing or sublimation may cause soil to detach from the slope and drop or roll to the base of the slope. In due course, water flow may remove the eroded soil. Sublimation can be quite active along banks aligned east-west, since they face the winter sun.

The flow of melting water from soil pores and lenses may further weaken thawing soil by reducing its angle of internal resistance and cohesion. This process is especially significant if the melt water accumulates on the underlying, still-frozen soil. It is also important when an impervious layer of clay or rock underlies the saturated thawed soil.

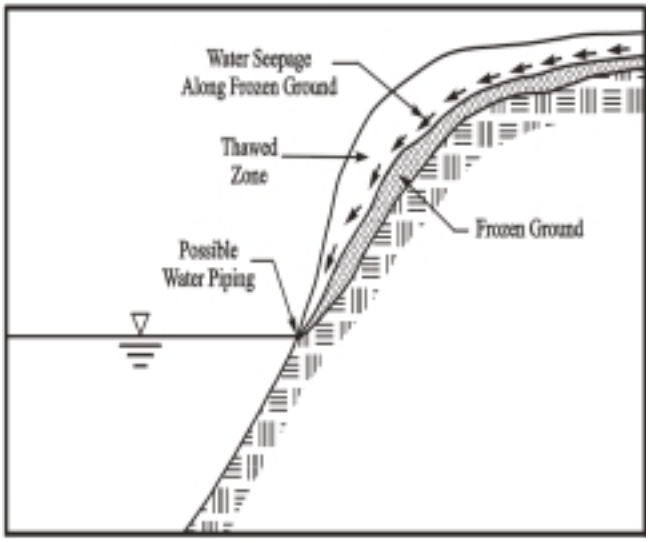

Figure 129-- Several features of riverbank thawing. Thawing progresses from the top and water seeps along the upper surface of the frozen ground.

Under this circumstance the thawed soil is prone to slip failure or flow failure. In the latter case, a mass of soil washes out from the bank.

Flow elevation and water temperature in a river may influence the freezing and thawing of riverbanks. The exact details of the influence have yet to be thoroughly investigated. They clearly depend on bank condition (material, vegetation, snow, etc.), the relative elevations of water-table and river water and the relative temperatures of groundwater and river water. Border-ice growth also plays an important role that remains to be investigated. Its role is interactive with bank freezing and thawing. For example, border ice is anchored to the bank. The strength of anchoring depends on the relative elevation of the water table and the river water. A relatively warm (i.e. several degrees above the freezing temperature) flow of groundwater into the river will hamper border-ice growth and weaken its hold on the bank, as conceptually indicated in Figure 130a. The growth of a thick fringe of border ice, on the other hand, may affect seepage flow through the bank, possibly constricting it and slightly raising the water table, as conceptually indicated in Figure 130b.

Also, ice-cover formation on a river will raise the water level in the river. The rise perhaps being as much as 30% of the equivalent openwater flow depth, plus an additional 0.92 times the ice cover thickness (see Figure 101). This and other important details have yet to be investigated rigorously. They are especially significant for regulated rivers, for which flows do not diminish during winter.

Fluctuations in flow elevation may influence bank stability. It is well known (e.g. Lawson, 1985) that a rapid drop in river level may momentarily reduce bank stability by increasing seepage pressures and, therefore, reducing the shearing resistance of the material comprising the bank. Ice cover formation and breakup, by raising the water level then lowering it abruptly, may weaken banks in this manner. At present, no detailed investigation of this interaction appears to have been conducted.

Freeze-Thaw/Sublimation Effects on Banks along the Lower Missouri River

As with any river that experiences frigid winters, the banks of the lower Missouri River are subject to freeze-thaw and freeze-sublimation weakening. Based on observations made during site visits in mid-February 1998, it would seem that freeze-thaw weakening may potentially influence bank erosion significantly and therefore perhaps channel morphology. Freeze-sublimation weakening seemed to be at work deteriorating the exposed face of banks. The soils comprising the river's banks contain sufficient amounts of silts and fine sands to make them prone to freeze-thaw/sublimation weakening. The extent to which the weakening influences rates of riverbank recession has yet to be determined, however, three erosion features were evident at some locations during the site visit:

1. Bank soil deposited on the ice cover flanking the banks;
2. Overall weakening of soil exposed at the bank face; and
3. Ice-filled cracks along the bank crest.

Figures 91 and 117, views of a severely eroded bank near River Mile 1625 at the Tveit-Johnson site, show deposits of bank soil dropped on the ice sheet. This sight is

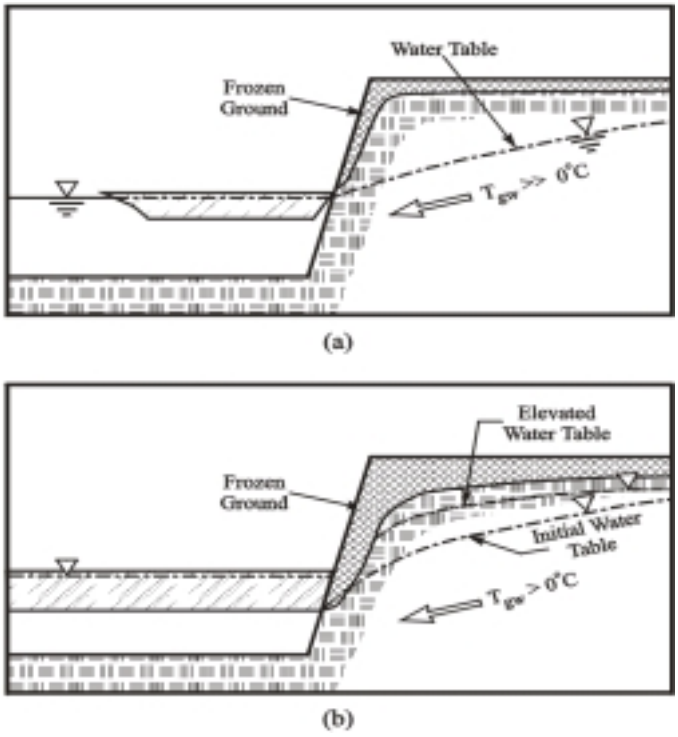

Figure 130--Border-ice growth and bank freezing are affected by water-table elevation and groundwater temperature; e.g., (a) groundwater relatively warm and water table above river level, (b) water table lower and groundwater cool. In the former case, border-ice growth is thin near the bank. In the latter case, thick border-ice

quite common along the lower Missouri River. Several explanations may be given for the way in which the soil detached from the bank and was deposited on the ice. A probable explanation is localized expansion and collapse of exposed bank soil consequent to soil freezing and sublimation of pore water exposed at the bank face. The bank shown in Figures 91 and 117 faces the sun during winter. The soil may simply have detached through drying without significant freeze-induced expansion. In either case, the amount of soil deposited is relatively small. It signifies that the bank faces continue to crumble during winter.

Soil deposited on the ice cover probably does not result from bank undercutting due to local concentration of flow under a stationary ice cover. The ice cover and the frozen bank attached to it would prop the bank if such undercutting occurred. Local bank collapse due to undercutting would occur once the ice sheet broke up and ceased to support the bank. Further evidence is that similar soil deposits on the ice cover occur at other sites where flow is rather shallow near the bank (e.g., River Mile 1631, the Vournas site). The significance of the soil deposition is the overall weakening of the bank face and crest that continues during winter. The lack of protective vegetation, sublimation-drying of exposed soil and the in-filling with snow and frozen water of cracks along the bank crest all weaken the bank face and crest.

Ice-wedge formation accelerates the detachment of large blocks of bank. The large crack shown in Figure 131 probably developed due to an overall structural weakening of the bank. Once formed, however, the crack would be weakened further by freeze-thawing of accumulated water, which would weaken soil surrounding the crack and cause it to enlarge. In this regard, frigid winter conditions may not slow bank erosion, or at least it may not significantly slow the deterioration of a bank.

Erosion Mitigation

As mentioned throughout this section, the extents to which ice contributes to problems of riverbank erosion and channel changes at sites along the river vary with flow and weather conditions, as well as with factors related to bank and channel conditions. Additionally, the adverse effects of ice would inherently vary over a range of scales in distance and time. In principle, the methods used to mitigate ice effects might also correspondingly vary in scale. However, as a practical matter for the lower Missouri River, it is likely that most mitigation activities would have to be limited to controlling problems at specific sites. Lessons learned from those sites might, though, be applied to other sites along the river and to rivers elsewhere. One very important, larger-scale action toward mitigation that should be considered is development of better understanding of ice-related erosion mechanisms. Better understanding of those processes will enhance the design of local mitigative measures and the regulation of flow in the river. It is not at all clear that the possible effects of ice have been fully taken into account in flow regulation plans for the river (Pokrefke *et al*., 1998) or in the design of methods for local bank control (LaGrone and Remus, 1998).

Consequently, an important practical step towards improved understanding is to monitor the overall characteristics of the ice cycle on the lower Missouri River, and to select several critical sites for diagnostic monitoring where bank erosion and changes in channel morphology are especially acute. The monitoring should lead to the clear

Figure 131--Crack development along the riverbank crest near River Mile 1716, the Pipal site.

determination of candidate methods for mitigating the adverse effects of ice at the monitored sites and at similar sites generally. The subsequent section indicates the information to be obtained during the monitoring.

The exact nature of further steps toward erosion mitigation depends on a number of considerations that extend beyond the scope of this section. In principle the possible mitigative methods fall into two categories: structural and operational. A third category, bathymetric methods, would probably not be effective for the river. Bathymetric methods entail excavation or dredging to modify flow alignment and channel dimensions. An excavated or dredged channel would be difficult to maintain in a channel as dynamic as the lower Missouri River between Fort Peck Dam and Lake Sakakawea. Possible conceptual structural and operational methods are discussed below, after several critical sites are nominated for diagnostic monitoring.

Critical Sites

The following sites might be selected as critical and considered for diagnostic monitoring of erosion concerns.

1. River Mile 1716 (Pipal)
2. River Mile 1646 (Mattelin)
3. River Mile 1631 (Vournas)
4. River Mile 1624 (Tveit-Johnson)

These sites are not the only critical sites along the river. They are selected because they show the effects of the erosion mechanisms described above. The monitoring of ice-related processes at these sites should be tied to the overall description of ice formation, extent of coverage and breakup on the lower Missouri River. The mitigative methods identified for them may be appropriate for other sites along the river.

Structural Methods

Structural methods to mitigate the adverse effects of river ice entail the use of flow-guidance and bank-protection structures. Such structures are used to maintain flow in a favorable orientation, usually so that it does not impinge against a bank or accelerate thalweg shifting. It is premature at this moment to recommend specific deployments of structural methods to mitigate possible adverse effects of ice. The significance of those effects must first be defined. Structures to be considered for flow-distribution control include groins, submerged groins, hard-points, guide-banks and vanes. Hard-points and groins have already been placed at some locations along the river, notably at River Mile 1716, the Pipal site (LaGrone and Remus, 1998). Riprap, armor-boulder and riparian vegetation methods might be considered for bank protection. Vanes have been used successfully to mitigate bank erosion in several small rivers (e.g., Odgaard and Mosconi, 1987). Long, submerged groins have been used to inhibit bank erosion and channel shifting on larger rivers, such as the Mississippi (Derrick *et al*. 1994). Whichever method is considered, it would need to be sufficiently robust to withstand ice loads.

Structural methods may also entail control of drainage in riverbanks, to the extent

feasible. Drainage control would seek to ensure that the water table in a bank remained at an appropriate level and that seepage pressures did not become excessive.

Operational Methods

Most of the adverse effects of ice on bank erosion and channel morphology are likely associated with high and fluctuating flow rates. Also of potential concern are water-table elevation and pore-water pressure in the banks. Ideally, from the standpoint of minimizing ice effects on bank erosion and channel change, flows should be relatively low during the ice cycle. If they are relatively high at any phase of the cycle they may amplify the effects of the ice.

It is premature at this moment to suggest optimal flow rates and stages regulated to mitigate the possible adverse effects of ice. The possibility of regulating flows to mitigate ice effects may in fact be moot, because of regulation constraints related to electric-power production and overall management of the annual water budget of the lower Missouri River. Nonetheless, it is of interest to determine whether flow regulation might be tailored during freeze-up and break-up to minimize the possible ice effects if they are significant. An optimal freeze-up flow might be established. Ideally, that flow (or range of flows) might be established using a numerical model in consort with a geographical information system (GIS), to map the river's channel and banks.

BANK-STABILITY INDEX

The nature of the subject matter in this report required a highly technical approach to quantitative analysis of bank-stability issues along the Missouri River below Fort Peck Dam. Because it is virtually impossible to sample, survey and analyze every foot of streambank along the reach, we selected "representative" banks between the dam and the North Dakota border. This approach has merit in that generalizations can be made about processes and conditions along the study reach. In addition, the detailed investigations at 17 study sites have provided a wealth of specific information about those sites. As an intermediate approach and to enable further evaluation of additional sites, we have developed a semi-quantitative index of bank stability that can be used at other sites along the river reach.

The bank-stability index (I_s) is founded on 15 physically-based criteria from several disciplines. A list of the variables used in the ranking procedure and the assigned values for the range of conditions encompassing a given variable are shown in Table 43. Note that the assigned values are not weighted but simply increase as the condition or value of a given variable indicates a greater tendency for bank instability. For example, in variable number 5, bank height, assigned values increase as bank height increases. Similarly, the assigned value increases as bank angle increases from the horizontal. No single variable can attain a value greater than 3. The value attained for a particular site is the sum of the values assigned to each variable at the site. The greater the value of I_s, the greater the potential for bank instability at the site. Sites with a bank-stability index greater then 20 are generally unstable. Values greater than 25 indicate the potential for rapid bank erosion by mass wasting while sites with an I_s value less than 15 are considered relatively stable under non ice-effected conditions. The maximum possible I_s value is 34.5.

An attempt has been made not to exaggerate the importance of one group of variables (such as driving forces, bank height and angle) at the expense of others (such as form variables, site location and position in meander). It should be emphasized that this index is not designed to predict rates of bank erosion or to insinuate that a streambank with an index value of 30 is twice as likely to fail as a site with an index value of 15.

Each of the 15 criteria shown in Table 43 are evaluated for a given site and assigned a value according to the key provided. If there is indecision in assigning a given variable because both conditions may exist, the average of the two values can be used for that variable. Values assigned for individual variables are ranked according to their potential for indicating or contributing to bank instability. The relative rankings of these variables are based on field and analytic experience as well as on the results of shear-strength tests of representative bank materials. The conceptual basis for the assigned values of each variable is self explanatory in most cases. Several variables merit further discussion.

Variable number 7, "*Upper soil unit (shear strength)*" is based on the weighted-mean values of cohesive strength as used in the Culman analysis (Table 33). Because several of the sites shown in Table 33 are composed of the same soil series (such as Havrelon located at River Miles 1589, 1621, 1630, and 1716) average values of effective and apparent cohesion for each soil series were obtained (Table 44).

It needs to be reiterated here that these rankings and the assignation of index values are based on the weighted-mean cohesive strengths of the entire bank, but are

Table 43-- Bank-stability index key, showing diagnostic variables and assigned point values for given conditions of each variable.

Criteria	Points
1. Type of bank failures observed	
None-stable	0
Dormant failures (with established vegetation)	1.5
Recent failures (no established vegetation)	3
2. Condition of bank toe	
Stable and/or vegetated	0
Failed material (or failure plane)	1
Undercut	2
3. Location of site	
Straight reach	1
Outside bend	2
Inside bend	0
4. Position in meander	
Not applicable	0
At apex	2
Upstream of apex	0
Downstream of apex	1
5. Bank height above mean low water	
0 – 5 feet	0
6 – 10 feet	.5
11 – 15 feet	1
16 - 20 feet	2
21 - 30 feet	2.5
Greater than 30 feet	3
6. Bank angle (from horizontal) above mean low water	0
$0 – 25^o$	1
$26 – 50^o$	2
$51 – 75^o$	3
$76 - 90^o$	
7. Upper soil unit (shear strength)	
Lohler	0
Shambo	0
Gerdrum	.5
Harlem	.5
Havrelon	1
Havre-Harlem	2
Banks	2.5
Trembles	3
Riverwash	3
8. Bank-toe material	

Rock-toe or other protection	0
Cohesive *in situ* material	1
Failed cohesive blocks	2
Gravel	2.5
Sand	3
9. Observed vertical cracks	
None observed	0
Some surface (desiccation) cracks	1
Tension cracks to 3-feet deep	1
Tension cracks > 3-feet deep	2
10. Density of bank vegetation on bank top	
None	2
Sparse	1
Dense	0
11. Rooting depth of bank vegetation	
Less than 3 feet	1
Greater than 3 feet	0
12. Root exposure	
Not applicable (if no vegetation)	0
Not exposed on face	0
Exposed on face	1
13. Depth to "normal" water table (low-water surface) from top bank	
0 – 5 feet	3
6 – 10 feet	2
11 – 15 feet	1
16 – 20 feet	0.5
Greater than 20 feet	0
14. Depth to worst-case (highest) water table from top bank	
0 – 5 feet	3
6 – 10 feet	2
11 – 15 feet	1
16 – 20 feet	0.5
Greater than 20 feet	0
15. Location and type of channel bars	
Point bar on same side as bank	0
Point bar on opposite bank	1
Mid-channel bar	1.5

The I_s value attained for a particular site is the sum of the values assigned to each variable at the site. The greater the value of I_s, the greater the potential for bank instability at the site. Sites with a bank-stability index greater then 20 are generally unstable. Values greater than 25 indicate the potential for rapid bank erosion by mass wasting while sites with an I_s value less than 15 are considered relatively stable under non ice-effected conditions. The maximum possible I_s value is 35.

Table 44-- Ranking of strongest to weakest streambanks based on cohesive strengths.

Soil Series	c'	Rank	Soil Series	c_a	Rank	Soil Series	Mean	Rank
Shambo	332	1	Lohler	494	1	Lohler	392	**1**
Harlem	293	2	Shambo	432	2	Shambo	382	**2**
Lohler	292	3	Gerdrum	357	3	Gerdrum	324	**3**
Gerdrum	290	4	Harlem	349	4	Harlem	321	**4**
Havrelon	213	5	Havrelon	280	5	Havrelon	247	**5**
Havre-Harlem	118	6	Banks	153	6	Havre-Harlem	118	**6**
Banks	82	7	Havre-Harlem	118	7	Banks	117	**7**
Trembles	76	8	Trembles	114	8	Trembles	95	**8**
Riverwash	0	9	Riverwash	0	9	Riverwash	0	**9**

being represented by a soil series. With regard to individual soil series, therefore, these strength rankings and average values should only be considered estimates and should not be used for engineering design. The final rankings of the individual soil series are based on the average between the effective and apparent cohesive strengths (Table 44). Actual site design of erosion-control measures requires detailed site specific design information. The bank-stability index cannot be used for engineering design.

Bank-Stability Index at the Study Sites: Application

The bank-stability index was applied to the 17 study sites. Field data collected during 1996 and 1997, analytic results and recent aerial photography were used to evaluate each index variable. Information useful in developing the I_s values for the study sites are provided in Table 45. Much of this has been presented elsewhere but is repeated here for the convenience of the reader.

The evaluation results for each index variable at each site is shown in Table 46. This provides direct evidence of the conditions that comprise the I_s -value for a given site. The maximum I_s value attained along the study reach was 26.5 for sites at River Miles 1631 (Vournas) and 1716 (Pipal) (Table 47). These sites have been shown to be particularly unstable using more rigorous analytic techniques. The lowest values (12 and 12.5) were calculated for sites at River Miles 1744 (Little Porcupine) and 1762 (Milk River). Similarly, these sites have been shown to be particularly stable in the bank-stability modeling described in this report. It is not surprising that most of the I_s values are close to, or greater than 20 (indicating instability) since problematic outside bends were targeted for study. Thus, the bank-stability index developed here seems to do a reasonably good job in evaluating the relative stability/instability of the streambanks in the reach.

Comparison with Local "Activity" Rates

Local erosion rates at the 16 main study sites were calculated as the difference in area encompassed by digitized banklines covering time periods from 20 to 42.5 years. The specific topographic and aerial photographic coverage used to calculate the local rates are shown in Appendix E. In addition, the 1971 and 1991 banklines are shown on two sets of color maps, one displaying soil types (Appendix B) and the other displaying vegetation types (Appendix F). The length of the sub-reach used for analysis was about 1.0 mile. The net area encompassed by the banklines divided by the mean bank length provided an average distance that the bank had migrated over the period.

Given the estimated error inherent in the analysis (Table 48), average migration distances ranged from no migration for two sites near the dam to close to 100 feet at River Mile 1631 (Vournas). It is interesting to note that the Vournas site has the highest I_s value and that one of the sites having the lowest I_s value (Milk River), was one of the sites with no migration. These total distances, however, represent different time periods. Dividing by the number of years between surveys normalizes the data and results in the rate of migration in ft/yr (Table 48). Average and maximum local-erosion rates are plotted against River Mile and compared with the calculated I_s values in Figure 132.

Table 45--Study site information useful in applying bank-stability index.

River mile	Bank-toe material	Bank angle [1]	Bank height [2]	Depth to worst-case water table[3]
		(degrees)	(feet)	(feet)
1589	CH-CL	85.0	18.0	5.48
1604	SM	77.8	24.1	13.2
1621	CL	78.0	18.3	9.12
1624 (LT)	SP	64.2	11.2	7.90
1624	SM	74.8	19.2	1.18
1630	CL	73.1	14.1	3.18
1631	SP	73.0	13.9	3.70
1646	SP	70.7	16.1	7.78
1676	SP	70.9	19.3	12.9
1682	CL	59.5	32.0	22.7
1701	CL	76.6	19.3	10.1
1716	SM	80.7	18.1	8.53
1728	SM	75.4	20.0	11.3
1737	CL	61.0	15.4	6.59
1744	CL	61.5	19.8	11.4
1762	CH	50.0	13.6	5.56
1765	SM	63.7	19.8	11.4

[1] Weighted bank angle over the length of the planar failure surface

[2] Distance from the top of the bank to the 5,000 ft^3/s water surface

[3] Worst-case water table corresponds to a river stage of 26,000 ft^3/s

Table 46- Bank-instability index key showing assigned values for each study site.

Criteria	Points	1589	1604	1621	1624 -LT	1624	1630	1631	1646	1676	1682	1701	1716	1728	1737	1744	1762	1765
1. Type of bank failures observed																		
None-stable	0															0	0	
Dormant failures (with established vegetation)	1.5										1.5				1.5			
Recent failures (no established vegetation)	3	3	3	3	3	3	3	3	3	3		3	3	3				3
2. Condition of bank toe																		
Stable and/or vegetated	0																	
Failed material (or failure plane)	1	1	1			1	1	1		1	1	1	1	1	1	1	1	1
Undercut	2			2	2				2									
3. Location of site																		
Straight reach	1	1					1											
Outside bend	2		2	2	2	2		2	2	2	2	2	2	2	2	2	2	2
Inside bend	0																	
4. Position in meander																		
Not applicable	0	0					0											
At apex	2		2					2	2	2			2	2	2	0	0	
Upstream of apex	0										0							
Downstream of apex	1			1	1	1						1						1
5. Bank height above mean low water																		
0 – 5 feet	0																	
6 – 10 feet	.5																	
11 – 15 feet	1				1		1	1									1	
16 - 20 feet	2	2		2		2			2	2		2	2	2	2	2		2
21 - 30 feet	2.5		2.5															
Greater than 30 feet	3										3							
6. Bank angle above mean low water																		
0 – 25^{o}	0																	

26 – 50°	1															1	
51 – 75°	2				2	2	2	2	2	2	2				2	2	2
76 - 90 °	3	3	3	3								3	3	3			
7. Upper soil unit (shear strength)																	
Lohler	0		0			0											
Shambo	0										0						
Gerdrum	.5											.5		.5	.5	.5	.5
Harlem	.5																
Havrelon	1	1		1			1										
Havre-Harlem	2												2				2
Banks	2.5							2.5									
Trembles	3								3	3							
Riverwash	3				3												
8. Bank-toe material																	
Rock-toe or other protection	0																
Cohesive *in situ* material	1			1			1				1	1			1	1	1
Failed cohesive blocks	2	(1.5)				(1.5)								2			
Gravel	2.5		(2.5)					(2.5)					(2.5)				(2.5)
Sand	3				3				3	3							
9. Observed vertical cracks																	
None observed	0		0	0	0				0	0					0	0	0
Some surface (dessication) cracks	1															1	
Tension cracks to 3-feet deep	1						1					1		1			
Tension cracks > 3-feet deep	2	2				2		2			2		2				
10. Density of bank vegetation on bank top																	
None	2						2										
Sparse	1	1	1	1		1		1	1	1	1		1			1	1
Dense	0				0							0		0	0	0	
11. Rooting depth of bank vegetation																	
Less than 3 feet	1	1		1	1	1	1	1	1	1	1	1	1	1			1	1

Greater than 3 feet	0		0												0	0		
12. Root exposure																		
Not applicable (if no vegetation)	0						0										0	
Not exposed on face	0																	
Exposed on face	1	1	1	1	1	1		1	1	1	1	1	1	1	1	1		1
13. Depth to water table (low-water surface) from top bank																		
0 – 5-feet	3																	
6 – 10-feet	2																	
11 – 15-feet	1				1		1	1							1		1	
16 – 20-feet	0.5	.5		.5		.5			.5	.5		.5	.5	.5		.5		.5
Greater than 20 feet	0		0								0							
14. Depth to worst-case water table from top bank																		
0-5-feet	3	3			3		3	3										
6-10-feet	2			2		2			2			2	2		2		2	
11-15-feet	1		1							1				1		1		1
16-20-feet	0.5																	
Greater than 20 feet	0										0							
15. Location and type of channel bars																		
Point bar on same side as bank	0	0					0										0	
Point bar on opposite bank	1		1		1				1	1		1			1	1		1
Mid-channel bar	1.5			1.5		1.5		1.5			1.5		1.5	1.5				
Sum of values (I_i)	**35**	**21**	**20**	**22**	**24**	**20.5**	**18**	**26.5**	**26**	**23.5**	**17**	**20**	**26.5**	**21.5**	**17**	**12**	**12.5**	**21**

Table 47—Bank-instability index for study sites, ranked from most unstable to stable.

River Mile	Soil Series	Site Name	Date Tested	Bank-Instability Index
1631	Banks	Vournas	8/20/96	26.5
1716	Havre	Pipal	8/21/96	26.5
1646	Trembles	Mattelin	8/21/96	26.0
1624 (LT)	River Wash	Tveit-Johnson	8/19/96	24.0
1676	Trembles	Woods Peninsula	9/10/97	23.5
1621	Havrelon	Culbertson	9/8/97	22.0
1728	Harlem	Flynn Creek	8/22/96	21.5
1589	Havrelon	Nohly	9/9/97	21.0
1765	Havre-Harlem	Garwood	9/17/97	21.0
1624	Lohler	Tveit-Johnson	8/19/96	20.5
1604	Lohler	Hardy	9/10/97	20.0
1701	Gerdrum	Wolf Point	9/12/97	20.0
1630	Haverlon	Iverson	8/20/96	18.0
1682	Shambo	McCrae	9/11/97	17.0
1737	Harlem	Fraizer Pump	9/15/97	17.0
1762	Harlem	Milk River	9/16/97	12.5
1744	Harlem/Till	L. Porcupine	9/15/97	12.0

Table 48-- Local erosion rates calculated from the area between 2 sets of digitalized banklines

River Mile	Site Name	Site #	Net area, ft^2	Mean bank length, ft	Mean distance, ft	Max distance, ft	Time, yr	Mean rate, ft/yr	Max rate, ft/yr	Error,ft	Error, ft/yr	Mean rate 1977- 83*, ft/yr
1589	Nohly	1	15,050	1,224	**12.3**	**31.8**	24.0	**0.51**	**1.32**	5.03	0.21	5.45
1604	Hardys	2	6,779	467	**14.5**	**30.3**	22.5	**0.64**	**1.34**	7.72	0.34	**
1604	Hardys II	2	34,034	1,298	**26.2**	**255**	22.5	**1.17**	**11.3**	7.72	0.34	**
1621	Culbertson	3	23,529	1,224	**19.2**	**26.8**	23.0	**0.84**	**1.16**	21.8	0.95	**
1624 (Low Terrace)	Tveit-Johnson	4	42,111	1,233	**34.2**	**62.8**	23.0	**1.49**	**2.73**	7.94	0.35	1.74
1624	Tveit-Johnson	5	42,111	1,233	**34.2**	**62.8**	23.0	**1.49**	**2.73**	7.94	0.35	1.74
1630	Iverson	6	71,028	1,237	**57.4**	**139**	23.0	**2.50**	**6.03**	5.03	0.22	**
1631	Vournas	7	115,526	1,223	**94.5**	**328**	23.0	**4.11**	**14.3**	5.03	0.22	26.5
1646	Mattelin	8	91,426	1,223	**74.7**	**125**	42.5	**1.76**	**2.95**	11.7	0.28	**
1676	Woods Peninsula	9	25,530	1,233	**20.7**	**38.3**	20.0	**1.04**	**1.91**	10.8	0.54	1.36
1682	McCrae	10	25,008	1,246	**20.1**	**59.1**	20.0	**1.00**	**2.96**	6.69	0.33	1.02
1701	Wolf Point	11	39,866	1,242	**32.1**	**69.0**	20.0	**1.60**	**3.45**	6.47	0.32	3.64
1716	Pipal	11.5	16,702	1,150	**14.5**	**30.5**	20.0	**0.73**	**1.52**	8.40	0.42	4.55
1728	Flynn Creek	12	17,554	1,064	**16.5**	**31.6**	20.0	**0.83**	**1.58**	6.70	0.34	1.03
1737	Fraizer Pump	13	21,744	1,249	**17.4**	**32.7**	20.0	**0.87**	**1.64**	6.10	0.30	0.69
1744	L. Porcupine	14	2,028	1,226	**1.65**	**14.9**	20.0	**0.08**	**0.74**	8.57	0.43	**
1762	Milk River	15	-281	382	**-0.74**	**41.3**	20.0	**-0.04**	**2.06**	7.83	0.39	**
1765	Garwood	16	-6,971	1,236	**-5.64**	**15.7**	20.0	**-0.28**	**0.78**	9.42	0.47	**

* Modified from U.S. Army Corps of Engineers (1986)

** The erosion losses during this 8-year period were very minor; however, past erosion estimated frrom aerial photography, along with anticipated future erosion losses based on field observation warrant the inclusion of these areas as erosion problem sites.

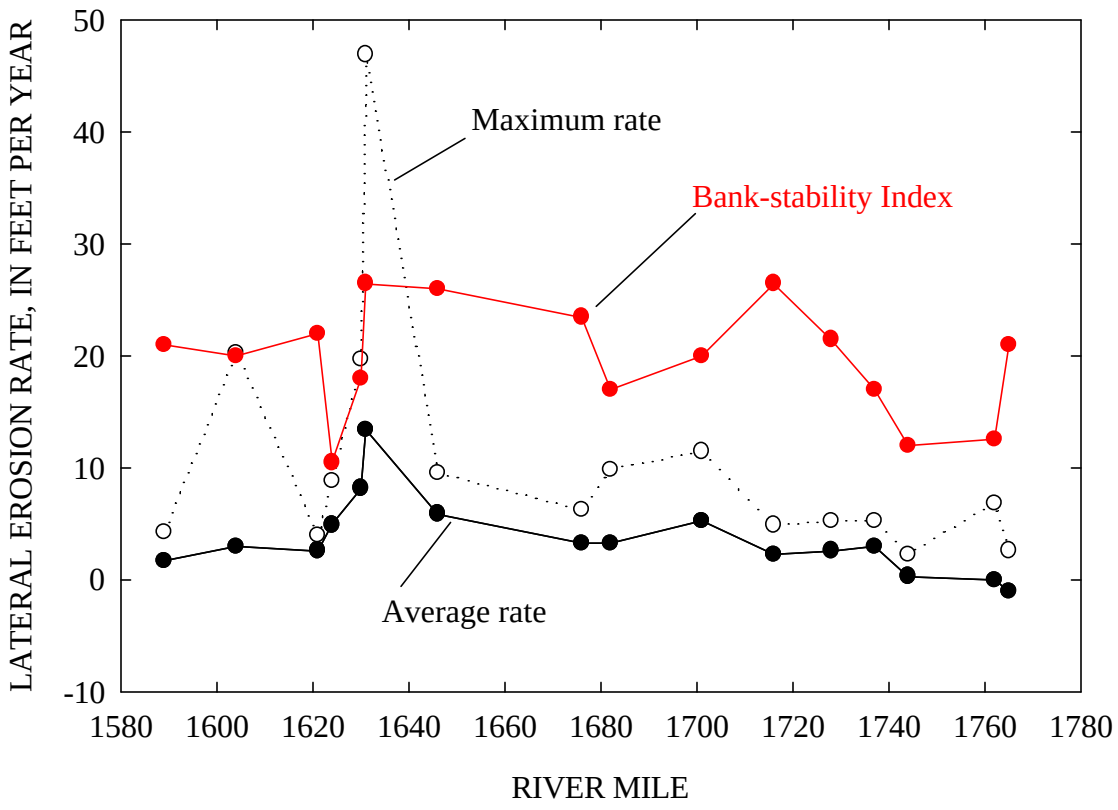

Figure 132--Lateral (local) erosion rates compared to the bank-stability index I_s for the study reach, showing a similar general trend.

Although there are no reliable statistical relations between long-term migration rates and I_s values, or migration rates and any of a variety of cohesive strength, bank height, and toe-material variables, Figure 132 does display some parallel trends between migration rates and I_s values. There are many possible reasons as to why these two variables are not statistically related at a significant level. These are particularly related to possible changes with time in the resistance of the boundary sediments and in the driving (erosive) forces as the channel migrates across the flood plain. For instance, migration and erosion through a flood-plain deposit of a given shear strength could then be followed by impingement on a terrace characterized by greater bank heights and potentially, vastly different shear strength and bank-toe characteristics. Clearly, the local erosion-rate values are an integration of force-resistance relations through time, leading to a homogenization of long-term erosion rates and, therefore, low statistical significance with current bank and channel characteristics.

DEVELOPMENT OF NEW SURFACES AND NEW SOILS

Channel incision along the Missouri River below Fort Peck Dam occurred as a result of the reduction of the upstream supply of sediment. Lowering of the channel bed results in a corresponding lowering of the water surface for a given discharge and can result in previous flood-plain levels being abandoned by the river for lower surfaces. In fact, this is one of the purposes of the Fort Peck or many other dams, to reduce or prevent the inundation of flood-plain surfaces. Sand- and gravel-sized sediment eroded from the channel bed in the 55 miles below Fort Peck Dam is transported to reaches further downstream. Deposition of this sediment may occur across the channel bed over time causing the general raising of the channel bed (aggradation). Deposition also occurs as bars that develop on the inside of meander bends or in mid-channel due to divergent flow streams. Mid-channel bars can be extremely dynamic, changing shape and size in response to changes in flow. Other bars may become semi-permanent features as they increase in height and length by vertical and lateral accretion of sediments. Riparian vegetation establishes on these surfaces and aids in their permanence by providing increased resistance to erosion by root reinforcement. With time, extension and coalescence of these features can form berms and incipient flood-plain surfaces at an elevation lower than the previous flood plain.

Ages of Recent Geomorphic Surfaces

Several geomorphic surfaces of different ages and relative elevations have been identified by the dating of trees established on these surfaces. It seems that the river is creating a new flood plain at an elevation lower than the previous flood-plain surface. The pre-dam flood plain is identified with tree ages of 55 years and greater. Some trees were dated as old as 115 years. This surface is now considered a terrace, in that it is not regularly inundated by the river. At a lower elevation is a relatively new surface identified by riparian trees generally between 32 and 39 years old. This surface was identified at five different locations, all at or upstream of River Mile 1682. We believe that this surface represents the new, incipient flood plain of the Missouri River in that it is found emanating from the base of the pre-dam flood-plain surface containing trees older than 60 years. The vertical difference in elevation between these two surfaces is generally 4-10 feet, approximately equal to the average amount of bed-level incision over the study reach.

There is additional evidence of revegetation of portions of this newer flood-plain surface in the 1970's, particularly in areas close to the channel. Trees 20 to 25 years old are commonly found above the surface occupied by bars and below the terrace (pre-dam flood-plain surface). This indicates that high magnitude flows during the 1970's (particularly in 1976-1979) probably did considerable damage to incipient flood-plain areas. New vegetation subsequently established itself after these flows resulting in a progression of younger tree ages as one moves from the base of the terrace (pre-dam flood plain) towards the channel. An idealized representation of the general setting and ages of these surfaces is provided in Figure 133. An overview of vegetation types bordering the river is shown in Appendix F.

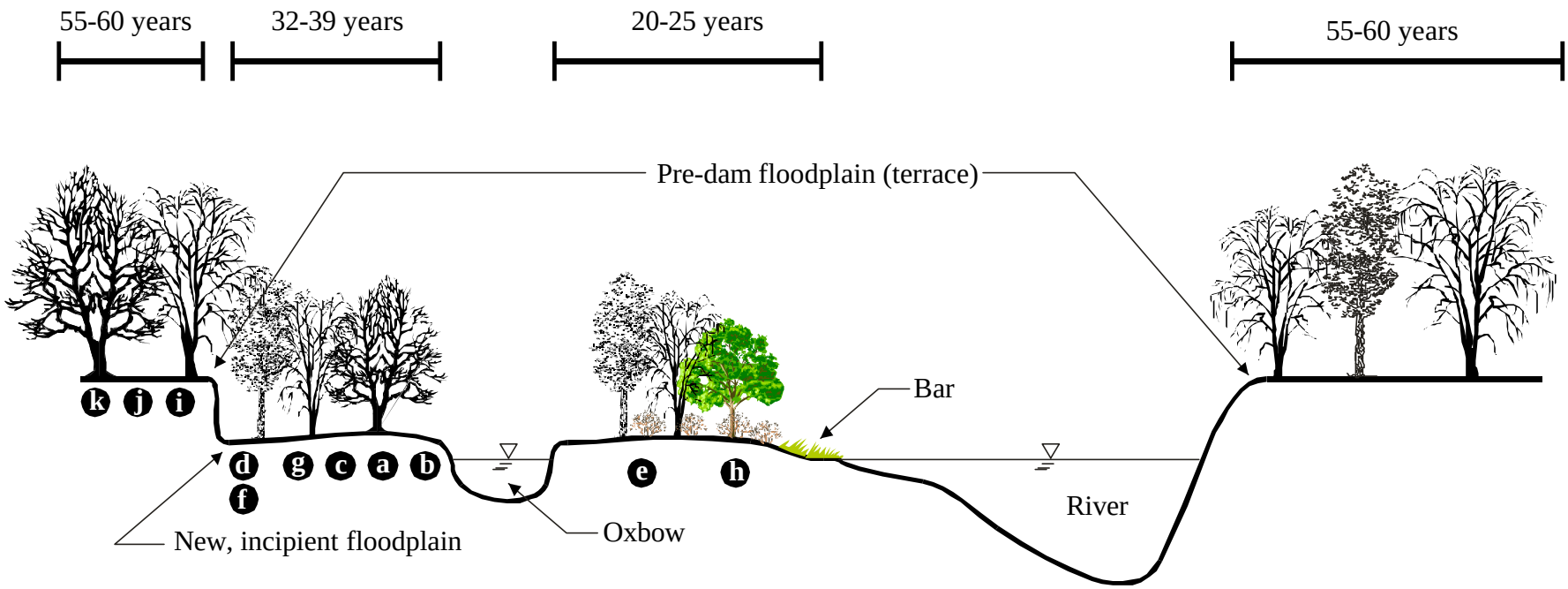

a	Green Ash	36 years old
b	Tilted Willow	37 years old
c	Willow	31 years old
d	Green Ash	34 years old
e	Cottonwood	19-20 years old
f	Ash	46-49 years old

g	Ash?	35 years old
h	Willow?	8-9 years old
i	Cottonwood	66 years old
j	Willow	53 years old
k	Cottonwood	62-64 years old

Figure 133 --Idealized drawing based on field sketch of Missouri River channel in the vicinity ofrivermile 1701 showing various geomorphic surfaces and their ages as determined fromtree-ring evidence.

Characteristics of "New" and "Old" Soils

Recently formed soils (since dam closure) on these low incipient flood-plain surfaces are different to the soils making up the pre-dam flood plain. Samples of these soils were collected to a depth of 5 feet by NRCS soil scientists in 1996 and 1998 between River Miles 1627.5 and 1687.3 (Table 49). The purpose of the sampling was to determine any differences in grain size between these "new" soils and the surficial soils composing the terraces currently under cultivation. This was accomplished by comparing these data with flood plain (bank-material) data representing the upper five feet of the sequence (Table 50). Average sampling depth of the two subsets is 1.6 feet. for the "new" soils (35 samples) and 3.1 feet for the "old" soils (12 samples).

In general, the soils formed in recent alluvium on low terraces at or near the water level have a higher average percentage of total sand (35.4%; std. error S_e = 4.6) than the more stable alluvial terraces (20.8%; S_e = 8.4), which lie above the present flood plain (Tables 29 and 49). If all of the bank samples are considered, the average percentage of sand is 9% (S_e = 2.4). Differences are even more striking if the median values are considered. Median sand content for the "new" soils is 27.4% compared to 5% for the upper 5 feet of the "old" soils. The marked difference between these materials is also portrayed in the average sand to clay ratios; 2.4 (S_e = 0.7) for the "new" soils and 0.38 (S_e = 0.25) for the "old" soils. The sand fraction of the "new" soils is dominated by very fine and fine sand in the 0.05 to 0.25-mm range. These soils are particularly susceptible to freeze-thaw processes, making them even more erodible than the "older" soils due to their low shear strength due to a lack of cohesive properties.

Table 49-- Summary of particle-size distributions of "new" soils materials.

River Mile	Date	Sample ID	Depth In Feet	% In Size Class			SP/CL
				Sand	Silt	Clay	
1627.5	1998	98MT083-001	0.25	51	39	10	5.07
1627.5	1998	98MT083-001	0.42	16	52	32	0.49
1627.5	1998	98MT083-001	0.58	16	54	30	0.52
1627.5	1998	98MT083-001	0.75	27	57	16	1.70
1627.5	1998	98MT083-001	2.50	14	57	29	0.47
1627.5	1998	98MT083-001	4.00	86	10	4	22.74
1627.5	1998	98MT083-002	0.17	45	46	10	4.55
1627.5	1998	98MT083-002	0.92	13	52	36	0.35
1627.5	1998	98MT083-002	1.83	27	55	18	1.56
1627.5	1998	98MT083-002	3.50	94	6	0	-
1623.5	1998	98MT083-003	0.5	14	47	39	0.35
1623.5	1998	98MT083-003	1.0	9	59	32	0.27
1623.5	1998	98MT083-003	1.2	83	6	11	7.83
1623.5	1998	98MT083-003	2.5	42	42	17	2.52
1637.3	1998	98MT055-001	0.5	7	44	50	0.13
1637.3	1998	98MT055-001	1.3	11	48	41	0.26
1637.3	1998	98MT055-001	2.3	65	24	11	6.17
1637.3	1998	98MT055-001	2.7	39	43	18	2.24
1637.3	1998	98MT055-001	4.0	94	6	0	-
1687.3	1998	98MT055-002	0.7	14	36	50	0.29
1687.3	1998	98MT055-002	3.0	94	6	0	-
1631 Vournas	1998	98MT661-001	0.3	24	43	33	0.73
1631 Vournas	1998	98MT661-001	0.4	49	39	12	4.00
1631 Vournas	1998	98MT661-001	1.7	7	60	33	0.23
1631 Vournas	1998	98MT661-001	3.2	27	53	19	1.43
1631 Vournas	1998	98MT661-001	4.0	12	56	32	0.37
1631.4 Vournas 4	1996	96MT083-004	0.5	46	34	21	2.22
1631.4 Vournas 4	1996	96MT083-004	1.0	49	36	16	3.08
1631.4 Vournas 4	1996	96MT083-004	2.0	42	41	18	2.34
1631.2 Vournas 4B	1996	96MT083-004B	0.5	38	37	25	1.49
1631.2 Vournas 4B	1996	96MT083-004B	1.5	7	40	53	0.14
1631.2 Vournas 4B	1996	96MT083-004B	2.0	11	57	32	0.35
1631.2 Vournas 4C	1996	96MT083-004C	0.3	12	47	42	0.28
1631.2 Vournas 4C	1996	96MT083-004C	0.8	47	36	17	2.74
1631.2 Vournas 4C	1996	96MT083-004C	2.0	9	37	54	0.16

Table 50-- Comparison between “new” soils and upper 5 feet of “old” soils.

		Average Values					
Material	**Samples**	**Depth** (feet)	**Gravel** %	**Sand** %	**Silt** %	**Clay** %	**SP/CL**[1]
“New” Soil	35	1.6	-	35.4	40.1	24.5	2.4
“Old” Soil	12	3.1	2.5	20.8	49.3	27.6	0.38

[1] Sand to clay ratio

RECOMMENDATIONS FOR FUTURE INFORMATION NEEDS

In this report, analysis of field data collected in 1996 and 1997 and the historical data on flow, channel morphology, sediment characteristics, bank stability and ice effects have addressed a number of issues critical to the lower Missouri River Coordinated Resource Management group. Although a large amount of data on the river itself has been collected historically by the U.S. Army Corps of Engineers and on surficial soils by the ongoing soil survey program of the NRCS, results of this study have identified a genuine void in the information regarding bank erosion. To reduce the uncertainty of some of the quantitative analyses and to encourage improved predictability of erosion effects, rates, damage to pump sites and erosion mitigation, the collection of more detailed information on specific processes is recommended.

Regarding changes in channel morphology, two of the principle concerns of the CRM group are the loss of agricultural land and irrigation systems from bank instabilities and the silting-in of pump sites due to channel shifting. Additional information needs, therefore, can separated into those that address bank-stability issues and those that affect hydraulic and sediment-transport changes in the river.

Bank Instability and Pore-Water Pressures

This study has shown clearly the overwhelming effect of both positive and negative pore-water pressures in determining the strength and stability of streambanks. Negative pore-water pressures occur above the water table and provide enhanced strength to streambanks through suction. Preliminary findings suggest that the negative pore-water pressures (matric suction) that occur in the unsaturated zone of streambanks along the Missouri River can cause increases in apparent cohesion ranging from 0% of effective cohesion for low-plasticity clays (CL) near saturation, to more than 100% for relatively dry silty sand (SM) or clayey sand (SC). Thus, a loss of matric suction causes a loss of bank strength and can potentially result in bank failure. In this report, matric suction was evaluated for each site with limited data from two weeks of field work in 1997 and by assuming a given distribution above the water table.

Positive pore-water pressures occur below the water table and create weaker banks by reducing the frictional strength of the bank material. The magnitude of these forces varies through time and for different soils. Data collected at selected sites during this study were not adequate to account for variations in this important parameter, particularly during critical periods such as high, steady flows. Additionally, the effects of bank freezing and subsequent thawing on pore-water pressures is not known. It is during these periods of high-sustained flow and frozen banks that monitoring of pore-water pressures are the most critical, since it is at these times and immediately following them when bank failures generally occur. Mitigation strategies can also be monitored and tested by the monitoring of pore-water pressures.

The effects of bank vegetation on pore-pressure distributions are also poorly understood. Data collected during this study are able to address conventional bank-stability factors for static conditions without the effects of vegetation. To account for dynamic moisture effects and the effects of vegetation, pore-water pressures need to be monitored over a range of conditions.

Pore-water pressures in streambanks are influenced by many factors related to moisture content and water level. Irrigation and water usage by crops affects pore-water pressures. High river stages cause water to seep into the bank, particularly if dam releases are maintained at high levels for an extended period of time. Rapid drawdown of the river tends to cause excess pore-water pressures in the bank because the confining pressure afforded by the river stage has been removed. This results in greatly weakened bank material. At times, the releases from Fort Peck Dam can vary up to 50% from one day to the next, depending on the need for downstream water use and during peak energy demands. These rapid changes in releases from Fort Peck Dam can, therefore, affect the downstream river elevations.

The woody and herbaceous vegetation growing on streambanks affects the stability of streambanks by altering the hydrologic and mechanical characteristics of the bank material. Roots provide reinforcement but also provide conduits for more rapid movement of water into the bank. In some cases, bank vegetation may prove beneficial to bank stability by removing water from the bank through evapotranspiration. In other cases, however, bank vegetation may decrease the stability of the bank by causing greater moisture contents and lower suction values.

The conditions under which vegetation is beneficial or unfavorable to bank stability must be determined to properly plan and design erosion control measures. These data have not yet been obtained and the magnitude and variability of pore-water pressures have not been determined. Data collected over a range of moisture conditions, river elevations, and weather cycles are necessary to help determine the patterns and effects of vegetation and pore-water pressure. These data will provide far greater certainty in determining the specific causes of bank instability and can be used to maintain stable banks during the year along this stretch of the Missouri River.

To accomplish these goals, it is recommended that a number of streambank sections be instrumented at various depths with pressure-transducer tensiometers to gather data on the pore-water pressures. These data will be combined with data on lateral and vertical depths of freezing, as well as rainfall and river-stage data collected simultaneously and stored on a data logger at each of the sites. The effects of bank vegetation will be evaluated by physically testing root strengths and by mapping root areas in the same reach as the tensiometer network. Additional tensiometers will be installed in and around the root zones of specific species to determine pore-water conditions around bank vegetation.

The benefit of acquiring these additional data centers on the application of pore-water pressure data for:

1) Determining the magnitude and frequency of near-bank groundwater levels;
2) Determining the magnitude and duration of flows which cause elevated groundwater levels;
3) Assessing bank shear strength during critical periods of high-sustained flow;
4) Determining the effects of freezing and thawing on pore-water pressures and shear strength;
5) Determining the effects of bank vegetation on root reinforcement and bank drainage;
6) Determining the magnitude and frequency of flows needed to reduce the generation of positive pore-water pressures and the loss of matric suction; and

7) Evaluating reduction of land loss and mitigation of erosion problems through innovative bank-stabilization techniques.

Information Needs on Ice Effects

As is evident throughout the section on ice effects, at present, it is only possible to hypothesize how ice may influence rates of bank erosion and channel change. For example, no evidence exists that ice hastens or slows large-scale changes, such as the migration of a series of meander loops. Such evidence is hard to obtain, since ice is one of several factors influencing the dynamic balance between flow, slope and sediment in an alluvial channel. Changes in channel geometry (e.g., width, statistical properties of meander wavelengths and radii) may occur in response to diverse changes in flow rate and sediment supply. Some evidence exists that ice may influence mid-scale features of alluvial channels. For example, ice jams may lead to meander-loop cutoffs. However, at this scale, ice effects are still subject to considerable hypothesis. At the local (or site) scale it is possible to identify several mechanisms whereby ice may hasten bank erosion and channel shifting. Two such mechanisms, for example, are flow concentration beneath an ice cover and bank/bed gouging by an ice run. Yet, questions remain as to whether these mechanisms prevail over other processes and conditions and as to exactly how they work.

To develop appropriate mitigation measures, significantly improved understanding of the ice-related erosion processes and the extent to which they occur in the lower Missouri River are needed. That understanding would not only help to address erosion concerns along the river's Montana reach, but it would also help to address similar concerns along other reaches of the river and for flow-regulated rivers in cold regions generally.

The information needs essentially fall into two categories: the effects of ice on changes in bank and channel conditions at selected sites and the overall effects of ice on the river's morphology. The first category is considered herein. It relates to specific, immediate concerns that have to be addressed; i.e. locally severe bank erosion, sedimentation difficulties with pump operation, possible flooding and meander-loop cutoff attributable to ice jams. The second category, though relevant and intriguing, is still in the realm of fluvial philosophy. It requires extensive data from other cold-regions rivers besides the lower Missouri River; i.e. the data should encompass wide ranges of the parameters characterizing channel geometry, bank conditions, flow magnitudes, and ice conditions.

The following tasks are required to obtain the information needed to establish whether indeed ice has significant adverse effects on bank and channel conditions at specific sites along the lower Missouri River, and to determine how those effects might be mitigated:

1. Prepare an overall description of ice formation, presence and breakup along the lower Missouri River;
2. Monitor changes in bank and channel conditions at selected sites over one or more winter cycles, to assess whether ice significantly affects those conditions;

3. By means of modeling, confirm ice effects found from field monitoring (Task 2) to have substantial adverse consequences for bank and channel conditions at the selected sites; and,
4. In conjunction with Task 3, establish practical methods for mitigating the adverse effects of ice.

Task 1 is needed to provide the overview context of ice formation, duration of presence and breakup along the river. Task 2 comprises a set of diagnostic investigations focused on specific ice-related concerns at selected sites. Together, Tasks 1 and 2 comprise a second phase (Phase II) of work aimed at extending the preliminary evaluation presented in this report.

Tasks 3 and 4 comprise a third phase of work (Phase III) to be considered in the future, if work under Phase II shows that ice has significant adverse effects for bank and channel conditions at the selected sites. If the decision is made to mitigate the effects, Phase III would be tailored to the selected sites and would evolve once more becomes known about each site.

Task 1: Monitoring Ice on the Lower Missouri River

Table 51 lists the information needed to develop a composite description of ice and its effects on the lower Missouri River. The information sought comprises data and observations that will enable features of ice cover formation, presence and breakup to be related to flow and weather conditions and to channel morphology. The composite description would meet educational and diagnostic needs.

The resulting description would document and substantially extend the scant information that exists on ice on the river, which exists mainly in oral, anecdotal format. The description would help people living and working along the river to better understand ice processes along it. Not to be under-valued are the safety-related benefits that the description would produce by promoting informed use of the river.

The description would also be of use to the Corps of Engineers, who operate Fort Peck Dam and have responsibilities for channel stability by providing specific information about how the river responds to regulation of winter flows. That knowledge is needed as the Corps considers enhancements to the Current Water Control Plan (CWCP) for the river. The preferred alternative to the CWCP apparently may entail increasing flow releases from Fort Peck Dam during winter (Pokrefke, *et al*. 1998). Ice seems not to have figured prominently in determining that alternative plan.

The set of diagnostic investigations of specific ice concerns at the selected monitoring sites (Task 2), requires an overall description of the ice conditions prevailing on the river. Some of the local processes to be investigated cannot be considered in isolation of the ice and flow conditions occurring on a larger scale on the river. For example, flow level, hydrograph attenuation, extent of ice-cover formation, ice-cover characteristics and ice-run effects all have a bearing on local bank and channel conditions.

Conducting Task 1 entails collection and synthesis of data and observations. The activities associated with it are not onerous. Some of the data would already be known and documented; e.g. rates and temperatures of water released from Fort Peck Dam and water levels at the Wolf Point and Culbertson gauges. Other data and observations can

Table 51--Information to be obtained from Task 1: ice on the lower Missouri River.

Ice Process	Information	Comments
A description of ice-cover formation during a typical year.	• Times and locations where ice cover first forms • Notes on how cover progresses upstream • Ice-cover thickness variation once cover formed • Record of flow rate and temperature at Fort Peck Dam • Record of air temperature and wind speed at one or two sites (e.g., Wolf Point, Culbertson)	The information here will help to develop an overall understanding of how ice forms on the river. It will help relate channel and bank condition to ice-cover formation
Ice cover effects on flow stage	• Stage-discharge record at Wolf Point and Culbertson gauges	This information will help assess the flow resistance attributable to the ice cover and the cover's affect on sediment-transport rates
Ice-cover breakup	• Notes (with photos and sketches) of where and how the ice cover starts to breakup. See Tables 52 and 53 for further information needs related to erosion mechanisms • Record of flow • Record of air temperature and wind speed	This information is needed to develop an overall understanding of the ice cycle for the river. It will help in assessing the severity of border-ice rotation and ice abrasion.
Breakup ice-jam formation	• Notes (with photos and sketches) of where and how a breakup jam forms. • Flow rate and elevation	This information is needed to understand how ice moves through the river. It also is needed for assessing jam mitigative methods.

be readily obtained by means of observation; e.g. locations where the ice cover begins forming, the manner in which it progresses upstream and the manner in which it breaks up. Certain data may require the use of simple temporary instrumentation; e.g. a temporary water-level post at a few selected sites along the river, augers for getting ice-thickness. The main effort associated with this task is coordination of data collection and the synthesis of these data into useful information.

One means whereby ice may adversely affect bank erosion and channel morphology is by damaging riparian vegetation, which usually helps to stabilize banks and channels. Elevated freeze-up and ice runs can be particularly damaging in this regard since they retard vegetation growth. It would be of interest, while developing a description of the ice cycle on the lower Missouri River, to determine whether riparian vegetation along the river is less developed than along reaches of unregulated rivers in the upper tier states of the US. Additionally, it would be of interest to compare reaches along the lower Missouri River to assess whether poorly developed riparian vegetation reflects severe ice effects. This information would form an interesting adjunct to the description of ice on the river and to the diagnostic investigations conducted as Task 2.

Task 2: Monitoring Selected Sites

This task entails a set of activities aimed expressly at determining if and how the ice-related erosion mechanisms discussed above affect bank and channel conditions at sites of immediate concern along the lower Missouri River. Each site would be monitored to address the following questions:

1. What evidence exists that the ice-related erosion mechanisms are active at the site?
2. How do the erosion mechanisms appear to affect the site?
3. If indeed the mechanisms appear significant, what structural or bathymetric methods would mitigate them?
4. What operational methods would mitigate them?
5. What further study would be needed to confirm the mechanisms and establish the methods identified to mitigate them?

Table 52 lists the erosion mechanisms associated with river ice and indicates selected sites for which there exists tentative evidence that the ice may adversely affect bank and channel conditions. It also summarizes the information needed to evaluate the erosion mechanisms. Table 53 does the same for freeze-thaw effects on bank erodibility.

It would be moderately expensive to conduct a detailed investigation of all the sites indicated in Tables 52 and 53. Therefore, an issue to be resolved is the number of sites to be monitored and the level of monitoring to be conducted. One way to resolve the issue is to select sites where bank- and channel-change concerns are most acute and where ice is perceived as a factor exacerbating them. The main concerns are bank erosion, pump-site sedimentation and meander-loop cutoff by ice jams. Impaired riparian vegetation and river habitat might also be mentioned as additional concerns. The investigative activities of Task 2 should indirectly illuminate some of the effects that ice has on the condition of riparian vegetation.

Table 52--Information sought from Task 2: river-ice erosion processes.

Ice-Related Erosion Mechanism	Information	Comments
1. Elevated Freeze-Up	• Bank Condition - location - soils - vegetation • River-Level Record - level before, during, and after freeze up • Water-Table Record - level before, after, and during freeze-up • Location of Border Ice - elevation - width of border ice - thickness of border ice • Bank Freezing - extent of frozen ground at border-ice root • Border-Ice Collapse Process - size of border ice pieces - failure process - disturbance of bank soil	Select one or two sites; e.g., - River Mile 1716 Pipal perhaps - River Mile 1632 Vournas - River Mile 1625 Tveit-Johnson This process should be monitored in conjunction with bank-freezing, whose details are indicated in Table 53. Instrumentation needs are minor; water-level gauge, simple tools for determining extents of ice. Observations of bank condition at border-ice root are important.
2. Flow distribution	• Bathymetry - openwater before winter (Early November) - ice-covered late in winter (Mid-March) - openwater mid spring and summer (late April and July) • Flow Rates - daily variation • Ice-Cover - thickness distribution • Flow Distribution - flow distribution for openwater	Select one or two sites; e.g., - River Mile 1646 Mattelin perhaps - River Mile 1620 Culbertson water intake This process should be monitored in conjunction with bank-freezing, whose details are indicated in Table 4. Instrumentation needs are for flow-depth measurement, ice-thickness measurement. Flow velocities would be nice, but are not critical.

	- flow distribution for ice cover	
2. Local Scour	• Photo series during ice-cover front progression upstream along a reach with a severely eroded bank • Flow Record	Select one or two sites for monitoring; e.g., - River Mile 1624 Tveit-Johnson perhaps - River Mile 1632 Vournas
3. Ice gouging and abrasion during Ice Run	• Date of ice run • Photo series of ice run, when it occurs • Flow Record • Ice Thickness	This mechanism may be difficult to observe due to the abrupt nature of ice runs. However, the effects of an ice run, if one occurs, should be observable.
4. Ice Jam	• Date • Bathymetry of jam location • Photos of ice movement through reach. If possible, photos of ice-jam development • Flow Record • Flow stages at site	River Mile 1632 Vournas site seems to be a recurring location. Only observations needed. Flow record is available from Dam. Flow stages obtainable from observations relative to fixtures at jam site.

Table 53--Information sought from Task 2: freeze-thaw erosion processes.

Process	Information	Comments
1. Freeze-Thaw Weakening	• Bank soils • Bank position • Water table record • Pore-pressure record • Vegetation features • Changes in soil structure during ice cycle • Rate of soil loss	Select one or two sites for monitoring; e.g., - River Mile1625 Tveit-Johnson perhaps - River Mile 1716 Pipal - River Mile 1632 Vournas
2. Ice Wedging	• All of the above • Presence of cracks along top of bank	Sites as above

The Tveit-Johnson, Vournas and Pipal sites are representative of bank erosion along this reach. Pump sedimentation problems reportedly occur at the Mattelin Farm and at the Culbertson water intake. A jam occurs on occasional years at the Vournas Farm. These five locations could form a set of monitoring sites. Three of the sites could be selected for close monitoring; i.e. the Pipal, Mattelin, and Tveit-Johnson sites. These three sites appear most prone to the adverse effects of elevated freeze-up, thalweg shifting and freeze-thaw weakening of bank soil. The Vournas and Culbertson water intake sites could be designated for observational monitoring only. Perhaps the Culbertson Water Intake site could be an alternative to the Mattelin Farm site if CRM considers it of greater concern. The unique feature of the Vournas site is occasional ice jamming accompanied by flooding. However, a formal jam-monitoring program is not suggested here, because of the relative infrequency with which they occur. Only observations and photographs are needed at this phase.

Tables 52 and 53 indicate the instrumentation requirements for Task 2. Instrumentation and equipment for obtaining channel cross sections, ice augering and flow-velocity measurements are needed to monitor flow distribution. The extent of bank-soil freezing could be determined by means of an auger and hand-tools; temperature sensors need not be used.

The information obtained from the monitoring should be documented in a single technical report, which would provide a substantiated assessment of ice effects on bank and channel conditions along the lower Missouri River. The insights obtained should be generalized, to the extent possible, for the river as a whole.

Tasks 3 and 4: Modeling of Processes and Sites

It is premature to elaborate on these tasks in detail at this time. However, it is appropriate to point out that modeling may be needed to determine and quantify some key processes concerning ice effects on bank erosion and channel morphology. In particular, modeling may be necessary to confirm and further investigate significant ice-related mechanisms incompletely observed at the monitoring sites, and to identify ways to mitigate the adverse effects of those mechanisms.

Modeling may also be used to develop and confirm an effective mitigation method for bank and channel stabilization at critical sites. The complex, three-dimensional flow features and sediment-movement patterns at the site, as well as the effect of the prospective mitigation method, may not be determined by any other means.

Modeling could entail the use of hydraulic models of the ice-related processes or of the monitoring sites. It could be conducted in a typical hydraulics laboratory or in a low-temperature-flow laboratory, in accordance with the process under investigation. In most instances, the cost of modeling is more than recovered by reductions in land loss and by the improved efficiency of the mitigation method developed.

ACKNOWLEDGMENTS

The authors would like to express their sincere gratitude to the members of the Lower Missouri River Coordinated Resources Management Group, particularly Boone Whitmer and Buzz Mattelin for helping to bring together the people and to address concerns about channel erosion downstream from Fort Peck Dam. We thank Jerry Bernard, NRCS, Washington, D.C., James Suit, NRCS, Bozeman, MT and Carlos Alonso, ARS, National Sedimentation Laboratory (NSL), Oxford, MS for providing the necessary funding and overall interagency coordination to conduct this study.

The efforts of Dick Iverson and his staff, particularly Rhonda Knudsen, NRCS, Culbertson, MT, for assisting in the field and for making arrangements that resulted in some of the most efficient fieldwork we have ever known. Those of us from the ARS, Oxford, MS who were involved in the 1996 and 1997 fieldwork owe an enormous debt of gratitude to Marie Marshall Garsjo, Mark Yerger, and George (Tony Montana) Rolfes for their professional and efficient drilling and logging of test holes. Without their capable assistance, we would still be on the banks of the Missouri, hand augering boreholes.

The field assistance provided by technical staff from the National Sedimentation Laboratory, including Steve Darby, Mark Griffith, and Keith Parker, and from the University of Nottingham, UK, including John Bromley and Anna Wood is greatly appreciated.

Data was provided to us from staff of the Montana NRCS, from John Remus, U.S. Corps of Engineers, Omaha District and staff from the U.S. Geological Survey, Montana District. Cathy Maynard, NRCS Helena, MT produced the GIS-based color maps. Lance Yarbrough, ARS/NSL, Oxford, MS produced the bank profiles and the cover page. A special thanks goes to Brian Bell, ARS/NSL, Oxford, MS for unyielding patience and dedication to getting this report “out the door.” F. Douglas Shields would like to thank P. D. Mitchell, Martin Doyle and Charles Butts for assistance with analysis of maps and photographs and associated computations. Jennifer Kulick assisted with manuscript preparation.

There are numerous other people that helped us in the field in eastern Montana and became friends to us during the weeks we spent along the river. There are also probably additional names that have been inadvertently left off this list. To you we apologize. This study could not have been successfully completed without all of your help.

REFERENCES

Ambrose, S.E., 1996, *Undaunted Courage*, Simon and Schuster, 521 p.

Andersland, O.B. and Anderson, D.M., 1990, *Geotechnical Engineering for Cold Regions*, McGraw Hill, NY.

Beatty, D. A. 1984. Channel migration and incision of the Beatton River. *Journal of Hydraulic Engineering* 110(11): 1681-1684.

Beeson, C.E. and Doyle, P.F., 1995, Comparison of bank erosion at vegetated and non-vegetated channel bends. *Water Resources Bulletin* 31(6): 983-990.

Beltaos, S., 1981, Field Investigations of a Hanging Ice Dam, Ice Symposium, Quebec City, Quebec, *International Association of Hydraulic Research*: II: 485-449.

Beltaos. S., 1995, *River Ice Jams*. Water Resources Publications, Highlands Ranch, CO.

Begin, Z. B. 1986. Curvature ratio and rate of river bend migration-update. *Journal of Hydraulic Engineering* 112(10): 904-908.

Bergantino, R. N., 1992, Groundwater in Quaternary deposits in the Wolf Point 1^{o} x 2^{o} Quadrangle, *Montana Bureau of Mines and Geology*, Montana Atlas 5-C.

Bergantino, R. N., Wilde, E. M., 1994, Geologic map of the Wolf Point 1^{o} x 2^{o} Quad, *Montana Bureau of Mines and Geology* Open-File Report 294.

Bernard, J. M., Shields, F. D., Jr., Munsey, T., and Steffen, L. 1997. The Missouri River below Fort Peck Dam, Montana: To Fix the River or To Fix the Banks? Wang, S.Y., Langendoen, E., and Shields, F. D. Jr. (eds.), *Management of Landscapes Disturbed by Channel Incision, Stabilization, Rehabilitation, and Restoration*, Center for Computational Hydroscience and Engineering, University of Mississippi, University, Mississippi. 781-787.

Biedenharn, D. S., Combs, P. G., Hill, G. J., Jr., Pinkard, C. F., and Pinkston, C. B. 1989. Relationship between channel migration and radius of curvature on the Red River. *In* Wang, S.Y. (ed.), *Sediment Transport Modeling: Proceedings of the International Symposium*, New York: American Society of Civil Engineers. 536-541.

Bird, J.B., 1974. Geomorphic processes in the Arctic. Chap. 12(A), *Arctic and Alpine Environments*, Ives, J.D. and Barry, R.G., (Eds), Methuen, London, 703-720.

Borland, W. M., 1959. Ice gorging and flooding on the Missouri River in the vicinity of Townsend, Montana." Internal Report, US Bureau of Reclamation, Denver, CO.

Bradley, C. and Smith, D. G. 1984. Meandering channel response to altered flow regime: Milk River, Alberta and Montana. *Water Resources Research* 20(12): 1913-1918.

Bravard, J. P., Amoros, C., Pautou, G., Bornette, G., Bournaud, M., Creuze des Chatelliers, M., Gibert, J., Peiry, J. L., Perrin, J. F., and Tachet, H. 1997. River incision in South-East France: Morphological phenomena and ecological effects. *Regulated Rivers: Research & Management*. 13:75-90.

Bravard, Jean-Paul, Amoros, Claude, and Pautou, Guy. 1986. Impact of Civil Engineering Works on the Successions of Communities in a Fluvial System. *OIKOS* 47(1):92-111.

Brice, J. C. 1982. *Stream channel stability assessment*. Rep. FHWA/RD-82/021, U.S. Department of Transportation Federal Highway Administration, Washington, D. C., 42pp.

Brice, J. C. 1984. Planform properties of meandering rivers. In Elliott, C. M. (ed.) *River Meandering, Proceedings of the Conference Rivers '83,* American Society of Civil Engineers, New York, 1-15.

Brooks, G.R., 1993. Characteristics of an ice-scoured river bank near Keele River confluence, Mackenzie Valley, Northwest Territories. *Current Research*, Part B: Geological Survey of Canada, Paper 93-1, 21-27.

Bull, W. B., 1979. Threshold of critical power in streams, *Geological Society of America Bulletin*, 90, 453-464.

Burrows, R.L. and Harrold, P.E., 1983. Sediment transport in the Tanana River near Fairbanks, Alaska, 1980-1981. *U.S. Geological Survey Water Resources Investigations Report* 83-4064.

Carson, M. A. 1986. Characteristics of high-energy meandering rivers: The Canterbury Plains, New Zealand. *Bulletin of the Geological Society of America* 97: 886-895.

Carson, M.A., and Kirkby, 1972, *Hillslope Form and Process*. Cambridge University Press, 475 p.

Casagli, N., 1994, Determinazione del fattore di sicurezza per scivolamenti planari nelle sponde fluviali. *Studi di Geologia Applicata e Geologia dell'Ambiente,* **N. 30**, Dipartimento Scienze della Terra, Universita degli Studi di Firenze.

Casagli, N., Curini, A., Gargini, A., and Rinaldi, M., in press, Monitoring of streambank instability processes *Earth Surface Processes and Landforms*.

Casagli, N., Curini, A., Gargini, A., Rinaldi, M., Simon, A., 1997, Effects of pore pressure on the stability of streambanks: Preliminary results from the Sieve River, Italy. In. S.S.Y. Wang, E.J. Langendoen, and F.D. Shields Jr., (eds.) *Management of Landscapes Disturbed by Channel Incision*, 243-248.

Chamberlain, E.J., 1981. Frost susceptibility of soil: review of index tests. Monograph 81-2, U.S. Army Corps of Engineers, Cold Regions Research and Engineering Laboratory, Hanover, NH.

Chang, H. H. 1988. *Fluvial Processes in River Engineering*. Krieger Publishing Company, Malabar, Flordia.

Cherry, D. S., Wilcock, P. R., and Wolman, M. G. 1996. *Evaluation of methods for forecasting planform change and bankline migration in flood-control channels*. U.S. Army Engineer Waterways Experiment Station, Vicksburg, MS.

Chitale, S. V. 1973. Theories and relationships of river channel patterns. *Journal of Hydrology* 19: 285-308.

Church, M. and Miles, M.J., 1982. Discussion of Chap. 9, Processes and mechanisms of bank erosion. In *Gravel-Bed Rivers*, Hey, R.D., Bathhurst, and Thorne, C.R. (Eds), Wiley and Sons, New York, 259-271.

Colby, B.R. and Scott, C.H., 1965. Effects of temperature on discharge of bed material. *U. S. Geological Survey Professional Paper* 462-G.

Collison, A.J.C., and Anderson, M.G., 1996, Using a combined slope hydrology/stability model to identify suitable conditions for landslide prevention by vegetation in the humid tropics. *Earth Surface Processes and Landforms*: 21: 737-747.

Collinson, J.D., 1971. Some effects of ice on a river bed. *Journal of Sedimentary Petrology*: 41 (2): 557-564.

Colton, R. B., Bateman, F. A., 1956, Geologic and structure contour map of the Fort Peck Indian Reservation and vicinity, Montana*: U. S. Geological Survey Miscellaneous Investigations Map* I-225.

Curini, A., 1998, *Analisi dei processi di erosione di sponda nei corsi d'acqua*, Universita degli Studi di Firenze, Dipartimento di Scienze della Terra, 147, unpublished thesis.

Daniels, R.B., 1960, Entrenchment of the Willow Drainage Ditch, Harrison County, Iowa: *American Journal of Science*: 258: 161-176.

Danilov, I.D., 1972. Ice as a factor of relief formation and sedimentation. Problemy Krioliltogii, 2: 137-143.

Darby, S.E., 1994, A physically-based numerical model of river channel widening: PhD thesis, University of Nottingham, UK, 276 p.

Darby, S. E., and Thorne, C. R. 1996. Bank stability analysis for the Upper Missouri River. Unpublished report submitted to US Army Engineers Waterways Experiment Station, Vicksburg, MS.

Derrick, D.L., Pokrefke. T.J, Boyd, M.B., Crutchfield, J.P., and Henderson, R.R., 1994. Design and development of bendway weirs for Dogtooth Bend Reach, Mississippi River. Technical Report HL-94-10, US Army Corps of Engineers Waterways Experiment Station, Vicksburg, MS.

Dionne, C.-J., 1974, "How Ice Shapes the St. Lawrence. *Canadian Geographical Journal*:88 (2): 4-9.

Donovan, J. J., 1988, Ground-water geology and high-yield aquifers of Northeastern Montana, *Montana Bureau of Mines and Geology Open-File Report* 209.

Doyle, P.F., 1988. Damage from a sudden river ice breakup. *Canadian Journal of Civil Engineering:* 15: 609-615.

Dupre, W.R. and Thompson, R., 1979. The Yukon Delta: a model for deltaic sedimentation in an ice-dominated environment. *11th Annual Offshore Technology Conference*, 657-664.

Eardley, A.J., 1938. Yukon channel shifting. Bulletin of the Geological Society of America: 49: 343-358.

Elliott, J.G., 1979, Evolution of large arroyos, the Rio Puerco of New Mexico. Colorado State University, Fort Collins, Colorado, Master of Science thesis, 106 p.

Emerson, J.W., 1971, Channelization: A case study: *Science*:172: 325-326.

Englehardt, B. and Waren, K. 1991. Upper Missouri River Bank Erosion. North Dakota State Water Commission, Bismarck, and *Montana Department of Natural Resources and Conservation*, Helena, 54p.

Ettema, R. and Braileanu, F., 1998. A method for calculating sediment transport rates in ice-covered channels. *Proc. IAHR Ice Symposium*, Potsdam, NY.

Ettema, R., Muste, M., and Kruger, A., (in press). Ice jams at river confluences. *CRREL Report* -, U.S. Army Corps of Engineers, Cold Regions Research and Engineering Laboratory, Hanover, NH.

Fischer, K. J. 1994. Fluvial geomorphology and flood control strategies: Sacramento River, California. *The Variability of Large Fluvial Rivers.* American Society of Civil Engineers Press, New York, 115-128.

Fisk, H. N. 1947. Fine-grained alluvial deposits and their effects on Mississippi River activity. *U. S. Army Engineer Waterways Experiment Station*, Vicksburg, Miss.

Fredlund, D.G., Morgenstern, N.R., and Widger, R.A., 1978, The shear strength of unsaturated soils. *Canadian Geotechnical Journal*:15: 313-321.

Fredlund, D.G., and Rahardjo, H., 1991, Use of linear and nonlinear shear strength versus matric suction relations in slope stability analyses. In Bell (ed.), *Landslides*, Balkema, Rotterdam, 531-537.

Fredlund, D.G., and Rahardjo, H., 1993, *Soil Mechanics of Unsaturated Soils*. John Wiley & Sons, Inc., New York, 517.

Garcia, M. H., Bittner, L., and Nino, Y. 1994. Mathematical modeling of meandering streams in Illinois: A tool for stream management and engineering. Urbana, Illinois: University of Illinois.

Gatto, L. W., 1988, "Techniques for Measuring Reservoir Bank Erosion," Special Report 88-3, *U.S. Army Cold Regions Research and Engineering Laboratory*, Hanover, NH.

Gatto, L. W., 1995, "Soil Freeze-Thaw Effects on Bank Erodibility and Stability," Special Report 95-24, *U.S. Army Cold Regions Research and Engineering Laboratory*, Hanover, NH.

Geo-Slope, 1995, User's Guide, SLOPE/W for slope stability analysis, Version 3. GEO-SLOPE International Ltd., Calgary, Alberta, Canada.

Graf, W.L., 1977, The rate law in fluvial geomorphology*: American Journal of Science*:277: 178-191.

Hamelin, L.-E., 1979. The bechevnik: a river bank feature from Siberia. *The Musk Ox*: 25: 70-72.

Handy, R.L., and Fox, J.S., 1967, A soil borehole direct-shear device, *Highway Research News*: 27: 42-51.

Harlan, R.L. and Nixon, J.F., 1978. Ground thermal regime. Section 3 *in Geotechnical Engineering for Cold Regions*, Ed. Andersland, O.B. and Anderson, D.M., McGraw Hill, NY.

Hasegawa, K. 1989. Universal bank erosion coefficient for meandering rivers. *Journal of Hydraulic Engineering* 115(6): 744-765.

Hickin, E. J. and Nanson, G. C. 1975. The character of channel migration on the Beatton River, Northeast British Columbia, Canada. *Geol. Soc. Am. Bull*. 86: 487-494.

Hickin, E. J. and Nanson, G. C. 1984. Lateral migration rates of river bends. *Journal of Hydraulic Engineering* 110(11): 1557-1565.

Hirsch, R. M., Walker, J. F., Day, J.C., and Kallio, R. 1990. The influence of man on hydrologic systems. Wolman, M. G. and Riggs, H. C. (eds.), *Surface Water Hydrology*. Boulder, CO: Geological Society of America. V. 0-1, 329-359.

Hong, R.-J., Karim, F., and Kennedy, J.F., 1984. Low-temperature effects on flow in sand-bed streams. *ASCE Journal of Hydraulic Engineering*:110 (2): 109-125.

Hooke, J. M. 1980. Magnitude and distribution of rates of river bank erosion. *Earth Surface Processes* 5: 143-157.

Hooke, J. M. 1984. Changes in river meanders: A review of techniques and results of analyses. *Progress in Physical Geography,* London, England: Edward Arnold, 473-508.

Hooke, J. M. 1987. Changes in meander morphology. Gardiner, V. (ed.), *International Geomorphology, Part I*, John Wiley and Sons, Ltd., Chichester, 591-609.

Hooke, J. M. 1995. Processes of channel planform change on meandering channels in the UK. Gurnell, A. and Petts, G. (eds.), *Changing River Channels*. 87-115.

Hooke, J. M. and Redmond C. E. 1992. Causes and nature of river planform change. Billi, P., Hey, R., Thorne, C., and Tacconi, P. (eds.), *Dynamics of Gravel-Bed Rivers*. 558-571.

Howard, A. D. 1992. Modeling channel migration and flood plain sedimentation in meandering streams. Carling, P. and Petts, G. (eds.), *Lowland Flood plain Rivers: Geomorphological Perspectives*, John Wiley and Sons, Ltd., Chichester, 1-41.

Ikeda, S., Parker, G., and Sawai, K. 1981. Bend theory of river meanders, 1, Linear development. *Journal of Fluid Mechanics* 112: 363-377.

Interagency Task Force. 1998. *Stream Corridor Restoration: Principles, Processes, and Practices*. Federal Interagency Stream Restoration Working Group (ISBN-0934213-59-3), Washington, D. C.

Ireland, H.A., Sharpe, C.F.S., and Eargle, D.H., 1939, Principles of gully erosion in the Piedmont of South Carolina: *U.S. Department of Agriculture Technical Bulletin* 633, 142 p.

Jacobson, R.B., 1995, Spatial controls on patterns of land-use induced stream disturbance at the drainage-basin scale--An example from gravel-bed streams of the Ozark Plateaus, Missouri. in Costa, J.E., Miller, A.J., Potter, K.W., and Wilcock, P.R., (eds.), *Natural and Anthropogenic Influences in Fluvial Geomorphology*: American Geophysical Union, Geophysical Monograph 89, 219-239.

Jensen, F. and Varnes, Helen, 1964, Geology of the Fort Peck Area, Garfield, McCone, and Valley Counties, Montana: *U. S. Geological Survey Professional Paper* 414-F, 48 p.

Jiongxin, X. 1997. Evolution of mid-channel bars in a braided river and complex response to reservoir construction: An example from the middle Hanjiang River, China. *Earth Surface Processes and Landforms* 22: 953-965.

Johannesson, H. and Parker, G. 1985. Computer simulated migration of meandering rivers in Minnesota. Project Report No.242, St. Anthony Falls Hydraulic Laboratory, University of Minnesota.

Johnson, W. C. 1992. Dams and riparian forests: Case study from the upper Missouri River. *Rivers* 3(4): 229-242.

Johnson, W. Carter; Burgess, Robert L., and Keammerer, Warren R. 1976. Forest Overstory Vegetation and Environment on the Missouri River Flood plain in North Dakota. *Ecological Monographs* 46(1):59-84.

Keller, E.A., 1972, Development of alluvial stream channels: A five-stage model: *Geological Society of America Bulletin*,83: 1531-1536.

Kellerhals, R. and Church, M, 1980. Comment on "Effects of channel enlargement by river ice processes on bankfull discharge in Alberta, Canada," by Smith, D,G. in *Water Resources Research*: 16 (6), 1131-1134.

Kindle. E.M., 1918. Notes of sedimentation in the Mackenzie River Basin. *Journal of Geology*: 26, 341-360.

King, W.A. and Martini, I.P., 1984. Morphology and recent sedimentations of the anastomizing reaches of the Attawapiskat River, James Bay, Ontario, Canada. *Sedimentary Geology*: 37 (4): 295-320.

Koutaniemi, L., 1984. The role of frost, snow cover, ice breakup and flooding in the fluvial processes of the Oulanka River, NE Finland. *Fennia*: 162 (2): 127-161.

Langbein, W. B. and Leopold, L. B. 1966. River Meanders—Theory of minimum variance. *U. S. Geological Survey Professional Paper* 422-H, 15 p.

LaGrone, D.L. and Remus, J.L., 1998. Nontraditional erosion control projects constructed on the Missouri River. *Proc. ASCE Conference Water Resources Engineering*, Memphis, TN, 399-404.

Lane, E.W., 1955, Design of stable alluvial channels, *Transactions, American Society of Civil Engineers*, 120:, paper no. 2776, 1234-1260.

Lau, Y.L. and Krishnappan, B.G., 1985. Sediment transport under ice cover. *ASCE Journal of Hydraulics Division*: 111 (6): 934-950.

Lawson, D.E., 1983. Erosion of perenially frozen streambanks. CRREL Report 83-29, U.S. Army Corps of Engineers, Cold Regions Research and Engineering Laboratory, Hanover, NH.

Lawson, D. E., 1985, "Erosion of Northern Reservoir Shores: Analysis and Application of Pertinent Literature," Monograph 85-1, *U.S. Army Cold Regions Research and Engineering Laboratory*, Hanover, NH.

Lawson, D.E, Chacho, E.F., Brockett, B.E., Wuebben, J.L., Collins, C.M., Arcone, S.A., and Delaney, A.J. (1986). Morphology, Hydraulics and Sediment Transport of an Ice-Covered River: Field Techniques and Initial Data. Report 86-11, *U.S. Army Corps of Engineers, Cold Regions Research and Engineering Laboratory*, Hanover, New Hampshire

Leopold, L. B. and Wolman, M. G. 1957. River channel patterns—braided, meandering, and straight. *U. S. Geological Survey Professional Paper* 422-H, 84 p.

Ligon, F., Dietrich, W. E. and Trush, W. J. 1995. Downstream ecological effects of dams: A geomorphic perspective. *BioScience* 45(3): 183-192.

Luttenegger, J. A. and Hallberg, B. R. 1981. 'Borehole shear test in geotechnical investigations', *American Society of Testing Materials*, Special Publication 740, 566-578.

Lutton, R.J., 1974, Use of loess soil for modeling rock mechanics: *U.S. Army Corps of Engineers Waterways Experiment Station Reports* S-74-28, Vicksburg.

MacDonald, T. E., Parker, G., and Leuthe, D. P. 1991. Inventory and analysis of stream meander problems in Minnesota. Minneapolis, MN: St. Anthony Falls Laboratory. 37 p.

MacDonald, T. and Parker, G. 1994. *User's Manual for Computer Program "MEANDER": External Memorandum No. M-240*. St. Paul, MN: University of Minnesota St. Anthony Falls Laboratory.

Mackay, D. K., Sherstone, D.A., and Arnold, K.C., 1974, "Channel Ice Effects and Surface Water Velocities From Aerial Photography of MaKenzie River Break-up," in *Hydrological Aspects of Northern Pipeline Development*, Report No. 74-12. Task Force on Northern Oil Development, Environmental-Social Program, Northern Pipelines, Saskatoon, Saskatchewan.

Mackay, J.R. and Mackay, D.K., 1977. The stability of ice-push features, Mackenzie River, Canada. *Canadian Journal of Earth Sciences*: 14 (10): 2213-2225.

Marston, R. A., Girel, J., Pautou, G., Piegay, H., Bravard, J. P., and Arneson, C. 1995. Channel metamorphosis, flood plain disturbance, and vegetation development: Ain River, France. *Geomorphology* 13(1995):121-131.

Martinson, C., 1980. Sediment displacement in the Ottauquechee River - 1975-1978. *CRREL Special Report* 80-20, U.S. Army Corps of Engineers, Cold Regions Research and Engineering Laboratory, Hanover, NH.

Marusenko, Ya. I., 1956. The action of ice on river banks. *Priroda*: 45 (12): 91-93.

McGregor, K. C., Cooper, C. M., and Cullum, R. F. 1996. Sedimentation of reservoirs - Case histories on large United States rivers. Molinas, A., Hotchkiss, R., and Albertson, M. L. (eds.), *Proceedings of the International Conference on Reservoir Sedimentation*, Mississippi State, MS. 1277-1291.

McKenzie, I.L.S. and Walker, H.J., 1974. Morphology of an Arctic River Bar. *Technical Report No. 172, Coastal Studies Institute*, Center for Wetland Resources, Louisiana State University, Baton Rouge, LA.

Mercer, A.G. and Cooper, R.H., 1977. River bed scour related to the growth of a major ice jam. *Proc. of the 3rd National Hydrotechnical Conference*, University of Laval, Quebec, 291-308.

Michel, B., 1978. *Ice Mechanics*. University of Laval Press, Laval, Quebec, Canada.

Milburn, D. and Prowse, T.D., 1998. The role of an ice cover on sediment transport and deposition in a northern delta. *Proc. IAHR Ice Symposium*, Potsdam, NY.

Mosselman, E. 1995. A review of mathematical models of river planform changes. *Earth Surface Processes and Landforms* 20: 661-670.

Nanson, G. C. and Hickin, E. J. 1983. Channel migration and incision on the Beatton River. *Journal of Hydraulic Engineering* 109(3): 327-337.

Nanson, G. C. and Hickin, E. J. 1986. Statistical analysis of bank erosion and channel migration in Western Canada. *Geological Society of America Bulletin*, 97(4): 497-504.

Neill, C. R., 1976. Scour holes in a wandering gravel river. *Proc. Symposium on Inland Waterways for Navigation, Flood Control, and Water Diversions*, 3rd Annual Conf. Of ASCE Waterways, Harbors and Coastal Engineering Division, New York, pp 1301-1317.

Newbury, R., 1968, The Nelson River: *A Study of Subarctic River Processes*, Ph.D. Thesis, Johns Hopkins Univ. Baltimore, MD.

Newbury, R.W., 1982. The Nelson River: a study of sub-Arctic of processes. John Hopkins University Press, Baltimore, MD.

Newbury, R.W. and McCullough, G.K., 1983. Shoreline erosion and restabilization in a permafrost-affected impoundment. *Permafrost: Proc. 4th International Conference*, National Academy Press, 918-923.

Odgaard, A. J. 1987. Streambank erosion along two rivers in Iowa. *Water Resources Research* 23(7): 1225-1236.

Odgaard, A.J. and Mosconi, C., 1987. Streambank control by submerged vanes. *ASCE Journal of Hydraulic Engineering*: 113 (4): 520-536.

Osman, A. M., and Thorne, C. R. 1988. Riverbank stability analysis. I: Theory, *Journal of Hydraulic Engineering*:114(2): 134-150.

Patrick, D. M., Smith, L. M., and Whitten, C. B. 1982. Methods for studying accelerated fluvial change. Bathurst, J. C., Thorne, C. R., and Hey, R. D. (eds.), *Gravel-Bed Rivers*. New York, NY: John Wiley and Sons, Ltd., 783-812.

Perry, E. S., 1934,Geology and artesian water resources along Missouri and Milk Rivers in northeastern Montana: *Montana Bureau of Mines and Geology Memoir* 11

Pokrefke, T. J., Abraham, D. A., Hoffman, P. H., Thomas, W. A., Darby, S. E., and Thorne, C. R. 1998. Cumulative erosion impacts analysis for the Missouri River master water control manual review and update study. *Technical Report No. CHL-98-7, U. S. Army Engineer Waterways Experiment Station*, Vicksburg, MS, 288 pp.

Prowse, T.D., 1993. Suspended sediment concentration during river ice breakup. *Canadian Journal of Civil Engineering*: 20: 872-875.

Prowse, 1998, River Ice Ecology, a chapter in *River Ice*, (Ed H. T. Shen), A.A. Balkema for International Association for Hydraulic Research, in press.

Rahn, P. H. 1977. Erosion below main stem dams on the Missouri River. *Bulletin of the Association of Engineering Geologists* 14(3), 157-181.

Reid, J.R., 1985. Bank-erosion processes in a cool-temperate environment, Orwell Lake, Minnesota. *Geological Society of America Bulletin*: 96 (6): 781-792.

Richards, K. 1982. *Rivers, Form and Process in Alluvial Channels*. New York: Methuen and Company.

Rinaldi, M., 1994 *Dinamica di un alveo fluviale antropizzato: Il Fiume Sieve (Toscana)*. Dottorato di Ricera in Geologia Applicata, Geomorfologia e Idrogeologia, Universita degle Studi di Perugia, Firenze e Camerino, VII Ciclo 1991-1994, unpublished

Rosen, P.S., 1979. Boulder barricades in central Labrador. *Journal of Sedimentary Petrology*: 49 (4):1113-1124.

Sayre, W.W. and Song, G.B., 1979. Effects of ice covers on alluvial channel flow and sediment transport processes. *IIHR Report* No. 218, Iowa Institute of Hydraulic Resarch, The University of Iowa, Iowa City, IA.

Schumm, S.A., and Hadley, R.F., 1957, Arroyos and the semiarid cycle of erosion. *American Journal of Science*: 225: 161-174.

Schumm, S.A., Harvey, M.D., and Watson, C.C., 1984, *Incised Channels, Morphology, Dynamics and Control*, Water Resources Publications, Littleton, Colorado, 200 p.

Schumm, S.A. and Khan, H.R., 1972. Experimental Study of Channel Patterns. *Geological Society of America Bulletin*: 83:1755-1770.

Schumm, S.A., and Lichty, R. 1963, Channel widening and flood plain construction along the Cimarron River in south-western Kansas. *U.S. Geological Survey Professional Paper* 352D, 71-88.

Scott, K.M., 1978. Effects of permafrost on stream channel behavior in Arctic Alaska. *U. S. Geological Survey Professional Paper* 1068

Scrimgeour, G.J., Prowse, T.D., Culp, J.M., and Chambers, P.A., 1994. Ecological effects of river ice break-up: a review and perspective. *Freshwater Biology*: 32: 261-275.

Selby, M. J. 1982. *Hillslope Materials and Processes*, Oxford University Press, Oxford, UK.

Shields, F. D., Jr. Cooper, C. M., and Testa, S. 1995. Towards greener riprap: environmental considerations from microscale to macroscale. *In* C. R. Thorne, S. R. Abt, F. B. J. Barends, S. T. Maynord, and K. W. Pilarczyk. (eds.). *River, coastal and shoreline protection: erosion control using riprap and armourstone*. John Wiley & Sons, Ltd., Chichester, U. K., 557-574.

Shields, F. D., Jr., Simon, A. and Steffen, L. J. In review. Reservoir Effects on River Channel Migration. Manuscript for submission to *Environmental Conservation*.

Simon, Andrew, 1989, A model of channel response in disturbed alluvial channels: *Earth Surface Processes and Landforms*:14: 11-26.

Simon, Andrew, 1992, Energy, time, and channel evolution in catastrophically disturbed fluvial systems, in Phillips J.D., and Renwick, W.H., (eds.), *Geomorphic Systems: Geomorphology*: 5: 345-372.

Simon, Andrew, 1994a, Gradation processes and channel evolution in modified West Tennessee streams: process, response, and form: *U.S. Geological Survey Professional Paper* 1470, 84 p.

Simon, A., Curini, A., Darby, S.E., and Langendoen, E., 1999, Streambank mechanics and the role of bank and near-bank processes in incised channels. In, S. E. Darby and A. Simon (eds.) *Incised Channels: Processes, Forms, Engineering, and Management*, John Wiley & Sons Inc., Chichester, 123-152.

Simon, A., and Curini, A., 1998, Pore pressure and bank stability: The influence of matric suction, In Abt, S.R., Young-Pezeshk, J., and Watson, C.C., (eds.) *Water Resources Engineering '98*: ASCE: 1: 358-363.

Simon, A., and Darby, S.E., 1996, Preliminary analysis of bank stability problems on the upper Missouri River below Fort Peck Dam. Unpublished report submitted to Natural Resources Conservation Service, Oxford, Mississippi.

Simon, Andrew, and Hupp, C.R., 1986, Channel evolution in modified Tennessee channels. Proceedings, *Fourth Federal Interagency Sedimentation Conference*, Las Vegas, March 24-27, 1986: 2: 5-71 to 5-82.

Simon, Andrew, and Hupp, C.R., 1992, Geomorphic and vegetative recovery processes along modified stream channels of West Tennessee*: U.S. Geological Survey Open-File Report* 91-502, 142 p.

Simon, Andrew, Rinaldi, M., and Hadish, G., 1996, Channel evolution in the loess area of the midwestern United States. *Proceedings, Sixth Federal Interagency Sedimentation Conference*, Las Vegas, March 10-14, 1996, 345-357.

Simon, A., Wolfe, W. J., and Molinas, A. 1991. Mass wasting algorithms in an alluvial channel model, *Proc. 5th Federal Interagency Sedimentation Conference*, Las Vegas, Nevada, 2: 8-22 to 8-29.

Smith, D.G., 1979. Effects of channel enlargement by river ice processes on bankfull discharge in Alberta, Canada. *Water Resources Research*: 15, (2): 469-475.

Smith, B. and Ettema, R., 1997. Flow resistance in ice-covered alluvial channels. *ASCE Journal of Hydraulic Engineering*: 123 (7): 592-599.

Soller, D. R., 1994, Map showing the thickness and character of Quaternary sediments in the glaciated United States east of the Rocky Mountains--Northern Plains states west of 102^{o} west longitude*): U. S. Geological Survey Miscellaneous Investigations Map* I-1970-D.

Straub, L.G., Effect of water temperature on suspended sediment load in an alluvial river. *Proc. 6th General Meeting of IAHR*, The Hague, The Netherlands, D25-1 to D25-5.

Swenson, F., 1955, Geology and Groundwater Resources of the Missouri River Valley in Northeastern Montana: *U. S. Geological Survey Water-Supply Paper* 1263.

Thorne, C.R., 1982, Processes and mechanisms of river bank erosion. In. R.D. Hey, J.C., Bathurst and C.R., Thorne, (eds.), *Gravel-Bed Rivers*, John Wiley and Sons, Chichester, England, 227-271.

Thorne, C.R., 1990, Effects of vegetation on riverbank erosion and stability, in J.B. Thornes, (ed.), *Vegetation and Erosion*, Chichester, England, John Wiley & Sons, 125-144.

Thorne, C. R. 1992. Bend scour and bank erosion on the meandering Red River, Louisiana. In Carling, P. A. and Petts, G. E. (eds.), *Lowland Flood plain Rivers: Geomorphological Perspectives.* John Wiley and Sons, Ltd., 95-115.

Thorne, C.R., Murphey, J.B., and Little, W.C., 1981, *Stream channel stability, Appendix D, Bank stability and bank material properties in the bluffline streams of northwest Mississippi*: Oxford, Mississippi, U.S. Department of Agriculture Sedimentation Laboratory, 257 p.

Tietze, W., 1961, Uber die Erosion von unter Eis Fliessendem Wasser, in *Mainzer Geographische Studien*, pp 125-141, pub. Georg Westermann, Mainz, Germany.

Tsai, W.-F. and Ettema, R., 1994. Ice cover influence on transverse bed slopes in a curved alluvial channel. *IAHR Journal of Hydraulic Research*: 32(4): 561-581.

Tuthill, A. and Mamone, A.C., 1997. Selection of confluence sites with ice problems for structural solutions. *CRREL Special Report* 97-4. U.S. Army Corps of Engineers, Cold Regions Research and Engineering Laboratory, Hanover, NH.

Tywonik, N, and Fowler, J.L., 1973. Winter measurement of suspended sediments. *Proc. IAHS Conf. The Role of Snow and Ice in Hydrology*, Banff, Alberta, 814-827.

U. S. Army Engineer District, Omaha. Undated. Missouri River, Fort Peck Dam to Williston, Aerial Mosaic. U. S. Corps of Engineers, Omaha, NE, 25 pp.

U. S. Corps of Engineers. 1995. *Missouri River main stem reservoirs annual operating plan and summary of actual 1994-1995 operations*. Omaha, NE: Corps of Engineers, Missouri River Division.

U. S. Corps of Engineers. 1984. Missouri River bank erosion study Fort Peck Dam to the Yellowstone River for Period July 1975 to August 1983, McCombs-Knutson Associates, Inc., 74 pp.

U. S. Corps of Engineers, 1983. Galena Streambank Protection. Galena, Alaska Section 14 Reconnaisance Report. US Army Corps of Engineers, Alaska District, Anchorage, AK.

U. S. Corps of Engineers. 1976. Fort Peck Dam to Yellowstone River Bank Erosion Study. Bank Erosion Rates for Period 1938 to 1975. Unpublished computation sheets (MRD form 68), U. S. Army Corps of Engineers, Omaha, NE.

U. S. Corps of Engineers. 1952. Report on degradation observations Missouri River downstream from Fort Peck Dam, 39 pp.

U. S. Corps of Engineers. 1945. Report on retrogression observations Missouri River below Fort Peck Dam. U. S. Army Corps of Engineers, Fort Peck, Montana.

U. S. Corps of Engineers. 1933. Report on Missouri River and tributaries. House Document 238, 308 Report, Congressional Documents, 73rd Congress, second Session 1933-34, United States Government Printing Office, Washington, D. C.

U. S. Department of Agriculture, Natural Resources Conservation Service, Soil Survey of McCone County, Montana, July, 1984.

U. S. Department of Agriculture, Natural Resources Conservation Service, Soil Survey of Richland County, Montana, August, 1980.
U. S. Department of Agriculture, Natural Resources Conservation Service, Soil Survey of Roosevelt and Daniels Counties, Montana, May, 1985.
U. S. Department of Agriculture, Natural Resources Conservation Service, Soil Survey of Valley County, Montana, September, 1984.
Uunila, L.S., 1997. Effects of river ice on bank morphology and riparian vegetation along the Peace River, Clayhurst to Fort Vermilion. *Proc. 9th Workshop on River Ice*, Fredericton, New Brunswick., 315-334.
Vanoni, V. A.(ed.) 1975. *Sedimentation Engineering*. American Society of Civil Engineers, New York.
Vidal, H., 1969, The principle of reinforced earth, *Highway Research Record*: 282:1-16.
Walker, H.J., 1969. Some aspects of erosion and sedimentation in an Arctic delta during breakup. *Proc. IAHS Symposium on the Hydrology of Deltas*, Bucharest, Romania, Publication 90, 209-219.
Wei, T. C. 1997. Downstream channel and sediment trends study. Prepared for U. S. Army Corps of Engineers, Omaha, NE., Midwest International Inc., 55 pp.
Weissmann, G. 1990a. Skinner's Island Riverbed, T27N, R51E, (File R-013), Department of State Lands, State of Montana, Helena.
Weissmann, G. 1990b. Holen (aka, Budak) Riverbed Determinations, (File R-013), Township 27 North, Range 49 East, Department of State Lands, State of Montana, Helena.
Weismann, G. 1993. Geological opinion on Missouri River Channel History, Panasuk (Little Muddy Creek) Riverbed. Sections 25, 26, 27, 35, 36, T27N, R583, Roosevelt County, Montana, Montana Department of State Lands, Helena.
Wentworth, C.K., 1932. The geologic work of ice jams in sub-Arctic river. In *Contributions in Geology and Geography*, Washington University Studies, Science and Technology No. 7, Washington University, St Louis, Thomas, L.F. (ed.), 49-82.
Williams, G. P. 1986. River meanders and channel size. *Journal of Hydrology* 88: 147-164.
Williams, G.P. and Mackay, D.K., 1973. The characteristics of ice jams. *Proc. Seminar on Ice Jams in Canada*, National Research Council of Canada, University of Alberta, Edmonton, 17-35.
Williams, G. P. and Wolman, M. G. 1984. Downstream effects of dams on alluvial rivers. *U. S. Geological Survey Professional Paper* 1286 83 p.
Wuebben, J.L., 1986. A laboratory study of flow in an ice-covered sand bed channel. Proc. 8th *IAHR Symposium on Ice*, Iowa City, IA, 1-8.
Wuebben, J.L., 1988. Effects of an ice cover on flow in a movable bed channel. Proc. 9th *IAHR Symposium on Ice*, Sapporo, Hokkaido, Japan, 137-146.
Wuebben, J.L., 1988. A preliminary study of scour under an ice jam. *Proc. of 5th Workshop on Hydraulics of River Ice/Ice Jams*, Winnipeg, Manitoba, 177-190.
Wuebben, J.L. and Gagnon, J.J., 1995. Ice jam flooding on the Missouri River near Williston, North Dakota. *CRREL Report* 95-19. U.S. Army Corps of Engineers, Cold Regions Research and Engineering Laboratory, Hanover, NH.

Wuebben, J.L., 1995. Ice effects on riprap. Section 31 in *River, Coastal and Shoreline Protection: Erosion Control Using Riprap and Armourstone*, Ed. by Thorne, C.R., Abt, S., Barends, S.T. and Pilarczyk, K.W., John Wiley & Sons Ltd., New York.

APPENDIX A

Average of the Mean-Daily Flows at the Wolf Point Gage for Specified Time Periods (See Figures 6-10)

Appendix A-- Average of the mean-daily flows at the Wolf Point gage for specified time periods (flow rates in cubic feet per second)							
Date	**Pre-dam average**	**1938-1956**	**1938-1956***	**1958-68**	**1970-95**	**1970-95****	
10/1/28	4190	17384	18893	7737	10621	10441	
10/2/28	4664	17388	19042	7659	10648	10470	
10/3/28	4567	17407	19063	7615	10352	10256	
10/4/28	4391	17566	19184	7606	10263	10115	
10/5/28	4344	17852	19297	7621	10121	9995	
10/6/28	4271	17690	19083	7627	10122	9978	
10/7/28	4367	17871	18899	7624	10510	10429	
10/8/28	4423	17963	18748	7506	10478	10394	
10/9/28	4496	17831	18796	7635	10495	10431	
10/10/28	4324	17425	18557	7635	10483	10426	
10/11/28	4386	17278	18559	7645	10496	10450	
10/12/28	4457	17500	18894	7537	10431	10379	
10/13/28	4570	17355	18821	7507	10237	10158	
10/14/28	4637	17282	18674	7583	10119	10012	
10/15/28	4597	17204	18543	7598	9909	9810	
10/16/28	4759	17191	18618	7650	9908	9791	
10/17/28	4763	17070	18624	7090	10085	9993	
10/18/28	4437	17153	18586	6793	10061	9966	
10/19/28	4439	17409	18860	6755	10094	9985	
10/20/28	4527	17290	18728	6767	9891	9808	
10/21/28	4440	17185	18642	6838	9757	9635	
10/22/28	4476	17630	19094	7100	9712	9585	
10/23/28	4661	17537	19101	7082	9547	9511	
10/24/28	4796	16769	18248	6913	9677	9638	
10/25/28	4861	16343	17746	6808	9418	9355	
10/26/28	4856	15907	17212	6906	9238	9150	
10/27/28	4771	15528	16703	6972	9273	9161	
10/28/28	4637	14944	16191	7079	9493	9311	
10/29/28	4567	14948	16167	6825	9512	9358	
10/30/28	4584	14658	15883	6893	9503	9330	
10/31/28	4597	14531	15732	6942	9398	9234	
11/1/28	4533	14120	15276	7003	9521	9368	
11/2/28	4496	13594	14691	7258	9668	9565	
11/3/28	4524	13161	14191	7174	9547	9487	
11/4/28	4571	12835	13744	7239	9512	9431	
11/5/28	4689	12311	13247	7140	9587	9504	
11/6/28	4756	11735	12663	7066	9678	9575	
11/7/28	4829	11206	12076	6953	9924	9799	
11/8/28	5154	10660	11469	6894	9578	9413	

11/9/28	5149	10287	11046	6939	9194	9003	
11/10/28	5221	9936	10707	6903	9558	9473	
11/11/28	5236	9529	10156	6943	9675	9678	
11/12/28	5166	9209	9882	7071	9671	9632	
11/13/28	5186	8947	9574	6939	9878	9758	
11/14/28	5083	8811	9397	6781	9967	9918	
11/15/28	4921	8437	8961	6634	9873	9895	
11/16/28	4896	8050	8541	6706	10073	9962	
11/17/28	4639	7714	8204	6740	10228	10157	
11/18/28	4540	7390	7894	6898	10029	9977	
11/19/28	4433	7370	7950	7156	9891	9817	
11/20/28	4566	7015	7628	7094	9944	9866	
11/21/28	4334	7137	7802	7543	10044	9948	
11/22/28	4169	6813	7448	7719	9845	9785	
11/23/28	4094	6408	6998	7707	9961	9903	
11/24/28	4161	6328	6887	7830	9755	9678	
11/25/28	4216	6306	6857	7929	9648	9597	
11/26/28	4281	6398	6981	8191	9442	9419	
11/27/28	4850	6259	6832	8478	9793	9747	
11/28/28	4426	6018	6582	8482	10054	10005	
11/29/28	4286	6083	6666	8599	10404	10395	
11/30/28	4061	6299	6843	8547	10403	10450	
12/1/28	3951	6254	6799	8671	9848	9806	
12/2/28	3961	6380	6956	8585	9701	9674	
12/3/28	3859	6265	6850	8448	9523	9462	
12/4/28	3901	6227	6802	8678	9358	9300	
12/5/28	3789	6101	6651	8763	9478	9465	
12/6/28	3744	5852	6386	8847	9697	9725	
12/7/28	3597	5862	6397	8757	10040	10085	
12/8/28	3636	5793	6320	8615	10097	10146	
12/9/28	3689	6034	6593	8443	10046	10072	
12/10/28	3664	5658	6159	8216	9949	9959	
12/11/28	3423	5965	6494	8027	9814	9827	
12/12/28	3440	6052	6597	7997	9924	9927	
12/13/28	3466	5881	6401	8083	10011	10029	
12/14/28	3370	5878	6392	8296	10258	10282	
12/15/28	3296	5876	6390	8391	10028	10109	
12/16/28	3250	5946	6473	8208	10103	10118	
12/17/28	3267	5732	6241	8345	10393	10491	
12/18/28	3191	5517	6002	8363	10458	10491	
12/19/28	3221	5300	5767	8310	10320	10364	
12/20/28	3239	5422	5902	8428	10299	10336	
12/21/28	3521	5524	6010	8660	10310	10364	
12/22/28	3517	5566	6062	8818	10441	10482	

12/23/28	3524	5632	6141	8920	10377	10489	
12/24/28	3573	5660	6161	9018	10591	10664	
12/25/28	3569	5749	6154	9062	10467	10545	
12/26/28	3427	5599	5899	8986	10047	10200	
12/27/28	3439	5370	5611	8910	10130	10291	
12/28/28	3457	5426	5640	8860	10268	10418	
12/29/28	3500	5351	5662	8830	10312	10491	
12/30/28	3531	5355	5688	8760	10285	10473	
12/31/28	3550	5311	5567	8750	10365	10500	
1/1/29	3843	5306	5595	8760	10531	10618	
1/2/29	3843	4886	5162	8760	10398	10536	
1/3/29	3857	4343	4603	8630	10545	10664	
1/4/29	3873	4189	4393	8740	10713	10800	
1/5/29	3880	3990	4194	8910	10808	10918	
1/6/29	4173	4091	4295	8940	10935	11100	
1/7/29	4150	4192	4318	8820	11137	11255	
1/8/29	4271	4268	4354	8690	10938	11082	
1/9/29	4369	4478	4570	8650	10967	11127	
1/10/29	4367	4709	4832	8730	10867	11036	
1/11/29	4241	4779	4910	8710	10983	11155	
1/12/29	4171	4823	5019	8710	11042	11200	
1/13/29	4183	4956	5140	8770	11283	11400	
1/14/29	4170	4914	5104	8830	11683	11655	
1/15/29	4216	4794	4921	8890	11742	11609	
1/16/29	4169	4756	4896	9000	11942	11773	
1/17/29	4147	4893	5048	9010	11792	11600	
1/18/29	4163	4957	5163	9020	11683	11491	
1/19/29	4057	4892	5158	8790	12142	12009	
1/20/29	4071	4782	5102	8890	12408	12309	
1/21/29	3786	4597	4947	8960	12392	12282	
1/22/29	3900	4596	4968	9030	12517	12427	
1/23/29	3856	4449	4816	9150	12742	12682	
1/24/29	3924	4486	4857	9230	12867	12809	
1/25/29	3870	4588	4970	9250	13092	13045	
1/26/29	3780	4575	4956	9170	13025	13027	
1/27/29	3734	4839	5249	9050	12942	12955	
1/28/29	3969	4998	5431	8920	12717	12736	
1/29/29	4057	5128	5581	9350	12625	12673	
1/30/29	4136	4986	5438	9520	12892	13018	
1/31/29	4370	4871	5314	9620	12525	12655	
2/1/29	5069	4871	5290	9730	12408	12555	
2/2/29	5060	4877	5297	9900	12017	12145	
2/3/29	5080	4700	5094	10060	12083	12236	
2/4/29	5100	4411	4768	10120	11958	12109	

2/5/29	5463	4000	4317	10120	12042	12209	
2/6/29	5509	4067	4402	9940	12292	12445	
2/7/29	5546	3885	4208	9980	12350	12482	
2/8/29	5117	3949	4277	10070	12350	12400	
2/9/29	4944	4017	4352	9940	12392	12400	
2/10/29	4904	3931	4268	9940	12800	12791	
2/11/29	5359	3781	4103	9910	13083	13091	
2/12/29	5666	3370	3647	9950	12925	12909	
2/13/29	5933	3366	3643	9860	12875	12845	
2/14/29	5971	3375	3650	9800	12833	12800	
2/15/29	5986	3400	3672	9680	12792	12773	
2/16/29	5857	3353	3617	9610	12842	12827	
2/17/29	5960	3445	3717	9560	13283	13327	
2/18/29	5993	3388	3648	9620	13183	13273	
2/19/29	5993	3401	3651	9550	13250	13364	
2/20/29	6019	3343	3587	9620	13242	13373	
2/21/29	6120	3190	3417	9660	13175	13309	
2/22/29	5963	3296	3534	9640	13058	13182	
2/23/29	5891	3372	3619	9750	12950	13064	
2/24/29	5753	3427	3680	9900	12667	12764	
2/25/29	5671	3408	3653	9860	12467	12555	
2/26/29	5683	3420	3683	10040	12467	12527	
2/27/29	5573	3341	3603	10030	12342	12391	
2/28/29	5501	3356	3562	9990	12150	12182	
3/1/29	6023	3427	3541	9990	11867	11891	
3/2/29	6424	3655	3711	9880	11792	11818	
3/3/29	6339	3645	3744	9855	11192	11182	
3/4/29	6341	3745	3661	9515	11142	11127	
3/5/29	6430	4566	3518	9430	11242	11236	
3/6/29	7201	4644	3404	9335	11033	11018	
3/7/29	7156	4472	3336	9480	10867	10855	
3/8/29	7134	4370	3300	9665	10525	10482	
3/9/29	7066	4406	3384	9795	10108	10045	
3/10/29	7219	4620	3500	9870	10000	9927	
3/11/29	6309	4915	3483	9745	10244	10194	
3/12/29	6157	5504	3660	9630	10267	10209	
3/13/29	6480	4891	3679	9550	10187	10131	
3/14/29	7204	5441	4323	9388	9985	9911	
3/15/29	8176	6897	4908	9154	10011	9939	
3/16/29	7243	6844	5049	8899	10149	10099	
3/17/29	7167	7448	5098	8931	9661	9585	
3/18/29	7063	7533	4792	9028	9671	9732	
3/19/29	7131	7734	4838	9079	9584	9674	
3/20/29	7391	7821	4923	9424	9560	9665	

3/21/29	8100	7356	4707	9802	9324	9426	
3/22/29	8954	7272	4947	10197	9200	9300	
3/23/29	9521	6989	4954	10390	9094	9175	
3/24/29	9936	6680	4933	10942	9302	9402	
3/25/29	9937	6127	4786	11570	9208	9282	
3/26/29	10843	5529	4477	11574	9175	9209	
3/27/29	10307	4850	4342	11687	9190	9125	
3/28/29	10060	5017	4721	12013	9438	9042	
3/29/29	11069	5061	4984	11712	9466	9099	
3/30/29	9990	4796	5027	11213	9418	9065	
3/31/29	9040	4880	5261	10873	9433	9126	
4/1/29	9609	5017	5419	10799	9315	9089	
4/2/29	9730	5309	5732	10965	8986	8821	
4/3/29	9703	5450	5672	10895	8937	8895	
4/4/29	9896	5323	5472	10830	8738	8777	
4/5/29	10300	5379	5493	10656	8660	8729	
4/6/29	10416	5929	6114	10396	8477	8556	
4/7/29	10263	6635	6988	10322	8489	8588	
4/8/29	9981	7485	7974	10204	8547	8651	
4/9/29	9600	9040	9736	10000	8665	8771	
4/10/29	9680	9275	10012	9812	8568	8660	
4/11/29	9346	9009	9693	9980	8569	8669	
4/12/29	8817	8858	9500	9614	8435	8513	
4/13/29	8841	8906	9482	9383	8437	8525	
4/14/29	9016	9102	9691	9544	8638	8751	
4/15/29	9267	9379	10008	9699	9079	9161	
4/16/29	9589	9960	10663	9251	9469	9527	
4/17/29	9849	10221	10914	8777	9501	9566	
4/18/29	10369	10343	11040	8604	9633	9660	
4/19/29	10150	10703	11499	8811	9905	9742	
4/20/29	10013	11048	11918	7999	9948	9679	
4/21/29	10067	10572	11413	8155	9524	9399	
4/22/29	9951	9854	10616	8366	9289	9197	
4/23/29	10221	9593	10358	8421	9378	9267	
4/24/29	10930	9269	9982	8180	9329	9186	
4/25/29	11510	8887	9573	8628	9162	9109	
4/26/29	12854	8360	9033	8764	9002	8933	
4/27/29	12554	7922	8576	8498	9029	8805	
4/28/29	12513	7478	8112	8258	8763	8596	
4/29/29	12223	7216	7838	8072	8437	8318	
4/30/29	12593	7232	7867	8086	8763	8641	
5/1/29	12914	7427	8093	8327	8883	8545	
5/2/29	12877	7734	8434	8374	9253	8930	
5/3/29	12671	7619	8317	8332	9171	8886	

5/4/29	12176	7362	8041	8120	8732	8525	
5/5/29	12086	7152	7788	8162	8723	8637	
5/6/29	11919	6921	7510	8910	8868	8693	
5/7/29	11830	6943	7550	9816	8667	8427	
5/8/29	12501	6708	7300	10284	8978	8621	
5/9/29	13187	6522	7098	10509	9443	8829	
5/10/29	13336	5956	6464	10605	9517	8764	
5/11/29	12533	5702	6177	10504	9253	8422	
5/12/29	12269	5548	6011	10155	9410	8593	
5/13/29	12146	5346	5766	9857	9737	8931	
5/14/29	12220	5345	5748	9713	9918	9138	
5/15/29	12384	5691	6127	9379	10093	9301	
5/16/29	12231	5305	5681	9139	10203	9157	
5/17/29	11476	5287	5678	8943	10430	9405	
5/18/29	11539	5033	5407	8745	10362	9340	
5/19/29	11713	4896	5254	8825	10239	9225	
5/20/29	11699	4808	5168	8855	10353	9349	
5/21/29	13116	4491	4821	8967	10263	9277	
5/22/29	13826	4006	4282	8856	10101	9128	
5/23/29	13766	3970	4237	8769	10147	9224	
5/24/29	17367	4036	4304	8660	9888	9005	
5/25/29	13996	3801	4038	8613	9880	9033	
5/26/29	13296	3711	3938	8594	9943	9146	
5/27/29	13830	3832	4061	8599	9894	9121	
5/28/29	14287	3735	3930	8520	10098	9379	
5/29/29	14794	3688	3864	8395	10112	9440	
5/30/29	14309	3591	3763	8561	10000	9382	
5/31/29	13671	3569	3717	8760	10381	9688	
6/1/29	14261	3453	3588	8759	10529	9568	
6/2/29	13697	3436	3621	8589	10939	9888	
6/3/29	14281	3478	3684	8639	10844	9803	
6/4/29	14427	3450	3642	8629	10761	9730	
6/5/29	15201	3509	3634	8299	10906	9897	
6/6/29	15393	4143	3848	8097	10918	9819	
6/7/29	14957	4478	4098	8176	11143	9838	
6/8/29	15510	4763	4414	8078	11160	9765	
6/9/29	16866	4859	4412	8236	11074	9699	
6/10/29	19890	5192	4722	8327	10989	9661	
6/11/29	20386	5427	4852	8362	11167	9909	
6/12/29	19529	5663	5114	8302	11365	10162	
6/13/29	20757	5160	4556	8145	11657	10480	
6/14/29	20879	5537	4830	8128	11407	10198	
6/15/29	21271	5643	5037	8134	11262	10040	
6/16/29	19920	5276	5268	8173	11493	10301	

6/17/29	19529	5227	5356	8185	11675	10482	
6/18/29	18776	5219	5357	8333	11506	10315	
6/19/29	19354	5833	5370	8824	11278	10039	
6/20/29	18834	5250	5350	9178	10993	9719	
6/21/29	18040	5661	5257	8995	10830	9569	
6/22/29	18079	6638	5531	8554	10528	9258	
6/23/29	17594	6631	5257	8395	10703	9404	
6/24/29	16614	6539	5010	8320	10972	9560	
6/25/29	15874	6427	4974	8723	11335	9629	
6/26/29	14927	6773	5270	8820	11882	10062	
6/27/29	13717	6901	5357	9003	11826	10028	
6/28/29	12747	7222	5669	8606	11793	9865	
6/29/29	11877	7200	5544	8794	11979	9914	
6/30/29	11149	7197	5441	9278	11692	9591	
7/1/29	10501	7676	5873	9452	11643	9501	
7/2/29	9823	7843	6059	9398	11918	9747	
7/3/29	9154	8360	6433	10023	11905	9796	
7/4/29	8881	8915	7006	9692	12212	10140	
7/5/29	8887	9100	7300	9504	12108	10018	
7/6/29	8613	8458	6731	9046	12212	10067	
7/7/29	8467	7964	6393	8991	12531	10297	
7/8/29	7990	7263	5848	9211	12347	10196	
7/9/29	9064	7315	5894	9132	12337	10231	
7/10/29	8323	7748	6276	9000	12304	10232	
7/11/29	7990	8301	6757	8600	12185	9956	
7/12/29	7613	8588	7131	8447	12348	9998	
7/13/29	7146	8538	7320	8291	12172	9933	
7/14/29	6290	8640	7222	8311	12172	9924	
7/15/29	5871	8527	7241	8319	12103	9848	
7/16/29	5700	8475	7172	8223	12245	10004	
7/17/29	5326	8699	7421	8462	12487	10240	
7/18/29	5343	8642	7847	8382	12522	10278	
7/19/29	5194	8370	7967	8473	12503	10295	
7/20/29	5074	8471	8034	8449	12487	10285	
7/21/29	5041	8903	8481	8469	12619	10448	
7/22/29	5291	9611	8901	8009	12729	10568	
7/23/29	5147	10193	9303	8086	12523	10352	
7/24/29	5053	10814	10038	8430	12321	10132	
7/25/29	5381	11777	10774	8563	12083	9909	
7/26/29	5400	12686	11873	8131	12282	10135	
7/27/29	5104	13028	12620	7835	11983	9790	
7/28/29	4859	13105	13394	7893	12035	9865	
7/29/29	4686	13497	13652	7887	12275	10118	
7/30/29	4494	13941	14246	7837	12763	10651	

7/31/29	4370	14607	14574	7656	12503	10312	
8/1/29	4374	14793	14692	7776	12399	10217	
8/2/29	4311	14912	14780	7929	12243	10128	
8/3/29	4383	15307	15263	7887	12268	10128	
8/4/29	4247	15731	16123	7913	11945	9776	
8/5/29	4031	17205	17372	7785	12013	9868	
8/6/29	3894	17413	17803	7742	11921	9795	
8/7/29	3816	17391	17634	7885	11863	9760	
8/8/29	3816	17165	17517	7790	11501	9637	
8/9/29	3784	17700	17944	7893	10957	9498	
8/10/29	3753	18650	18944	7874	10419	9403	
8/11/29	3713	19010	19389	7790	9894	9275	
8/12/29	3697	18750	19233	7775	9723	9197	
8/13/29	4796	18450	18933	7762	9433	8863	
8/14/29	4649	18080	18433	7786	9523	8988	
8/15/29	4737	17920	18300	7964	9665	9189	
8/16/29	4299	18090	18400	7752	9790	9335	
8/17/29	3893	17980	18333	7389	9799	9435	
8/18/29	3611	18060	18456	7527	9829	9459	
8/19/29	3541	18110	18478	7673	9737	9358	
8/20/29	3710	18030	18433	7619	9908	9526	
8/21/29	3800	17760	18178	7668	9846	9495	
8/22/29	3799	17680	18011	7705	10026	9628	
8/23/29	3900	17680	18056	7619	10073	9679	
8/24/29	3891	17720	18067	7590	10120	9685	
8/25/29	4250	17910	18267	7828	10238	9751	
8/26/29	5860	18390	18800	7885	10357	9889	
8/27/29	6431	18740	19211	7874	10178	9785	
8/28/29	6867	19150	19656	7698	10048	9662	
8/29/29	6957	19160	19667	7883	10051	9574	
8/30/29	6164	19310	19833	7924	10060	9529	
8/31/29	5426	19100	19667	7850	10011	9457	
9/1/29	4876	18800	19322	7710	10171	9668	
9/2/29	4496	18460	18889	7606	10125	9609	
9/3/29	4266	17849	18210	7949	10381	9897	
9/4/29	4436	17090	17378	7770	10271	9795	
9/5/29	4583	16202	16436	7790	10143	9647	
9/6/29	4204	15624	15749	7858	9888	9377	
9/7/29	4041	15669	15799	7888	9789	9279	
9/8/29	3796	15274	15482	7809	9763	9260	
9/9/29	3726	15183	15514	7601	9801	9292	
9/10/29	3661	15151	15457	7537	9856	9288	
9/11/29	3711	15199	15510	7530	9899	9335	
9/12/29	3431	15138	15242	7810	9713	9169	

9/13/29	3547	15971	16179	7833	9584	9155	
9/14/29	3737	15843	16137	7985	9608	9117	
9/15/29	3717	16441	16768	8076	9558	9064	
9/16/29	3680	16787	17130	8192	9524	9035	
9/17/29	3606	16622	16947	8559	9440	8989	
9/18/29	3689	16257	16452	8747	9366	8954	
9/19/29	3679	16145	16328	8816	9398	8961	
9/20/29	3647	15951	16112	8743	9453	9039	
9/21/29	3754	15904	16127	8722	9477	9056	
9/22/29	4133	15804	15993	8600	9216	8763	
9/23/29	4323	15826	15940	8640	9264	8815	
9/24/29	3860	16094	15904	8589	9324	8872	
9/25/29	3897	16338	16142	8252	9222	8733	
9/26/29	4140	16024	15838	8479	9175	8682	
9/27/29	4137	16038	15898	8505	9166	8699	
9/28/29	4133	16185	16017	8540	9060	8602	
9/29/29	4181	16235	15939	8617	9151	8701	
9/30/29	4004	16900	16344	8530	9383	8936	
* w/out 1938							
**w/out 1975							

APPENDIX B

GIS-Based Maps of Soil Types Bordering the Missouri River*

* These maps are available from the U.S. Department of Agriculture, Agricultural Research Service, National Sedimentation Laboratory, Oxford, Mississippi. Requests should be brought to the attention of Dr. Andrew Simon, simon@sedlab.olemiss.edu.

APPENDIX C

Plots of Changes in Thalweg Elevations for Different 5 Time Periods

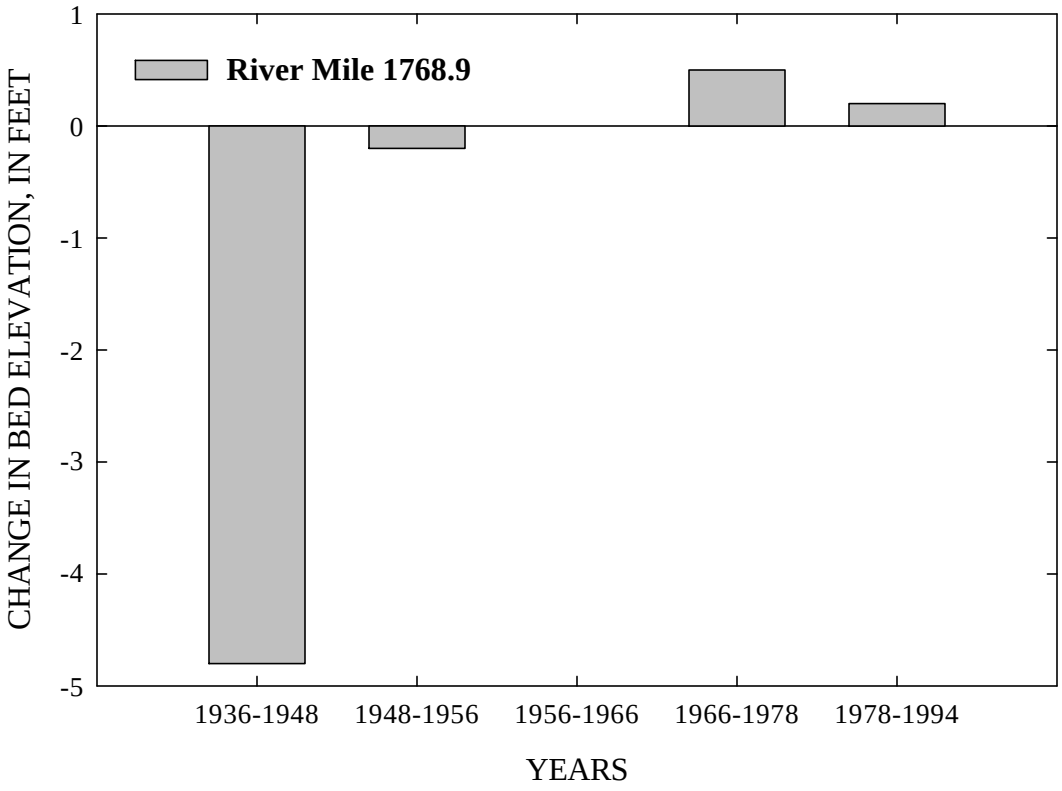
River Mile 1768.9
CHANGE IN BED ELEVATION, IN FEET
1
0
-1
-2
-3
-4
-5
1936-1948
1948-1956
1956-1966
1966-1978
1978-1994
YEARS

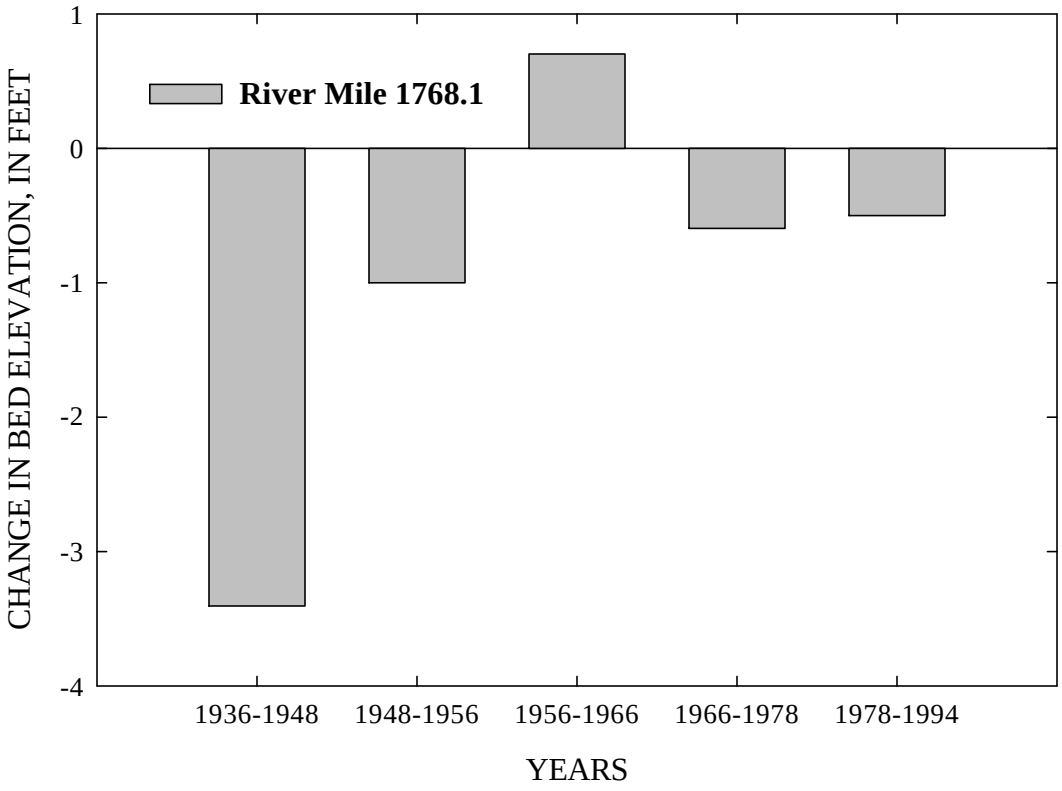
River Mile 1768.1
CHANGE IN BED ELEVATION, IN FEET
1
0
-1
-2
-3
-4
1936-1948
1948-1956
1956-1966
1966-1978
1978-1994
YEARS

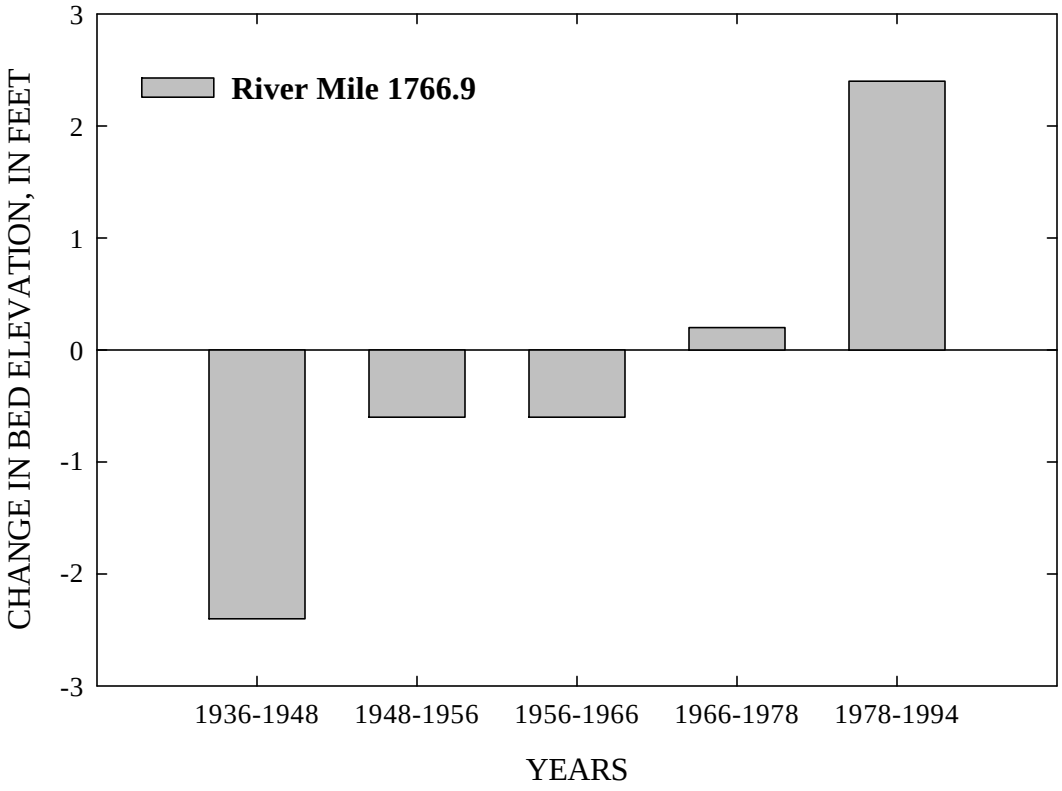
River Mile 1766.9
CHANGE IN BED ELEVATION, IN FEET
3
2
1
0
-1
-2
-3
1936-1948
1948-1956
1956-1966
1966-1978
1978-1994
YEARS

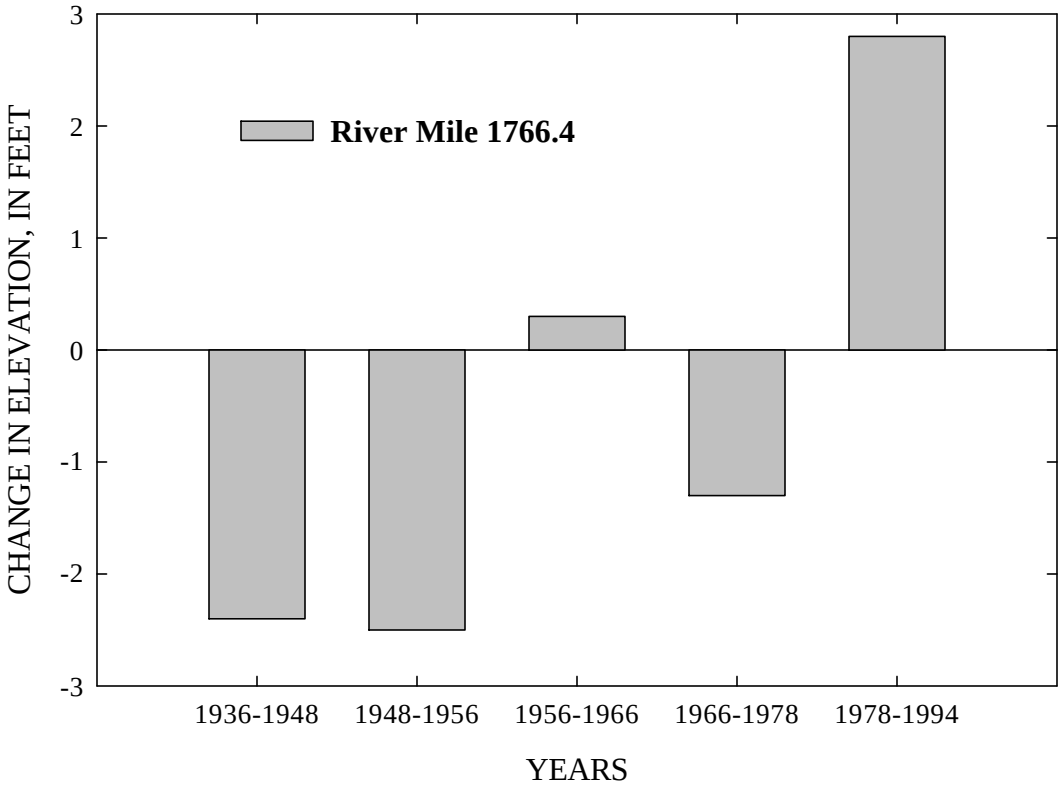
River Mile 1766.4
CHANGE IN ELEVATION, IN FEET
3
2
1
0
-1
-2
-3
1936-1948
1948-1956
1956-1966
1966-1978
1978-1994
YEARS

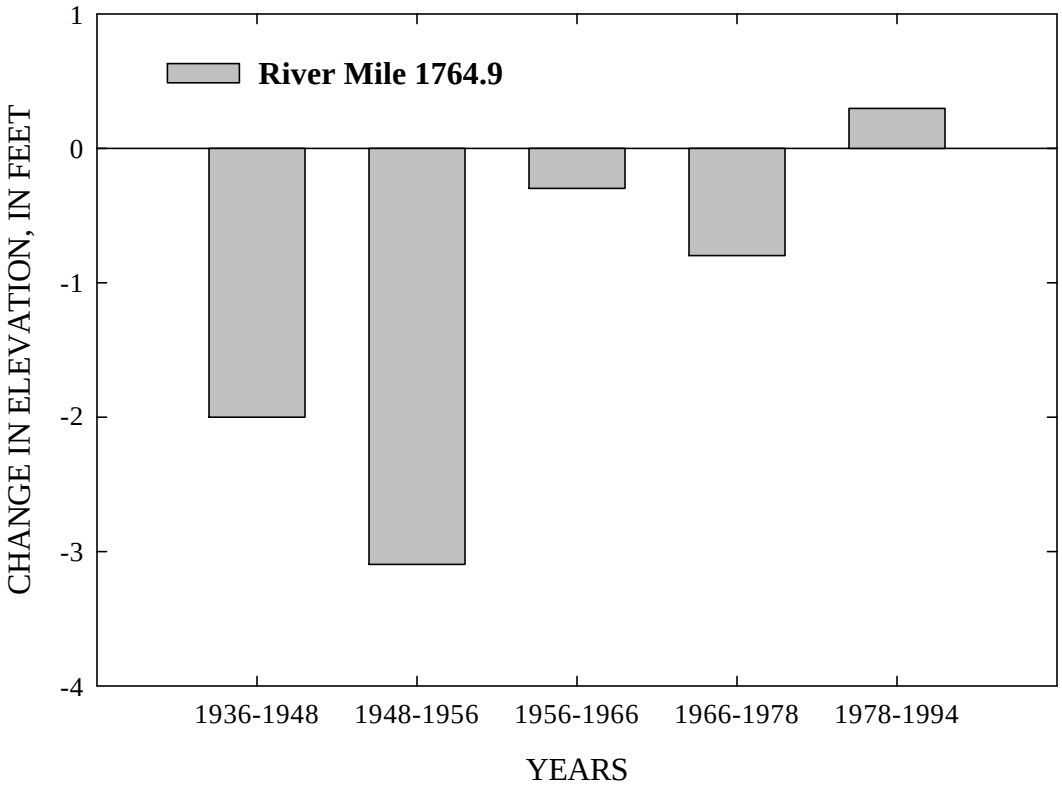
River Mile 1764.9
CHANGE IN ELEVATION, IN FEET
1
0
-1
-2
-3
-4
1936-1948
1948-1956
1956-1966
1966-1978
1978-1994
YEARS

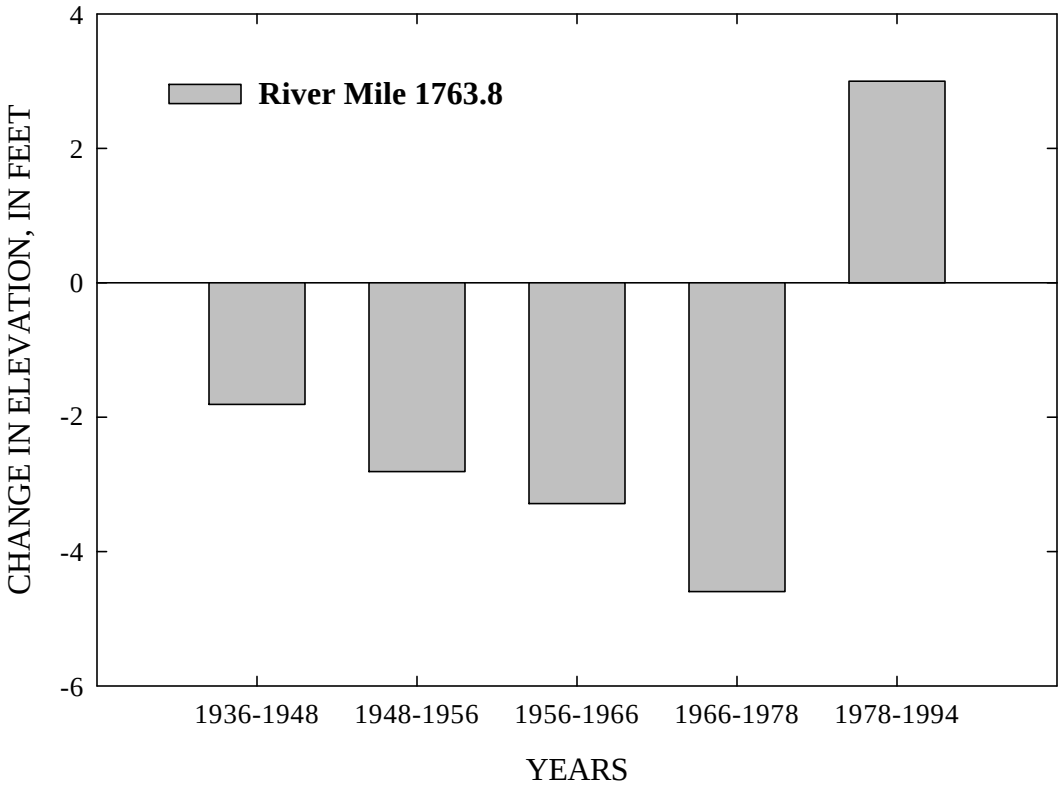
River Mile 1763.8
CHANGE IN ELEVATION, IN FEET
4
2
0
-2
-4
-6
1936-1948
1948-1956
1956-1966
1966-1978
1978-1994
YEARS

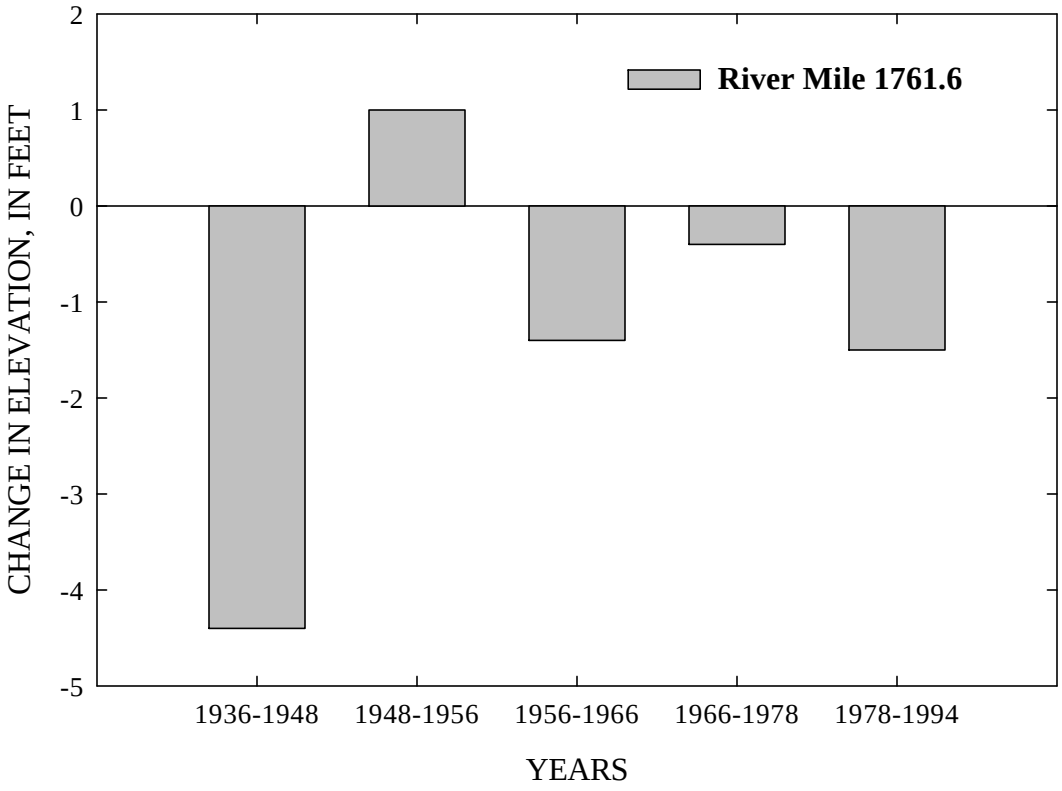
River Mile 1761.6
CHANGE IN ELEVATION, IN FEET
2
1
0
-1
-2
-3
-4
-5
1936-1948
1948-1956
1956-1966
1966-1978
1978-1994
YEARS

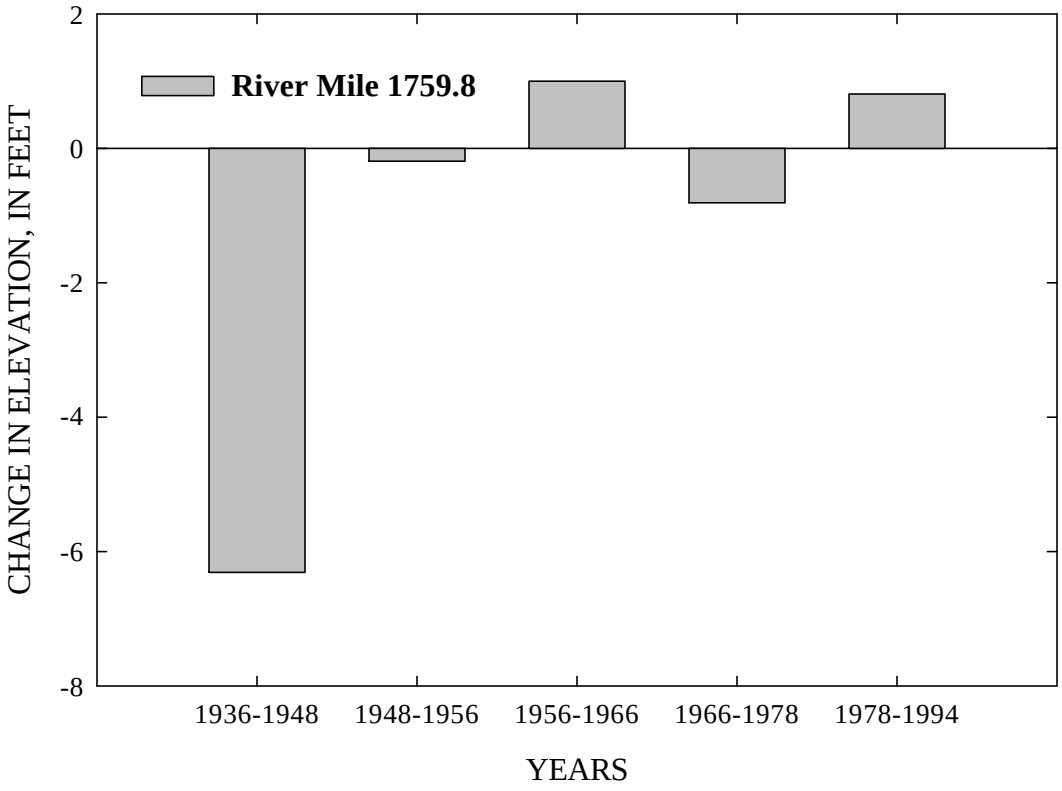
River Mile 1759.8
2
0
-2
-4
-6
-8
CHANGE IN ELEVATION, IN FEET
1936-1948
1948-1956
1956-1966
1966-1978
1978-1994
YEARS

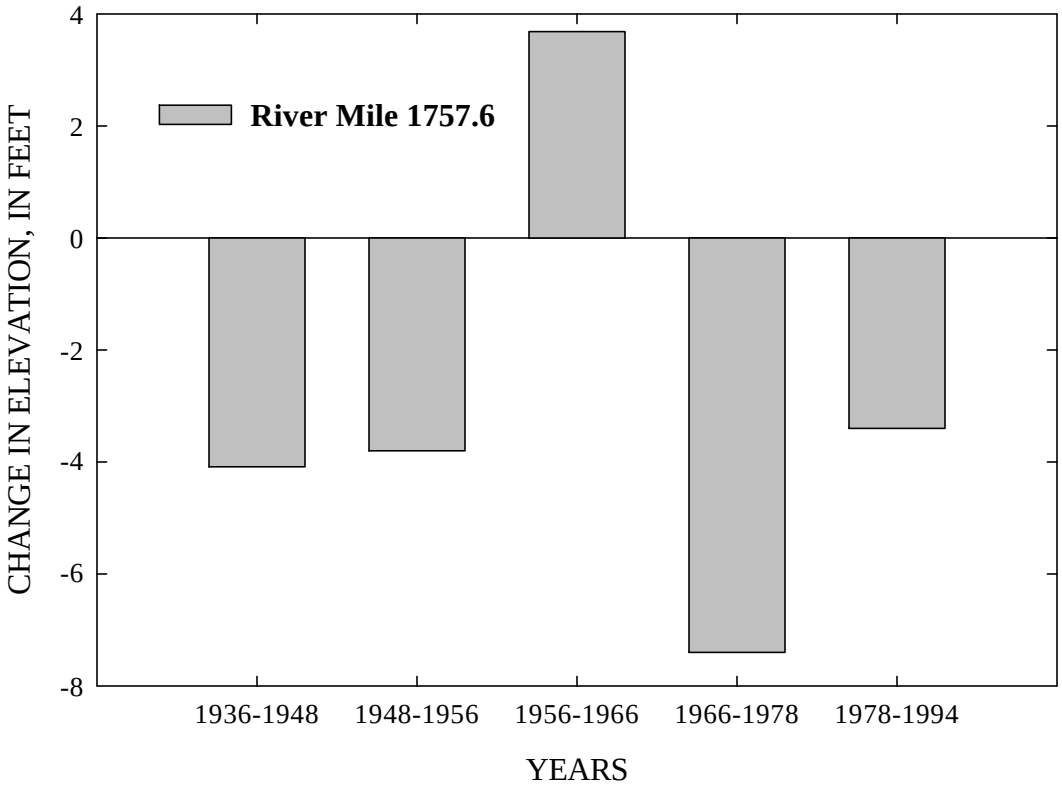
River Mile 1757.6
CHANGE IN ELEVATION, IN FEET
4
2
0
-2
-4
-6
-8
1936-1948
1948-1956
1956-1966
1966-1978
1978-1994
YEARS

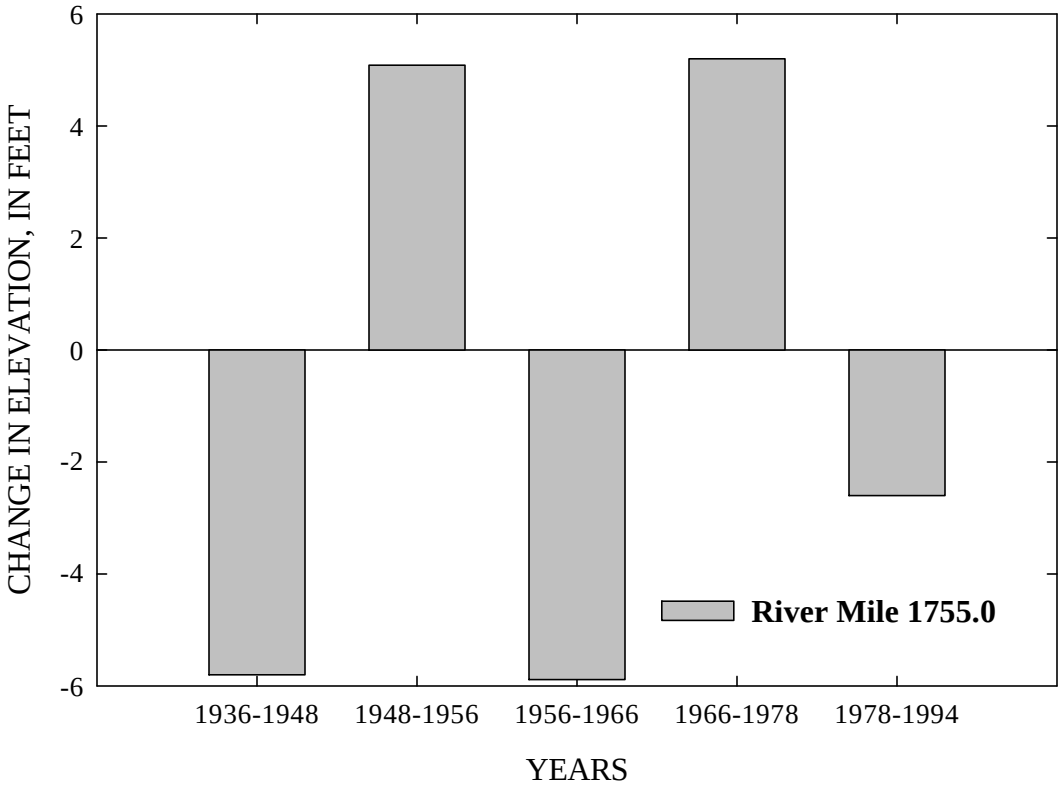
6
4
2
0
-2
-4
-6
CHANGE IN ELEVATION, IN FEET
1936-1948
1948-1956
1956-1966
1966-1978
1978-1994
YEARS
River Mile 1755.0

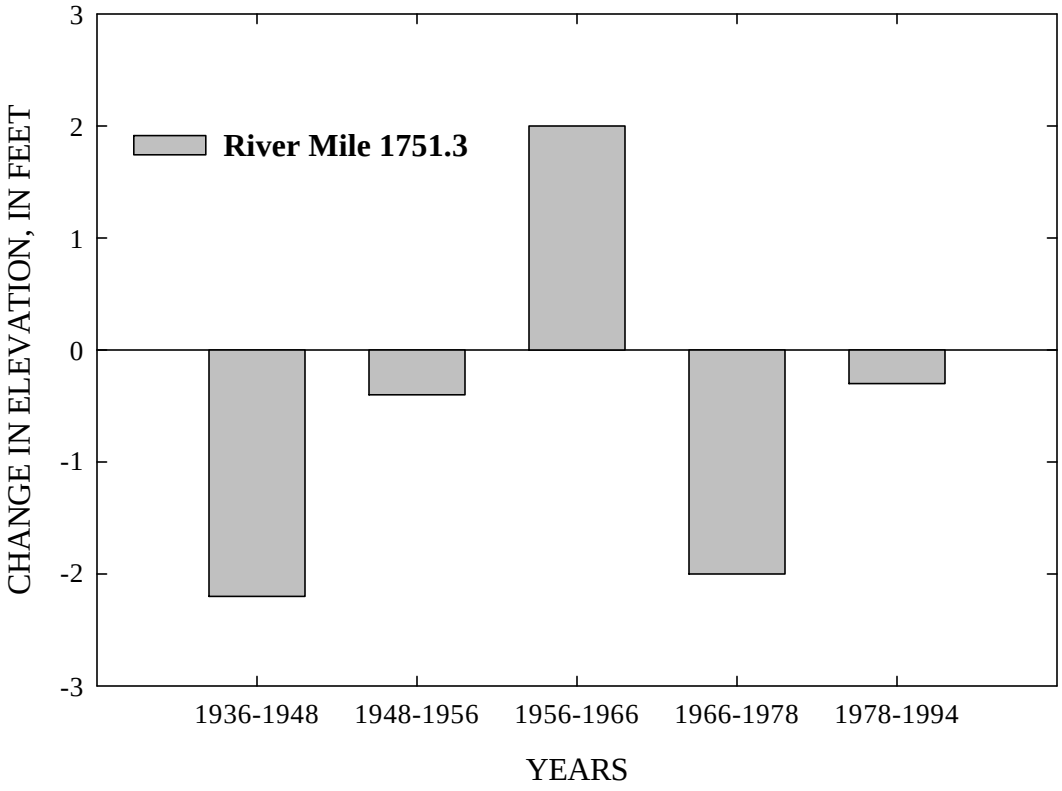
River Mile 1751.3
CHANGE IN ELEVATION, IN FEET
3
2
1
0
-1
-2
-3
1936-1948
1948-1956
1956-1966
1966-1978
1978-1994
YEARS

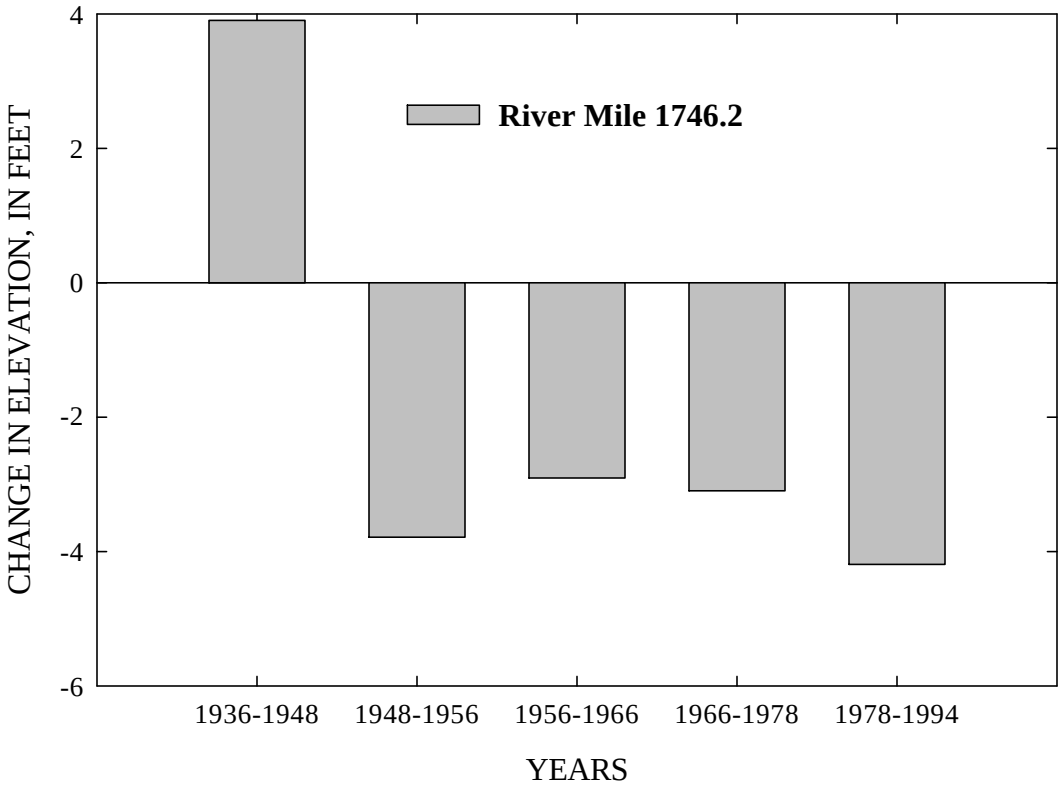
River Mile 1746.2
CHANGE IN ELEVATION, IN FEET
4
2
0
-2
-4
-6
1936-1948
1948-1956
1956-1966
1966-1978
1978-1994
YEARS

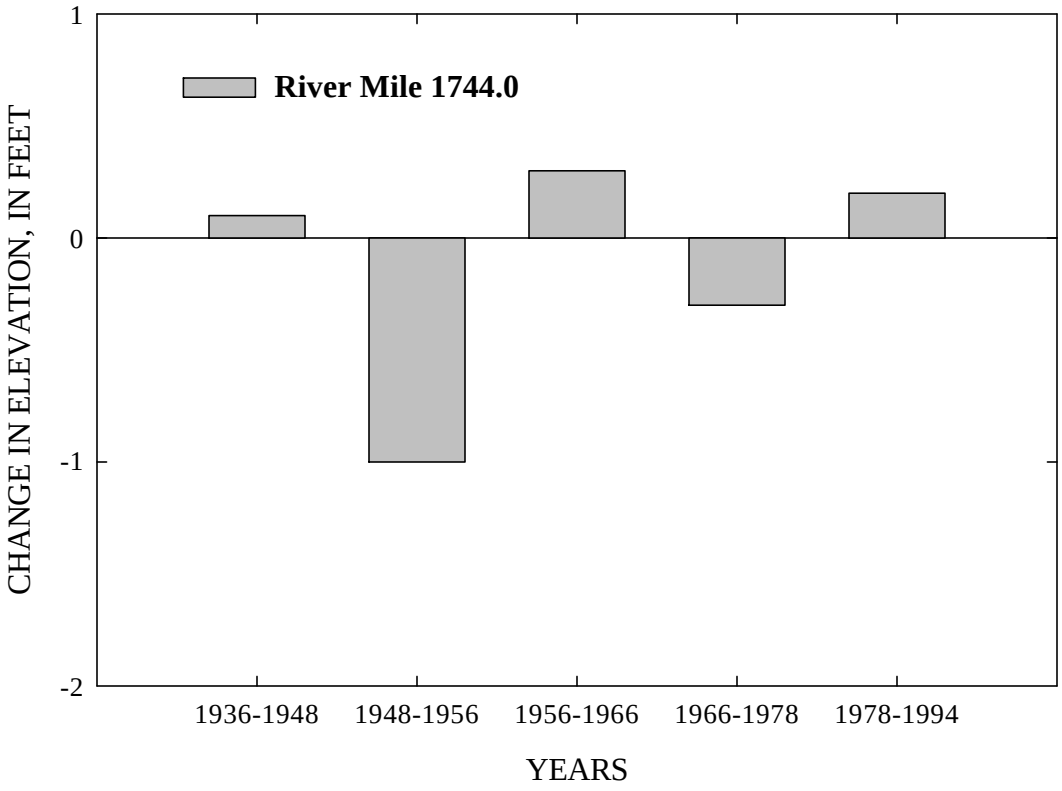
River Mile 1744.0
CHANGE IN ELEVATION, IN FEET
1
0
-1
-2
1936-1948
1948-1956
1956-1966
1966-1978
1978-1994
YEARS

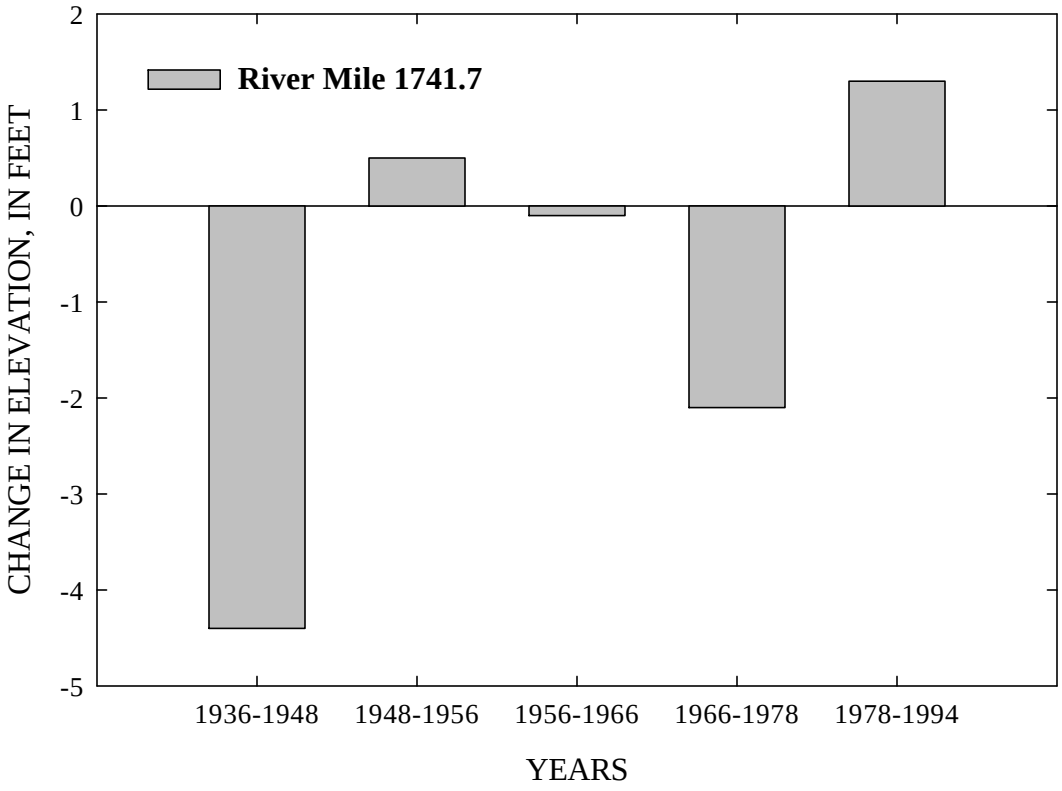
River Mile 1741.7
CHANGE IN ELEVATION, IN FEET
2
1
0
-1
-2
-3
-4
-5
1936-1948
1948-1956
1956-1966
1966-1978
1978-1994
YEARS

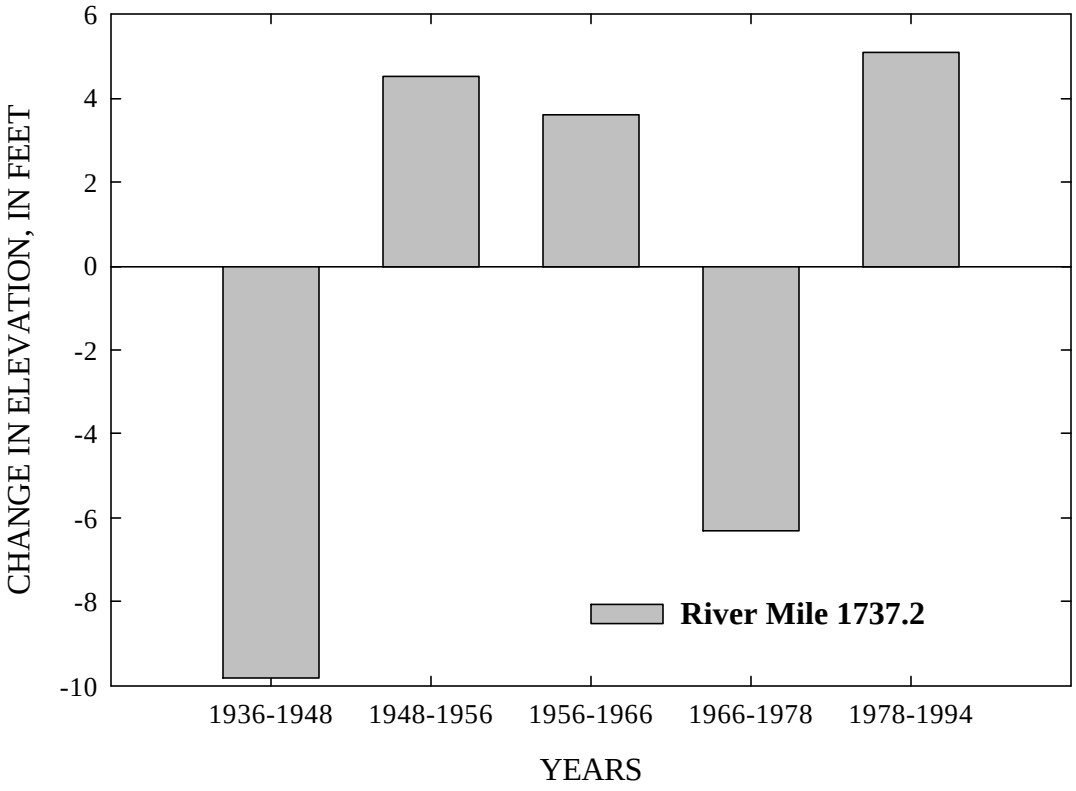
6
4
2
0
-2
-4
-6
-8
-10
CHANGE IN ELEVATION, IN FEET
1936-1948
1948-1956
1956-1966
1966-1978
1978-1994
YEARS
River Mile 1737.2

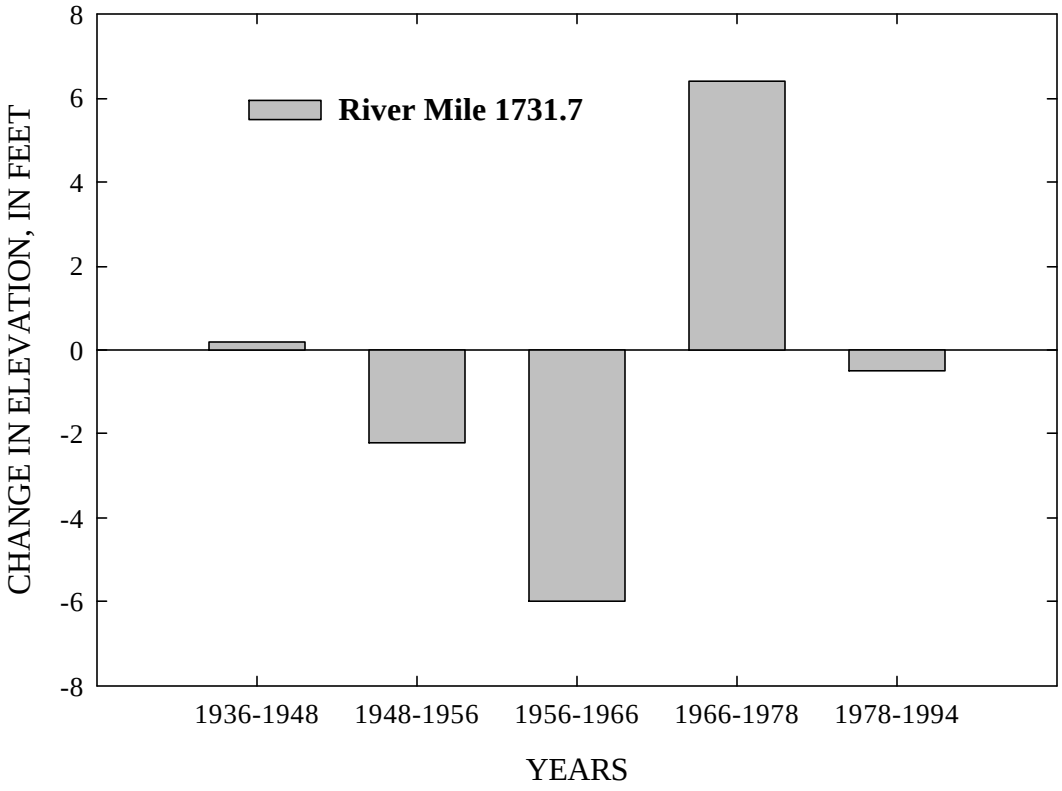
River Mile 1731.7
CHANGE IN ELEVATION, IN FEET
8
6
4
2
0
-2
-4
-6
-8
1936-1948
1948-1956
1956-1966
1966-1978
1978-1994
YEARS

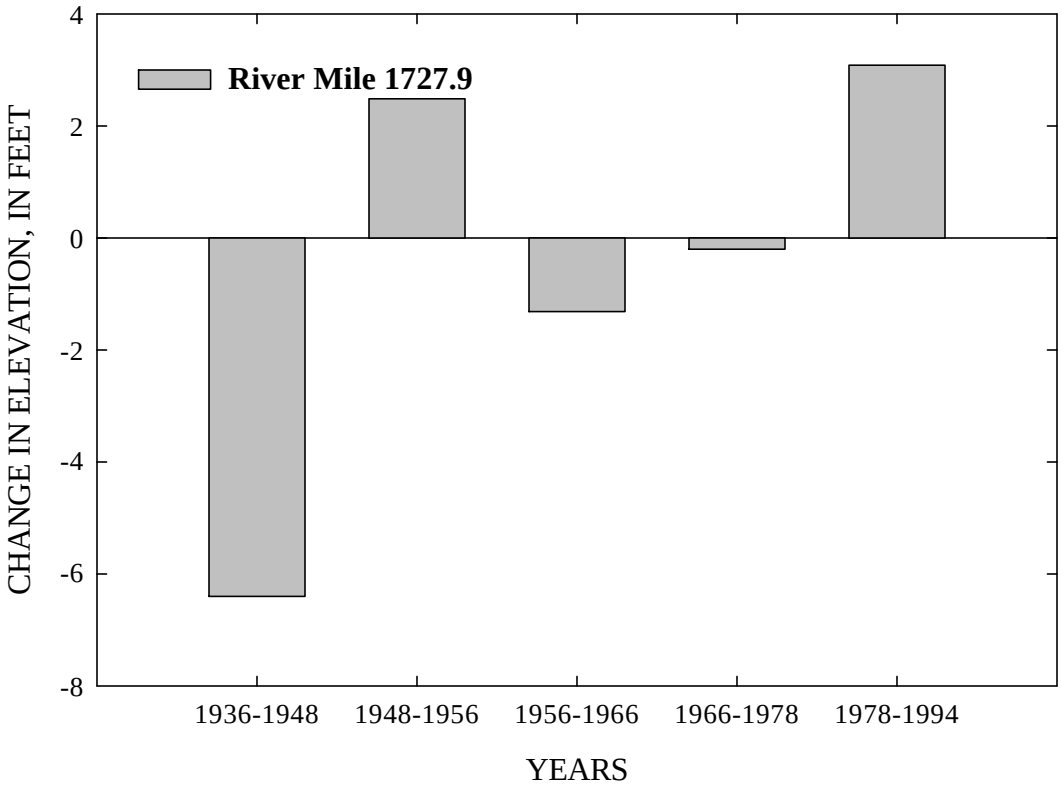
River Mile 1727.9
CHANGE IN ELEVATION, IN FEET
4
2
0
-2
-4
-6
-8
1936-1948
1948-1956
1956-1966
1966-1978
1978-1994
YEARS

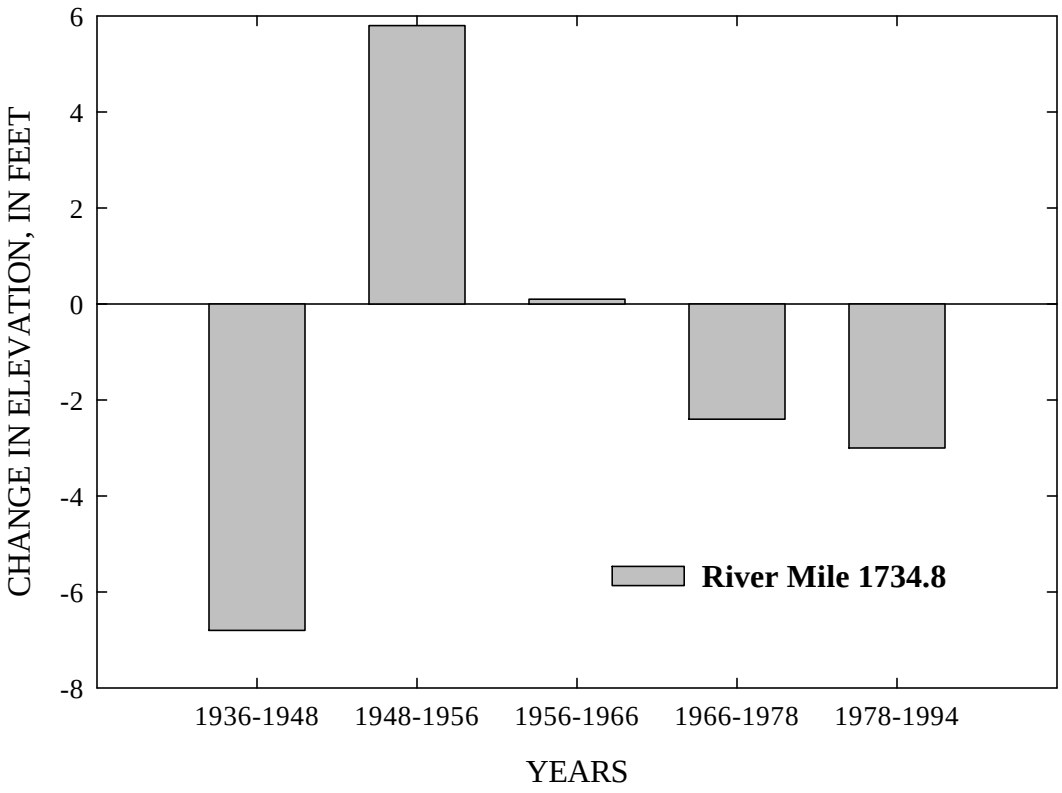
6
4
2
0
-2
-4
-6
-8
CHANGE IN ELEVATION, IN FEET
1936-1948
1948-1956
1956-1966
1966-1978
1978-1994
YEARS
River Mile 1734.8

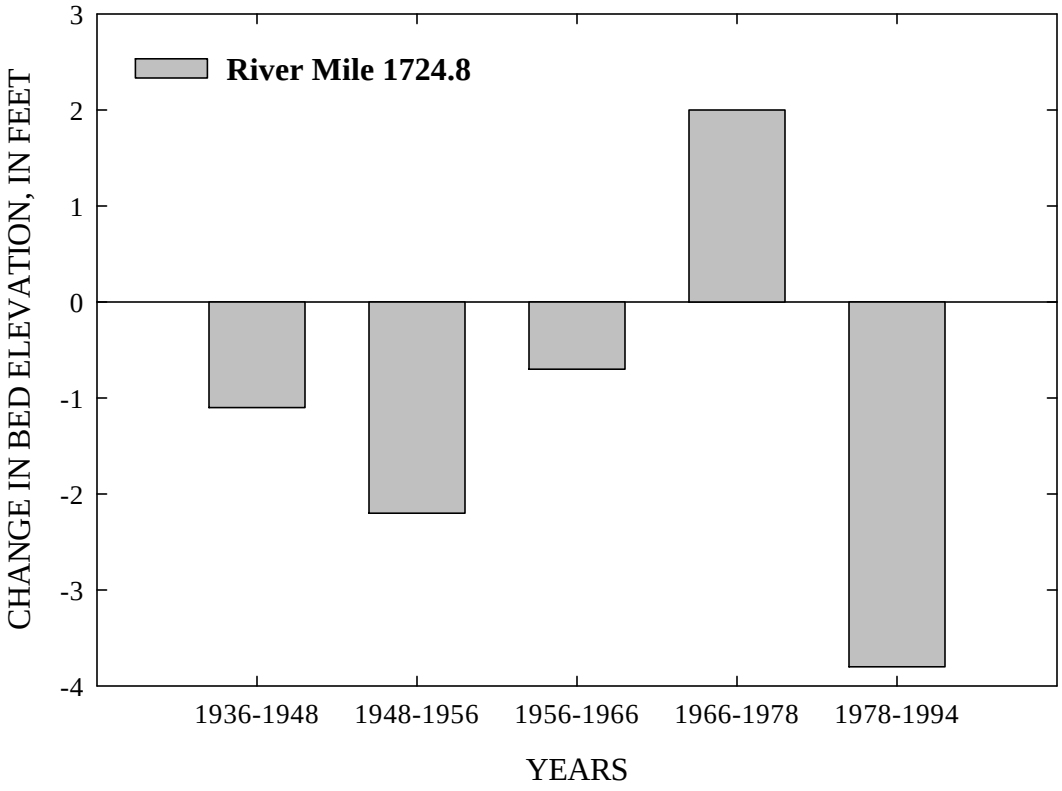
River Mile 1724.8
CHANGE IN BED ELEVATION, IN FEET
3
2
1
0
-1
-2
-3
-4
1936-1948
1948-1956
1956-1966
1966-1978
1978-1994
YEARS

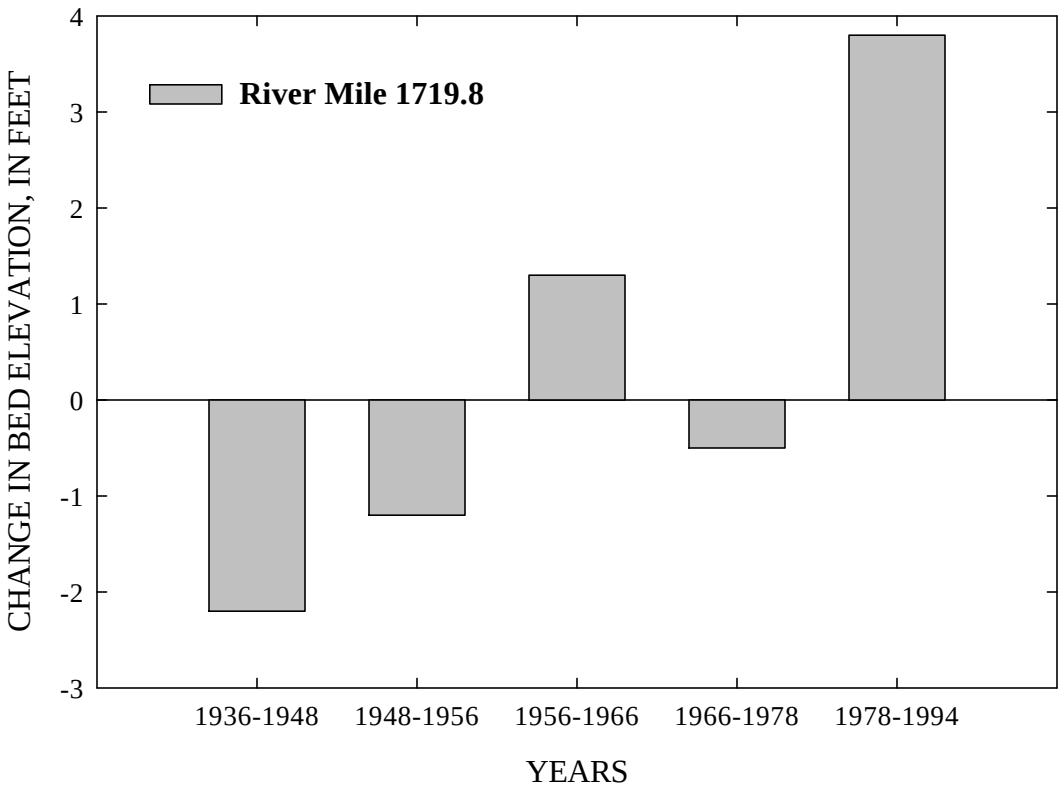
River Mile 1719.8
CHANGE IN BED ELEVATION, IN FEET
4
3
2
1
0
-1
-2
-3
1936-1948
1948-1956
1956-1966
1966-1978
1978-1994
YEARS

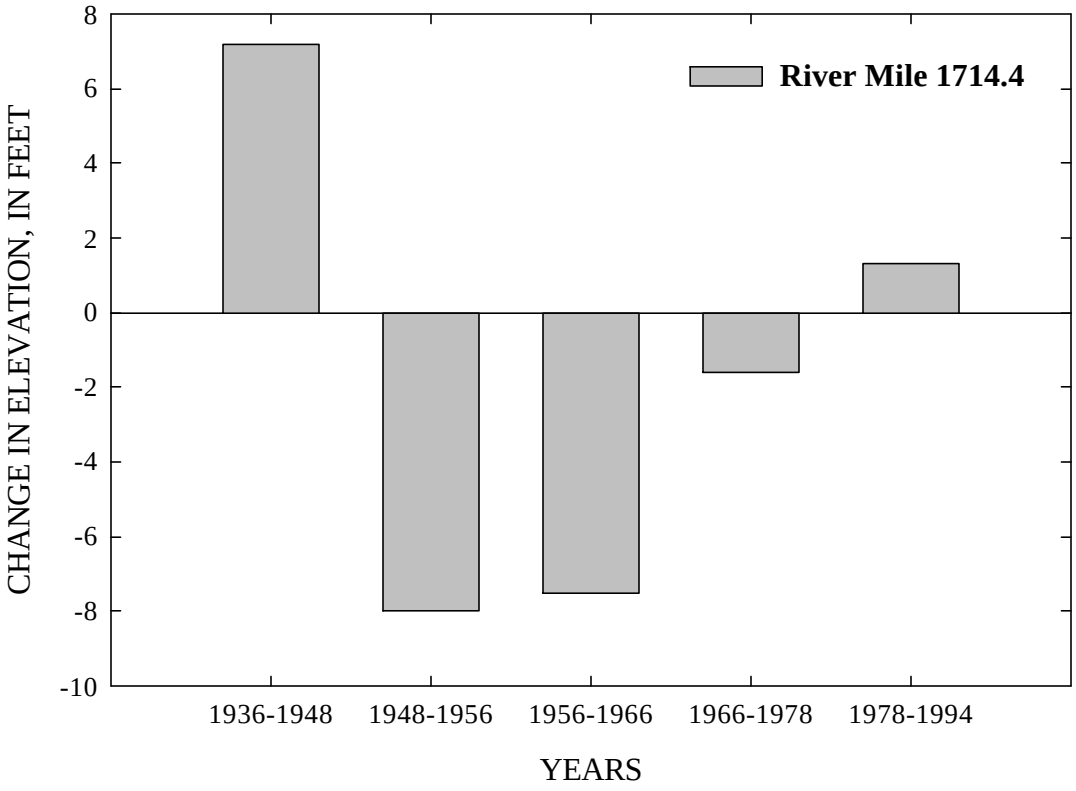
River Mile 1714.4
CHANGE IN ELEVATION, IN FEET
8
6
4
2
0
-2
-4
-6
-8
-10
1936-1948
1948-1956
1956-1966
1966-1978
1978-1994
YEARS

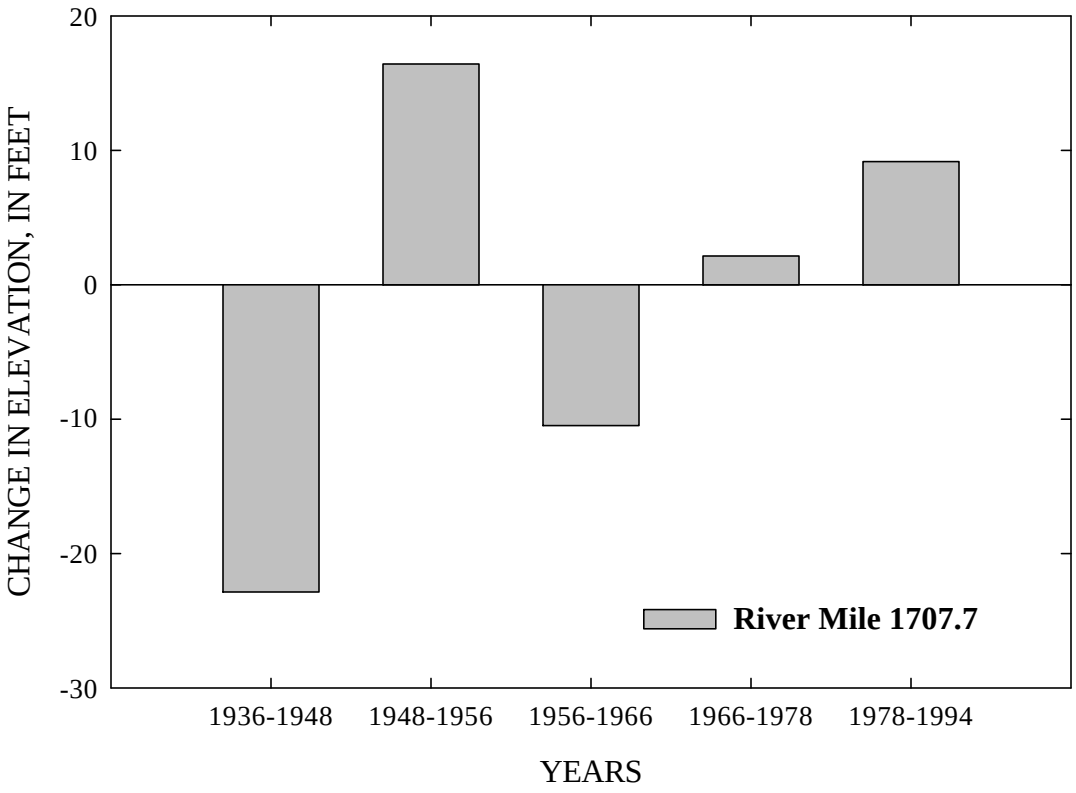
20
10
0
-10
-20
-30
CHANGE IN ELEVATION, IN FEET
1936-1948
1948-1956
1956-1966
1966-1978
1978-1994
YEARS
River Mile 1707.7

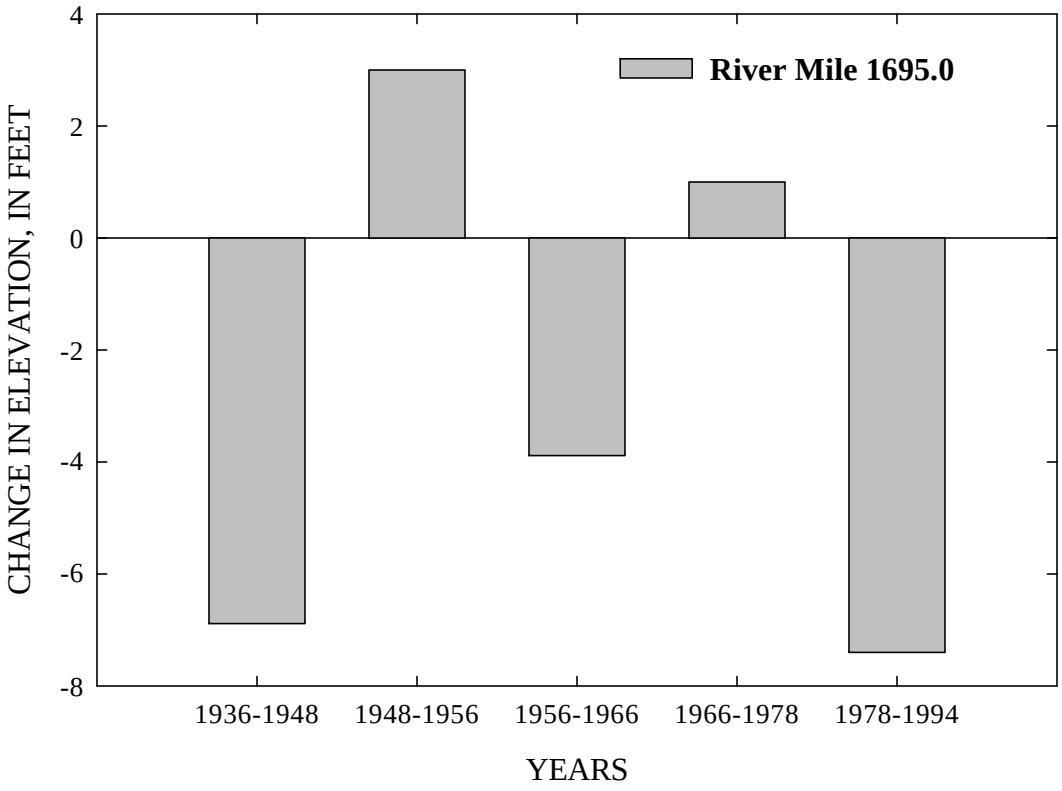
River Mile 1695.0
CHANGE IN ELEVATION, IN FEET
4
2
0
-2
-4
-6
-8
1936-1948
1948-1956
1956-1966
1966-1978
1978-1994
YEARS

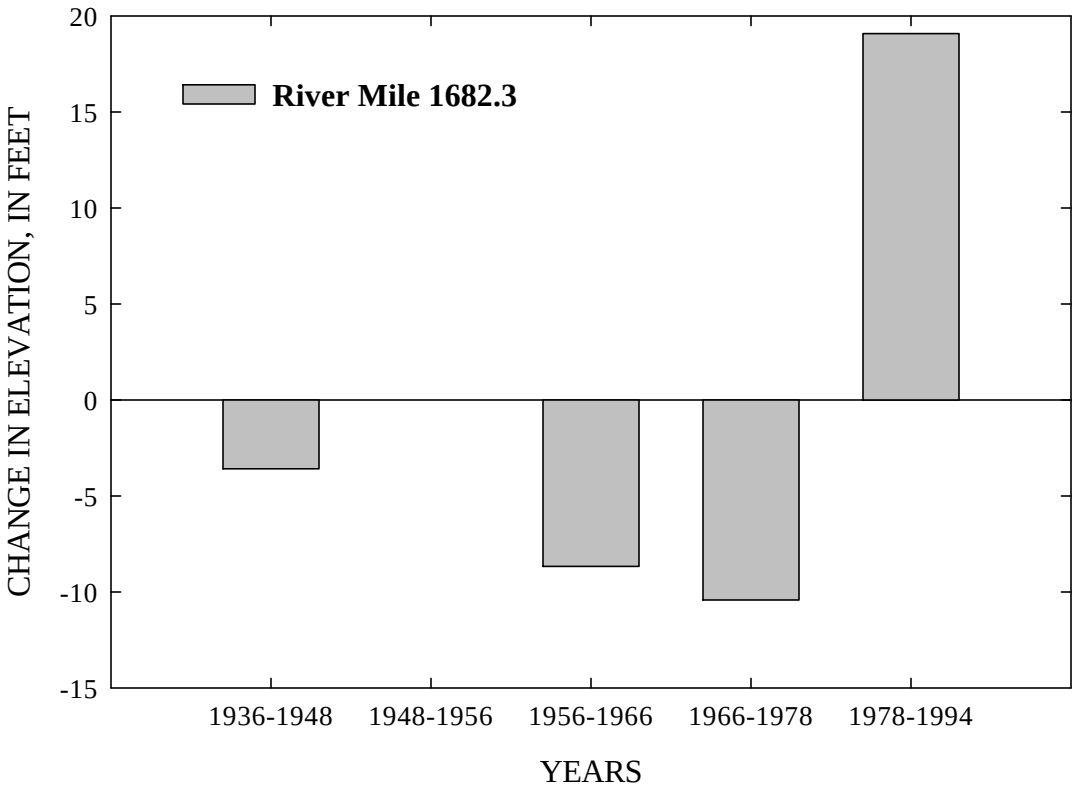
River Mile 1682.3
CHANGE IN ELEVATION, IN FEET
20
15
10
5
0
-5
-10
-15
1936-1948
1948-1956
1956-1966
1966-1978
1978-1994
YEARS

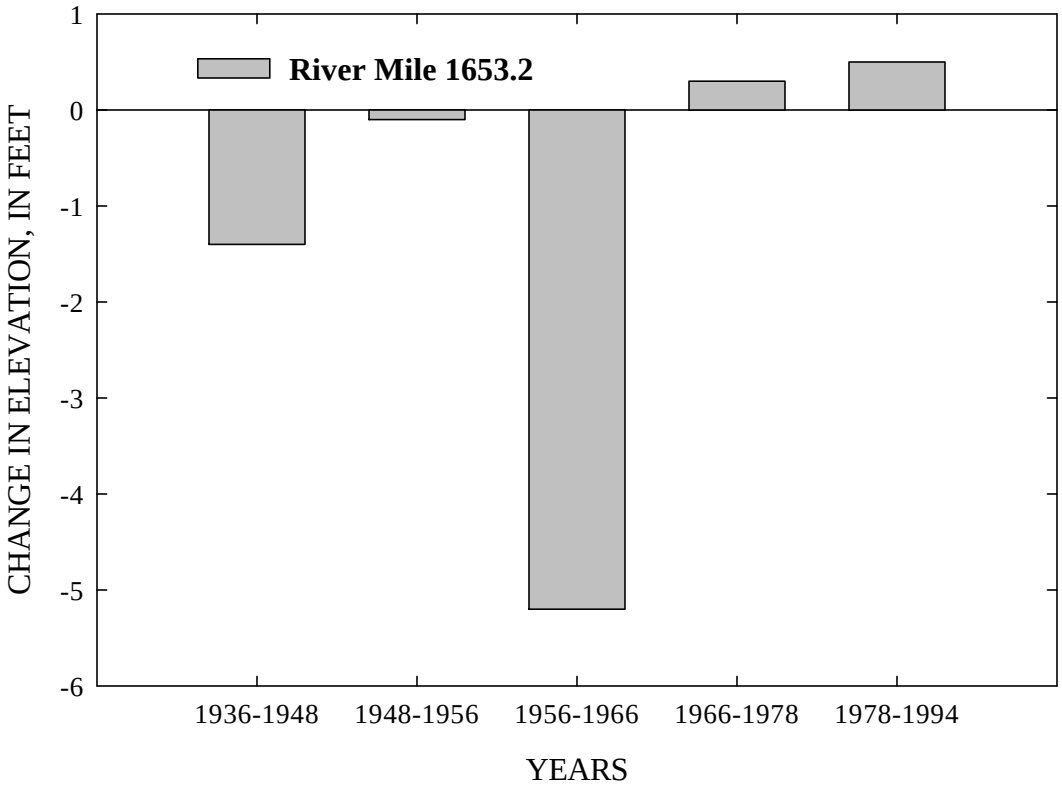
River Mile 1653.2
CHANGE IN ELEVATION, IN FEET
1
0
-1
-2
-3
-4
-5
-6
1936-1948
1948-1956
1956-1966
1966-1978
1978-1994
YEARS

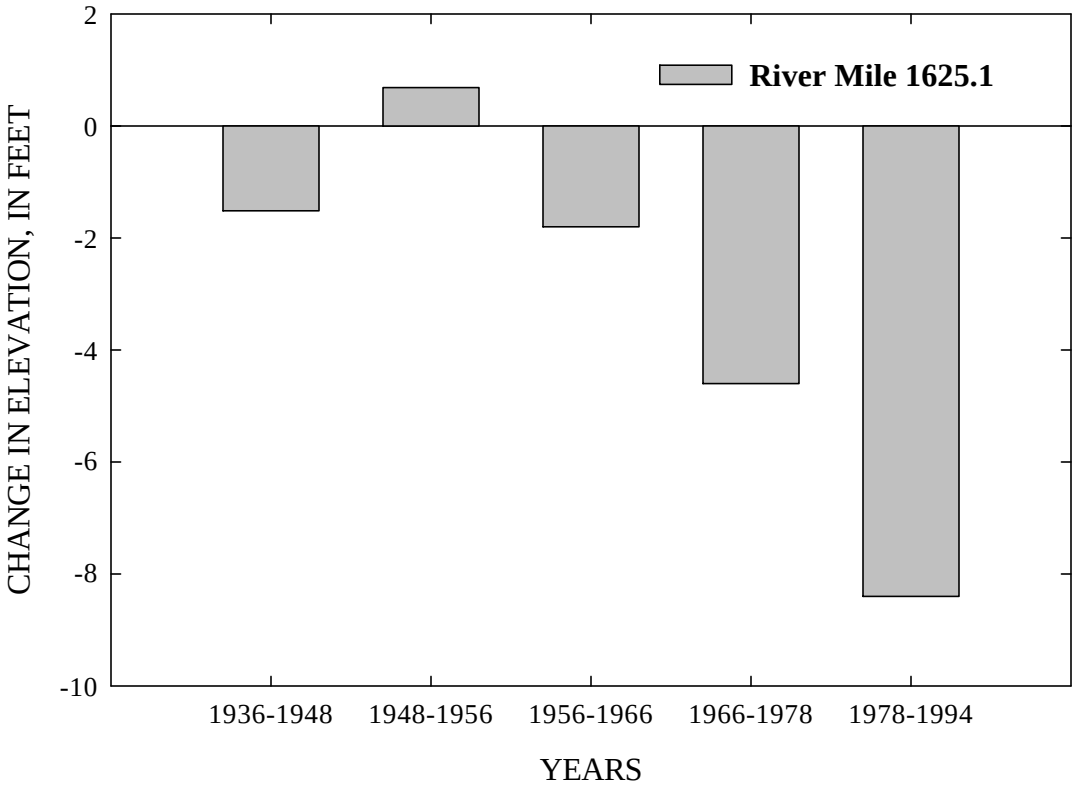
River Mile 1625.1
2
0
-2
-4
-6
-8
-10
CHANGE IN ELEVATION, IN FEET
1936-1948
1948-1956
1956-1966
1966-1978
1978-1994
YEARS

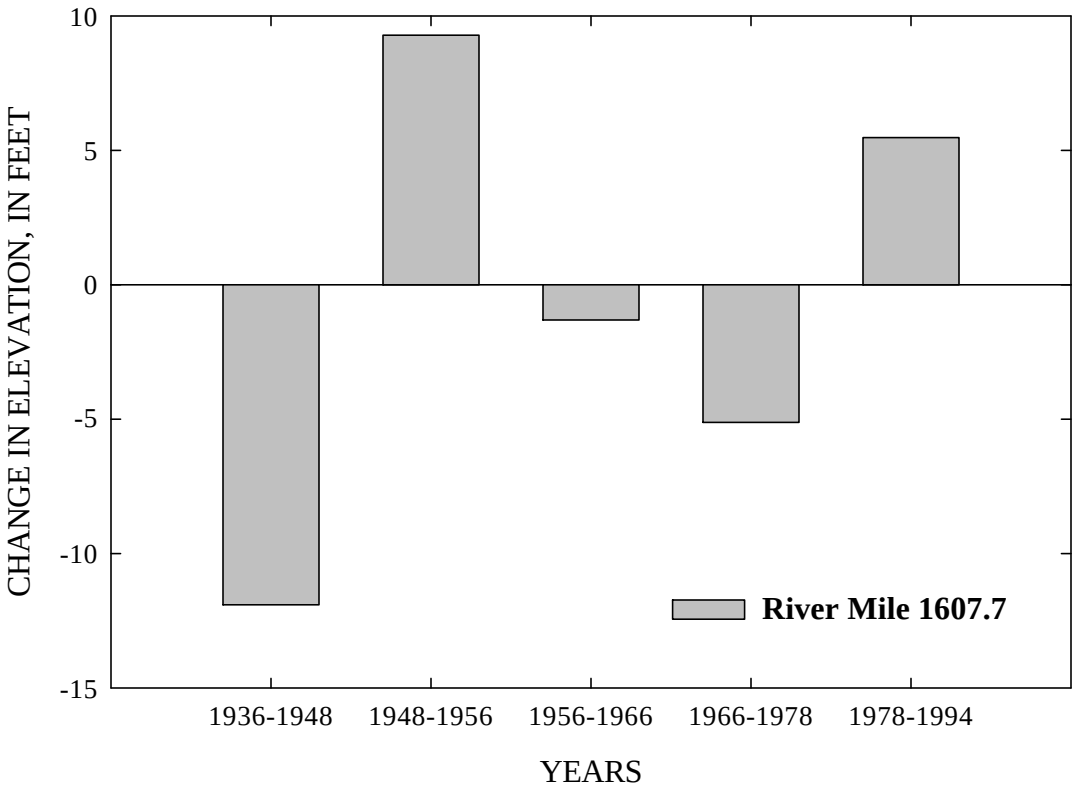
10
5
0
-5
-10
-15
CHANGE IN ELEVATION, IN FEET
1936-1948
1948-1956
1956-1966
1966-1978
1978-1994
YEARS
River Mile 1607.7

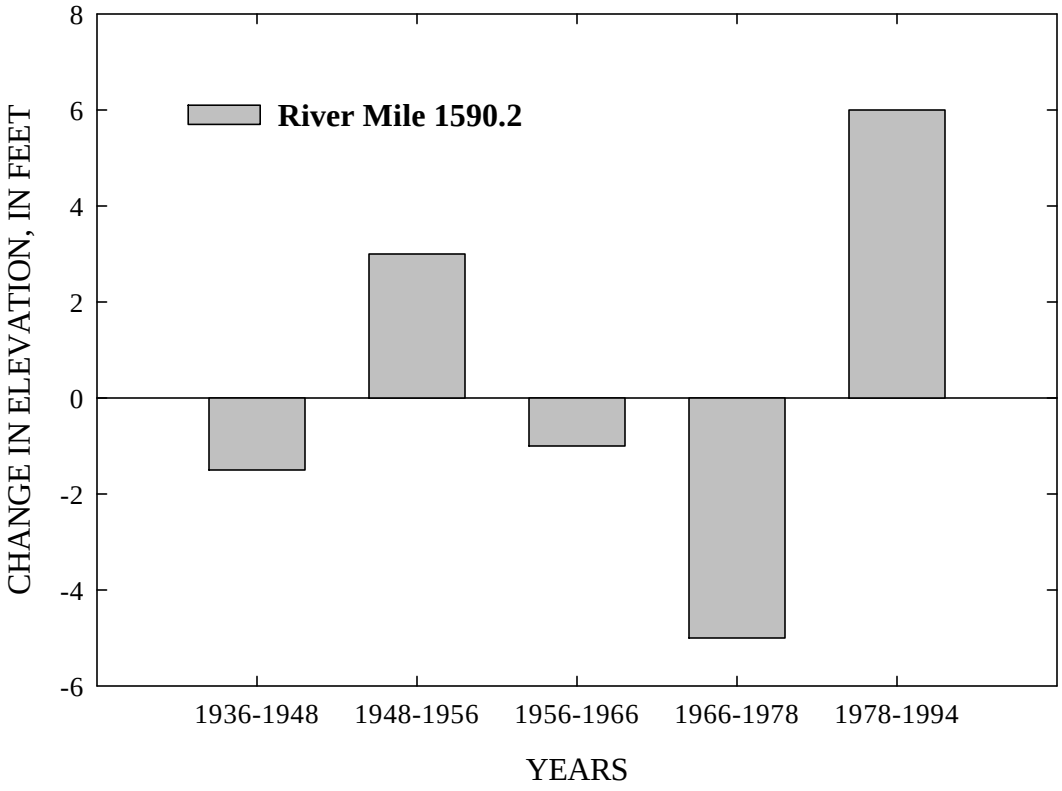
River Mile 1590.2
CHANGE IN ELEVATION, IN FEET
8
6
4
2
0
-2
-4
-6
1936-1948
1948-1956
1956-1966
1966-1978
1978-1994
YEARS

APPENDIX D

List of Maps and Photographs Used for Analysis of Rates of Channel Activity

Appendix D1-- Map coverages used for analysis of rates of channel activity

Quad Name	Year	Scale	Degrees	Minutes	Seconds	Scale	Source	Map Number	coverage				year	coverage
RG77-CWMF-Q271- #3	1874		105	0	0	1:253440	US Northern Boundary Commission	3	1				1874	1
RG77-CWMF-Q271- #4	1874		103	0	0	1:253440	US Northern Boundary Commission	4	1				1891	2
LXIII	1890	1:63,360	105	18	0	1:63360	Missouri River Commission	63	1				1913	3
LXIV	1890	1:63,360	105	48	0	1:63360	Missouri River Commission	64	1				1915	3
LXV	1890	1:63,360	106	12	0	1:63360	Missouri River Commission	65	1				1916	3
LX	1891	1:63,360	103	54	0	1:63360	Missouri River Commission	60	2				1950	4
LXI	1891	1:63,360	104	21	0	1:63360	Missouri River Commission	61	2				1968	4
LXII	1891	1:63,360	104	51	0	1:63360	Missouri River Commission	62	2				1972	4
Chelsea	1910	1:62,500	105	15	0	1:62500	USGS	5	2				1989	5
Poplar	1910	1:62,500	105	0	0	1:62500	USGS	6	2				1991	6
Brockton	1911	1:62,500	104	45	0	1:62500	USGS	7	2					
Wolf Point	1913	1:62,500	105	30	0	1:62500	USGS	4	3					
Frazer	1913	1:62,500	106	0	0	1:62500	USGS	3-2	3					
Oswego	1913	1:62,500	105	45	0	1:62500	USGS	3-3	3					
Nashua	1914	1:62,500	106	15	0	1:62500	USGS	3-1	3					
Fort Kipp	1949	1:24000	104	37	30			15 a	4					
Calais	1950	1:24000	104	45	0	1:24000	USGS	14 a	4					
Bainville SE	1967	1:24000	104	0	0	1:24000	USGS	20	4					
Dore	1967	1:24000	104	0	0	1:24000	USGS	20 a	4					
Twomile Creek	1968	1:24000	104	37	30	1:24000	USGS	15	4					
Dugout Creek	1968	1:24000	104	30	0	1:24000	USGS	16	4					
Three Buttes	1968	1:24000	104	22	30	1:24000	USGS	17	4					
Cedar Coulee	1968	1:24000	104	15	0	1:24000	USGS	18	4					
Culbertson	1968	1:24000	104	30	0	1:24000	USGS	16 a	4					
Bainville SW	1969	1:24000	104	7	30	1:24000	USGS	19	4					
Fort Peck	1971	1:24000	106	22	30	1:24000	USGS	1	4					
Milk River Hills	1971	1:24000	106	15	0	1:24000	USGS	2	4					
Kintyre	1971	1:24000	106	7	30	1:24000	USGS	3	4					
Frazer	1971	1:24000	106	0	0	1:24000	USGS	4	4					
Oswego	1971	1:24000	105	52	30	1:24000	USGS	5	4					
Flynn Creek	1971	1:24000	105	45	0	1:24000	USGS	6	4					
Wolf Point	1971	1:24000	105	37	30	1:24000	USGS	7	4					
Macon	1971	1:24000	105	30	0	1:24000	USGS	8	4					
Nickwall	1971	1:24000	105	15	0	1:24000	USGS	10	4					
Poplar	1971	1:24000	105	7	30	1:24000	USGS	11	4					
Sprole	1971	1:24000	105	0	0	1:24000	USGS	12	4					
Mortarstone Bluff	1971	1:24000	104	52	30	1:24000	USGS	13	4					
Frog Coulee	1971	1:24000	104	45	0	1:24000	USGS	14	4					
Brockton	1971	1:24000	104	52	30	1:24000	USGS	13 a	4					
Chelsea SW	1972	1:24000	105	22	30	1:24000	USGS	9	4					
Flynn Creek	1989	1:24000	105	45	0	1:24000	USGS	6	5					
Wolf Point	1989	1:24000	105	37	30	1:24000	USGS	7	5					
Poplar	1989	1:24000	105	7	30	1:24000	USGS	11	5					
Sprole	1989	1:24000	105	0	0	1:24000	USGS	12	5					
Mortarstone Bluff	1989	1:24000	104	52	30	1:24000	USGS	13	5					
Frog Coulee	1989	1:24000	104	45	0	1:24000	USGS	14	5					
Twomile Creek	1989	1:24000	104	37	30	1:24000	USGS	15	5					
Dugout Creek	1989	1:24000	104	30	0	1:24000	USGS	16	5					
Three Buttes	1989	1:24000	104	22	30	1:24000	USGS	17	5					
Cedar Coulee	1989	1:24000	104	15	0	1:24000	USGS	18	5					
Bailville SW	1989	1:24000	104	7	30	1:24000	USGS	19	5					
Bainville SE	1989	1:24000	104	0	0	1:24000	USGS	20	5					
Calais	1989	1:24000	104	45	0	1:24000	USGS		5					
Brockton	1989	1:24000	104	52	30	1:24000	USGS		5					
Culbertson	1989	1:24000	104	30	0	1:24000	USGS		5					
Fort Kipp	1989	1:24000	104	37	30	1:24000	USGS		5					

Appendix D2-- Photographic coverage used for analysis of channel activity			
ID Number	**Date**	**Nominal Scale**	**Source**
3730-70	06/12/91	1:24000	NAPP
3731-7	06/12/91	1:24000	NAPP
3731-282	06/12/91	1:24000	NAPP
3732-12	06/12/91	1:24000	NAPP
3671-172	07/13/91	1:24000	NAPP
3700-064	07/13/91	1:24000	NAPP
3700-125	07/13/91	1:24000	NAPP
3700-273	07/13/91	1:24000	NAPP
3672-201	07/28/91	1:24000	NAPP
3672-231	07/28/91	1:24000	NAPP
3673-017	08/04/91	1:24000	NAPP
3673-112	08/04/91	1:24000	NAPP
3673-103	08/04/91	1:24000	NAPP
3264-033	08/10/91	1:24000	NAPP
3703-015	08/11/91	1:24000	NAPP
3675-036	08/12/91	1:24000	NAPP
3675-096	08/12/91	1:24000	NAPP
3675-177	08/12/91	1:24000	NAPP
3704-095	08/18/91	1:24000	NAPP
3704-157	08/18/91	1:24000	NAPP
3705-011	08/18/91	1:24000	NAPP
3707-044	08/21/91	1:24000	NAPP
3707-072	08/21/91	1:24000	NAPP
3707-137	08/21/91	1:24000	NAPP
3707-192	08/21/91	1:24000	NAPP
3681-009	08/31/91	1:24000	NAPP
3735-194	09/18/91	1:24000	NAPP
3735-192	09/18/91	1:24000	NAPP
3736-137	09/18/91	1:24000	NAPP
3736-71	09/18/91	1:24000	NAPP
3683-76	08/13/92	1:24000	NAPP
3683-139	08/13/92	1:24000	NAPP
3687-8	08/18/92	1:24000	NAPP
3687-6	08/18/92	1:24000	NAPP
3711-12	08/18/92	1:24000	NAPP
3711-104	08/18/92	1:24000	NAPP
3711-152	08/18/92	1:24000	NAPP
3712-28	08/19/92	1:24000	NAPP
3688-22	08/26/92	1:24000	NAPP

APPENDIX E

Site Locations for Analysis of Rates of Local Channel Activity

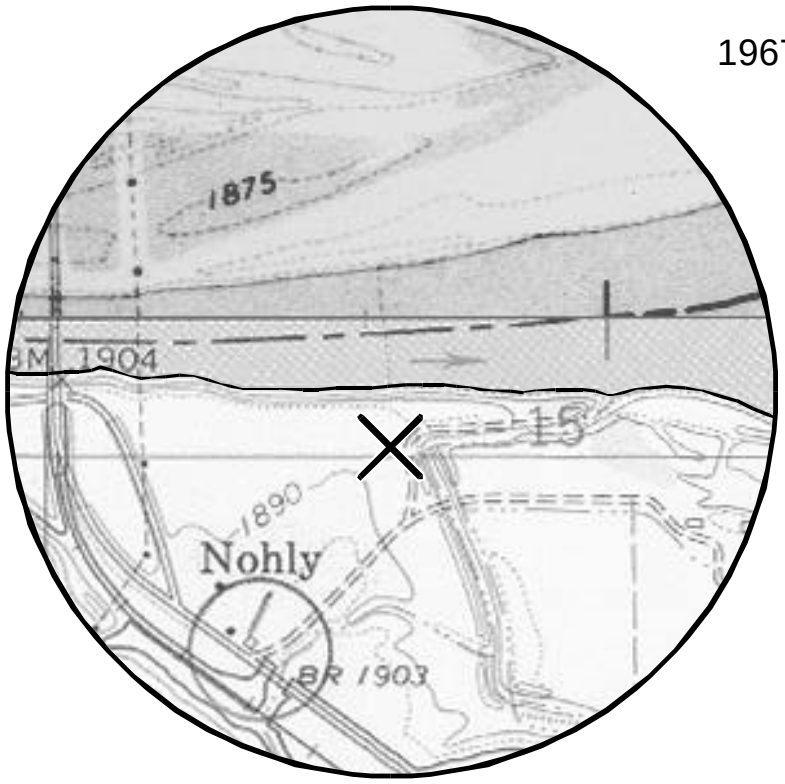

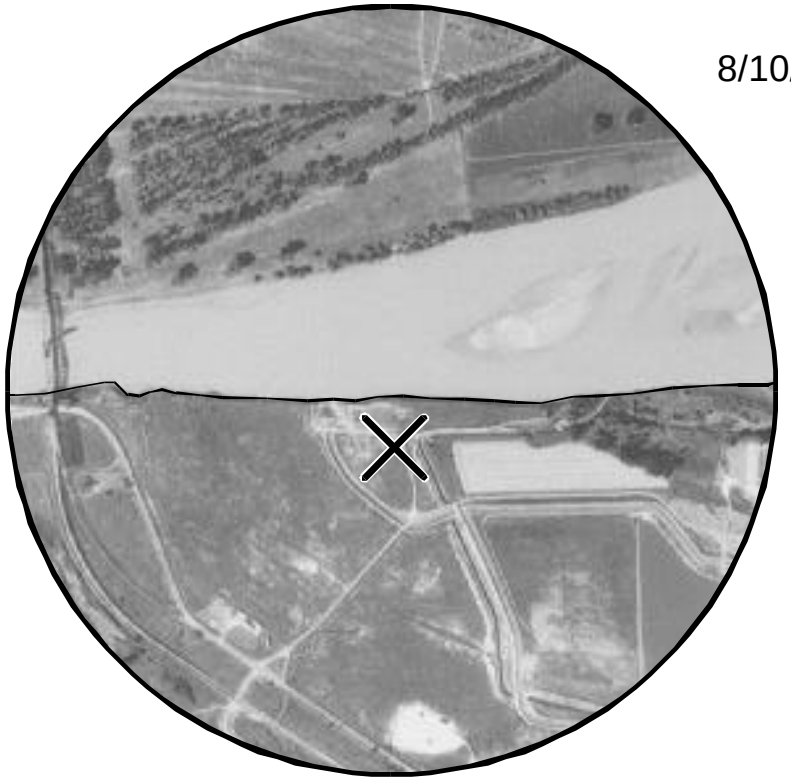

U.S.Geological Survey topographic map and NationalHighAltitude Photography Program coverage of local erosion rate site 1, RM 1590 (Nohly site).

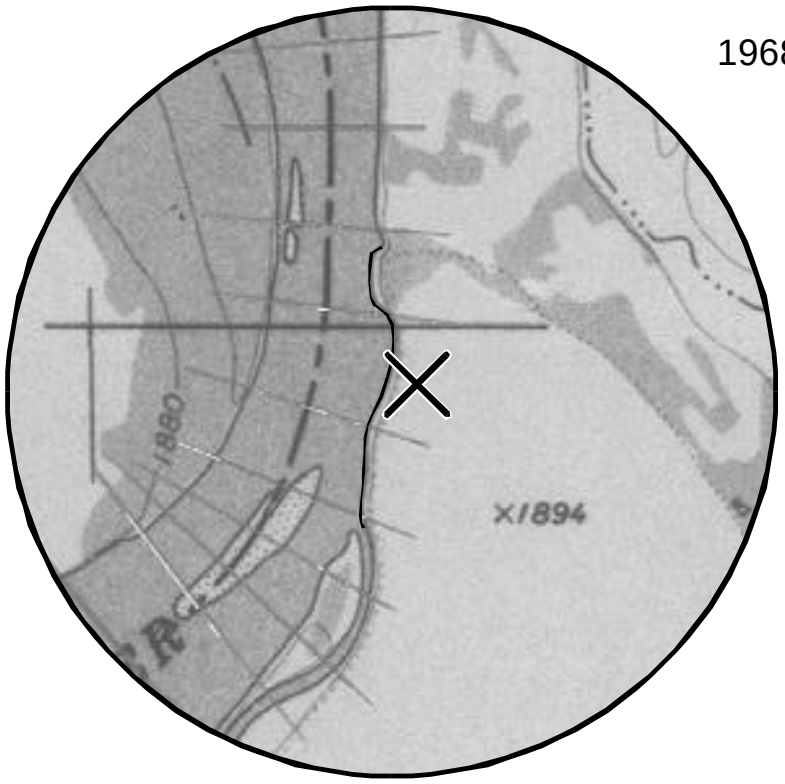

U.S. Geological Survey topographicmapandNational High Altitude Photography Program coverage of local erosion rate site 2, RM1604 (Hardy site).

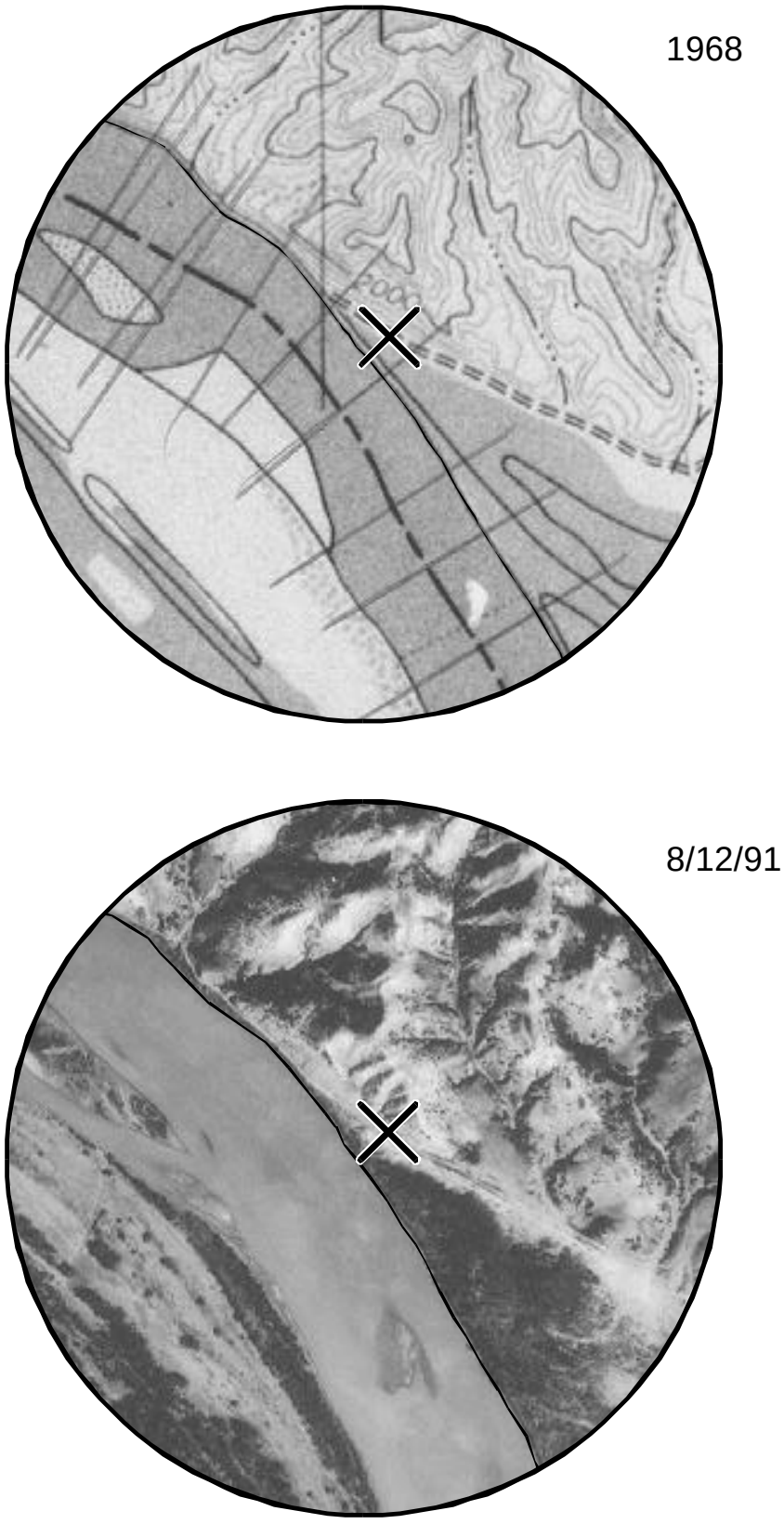

U.S. Geological Survey topographic map and NationalHighAltitude Photography Program coverage of local erosion rate site 3, RM 1621 (Culbertson site).

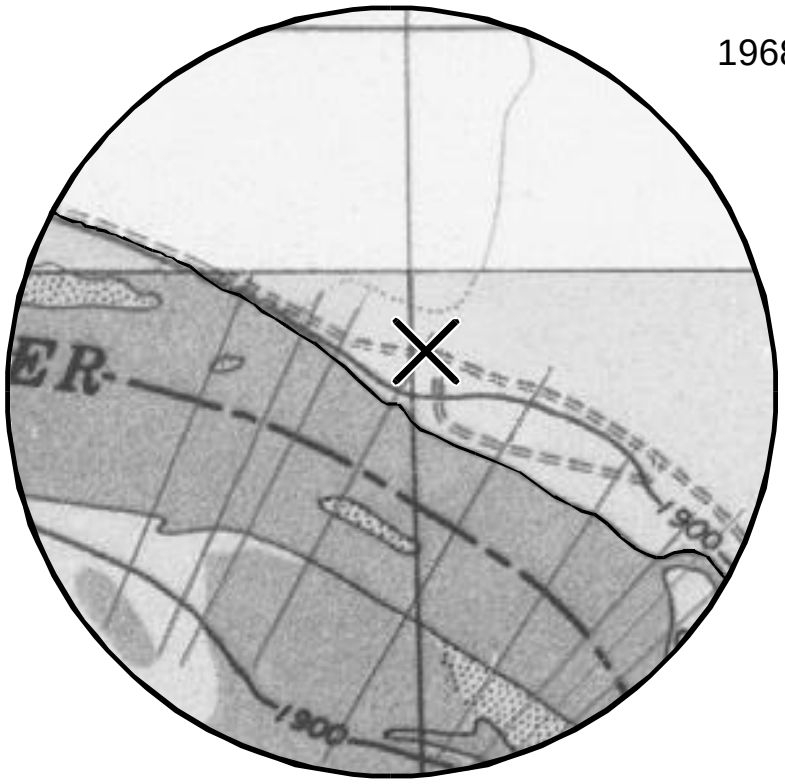

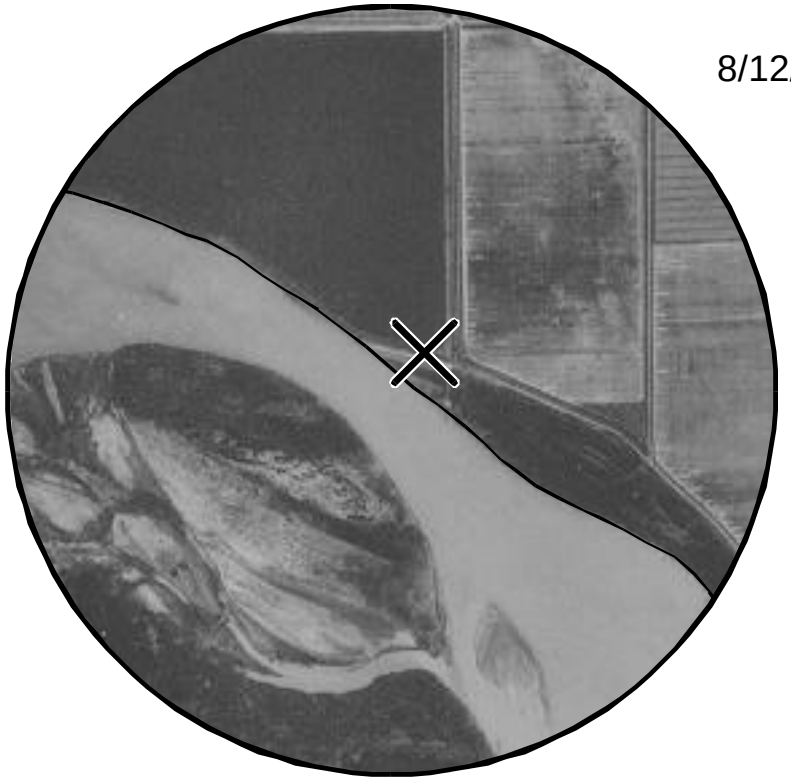

U.S. Geological Survey topographic map and NationalHighAltitude Photography Program coverage oflocalerosion rate sites 4 and 5, RM 1624 (Tveit-Johnson site).

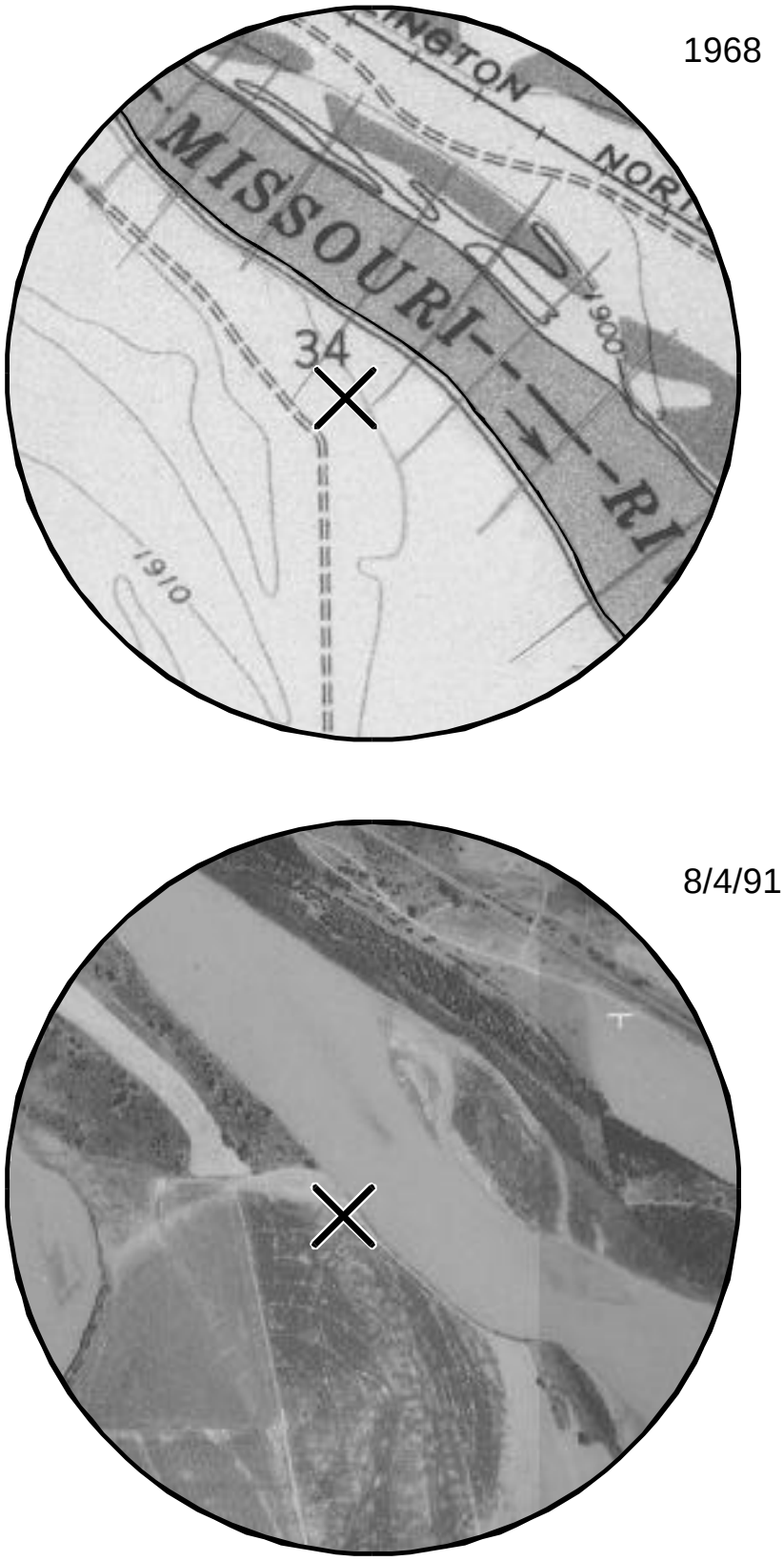

U.S. Geological Survey topographic map and NationalHighAltitude Photography Program coverage oflocalerosion rate site 6, RM 1630 (Iverson site).

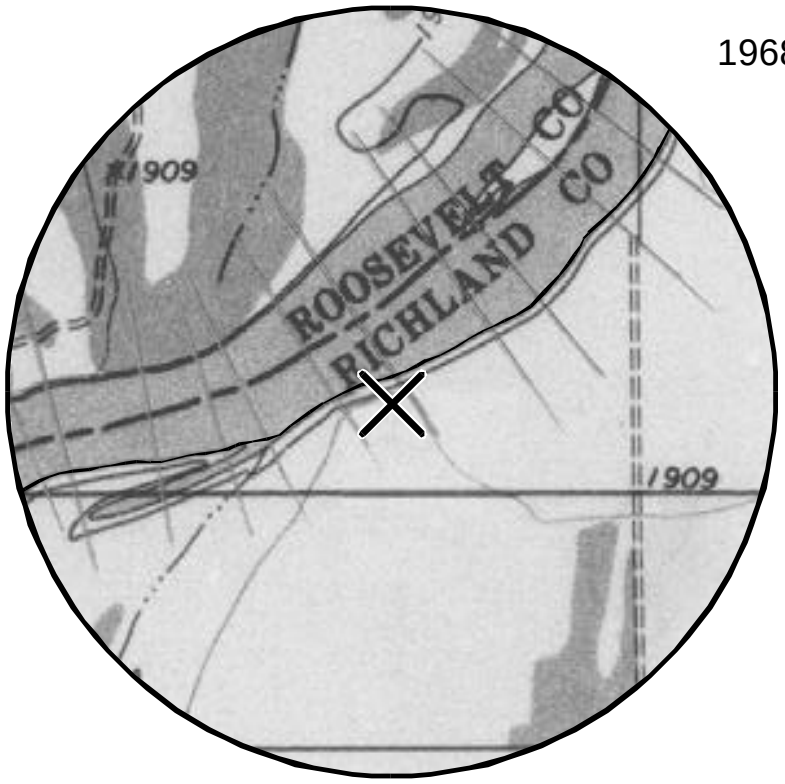

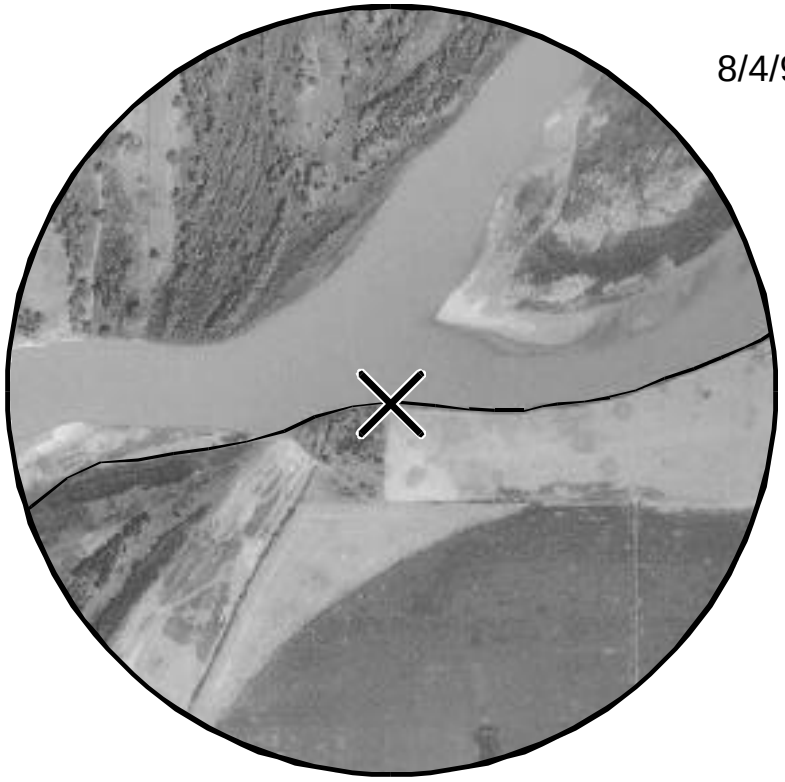

U.S. GeologicalSurvey topographic map and National High Altitude Photography Program coverage of local erosion rate site 7, RM 1631 (Vournassite).

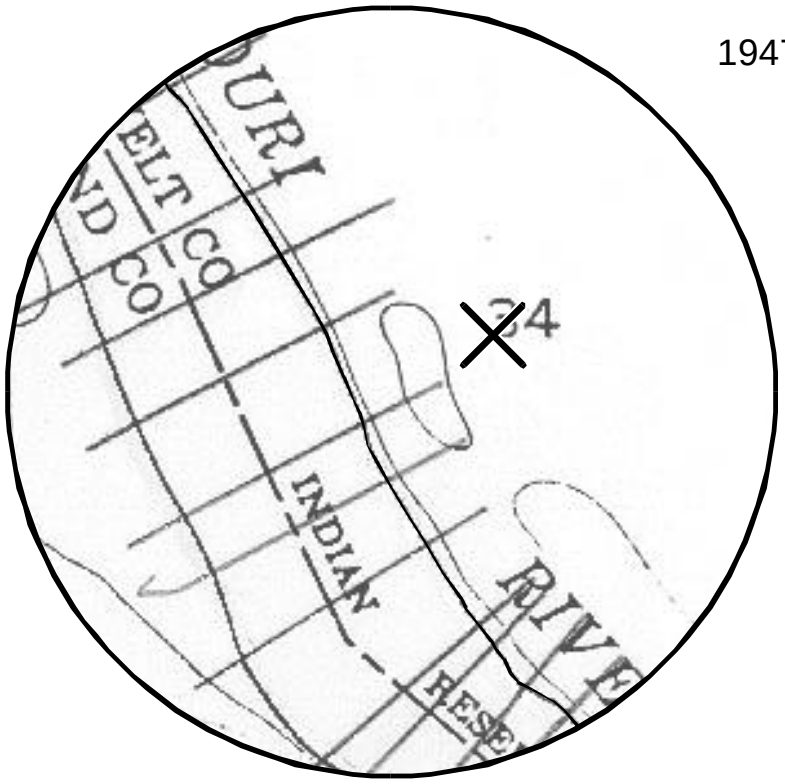

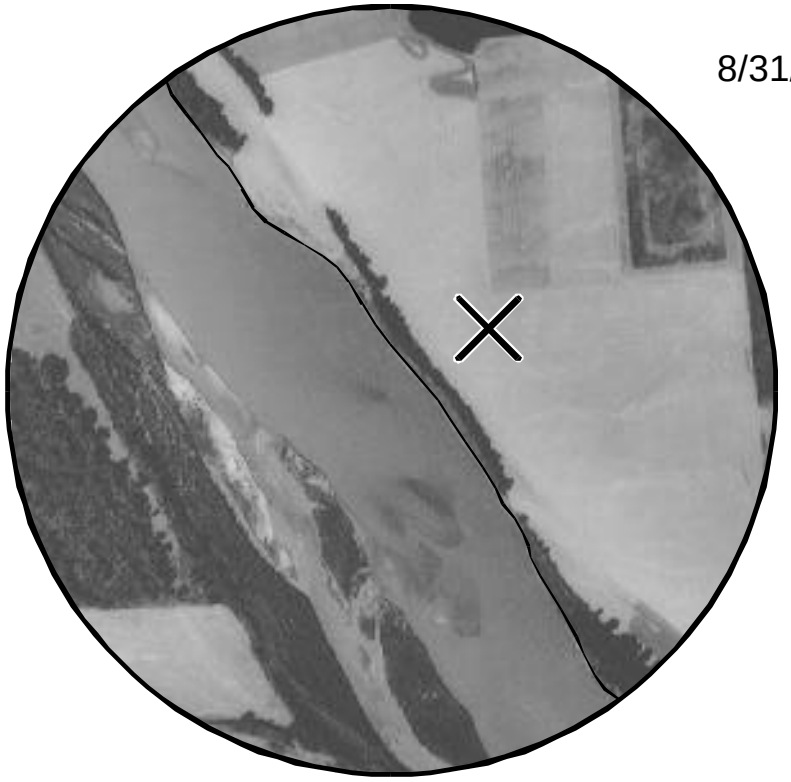

U.S. Geological Survey topographic map and National High Altitude Photography Program coverage of local erosion rate site 8, RM 1646 (Mattelin site).

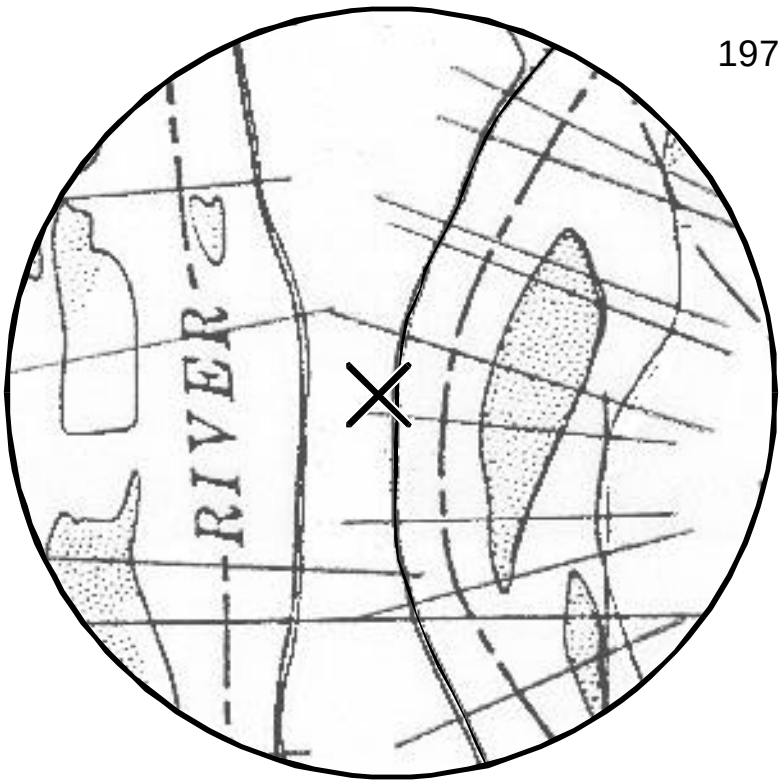

U.S. Geological Survey topographicmapandNational High Altitude Photography Program coverage of local erosion ratesite 9, RM1676 (Woods Peninsula site).

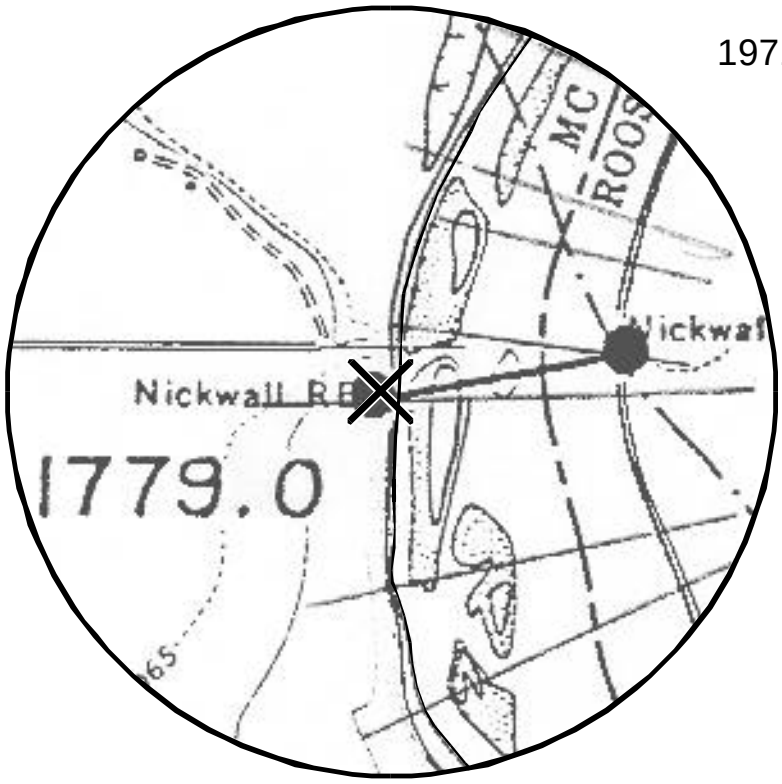

U.S. Geological Survey topographicmapandNational High Altitude Photography Program coverage of local erosion ratesite 10, RM1682 (McCraesite).

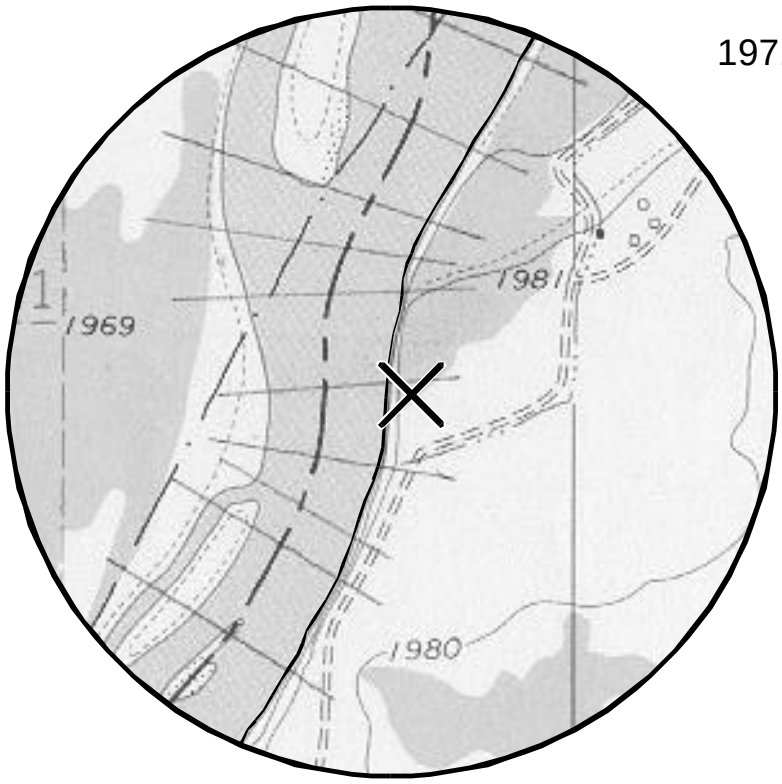

U.S. Geological Survey topographic map and NationalHighAltitude Photography Program coverage oflocalerosion rate site 11 RM 1701 (Wolf Point site).

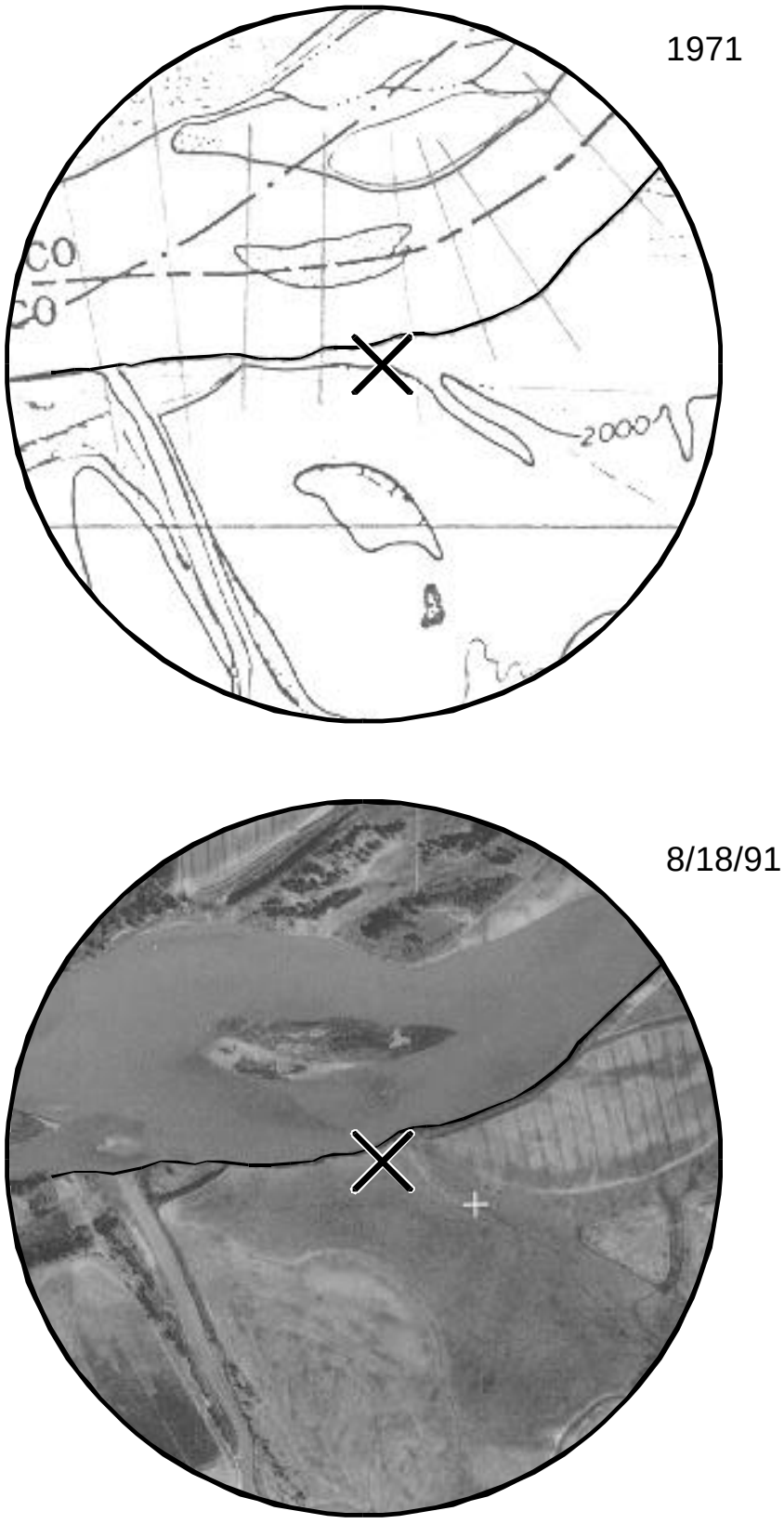

U.S. Geological Survey topographic map and NationalHighAltitude Photography Program coverage oflocalerosion rate site 11.5, RM 1716 (Pipal site).

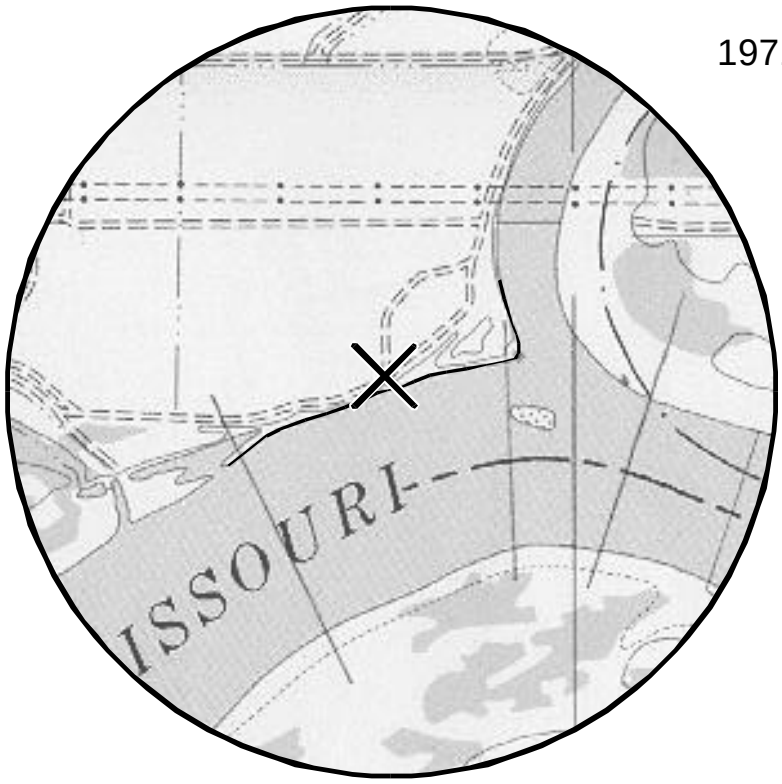

U.S. GeologicalSurvey topographic map and National High Altitude Photography Program coverage of local erosion rate site 15, RM 1762 (Milk River site).

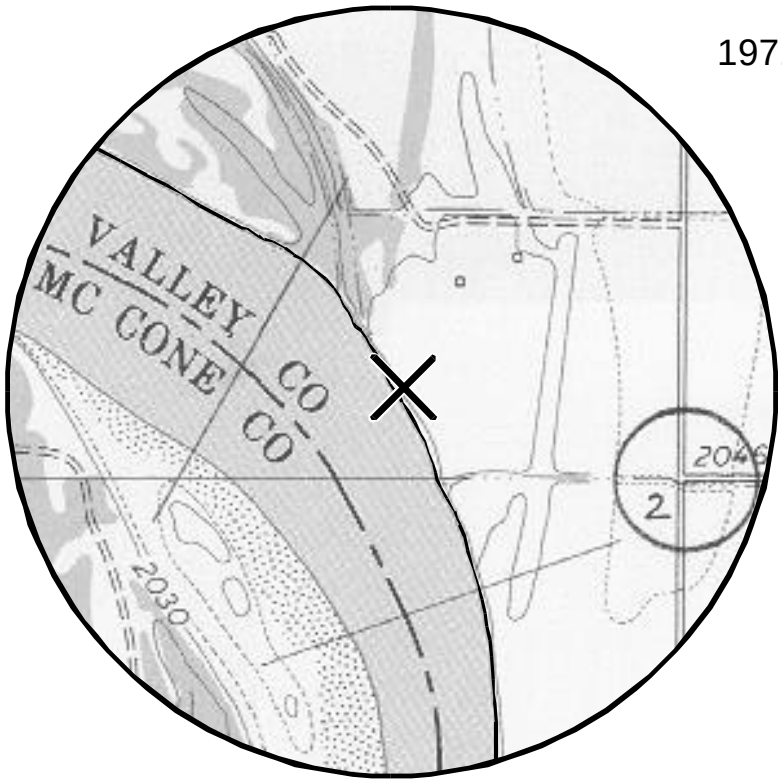

U.S. Geological Survey topographic map and National High Altitude Photography Program coverage of local erosion rate site 16, RM1765 (Garwood site).

APPENDIX F

GIS-Based Maps on Vegetation Types and Location of 1971 and 1991 Banklines*

* These maps are available from the U.S. Department of Agriculture, Agricultural Research Service, National Sedimentation Laboratory, Oxford, Mississippi. Requests should be brought to the attention of Dr. Andrew Simon, simon@sedlab.olemiss.edu.